

**OFFICE OF CIVILIAN RADIOACTIVE WASTE MANAGEMENT
ANALYSIS/MODEL COVER SHEET**

1. QA: QA

Page: 1 of 576

Complete Only Applicable Items

<p><input type="checkbox"/> Analysis Check all that apply</p> <table border="1" style="width:100%; border-collapse: collapse;"> <tr> <td style="width:20%;">Type of Analysis</td> <td> <input type="checkbox"/> Engineering <input type="checkbox"/> Performance Assessment <input type="checkbox"/> Scientific </td> </tr> <tr> <td>Intended Use of Analysis</td> <td> <input type="checkbox"/> Input to Calculation <input type="checkbox"/> Input to another Analysis or Model <input type="checkbox"/> Input to Technical Document <input type="checkbox"/> Input to other Technical Products </td> </tr> <tr> <td colspan="2">Describe use:</td> </tr> </table>	Type of Analysis	<input type="checkbox"/> Engineering <input type="checkbox"/> Performance Assessment <input type="checkbox"/> Scientific	Intended Use of Analysis	<input type="checkbox"/> Input to Calculation <input type="checkbox"/> Input to another Analysis or Model <input type="checkbox"/> Input to Technical Document <input type="checkbox"/> Input to other Technical Products	Describe use:		<p>3. <input checked="" type="checkbox"/> Model Check all that apply</p> <table border="1" style="width:100%; border-collapse: collapse;"> <tr> <td style="width:20%;">Type of Model</td> <td> <input type="checkbox"/> Conceptual Model <input type="checkbox"/> Abstraction Model <input type="checkbox"/> Mathematical Model <input checked="" type="checkbox"/> System Model <input type="checkbox"/> Process Model </td> </tr> <tr> <td>Intended Use of Model</td> <td> <input type="checkbox"/> Input to Calculation <input type="checkbox"/> Input to another Model or Analysis <input type="checkbox"/> Input to Technical Document <input checked="" type="checkbox"/> Input to other Technical Products </td> </tr> <tr> <td colspan="2">Describe use: Forecast the performance of a proposed repository at Yucca Mountain for Site Recommendation.</td> </tr> </table>	Type of Model	<input type="checkbox"/> Conceptual Model <input type="checkbox"/> Abstraction Model <input type="checkbox"/> Mathematical Model <input checked="" type="checkbox"/> System Model <input type="checkbox"/> Process Model	Intended Use of Model	<input type="checkbox"/> Input to Calculation <input type="checkbox"/> Input to another Model or Analysis <input type="checkbox"/> Input to Technical Document <input checked="" type="checkbox"/> Input to other Technical Products	Describe use: Forecast the performance of a proposed repository at Yucca Mountain for Site Recommendation.	
Type of Analysis	<input type="checkbox"/> Engineering <input type="checkbox"/> Performance Assessment <input type="checkbox"/> Scientific												
Intended Use of Analysis	<input type="checkbox"/> Input to Calculation <input type="checkbox"/> Input to another Analysis or Model <input type="checkbox"/> Input to Technical Document <input type="checkbox"/> Input to other Technical Products												
Describe use:													
Type of Model	<input type="checkbox"/> Conceptual Model <input type="checkbox"/> Abstraction Model <input type="checkbox"/> Mathematical Model <input checked="" type="checkbox"/> System Model <input type="checkbox"/> Process Model												
Intended Use of Model	<input type="checkbox"/> Input to Calculation <input type="checkbox"/> Input to another Model or Analysis <input type="checkbox"/> Input to Technical Document <input checked="" type="checkbox"/> Input to other Technical Products												
Describe use: Forecast the performance of a proposed repository at Yucca Mountain for Site Recommendation.													

4. Title:

Total System Performance Assessment (TSPA) Model for Site Recommendation

5. Document Identifier (including Rev. No. and Change No., if applicable):

MDL-WIS-PA-000002 REV 00

6. Total Attachments:

9

7. Attachment Numbers - No. of Pages in Each:

I-6, II-78, III-8, IV-12, V-8, VI-12, VII-68, VIII-12, IX-14

	Printed Name	Signature	Date
8. Originator	Patrick D. Mattie Steven P. Miller	<i>Patrick D. Mattie</i> <i>Jerry A. McNeish for S. Miller</i>	12/6/00 12-6-00
9. Checker	Norman Graves	<i>Norman L. Graves</i>	12/6/00
10. Lead/Supervisor	Jerry McNeish	<i>Jerry A. McNeish</i>	12-6-00
11. Responsible Manager	Jerry McNeish	<i>Jerry A. McNeish</i>	12-6-00

12. Remarks:

WM-11
N12507

**OFFICE OF CIVILIAN RADIOACTIVE WASTE MANAGEMENT
ANALYSIS/MODEL COVER SHEET**

1. QA: QA
Page: 1 of 576

Complete Only Applicable Items

<p><input type="checkbox"/> Analysis Check all that apply</p> <table border="1" style="width:100%; border-collapse: collapse;"> <tr> <td style="width:20%;">Type of Analysis</td> <td> <input type="checkbox"/> Engineering <input type="checkbox"/> Performance Assessment <input type="checkbox"/> Scientific </td> </tr> <tr> <td>Intended Use of Analysis</td> <td> <input type="checkbox"/> Input to Calculation <input type="checkbox"/> Input to another Analysis or Model <input type="checkbox"/> Input to Technical Document <input type="checkbox"/> Input to other Technical Products </td> </tr> <tr> <td colspan="2">Describe use:</td> </tr> </table>	Type of Analysis	<input type="checkbox"/> Engineering <input type="checkbox"/> Performance Assessment <input type="checkbox"/> Scientific	Intended Use of Analysis	<input type="checkbox"/> Input to Calculation <input type="checkbox"/> Input to another Analysis or Model <input type="checkbox"/> Input to Technical Document <input type="checkbox"/> Input to other Technical Products	Describe use:		<p>3. <input checked="" type="checkbox"/> Model Check all that apply</p> <table border="1" style="width:100%; border-collapse: collapse;"> <tr> <td style="width:20%;">Type of Model</td> <td> <input type="checkbox"/> Conceptual Model <input type="checkbox"/> Abstraction Model <input type="checkbox"/> Mathematical Model <input checked="" type="checkbox"/> System Model <input type="checkbox"/> Process Model </td> </tr> <tr> <td>Intended Use of Model</td> <td> <input type="checkbox"/> Input to Calculation <input type="checkbox"/> Input to another Model or Analysis <input type="checkbox"/> Input to Technical Document <input checked="" type="checkbox"/> Input to other Technical Products </td> </tr> <tr> <td colspan="2">Describe use:</td> </tr> </table> <p>Forecast the performance of a proposed repository at Yucca Mountain for Site Recommendation.</p>	Type of Model	<input type="checkbox"/> Conceptual Model <input type="checkbox"/> Abstraction Model <input type="checkbox"/> Mathematical Model <input checked="" type="checkbox"/> System Model <input type="checkbox"/> Process Model	Intended Use of Model	<input type="checkbox"/> Input to Calculation <input type="checkbox"/> Input to another Model or Analysis <input type="checkbox"/> Input to Technical Document <input checked="" type="checkbox"/> Input to other Technical Products	Describe use:	
Type of Analysis	<input type="checkbox"/> Engineering <input type="checkbox"/> Performance Assessment <input type="checkbox"/> Scientific												
Intended Use of Analysis	<input type="checkbox"/> Input to Calculation <input type="checkbox"/> Input to another Analysis or Model <input type="checkbox"/> Input to Technical Document <input type="checkbox"/> Input to other Technical Products												
Describe use:													
Type of Model	<input type="checkbox"/> Conceptual Model <input type="checkbox"/> Abstraction Model <input type="checkbox"/> Mathematical Model <input checked="" type="checkbox"/> System Model <input type="checkbox"/> Process Model												
Intended Use of Model	<input type="checkbox"/> Input to Calculation <input type="checkbox"/> Input to another Model or Analysis <input type="checkbox"/> Input to Technical Document <input checked="" type="checkbox"/> Input to other Technical Products												
Describe use:													

4. Title:

Total System Performance Assessment (TSPA) Model for Site Recommendation

5. Document Identifier (including Rev. No. and Change No., if applicable):

MDL-WIS-PA-000002 REV 00

6. Total Attachments:

9

7. Attachment Numbers - No. of Pages in Each:

I-6, II-78, III-8, IV-12, V-8, VI-12, VII-68, VIII-12, IX-14

	Printed Name	Signature	Date
8. Originator	Patrick D. Mattie Steven P. Miller	<i>Patrick D. Mattie</i> <i>Steven P. Miller for S. Miller</i>	12/6/00 12-6-00
9. Checker	Norman Graves	<i>Norman Graves</i>	12/6/00
10. Lead/Supervisor	Jerry McNeish	<i>Jerry McNeish</i>	12-6-00
11. Responsible Manager	Jerry McNeish	<i>Jerry McNeish</i>	12-6-00

12. Remarks:

INFORMATION COPY
LAS VEGAS DOCUMENT CONTROL

**OFFICE OF CIVILIAN RADIOACTIVE WASTE MANAGEMENT
ANALYSIS/MODEL REVISION RECORD**

Complete Only Applicable Items

1. Page: 2 of: 576

2. Analysis or Model Title:

Total System Performance Assessment (TSPA) Model for Site Recommendation

3. Document Identifier (including Rev. No. and Change No., if applicable):

MDL-WIS-PA-000002 REV 00

4. Revision/Change No.

5. Description of Revision/Change

Rev. 00

Initial Issue

ACKNOWLEDGMENTS

SUPPORTING AUTHORS

P.D. Mattie (Lead), S.P. Miller (Lead), S.D. Sevougian, D.A. Kalinich, S. Mehta, E. Devonec, K.P. Lee, D.R. Myers, C. Li, N.J. Erb, A.R. Loch.

CHECKERS

N. Graves (Discipline Primary Checker), B.W. Arnold, A. Behie, B.E. Bullard, G.B. Evans, N.D. Francis, M. Gross, W.R. Hunt (PCG Lead), T. Jones, J. Kingston, R. Metcalf, E.J. Nowak, H.W. Papenguth, L.C. Powell, B. Ramarao, E.R. Siegmann, C. Smith, M.L. Wilson, R. Zimmerman (PCG).

REVIEWERS

B. Bodvarsson, N. Brodsky, D. Dobson, A.A. Eddebbarh, J. Kam, J. King, J. Lee, A. Orrell, J. Schmitt, J. Snyder, C. Stockman, S. Swenning.

TECHNICAL SUPPORT

L.L. Mays, M.W. Lee, J.D. Matties, L.K. Henderson

INTENTIONALLY LEFT BLANK

CONTENTS

	Page
1. PURPOSE	25
2. QUALITY ASSURANCE	26
3. COMPUTER SOFTWARE AND MODEL USAGE	27
3.1 SOFTWARE	27
3.1.1 GoldSim	29
3.1.2 FEHM	30
3.1.3 T2_BINNING	30
3.1.4 WT_BINNING	30
3.1.5 MAKEPTRK	31
3.1.6 WAPDEG	31
3.1.7 ASHPLUME	31
3.1.8 SZ_CONVOLUTE	32
3.1.9 SEEPDLL	32
3.1.10 SOILEXP	32
3.1.11 GVP (Gaussian Variance Partitioning)	33
3.1.12 MFD (Manufacturing Defects Calculation)	33
3.1.13 SCCD (Stress Corrosion Cracking Dissolution)	33
3.1.14 PREWAP	34
3.1.15 mView	34
3.1.16 SATOOL	34
3.1.17 PDFSENS	34
3.2 MODELS	34
4. INPUTS	37
4.1 DATA AND PARAMETERS	37
4.2 CRITERIA	37
4.2.1 NRC Review and Acceptance Criteria	37
4.3 CODES AND STANDARDS	52
5. ASSUMPTIONS	53
5.1 INTRODUCTION	53
5.2 TSPA-SR MODEL ASSUMPTIONS	53
5.3 ASSUMPTIONS FROM INPUTS TO THE TSPA-SR MODEL	56
5.3.1 Unsaturated Zone Flow	57
5.3.2 Near Field Environment	59
5.3.3 Waste Package Degradation	62
5.3.4 Waste Form Degradation And Mobilization	64
5.3.5 Engineered Barrier System Transport	69
5.3.6 Unsaturated Zone Transport	71
5.3.7 Saturated Zone Transport	72
5.3.8 Biosphere	76

CONTENTS (Continued)

	Page
5.3.9 Disruptive Events	77
6. TSPA-SR MODEL	80
6.1 INTRODUCTION	80
6.1.1 TSPA Previous Work	81
6.1.2 TSPA-SR Model Importance	81
6.2 MODEL STRUCTURE AND DESIGN	97
6.2.1 Information Flow between Component Models	97
6.2.2 Model Architecture	104
6.3 COMPONENTS OF THE TSPA MODEL	112
6.3.1 Unsaturated Zone Flow	115
6.3.2 Near Field Environment	148
6.3.3 Waste Package Degradation	197
6.3.4 Waste Form Degradation and Mobilization	224
6.3.5 Engineered Barrier System Transport	349
6.3.6 Unsaturated Zone Transport	369
6.3.7 Saturated Zone Transport	405
6.3.8 Biosphere	437
6.3.9 Disruptive Events	454
6.4 SIMULATION SETTINGS	534
6.5 MODEL VALIDATION	542
6.5.1 Integrated Model Testing	543
6.5.2 Phase-1: Verification of the TSPA-SR Model	544
6.5.3 Phase-2: Verification of GoldSim TSPA-SR Model	546
6.5.4 Summary of Integrated Model Testing	550
6.5.5 Peer Review	551
7. CONCLUSIONS	558
8. REFERENCES	560
8.1 DOCUMENTS CITED	560
8.2 CODES, STANDARDS, AND REGULATIONS	569
8.3 DATA, LISTED BY DATA TRACKING NUMBER	570
8.3.1 Source Data	570
8.3.2 DTNs That Superseded Source Data	575
ATTACHMENT I - GOLDSIM GRAPHICAL ELEMENTS	I-1
ATTACHMENT II - SEEPDLL AVERAGE SEEPAGE FLUX AND SEEPAGE FRACTION	II-1
ATTACHMENT III - SOILEXP SOIL EROSION DLL	III-1
ATTACHMENT IV - SOFTWARE ROUTINE T2_BINNING V. 1.0	IV-1

CONTENTS (Continued)

	Page
ATTACHMENT V - SOFTWARE ROUTINE WT_BINNING V. 1.0.....	V-1
ATTACHMENT VI - SOFTWARE ROUTINE MAKEPTRK V. 2.0	VI-1
ATTACHMENT VII - PREWAP SOFTWARE ROUTINE REPORT	VII-1
ATTACHMENT VIII - TSPA-SR MODEL DATA SUBMITTAL 'README' FILE.....	VIII-1
ATTACHMENT IX - DLL OUTPUT FILES FOR MODEL VALIDATION	IX-1

FIGURES

	Page
6-1. Hierarchy of Analyses and Models Supporting the Total System Performance Assessment-Site Recommendation	83
6-2. Total System Performance Assessment Model: Hierarchy of Analyses and Models Supporting the Waste Package Degradation Model of Total System Performance Assessment-Site Recommendation - Part A	84
6-3. Total System Performance Assessment Model: Hierarchy of Analyses and Models Supporting the Waste Package Degradation Model of Total System Performance Assessment-Site Recommendation - Part B	84
6-4. Total System Performance Assessment Model: Hierarchy of Analyses and Models Supporting the Waste Package Degradation Model of Total System Performance Assessment-Site Recommendation - Part C	85
6-5. Total System Performance Assessment Model: Hierarchy of Analyses and Models Supporting the Waste Package Degradation Model of Total System Performance Assessment-Site Recommendation - Part D	86
6-6. Total System Performance Assessment Model: Hierarchy of Analyses and Models Supporting the Waste Form Model of Total System Performance Assessment-Site Recommendation - Part A.....	87
6-7. Total System Performance Assessment Model: Hierarchy of Analyses and Models Supporting the Waste Form Model of Total System Performance Assessment-Site Recommendation - Part B.....	88
6-8. Total System Performance Assessment Model: Hierarchy of Analyses and Models Supporting the Waste Form Model of Total System Performance Assessment-Site Recommendation - Part C.....	89
6-9. Total System Performance Assessment Model: Hierarchy of Analyses and Models Supporting the Waste Form Model of Total System Performance Assessment-Site Recommendation - Part D.....	90
6-10. Total System Performance Assessment Model: Hierarchy of Analyses and Models Supporting the EBS Transport Model of Total System Performance Assessment-Site Recommendation - Part A.....	91
6-11. Total System Performance Assessment Model: Hierarchy of Analyses and Models Supporting the EBS Transport Model of Total System Performance Assessment-Site Recommendation - Part B.....	91
6-12. Total System Performance Assessment Model: Hierarchy of Analyses and Models Supporting the EBS Transport Model of Total System Performance Assessment-Site Recommendation - Part C.....	92
6-13. Total System Performance Assessment Model: Hierarchy of Analyses and Models Supporting the Unsaturated Zone Transport Model of Total System Performance Assessment-Site Recommendation.....	93
6-14. Total System Performance Assessment Model: Hierarchy of Analyses and Models Supporting the Saturated Zone Transport Model of Total System Performance Assessment-Site Recommendation.....	94

FIGURES (Continued)

	Page
6-15. Total System Performance Assessment Model: Hierarchy of Analyses and Models Supporting the Biosphere Model of Total System Performance Assessment-Site Recommendation - Part A.....	95
6-16. Total System Performance Assessment Model: Hierarchy of Analyses and Models Supporting the Biosphere Model of Total System Performance Assessment-Site Recommendation - Part B.....	96
6-17. Major Sources of Information Used in the Development of the TSPA-SR.....	100
6-18. Simplified Representation of Information Flow in the TSPA-SR between Data, Process Models, and Abstracted Models.....	101
6-19. Detailed Representation of Information Flow in the TSPA-SR.....	102
6-20. Detailed Representation of Information Flow in the Waste Form and Waste Package Models of the TSPA-SR	103
6-21. TSPA-SR Model Code Architecture: Information Flow Among Component Computer Codes.....	111
6-22. Major Components of the Total System Performance Assessment Model.....	114
6-23. Conceptual Drawing of Unsaturated Zone Flow Processes at Different Scales	116
6-24. A Graphical Illustration of the TSPA Model Implementation of the Climate Model	120
6-25. TSPA Implementation of the Infiltration Rate Map Weighting Factors.....	121
6-26. Result of a Simulation of the Climate State Model.....	122
6-27. Diagram of the GoldSim Seepage Model	135
6-28. Illustration of the Contents of the <i>Seepage_Flux_multi</i> Container Showing Tables Containing Time-Varying Seepage Flow for Always and Intermittent Seepage in Each Infiltration Bin for CSNF and CDSP Waste Packages	136
6-29. The Contents Of The <i>No_Backfill</i> Container Showing Tables Containing Median-Value Time-Varying Seepage Flow for Always and Intermittent Seepage in Each Infiltration Bin for CSNF and CDSP Waste Packages	137
6-30. The Contents of the <i>Backfill</i> Container Showing Tables Containing Median-Value Time-Varying Seepage Flow for Always and Intermittent Seepage in Each Infiltration Bin for CSNF and CDSP Waste Packages	138
6-31. The Selector Switches In the <i>Seepage_Flux</i> Container that are Used to Determine Whether Values are Chosen from <i>Seepage_Flux_median</i> or <i>Seepage_Flux_multi</i> Look-Up Tables.....	139
6-32. The Contents of the <i>Seepage_Fraction</i> Container Showing Data Elements Containing the Fraction of CDSP and CSNF Waste Packages that Always, Intermittently, and Never See Seepage in Each of the Infiltration Bins	140
6-33. The Contents of the <i>Median_Seep_Fractions</i> Container Showing Data Elements Containing the Fraction of CDSP and CSNF Waste Packages that Always, Intermittently, and Never See Seepage in Each of the Infiltration Bins for Backfill and No Backfill Median Value Cases	140
6-34. Intermittent Seepage for Bin 4 Containing CSNF	141
6-35. Always Seeping Conditions for Bin 4 Containing CDSP	141

FIGURES (Continued)

		Page
6-36.	Stratigraphy and Mesh for Mountain-Scale Flow Model.....	146
6-37.	A Graphical Illustration of the TSPA Model Implementation of the UZ Flow Model	147
6-38.	The TSPA-SR Model Organization for TH Implementation	169
6-39.	Graphical Representation of the Temperature Profiles for the TH Model.....	169
6-40.	Illustration of the CSNF Waste Package Surface Temperature Implementation	170
6-41.	CSNF Waste Package Surface Temperature, Low Infiltration, No Backfill Design	170
6-42.	CSNF Waste Package Surface Temperature, Mean Infiltration, No Backfill Design.....	171
6-43.	CSNF Waste Package Surface Temperature, High Infiltration, No Backfill Design.....	171
6-44.	CSNF Invert Temperatures, Low Infiltration, No Backfill Design.....	172
6-45.	CSNF Invert Temperatures, Mean Infiltration, No Backfill Design.....	172
6-46.	CSNF Invert Temperatures, High Infiltration, No Backfill Design	173
6-47.	CSNF Invert Relative Humidities, Low Infiltration, No Backfill Design	173
6-48.	CSNF Invert Relative Humidities, Mean Infiltration, No Backfill Design.....	174
6-49.	CSNF Invert Relative Humidities, High Infiltration, No Backfill Design.....	174
6-50.	CSNF Invert Evaporation Flux, Low Infiltration, No Backfill Design.....	175
6-51.	CSNF Invert Evaporation Flux, Mean Infiltration, No Backfill Design.....	175
6-52.	CSNF Invert Evaporation Flux, High Infiltration, No Backfill Design	176
6-53.	CSNF Invert Saturation, Low Infiltration, No Backfill Design	176
6-54.	CSNF Invert Saturation, Mean Infiltration, No Backfill Design	177
6-55.	CSNF Invert Saturation, High Infiltration, No Backfill Design	177
6-56.	CSNF Invert Flux, Low Infiltration, No Backfill Design	178
6-57.	CSNF Invert Flux, Mean Infiltration, No Backfill Design	178
6-58.	CSNF Invert Flux, High Infiltration, No Backfill Design.....	179
6-59.	CSNF Waste Package Surface Temperature Profile for the Median Value Simulation	179
6-60.	CSNF Invert Temperature Profiles for the Median Value Simulation.....	180
6-61.	CSNF Invert Relative Humidity Profiles for the Median Value Simulation	180
6-62.	CSNF Invert Evaporation Rate Profiles for the Median Value Simulation	181
6-63.	CSNF Invert Liquid Saturation Profiles for the Median Value Simulation.....	181
6-64.	CSNF Invert Liquid Flux Profiles for the Median Value Simulation.....	182
6-65.	Comparison of the Median Value Simulation Model Results and the Predicted Results: CSNF Waste Package Surface Temperature	182
6-66.	A Graphical Illustration of the Bin-Level In-Drift Chemistry Model.....	193
6-67.	A Graphical Illustration of In-Drift Chemistry at the EBS Level of the Model	194
6-68.	Illustration of Selection of In-drift Ionic Strength for Relative Humidities Less Than 50 percent (Ionic_Str_invert_bound)	195

FIGURES (Continued)

	Page
6-69. Illustration of Selection of In-drift pH for Relative Humidities Less Than 50 percent (pH_invert_bound) and Relative Humidities Between 50 and 85 percent (pH_drip_case2)	195
6-70. Model Logic for Determining the Ionic Strength of the Invert when the Relative Humidity is Greater than or Equal to 50 Percent	196
6-71. Model Logic for Determining the pH of the Invert When the Relative Humidity is Greater than or Equal to 50 Percent.....	196
6-72. The Waste Package Degradation Component of the TSPA-SR Model	217
6-73. Illustration of the Six GVP DLL Calls from the TSPA-SR Model.....	217
6-74. Illustration of the TSPA-SR / GVP.dll Interface.....	218
6-75. Two Calls to MFD.dll	218
6-76. TSPA-SR / MFD.dll Interface.....	219
6-77. Illustration of the Two Calls to the SCCD.dll.....	219
6-78. Illustration of the TSPA-SR / SCCD.dll Interface	220
6-79. Illustration of the Slip Dissolution Component in the SCCD Component	221
6-80. Graphical Illustration of the Input Variance Sharing Distribution for the WAPDEG DLL	221
6-81. Drip Shield and Waste Package Failure Curves for the Median Value Simulation.....	222
6-82. Time History of the Evolution of Patch, Pit, and Crack Formations on the Drip Shield and Waste Packages for the Median Value Simulation	223
6-83. Time History of the Number of Failed Packages in Each Bin 4 Environment for the Median Value Simulation.....	224
6-84. Major Components and Inputs of the Waste Degradation Model.....	226
6-85. Graphical Representation of the Three Different Fuel Inventories as Implemented in GoldSim	245
6-86. Graphical Representation of the Calculation of Fraction of CSNF and CDSP Waste Packages in Each Bin from the GoldSim container <i>Num_Packages</i> in the <i>WastePackage_Dripshield</i> container	246
6-87. Illustration of the Adjustment for Round-off Error in the Calculation of Number of CSNF and CDSP Waste Packages in Each Infiltration Bin.....	247
6-88. Graphical Representation for the Calculation of Number of Waste Packages in Each Seepage Group	248
6-89. Verification of GoldSim Calculations for the Number of Waste Packages Present within Infiltration Bins and Seepage (Dripping Environment) Groups	249
6-90. Separation of CSNF and CDSP Waste Packages for the pH Calculations	267
6-91. Grouping of Waste Package by Bins.....	268
6-92. Grouping of Waste Packages by Environments within a Bin	268
6-93. Calculations within One Bin Environment	269
6-94. Organization of the In-Package Chemistry Calculations	269
6-95. Illustration of the pH Calculation within One Bin Environment	270
6-96. Globally Defined In-Package Chemistry Parameters.....	271
6-97. Locally Defined In-Package Ionic Strength.....	272
6-98. Average Package Failure Time Calculation.....	272

FIGURES (Continued)

	Page
6-99. Temporal Profile of the In-Package pH of a CSNF Waste Package in Bin 4	273
6-100. Temporal Profile of In-Package pH of a CDSP Waste Package in Bin 4	274
6-101. Temporal Profile of the Total Carbonate within a CSNF Waste Package in Bin 4	275
6-102. Temporal Profile of the Ionic Strength Inside a CSNF Waste Package in Bin 4	276
6-103. Temporal Profile of the Package Failures and Average Package Failure Time (CSNF, Bin 4, Intermittent Drip)	276
6-104. Overview of the TSPA Cladding Degradation Model	289
6-105. The Clad Container Includes the Containers for the Determining Localized Corrosion of the Cladding and the Intrinsic Dissolution Rate of the Fuel Matrix	290
6-106. Cladding Model Parameters that are Defined Globally in the TSPA-SR Model	290
6-107. Global Parameters within the <i>Cladding_Uncertainty_Parms</i> Container	291
6-108. TSPA-SR Model Implementation of Creep and SCC Failures	291
6-109. TSPA Model Implementation of Local Cladding Corrosion	292
6-110. TSPA Model Implementation of CSNF Cladding Dissolution Rate	292
6-111. TSPA Model Implementation of the CSNF Cladding Unzipping	293
6-112. An Illustration of Implementation of the Calculation of the Average Amount of Failed CSNF Cladding	293
6-113. Calculation of the In-growth of ^{238}U from the Decay of ^{242}Pu ; used in Calculating Average Cladding Exposed	294
6-114. CSNF Unzipping Rate, Bin 4, Intermittent Seepage	294
6-115. Time History of the Average Fuel Exposed for Bin 4, Intermittent Drip (Median Value Simulation)	295
6-116. Illustration of the HLW Glass Dissolution Rate Parameters	303
6-117. Representation of the HLW Glass Dissolution Rate Calculation	303
6-118. Illustration of the Exponential Term Calculation for the HLW Glass Dissolution Rate and DSNF Degradation Rate	304
6-119. Illustration of the HLW Glass Dissolution Rate Calculation	304
6-120. Temporal Profile of the HLW Glass Dissolution Rate in Bin 4	305
6-121. Glass Degradation Rate Comparison Using Parameters Defined for Both Low and High pH Conditions with the Model Output	306
6-122. Illustration of the Globally Defined Solubility Limits in the TSPA-SR Model	317
6-123. Graphical Representation of the Localized Solubility Limit Calculations for an Environment	317
6-124. Calculated Solubility Limits of the Selected Radionuclides for the Median Value Simulation, Bin 4 Always Drip Environment: CSNF Waste Packages and Invert	318
6-125. Calculated Solubility Limits of the Selected Radionuclides for the Median Value Simulation, Bin 4 Always Drip Environment: CDSP Waste Packages and Invert	319
6-126. Waste Form Colloid Formation Flow Charts of Model Logic	334
6-127. Iron-(Hydr)oxide Colloid Formation Flow Charts of Model Logic	335
6-128. Groundwater Colloid Formation Flow Charts of Model Logic	336
6-129. Representation of the Definition of Colloid Model Component Inputs	337
6-130. Illustration of the Waste Form Colloids Implementation	338
6-131. Representation of the Calculation for Irreversibly Bound Am Species	339

FIGURES (Continued)

	Page
6-132. Representation of the Iron-(hydr)oxide Colloids Calculation for Waste Packages	339
6-133. Illustration of the Iron-(hydr)oxide Colloid Formation in the Invert Cell	340
6-134. Illustration of the Groundwater Colloids Calculation for Waste Packages	340
6-135. Graphical Illustration of the Groundwater Colloids Calculation for the Invert Cell	340
6-136. Graphical Illustration of the Model Implementation for Removing Species Mass as Irreversible Colloids.....	341
6-137. Illustration of the Definition of Colloid Solids	342
6-138. Plot of the In-Package Ionic Strength Conditional Statements for Waste Form Colloids	343
6-139. Concentration of Pu Irreversibly Bound on Waste Form Colloids in the Waste Package.....	344
6-140. Comparison of Ionic_Str_Invert and Conditional Statements for Waste Form Colloid Formation	344
6-141. Pu and Am Species Irreversibly Bound to Waste Form Colloids in the Waste Package.....	345
6-142. Ionic Strength Comparison to Conditional Statements for the Formation of Iron-(hydr)oxide Colloids in the Waste Package	345
6-143. Ionic Strength Comparison to Conditional Statements for the Formation of Iron-(hydr)oxide Colloids in the Invert.....	346
6-144. Mass of Stable Iron-(hydr)oxide Colloids Formed in the Waste Package and in the Invert	346
6-145. Mass of Stable Groundwater Colloids Formed in the Waste Package and in the Waste Package.....	347
6-146. Mass of Stable Groundwater Colloids Formed in the Waste Package and in the Invert	348
6-147. Mass of Model Species Produced and Lost Due to Irreversible Colloids.....	349
6-148. Graphical Representation of Important Processes that affect EBS Transport of Radionuclides	352
6-149. The Cells Defined for EBS Transport from Each Unique Source Term.....	361
6-150. Graphical Representation of Thirty Unique Source Terms for the Total System Model in GoldSim.....	362
6-151. Cells at the Edge of the EBS that Feed The UZ Model	362
6-152. Comparison of Mass Release of Np-237 from EBS for each Infiltration Bin	367
6-153. Comparison of Mass Release of Tc-99 from EBS for each Infiltration Bin	368
6-154. Location of Nodes within Each Infiltration Bin in the Repository Footprint	389
6-155. Location of Four Regions for UZ/SZ Interface.....	390
6-156. Influence of Dispersivity on the Transport of Tc99 in the UZ Under the Glacial Transitional Climate Condition. The Water Table was at 850 m.....	391
6-157. Influence of Dispersivity on Normalized Cumulative Breakthrough Curves of Tc-99 Under Glacial Transitional Climate Condition. The Water Table was Set at 850 m.....	392
6-158. Flow Chart of FEHM-GOLDSIM Coupling.....	399
6-159. Flow Chart of GoldSim-FEHM Coupling and FEHM Simulation Processes.....	400

FIGURES (Continued)

	Page
6-160. Structure of the GoldSim End Array.....	401
6-161. Structure of out[] Array for Sending FEHM Simulation Results Back to GoldSim.....	401
6-162. Input Parameters for UZ Transport Model.....	401
6-163. Engineered Barrier Connection Cells for the Five Infiltration Bins	402
6-164. Cells and Parameters for Unsaturated Zone Transport	402
6-165. Radionuclide EBS Release for Selected Species	403
6-166. Radionuclide Mass Flux at the UZ Outflow Boundary for Selected Species	404
6-167. Evaluation of the Migration of Radionuclides from Their Introduction at the Water Table below the Repository to the Release Point to the Biosphere.....	425
6-168. The Geosphere/Biosphere Interface which is assumed to be located 20 km from the Repository	426
6-169. Illustration of Saturated Zone One-dimensional Pipe Model and Convolution Integral Model Implementation.....	427
6-170. Look-up Tables for Multiple Realization Simulation Residing in SZ_Input_Parameters Container	428
6-171. Contents of SZ_1DModel_Parameters Container.....	429
6-172. Contents of Median_Values_SZ_Parameters Container.....	429
6-173. Contents of Alluvium_Properties Container.....	430
6-174. Contents of Volcanic_Properties Container.....	431
6-175. Scaling of Discharge_5km by Factor1 to Account for Changes in Groundwater Flux Due to Climate	431
6-176. Np ²³⁷ Transport through the SZ Convolution Integral Model in Grams/Year Compared to Total UZ Release in Grams/Year	432
6-177. Time History Result for SZ Convolution Integral Model Mass Release in grams/year Compared to Total UZ Mass Release for Pu ²³⁹	433
6-178. Time History Result for SZ Pipe Model Mass Release in grams/year Compared to Total UZ Mass Release for Th ²²⁹	434
6-179. Time History Result for SZ Pipe Model Mass Release in Grams/Year Compared to Total UZ Mass Release for U ²³³ (Parent Species for Th ²²⁹)	435
6-180. Time History Result for SZ Convolution Integral Model Mass Release in Grams/Year Compared to Total UZ Mass Release for Tc ⁹⁹	436
6-181. Time History Result for SZ Convolution Integral Model Mass Release in Grams/Year Compared to Total UZ Mass Release for Ic ²³⁹ (Irreversible Pu colloid)	437
6-182. Graphical Illustration of the Biosphere Component	449
6-183. Biosphere Dose Conversion Factors in the TSPA-SR Model.....	450
6-184. Graphical Illustration of the GWPC_Results Container: calculation of alpha_activity	451
6-185. Dose Rate from Each Radionuclide for the Median Value of all Input Parameters	451
6-186. Overview of the TSPA Annual Groundwater Usage Model (Screen Capture from model file, refer to Attachment I for description of GoldSim Elements)	453
6-187. Disruptive Events Model within GoldSim.....	473
6-188. Implementation of the Volcanic Release Event in the TSPA Model.....	473

FIGURES (Continued)

	Page
6-189. Calculations for Determining the Total Waste Inventory Affected by a Volcanic Release Event	474
6-190. Calculation of the Source Term from Direct Volcanic Release	475
6-191. Volcanic Direct Release Dose Calculation	476
6-192. Dose From Direct Volcanic Release, <i>Ash_Dose</i> (not probability weighted)	477
6-193. Probability Weighted Total Dose From Direct Volcanic Release	477
6-194. Cumulative Distribution Function for Intrusive Indirect Events	500
6-195. Cumulative Distribution Function for the Number of Zone 1 Waste Packages Hit by an Intrusive Indirect Event	500
6-196. Cumulative Distribution Function for the Number of Zone 1 and 2 Waste Packages Hit by an Intrusive Indirect Event	501
6-197. The Disruptive Event Component in the TSPA-SR Model	501
6-198. Zone 1 Intrusive Indirect Release Component in the TSPA-SR Model	502
6-199. Zone 2 Intrusive Indirect Release Component in the TSPA-SR Model	502
6-200. Intrusive indirect event Initiation Switch	502
6-201. The Bin Selector for Intrusive indirect event Releases	503
6-202. The Calculation of Impacted Packages	503
6-203. The FEHMN Nodes Calculation Container for an Intrusive Indirect Release	504
6-204. An Illustration of the Intrusive Indirect Event Impacting CSNF Waste Package Release from the EBS	505
6-205. The In-Drift Chemistry Component within the Intrusive Indirect Event Component	506
6-206. Graphical Representation of the Invert Properties Container within the Intrusive Indirect Event Component	506
6-207. The Matrix Degradation Rate Container within the Intrusive Indirect Event Component	507
6-208. Seepage Flux Through the Drift in the Intrusive Indirect Event Component of the TSPA-SR Model	507
6-209. In-Package Chemistry Component Implementation for Intrusive Indirect Releases	508
6-210. Illustration of the Calculation of Mass Released from the EBS to the UZ for an Intrusive Indirect Event	509
6-211. Illustration of the Calculation of CDSP Waste Form Dissolution Rates for an Intrusive Indirect Event	509
6-212. Time History Result of the Number of Failed Waste Packages Impacted by an Indirect Intrusive Event: Median Value Simulation	510
6-213. Time History Result of the Mass Released from Zone 1 CSNF Packages by an Indirect Intrusive Event: Median Value Simulation	510
6-214. Time History Result of the CSNF Matrix Degradation Rate in the Indirect Intrusive Indirect Event Component: Median Value Simulation	511
6-215. Time History Result of the Mass Released from CDSP EBS by an Indirect Intrusive Indirect Event: Median Value Simulation	511

FIGURES (Continued)

	Page
6-216. Time History Result of the CDSP HLW Glass Degradation Rate in the Indirect Intrusive Indirect Event Component: Median Value Simulation.....	512
6-217. Time History Result of the Igneous Intrusive Event CSNF Waste Form Uranium Concentration and Solubility.....	512
6-218. Overview of Human Intrusion Case GoldSim File	522
6-219. Human Intrusion Scenario Parameters in the Human_Intrusion_Parameters Container	523
6-220. An Illustration of the Human Intrusion Case for CSNF at the EBS Level	523
6-221. An Illustration of the Human Intrusion Case for CDSP at the EBS Level	524
6-222. The Human Intrusion Case for CSNF at the Environment Level	524
6-223. The Human Intrusion Case for CDSP at the Environment Level	525
6-224. An Illustration of In-Package Chemistry for the Human Intrusion Scenario.....	526
6-225. Selection of NFE Parameters for the Human Intrusion Scenario.....	526
6-226. Selection of Seepage Flux for the Human Intrusion Scenario	527
6-227. An Illustration of Source Term Transport from the EBS to the Borehole for the Human Intrusion Case	527
6-228. An Illustration of the Borehole between the EBS and the SZ in the Human Intrusion Case.....	528
6-229. The Human Intrusion Case Borehole Kds.....	528
6-230. The Human Intrusion Case BDCFs.....	529
6-231. Plot of Parameter <i>HumanIntr_WP_Failure</i> vs. Simulation Time.....	530
6-232. Plot of Human Intrusion Waste Package Failure time vs. Simulation Time.....	530
6-233. Cladding Model Parameters that are Defined Globally in the TSPA-SR Model.....	533
6-234. Time History of the Average Cladding Exposed for Bin 4, Intermittent Drip (Median Value Simulation).....	533
6-235. Simulation Settings and Switch in the <i>Simulation_Settings</i> Container for the TSPA-SR Model	539
6-236. Simulation Settings and Switch for the TSPA-SR Model.....	540
6-237. File Elements in the <i>External_Files</i> Container	540
6-238. File Elements in the <i>Multiple_Realization_Files</i> Container	540
6-239. Simulation Settings Pulldown Menu for the Nominal Case, 1E5 years, 100 Realizations	541
6-240. Timestep Settings for Nominal Case, 1E5, 100 Realizations	542
6-241. Validation of the Integrated Model: Two Phases.....	552
6-242. Validation of the Integrated Model: Phase 1	552
6-243. Validation of TSPA Model Codes: Stages 1 and 2	553
6-244. Verification of Integrated TSPA Model: Stage 3.....	554
6-245. Validation of the TSPA-SR Model: Stage 3. Fraction of Failed Packages (from WAPDEG DLL) Versus Number of Failed Packages in a GoldSim Source Term Group (CSNF BIN 4 Intermittent Drip).....	555
6-246. Validation of the TSPA-SR Model: Stage 3. pH in the Waste Package Versus the Number of Failed Packages (CSNF BIN 4 Intermittent Drip).....	555

FIGURES (Continued)

	Page
6-247. Validation of the TSPA-SR Model: Stage 3. Clad Unzipping Rate Versus pH in the Waste Package (CSNF BIN 4 Intermittent Drip).....	556
6-248. Validation of the TSPA-SR Model: Stage 3. Flux Through the Drip Shield (Q_{flux_DS}) Versus Drip Shield Patch Failure Fraction. Also, Shown are Seepage into the Drift and Fraction of Failed Dripshields (CSNF BIN 4 Intermittent Drip)	556
6-249. Validation of the TSPA-SR Model: Stage 3. Cumulative ^{99}Tc Mass Released from Various Submodels of the Total Integrated System Model; Compared to the CDF of Waste Package Failures.....	557
6-250. Validation of the TSPA-SR Model: Stage 3. Cumulative ^{237}Np Mass Released from Various Submodels of the Total Integrated System Model; Compared to the CDF of Waste Package Failures.....	557

TABLES

	Page
3-1. Software and Software Routines	27
3-2. Computer Systems.....	28
3-3. Models Used in this Analysis.....	35
4-1. General Listing of Inputs to the Total System Performance Assessment-Site Recommendation Model	38
4-2. Source Data Tracking Numbers	48
4-3. A Listing of TSPA-SR Model Inputs That Were Superseded After the Completion of the TSPA-SR Simulations but Before Final Production of This AMR.....	49
6-1. Climate State Durations Used in the TSPA Model.....	118
6-2. Infiltration Case Weighting Factors Used in the TSPA Model.....	119
6-3. Basis for Selection of Infiltration Bins.....	123
6-4. Uncertainty in Seepage Fraction, Mean Seep Flow Rate, and Seep Flow Rate Standard Deviation as a Function of Percolation Flux.....	125
6-5. SEEPDLL Input Parameters Directly Implemented in GoldSim.....	125
6-6. SEEPDLL Input Parameters Generated by Median Value, One Million-Year Simulation	132
6-7. <i>Seepage_Flux Switch</i> Input Parameters Generated by the Median Value, No Backfill Simulation at One Million Years.....	133
6-8. Seepage Time History Results of Median Value, No Backfill, One Million-Year Simulation	134
6-9. List of Input Parameters used from TSPA-SR Model to Select the Flow Fields used in the UZ Transport Calculations and the Names and Source for the Flow Field Files.....	144
6-10. Five Infiltration Rate Bins Based Upon Percolation Flux as Defined by Thermal Hydrology Calculations.....	151
6-11. Input Parameters for the Thermal Hydrology Calculations	152
6-12. Input Parameters to the In-Drift Chemistry Model	185
6-13. Lookup Table for In-Drift pH and Ionic Strength for Time Period	186
6-14. Lookup Table for In-Drift p and Ionic Strength for Time Periods 3 and 5.....	187
6-15. Lookup Table for In-Drift pH and Ionic Strength for Time Period 4	188
6-16. Input Parameters for the GVP Calculation.....	201
6-17. Input Parameters for the MFD Calculation	202
6-18. Input Parameters for the SCCD Calculation	203
6-19. File Description and Index Cross-Reference for TSPA-SR DLL Inputs and Outputs	205
6-20. Inputs to the Waste Package Degradation Model Component.....	206
6-21. Input Parameters for the WAPDEG Calculations	207
6-22. Cross-Reference Table for WAPDEG Results Tabulated in <i>Failure_Openings</i>	212
6-23. List of WAPDEG Results for Performance Analysis	213

TABLES (Continued)

	Page
6-24. Supplemental TSPA-SR Parameters for Drip Shield and Waste Package Degradation Calculations	214
6-25. Inventory for 1,000,000-Year Nominal Igneous Groundwater Release Scenarios [†]	228
6-26. Decay Rates for the Radionuclides [†]	229
6-27. Specific Activities for the Radionuclides [†]	230
6-28. Disposition of Radionuclides for 1,000,000-Year Nominal and Igneous Groundwater Release Scenarios.....	234
6-29. Disposition of Radionuclides for 10,000- to 100,000-Year Human Intrusion Groundwater Release Scenarios.....	238
6-30. Disposition of Radionuclides for 10,000-Year to 100,000-Year Eruptive Release Scenario	241
6-31. Various TSPA Model Input Parameters used for Dividing the Waste Inventory into Groups Based on Infiltration.....	242
6-32. Fraction of Waste Packages in the Five Infiltration Bins as a Function of the Infiltration Scenario.....	242
6-33. Contents of the Data Element <i>CSNF_Pkg_Adjust</i>	243
6-34. Contents of the Data Element <i>Num_Pkgs_Adjust</i>	244
6-35. Response Surface Characteristics.....	253
6-36. pH Response Surface Parameters for CSNF Waste Packages	254
6-37. pH Response Surface Parameters for CDSP Waste Packages	254
6-38. Input Parameters for In-Package Chemistry Calculations	255
6-39. Bounding Waste Package Flux Rates for pH Calculations	257
6-40. Parameter Details for Supplemental TSPA-SR Parameters	260
6-41. Other TSPA-SR Model Parameters with In-Package Chemistry Component Impacts	262
6-42. pH Calculation Verification for the Median Value Simulation	265
6-43. Total Carbonate Concentration Calculation Verification for the Median Value Simulation	266
6-44. Data Inputs to the TSPA Model for Cladding Degradation	278
6-45. Fraction of Rods Perforated from Creep as a Function of Peak Waste Package Surface Temperature	281
6-46. CSNF Intrinsic Dissolution Rate Equation Coefficients as a Function of pH	283
6-47. GoldSim Results for the Fraction of Cladding that has Perforated in Bin 4 (Intermittent Dripping) Versus Time for a Median Value Simulation.....	286
6-48. Cumulative Seepage into CSNF Waste Package (Bin 4, Intermittent Drip).....	286
6-49. TSPA Model Results for the CSNF Cladding Intrinsic Dissolution Rate and Unzipping Rate in Bin 4, Intermittent Drip.....	288
6-50. TSPA Model Results for the In-package Chemistry and Thermohydrology Values Used in the Cladding Unzipping Rate Verification Calculation.....	288
6-51. Parameter Values for the HLW Glass Dissolution Rate Calculation.....	297
6-52. Parameter Details for Supplemental HLW Glass Dissolution Calculations	299
6-53. Other TSPA-SR Model Parameters with HLW Glass Dissolution Impacts	300

TABLES (Continued)

	Page
6-54. Verification of HLW Glass Dissolution Rate Calculation for the Median Value Simulation	301
6-55. Solubility Limits for the Elements Considered in the TSPA-SR Model.....	308
6-56. Coefficients for the Am Solubility Function.....	309
6-57. Supplemental TSPA-SR Model Parameters for Solubility Limit Calculations	311
6-58. Other TSPA-SR Model Parameters with Solubility Limit Calculation Impacts.....	314
6-59. Solubility Limits for Tc, Th, C, I, Sr, and Cs.....	314
6-60. Verification of the TSPA-SR Model Solubility Limit Calculations for U, Am, and Np	316
6-61. Input Parameters for the Colloid Model Calculations.....	321
6-62. Other TSPA-SR Parameters with Colloid Generation Calculation Impacts	330
6-63. Parameters Defining the Waste Form Cells	353
6-64. Parameters Defining the Invert Cells	355
6-65. Parameters Defining the Collector Cells.....	356
6-66. Parameters Defining the EBS Bin Out Cells.....	357
6-67. Parameters Defining Flux through Drip Shields, Waste Packages, and Invert.....	360
6-68. Values and Sources for EBS Transport Parameters	363
6-69. Description of the Components of the Total System Model that are Connected to EBS Transport	366
6-70. Grid File used in TSPA Simulations	370
6-71. FEHM Stiffness Matrix Files used in TSPA Simulations.....	371
6-72. Input Data used for Generating Repository Release Bins and Water Table Collect Bins.....	371
6-73. Zone Files used in FEHM	373
6-74. Fracture and Matrix Dispersivities used in TSPA Simulations	375
6-75. Matrix Rock Porosity and Density Values.....	376
6-76. Sorption-Coefficient Distributions for Unsaturated Zone Units	377
6-77. Sampled Matrix Adsorption Coefficient Data	378
6-78. Matrix Diffusion Coefficient Distribution for Unsaturated Zone	379
6-79. Sampled Matrix Diffusion Coefficient Data	379
6-80. Fracture γ Parameter for Low Day Infiltration Scenario.....	379
6-81. Fracture γ Parameter for Medium Infiltration Scenario	380
6-82. Fracture γ Parameter for High Infiltration Scenario.....	381
6-83. List of Fracture Porosity Values used in TSPA Simulations	382
6-84. Fracture Spacing Values used in TSPA Simulations	383
6-85. Fracture Aperture Distribution in Each Rock Layer	384
6-86. Fracture Surface Retardation Factor used in TSPA	384
6-87. Cumulative Probabilities for Colloid Transport at Matrix Interfaces	385
6-88. Colloid Size Distribution.....	385
6-89. K_c for Irreversible Colloid.....	386
6-90. Adsorption Coefficient for Reversible Sorption of Radionuclide to Waste Form Colloids	387
6-91. Colloid K_c Values in FEHM File	387

TABLES (Continued)

	Page
6-92. Filtration Factor used in FEHM for Size Exclusion Calculation	387
6-93. Radionuclide Half-Life and Daughter Products used in TSPA.....	388
6-94. GoldSim Parameters used in TSPA-SR Saturated Zone Transport Model	406
6-95. GoldSim Parameter Descriptions for both 1-D and 3-D SZ Transport Models	410
6-96. SZ Convolution Model Breakthrough Curves for each Radionuclide in the TSPA-SR Model	414
6-97. Model Median Value Saturated Zone Breakthrough Curves	415
6-98. Saturated Zone Breakthrough Curves for Probabilistic Simulations	417
6-99. Comparison of Abstraction Prescribed Input Parameter Values to those Selected for Median Value Simulation	419
6-100. Comparison of Abstraction Prescribed Input Parameter Values for Alluvium_Properties to Those Selected for Median Value Simulation	422
6-101. Comparison of Abstraction Prescribed Input Parameter Values for Volcanic_Properties to those Selected for Median Value Simulation	422
6-102. Comparison of Abstraction Prescribed Input Parameter Values for Flow_Properties to those Selected for Median Value Simulation	422
6-103. Comparison of Abstraction Prescribed Input Parameter Values for Pipe_Length to those Selected for Median Value Simulation	423
6-104. Comparison of Abstraction Prescribed Input Parameter Values to those Selected for Median Value Simulation	423
6-105. Best Fit Parameters for BDCF Distributions.....	439
6-106. Calculation of the Annual Mass of Each Radionuclide in the Groundwater Consumed.....	442
6-107. Details for TSPA Parameters in the Biosphere Component	446
6-108. Mass Concentration of U ²³⁸ and Th ²²⁹ in Groundwater for the Median Value Simulation	447
6-109. Activity Concentration of U ²³⁸ and Th ²²⁹ in Groundwater for the Median Value Simulation	447
6-110. Annual Receptor Dose of U ²³⁸ and Th ²²⁹ for the Median Value Simulation	447
6-111. Estimates of Annual Water Usage per Farm.....	452
6-112. Direct Volcanic Release Model Input Parameters	456
6-113. Vent Diameter and Initial Eruptive Velocity CDF.....	456
6-114. Number of Packages Hit per Drift per Vent CDF Sampled on Vent Diameter	457
6-115. Number of Drifts Hit per Vent CDF Sampled on Vent Diameter.....	458
6-116. Number of Vents Intersecting Waste Drifts PDF.....	458
6-117. Event Probability CDF	459
6-118. Data Inputs used by ASHPLUME	460
6-119. Ash Dispersion Controlling Constant CDF.....	462
6-120. Ash Mean Particle Diameter CDF	462
6-121. Ash Mean Particle Diameter Standard Deviation CDF	462
6-122. Wind Direction PDF.....	463
6-123. Wind Speed CDF	463
6-124. Event Power CDF.....	464

TABLES (Continued)

	Page
6-125. Eruptive Volume CDF	464
6-126. Soil Reduction Rate	464
6-127. Biosphere Dose Conversion Factors for Direct Volcanic Release	465
6-128. Mass of Waste Released in a Direct Volcanic Release for a Median Value Simulation	468
6-129. Dose from Direct Volcanic Release for the First 1,000 years (not probability weighted)	470
6-130. Surface Concentration of Radionuclides Following a Direct Volcanic Release (at the 500-year timestep)	471
6-131. BDCFs for a Median Value Simulation	471
6-132. Dose from Direct Volcanic Release at 500 Years (not probability weighted)	472
6-133. Dose from Direct Volcanic Release at 500 Years (probability weighted)	472
6-134. In-Package Chemistry Parameters for Intrusive Indirect Releases	479
6-135. Indirect Release Bin Placement Probabilities	481
6-136. Parameter Details for Supplemental TSPA-SR Parameters	487
6-137. Human Intrusion Scenario Regulatory Assumptions	514
6-138. General Human Intrusion Input Parameters	515
6-139. Human Intrusion Input Parameters for Infiltration of Water Down the Borehole	515
6-140. Human Intrusion Input Parameters for Mobilization and Release of Radionuclides	517
6-141. Human Intrusion Input Parameters for Transport of Radionuclides Down the Borehole	517
6-142. Human Intrusion Input Parameters for Transport of Radionuclides Through the SZ	518
6-143. Human Intrusion Input Parameters for the Biosphere	519
6-144. Data Inputs to the TSPA Model for Cladding Degradation	531
6-145. GoldSim Results for the Seismic Clad Event (number of events) Versus Time for a Median Value Simulation	532
6-146. Parameters in <i>Simulation_Settings</i> Container	535
6-147. Parameters in <i>Switches</i> Container	535
6-148. Parameters in <i>External_Files</i> Container	537
6-149. Time Option Settings	538

ACRONYMS AND ABBREVIATIONS

ACC	accession number
AEC	U.S. Atomic Energy Commission
AMR	Analysis and Model Report
ASTM	American Society for Testing and Materials
BDCF	biosphere dose conversion factor
CCDF	complementary cumulative distribution function
CDF	cumulative distribution function
CDSP	co-disposal waste packages
CFR	Code of Federal Regulations
CRWMS M&O	Civilian Radioactive Waste Management System Management and Operating Contractor
CSCI	Computer Software Configuration Item
CSNF	commercial spent nuclear fuel
DHLW	defense high-level waste
DI	document identifier
DIRS	Document Input Reference System
DLL	dynamic-link library
DOE	U.S. Department of Energy
DSNF	DOE-owned spent nuclear fuel
DTN	data tracking number
EBS	engineered barrier system
EIS	Environmental Impact Statement
EPA	U.S. Environmental Protection Agency
FEP	feature, event, or process
HLW	high-level waste
HRH	high relative humidity
IRSR	Issue Resolution Status Report
KTI	Key Technical Issue
LA	License Application
LHS	Latin Hypercube Sampling
LRH	low relative humidity
MIC	Microbiologically Induced Corrosion
NFE	Near Field Environment
NRC	U.S. Nuclear Regulatory Commission

ACRONYMS AND ABBREVIATIONS (Continued)

OCRWM	Office of Civilian Radioactive Waste Management
PAO	Performance Assessment Operations
PDF	probability distribution function
PMR	Process Model Report
QA	quality assurance
QARD	Quality Assurance Requirements and Description
RH	Relative Humidity
SR	site recommendation
SZ	saturated zone
TDMS	Technical Data Management System
TH	Thermal Hydrology
THC	Thermohydrological-Chemical
TSPA	total system performance assessment
TSPA&I	Total System Performance Assessment and Integration
TSPA-SR	Total System Performance Assessment-Site Recommendation
TSPA-VA	Total System Performance Assessment-Viability Assessment
USGS	U.S. Geological Survey
UZ	unsaturated zone
VA	Viability Assessment
YMP	Yucca Mountain Site Characterization Project

1. PURPOSE

As directed by a written technical work plan (CRWMS M&O 2000 [153289]), a model of the Yucca Mountain Total System Performance Assessment for Site Recommendation (TSPA-SR) is to be developed. The purpose of this model is to assist the Performance Assessment Operations (PAO) and its Engineered Barrier Performance Section in analyzing the performance of the repository system in isolating waste for long periods of time. This model will allow PAO to perform a detailed and complete analysis and to answer the key technical issues (KTI) raised in the Nuclear Regulatory Commission (NRC) *Issue Resolution Status Report: Key Technical Issue: Total System Performance Assessment and Integration*, Revision 2 (NRC 2000 [149372]).

The scope of this document is to describe the integration of information that represents different aspects of the repository, into one comprehensive model. The Yucca Mountain system has been divided into individual parts to make the overall system analyses manageable. Each of the individual parts or components represents a major process area. The process areas are the following:

- Unsaturated Zone Flow
- Thermal Hydrology
- Waste Package and Drip Shield Degradation
- Waste Form Degradation
- Engineered Barrier System Transport
- Unsaturated Zone Transport
- Saturated Zone Flow and Transport
- Biosphere
- Disruptive Events.

Process Model Reports (PMRs) and their associated Analysis Model Reports (AMRs) describe the development of the component models that define these process areas. This AMR provides detail as to how these component models are implemented in the TSPA-SR model.

Conclusions are presented in Section 7.

The intended use of this document is as a description of the TSPA-SR model files given in Section 3.

2. QUALITY ASSURANCE

The Quality Assurance (QA) program applies to the development of the TSPA-SR model. The Performance Assessment Operations responsible manager has evaluated the technical document development activity in accordance with AP-2.21Q, *Quality Determinations and Planning for Scientific, Engineering, and Regulatory Compliance Activities* [152174]. The AP-2.21Q activity evaluation, *Activity Evaluation for TSPA-SR* (CRWMS M&O 2000 [153283]), has determined that the preparation and review of this technical document is subject to *Quality Assurance Requirements and Description* (QARD) DOE/RW-0333P (DOE 2000 [149540]) requirements. Preparation of this AMR did not require the classification of items in accordance with QAP-2-3, *Classification of Permanent Items*. This activity is not a field activity, therefore, an evaluation in accordance with NLP-2-0, *Determination of Importance Evaluations*, was not required.

With regard to the development of this model, the control of electronic management of data was evaluated in accordance with AP-SV.1Q, *Control of the Electronic Management of Information* [153202] in the document *Technical Work Plan for Total System Performance Assessment* (CRWMS M&O 2000 [153289]). The evaluation determined that current work processes and procedures are adequate for the control of electronic management of data for this activity.

3. COMPUTER SOFTWARE AND MODEL USAGE

3.1 SOFTWARE

The software used in the TSPA-SR model along with the version number, qualification status and operating platform is listed in Table 3-1. Table 3-2, identifies the computer systems, including CPU number and location, that were used in developing and running these programs. MAKEPTRK and mView were used on the Sun Ultra Sparc, and the remaining codes were used on all the listed Dell servers and workstations.

Table 3-1. Software and Software Routines

Computer Code	Version	STN/CSCI	Qualification Status	Platform
GoldSim	6.0.4.007	10344-6.04.007-00	Qualified	Windows NT 4.0
FEHM ^a	2.1	10086-2.10-00	Unqualified	Windows NT 4.0
T2_BINNING	1.0	NA ^b	Documented in Attachment IV	Windows NT 4.0
WT_BINNING	1.0	NA ^b	Documented in Attachment V	Windows NT 4.0
MAKEPTRK	2.0	NA ^b	Documented in Attachment VI	Sun OS 5.7
WAPDEG ^a	4.0	10000-4.0-00	Qualified	Windows NT 4.0
ASHPLUME	1.4LVdII	10022-1.4LVdII-00	Qualified	Windows NT 4.0
SZ_CONVOLUTE ^a	2.0	10207-2.0-00	Qualified	Windows NT 4.0
SEEPDLL	1.0	NA ^b	Documented in Attachment II	Windows NT 4.0
SOILEXP	1.0	NA ^b	Documented in Attachment III	Windows NT 4.0
GVP	1.02	10341-1.02-00	Qualified	Windows NT 4.0
MFD	1.01	10342-1.01-00	Qualified	Windows NT 4.0
SCCD	2.0	10343-2.0-00	Qualified	Windows NT 4.0
PREWAP	1.0	NA ^b	Documented in Attachment VII	Windows NT 4.0
MVIEW	2.10	10072-2.10-00	Qualified	Irix 6.3 or greater, HP-UX 10.2, Solaris 2.6, Digital Unix V4
SATOOL	1.0	10084-1.0-00	Qualified	Windows 98
PDFSENS	1.0	10190-1.0-00	Qualified	Windows 98 Windows 95

NOTE: ^a This software qualification package contains program executable (.exe) and dynamic-linked library (.dll) versions of the code. It is the DLL version that is used in the TSPA-SR model simulations.

^b This software routine is documented in this AMR as a single use software routine per Section 5.1.1 of AP-SI.1Q [153201].

Table 3-2. Computer Systems

Computer Type	CPU Number	Location
Sun Ultra Sparc	R404810	DE&S Las Vegas, Nevada
Dell 6350 PowerEdge Server	114328	DE&S Las Vegas, Nevada
Dell 6350 PowerEdge Server	114329	DE&S Las Vegas, Nevada
Dell 6350 PowerEdge Server	114330	DE&S Las Vegas, Nevada
Dell 6350 PowerEdge Server	114331	DE&S Las Vegas, Nevada
Dell 6350 PowerEdge Server	114332	DE&S Las Vegas, Nevada
Dell 6350 PowerEdge Server	114333	DE&S Las Vegas, Nevada
Dell 6350 PowerEdge Server	114334	DE&S Las Vegas, Nevada
Dell 6350 PowerEdge Server	114335	DE&S Las Vegas, Nevada
Dell 6350 PowerEdge Server	117165	DE&S Las Vegas, Nevada
Dell 6350 PowerEdge Server	117166	DE&S Las Vegas, Nevada
Dell 6350 PowerEdge Server	117167	DE&S Las Vegas, Nevada
Dell 6350 PowerEdge Server	117168	DE&S Las Vegas, Nevada
Dell 6350 PowerEdge Server	117169	DE&S Las Vegas, Nevada
Dell 6350 PowerEdge Server	117170	DE&S Las Vegas, Nevada
Dell 6350 PowerEdge Server	117171	DE&S Las Vegas, Nevada
Dell 6350 PowerEdge Server	117172	DE&S Las Vegas, Nevada
Dell 6350 PowerEdge Server	117173	DE&S Las Vegas, Nevada
Dell Precision 620 Workstation	117322	DE&S Las Vegas, Nevada
Dell Precision 620 Workstation	117323	DE&S Las Vegas, Nevada
Dell Precision 620 Workstation	117324	DE&S Las Vegas, Nevada
Dell Precision 620 Workstation	117325	DE&S Las Vegas, Nevada

The TSPA-SR model file and associated external files necessary to reproduce the results documented in this AMR can be found in the Technical Data Management System (TDMS). Median-value realizations are contained under DTN: MO0009MWDMED01.020 [152838], and human intrusion cases are contained under DTN: MO0008MWDHUMAN.000 [152186].

For each case, the “.gsm” file is the GoldSim file that contains the TSPA-SR model, and the results of the simulation upon which this document is based. This file (along with the GoldSim code) is all that is needed to view the model and the results shown in the subsections below.

One base case and three disruptive event cases have been submitted under two data tracking numbers (DTNs). The following three cases (GoldSim files) have been submitted under DTN: MO0009MWDMED01.020 [152838]:

- “SR00_038ne6.gsm” is a 1,000,000-year median value simulation of the base case model.
- “SR00_037ne6.gsm” is a 1,000,000-year median value simulation of a seismic cladding disruptive event.

- “SR00_001ie5.gsm” is a 100,000-year median value simulation of an igneous disruptive event.

The DTN: MO0008MWDHUMAN.000 [152186] contains the GoldSim file “SR00_005hm5.gsm” which gives the results of a 100,000-year 100 realization simulation of the human intrusion scenario.

3.1.1 GoldSim

GoldSim version 6.04.007 was developed by Golder Associates as an update to the baselined software, RIP v.5.19.01. GoldSim is a Windows based program that is used as the “executive driver program” for simulations of the TSPA-SR model. GoldSim is computationally similar to RIP, which was used for TSPA calculations for the Viability Assessment (DOE 1998 [100550]). GoldSim is designed so that probabilistic simulations can be represented graphically. Models are created in GoldSim by manipulating graphical objects. The graphical objects (or graphical elements as they are called in GoldSim) represent the features, processes and events controlling the system that is being simulated.

The following lists four ways that component models may be coupled into GoldSim, from most complex to least complex, include the following:

- External function calls to detailed process software codes (e.g., WAPDEG)
- Cells, which are basically equilibrium batch reactors that, linked in series, can provide a reasonably accurate description of transport through selected parts of the system
- Response surfaces, which take the form of multidimensional tables representing the results of modeling with detailed process models before running model
- Functional or stochastic representations of a component model built directly into the GoldSim architecture.

The first and third items listed above merit further description. GoldSim is designed to dynamically link with external software (i.e., independent, stand-alone software) to perform certain calculations. The majority of the TSPA-SR model is treated within GoldSim. However, some TSPA calculations (e.g., waste package degradation, seepage into drifts, UZ transport, SZ transport) are too complex to be performed by GoldSim. In these cases, dynamic-linked libraries (DLLs) are written to perform the calculations. A DLL is similar to an executable program, except that instead of being run as a stand-alone program, a DLL is run by another program (in this case GoldSim). When GoldSim runs a DLL, data are transferred between GoldSim and the DLL via blocks of shared memory. One memory block is assigned for DLL input and one for DLL output. For example, when GoldSim calls the *soilexp* DLL four parameter values (*Etime*, *Volcano_Period*, *Closure_Time*, and *Soil_Removal*) are passed from GoldSim to the DLL’s input memory block. The *soilexp* DLL reads the data from its input memory block, performs its calculations, and then passes its output to its output memory block. GoldSim then reads the data the DLL’s output memory block and assigns it to the *Soil_Removal_Factor* data element. At no time during this process are the GoldSim or the *soilexp* DLL binary files altered.

For the TSPA-SR model simulations, GoldSim calls the following DLLs: ASHPLUME, FEHM, GVP, MFD, SCCD, seepdll, soilxp, SZ_CONVOLUTE, and WAPDEG. Each of these is discussed in the following sections.

As described above for the third coupling method, much of the computational work that goes into the TSPA-SR model is done outside of GoldSim, before running the actual total system computations. The results of these detailed process-level runs were provided as multidimensional tables that are read into GoldSim at run time. Refer to Section 6.2 *Model Structure and Design* for further details on how the TSPA-SR model simulations are executed.

Another important feature of GoldSim is distributed parallel processing. Since each realization of a multi-realization simulation is independent from the others, GoldSim can run on a network where multiple realizations can be carried out on different processors. This feature greatly facilitates probabilistic simulation of highly complex systems in which a single realization can take hours to complete.

GoldSim was obtained from software configuration management, it is appropriate for this application, and it is used only within the range of validation in accordance with OCRWM Procedure AP-SI.1Q, *Software Management* [153201].

3.1.2 FEHM

At each time step FEHM reads a set of pre-generated flow fields and performs the unsaturated zone particle transport simulation. The results of the simulation are used as input by GoldSim for the saturated zone model. FEHM Version 2.10 is currently undergoing qualification under AP-SI.1Q. The FEHM software qualification package contains program executable (.exe) and dynamic-linked library (.dll) versions of the code. It is the DLL version (filename fehm_sr.dll) that is used in the TSPA-SR model simulations. FEHM was obtained from software configuration management in accordance with AP-SI.1Q [153201].

3.1.3 T2_BINNING

T2_BINNING version 1.0 was used to generate repository release bins based on surface infiltration information. T2_BINNING groups nodes into five bins that correspond to prescribed infiltration ranges. The nodes belong to a pre-defined repository region from the 3-D site-scale unsaturated zone model. T2_BINNING is qualified as a single use software routine in accordance with Section 5.1.1 of AP-SI.1Q [153201] (see Attachment IV). It is appropriate for this application, and is used only within the range of validation in accordance with AP-SI.1Q [153201].

3.1.4 WT_BINNING

WT_BINNING version 1.0 was used to generate UZ radionuclide collect bins at the UZ-SZ interface. WT_BINNING groups nodes at or below a prescribed water table into one of four quadrants defined for the saturated zone model. WT_BINNING is qualified as a single use software routine in accordance with Section 5.1.1 of e AP-SI.1Q [153201] (see Attachment V). It is appropriate for this application, and is used only within the range of validation in accordance with AP-SI.1Q [153201].

3.1.5 MAKEPTRK

MAKEPTRK version 2.0 provides input information required by the code FEHM to define transport models and nodal assignments. For TSPA, only the nodal assignments were used. MAKEPTRK is qualified as a single use software routine in accordance with Section 5.1.1 of AP-SI.1Q [53201] (see Attachment VI). It is appropriate for this application, and is used only within the range of validation in accordance with AP-SI.1Q [153201].

3.1.6 WAPDEG

WAPDEG version 4.0 was developed to simulate waste package degradation utilizing a stochastic approach. It is an improved version of WAPDEG 3.09, which was used for waste package degradation analysis for the Viability Assessment (VA) of the Yucca Mountain repository (DOE 1998 [100550]). WAPDEG consists of two parts: the WAPDEG dynamic link library (DLL) and the WAPDEG executable program. The WAPDEG DLL (filename wapdeg.dll) is designed to be called by the GoldSim program. It evaluates and applies initiation thresholds of various corrosion and other degradation processes as a function of time-dependent exposure conditions. The penetration rate of active degradation processes as a function of exposure conditions is also evaluated. WAPDEG generates output for time-histories of failures and subsequent degradation (i.e., number of penetrations) for each waste package barrier. WAPDEG is appropriate for this application, and is used only within the range of validation in accordance with AP-SI.1Q [153201]. WAPDEG was obtained from software configuration management in accordance with AP-SI.1Q [153201].

3.1.7 ASHPLUME

ASHPLUME version 1.4LV was selected in the AMR *Igneous Consequence Modeling for TSPA-SR* (CRWMS M&O 2000 [139563]) for modeling volcanic ash dispersion and deposition to evaluate the consequences of extrusive volcanic events through the Yucca Mountain Repository. The software estimates the distribution of ash and radioactive waste released into the biosphere during volcanic events that intercept the repository. ASHPLUME uses a variety of important eruption and environmental parameters as input and returns ash and radioactive waste concentrations at selected locations on the ground surface as output.

ASHPLUME version 1.4LVdll is a modified version of ASHPLUME version 1.0 (Jarzemba et al. 1997 [100987]), a model developed by the Southwest Research Institute Center for Nuclear Waste Regulatory Analyses (CNWRA) in San Antonio, Texas, to support Nuclear Regulatory Commission (NRC) performance assessments. ASHPLUME version 1.4LVdll (filename ashdll.dll) is a recompiled version of ASHPLUME version 1.4LV (into a DLL) for direct linking to GoldSim. This version is identical to version 1.4LV with the exception that version 1.4LVdll was compiled to receive its inputs from GoldSim and return its results to GoldSim.

ASHPLUME was obtained from Configuration Management, is appropriate for this application, and is used only within the range of validation in accordance with its qualification under AP-SI.1Q [153201].

3.1.8 SZ_CONVOLUTE

SZ_CONVOLUTE version 2.0 was developed to calculate saturated-zone response curves based on unsaturated-zone radionuclide source terms, generic saturated-zone responses, and the expected climate scenario. SZ_CONVOLUTE version 2.0 is the result of minor modifications made to SZ_CONVOLUTE version 1.0 (CRWMS M&O 1998 [101112]). The modifications include a change to the format of the breakthrough curve input file. SZ_CONVOLUTE version 1.0 read the breakthrough curve for each of 100 realizations from 100 separate files. SZ_CONVOLUTE version 2.0 reads the breakthrough curves for all 100 realizations from a single file. SZ_CONVOLUTE version 2.0 includes a provision to allow GoldSim to track a subset of the total radionuclide inventory. SZ_CONVOLUTE version 2.0 incorporates an approximate method for computing concentration and dose at the accessible environment that used the generic saturated-zone transport calculation as a basis. It requires input of data files containing generic saturated-zone breakthrough curves that have been calculated for a constant mass flux input. Any number of nuclides, source regions, and breakthrough monitoring locations may be used. Unsaturated-zone mass flux information is required for each nuclide at each source location. Generic saturated-zone breakthrough curves are also required for each nuclide originating at each source region and reaching each monitoring location. Information concerning the unsaturated-zone breakthrough concentration, the current simulation time, the current climate state, and the number of radionuclides are supplied through the routine call from GoldSim. The output information returned to GoldSim through the routine call is the breakthrough concentration multiplied by the current time step at each time. Breakthrough information is supplied for each nuclide origination at each source location and reaching each monitoring location.

The SZ_Convolute software qualification package contains program executable (.exe) and dynamic-linked library (.dll) versions of the code. It is the DLL version (filename szconv_sr.dll) that is used in the TSPA-SR model simulations. SZ_CONVOLUTE version 2.0, was obtained from Configuration Management, is appropriate for this application, and is used only within the range of validation in accordance with its qualification under AP-SI.1Q [153201].

3.1.9 SEEPDLL

Seepdll version 1.0 calculates the seepage fraction and flux of water that will enter the drift and could potentially contribute to the degradation of the engineered systems and release and transport radionuclides within the drifts. The routine was developed using an analysis abstracted from the seepage process modeling that generated probability distributions that represent the uncertainty and spatial variability of seepage. The resulting output is passed from the routine to GoldSim. Seepdll is qualified as a single use software routine in accordance with Section 5.1.1 of AP-SI.1Q [153201] (see Attachment II). Seepdll is appropriate for this application, and is used only within the range of validation in accordance with its qualification under AP-SI.1Q [153201].

3.1.10 SOILEXP

Soilexp version 1.0 calculates the cumulative soil removal factor used to calculate radionuclide concentration at deposition points over the life of the repository. The soilexp routine receives

input from GoldSim, calculates the cumulative soil removal factor for the time interval, and passes the result back to GoldSim. Soilexp is qualified as a single use software routine in accordance with Section 5.1.1 of AP-SI.1Q [153201] (see Attachment III). Soilexp is appropriate for this application, and is used only within the range of validation in accordance with its qualification under AP-SI.1Q [153201].

3.1.11 GVP (Gaussian Variance Partitioning)

GVP version 1.02 was developed to incorporate measurement uncertainty and corrosion rate variability into the calculations of waste package degradation. In order to assess waste package failure distribution over time in the repository, only the fraction of the total variance is needed because of variability in the waste package degradation simulations. Gaussian Variance Partitioning is applied to separate the contributions of uncertainty from their elicited distributions. The routine accesses corrosion rates located in an external file and GoldSim stochastic variables. The output of GVP is a distribution table of variability in uncertainty. GVP provides a clearer demonstration of the sensitivity of the TSPA-SR model to uncertainty and variability. GVP is qualified as a multiple use software routine in accordance with Section 5.1.2 of AP-SI.1Q [153201]. GVP is appropriate for this application, and is used only within the range of validation in accordance with its qualification under AP-SI.1Q [153201]. GVP was obtained from software configuration management in accordance with AP-SI.1Q [153201].

3.1.12 MFD (Manufacturing Defects Calculation)

MFD version 1.01 was developed to calculate the frequency of occurrence and size of flaws potentially found in the waste package closure welds based on uncertainties within the repository. Flaw density and size distributions are utilized as the parameter for a Poisson distribution used to represent the frequency of occurrence of flaws in a given length of closure weld. Its output, flaw sizes as a probability density function on each closure weld, is used to support WAPDEG analysis and is linked to GoldSim. MFD version 1.01 is qualified as a multiple use software routine in accordance with Section 5.1.2 of AP-SI.1Q [153201]. MFD is appropriate for this application, and is used only within the range of validation in accordance with its qualification under AP-SI.1Q [153201]. MFD was obtained from software configuration management in accordance with AP-SI.1Q [153201].

3.1.13 SCCD (Stress Corrosion Cracking Dissolution)

SCCD version 2.00 was developed to predict crack initiation and propagation in closure weld manufacturing defects and incipient weld cracks. A reference table based on stress/strain intensity as a function of crack depth is modified by SCCD and used as input to WAPDEG. The resulting waste package failure histories are then returned to GoldSim. SCCD is qualified as a multiple use software routine in accordance with Section 5.1.2 of AP-SI.1Q [153201]. SCCD is appropriate for this application, and is used only within the range of validation in accordance with its qualification under AP-SI.1Q [153201]. SCCD version 2.00 was obtained from software configuration management in accordance with AP-SI.1Q [153201].

3.1.14 PREWAP

PREWAP version 1.0 is an executable file developed for constructing the WAPDEG input file by using pH, Cl, and thermohydrology data extracted from various tables to generate reformatted output tables of in-drift (drip shield and waste package) and in-package chemistry parameters that are used as input to the WAPDEG routine. The PREWAP file is executed to generate the WAPDEG data file before invoking the TSPA-SR model. PREWAP is qualified as a single use software routine in accordance with Section 5.1.1 of AP-SI.1Q [153201] (see Attachment VII). PREWAP is appropriate for this application, and is used only within the range of validation in accordance with its qualification under AP-SI.1Q [153201].

3.1.15 mView

mView version 2.10 is designed to transform text data describing numeric model geometry and numeric model output into two dimensional and three dimensional visual representations. For TSPA-SR, it is used for the visualization of radionuclide concentrations as they travel from the engineered barrier system through the unsaturated zone. It obtains its input from FEHM output data sets. mView is appropriate for this application, and is used only within the range of validation in accordance with its qualification under AP-SI.1Q [153201]. mView was obtained from software configuration management in accordance with AP-SI.1Q [153201].

3.1.16 SATOOL

SATOOL version 1.0 was developed for use in sensitivity analyses following the uncertainty analysis by Monte Carlo simulations of the TSPA-SR by GoldSim or of WAPDEG. The sensitivity analysis identifies those input variables whose variance contributes dominantly to the variance in the output. The code uses step-wise regression for identifying a set of the most sensitive variables. SATOOL was obtained from CM, is appropriate for the application, and is used only within the range of validation in accordance with its qualification under AP-SI.1Q [153201].

3.1.17 PDFSENS

PDFSENS version 1.0 is designed to compute the mean and the cumulative distribution function (CDF) of the output in a Monte Carlo simulation (MCS) when the probability distribution function (PDF) of one or more input variables is modified from their original PDFs used in the MCS, without recourse to re-simulation in the MCS. The code will be used for post processing of the TSPA-SR results. Sensitivity studies will be conducted by varying the PDFs from the TSPA-SR results in the different scenarios to calculate new doses without rerunning the GoldSim code. PDFSENS was obtained from CM, is appropriate for the application, and is used only within the range of validation in accordance with its qualification under AP-SI.1Q [153201].

3.2 MODELS

The YMP repository is comprised of a complex system of engineered and natural barriers that will confine the wastes stored in the repository. The TSPA-SR model incorporates models of these individual barriers and processes (submodels) into a comprehensive integrated model of the

total repository system. A guide to detailed information regarding these submodels (or components) of the TSPA-SR model is presented in Table 3-3 which gives the section of this document where each submodel and its intended use is described. Data generated by these submodels that are utilized in the TSPA-SR are discussed in Section 4.

The submodels have been developed and validated in accordance with AP-3.10Q [152363] and have been used only within their range of validation. Each of the submodels is appropriate for this application because their design was specifically intended for use in TSPA-SR support. Submodel output file DTNs are provided in Table 3-3 because Model Warehouse DTNs were not available at the time this document was produced.

Table 3-3. Models Used in this Analysis

Submodel	Section	Supporting AMR	Submodel Output File DTN (TSPA-SR Model Input)
Seepage Model	6.3.1.2	Abstraction of Drift Seepage (CRWMS M&O 2000 [142004])	SN9912T0511599.002 [146902]
In-drift Geochemical Environment Model	6.3.2.2	In-Drift Precipitates/Salts Analysis (CRWMS M&O 2000 [127818])	MO0002SPALOO46.010 ^a [149168]
Waste Package Degradation Model	6.3.3	WAPDEG Analysis of Waste Package and Drip Shield Degradation (CRWMS M&O 2000 [151566])	MO0004SPASUP01.004 [153127]
In Package Chemistry Model	6.3.4.2	In-Package Chemistry Abstraction (CRWMS M&O 2000 [129287])	MO9911SPACDP37.001 [139569]
Dissolution Rate Model	6.3.4.4	Defense High Level Waste Glass Degradation (CRWMS M&O 2000 [143420])	LL000210651021.121 [145943]
Dissolved Concentration Limits	6.3.4.5	Summary of Dissolved Concentration Limits (CRWMS M&O 2000 [143569])	MO0004SPASOL10.002 [151713]
Colloid Model	6.3.4.6	Waste Form Colloid-Associated Concentration Limits-Abstraction and Summary (CRWMS M&O 2000 [125156])	MO0003SPAHIG12.002 [147949] MO0003SPAHLO12.004 [147952] MO0003SPAION02.003 [147951] MO0003SPALOW12.001 [147953]
EBS Flow and Transport Paths	6.3.5.1	EBS Radionuclide Transport Abstraction (CRWMS M&O 2000 [129284])	SN9908T0872799.004 [108437] ^a
EBS Transport Parameters	6.3.5.2	EBS Radionuclide Transport Abstraction (CRWMS M&O 2000 [129284])	SN9908T0872799.004 [108437] ^a LL000207751021.119 [145940] ^b
Unsaturated Zone Transport Parameters	6.3.6.1	Unsaturated Zone and Saturated Zone Transport Properties (U0100) (CRWMS M&O 2000 [152773])	LA0003JC831362.001 [149557]
Particle Tracking Model	6.3.6.2	Particle Tracking Model and Abstraction of Transport Processes (CRWMS M&O 2000 [141418]); Abstraction of Flow Fields for RIP (CRWMS M&O 2000 [123913])	SN9910T0581699.002 [126110]
Saturated Zone Transport Parameters	6.3.7.1	Input and Results of the Base Case Saturated Zone Flow and Transport Model for TSPA (CRWMS M&O 2000 [139440]); Uncertainty Distribution for Stochastic Parameters (CRWMS M&O 2000 [147972])	SN0004T0571599.004 [149254]

Table 3-3. Models Used in this Analysis (Continued)

Submodel	Section	Supporting AMR	Submodel Output File DTN (TSPA-SR Model Input)
Volcanic Direct Release Model	6.3.9.1	Igneous Consequence Modeling for the TSPA-SR (CRWMS M&O 2000 [139563])	SN0006T0502900.002 [150856]
Intrusive Indirect Release Model	6.3.9.2	Igneous Consequence Modeling for the TSPA-SR (CRWMS M&O 2000 [139563])	SN0006T0502900.002 [150856]

NOTES: ^aThe component model and associated TSPA-SR model inputs were developed in the AMR specified. These TSPA-SR model inputs were later updated and documented in a calculation. This DTN corresponds to that calculation.

^bThis data is from a transmittal letter from Lawrence Livermore National Laboratory (Steward 1999 [153328]).

4. INPUTS

NOTE: This document may be affected by technical product input information that requires confirmation. Any changes to the document or its conclusions that may occur as a result of completing the confirmation activities will be reflected in subsequent revisions. The status of the technical product input information quality may be confirmed by review of the DIRS database.

4.1 DATA AND PARAMETERS

The TSPA-SR model is a computer model that integrates all of the process models that were developed for the Yucca Mountain site characterization for site recommendation. Table 4-1 provides a summary of the major inputs to the TSPA-SR model. Each component model of the TSPA-SR model is presented individually in Section 6.3, and the complete set of inputs for each of these component models is presented there. Table 4-2 provides the output DTNs from the component models and analyses that are used as input to the TSPA-SR model. Not all the inputs to the TSPA-SR model are qualified at this time. Some of the input AMRs contain data that is in the process of being qualified. The qualification status of inputs to this model can be found in the Document Input Reference System (DIRS) database. These inputs are considered appropriate for this model.

The YMP TSPAs are intended to be iterative—as new data become available and as the underlying processes are better understood, the models and model inputs are refined. Because the TSPA process is an iterative one, these inputs, and therefore the simulation results, are a “snap-shot” of the information available at the time the simulations were run. In the time since the development of this version of the TSPA-SR model and the final production of this AMR, some of the inputs have been superceded by newer information as listed in Table 4-3. Indeed, many of the AMRs that provided inputs to the TSPA-SR model are currently undergoing updates. Because of this, after all the input AMRs that are undergoing updates have been completed, the TSPA-SR model will be updated to reflect those changes, and this AMR will be updated.

4.2 CRITERIA

4.2.1 NRC Review and Acceptance Criteria

A summary is listed of the NRC review and acceptance criteria outlined in the Issue Resolution Status Report (IRSR) that applies to the Total System Performance Assessment and Integration (TSPA&I) Key Technical Issues (KTIs) (NRC 2000 [149372]). The following four subissues are identified in the TSPA&I IRSR (NRC 2000 [149372], Section 2.0).

1. System Description and Demonstration of Multiple Barriers
2. Scenario Analysis
3. Model Abstraction
4. Demonstration of the Overall Performance Objective.

Table 4-1. General Listing of Inputs to the Total System Performance Assessment-Site Recommendation Model

Key System Attribute	Factor	Reference Document	Major Types of Input Parameters to the TSPA-SR	Refer to the Following Sections for a Detailed Listing of Parameters and Data Tracking Numbers
Limiting Water contacting waste package	Climate	<i>Future Climate Analysis</i> (USGS 2000 [136368])	Climate states Timing and sequence	Section 6.3.1.1
	Infiltration	<i>Analysis of Infiltration Uncertainty</i> (CRWMS M&O 2000 [143244])	Probabilities for different infiltration scenarios	Section 6.3.1.1
	UZ flow above potential repository	<i>Abstraction of Flow Fields for RIP (U0125)</i> (CRWMS M&O 2000 [123913])	Flow fields for different infiltration scenarios and climate states	Section 6.3.1.3
	Seepage into drifts	<i>Abstraction of Drift Seepage</i> (CRWMS M&O 2000 [142004])	Seepage flux and seepage fraction as a function of percolation flux	Section 6.3.1.2
		<i>Abstraction of NFE Drift Thermodynamic Environment and Percolation Flux</i> (CRWMS M&O 2000 [149860])	Percolation flux – f (multiple locations, waste type, time, climate)	Section 6.3.2.1
	Coupled processes - effects on UZ flow	<i>Drift Scale Coupled Processes (DST and THC Seepage) Models</i> (CRWMS M&O 2000 [142022])	Flow fields affected by TH	N/A – Background Information Only
	Coupled processes - effects on seepage	<i>Abstraction of Drift Seepage</i> (CRWMS M&O 2000 [142004])	Seepage flux and seepage fraction as a function of percolation flux	Section 6.3.1.2
		<i>Abstraction of NFE Drift Thermodynamic Environment and Percolation Flux</i> (CRWMS M&O 2000 [149860])	Percolation flux – f (multiple locations, waste type, time, climate)	Section 6.3.2.1
	In-drift physical and chemical environments	<i>Abstraction of NFE Drift Thermodynamic Environment and Percolation Flux</i> (CRWMS M&O 2000 [149860])	Temperature and relative humidity on the drip shield surface – f (multiple locations, waste type, time, climate)	Section 6.3.2.1

Table 4-1. General Listing of Inputs to the Total System Performance Assessment-Site Recommendation Model (Continued)

Key System Attribute	Factor	Reference Document	Major Types of Input Parameters to the TSPA-SR	Refer to the Following Sections for a Detailed Listing of Parameters and Data Tracking Numbers
Limiting water contacting waste package (Continued)	In-drift physical and chemical environments (Continued)	<i>In-Drift Precipitates/Salts Analysis</i> (CRWMS M&O 2000 [127818])	pH – f (region, time, response surface) Chloride – f (region, time) Ionic strength	Section 6.3.2.2
	In-drift moisture distribution	<i>EBS Radionuclide Transport Abstraction</i> (CRWMS M&O 2000 [129284])	Seepage flux through the drip shield Fraction of drip shield surface that is wet	N/A - Equations
	Performance of drip shield	<i>Environment on the Surfaces of the Drip Shield and Waste Package Outer Barrier</i> (CRWMS M&O 2000 [148460])	Threshold for general corrosion initiation	Section 6.3.3
		<i>Calculation of General Corrosion Rate of Drip Shield and Waste Package Outer Barrier to Support WAPDEG Analysis</i> (CRWMS M&O 2000 [147641])	General corrosion rate under drip and no-drip conditions	Section 6.3.3
		<i>WAPDEG Analysis of Waste Package and Drip Shield Degradation</i> (CRWMS M&O 2000 [151566])	Drip shield geometry and thickness Drip shield failure time history Number of penetration openings in drip shield by general corrosion, crevice corrosion, SCC, HIC, and other degradation modes.	N/A – Design information and WAPDEG Outputs

Table 4-1. General Listing of Inputs to the Total System Performance Assessment-Site Recommendation Model (Continued)

Key System Attribute	Factor	Reference Document	Major Types of Input Parameters to the TSPA-SR	Refer to the Following Sections for a Detailed Listing of Parameters and Data Tracking Numbers
Long waste package lifetime	Moisture, temperature, and chemistry effects on waste package	<i>In-Drift Precipitates/Salts Analysis</i> (CRWMS M&O 2000 [127818])	pH – f (region, time, response surface) Chloride – f (region, time, response surface) Ionic Strength	Section 6.3.2.2
		<i>Abstraction of NFE Drift Thermodynamic Environment and Percolation Flux</i> (CRWMS M&O 2000 [149860])	Average and maximum temperature on waste package surface – f (waste type, region, time, climate) Temperature and relative humidity on waste package surface – f (multiple locations, waste type, time, climate, infiltration)	Section 6.3.2.1
		<i>EBS Radionuclide Transport Abstraction</i> (CRWMS M&O 2000 [129284])	Seepage flux through waste package Fraction of waste package surface that is wet	N/A - Equations
	Performance of waste package barrier	<i>WAPDEG Analysis of Waste Package and Drip Shield Degradation</i> (CRWMS M&O 2000 [151566])	Waste package geometry Thickness of waste package barriers Waste package failure time history Number of penetration openings in waste package by general corrosion, crevice corrosion, SCC, and other degradation modes	N/A – Design Input and WAPDEG Output
		<i>Aging and Phase Stability of Waste Package outer Barrier</i> (CRWMS M&O 2000 [147639])	Kinetics of secondary phase formation in base metal and weld of waste package outer barrier Threshold secondary phase volume fraction above which corrosion resistance of waste package outer barrier is affected	N/A – Equations

Table 4-1. General Listing of Inputs to the Total System Performance Assessment-Site Recommendation Model (Continued)

Key System Attribute	Factor	Reference Document	Major Types of Input Parameters to the TSPA-SR	Refer to the Following Sections for a Detailed Listing of Parameters and Data Tracking Numbers
Long waste package lifetime (Continued)	Performance of waste package barrier (Continued)	<i>Environment on the Surfaces of the Drip Shield and Waste Package Outer Barrier</i> (CRWMS M&O 2000 [146460])	Threshold relative humidity for general corrosion initiation under drip (after drip shield failure) and no-drip conditions	Section 6.3.3
		<i>General Corrosion and Localized Corrosion of Waste Package Outer Barrier</i> (CRWMS M&O 2000 [144229])	General corrosion rate under drip (after drip shield failure) and no-drip conditions	Section 6.3.3
		<i>Abstraction of Models for Pitting and Crevice Corrosion of Drip Shield and Waste Package Outer Barrier</i> (CRWMS M&O 2000 [147648]) <i>Abstraction of models of Stress Corrosion Cracking of Drip Shield and Waste Package Outer Barrier and Hydrogen Induced Corrosion of Drip Shield</i> (CRWMS M&O 2000 [135773])	Crevice corrosion initiation threshold of waste package outer barrier Pit density (under crevice) Pit penetration rate (under crevice) Stress and stress intensity factor profile in waste package outer barrier SCC initiation threshold SCC crack density SCC crack growth rate Effect of material and manufacturing defects on SCC initiation and crack growth rate SCC crack penetration opening size Effect of phase stability and aging of waste package outer barrier on SCC initiation and crack growth rate	Section 6.3.3

Table 4-1. General Listing of Inputs to the Total System Performance Assessment-Site Recommendation Model (Continued)

Key System Attribute	Factor	Reference Document	Major Types of Input Parameters to the TSPA-SR	Refer to the Following Sections for a Detailed Listing of Parameters and Data Tracking Numbers
Long waste package lifetime (Continued)	Performance of waste package barrier (Continued)	<i>Calculation of the Probability and Size of defect flaws in the Waste Package closure welds to support WAPDEG Analysis</i> (CRWMS M&O 2000 [144551])	Probability of the occurrence of material and manufacturing defects Size of material and manufacturing defects	Section 6.3.3
Limiting radionuclide mobilization and release from the engineered barrier system	Moisture, temperature, and chemistry effects within waste package	<i>In-Package Chemistry Abstraction</i> (CRWMS M&O 2000 [129287])	pH – f (region, time) Total dissolved carbonate (CO_3^{2-}) – f (region, time) Oxygen fugacity – f (region, time) Ionic strength – f (region, time) Fluoride – f (region, time) CO_2 fugacity	Section 6.3.4.2
		<i>In-Package Source Term Abstraction</i> (CRWMS M&O 2000 [144167])	Volume of water in the waste package/waste form cell, calculated internal to GoldSim	N/A – calculated internal to GoldSim
	Commercial Spent Nuclear Fuel (CSNF) waste form (with cladding or canister) performance	<i>Inventory Abstraction</i> (CRWMS M&O 2000 [136383])	Number of packages Zircaloy-clad fuel Stainless steel-clad fuel Inventory per package (actual and adjusted for ingrowth) Mass fraction	Section 6.3.4.1

Table 4-1. General Listing of Inputs to the Total System Performance Assessment-Site Recommendation Model (Continued)

Key System Attribute	Factor	Reference Document	Major Types of Input Parameters to the TSPA-SR	Refer to the Following Sections for a Detailed Listing of Parameters and Data Tracking Numbers
Limiting radionuclide mobilization and release from the engineered barrier system (Continued)	Commercial Spent Nuclear Fuel (CSNF) waste form (with cladding or canister) performance (Continued)	<i>Clad Degradation - Summary and Abstraction</i> (CRWMS M&O 2000 [147210])	Fraction of surface area of Zircaloy-clad CSNF exposed as a function of time	Section 6.3.4.3
		<i>CSNF Waste Form Degradation: Summary Abstraction</i> (CRWMS M&O 2000 [136060])	CSNF intrinsic dissolution rate equation	N/A - Equation
	DOE Spent Nuclear Fuel (DSNF) and plutonium disposition waste form performance	<i>Inventory Abstraction</i> (CRWMS M&O 2000 [136383])	Number of packages Inventory per package (actual and adjusted for ingrowth) Mass fraction	Section 6.3.4.1
		<i>DSNF and Other Waste Form Degradation Abstraction</i> (CRWMS M&O 2000 [144164])	DSNF constant dissolution rate DSNF fuel surface area	Section 6.3.4.4
	High Level Waste (HLW) glass waste form (including canister) performance	<i>Inventory Abstraction</i> (CRWMS M&O 2000 [136383])	Number of packages Inventory per package (actual and adjusted for ingrowth) Mass fraction	Section 6.3.4.1
		<i>Defense High Level Waste Glass Degradation</i> (CRWMS M&O 2000 [143420])	HLW intrinsic dissolution rate equation Specific surface area	Section 6.3.4.4
	Dissolved radionuclide concentration limits	<i>Summary of Dissolved Concentration Limits</i> (CRWMS M&O 2000 [143569])	Concentration limits (solubilities) for all isotopes included in TSPA	Section 6.3.4.5

Table 4-1. General Listing of Inputs to the Total System Performance Assessment-Site Recommendation Model (Continued)

Key System Attribute	Factor	Reference Document	Major Types of Input Parameters to the TSPA-SR	Refer to the Following Sections for a Detailed Listing of Parameters and Data Tracking Numbers
Limiting radionuclide mobilization and release from the engineered barrier system (Continued)	Colloid-associated radionuclide concentrations	<i>Waste Form Colloid-Associated Concentration Limits: Abstraction and Summary</i> (CRWMS M&O 2000 [125156])	Types of waste form colloids Concentration of colloids K_d and/or K_c for various colloid types Fraction of inventory that travels as irreversibly attached to colloids	Section 6.3.4.6
	EBS radionuclide migration—transport through invert	<i>Abstraction of NFE Drift Thermodynamic Environment and Percolation Flux</i> (CRWMS M&O 2000 [149860])	Thermally perturbed saturation in the invert – f (waste type, region, time, climate) Saturation in the invert after thermal pulse – $f(\text{time})$	Section 6.3.2.1
		<i>EBS Radionuclide Transport Abstraction</i> (CRWMS M&O 2000 [129284])	Invert geometry Porosity of the invert Diffusion coefficient	Section 6.3.5
Slow transport away from the engineered barrier system	UZ flow and transport—advective pathways	<i>Particle Tracking Model and Abstraction of Transport Processes</i> (CRWMS M&O 2000 [141418])	FEHM particle-tracking model coupled to GoldSim (LANL 1999) Grid nodes for each bin	N/A – not data
		<i>Unsaturated Zone and Saturated Zone Transport Properties (U0100)</i> (CRWMS M&O 2000 [152773])	Transport parameters Fracture aperture in different units Dispersivity of fractures Dispersivity of matrix	Section 6.3.6.1
		<i>Abstraction of Flow Fields for RIP (ID:U0125)</i> (CRWMS M&O 2000 [123913])	Flow fields for different infiltration scenarios and climate states (FEHM input files for the particle-tracking model [LANL])	Section 6.3.1.3 and Section 6.3.6.1

Table 4-1. General Listing of Inputs to the Total System Performance Assessment-Site Recommendation Model (Continued)

Key System Attribute	Factor	Reference Document	Major Types of Input Parameters to the TSPA-SR	Refer to the Following Sections for a Detailed Listing of Parameters and Data Tracking Numbers
Slow transport away from the engineered barrier system (Continued)	UZ flow and transport—sorption and matrix diffusion	<i>Unsaturated Zone and Saturated Zone Transport Properties (U0100)</i> (CRWMS M&O 2000 [152773])	K_d for all isotopes included in TSPA Matrix diffusion coefficients – f (isotopes, units)	Section 6.3.6.1
	UZ flow and transport—colloid-facilitated transport	<i>Unsaturated Zone Colloid Transport Model</i> (CRWMS M&O 2000 [122799])	K_c and/or kinetic colloid parameters for plutonium, americium, thorium, etc. Colloid filtration factor	Section 6.3.6.1*
	Coupled processes—effects on UZ transport	<i>Unsaturated Zone and Saturated Zone Transport Properties (U0100)</i> (CRWMS M&O 2000 [152773])	$K_d s - f$ (isotopes, rock type)	Section 6.3.6.1
	SZ flow and transport—advective pathways	<i>Input and Results of the Base Case Saturated Zone Flow and Transport Model for TSPA</i> (CRWMS M&O 2000 [139440])	Breakthrough curves – f (radionuclide, region) Input parameters for convolution code Climate change flux multiplication factor Transport parameters Dispersivity (longitudinal, horizontal transverse, and vertical transverse) Boundary definition of the alluvium K_d for all isotopes included in TSPA Matrix porosity Flowing-interval spacing Effective diffusion coefficient Flowing interval Bulk density Source region definition Horizontal anisotropy K_c and/or kinetic parameters for plutonium desorption	Section 6.3.7.1

Table 4-1. General Listing of Inputs to the Total System Performance Assessment-Site Recommendation Model (Continued)

Key System Attribute	Factor	Reference Document	Major Types of Input Parameters to the TSPA-SR	Refer to the Following Sections for a Detailed Listing of Parameters and Data Tracking Numbers
Slow transport away from the engineered barrier system (Continued)	Wellhead dilution	<i>Groundwater Usage by the Proposed Farming Community</i> (CRWMS M&O 2000 [144056])	Annual groundwater use	Section 6.3.8.2
	Biosphere transport and uptake	<i>Abstraction of BDCF Distributions for Irrigation Periods</i> (CRWMS M&O 2000 [144054])	Biosphere dose conversion factor – f (radionuclide, irrigation time)	Section 6.3.8.1
		<i>Distribution Fitting to the Stochastic BDCF Data</i> (CRWMS M&O 2000 [144055])	Biosphere dose conversion factor – f (radionuclide, irrigation time)	Section 6.3.8.1
Addressing effects of disruptive events	Intrusive indirect release	<i>Igneous Consequence Modeling for the TSPA-SR</i> (CRWMS M&O 2000 [139563])	Number of waste packages damaged by intrusion (for groundwater transport source term) In-drift chemical conditions	Section 6.3.9.2
	Volcanic direct release	<i>Characterize Framework for Igneous Activity at Yucca Mountain, Nevada (T0015)</i> (CRWMS M&O 2000 [141044])	Annual probability of igneous intrusion into the waste	Section 6.3.9.1
		<i>Igneous Consequence Modeling for the TSPA-SR</i> (CRWMS M&O 2000 [139563])	Input parameters for ASHP LUME Probability that an intrusion into the waste will result in one or more eruptive vents through the waste Number of vents through the waste for intrusions that result in one or more vents through the waste Wind direction factor	Section 6.3.9.1
		<i>Disruptive Event Biosphere Dose Conversion Factor Analysis</i> (CRWMS M&O 2000 [143378])	Biosphere dose conversion factors – f (radionuclide)	Section 6.3.9.1

Table 4-1. General Listing of Inputs to the Total System Performance Assessment-Site Recommendation Model (Continued)

Key System Attribute	Factor	Reference Document	Major Types of Input Parameters to the TSPA-SR	Refer to the Following Sections for a Detailed Listing of Parameters and Data Tracking Numbers
Addressing effects of disruptive events (Continued)	Volcanic direct release (Continued)	<i>Evaluate Soil/Radionuclide Removal by Erosion and Leaching</i> (CRWMS M&O 2000 [136281])	Factor to account for radionuclide removal from soil	Section 6.3.9.1
	Seismic activity	<i>Characterize Framework for Seismicity and Structural Deformation at Yucca Mountain, Nevada</i> (CRWMS M&O 2000 [142321])	Probability of seismicity and structural deformation	Section 6.3.9.4

NOTE: N/A = not applicable.

Table 4-2. Source Data Tracking Numbers

Section	Input DTNs	
6.3.1.1 Climate and Infiltration	GS000308315121.003 [151139]	SN0003T0503100.001 [149556]
6.3.1.2 Seepage into Drifts	SN9912T0511599.002 [146902]	
6.3.1.3 Mountain-Scale Unsaturated Zone Flow	SN9910T0581699.002 [126110]	
6.3.2.1 Thermal Hydrology	SN0007T0872799.014 [152545]	SN0001T0872799.006 [147198]
6.3.2.2 In-drift Geochemical Environment	MO0002SPALOO46.010 [149168]	MO0003MWDTAB45.013 [146857]
6.3.3 Waste Package Degradation	MO0010MWDWAP01.009 [153127]	
6.3.4.1 Radionuclide Inventory	SN0005T0810599.012 [152110] MO0004SPAFRE00.003 [151062] MO0008MWDNM501.005 [151714]	MO0004SPADEC00.002 [151063] MO0009MWDNM601.018 [152839]
6.3.4.2 In-Package Chemistry	MO9911SPACDP37.001 [139569]	
6.3.4.3 Cladding Degradation Model	MO0009MWDMED01.020 [152838]	MO0004SPACLD07.043 [151368]
6.3.4.4 Dissolution Rate Model	MO0007RIB00091.000 [151712]	LL000210651021.121 [145943]
6.3.4.5 Dissolved Concentration Limits	MO0004SPASOL10.002 [151713]	
6.3.4.6 Colloids	MO0003SPAION02.003 [147951] MO0003SPAFIG12.002 [147949] MO0004SPAKDS42.005 [148810]	MO0003SPAHL012.004 [147952] LL991109851021.095 [142902] MO0003SPALOW12.001 [147953]
6.3.5.2 EBS Transport Parameters	LL000207751021.119 [145940] MO0006SPASTR01.003 [153029]	MO0002SPASDC00.002 [148338] SN9908T0872799.004 [108437]
6.3.6.1 UZ Transport Model Components and Input Parameters	SN9907T0872799.004 [111485] LB990501233129.001 [106787] LB990801233129.007 [118710] LB990801233129.009 [118717] LB990801233129.011 [118722] LB997141233129.001 [104055] SN9912T0581699.003 [146903] SN0005T0581699.005 [151514] LA0003MCG12213.002 [147285] LL000122051021.116 [142973] LA0007MCG12213.001 [153251] MO0003SPAHL012.004 [147952] MO0004SPAKDS42.005 [148810]	SN9910T0581699.002 [126110] LB990701233129.001 [106785] LA0003AM831341.001 [148751] LA0003JC831362.001 [149557] LB997141233129.003 [119940] LB991091233129.004 [126111] LB997141233129.002 [119933]
6.3.7.1 Saturated Zone Transport Parameters	MO0003SPAFIG12.002 [147949] MO0004SPAKDS42.005 [148810] SN0004T0501600.004 [149288] MO0003SPAION02.003 [147951]	MO0003SPAHL012.004 [147952] LL991109851021.095 [142902] MO0003SPALOW12.001 [147953] SN004T0501600.005 [151515] SN004T0571599.004 [149254]
6.3.8.1 Biosphere Dose Conversion Factors	MO0002SPACRI02.002 [150040] MO0006SPABDC01.007 [152837]	MO0003SPAABS08.004 [148453] MO0003SPAABS07.006 [148872]
6.3.8.2 Annual Groundwater Usage	MO0003SPASGU01.003 [151075]	
6.3.9.1 Volcanic Release	MO0008MWDVEB03.003 [151547] SN9912T0512299.002 [136370]	SN0006T0502900.002 [150856]
6.3.9.2 Intrusive Indirect Release	MO9912SPAPAI29.002 [148596]	SN0006T0502900.002 [150856]
6.3.9.3 Human Intrusion	MO0003SPAABS07.006 [148872] LA0003AM831341.001 [148751]	GS000308311221.005 [147613] MO0008MWDHUMAN.000 [152186]
6.3.9.4 Seismic Cladding Event	MO0004SPACLD07.043 [151368]	

Table 4-3. A Listing of TSPA-SR Model Inputs That Were Superseded After the Completion of the TSPA-SR Simulations but Before Final Production of This AMR

Section	Input DTNs	Superseded By
6.3.4.1 Radionuclide Inventory	SN0005T0810599.012 [152110] SN0003T0810599.010 [151021]	SN0011T0810599.023 [152993] SN0009T0810599.014 [152980]
6.3.8 1 Biosphere Dose Conversion Factors	MO0003SPAABS08.004 [148453] MO0003SPAABS07.006 [148872]	MO0010SPAABS08.007 [153267] MO0011SPAABS07.009 [153268]
6.3.9.3 Human Intrusion	MO0003SPAABS07.006 [148872]	MO0011SPAABS07.009 [153268]

4.2.1.1 Acceptance Criteria Applicable to All Four Subissues

1. The collection, documentation, and development of data, models, and/or computer codes have been performed under acceptable quality assurance procedures, or if the data, models and/or computer codes were not subject to an acceptable QA procedure, they have been appropriately qualified (NRC 2000 [149372], Section 4.0).
2. Expert elicitations can be used to support data synthesis and model development for the TSPA, provided that the elicitations are conducted and documented under acceptable procedures (NRC 2000 [149372], Section 4.0).

4.2.1.2 Acceptance Criteria for System Description and Demonstration of Multiple Barriers

1. Documents and reports are required to be complete, clear, and consistent (NRC 2000 [149372], Section 4.1).
2. Information is required to be amply cross-referenced (NRC 2000 [149372], Section 4.1).
3. The screening process by which FEPs were included or excluded from the TSPA is required to be fully described (NRC 2000 [149372], Section 4.1).
4. Relationships between relevant FEPs are required to be fully described (NRC 2000 [149372], Section 4.1).
5. The levels and method(s) of abstraction are required to be described starting from assumptions defining the scope of the assessment down to assumptions concerning specific processes and the validity of given data (NRC 2000 [149372], Section 4.1).
6. Mapping (e.g., a road map diagram, a traceability matrix, a cross-reference matrix) is to be provided to show what conceptual features (e.g., patterns of volcanic events) and processes are represented in the abstracted models, and by what algorithms (NRC 2000 [149372], Section 4.1).

7. Explicit discussion of uncertainty is to be provided to identify which issues and factors are of most concern or are key sources of disagreement among experts (NRC 2000 [149372], Section 4.1).
8. The pedigree of data from laboratory tests, natural analogs, and the site is to be clearly identified (NRC 2000 [149372], Section 4.1).
9. Input parameter development and basis for their selection is required to be described (NRC 2000 [149372], Section 4.1).
10. A thorough description of the method used to identify performance confirmation program parameters is required (NRC 2000 [149372], Section 4.1).
11. It is required that the TSPA results (i.e., the peak expected annual dose within the compliance period) can be traced back to applicable analyses that identify the FEPs, assumptions, input parameters, and models in the TSPA (NRC 2000 [149372], Section 4.1).
12. It is required that the TSPA results include a presentation of intermediate results that provide insight into the assessment (e.g., results of intermediate calculations of the behavior of individual barriers) (NRC 2000 [149372], Section 4.1).
13. The flow of information (input and output) between the various modules is required to be clearly described (NRC 2000 [149372], Section 4.1).
14. Supporting documentation (e.g., user's manuals, design documents) is required to clearly describes code structure and relationships between modules (NRC 2000 [149372], Section 4.1).

4.2.1.3 Acceptance Criteria for Scenario Analysis

1. A comprehensive list is required to (i): identify the processes and events that are present or might occur in the region and (ii) includes those processes and events that have the potential to influence repository performance (NRC 2000 [149372], Section 4.2).
2. It is required that adequate documentation be provided to identify how the initial list of processes and events has been grouped into categories (NRC 2000 [149372], Section 4.2).
3. It is required that the categorization of processes and events is compatible with the use of categories during the screening of processes and events (NRC 2000 [149372], Section 4.2).
4. Categories of processes and events that are not credible for the repository because of waste characteristics, repository design, or site characteristics are require to be identified and sufficient justification is to be provided for those conclusions (NRC 2000 [149372], Section 4.2).

5. It is required that the probability assigned to each category of processes and events not screened based on above criteria is consistent with site information, well documented, and appropriately considers uncertainty (NRC 2000 [149372], Section 4.2).
6. It is required that Processes and events that are screened from the TSPA on the basis of their probability of occurrence have been demonstrated to have a probability of less than one chance in 10,000 of occurring over 10,000 years (NRC 2000 [149372], Section 4.2).
7. It is required that categories of processes and events omitted from the TSPA on the basis that their omission does not significantly change the calculated expected annual dose have been demonstrated to cause no significant change in the calculated expected annual dose (NRC 2000 [149372], Section 4.2).
8. It is required that adequate documentation be provided that identifies: (i) whether processes and events have been addressed through consequence model abstraction or scenario analysis and (ii) how the remaining categories of processes and events have been combined into scenario classes (NRC 2000 [149372], Section 4.2).
9. It is required that the set of scenario classes is mutually exclusive and complete (NRC 2000 [149372], Section 4.2).
10. It is required that scenario classes that are not credible for the repository because of waste characteristics, repository design, or site characteristics (individually or in combination) are identified and sufficient justification is provided for those conclusions (NRC 2000 [149372], Section 4.2).
11. The probability assigned to each scenario class is required to be consistent with site information, well documented, and appropriately considers uncertainty (NRC 2000 [149372], Section 4.2).
12. Scenario classes that combine categories of processes and events may be screened from the TSPA on the basis of their probability of occurrence, provided: (i) the probability used for screening the scenario class is defined from combinations of initiating processes and events and (ii) they have been demonstrated to have a probability of less than one chance in 10,000 of occurring over 10,000 years (NRC 2000 [149372], Section 4.2).
13. Scenario classes may be omitted from the PA on the basis that their omission would not significantly change the calculated expected annual dose, provided DOE has demonstrated that excluded categories of processes and events would not significantly change the calculated expected annual dose (NRC 2000 [149372], Section 4.2).

4.2.1.4 Acceptance Criteria for Model Abstraction

1. **Data and Model Justification:** It is required that sufficient data (field, laboratory, or natural analog data) are available to adequately support the conceptual models, assumptions, and boundary conditions and to define all relevant parameters implemented in the TSPA. Where adequate data do not exist, other information sources such as expert elicitation have been appropriately incorporated into the TSPA (NRC 2000 [149372], Section 4.3).
2. **Data Uncertainty:** It is required that parameter values, assumed ranges, probability distributions, and bounding assumptions used in the TSPA are technically defensible and reasonably account for uncertainties and variability (NRC 2000 [149372], Section 4.3).
3. **Model Uncertainty:** It is required that alternative modeling approaches consistent with available data and current scientific understanding are investigated and results and limitations appropriately considered in the abstractions (NRC 2000 [149372], Section 4.3).
4. **Model Support:** Models implemented in the TSPA are required to provide results consistent with output of detailed process models or empirical observations (laboratory testing, natural analogs, or both) (NRC 2000 [149372], Section 4.3).
5. **Integration:** Is required that the TSPA adequately incorporate important design features, physical phenomena, and couplings and uses consistent and appropriate assumptions throughout the abstraction process (NRC 2000 [149372], Section 4.3).

4.2.1.5 Acceptance Criteria for Demonstration of the Overall Performance Objective

No acceptance criteria associated with the calculation of the overall performance objective have been included in the TSPA&I IRSR (NRC 2000 [149372], Section 4.4). In the absence of such acceptance criteria, the expected annual dose to the average member of the critical group can be calculated using an approach provided in the TSPA&I IRSR for informational purposes.

4.3 CODES AND STANDARDS

This AMR was prepared to comply with the DOE interim guidance (Dyer 1999 [105655]) which directs the use of specified Subparts/Sections of the proposed NRC high-level waste rule, 10 CFR Part 63 (64 FR 8640 [101680]). Subparts of this proposed rule that are applicable to data include Subpart B, Section 15 (Site Characterization) and Subpart E, Section 114 (Requirements For Performance Assessment). The subpart applicable to models is also outlined in Subpart E Section 114.

5. ASSUMPTIONS

5.1 INTRODUCTION

This section presents two distinct sets of assumptions. One set are those that were used to create the TSPA-SR model from the component models. These assumptions are given in Section 5.2. The second set presented are those that were used by the analysts who created each of the component models that are used in the TSPA-SR model. These assumptions are given for background information, and they are listed in Section 5.3.

5.2 TSPA-SR MODEL ASSUMPTIONS

The assumptions given in this section were required to develop the TSPA-SR model and to use the available information as input to the model.

1. *The waste form temperature was assumed to be the same as the waste package surface temperature.* Basis: The content of the waste package is used to determine the waste package surface temperature, and so this surface temperature should be close to the waste form temperature. Potential differences between the surface temperature of the waste package and the temperature of the waste form are insignificant compared to the sensitivity of the TSPA-SR model to temperature. This assumption is used in Section 6.3.4.
2. *In current TSPA-SR simulations, all the fracture surface retardation factors are set to 1.0 (no fracture surface retardation).* Basis: Because few data are available on fracture surface retardation factors, no fracture surface retardation is simulated in TSPA-SR. This is conservative because it overestimates the release rate to the critical group. This assumption is used in Section 6.3.6.
3. *For times beyond 100,000 years, period 3 in drift chemistry conditions are assumed.* Basis: For in-drift chemistry, given that data beyond 100,000 years does not exist, it is believed that the transitional chemistry state (Period 3) would be reasonably conservative to use for times beyond 100,000 years. This assumption is used in Section 6.3.2.2.
4. *Secular equilibrium is assumed for parent nuclides that had a considerably longer half-life than their decay products.* Basis: The decay product's mass, determined by its half-life, increases exponentially while no significant decrease in the quantity of mass of the parent occurs for an extended period of time. The ratio of parent mass to decay product mass approaches a constant value and the rate of decay of the daughter becomes equal to that of its parent. This condition is known as secular equilibrium and was assumed for ^{227}Ac with ^{231}Pa , for ^{210}Pb with ^{226}Ra , for ^{226}Ra with ^{230}Th and for ^{228}Ra with ^{232}Th . This assumption is used in Section 6.3.4.1.
5. *The entire surface of both the HLW and the DSNF waste forms are exposed to the near-field environment and completely covered by a thin film of water as soon as the waste package breaches.* Basis: This is conservative in that the entire waste form surface is covered with a water film capable of degrading the waste form. The entire

waste form surface is available for dissolution rather than just the area around the package breach. This assumption is used in Section 6.3.4.4.

6. *The dissolution rate of DSNF is a constant value that results in the complete dissolution of the fuel in a single time step.* Basis: This assumption releases the entire DSNF inventory in the package as soon as the package is breached, and is therefore conservative. This assumption is used in Section 6.3.4.4.
7. *Daughter products of ^{242}Pu , ^{240}Pu , and ^{239}Pu are ignored when modeling colloidal radionuclides.* Basis: For irreversible colloids of ^{242}Pu , ^{240}Pu , and ^{239}Pu , the combined dose of the daughters and granddaughters within the colloid is several orders of magnitude less than the dose of the parent during the travel time within the natural barriers. (This assumes the travel time is about 75,000 years or less for irreversible colloids.) This assumption is used in Section 6.3.4.6.
8. *Irreversible colloid species ^{241}Am and ^{238}Pu are each decayed to a daughter (^{237}Np and ^{234}U , respectively) that is irreversibly bound within the colloid.* Basis: This assumption results in the transport of the daughter products with the colloidal material and is conservative. This assumption is used in Section 6.3.4.6.
9. *Irreversible colloid species ^{243}Am is decayed to ^{239}Pu , but the daughters of irreversible colloid species ^{239}Pu are neglected.* Basis: The combined dose of daughters and granddaughters within the colloid is negligible compared to the ^{239}Pu dose, as discussed in Assumption 26 of this section. This assumption is used in Section 6.3.4.6.
10. *The volume of water in the waste form cell is $1.0 \times 10^{-6} \text{ m}^3$ when the calculated value (Vol_watera) is less than or equal to zero.* Basis: At times prior to waste package breach the volume of water in the waste form cell is not calculated, i.e., its value is zero. Due to limitations of GoldSim code and artifacts of how the radionuclide transport calculations are solved, the model will produce a divide by zero error and end its simulation prematurely if the volume of the waste form cell is allowed to be zero or less. To prevent this from happening and arbitrarily small number, $1.0 \times 10^{-6} \text{ m}^3$ was selected for the volume of the cell at times when there is no valid calculated value. There is no impact of this number on any of the results. This assumption is used in Section 6.3.5.
11. *The volume of water in the collector and EBS_Bin_Out cells is $1.0 \times 10^{-6} \text{ m}^3$. Flux out of these cells is $1.0 \times 10^5 \text{ m}^3/\text{yr}$.* Basis: Computationally, this assumption creates a swept away boundary with minimal radionuclide concentration and effectively no residence time in the cell. This assumption is conservative due to the fact the volume of water in the cell is so small that at the assumed flux of $1.0 \times 10^5 \text{ m}^3/\text{yr}$ the entire volume of the cell would be replaced every 3.15576×10^{-4} seconds or 1.0×10^{11} times a year. Physically, this is unrealistic and is only used as a method to pass a combined advective and diffusive total mass flux from the EBS transport model to the UZ transport model without introducing any artificial delay due to the presence of the collector cell. This assumption is used in Section 6.3.5.

12. *For the human intrusion scenario, the intrusion occurs at 100 years.* Basis: There is no information to estimate the time at which there could be intrusion by waste package penetration without recognition by the drillers. An earlier intrusion time is assumed to produce larger doses since there has been less radioactive decay. This assumption is used in Section 6.3.9.3.
13. *The relative probability of intruding a CSNF package versus a CDSP package is proportional to the relative number of each type of waste package present in the repository.* Basis: The probability of intrusion is directly proportional to the relative horizontal areal dimensions. Since the two types of waste packages have approximately the same dimensions, the number of packages can be used as a surrogate to horizontal area. This assumption is used in Section 6.3.9.3.
14. *The penetrated waste package is assumed to reside in waste package infiltration bin 4.* Basis: Bin 4 is the most likely bin to contain the penetrated waste package (see Section 6.3.4.1, Table 6-31). Regardless of which bin the package is in, the TH properties which depend on the bin number have very little effect of the model results. This assumption is used in Section 6.3.9.3.
15. *The penetrated waste package is assumed to reside in a "sometimes dripping" environment.* Basis: The seepage environment only affects the seepage model. For human intrusion, borehole seepage is used instead of the seepage model. This assumption is used in Section 6.3.9.3.
16. *The intrusion borehole has a diameter of 20.3 cm (8 in) and a corresponding cross-sectional area of 0.0324 m².* Basis: This is the diameter of a typical water well in the Yucca Mountain region (Edward E. Johnson, Inc. 1966 [153112], p. 161). This assumption is used in Section 6.3.9.3.
17. *The distribution of borehole infiltration rates can be represented by the predicted distribution of infiltration in the Yucca Mountain region for the glacial transition climate.* Basis: Since it is the wettest of the three climate states, the distribution of infiltration for the glacial transition climate provides the most conservative estimate of infiltration and is the climate that is assumed to be in effect for the majority of the human intrusion simulation. This assumption is used in Section 6.3.9.3.
18. *All of the cladding in the penetrated waste package is assumed to be perforated during the drilling event.* Basis: This is a reasonable, conservative assumption (i.e., cladding cannot unzip until it is perforated). Typically, unzipping is not limited by unperforated cladding anyway, so this assumption should have little effect. This assumption is used in Section 6.3.9.3.
19. *The sorption in the rubblized borehole is represented by the K_d values for the devitrified units of the UZ.* Basis: Devitrified rock properties were assumed to be more representative of the rubblized rock in the borehole than vitric or zeolitic rock properties. Devitrified rock has lower sorption properties. Consequently this

assumption results in a higher estimated dose than would occur using vitric or zeolitic properties. This assumption is used in Section 6.3.9.3.

20. *The properties of the rubblized borehole (porosity, fluid saturation, and dispersivity) are represented by the matrix properties of a UZ fault.* Basis: The regulations suggest that the borehole provide a pathway no more severe than a ground water flow path (Dyer 1999 [105655], Section 113(d)). Fault properties are conservatively assumed because a fault is the fastest pathway in the UZ. This assumption is used in Section 6.3.9.3.
21. *The length of the borehole from the repository to the SZ is 190 m.* Basis: The water table is highest during the glacial transition climate, and this therefore provides the shortest borehole length between the repository and the SZ. This assumption is used in Section 6.3.9.3.
22. *The borehole is assumed to intersect the SZ in either region 1 or region 3.* Basis: The only two SZ source regions that underlie the repository footprint are regions 1 and 3. They each underlie approximately 50 percent of the footprint (see Section 6.3.6.3, Figure 6-163). This assumption is used in Section 6.3.9.3.
23. *The relative humidity threshold for initiation of glass dissolution is assumed to be 5 percent.* Basis: a) It is conservative because the dissolution is implemented to start once the relative humidity gets above 5 percent instead of 80 percent as assumed in the DHLW Glass Degradation AMR. b) To avoid sudden sharp variation in calculated dissolution rates when humidity becomes greater than 80 percent, which gets propagated in the model and causes instability (in other words, a gradual increase in glass dissolution is implemented here).
24. *^{238}U is used to determine the fraction of the waste form that has been exposed to form a rind.* Basis: ^{238}U has a long half-life (~4.5 billion years) and does not appreciably decay during the proposed repository operating period. Hence the exposed mass of ^{238}U can be considered to represent the amount of mass exposed for the entire waste form inventory initially present.
25. *Saturation of rind is always assumed to be one (that is fully saturated).* Basis: To conservatively calculate the maximum volume of water in the waste package per waste form cell. This also simplifies the volume calculations as uncertainties related to saturation and matric potential are avoided.

5.3 ASSUMPTIONS FROM INPUTS TO THE TSPA-SR MODEL

The component models that compose the TSPA-SR model explicitly include assumptions that are used to create these component models and/or their input data. The following subsections list the assumptions given in each of the component model AMRs. They are provided here as background information. For greater detail on any of these assumptions, including the basis, the source document should be consulted.

5.3.1 Unsaturated Zone Flow

Climate

The assumptions listed below are given in the AMR *Future Climate Analysis* (USGS 2000 [136368], Section 5). Refer to that AMR for additional information. These assumptions are used in Section 6.3.1.1.

1. *"Climate is cyclical, so past climates provide insight into potential future climates."*
2. *"A relation exists between the timing of long-term past climate change (the glacial/interglacial cycles) and the timing of changes in certain earth-orbital parameters. This establishes a millennial-scale climate-change clock, which provides a possible way to time future climate change."*
3. *"A relation exists between the characteristics of past climates and the sequence of those climates in the long, approximately 400,000-year, earth-orbital cycle."*
4. *"Long-term earth-based climate forcing functions, primarily tectonics, that operate on the million-year time scale have remained relatively unchanged during the last long earth climate cycle, and will remain relatively unchanged during the next 10,000 years. Consequently, the potential and unpredictable impact of long-term earth-based forcing functions on climate need not be considered for understanding climate change during the past 400,000 years or the next 10,000 years."*

Infiltration

The assumptions listed below are given in the AMR *Analysis of Infiltration Uncertainty* (CRWMS M&O 2000 [143244], Section 5). Refer to that AMR for additional information. These assumptions are used in Section 6.3.1.1.

1. *The sampled parameters are predominantly linear scaling factors, and are assumed to vary uniformly over the set of realizations independent of location.*
2. *"[A]ll watersheds have the same relative variability in their associated climatic, geological, and hydrological properties."*
3. *A spatially averaged infiltration rate is a reasonable approximation of infiltration rate in a subregion of a watershed.*
4. *Sampled input parameters vary independently.*
5. *The low and high values in normal and lognormal distributions for Latin Hypercube Sampling are the 1.0 and 99.0 percentiles, respectively.*
6. *"The glacial transition climate was chosen for estimation of the weighting factors as derived for the lower, middle, and upper bound infiltration rate maps because of the duration of this climate regime."*

Seepage into Drifts

The assumptions listed below are given in the AMR *Abstraction of Drift Seepage* (CRWMS M&O 2000 [142004], Section 5). Refer to that AMR for additional information. These assumptions are used in Section 6.3.1.2.

1. *"Seepage can be treated as a random process."*
2. *"The extent of flow focusing can be estimated using the active-fracture model."*
3. *"Effects of episodic flow on seepage can be neglected."*
4. *"Thermal-mechanical and thermal-chemical effects on seepage can be neglected."*
5. *"Seepage for non-convergent simulations can be bounded by 100 percent of the flow above a drift segment."*
6. *The standard deviation of $\log(\bar{k}/\alpha)$ (where \bar{k} is the geometric average of the permeability field in the seepage model and α is the van Genuchten α parameter for fractures) can be approximated by the standard deviation of $\log(\bar{k})$.*
7. *"Seepage is increased by 55 percent to account for the effects of drift degradation and rock bolts, and by another 10 percent to account for possible effects of correlation between α and k ."*

Mountain-Scale Unsaturated Zone Flow

The assumptions listed below are given in the AMR *Analysis of Base-Case Particle Tracking Results of the Base-Case Flow Fields* (CRWMS M&O 2000 [134732], Section 5). Refer to that AMR for additional information. These assumptions are used in Section 6.3.1.3.

1. *"We assume deterministic transport property values for two radionuclides in this analysis."*
2. *The flow field inputs for Analysis of Base-Case Particle Tracking Results of the Base-Case Flow Fields (DTN: SN9910T0581699.002 [126110]) represent the unsaturated flow system at Yucca Mountain.*
3. *"The number of particles used in both FEHM and DCPT [Dual Continuum Particle Tracker] is adequate to represent the probabilistic distributions of particle movement."*

The assumptions listed below are given in the AMR *UZ Flow Models and Submodels* (CRWMS M&O 1999 [122797], Section 5). Refer to that AMR for additional information. These assumptions are used in Section 6.3.1.3.

1. *"The water table is used as the bottom model boundary which is subject to constant water pressure (equal to the atmospherical pressure)."*

2. *"The bottom model boundary representing the water table is subject to fixed gas pressure."*
3. *"The bottom model boundary representing the water table is subject to spatially varying but constant temperature conditions."*
4. *"For simulations of barometric pumping, the bottom model boundary representing the water table is assumed to be a no-flow boundary."*
5. *"The lateral boundaries of the model domain are subject to no-flow boundary conditions."*
6. *"Perched water occurrence results from permeability barrier effects."*
7. *"Under steady flow conditions, moisture flow and tracer transport processes can be decoupled."*
8. *"Water flow through the UZ is assumed to occur under steady-state conditions."*
9. *"The dual-permeability formulation is assumed to be appropriate for simulating flow and transport through fractured tuffs."*
10. *"The time required for moisture conditions within the UZ to adjust to changes in the spatial and temporal distribution of net infiltration at land surface induced by climatic change is assumed to be short compared to the time over which climatic conditions change so that simulated conditions within the UZ reflect the present-day and estimated future net-infiltration rates imposed on the upper land-surface boundary of the UZ model."*
11. *"Regarding calcite deposition in the unsaturated zone, the following assumptions are made: (a) the gas phase is at a constant (atmospheric) pressure, and air flow is neglected for the purpose of solving water flow; (b) a constant infiltration rate and water chemistry over the entire simulation period is applied to the top boundary; (c) steady-state water flow condition remains during chemical transport and fluid-rock interactions."*

5.3.2 Near Field Environment

Thermohydrology

The assumptions listed below are given in the AMR *Abstraction of NFE Drift Thermodynamic Environment and Percolation Flux* (CRWMS M&O 2000 [149860], Section 5). Refer to that AMR for additional information. These assumptions are used in Section 6.3.2.1.

1. *The same infiltration rate bin definitions are applied to each of the three infiltration rate cases (low, mean, and high) considered in the multiscale TH model.*

2. *The five binning ranges selected apply to the glacial transition period of the future climate state.*
3. *It is assumed that the evaporation rates given in kg/yr can be converted to volume flow rates using a constant water density of 1000 kg/m³.*

In-drift Geochemical Environment

The assumptions listed below are given in the AMR *In-Drift Precipitates/Salts Analysis* (CRWMS M&O 2000 [127818], Section 5). Refer to that AMR for additional information. These assumptions are used in Section 6.3.2.2.

1. *Water is in the standard state.*
2. *Redox conditions within the drift are oxidizing at all times.*
3. *The model for in-drift precipitates and salts assumes equilibrium chemical conditions.*
4. *"The precipitates/salts model uses an approximation that [relative humidity (RH)] rises to 50 percent at about 200 years and up to 85 percent at about 1100 years."*
5. *"[R]elative humidity rises from 50 percent to 85 percent linearly with the logarithm of time."*
6. *The PT4 database for EQ3/6 was developed using assumptions analogous to those used in expanding the Pitzer model to cement pore water.*
7. *To develop the PT4 database from the PIT database, aqueous species from the HMW database were added using the Pitzer coefficients from the HMW database.*
8. *Species from the cement pore water extension of the Pitzer model were added to the PT4 database using the same binary and mixing coefficients developed for that work.*
9. *Unknown temperature derivatives of the cation-anion parameters were estimated by using a median of the known values.*
10. *Equilibrium constants calculated from Gibbs free energies for certain minerals are assumed not to threaten database consistency.*
11. *"Minerals that would likely either form very slowly or not form at all under the expected conditions within the drift are prevented from precipitating in the model when their saturation indices exceed zero."*
12. *"The [low relative humidity (LRH)] salts model assumes a constant seepage rate (Qs) and constant seepage composition."*
13. *"The dissolved solids in the seepage composition are restricted to Na, K, NO₃, SO₄, Cl, and CO₃."*

14. "[N]itrate salts accumulate until the RH in the reactor rises to 50 percent."
15. The mole fraction of salts (other than nitrate salts) dissolved in the LRH model increases exponentially from zero to one over time as RH increases from 50 percent to 85 percent.
16. The mass of water in the brine is determined from the moles of salt dissolved and the effective solubility of each salt species.
17. The effective solubility for nitrate salts is assumed to be 24.4 molal; the effective solubility for all other salts is assumed to be 3 to 4 molal.
18. "[T]he carbonate in the LRH salts model is assumed to be 'soluble' carbonate."
19. "To achieve the 0.85 activity of water endpoint, the carbonate concentration in the incoming seepage is adjusted to achieve a Na:CO₃ ratio equivalent to the ratio of the EQ3/6 model results at 0.85 activity of water."
20. "Na concentrations and moles in each phase and at each time increment are calculated by charge balance in the LRH salts model in a manner that maintains any original charge imbalance."
21. The valence of carbonate is between 1 and 2 and depends on the pH calculated by the EQ3/6 Pitzer model.
22. In the condensed water model, water composition is predicted by the equilibrium between pure water and the fugacity of CO₂ at a given temperature.

The assumptions listed below are given in the calculation document *Precipitates/Salts Model Results for THC Abstraction* (CRWMS M&O 2000 [151708], Section 3). Refer to that calculation for additional information. These assumptions are used in Section 6.3.2.2.

1. The predicted mean RH [relative humidity] history within the invert is a reasonable approximation for the LRH [low relative humidity] model simulations. This assumption replaces assumption 4 above.
2. "[T]he concentration ratio of nitrate to chloride in the THC-abstracted incoming seepage water is equivalent to that in average J-13 well water."
3. "[B]oth the incoming carbonate and sulfate concentrations used in the LRH model are assumed to be the soluble carbonate and sulfate concentrations determined by the HRH [high relative humidity] model at a water activity of 0.85."

5.3.3 Waste Package Degradation

The assumptions listed below are given in the AMR WAPDEG *Analysis of Waste Package and Drip Shield Degradation* (CRWMS M&O 2000 [151566], Section 5). Refer to that AMR for additional information. These assumptions are used in Section 6.3.3.

1. *The drip shield is approximated by 3 parallelepipeds with a total surface area of 3.607×10^7 mm² and a thickness of 15 mm.*
2. *"The variability in drip shield degradation is adequately characterized by modeling 400 waste package/drip shield pairs with 500 patches per drip shield."*
3. *The waste package is assumed to be the "Single CRM 21-PWR Waste Package" with an outer surface area of 2.346×10^7 mm².*
4. *"The variability in waste package outer barrier degradation is adequately characterized by modeling 400 waste package/drip shield pairs with 938 patches per waste package."*
5. *Alloy 22 is used as weld filler material for the Alloy 22 waste package outer barrier lid welds.*
6. *The stainless steel waste package inner layer is not included in the analysis.*
7. *Critical threshold RH and exposure temperature are related based on the assumption of a NaNO₃ salt film on waste package and drip shield surfaces.*
8. *Localized corrosion is not possible on the titanium grade 7 drip shield under all expected repository conditions.*
9. *Unqualified data for localized corrosion rates of titanium grade 7 can be used for the WAPDEG models.*
10. *Initiation criteria and localized corrosion models for Alloy 22 are included in the WAPDEG analysis.*
11. *Localized corrosion of the waste package outer barrier is assumed to initiate only under dripping conditions.*
12. *Drips resulting from condensation on the underside of the drip shield (if they occur) do not initiate localized corrosion.*
13. *Localized corrosion rates for Alloy 22 are log uniformly distributed.*
14. *The unqualified data for Alloy 22 localized corrosion can be used in the WAPDEG analyses.*

15. *Only surface-breaking defects are considered in crack penetration of the waste package closure lid welds.*
16. *"Only the closure lid weld of the waste package develops residual stresses high enough to cause stress corrosion cracking."*
17. *Defects are distributed randomly over space as represented by a Poisson process with a mean flaw density of 0.6839 flaws/meter (DTN: MO9910SPAFWPWF.001 [144565]) for the closure lid welds.*
18. *The fraction of surface-breaking flaws is a uniform distribution between the minimum and maximum fractions used to determine the average fraction.*
19. *Pre-inspection flaw sizes are log normally distributed with distribution parameters (dependent on weld thickness) given in Section 6.2.1 of Analysis of Mechanisms for Early Waste Package Failure.*
20. *The probability of non-detection is given as a function of flaw size.*
21. *All detected flaws are acceptably repaired or removed, and need not be considered in the failure analysis.*
22. *All fabrication welds other than closure lid welds are immune from stress corrosion cracking (SCC).*
23. *The hoop stress is the prevailing stress in closure lid welds that fail by SCC.*
24. *"The hoop stress and corresponding stress intensity factor profiles in the outer barrier inner lid welds from the process-level analysis are for a plane that is inclined at an angle of 37.5° with the outer surface of the outer barrier inner lid."*
25. *"The hoop stress and corresponding stress intensity factor profiles as a function of depth in the closure-lid welds from the process-level analyses represent the mean profiles."*
26. *The same degree of profile variability in hoop stress profiles and stress intensity factor profiles is applied equally to all waste packages in the repository. There is no variability between waste packages.*
27. *Re-distribution of stress and its mitigation of SCC initiation and crack propagation are not considered.*
28. *Manufacturing defect and incipient crack analyses are assumed applicable to closure lid welds that have undergone stress mitigation processes.*
29. *All incipient cracks are analyzed at the maximum size (0.05 mm) rather than allowing crack size variability.*

30. *The drip shield is not subject to SCC or microbiologically influenced corrosion (MIC).*
31. *Stress corrosion cracking of the closure lid welds can initiate as soon as the RH threshold is met.*
32. *The waste package can undergo MIC when RH is above 90 percent. Further, this corrosion is represented by a corrosion enhancement factor that varies between waste packages and varies between patches via a uniform distribution from 1 to 2.*
33. *The drip shield is immune to long-term aging, phase instability, and hydrogen induced cracking under expected repository conditions.*
34. *Thermal aging and phase instability effects on corrosion of the waste package outer barrier is represented by a general corrosion enhancement factor which varies uniformly from 1 to 2.5. This variation is both between waste packages and between patches on a given waste package.*
35. *The drip shield and the waste package outer barrier are not subject to radiolysis-enhanced corrosion under expected repository conditions.*

5.3.4 Waste Form Degradation And Mobilization

Radionuclide Inventory

The assumptions listed below are given in the *AMR Inventory Abstraction* (CRWMS M&O 2000 [136383], Section 5). Refer to that AMR for additional information. All of these assumptions are used in Section 6.3.4.1.

1. *"The time at which an exposure may occur is unknown."*
2. *"All waste forms disposed in the repository could contribute to the dose."*
3. *"Inhalation and ingestion exposure pathways could contribute to the dose."*
4. *"Even radionuclides that are traditionally treated as insoluble could find a migration pathway to the accessible environment."*
5. *"The dominant groundwater transport mechanism for radionuclide movements is unknown."*
6. *"Any radionuclide with a half-life less than twenty years will not contribute significantly to the dose for post-closure scenarios."*
7. *"A dose cut-off of 95 percent is adequate for the TSPA-SR."*

In-Package Chemistry

The assumptions listed below are given in the AMR *In-Package Chemistry Abstraction* (CRWMS M&O 2000 [129287], Section 5). Refer to that AMR for additional information. These assumptions are used in Section 6.3.4.2.

1. *System pH is a valid indicator of changes in system chemistry.*
2. *At some maximum value (determined by linear extrapolation) of flux, the pH of solution exiting the waste package will equal the pH of the J-13 well water (i.e., the solution entering the waste packages).*
3. *The time frame used is with regard to the time that a waste package first breaches.*
4. *The dissolution rate of the CSNF increases proportionally with hydrogen ion activity.*
5. *The dissolution rate of the CDSP increases when pH is above or below 7.*

Cladding Degradation Model

The first sixteen assumptions listed below are given in the AMR *Clad Degradation – Summary and Abstraction* (CRWMS M&O 2000 [147210], Section 5). The final assumption is from *Initial Cladding Condition* (CRWMS M&O 2000 [136045], Section 5). Refer to those AMRs for additional information. These assumptions are used in Section 6.3.4.3.

1. *Waste packages are loaded with spent fuel in the order of discharge from reactors as a function of calendar years.*
2. *Each failed Pressurized Water Reactor (PWR) fuel assembly has an average of 221 total rods and 2.2 failed rods initially.*
3. *All rods are exposed to dry storage at 350 °C for three weeks during shipping.*
4. *Four (4) is the uncertainty value for rod failure data.*
5. *BWR cladding degrades in a similar manner to PWR cladding.*
6. *Cladding degradation does not occur at the YMP surface facility.*
7. *Murty's correlation is used to analyze creep.*
8. *Creep failure distribution is determined experimentally.*
9. *Stress corrosion cracking fails any rod with stress exceeding 180 MPa.*

10. *Localized corrosion is fluoride limited and based on the amount of fluoride required to completely degrade a 10 mm length of cladding from the fuel rod. Further, all fuel rods are subject to fluoride corrosion and available fluoride is partitioned so that the maximum number of fuel rods are subject to the complete degradation of a 10 mm length.*
11. *A seismic event fails all cladding the center of the rod.*
12. *The absolute rate of fast release from a breached fuel rod is proportional to the length of the rod.*
13. *"Fuel reacts with water to form metaschoepite."*
15. *"[The reaction rate] of uranium dioxide with water is limited by the intrinsic dissolution rate of UO_2 ."*
16. *Cladding perforation occurs in the center of a fuel rod and propagates in both directions to the ends of the rod.*
17. *Stainless steel clad fuel is loaded into waste packages as it is received.*
18. *Commercial nuclear fuel with stainless steel cladding is considered as a separate type of clad fuel.*

Dissolution Rate Model

The assumptions listed below are given in the AMR *Defense High Level Waste Glass Degradation* (CRWMS M&O 2000 [143420], Section 5). Refer to that AMR for additional information. These assumptions are used in Section 6.3.4.4.

1. *"The dissolution rate of the glass provides an upper bound to the release rates of the radionuclides."*
2. *"The form of the rate expression for glass dissolution is adequate for calculating the glass dissolution rate."*
3. *"The dependence of the glass dissolution rate on pH and temperature is assumed to be the same for all waste glass compositions."*
4. *The influence of inclusion phases on dissolution are accounted for in the model parameter values.*
5. *The same rate expression can be used for all aqueous corrosion, including glass dissolution in humid air and in dripping water.*
6. *"The temperature dependence for glass degradation in humid air and in dripping water follows Arrhenius behavior."*

7. *"The glass corrosion rate is nil when glass is exposed to humid air at less than 80 percent relative humidity."*
8. *"Glass dissolution behavior upon contact by humid air or dripping water is a special case of aqueous corrosion at very high glass surface area/solution volume (S/V) ratios."*

Dissolved Concentration Limits

The assumptions listed below are given in the AMR *Summary of Dissolved Concentration Limits* (CRWMS M&O 2000 [143569], Section 5). Refer to that AMR for additional information. These assumptions are used in Section 6.3.4.5.

1. *There is no direct interaction between radioactive elements and either Cr or Ni.*
2. *Amorphous solids are the default solubility-controlling solids for radioactive elements which have no experimental identification of the actual controlling solids in the waste form.*
3. *There are no solubility-controlling solids for Tc, C, I, Cl, Cs, or Sr under the repository conditions and their solubility limits are arbitrarily set to 1mol/L as a conservative upper bound.*
4. *Schoepite is the solubility-controlling mineral for U.*
5. *$\text{Pu}(\text{OH})_4(\text{am})$ is the solubility-controlling mineral for Pu.*

Colloids

The assumptions listed below are given in the AMR *Waste Form Colloid-Associated Concentration Limits: Abstraction and Summary* (CRWMS M&O 2000 [125156], Section 5). Refer to that AMR for additional information. All of these assumptions are used in Section 6.3.4.6.

1. *All waste form colloids are assumed to be smectite or irreversibly bound to smectite.*
2. *All metal oxides and hydroxides are iron (hydr)oxides.*
3. *"Smectite colloids may form from spallation of altered phases from HLW as well as precipitation from solution."*
4. *"SNF produces colloids less readily under experimental conditions approximating repository conditions [because of the alteration mechanisms which operate on the SNF]."*
5. *Spent nuclear fuel (SNF) is a generic waste form that considers both DOE-SNF and commercial SNF.*

6. *A single GoldSim mixing cell represents waste form degradation in the TSPA-SR model. The processes adhere to the in-package geochemistry models and abstractions.*
7. *"The stability of smectite colloids will depend to varying degrees on their concentration and the composition, ionic strength, and pH of the solution."*
8. *Smectite stability is more pH sensitive at lower values of pH than at higher values of pH.*
9. *Am is assumed to mobilize from waste and form irreversible associations with smectite colloids and HLW clay layers in the same manner as Pu.*
10. *Colloidal smectite and iron (hydr)oxides have well-known properties that are applicable to the radionuclide-bearing colloids.*
11. *Iron (hydr)oxide colloid stability and concentration depend on the pH and ionic strength of the environment.*
12. *Waste form colloids formed at 90 °C are stable at 25 °C.*
13. *Some radionuclides released by waste form degradation are aqueous and available to sorb onto colloidal material, forming pseudocolloids.*
14. *"Smectite colloids contain entrained radionuclide-bearing phases; further, all discrete radionuclide-bearing colloid-sized phases (besides smectite) are entrained in the smectite colloids."*
15. *"Smectite colloids with or without entrained radionuclide-bearing phases may have adsorbed dissolved radionuclides."*
16. *"Pu, Am, Th, Pa, Cs, and Sr are assumed to be the most significant radionuclides available for colloids association; data indicate that smectite colloids may contain Pu, Am, Th, U, Cm, Np, and rare earth elements (REEs)." Pu is also shown to behave similarly to Th, Am, and REEs.*
17. *All radionuclide associations with colloids is irreversible in the waste package environment except for dissolved radionuclide-pseudocolloid associations.*
18. *Adsorption-desorption rates in pseudocolloid formation are based on experimentally determined rates for Am and Pu. The effective K_d incorporates both the adsorption and desorption rates.*
19. *"Desorption of Pu and Am from pseudocolloids is assumed to be slow relative to transport rates within the waste package."*
20. *Physical filtration of colloids is not considered.*

21. *Colloid sorption at the air-water interface within the waste package is not considered.*
22. *Gravitational settling of colloids within the waste package is not considered.*
23. *Colloid diffusion within the waste package is not considered.*
24. *Contaminant-microbe and contaminant-organic (where organic refers to such material as humic and fulvic acids) interactions are not considered.*
25. *"All stable colloids are assumed to leave the waste package through [a] failure opening."*

5.3.5 Engineered Barrier System Transport

The assumptions listed below are given in the AMR *EBS Radionuclide Transport Abstraction* (CRWMS M&O 2000 [129284], Sections 5 and 6.1.1). Refer to that AMR for additional information. All of these assumptions are used in Section 6.3.5.

1. *"Capillary fluxes are estimated assuming pressure equilibrium at the interface between the quartz sand backfill and the host rock."*
2. *"Condensation on the underside of the drip shield occurs when the temperature of the drip shield is less than the temperature of the invert."*
3. *"If condensation occurs, it is assumed that the condensation flux on the drip shield is equal to the evaporative flux in the invert."*
4. *"If condensation occurs, it is assumed that all the condensation flux drips from the crown of the drip shield onto the waste package."*
5. *"The advective flow (of water) in the backfill cannot reach the waste packages as long as the integrity of the drip shield is maintained."*
6. *"Once the integrity of the drip shield is compromised, backfill is assumed to fill the axial space surrounding the waste package."*
7. *"The total flux into the quartz sand [backfill] is equal to the sum of the seepage flux and the capillary flux multiplied by a factor between 0 and 1."*
8. *"Flow of water through the backfill is a quasi-steady [state] process in a homogeneous porous medium."*
9. *"The fluid flux through a patch or pit in the drip shield or waste package is proportional to the ratio of the length of the penetration in the axial direction to the total axial length of the drip shield or waste package. This assumption is equivalent to assuming that a patch or pit is always located on the side (90° from the crown) of the drip shield or waste package and that it can collect all fluid that flows from the crown towards the penetration if the axial locations of source and penetration coincide."*

10. *"Patch location on the upper or lower surface of the waste package is conservatively ignored. Similarly, the location of a stress corrosion crack (SCC) on the lid is conservatively ignored."*
11. *Patch area on the drip shield is $7.21 \times 10^4 \text{ mm}^2$ and patch area on the waste package is $2.346 \times 10^4 \text{ mm}^2$, and both are assumed to be square for the purposes of the flux splitting algorithm.*
12. *Diversion of flux around a breached drip shield or waste package is based on continuity of liquid flux. This assumption means that the sum of the diverted and penetrating flux is equal to the incident flux on either the waste package or the drip shield.*
13. *"[Stress corrosion cracks] through the welded lid are assumed to be in the radial direction."*
14. *"The width of the weld on the inner surface of the outer lid of the waste package is assumed to be 0.25 inches."*
15. *"The fluid flux onto the closure lid of the waste package is conservatively calculated assuming that the waste package is tilted at the maximum angle possible. This flux is given by the ratio of the projected length of the end cap in the axial direction to the projected length of the total waste package in the axial direction."*
16. *"All fluid that flows as a film on the closure lid of the waste package is assumed to flow through a SCC, if present."*
17. *"The potential for evaporation in and on the waste package is [conservatively] ignored."*
18. *"The stainless steel components of the waste package provide no resistance to corrosion or flow."*
19. *"Seismic damage to the waste package has been screened out because of low consequence to EBS performance."*
20. *Advective transport occurs only in the vertical direction (i.e., is one dimensional) and is always downward.*
21. *"There is no upward transport through the quartz sand backfill."*
22. *"The effects of longitudinal and transverse dispersion are ignored."*
23. *"The diffusion coefficient of all relevant radionuclides is bounded by the self-diffusion coefficient for water. [Further, the] diffusion coefficient for a radionuclide in a porous, partially saturated medium is given by the diffusion coefficient in water times the product of porosity and (liquid) saturation of the medium."*

24. *The sorption of radionuclides to stationary phases is ignored in the waste package and invert. The partition coefficients for all radionuclides are assumed to be zero.*
25. *"Radionuclide transport through a SCC [Stress Corrosion Crack] is limited to diffusive transport through a thin, continuous film that is always present."*
26. *"The invert is assumed to be adjacent to the waste package for diffusive release calculations."*
27. *"Adjacent drip shields can slip freely to relieve thermal stresses and seismic displacements."*
28. *"The maximum drip shield displacement from the 1-in-10,000-year earthquake is 250 mm."*
29. *"The sand backfill is effective in spreading the load from a rock fall."*
30. *"The impact of rock fall on the degraded drip shield has been screened out from Rev 00 of the TSPA-SR."*
31. *Flux that goes around the drip shield does not travel through the invert for EBS transport calculations.*

5.3.6 Unsaturated Zone Transport

The assumptions listed below are given in the AMR *Particle Tracking Model and Abstraction of Transport Processes* (CRWMS M&O 2000 [141418], Section 5). Refer to that AMR for additional information. These assumptions are used in Section 6.3.6.

1. *The cell-to-cell migration method of tracking particles developed for Particle Tracking Model and Abstraction of Transport Processes is sufficient for modeling purposes.*
2. *"Fracture frequency, aperture, and permeability are log-normally distributed."*
3. *"The cubic law is a valid approximation for gas permeability in fractured rock at Yucca Mountain."*
4. *"[The a]ctive fracture model appropriately accounts for reduced fracture/matrix interaction."*

The assumptions listed below are given in the AMR *Abstraction of Flow Fields for RIP* (CRWMS M&O 2000 [123913], Section 5). Refer to that AMR for additional information. These assumptions are used in Section 6.3.6.

1. *"The rock grain densities for perched water elements in 'pch1.rock' and 'pch2.rock' are conservatively assumed to be equal to the lowest rock grain density in the parameter set (2240 kg/m³)."*

2. *"Water table rise does not significantly affect liquid mass flow rates and transport above the water table."*
3. *"Mass sinks can be used below the prescribed water table in FEHM to signify locations where particles (radionuclides) leave the UZ and enter the SZ."*

The assumptions listed below are given in the AMR *Colloid-Associated Radionuclide Concentration Limits* (CRWMS M&O 2000 [147505], Section 5). Refer to that AMR for additional information. These assumptions are used in Section 6.3.6.

1. *"The measured waste form colloid characteristics (composition, size distribution, and rate of generation) are determined by the waste form and not the testing setup. Specifically, it was assumed that sorption of colloids onto the test vessel walls didn't effect the rate of colloid generation and that the sample holder configuration in the spent fuel (SF) tests does not effect the release of filterable material."*
2. *"The TEM [transmission electron microscopy] phase identification techniques provide data that are representative of waste form colloids."*
3. *"The filterable material (obtained from sequential filtration) is colloidal or particulate."*
4. *"Dynamic light scattering (DLS) provides an accurate representation of the size distribution of the waste form colloids."*
5. *"Ionic strength can be calculated from the major cations in solution."*
6. *"The normalized mass loss of B and Tc indicate the extent of glass and spent fuel corrosion, respectively."*

5.3.7 Saturated Zone Transport

Saturated Zone Transport Parameters

The assumptions listed below are given in the AMR *Input and Results of the Base Case Saturated Zone Flow and Transport Model for TSPA* (CRWMS M&O 2000 [139440], Section 5). Refer to that AMR for additional information. These assumptions are used in Section 6.3.7.1.

1. *"The interface between radionuclide transport in the UZ and the SZ is assumed to be a point source near the water table."*
2. *"The location of the point source of radionuclides for transport in the SZ site-scale flow and transport model is assumed to be randomly located within the four source regions defined at the water table."*
3. *"It is assumed that all radionuclide mass crossing the 20 km fence in the SZ is captured by pumping wells of the hypothetical farming community."*

4. *"The assumption is made that the average concentration of radionuclides in the groundwater supply of the hypothetical community is an appropriate estimate of radionuclide concentration for the calculation of radiological dose."*
5. *"Pumping of groundwater by the hypothetical farming community is assumed not to alter significantly the groundwater pathways or radionuclide travel times in the SZ."*
6. *"It is assumed that the uncertainty in groundwater flux in the volcanic aquifer near Yucca Mountain elicited from the SZ expert elicitation panel is applicable to the entire flowpath from the repository to the accessible environment."*
7. *"It is assumed that the potential anisotropy of permeability in the horizontal direction is adequately represented by a permeability tensor that is oriented in the north-south and east-west directions."*
8. *"The assumption is made that the horizontal anisotropy in permeability applies to the fractured and faulted volcanic units of the SZ system along the groundwater flowpath from the repository to the south and east of Yucca Mountain."*
9. *"It is assumed that potential anisotropy in permeability represents an alternative conceptual model of groundwater flow at the Yucca Mountain site."*
10. *"An assumption inherent to the convolution integral method is that the system being simulated exhibits a linear response to the input function."*
11. *"It is also assumed that the groundwater flow conditions in the SZ system are in steady state."*
12. *"It is assumed that the change in groundwater flow in the SZ from one climatic state to another occurs rapidly and is approximated by an instantaneous shift from one steady-state flow condition to another steady-state flow condition."*
13. *"Groundwater flow pathways in the SZ from beneath the repository to the accessible environment are assumed not to be significantly altered for wetter climatic states."*
14. *"The final radionuclide daughter product in three of the radionuclide decay chains simulated in the one-dimensional radionuclide transport model is assumed to be in secular equilibrium with its parent radionuclide."*
15. *"The groundwater flux within each one-dimensional 'pipe' segment used in the model is assumed to be constant along the length of the pipe."*
16. *The K_c equilibrium model, which combines radionuclide distribution coefficients and constant colloid mass concentration, will be used for the transport of radionuclides reversibly bound to colloids in unsaturated zone (UZ) and saturated zone (SZ) transport calculations.*

The assumptions listed below are given in the AMR *Uncertainty Distributions for Stochastic Parameters* (CRWMS M&O 2000 [147972], Section 5). Refer to that AMR for additional information. These assumptions are used in Section 6.3.7.

1. *Uniformly scaling the groundwater flux in the SZ site scale flow model adequately represents uncertainties in the saturated zone groundwater flow velocities.*
2. *"[T]he Hydrologic Framework Model is the basis for determining the uncertainty in the location of alluvium at the water table along the modeled flowpath."*
3. *"The uncertainty in the location of the contact between volcanic units and alluvium at the water table is uniformly distributed between the bounds placed on the possible location of the boundaries."*
4. *Uncertainty in effective porosity of alluvium can be represented with a truncated normal distribution with sampled values within the physical limits of porosity.*
5. *Porosity values from analogous geological deposits are valid for valley fill (unit 19) and undifferentiated alluvium (unit 7).*
6. *"Effective porosities are specified constants for the units that will not be in the transport pathway."*
7. *Units of the same basic rock type can be assigned the same descriptive values of physical attributes (such as bulk density, effective porosity, and matrix porosity) based on the values of a single referenced unit.*
8. *"Matrix Porosities are constant within hydrogeological units."*
9. *"Given a referenced matrix porosity value for one unit or group of units, other units of the same basic rock type can be assigned the same value (or average value)."*
10. *Boreholes are vertical.*
11. *"Not all fractured zones in the SZ transmit water."*
12. *"There is no correlation between flowing intervals and hydrogeological units."*
13. *"There is no correlation between flowing interval spacing and the dip angle of fractures."*
14. *"The fracture system can be represented as a series of parallel plates or intersecting parallel plates with characteristics equivalent to the mean fracture aperture, dip and frequency observed in core samples."*
15. *"Cores provide representative samples of the fracture system."*
16. *Fractures associated with the flowing intervals are sampled and measured.*

17. *"Specific yield represents the effective porosity."*
18. *"No flow occurred in the matrix porosity."*
19. *"Flowing interval thickness is known or conservatively estimated."*
20. *The size and charge of the ions considered could fall within wide ranges.*
21. *Laboratory scale diffusion experiments provide tortuosity values representative of field scale diffusion and bound the values of tortuosity found in the field due to matrix heterogeneity.*
22. *"Bulk densities are constant for the geologic units of concern."*
23. *"Given a referenced bulk density value for one unit or group of units, other units of the same basic rock type can be assigned the same value (or average value)."*
24. *The alluvium bulk density values are applicable to the SZ site-scale model.*
25. *Effective porosity values are valid substitutes for total porosity values in Equation 16 of Uncertainty Distributions for Stochastic Parameters.*
26. *The sorption model assumes a linear relationship between the aqueous phase and sorbed phase.*
27. *"[S]orption coefficients, K_d , can be grouped in terms three rock types and a grouping for and a grouping for iron oxides to represent the waste container."*
28. *"The waters from Wells J-13 and UE-25p#1 bound the chemistry of the groundwaters at Yucca Mountain."*
29. *Values obtained from the SZ expert elicitation for longitudinal dispersivity at 30 km are applicable at 20 km for TSPA-SR modeling purposes.*
30. *Dispersivity in volcanic and alluvial units are not differentiated.*
31. *There is a correlation between longitudinal and transverse dispersivity.*
32. *A permeability tensor oriented in the north-south and east-west directions adequately represents the potential anisotropy of permeability in the horizontal direction.*
33. *"[H]orizontal anisotropy in permeability applies to the fractured and faulted volcanic units of the SZ system along the groundwater flowpath from the repository to the south and east of Yucca Mountain."*
34. *"[P]otential anisotropy in permeability represents an alternative conceptual model of groundwater flow at the Yucca Mountain site."*

35. *Radionuclides that are irreversibly sorbed to colloids are embedded in the colloid and are part of the colloidal structure.*
36. *Matrix exclusion is assumed in the volcanic units.*
37. *Waste form colloids are representative of all the colloids in the groundwater.*
38. *Americium is representative of all the radionuclides with respect to transport via colloids.*
39. *The K_c parameter is determined adequately by the maximum colloid concentration.*
40. *A uniform distribution with a minimum of 0 and a maximum of 100 describes the K_d values for all actinides subject to colloidal transport.*
41. *"[P]hysical and chemical filtration have no retardation effect on transport by reversible colloids."*
42. *"[F]our source regions for radionuclide transport in the SZ are sufficient to represent the variability in transport pathways and characteristics of the SZ system."*

5.3.8 Biosphere

Biosphere Dose Conversion Factors

The first assumption listed below is given in the AMR *Abstraction of BDCF Distributions for Irrigation Periods* (CRWMS M&O 2000 [144054], Section 5). The last two assumptions listed below are given in the AMR *Distribution Fitting to the Stochastic BDCF Data* (CRWMS M&O 2000 [144055], Section 5). Refer to those AMRs for additional information. These assumptions are used in Section 6.3.8.1.

1. *The GENII-S model and the data fed to the model accurately and acceptably reflect the reference biosphere and the receptor, and the model is a valid calculation method for biosphere dose conversion factors.*
2. *"[T]he elementary statistical test known as the Chi Square (sometimes referred to as Chi Squared) test is adequate to demonstrate acceptable distribution fits to the stochastic BDCF data."*
3. *Soil build-up was considered in creating the radionuclide distributions only when the magnitude of the radionuclide build-up was greater than 15 percent.*

Annual Ground Water Usage

The assumptions listed below are given in the AMR *Groundwater Usage by the Proposed Farming Community* (CRWMS M&O 2000 [144056], Section 5). Refer to that AMR for additional information. These assumptions are used in Section 6.3.8.2.

1. *The predicted dose to the DOE/NRC specified receptor is proportional to the radionuclide concentration in water withdrawn from wells.*
2. *It is assumed that the hypothetical farming community located near Lathrop Wells has sufficient water usage to capture the entire contaminated plume.*
3. *The hypothetical farming community is based on the proposed Yucca Mountain rules and interim guidance from DOE, and not the actual population in nearby Amargosa Valley.*
4. *Both a farming community of 100 individuals and a community of 15 to 25 farms are analyzed, allowing the impact on both potential hypothetical communities to be evaluated.*
5. *The hypothetical farming community will be at a specific location and conditions in the community will be "consistent with current conditions of the region surrounding the Yucca Mountain site."*
6. *Land areas are combined under a single farming unit only to demonstrate that consolidation is a non-conservative approach.*

5.3.9 Disruptive Events

Volcanic Direct Release

The assumptions listed below are given in the AMR *Igneous Consequence Modeling for the TSPA-SR* (CRWMS M&O 2000 [139563], Section 5) for volcanic direct release events modeling. Refer to that AMR for additional information. These assumptions are used in Section 6.3.9.1.

1. *The current variability in wind speed and direction in the Yucca Mountain region are a suitable approximation for future variability in wind conditions in the region.*
2. *Wind speed and wind direction "are treated as uncorrelated parameters, even though they were collected as paired, fully-correlated parameters."*
3. *The wind speed and wind direction parameters do not include a component to account for altitude variation.*
4. *"All eruptions include a violent strombolian phase with fragmentation of the ascending magma into pyroclasts occurring below the repository horizon."*

5. *All waste packages and other components of the EBS that are partially or completely intersected by an eruptive conduit are completely destroyed, and all waste from intersected packages are available for entrainment in the eruption.*
6. *The EBS provides no protection to the waste form during an eruptive event, and waste particle diameter is estimated assuming direct exposure of the waste form to the magmatic environment.*
7. *"For the purposes of estimating waste particle diameters in the eruptive environment, all waste is assumed to be unaltered commercial spent fuel."*

Biosphere Dose Conversion Factors for Volcanic Direct Release

The assumptions listed below are given in the AMR *Disruptive Event Biosphere Dose Conversion Factor Analysis* (CRWMS M&O 2000 [143378], Section 5). Refer to that AMR for additional information. These assumptions are used in Section 6.3.9.1.

1. *The source of contamination for volcanic biological dose conversion factors is surface soil.*
2. *Doses are calculated based on an ash-soil mixture with the properties of soil.*
3. *Groundwater is assumed to be uncontaminated.*
4. *Air transport was not considered.*
5. *Surface water transport was not considered in the analysis.*
6. *All contaminated food is locally grown.*
7. *Biotic transport and waste form degradation were not considered in the analysis.*
8. *The receptor of interest for the reasonable representation is the average member of the critical group. The receptor for the bounding case is an individual who exhibits characteristics that maximize exposure.*
9. *Exposure pathways considered were the consumption of locally produced food, inadvertent soil ingestion, inhalation of resuspended particulate matter, and external exposure to contaminated soil.*
10. *The thickness of the surface soil has been determined to be 15 cm.*
11. *The thickness of the volcanic ash deposited on the soil surface was determined to be insignificant, when compared to the thickness of the surface soil.*

Intrusive Indirect Release

The assumptions listed below are given in the AMR *Igneous Consequence Modeling for the TSPA-SR* (CRWMS M&O 2000 [139563], Section 5) for intrusive indirect release events

modeling. Refer to that AMR for additional information. These assumptions are used in Section 6.3.9.2.

1. *"Any waste packages, drip shields, and other components of the engineered barrier system that are partially or completely intersected by an intrusive dike are fully destroyed. Furthermore, three waste packages on either side of the dike are also assumed to be fully destroyed."*
2. *All the material in the waste packages destroyed on either side of a dike are assumed available for incorporation into the UZ transport model, dependent on solubility limits and the availability of water.*

Seismic Cladding Event

The assumption listed below is given in the AMR Clad Degradation – Abstraction and Summary (CRWMS M&O 2000 [147210], Section 5.4). Refer to that AMR for additional information. This assumption is used in Section 6.3.9.4.

1. *"Seismic analysis showed that rods would fail from a very severe earthquake (a once per million years event) and that most of the rods would fail. Therefore, in the TSPA-SR, the seismic event is assumed to have a frequency of 1.1×10^{-6} /yr and it is assumed that all the cladding is failed at the rod center and available for clad unzipping when a seismic event occurs. Failing all the rods is an upper limit and failing the rods in the center minimizes the release time for unzipping."*

6. TSPA-SR MODEL

Performance assessment is a method of forecasting how a system or parts of a system will behave or perform over time. Its goal is to aid in determining whether the system can meet established performance requirements. A total system performance assessment (TSPA) is a set of performance assessment analyses in which all the components of a system are linked into a single analysis. The TSPA-SR model of Yucca Mountain is a computer model that integrates information from all of the various component models of the potential repository (e.g., unsaturated zone flow, waste package degradation, etc.) into one comprehensive model. The TSPA-SR model is then used to forecast the performance of a potential nuclear waste repository system at Yucca Mountain, Nevada for future times up to 1,000,000 years after closure of the repository.

6.1 INTRODUCTION

The Yucca Mountain TSPA combines information from a series of process models that are specific to the geologic and engineered environments at Yucca Mountain. The information from these process models is either used "as is" or is further reduced into abstracted models. Both process models and abstracted models, as appropriate, are then integrated into a single TSPA model that can be used to forecast the performance of the repository system. The primary output of the total system model is a forecasted range of possible annual dose rates to a human receptor living approximately 20 km downgradient of the repository site. A "range" of dose rates is the output of the model because the model framework is inherently probabilistic based on a certain amount of irreducible uncertainty in the model inputs. This uncertainty is inherent in large-scale geologic processes and in our knowledge of future conditions at the repository site. For this reason all TSPA analyses are probabilistic in nature and involve some sort of stochastic sampling algorithm, such as Monte Carlo or Latin Hypercube sampling, to generate a "full range" of outputs based on the stochastic input parameter distributions. For the TSPA-SR, GoldSim 6.04.007 (Golder Associates 2000 [143556]) is the graphical, object-oriented, computer program used as the integrating shell and statistical framework for linking the various component models together, sampling their inputs stochastically, and then generating a large number of realizations of the possible dose rate based on the sampled inputs.

Figure 6-1 shows the primary components of the TSPA-SR model and the information that feeds into these components. The primary components are highlighted in the center of the figure, within the dotted outline labeled "Run with GoldSim."

The primary outputs of the Yucca Mountain process models are described in a series of Analyses and Model Reports (AMRs). These outputs are input directly (or sometimes with minor postprocessing) into the total system model, illustrated in Figure 6-1 by the abstraction or submodel boxes above and beneath the primary TSPA model component boxes. The AMR number corresponding to the given abstraction (e.g., Seepage Flow Abstraction) or submodel (e.g., UZ Colloid Transport Model) is also listed on the figure. In effect, Figure 6-1 is a summary of Sections 6.3.1 to 6.3.9 of this chapter, which describe the links between the TSPA model and the underlying process models, described in the Process Model Reports (PMRs) and developed through the AMRs. Both Table 4-1 in Section 4 and Figure 6-1 depict the final analyses, model and data feeds into the TSPA-SR model. It is important to recognize that these

final feeds are built on a hierarchy of calculations, data and software contained in a family of supporting AMRs and their associated DTNs. Figure 6-2 through Figure 6-16 depict the entire hierarchy of AMRs and DTNs that form the entire scientific basis for the TSPA-SR model.

The subsections of this chapter provide details of the TSPA model structure and design, and the details of the individual component models and their implementation into the TSPA-SR model. The TSPA-SR model files and the input files for the DLLs necessary to reproduce the results documented in this AMR are in the Technical Data Management System (TDMS) under DTNs: MO0009MWDMED01.020 [152838] and MO0008MWDHUMAN.000 [152186]. The TSPA-SR cases "SR00_037ne6" and "SR00_038ne6" in DTN: MO0009MWDMED01.020 [152838] contain the TSPA-SR model and results for a nominal-scenario median-value simulation, with and without the implementation of seismic cladding failure, respectively. The case "SR00_001ie5" in DTN MO0009MWDMED01.020 [152838] is the median value simulation for the igneous scenario that includes both eruptive and groundwater release doses. Realization #1 in the case SR00_005hm5 in DTN: MO0008MWDHUMAN.000 [152186] was used to verify the human intrusion model described in Section 6.3.9.3. The four associated .gsm files (along with the GoldSim code, version 6.04.007) for these four cases are all that is needed to view the model and the results shown in the subsections below. Also, many of the figures in Section 6 make use of GoldSim icons. Attachment I describes these icons and will be a useful reference when reading Section 6.

6.1.1 TSPA Previous Work

To date, DOE has completed and documented four major iterations of probabilistic TSPAs for the Yucca Mountain site: TSPA-91 (Barnard et al. 1992 [100309]), TSPA-93 (Wilson et al. 1994 [100191]; CRWMS M&O 1994 [100111]), TSPA-95 (CRWMS M&O 1995 [100198]), and the *Total System Performance Assessment-Viability Assessment of a Repository at Yucca Mountain* TSPA-VA (DOE 1998 [100550], Volume 3). Each successive TSPA iteration has advanced the technical understanding of the performance attributes of the natural features and processes and enhanced engineering designs. The TSPA-SR model is the next major iteration of the Yucca Mountain TSPA. The probabilistic TSPA methodology used for TSPA-SR is generally accepted by the U.S. Nuclear Waste Technical Review Board (NWTRB), TSPA Peer Review (Budnitz et al. 1999 [102726]), and the international scientific community (NEA 1991 [100477], and OECD 1991 [100478]) as the appropriate basis for a TSPA model. This in turn lends scientific credibility to the probabilistic risk based methodology that is the basis for the TSPA-SR model. Finally, the probabilistic risk based approach is established as a direct modeling criteria as referenced in the NRC's TSPA IRSR (NRC 2000 [149372], Section 4.2) and in 10 CFR Part 63 (64 FR 8640, [101680], Section 4.3).

The integrated TSPA-SR model is considered appropriate for its intended use (see Section 6.5 below for model validation). Verification of the accuracy of individual components of the integrated model is presented in the various subsections of this chapter.

6.1.2 TSPA-SR Model Importance

Per YMP administrative procedures AP-3.10Q [152363] and AP-3.15Q [153184], the integrated TSPA-SR model described in the present AMR is assigned a primary (Level 1) importance

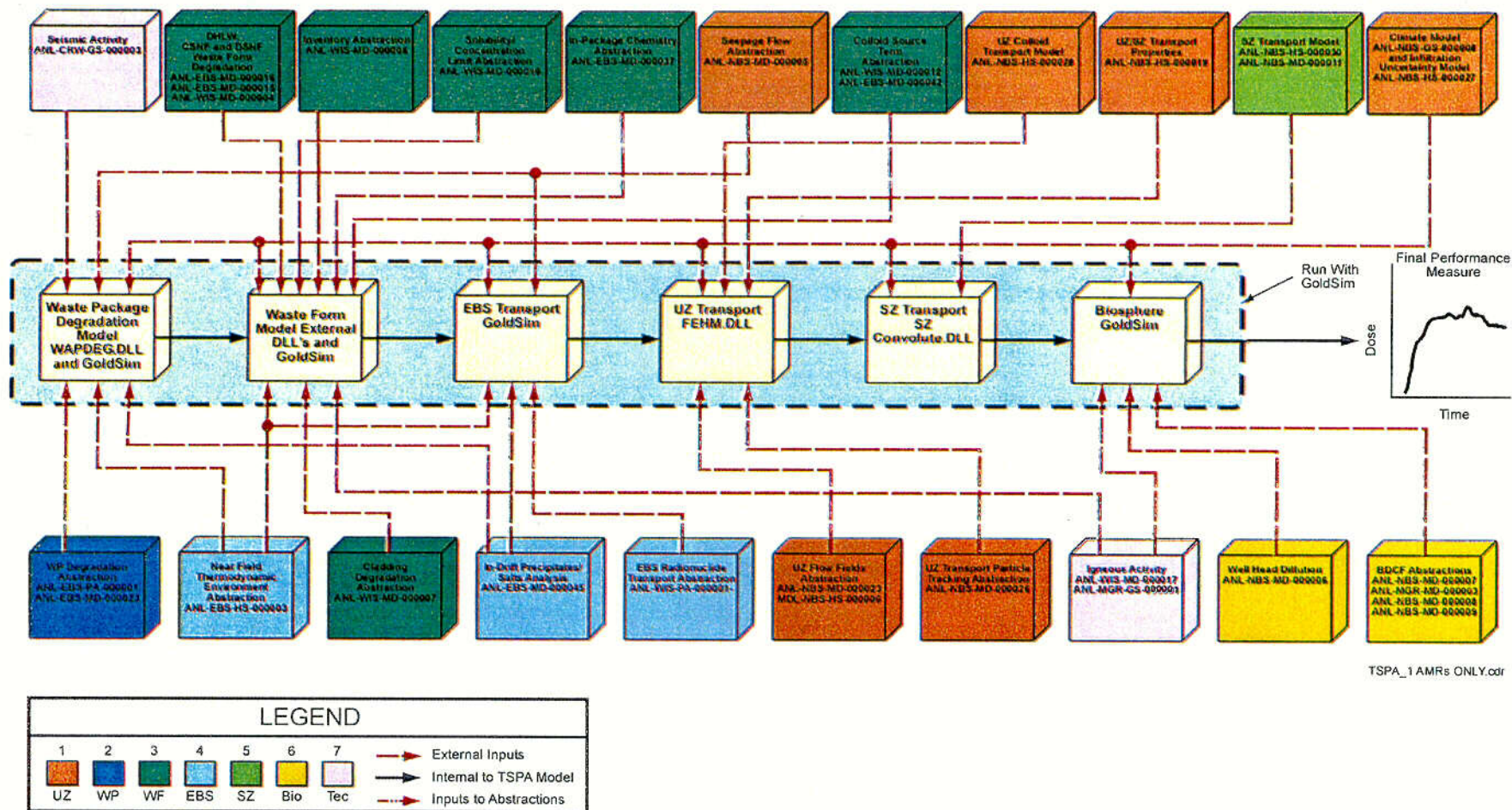
because the model is used to provide estimates of all the principal factors (Table ES-1, Volume II, CRWMS M&O 2000 [148713]) listed under the Screening Criteria for Grading of Data in AP-3.15Q [153184]:

- Seepage into drifts
- Solubility limits of dissolved radionuclides
- Solution of radionuclide concentrations in the geologic setting
- Retardation of radionuclide migration in the unsaturated zone
- Retardation of radionuclide migration in the saturated zone
- Performance of the drip shield
- Performance of the waste package barriers.

The TSPA-SR model also evaluates, or directly uses as input, all of the “other factors for the post-closure safety case” listed in AP-3.15Q [153184], except “coupled processes—effects on unsaturated zone flow,” which was screened out of the TSPA-SR integrated model at the AMR level.

In addition, the TSPA-SR model is used to examine the effects of potentially disruptive processes and events during the period of compliance for post-closure, specific disruptive processes and events investigated are human intrusion, water table rise, seismic activity, and igneous activity.

Total System Performance Assessment (TSPA) Model



TSPA_1 AMRs ONLY.cdr

Figure 6-1. Hierarchy of Analyses and Models Supporting the Total System Performance Assessment-Site Recommendation

COI

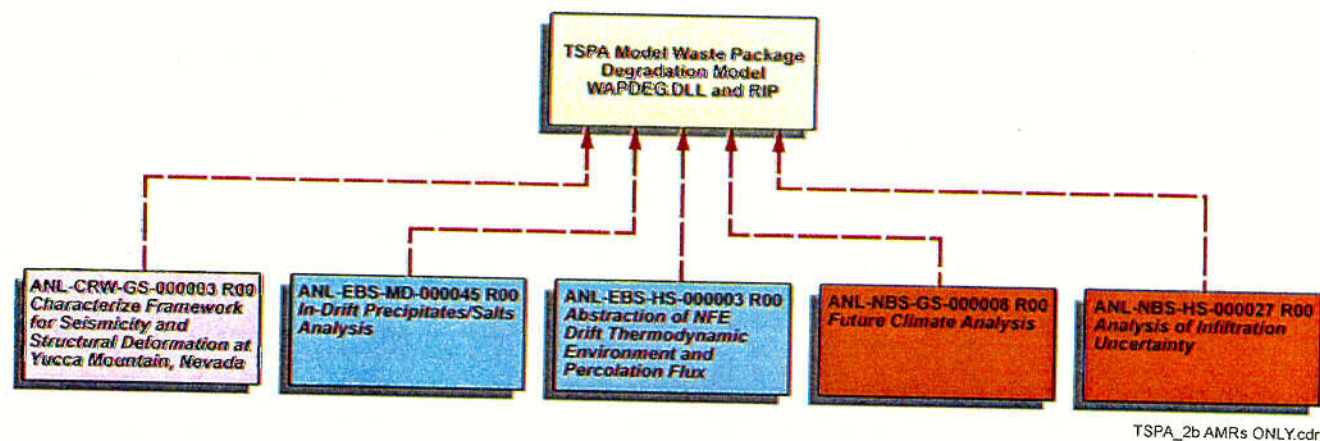


Figure 6-2. Total System Performance Assessment Model: Hierarchy of Analyses and Models Supporting the Waste Package Degradation Model of Total System Performance Assessment-Site Recommendation - Part A

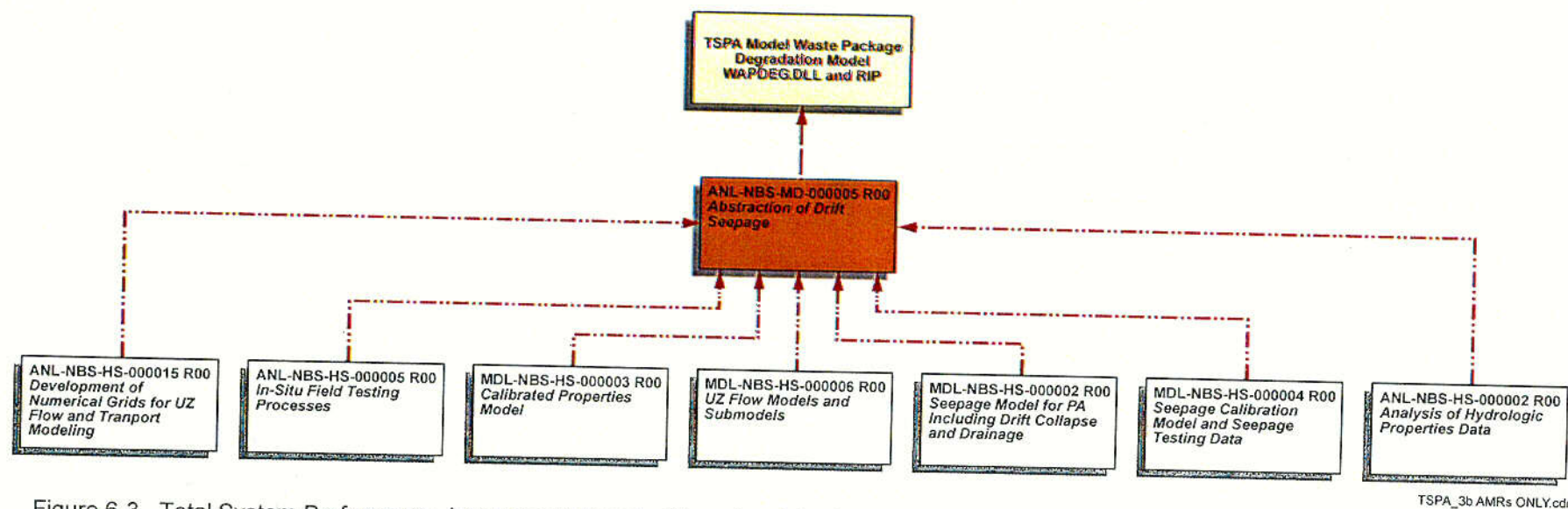


Figure 6-3. Total System Performance Assessment Model: Hierarchy of Analyses and Models Supporting the Waste Package Degradation Model of Total System Performance Assessment-Site Recommendation - Part B

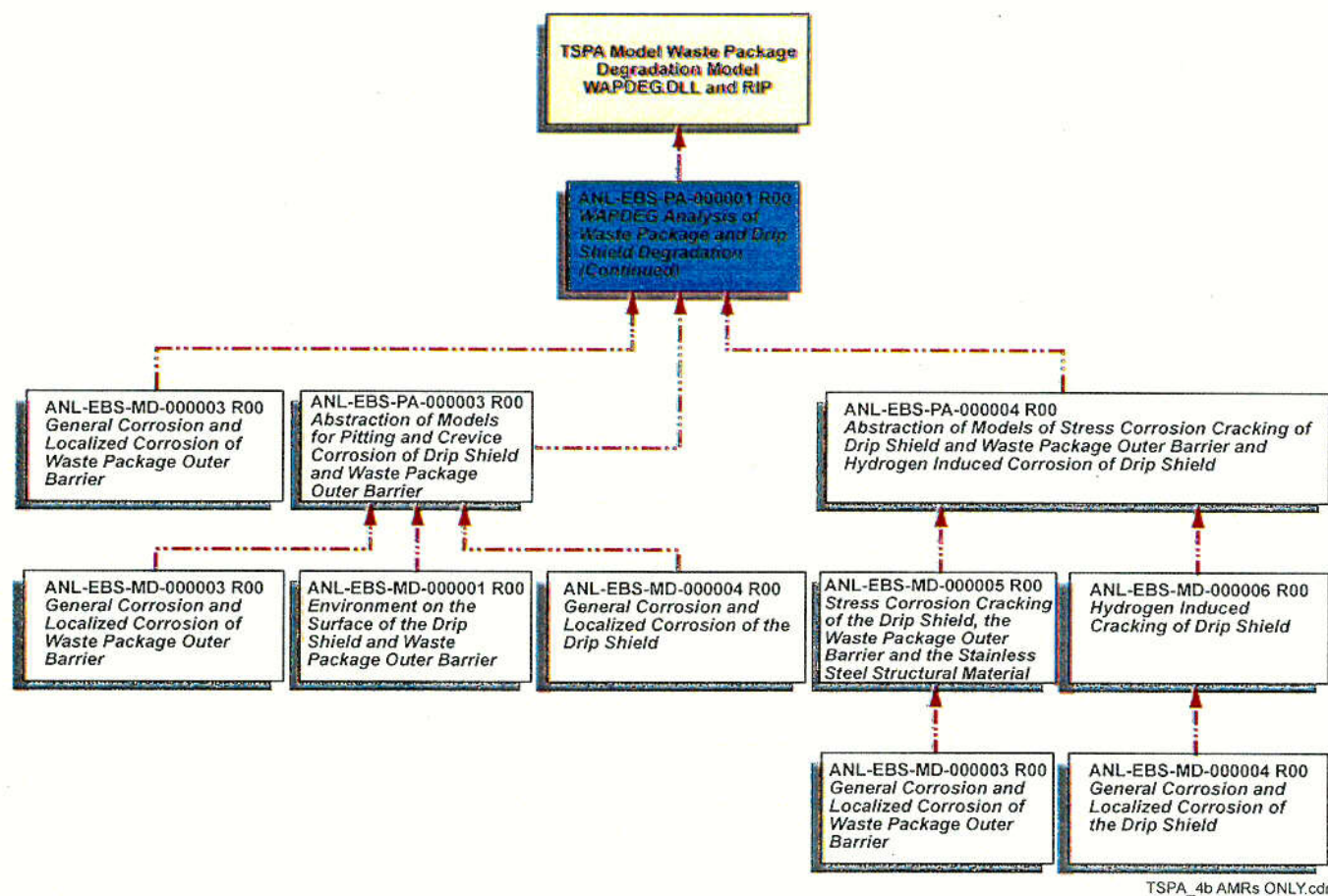


Figure 6-4. Total System Performance Assessment Model: Hierarchy of Analyses and Models Supporting the Waste Package Degradation Model of Total System Performance Assessment-Site Recommendation - Part C

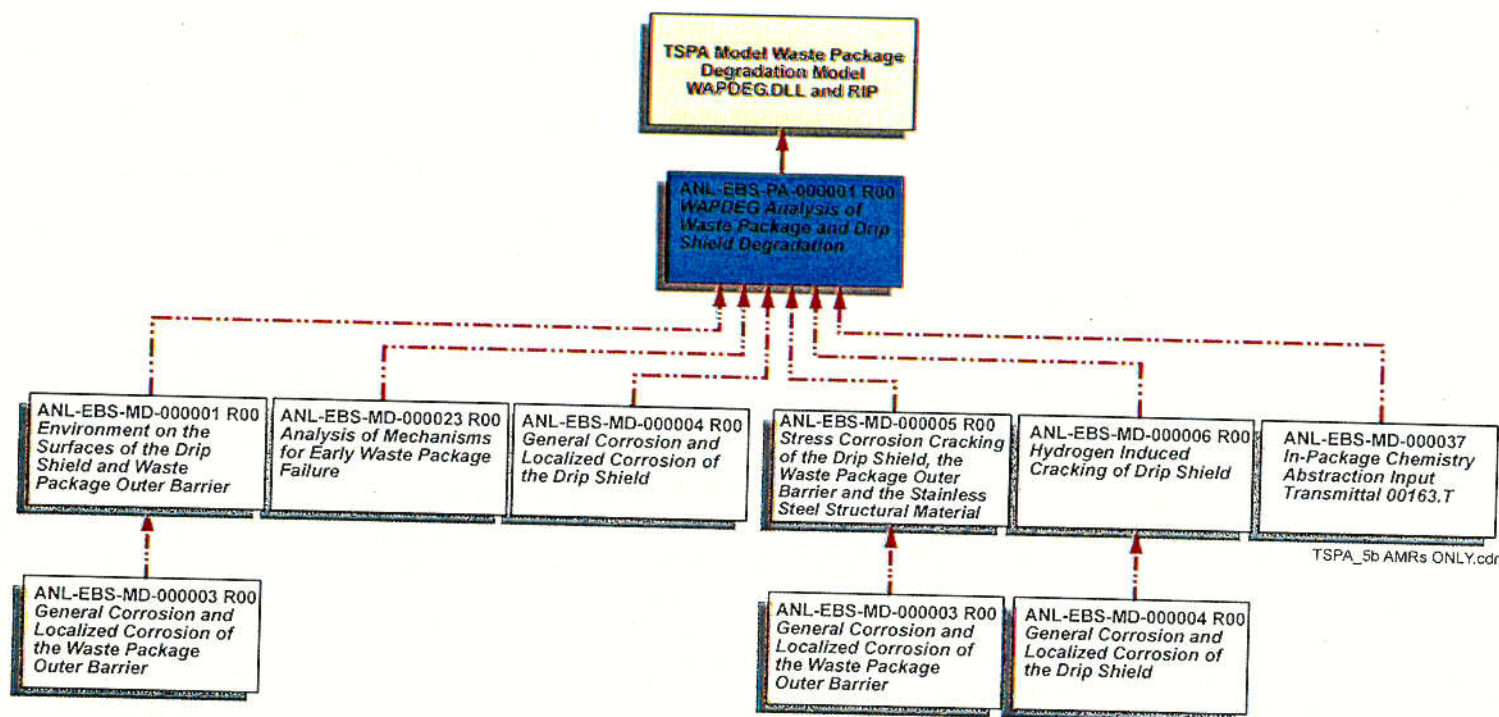


Figure 6-5. Total System Performance Assessment Model: Hierarchy of Analyses and Models Supporting the Waste Package Degradation Model of Total System Performance Assessment-Site Recommendation - Part D

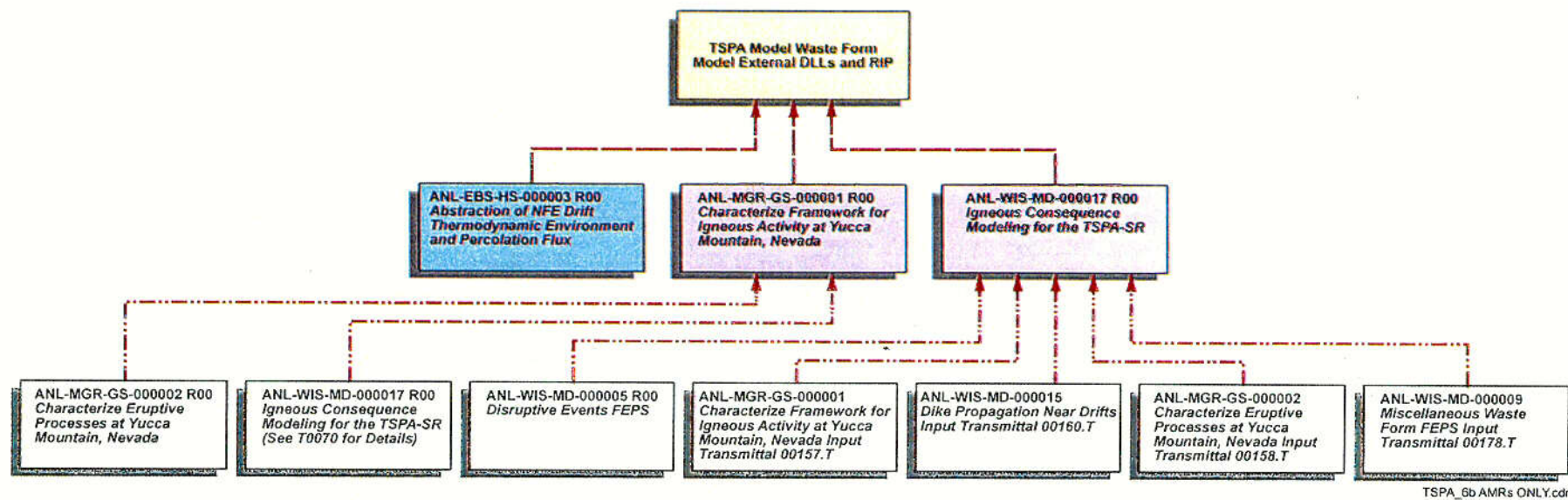


Figure 6-6. Total System Performance Assessment Model: Hierarchy of Analyses and Models Supporting the Waste Form Model of Total System Performance Assessment-Site Recommendation - Part A

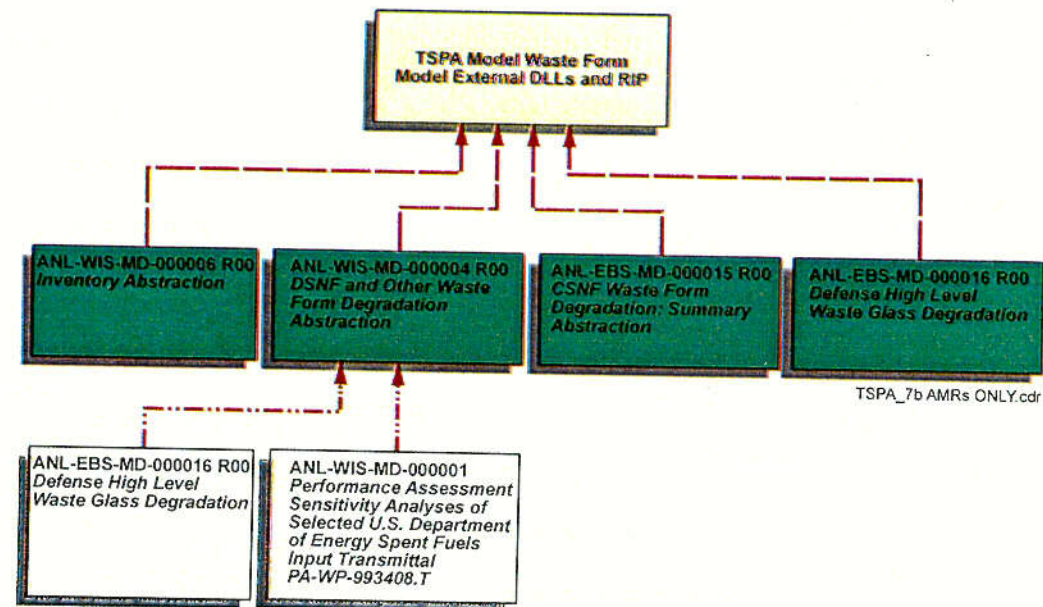


Figure 6-7. Total System Performance Assessment Model: Hierarchy of Analyses and Models Supporting the Waste Form Model of Total System Performance Assessment-Site Recommendation - Part B

C06

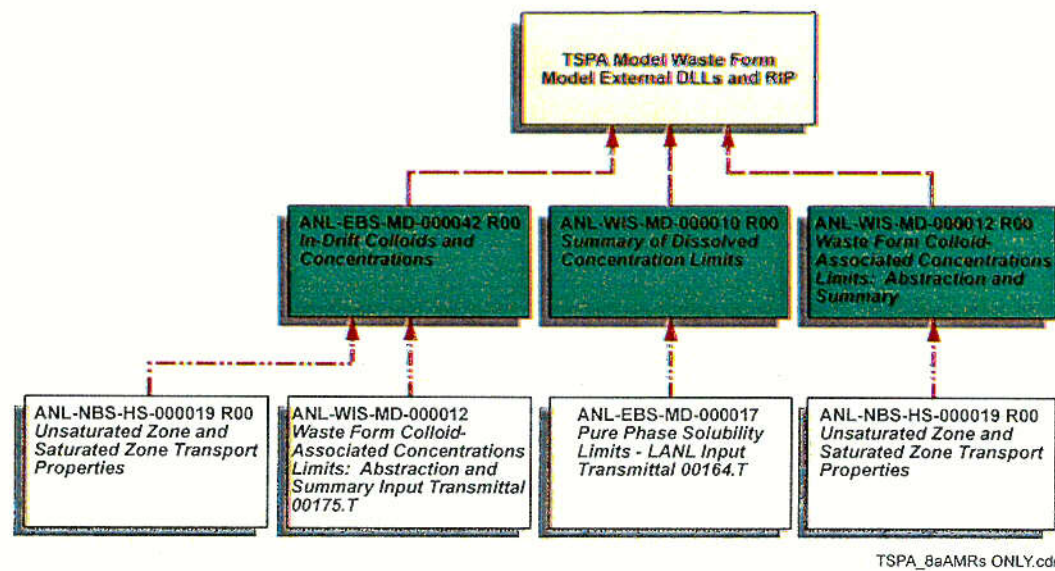


Figure 6-8. Total System Performance Assessment Model: Hierarchy of Analyses and Models Supporting the Waste Form Model of Total System Performance Assessment-Site Recommendation - Part C

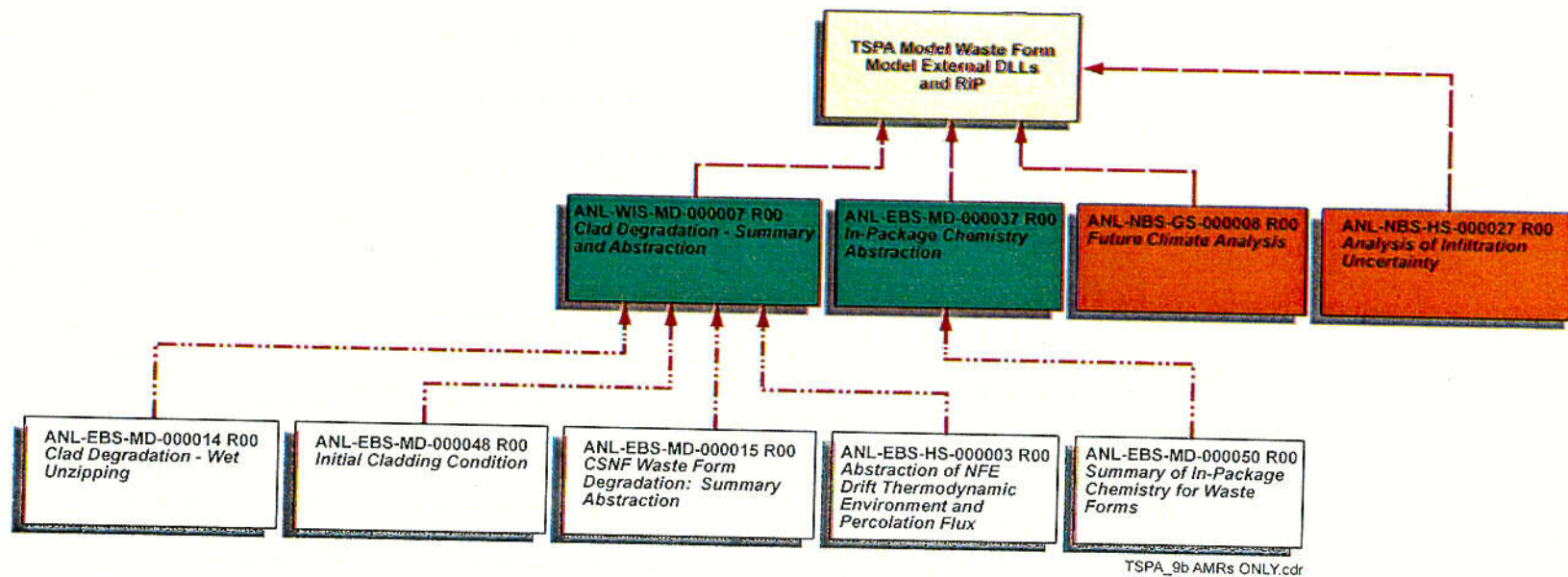


Figure 6-9. Total System Performance Assessment Model: Hierarchy of Analyses and Models Supporting the Waste Form Model of Total System Performance Assessment-Site Recommendation - Part D

C08

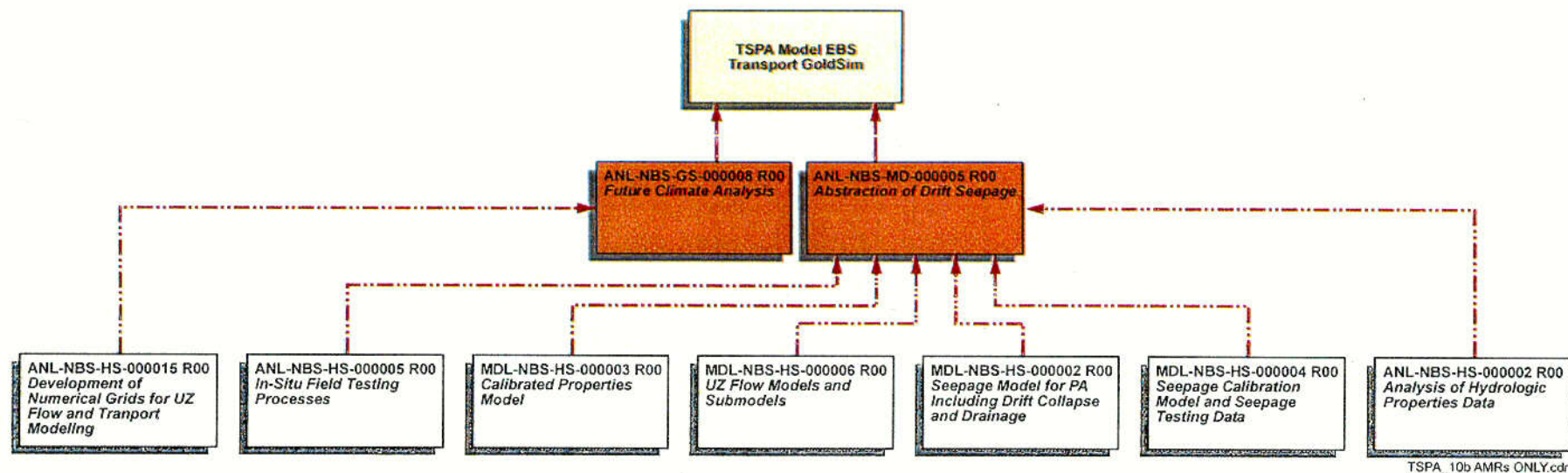


Figure 6-10. Total System Performance Assessment Model: Hierarchy of Analyses and Models Supporting the EBS Transport Model of Total System Performance Assessment-Site Recommendation - Part A

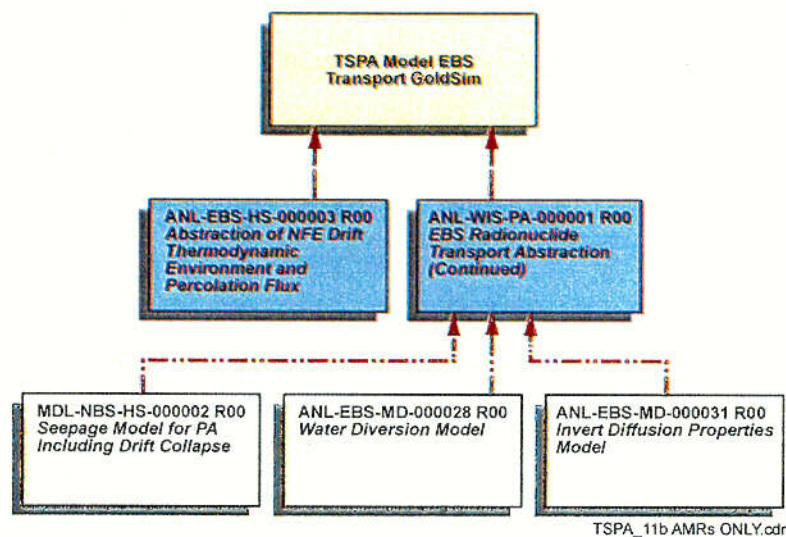


Figure 6-11. Total System Performance Assessment Model: Hierarchy of Analyses and Models Supporting the EBS Transport Model of Total System Performance Assessment-Site Recommendation - Part B

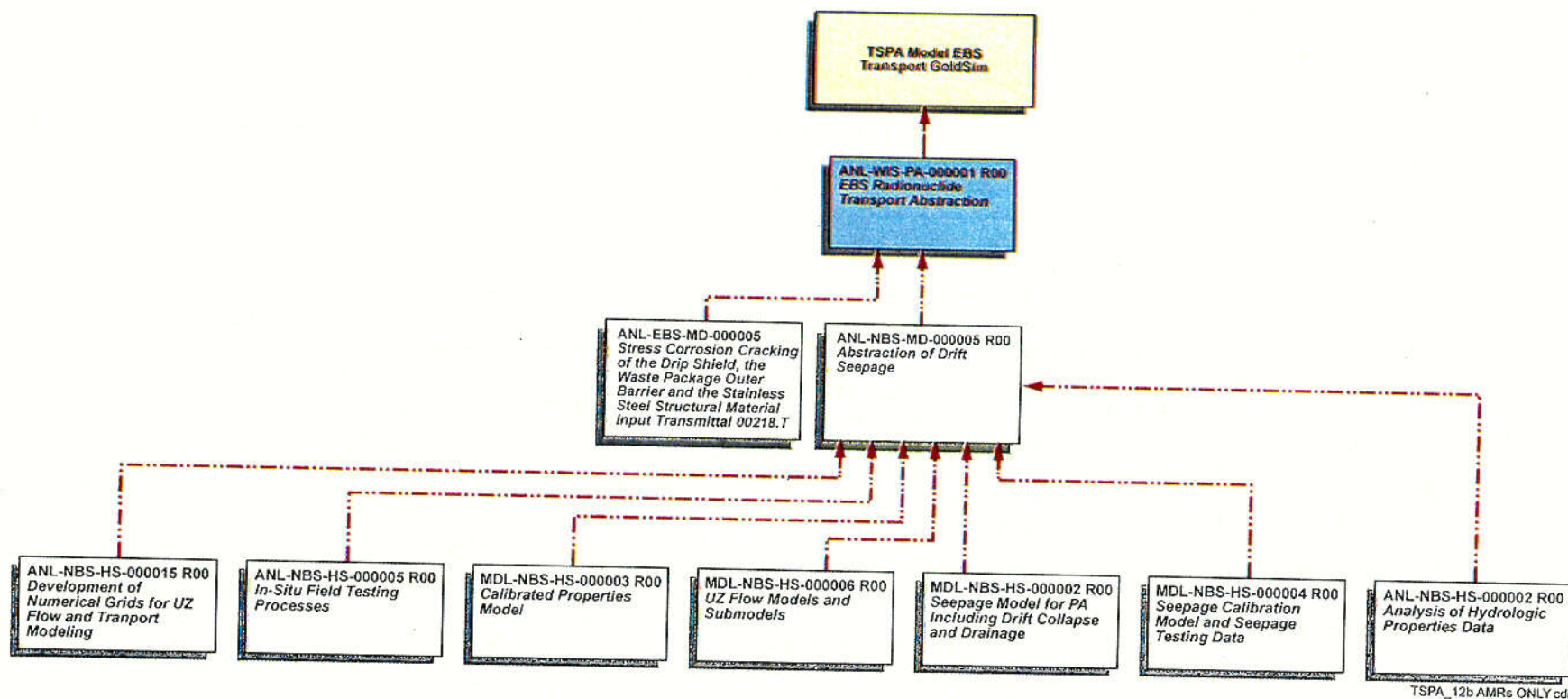


Figure 6-12. Total System Performance Assessment Model: Hierarchy of Analyses and Models Supporting the EBS Transport Model of Total System Performance Assessment-Site Recommendation - Part C

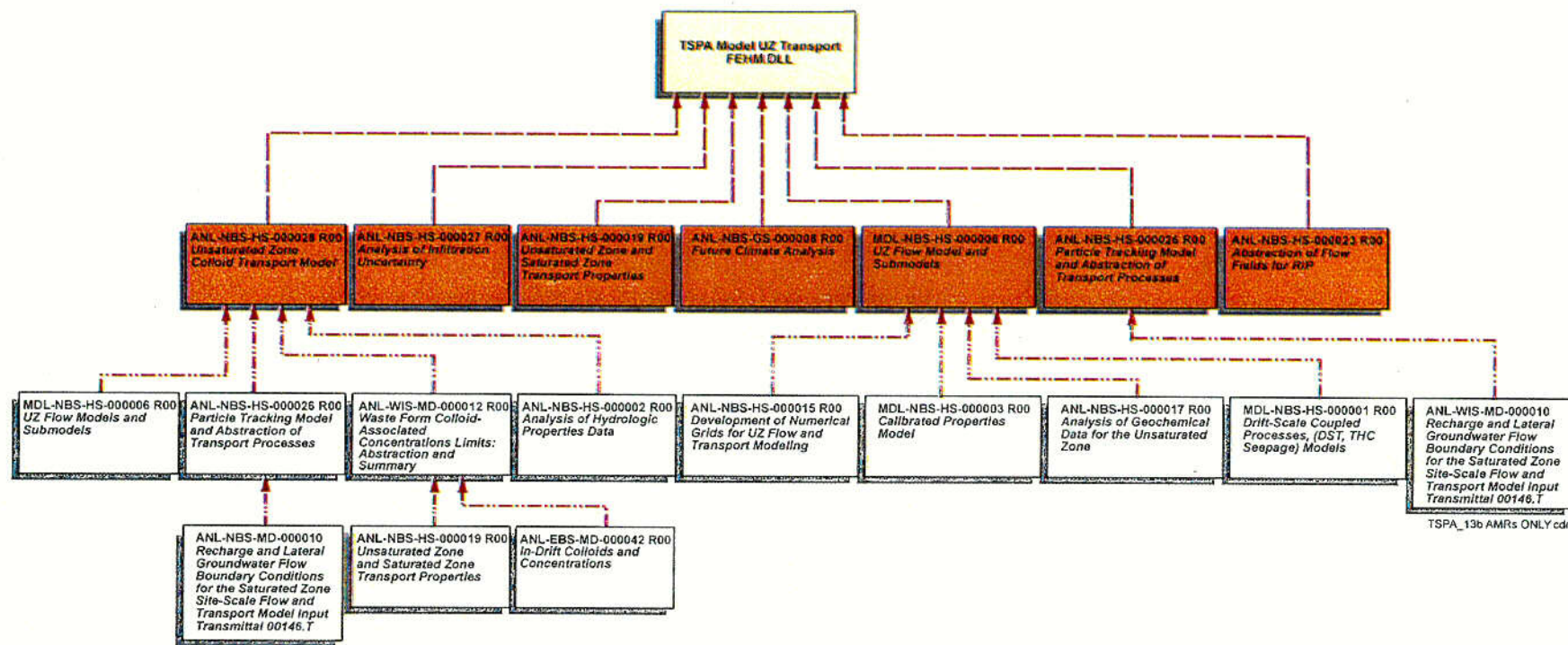


Figure 6-13. Total System Performance Assessment Model: Hierarchy of Analyses and Models Supporting the Unsaturated Zone Transport Model of Total System Performance Assessment-Site Recommendation

C11

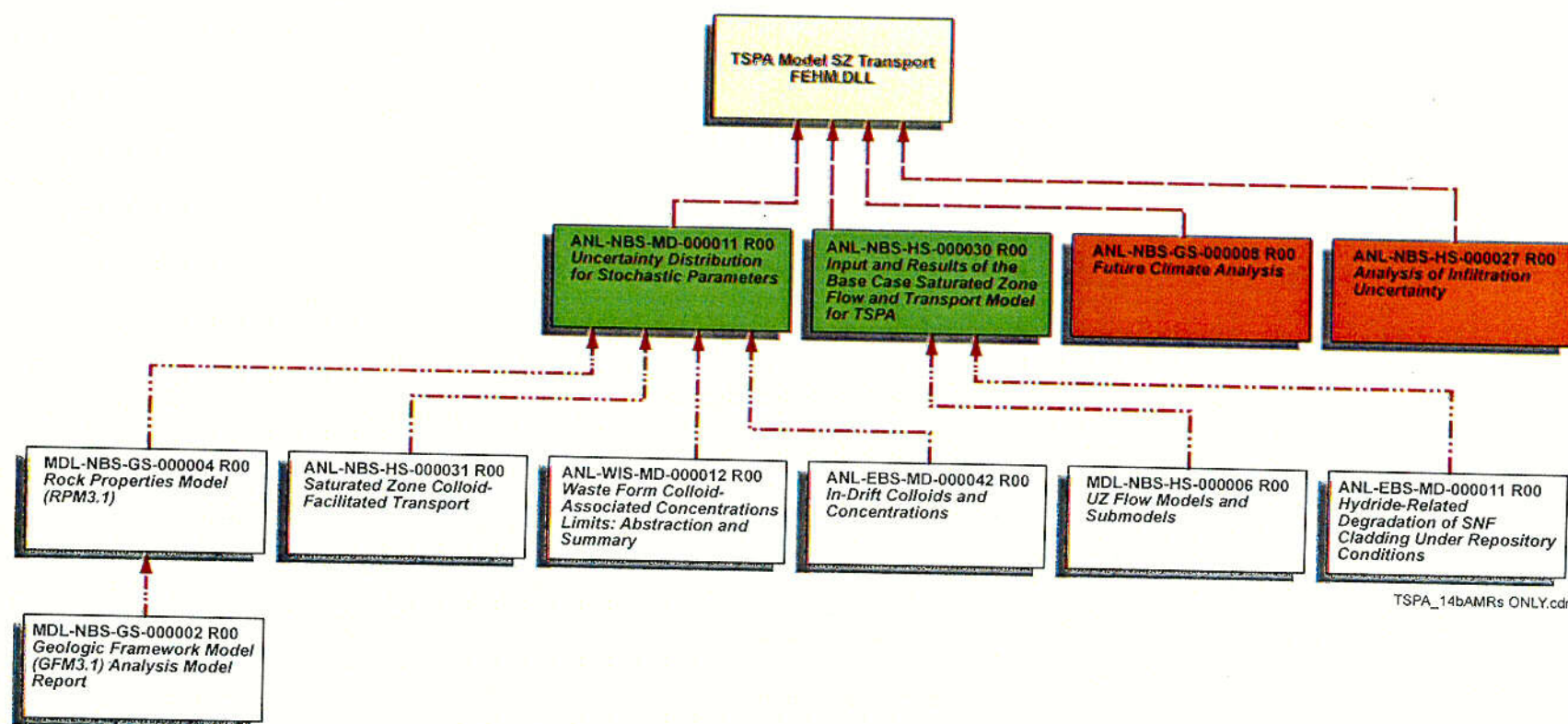


Figure 6-14. Total System Performance Assessment Model: Hierarchy of Analyses and Models Supporting the Saturated Zone Transport Model of Total System Performance Assessment-Site Recommendation

C12

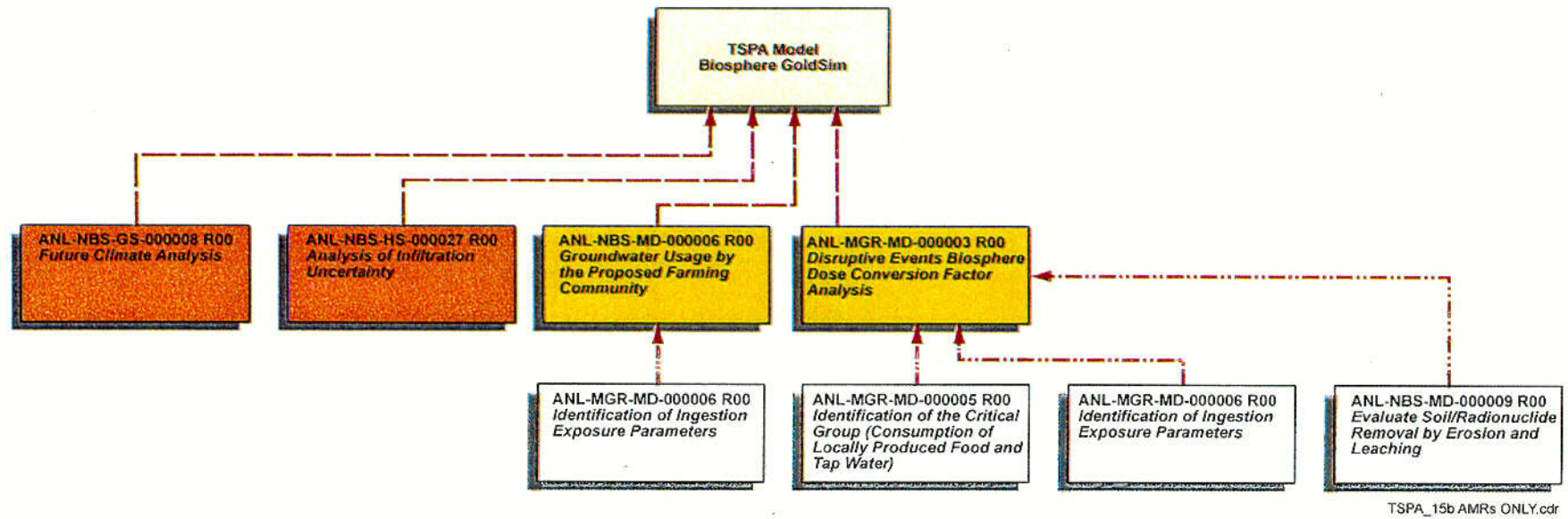


Figure 6-15. Total System Performance Assessment Model: Hierarchy of Analyses and Models Supporting the Biosphere Model of Total System Performance Assessment-Site Recommendation - Part A

C13

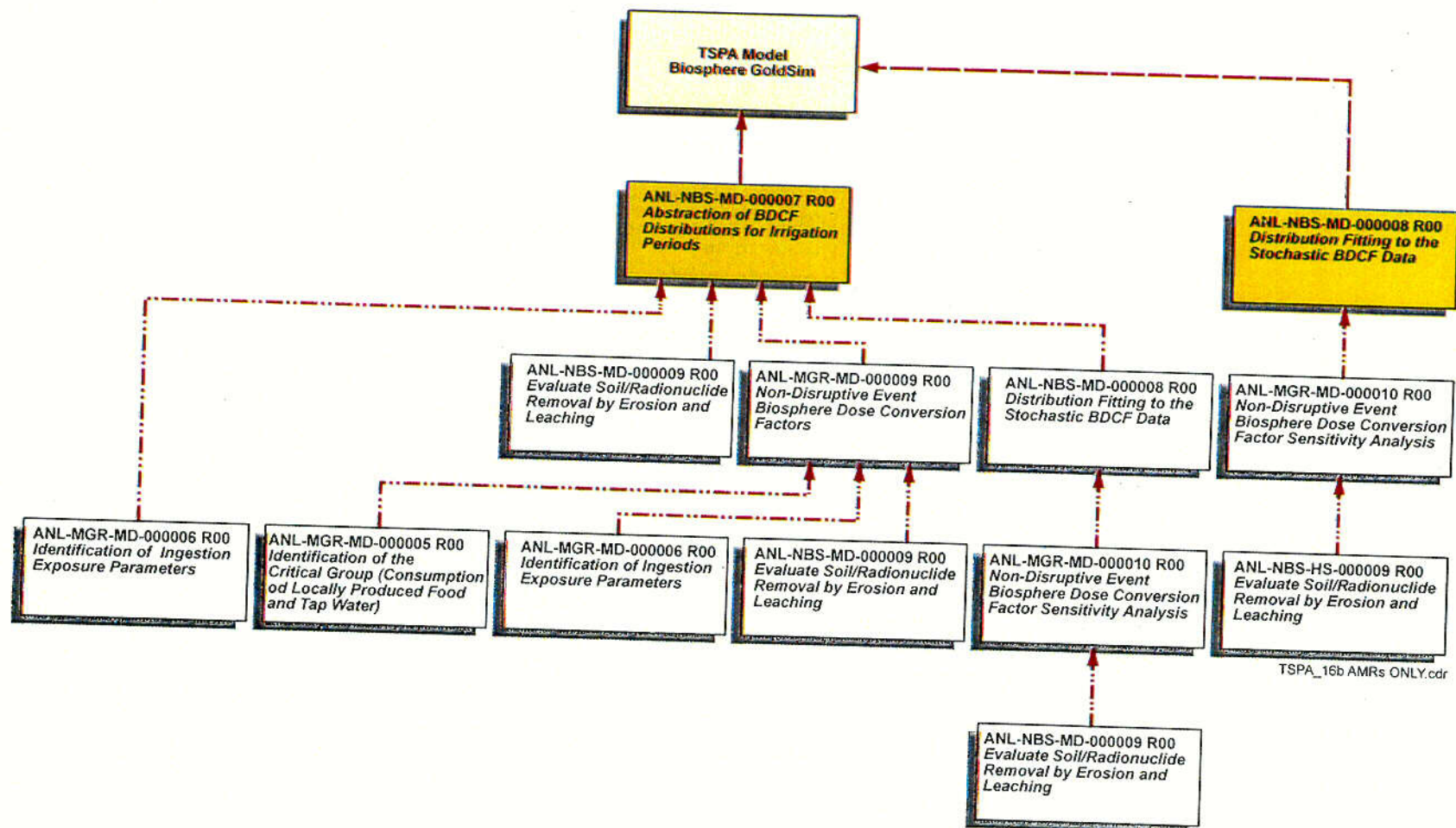


Figure 6-16. Total System Performance Assessment Model: Hierarchy of Analyses and Models Supporting the Biosphere Model of Total System Performance Assessment-Site Recommendation - Part B

C14

6.2 MODEL STRUCTURE AND DESIGN

The general approach of using probabilistic risk analysis for the TSPA-SR is appropriate because of the inherent uncertainties in predicting physical behavior many thousands of years into the future in a geologic system with properties that can never be fully characterized deterministically. Much of the modeling of the repository (and its components) is complex, uncertain, and variable, involving a variety of coupled processes (thermal-hydrologic-chemical and thermal-hydrologic-mechanical) operating in three spatial dimensions on a variety of different materials (e.g., fuel rods, waste packages, invert, and host rock) and changing over time. Because of the rather large number of uncertain parameters in the numerous component TSPA-SR models (about 250), probabilistic risk analysis involves a Monte Carlo method of multiple realizations of system behavior, which can require significant computational resources. For this reason, and because the lack of certain data makes some detailed models difficult to quantify, model abstractions or simplifications are often employed. The abstracted performance assessment models may have a one-to-one correspondence with the detailed process-level models or may represent a combined subsystem model covering several aspects of the overall system (see Figure 6-17).

This section presents an overview of the method for mathematical and numerical modeling of each physical process and repository system component, including their abstractions, uncertainty, and the approach for combining them into an overall model and computer code. The overview includes discussions about information flow between the models (Section 6.2.1) and the computer code architecture that facilitates the information flow (Section 6.2.2). This section also provides a road map showing how to re-couple the component models (e.g., unsaturated zone flow, waste package degradation, etc) into an integrated total system model, and understand the information flow between components that allows for evaluation of overall system performance.

6.2.1 Information Flow between Component Models

A stylized conceptualization of the total system performance assessment-site recommendation (TSPA-SR) model hierarchy and information flow is shown in Figure 6-17 and Figure 6-18. These figures indicate a continuum of information and models, from the most basic, detailed level to the level of the total system model. The data and associated conceptual models, and their integration into process-level (detailed numerical models) models, lie in the lower part of the pyramid in Figure 6-17. These process-level models may be simplified or abstracted¹, if necessary, to the next higher level of the pyramid, because of computational constraints or a lack of information. The need for simplification is particularly evident in the TSPA, which has a significant component of probabilistic risk analysis, requiring multiple realizations/simulations of the entire system and its associated component processes and models.

For the model abstraction process, there are two key factors in accurately representing the performance of the overall system. First, information and assumptions passed up the model pyramid must be consistent. For example, a surface infiltration flux used to generate liquid flow

¹“abstraction” is used to connote the development of a simplified mathematical and/or numerical model that reproduces and bounds the results of an underlying detailed process model.

fields from the detailed process model for the UZ must be used in all subsequent analyses based on those particular flow fields. The same infiltration flux must be used when calculating seepage flux in the abstracted seepage subsystem model (Section 6.3.1) and when calculating thermal-hydrologic response (temperature and relative humidity) in the near-field environment (Section 6.3.2). Second, the parameters that most affect performance in the detailed process models must be appropriately represented in the subsequent subsystem and total system models, including the appropriate uncertainty range of the parameters.

A key feature of the abstraction methodology is the approach used to pass uncertainty at one level to uncertainty at another level. Transfer of uncertainty must go in both directions, from bottom up and from top down. When analyzing uncertainty at the bottom levels (data, conceptual models, and process models), the analyses look at the effect of uncertain parameters on surrogate or subsystem performance measures, such as the amount of fracture flow in the UZ. The sensitivity of the surrogate measure to component model uncertainty is then used to decide whether to carry this uncertainty through to the total system analyses. However, important parameters at the subsystem level sometimes prove to be unimportant at the overall system level. This information is then passed down the pyramid to indicate the relative unimportance of collecting more physical data about this parameter.

Traceability of data transfer among models and quality assurance of the data are very important aspects of the information flow process. The PMRs and AMRs, which support the TSPA results presented here, explicitly identify the source and status of data, computer codes, and computer input and output files used in the Site Recommendation (SR). Following prescribed procedures, the U.S. Department of Energy (DOE) is reviewing the data, assumptions, computer codes, and information used in the TSPA analyses to ensure the models are valid, defensible, and appropriate. To be fully validated, there must be clear documentation that the TSPA models are supported by qualified data, and the numerical models and computer codes are documented and appropriately controlled.

Figure 6-18 is a more detailed, but still simplified, look at information flow among the component models: unsaturated zone (UZ) flow (and seepage), waste package and drip shield degradation, engineered barrier system (EBS) geochemical environment, thermal hydrology, waste form degradation, EBS transport, UZ transport, saturated zone (SZ) flow and transport, biosphere, and volcanism. This Figure does not show all of the couplings among TSPA-SR component models but does illustrate major model connections, abstractions, and information feeds.

The information transfer between component models is activated in several ways. One approach is use of a "response surface," which means a multidimensional table of output from one component model that is used as input to another component model. When interpolating among points in the table, linearity is generally assumed. Often a response surface has more than one independent variable (e.g., both time and percolation flux). However, in the usage in Figure 6-18, sometimes time is the only independent variable, and interpolation is not necessary between the time points (e.g., the data are provided directly "as is" to the next component model). Other approaches to information transfer include direct transfer of results from one component to another, or direct data or parameter feeds from one component to another.

A more detailed description of information flow in the TSPA-SR is shown in Figure 6-19 and Figure 6-20. These figures show the principal pieces of information passed between the various component models. Figure 6-19 shows the overall system, while Figure 6-20 shows the details of the EBS system. These details of information flow are explained in greater depth in the discussion of the TSPA-SR models architecture in Section 6.2.2. The conceptual and experimental basis for this depiction of information flow is given in detail in Section 6.3.

Decoupling of the physical-chemical processes into component models, shown in Figure 6-18, and in Figure 6-19 and Figure 6-20, is facilitated by a natural division of the repository system into a series of sequentially linked spatial domains (e.g., the waste package, emplacement drift, host rock near the drift, UZ between the drift and the water table, SZ, and biosphere). This division works best from the standpoint of radionuclide transport, which is the primary consideration of the TSPA model. The TSPA-SR model architecture and information flow becomes, therefore, a sequential calculation in which each spatially based transport model may be run in succession, with output as "mass versus time" from an upstream spatial domain serving as the input of mass versus time for the spatial domain immediately downstream.

A complexity to this approach to transport is brought on by the inclusion of the disruptive event, volcanism, and its effects on the system. For example, the systematic transport in the nominal groundwater-release scenario is entirely disrupted or disconnected when eruptive volcanic events are included in the model because the waste is transported through the atmosphere to the receptor rather than through the groundwater pathways. On the other hand, intrusive igneous events (e.g., a dike intersecting the repository) only disrupt some of the nominal models (e.g., waste package degradation) and the other nominal scenario models for groundwater transport remain applicable. Both eruptive and intrusive igneous scenarios are integrated into the TSPA-SR model, as described in Section 6.3.9.

Oversight

NRC Technical Exchanges, Appendix 7 Meetings
NWTRB Panel Meetings, Reports to Congress
State of Nevada; Affected Units of Local Government
Public

Prior TSPAs

DOE TSPA-91, 93, 95, VA
NRC IPA-1, -2, -3
EPRI TSPA Phases 1, 2, and 3

Process Model Abstraction

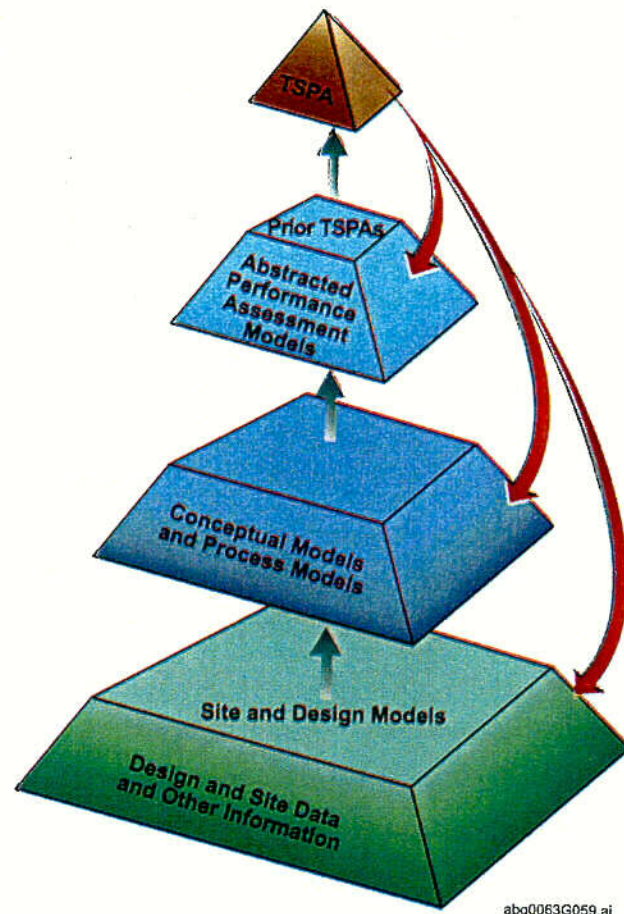
Unsaturated Zone Flow
Engineered Barrier System Environments
Waste Package & Drip Shield Degradation
Waste Form Degradation
Engineered Barrier System Transport
Unsaturated Zone Transport
Saturated Zone Flow and Transport
Disruptive Events
Biosphere

Process Models

Unsaturated Zone Flow Model
Seepage Model
Near Field Geochemistry Model
In-Drift Environment Model
Multi-Scale Thermal Hydrological Model
Waste Package and Drip Shield Corrosion Model
Unsaturated Zone Transport Model
Saturated Zone Flow and Transport Model
Volcanic Eruption Model

Site and Design Information

Site Description Document
Repository Design
Waste Package Design
Laboratory Data
In-Situ Data
Analog Data



abq0063G059.ai

Figure 6-17. Major Sources of Information Used in the Development of the TSPA-SR

c15

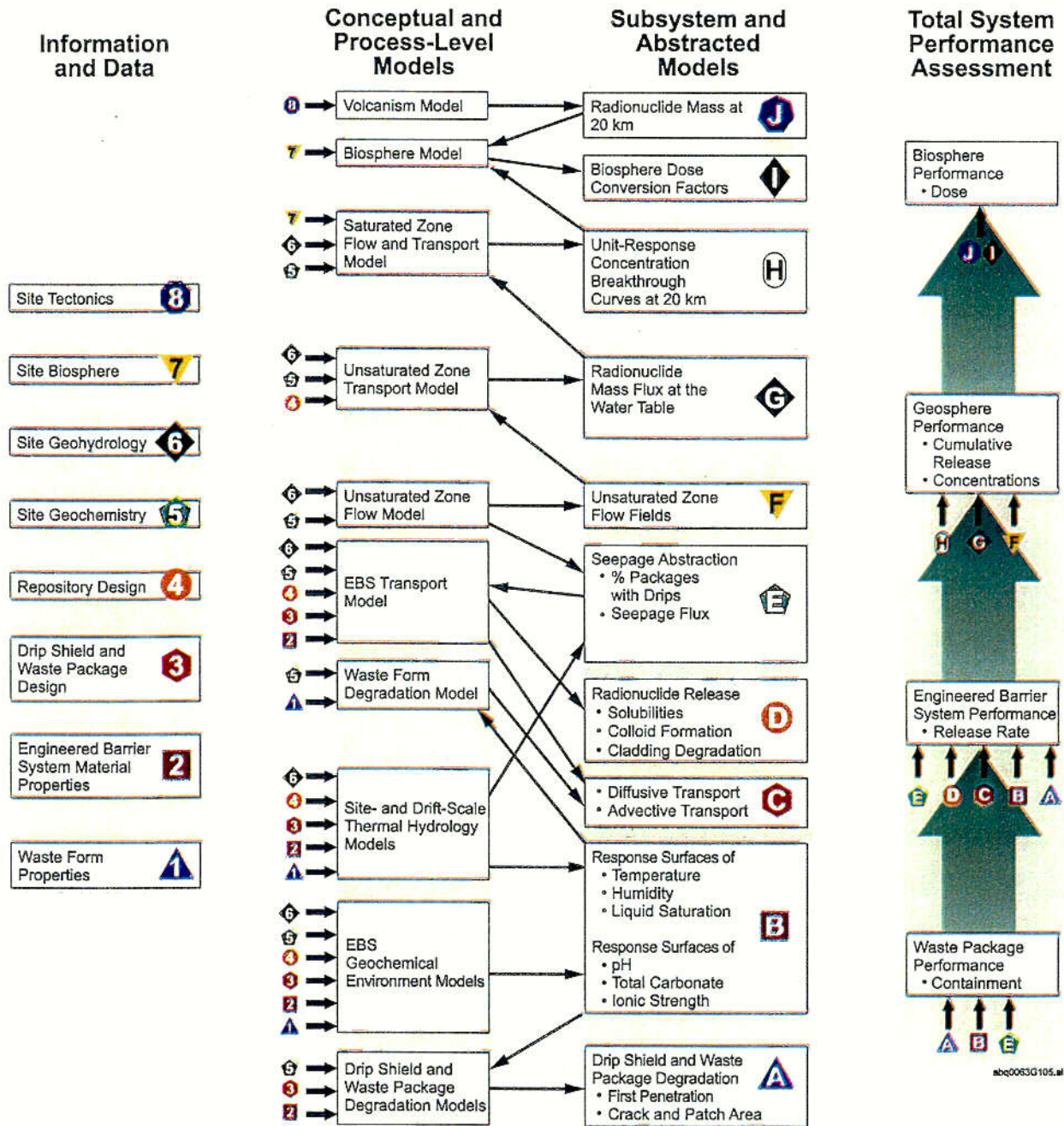
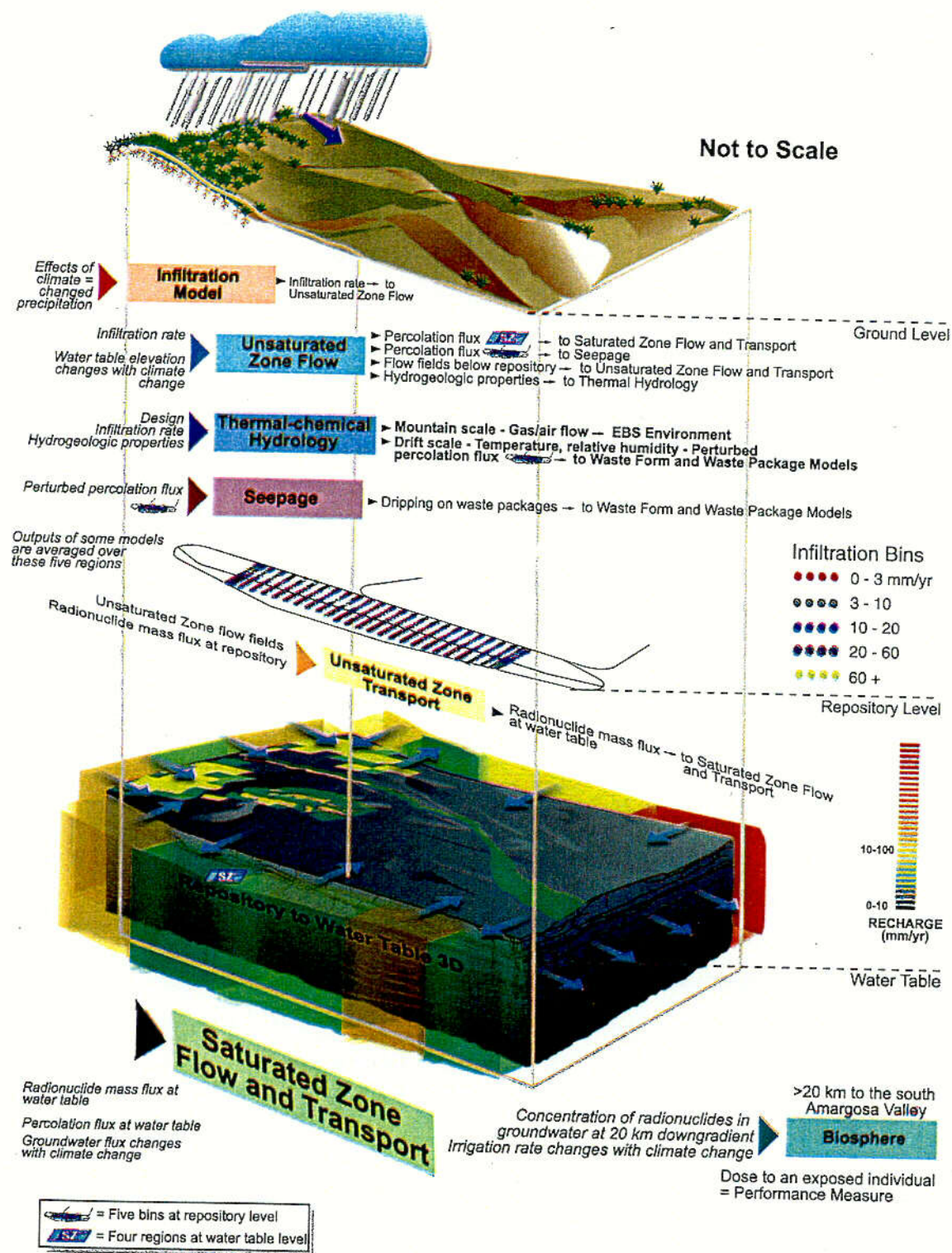


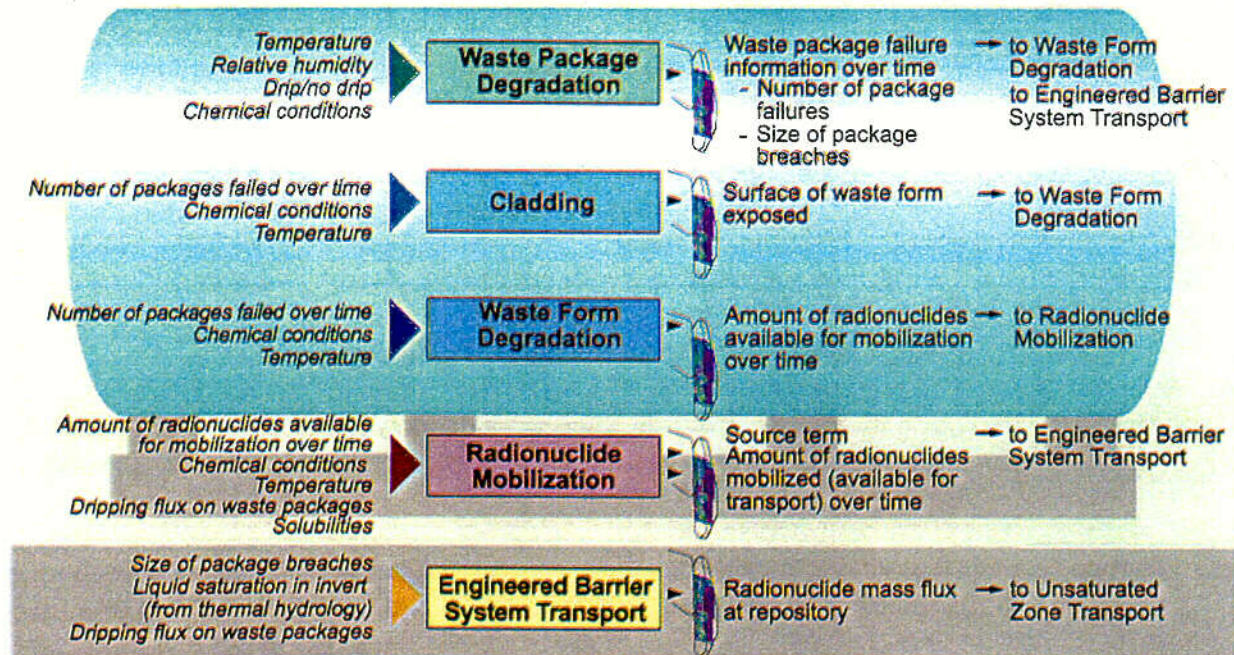
Figure 6-18. Simplified Representation of Information Flow in the TSPA-SR between Data, Process Models, and Abstracted Models



NOTE: The Figure is in two parts with the detail of the waste package and waste form models shown in Figure 6-20.

Figure 6-19. Detailed Representation of Information Flow in the TSPA-SR

Waste Form and Waste Package Models



abq0063G285.ai



Figure 6-20. Detailed Representation of Information Flow in the Waste Form and Waste Package Models of the TSPA-SR

C18.

6.2.2 Model Architecture

The overall information flow, discussed in Section 6.2.1, forms the basis for the architecture of the TSPA-SR computer model. The executive driver program, or integrating shell, that links the various component models or codes is GoldSim 6.04.007 (Golder Associates 2000 [151202]; Golder Associates 2000 [143556]). GoldSim is a probabilistic sampling program that ties all the component models, codes, and response surfaces together in a coherent structure that allows for consistent parameter sampling among the component models. The GoldSim program is used to conduct either single- or multi-realization runs of the entire system. The latter realizations yield a probability distribution of dose rate in the biosphere that shows uncertainty in dose rate based on uncertainty in all the component models.

The GoldSim program is very flexible in representing various component processes in the total system model. The four ways that component models may be coupled into GoldSim, from most complex to least complex, include the following:

- External function calls to detailed process software codes, e.g., UZ transport software (FEHM) or waste package degradation software (WAPDEG)
- Cells, which are basically equilibrium batch reactors that, linked in series, can provide a reasonably accurate description of transport through selected parts of the system, e.g., EBS transport
- Response surfaces, which take the form of multidimensional tables representing the results of modeling with detailed process models before running the TSPA code, e.g., thermal-hydrology input, such as temperature and RH in the invert
- Functional or stochastic representations of a component model directly built within the GoldSim code, e.g., cladding degradation or BDCFs, respectively.

The method used for each TSPA-SR component model is described briefly below and in greater detail in the corresponding parts of Section 6.3.

As described above for the third coupling method, much of the computational work that goes into the TSPA-SR model is done outside of GoldSim, before running the actual total system computations. For example, the UZ flow fields were computed using Transport of Unsaturated Groundwater and Heat (TOUGH2) (Pruess 1991 [100413]), a three-dimensional, finite-volume numerical simulator, representing the entire UZ model domain (for the dual-permeability model). Other component models that were also run outside of GoldSim are shown in Figure 6-21. The results of these detailed process-level runs were provided as multidimensional tables that are read into GoldSim at run time. Examples of these multidimensional tables include (1) liquid flux and velocity fields for the UZ as a function x , y , z , t , and infiltration flux (and other uncertain UZ rock property parameters), and (2) temperature and RH versus time as a function of location within the repository.

Figure 6-21, in conjunction with Figure 6-18, provides a better understanding of the TSPA-SR model architecture, i.e., the actual computer codes used and the connections (information

transfer) between codes. The model architecture includes the component models run in the first time step (e.g., ASHPLUME and WAPDEG), those run in real time that are coupled to GoldSim (e.g., external function calls such as FEHM), and those contained directly in GoldSim (e.g., coupled cells representing EBS transport or imbedded tables representing the thermal-hydrologic responses). Based on the schematic information transfer shown in Figure 6-21, some response surfaces generated by codes external to GoldSim only provide data to other codes external to GoldSim. Other response surfaces, such as liquid saturation, temperature, and seepage flux, provide data directly into GoldSim as response surfaces that influence such things as waste form degradation rates. Not all couplings or models are shown in Figure 6-21, (e.g., in-drift geochemical modeling is too complex to show all of its aspects in this figure).

Coupling of the various component models is affected by the climate model, which impacts almost all other component models in one way or another because it alters water flow throughout the system. The climate change is treated as a sequence of step changes between three different climate states in the first 10,000 years; present-day climate (from 0 to 600 years), monsoon climate (about twice the precipitation of dry climate, from 600 to 2,000 years), and glacial transition climate (colder than monsoon but similar precipitation, from 2,000 to 1,000,000 years). These climate shifts are implemented as a series of steady-state flow fields in the UZ and SZ, including changes in the water table elevation. The water table rise is 120 m when the climate shifts from present-day to monsoon. It remains at this 120 m increase for the glacial transition climate. Within the GoldSim program, these climate transitions require coordination among the coupled component models because they must all simultaneously change to the appropriate climate state.

In general terms, the coding methods and couplings used for the major components are discussed below.

Mountain-Scale, UZ Flow is modeled directly with the three-dimensional, site-scale, UZ flow model (Section 6.3.1), using the volume-centered, integral-finite-difference, numerical flow simulator, TOUGH2 (Pruess 1991 [100413]). Steady-state, three-dimensional flow fields are generated for three different infiltration boundary conditions, three different climate states, and several values of rock properties. These “pre-generated” flow fields (i.e., developed externally and before the TSPA-SR model simulations) are then placed in a library of files to be read by the FEHM computer code for UZ transport during the real time GoldSim simulations. Fracture and matrix liquid fluxes, along with liquid saturation, rock properties, and grid dimensions, are passed to FEHM in these flow field tables. To generate the library of flow fields, the inverse model, ITOUGH2 (Finsterle et al. 1996 [100393]) is used to calibrate the model-predicted liquid saturations to field-measured liquid saturations in the matrix.² The three calibrations for the three different infiltration conditions and corresponding rock properties are conducted at present-day climatic conditions. For future-climate conditions, flow fields are generated based on the present-day climate calibrations. Climate change is modeled within TSPA-SR UZ calculations by a series of step changes in boundary conditions, meaning that different flow fields are provided at the appropriate time with the imposition of instantaneous pressure equilibrium. Based on the defined history of climate changes, the UZ flow field library is

² Actually, there are many other parameters used in these calibrations. See, for example, (CRWMS M&O 2000 [150824]). Unsaturated Zone Flow and Transport Model Process Model Report.

interrogated for a different flow field whenever a step change in climate is indicated. This change in a flow field is applied instantaneously to the transport model. The validity of this approach is discussed in Section 3.2.3 of *Total System Performance Assessment For The Site Recommendation* (CRWMS M&O 2000 [143665]). The UZ flow fields are also provided to the TOUGH2 drift-scale seepage models (see Section 3.2.4 of *Total System Performance Assessment For The Site Recommendation* (CRWMS M&O 2000 [143665])) and the corresponding UZ hydrologic property sets are passed to the drift-scale, thermal-hydrology model (see Section 3.3.3 of *Total System Performance Assessment For The Site Recommendation* (CRWMS M&O 2000 [143665])).

Seepage of Water into Emplacement Drifts (i.e., Drift-Scale, UZ Flow) is also modeled externally (Section 6.3.1.2) before the TSPA-SR model simulations using TOUGH2 on a finely discretized grid around the drift and then abstracted for use in GoldSim. Simulations are conducted over a heterogeneous fracture permeability field based on permeability measurements in the Exploratory Studies Facility (CRWMS M&O 2000 [142004] and CRWMS M&O 2000 [122894]) at a variety of percolation rates (from the mountain-scale, UZ flow model), and a variety of mean values and standard deviations for the fracture permeability distribution and the fracture "alpha" distribution. These simulations become an uncertain response surface of seepage flux into the drift as a function of percolation flux and a response surface of the number of packages that are dripped on (by seeps) as a function of percolation flux (Section 6.3.1).

Drift-Scale, UZ Thermal Hydrology is modeled with the finite-difference computer program NUFT (Nitao 1998 [100474]) in one, two, and three dimensions before the TSPA-SR model simulations. The multi-scale thermal-hydrology model uses a complicated set of embedded abstractions at different levels of spatial and process detail (e.g., conduction-only versus conduction and convection), as described in Section 6.3.2 (also see Section 3.3.3 of *Total System Performance Assessment For The Site Recommendation* (CRWMS M&O 2000 [143665]) and CRWMS M&O 2000 [149862]). *Multiscale Thermohydrologic Model*. Submit to RPC URN-0574). Outputs include, but are not limited to (see individual sections of Section 6.3 for more details):

- Waste package and drip shield surface temperatures and waste package and drip shield surface relative humidities for two different package types (average CSNF and average co-disposal) in each of the five infiltration bins. These values are provided to drip shield, waste package, solubility, and waste form component models in the TSPA-SR model.
- Invert temperature, invert RH, and invert liquid saturation in each of the five infiltration bins. These values are provided to the solubility, colloid, and EBS transport component models in the TSPA-SR model.
- Liquid flux at 5 m above the crown of the drift. This is provided to the seepage component model in the TSPA-SR model (CRWMS M&O 2000 [149860]).

EBS Environment (i.e., Drift-Scale Thermal Chemistry) is modeled with a response surface (Section 6.3.2.2). The dependent variables of the response surface are pH and ionic strength and the independent variables are relative humidity in the drift, the ratio of water flux into the drift to

water evaporation out of the drift, and the chemical boundary conditions at the drift wall (specifically, $p\text{CO}_2$) through time, which was developed in the drift-scale thermal chemistry AMR (CRWMS M&O 2000 [142022]). Equilibrium batch-reaction calculations with EQ3/6 (Wolery 1992 [100836]; Wolery and Daveler 1992 [100097]) are performed at several values of the independent variables to develop a response surface of drift pH and ionic strength versus time. The response surface is used in the solubility and colloid models within the TSPA-SR model (CRWMS M&O 2000 [127818]; CRWMS M&O 2000 [143569]; CRWMS M&O 2000 [125156]).

Drip Shield and Waste Package Degradation is modeled during TSPA-SR model simulations using the computer code WAPDEG (CRWMS M&O 2000 [151566]), which includes corrosion-rate variability both on a given package and from package-to-package (Section 6.3.3). WAPDEG is linked to the GoldSim code and runs at the start of each realization to provide output in the form of several tables containing the cumulative number of package/dripshield failures per time, average patch area per package/dripshield versus time, average crack area per package versus time, and average pit area per package versus time.

Cladding Degradation by physical-chemical processes such as creep rupture and localized corrosion (CRWMS M&O 2000 [147210]) is modeled within the TSPA-SR model using functional relationships. The Model yields percentage values for failed cladding versus time (exposed waste form area versus time) (Section 6.3.4.3). Other cladding degradation modes such as seismic-induced mechanical failure are also modeled within the TSPA-SR model (Section 6.3.4.3 and 6.3.9).

Waste Form Degradation is modeled as an equation within the TSPA-SR model using empirical degradation-rate formulas developed from available data and experiments for the three different waste form types: commercial spent nuclear fuel (CSNF), DOE-owned spent nuclear fuel (DSNF), and high-level glassified waste (HLW) (Section 6.3.4). Output from the waste form degradation component model is the mass of waste form exposed per time, including the partitioning of the mass into various transportable forms including dissolved, reversibly sorbed onto colloids, and irreversibly sorbed onto colloids (CRWMS M&O 2000 [143420]; CRWMS M&O 2000 [144164]; CRWMS M&O 2000 [144167]; CRWMS M&O 2000 [111880]; CRWMS M&O 2000 [125156]).

There are a number of waste form cells in the GoldSim program that correspond to different waste types, different percolation-flux environments at the drift wall, and different seepage into the drift. As described in Section 6.3.1, the repository is divided into five infiltration bins based on spatial variability in the percolation flux above the drift as derived from the thermal-hydrology multi-scale model. Three types of local seepage or dripping environments are defined within each of the percolation environments: always drip, intermittent drip, and no-drip. Furthermore waste packages are divided into two types: CSNF and co-disposal (DSNF plus HLW). Although the DSNF and HLW waste types can have separate degradation rates and inventories in the TSPA-SR model, because they are co-disposed in the same package, their waste-form releases are mixed in the waste form cell and they experience identical environmental conditions. Based on infiltration, seepage (dripping), and waste package type, there are $5 \times 3 \times 2 = 30$ different waste form cells defined in the TSPA-SR model, each representing a large fraction of the approximately 12,000 waste packages envisioned in the SR

design. There is one additional waste-form cell representing stainless-steel clad CSNF. This cell is conservatively placed in the always drip environment in the medium and high infiltration scenarios and in the no-drip environment for the low infiltration scenario. This brings the total number of waste form cells to 31.

The entire waste inventory is composed of hundreds of different radionuclides (CRWMS M&O 2000 [136383]). Of these hundreds, 26 were found to potentially give a high enough dose or a high enough groundwater concentration to warrant modeling in the base-case component models of the TSPA.³ Not all of these were tracked through all component models because of various assumptions, such as secular equilibrium. For example, only 19 were tracked through the UZ. See Section 6.3.4.1 for details on the radionuclide inventory and which radionuclides were tracked in which models.

EBS Transport is modeled directly within the TSPA-SR model at run time using the GoldSim code cells algorithm. Modeling of the EBS is based on an idealized representation (basically a linked series of equilibrium batch reactors) of drip shield, waste package, waste form, and invert, and how radionuclides move through them via diffusion and advection (Section 6.3.5). Output from EBS transport is radionuclide mass flux (for each of the modeled radionuclides) at each time step, passed during the TSPA model simulations to the directly coupled, three-dimensional, dual-permeability, FEHM particle tracker (LANL 1999 [146971]) used for UZ transport. As shown in Figure 6-19, the repository area is divided into five bins based on infiltration rates. The mass releases from these five source-term groups enter the corresponding grid blocks in FEHM (Section 6.3.6). At early times, when few packages have failed, the number of FEHM grid blocks receiving releases from the EBS is dependent upon the number of packages that have failed. Once the number of failed packages exceeds the number of grid blocks in FEHM, mass is released uniformly from the EBS to the UZ FEHM model (Section 6.3.6). EBS transport is a function of the cell environment, of which there are 31 different environments based on the previous discussion regarding the waste form model. There are two mechanisms of transport through the EBS, diffusion and advection (CRWMS M&O 2000 [129284]). These transport mechanisms are implemented in the GoldSim cells through parameters related to the connection area between cells, the input and output liquid fluxes of the cells, the dimensions of the cell and amount of material in the cell, and the environment in the cell. Both transport mechanisms depend on the radionuclide concentration in the cell, which can be constrained by radionuclide concentration limits (Section 6.3.4.5) (CRWMS M&O 2000 [143569]; CRWMS M&O 2000 [125156]).

UZ Transport is modeled at run-time using the directly coupled, three-dimensional, dual-permeability, finite-element code FEHM (LANL 1999 [146971]), which is accessed as an external function by the GoldSim program. Flow fields and property sets for the UZ are accessed directly by FEHM from table files external to GoldSim residing in the run directory. The UZ transport model is based on the UZ flow model and uses the same flow fields (generated by the TOUGH2 UZ flow code) and the same climate states (CRWMS M&O 2000 [123913]). Transport is modeled with the FEHM dual-porosity particle tracker in three dimensions

³ As implemented in GoldSim, the actual number of separate species tracked was 34. This was because the modeling of nuclides irreversibly sorbed onto colloids required the addition of 8 additional "fictitious" species (see Section 6.3.4.6): 7 irreversibly sorbed nuclides and 1 "colloid particle" species.

(CRWMS M&O 2000 [141418]). The FEHM particle tracker transports particles on the same TOUGH2 spatial grid as used in the UZ flow model (using the same material properties, infiltration, and liquid saturation). When the climate shifts, a new TOUGH2 flow field is provided from the run-time file directory, and the particles are assumed to be instantly traveling with the new velocities. In addition, for multi-realization runs, an uncertainty matrix of UZ transport property values is created before simulation time by the GoldSim program and then accessed by FEHM during the simulations. The FEHM code steps through the uncertainty matrix row by row, where each row represents one realization of the uncertain UZ transport parameters, including K_d s for each radionuclide (K_d is the ratio of the mass of a given radionuclide sorbed or residing on the immobile rock phase to the mass dissolved in the aqueous phase), matrix diffusion coefficients, dispersivity, and K_c values (K_c is the ratio of the mass of a given radionuclide sorbed or residing on colloidal particles to the mass dissolved in the aqueous phase) (CRWMS M&O 2000 [152773]). Output from the FEHM code at each time step is radionuclide mass flux from the fractures and matrix at the water table for each of the 19 radionuclides tracked through the UZ⁴. The location of these output grid points is a vertical function of the climate state, increasing in elevation for wetter climates.⁵ The fracture and matrix mass fluxes from FEHM are combined in four GoldSim mixing cells corresponding to each of the four SZ capture zones (Section 6.3.7), and then fed to the SZ convolution integral, SZ_CONVOLUTE, at each TSPA-SR model time step.

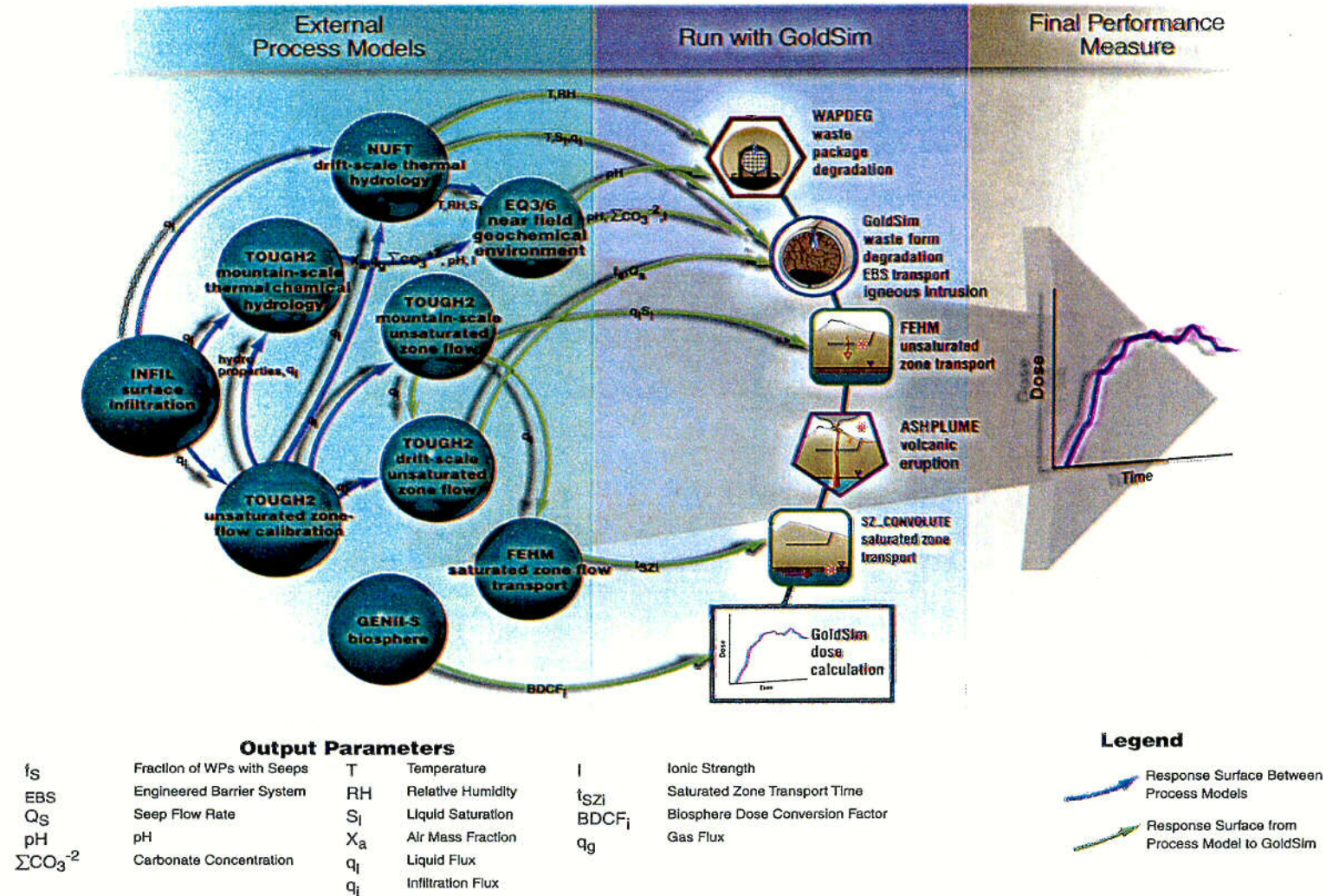
Saturated Zone Transport is modeled for most radionuclides by three-dimensional, dual-continuum, flow-and-transport simulations using the FEHM computer program and the associate SZ particle tracking algorithm (Section 6.3.7) (CRWMS M&O 2000 [139440]). Four sets of 3-D simulations are conducted based on the four source regions in the SZ beneath the repository. These flow and transport simulations are performed outside the GoldSim program for each of the selected radionuclides over 100 realizations of uncertain SZ model parameters (CRWMS M&O 2000 [152773]). The uncertain parameters include effective porosity in the tuff and alluvium, K_d s in the tuff and alluvium, colloid K_c , longitudinal dispersivity, fraction of flow path in the alluvium, and others (see Section 6.3.7). Although 13 radionuclides are transported through the SZ component model in the TSPA-SR,⁶ some of them share similar enough properties (e.g., K_d s) that it was only necessary to simulate 8 radionuclides in the 3-D FEHM model used to produce the breakthrough curves, and then use the results of these 8 for the other 5. The eight are a nonsorbing solute (e.g., C-14), Tc, I, U, Np, an irreversible colloid, a Th/Pu/Am reversible colloid (modeled with Am sorption properties), and a Cs/Sr reversible colloid. Output from the 3-D FEHM simulations is concentration versus time at 20-km (12-mi) for a constant mass-release-rate source term. Based on 100 realizations of the input variables along with 4 source regions and 8 nuclides, 3200 simulations were performed. The resulting breakthrough curves reside in 32 files in the TSPA model run time directory and these breakthrough curves are accessed when needed by the SZ_CONVOLUTE external function (which convolves, or integrates, the time-dependent source term with the pre-generated

⁴ Similarly to EBS transport through the GoldSim cells, 7 additional irreversible colloid species were tracked by FEHM. For example, transport of ²³⁹Pu required the modeling of two separate ²³⁹Pu species, ²³⁹Pu_{rev} and ²³⁹Pu_{irr}. This brought the actual total to 26 separate species tracked through the UZ (see Section 6.3.4.1 for more details).

⁵ An abrupt rise in water table, corresponding to a shift in climate state, results in a pulse of nuclides released from the UZ to SZ—the nuclide mass residing in the vertical distance of UZ suddenly overtaken by the water table.

⁶ Similarly to the EBS and UZ, 7 additional irreversible colloid species are also tracked through the 3-D SZ model, making the actual total equal to 20 in the 3-D SZ model (see Section 6.3.4.1 for more details).

unit breakthrough curves) called by the GoldSim program. The remaining 6 radionuclides tracked through the SZ (recall that 19 are tracked through the UZ) are modeled with the 1-D pipe model in the GoldSim code. This is necessary because these six radionuclides are daughters in a decay chain and SZ_CONVOLUTE cannot model chain decay.



abq0063G324.ai

Figure 6-21. TSPA-SR Model Code Architecture: Information Flow Among Component Computer Codes

C19

Biosphere Transport is modeled within TSPA-SR using biosphere dose-conversion factors (BDCFs) that convert SZ radionuclide concentration to individual radiation dose rates (Section 6.3.8) (CRWMS M&O 2000 [144054]; CRWMS M&O 2000 [144055]; CRWMS M&O 2000 [143378]). The BDCFs are developed outside the GoldSim program using a computer program named GENII-S (Leigh et al. 1993 [100464]). The BDCFs are then entered as table values in the TSPA model. These BDCFs are multiplied by the concentrations from the SZ models to compute individual doses, which are the end product of the TSPA calculations.

Disruptive Events, specifically igneous activity (both eruptive and intrusive volcanic effects), are modeled in a separate scenario from the nominal scenario (Section 6.3.9) (CRWMS M&O 2000 [139563]). Seismic activity is modeled in the cladding component model. Intrusive volcanism (also called indirect igneous activity) is modeled using the same components as the nominal-scenario TSPA groundwater release model. Eruptive volcanic activity (also called direct igneous activity, i.e., radionuclides carried through the atmosphere directly to the receptor) is modeled using the code ASHPLUME (LaPlante and Poor 1997 [101079]), which is directly coupled to the TSPA model and executed at run time. ASHPLUME is the first external code executed by the GoldSim code during a realization. Its time stepping and results are essentially independent of the actual TSPA model simulation that uses the cells and the external calls to FEHM and SZ_CONVOLUTE. The entire time history of the ASHPLUME results is generated prior to taking the first timestep with the rest of the TSPA model. (A similar description applies to WAPDEG, which is called just after ASHPLUME.)

Human Intrusion is also analyzed in a separate scenario from the nominal scenario. Modeling of human intrusion is consistent with the stylized scenario defined by the regulations, proposed 10 CFR Part 63 (64 FR 8640 [101680]) and proposed 40 CFR Part 197 (64 FR 46976 [105065]). The human intrusion model is developed within the TSPA-SR model utilizing GoldSim cell and pipe algorithms to calculate release and transport of radionuclides for various conditions of waste package breaches due to human intrusion. It uses the same SZ model as the nominal scenario (with the addition of two more short-lived radionuclides, ^{137}Cs and ^{90}Sr), but different UZ and EBS models (Section 6.3.9.3).

6.3 COMPONENTS OF THE TSPA MODEL

The Yucca Mountain total system model is divided into individual parts. These parts are delineated and defined by both physical-chemical processes and by the spatial location in the repository where the processes occur. Collectively, these individual parts of the TSPA analysis are called component models. The assumption is made that the components can be treated separately if a consistent set of boundary conditions and scenarios are rigorously maintained among all the related components.

The major component models, and some of their associated submodels, are illustrated in the context of the geologic setting and engineered barriers of the potential Yucca Mountain repository in Figure 6-22 (CRWMS M&O 2000 [143665], Figure 1.8-1). Submodels represent a further division of the major component models. These submodels can exist at various levels of complexity and computational detail. For example, submodels of the UZ flow and transport component model include a conceptual climate submodel based on interpretation of past climates, a numerical infiltration submodel that explicitly simulates relevant processes at Yucca

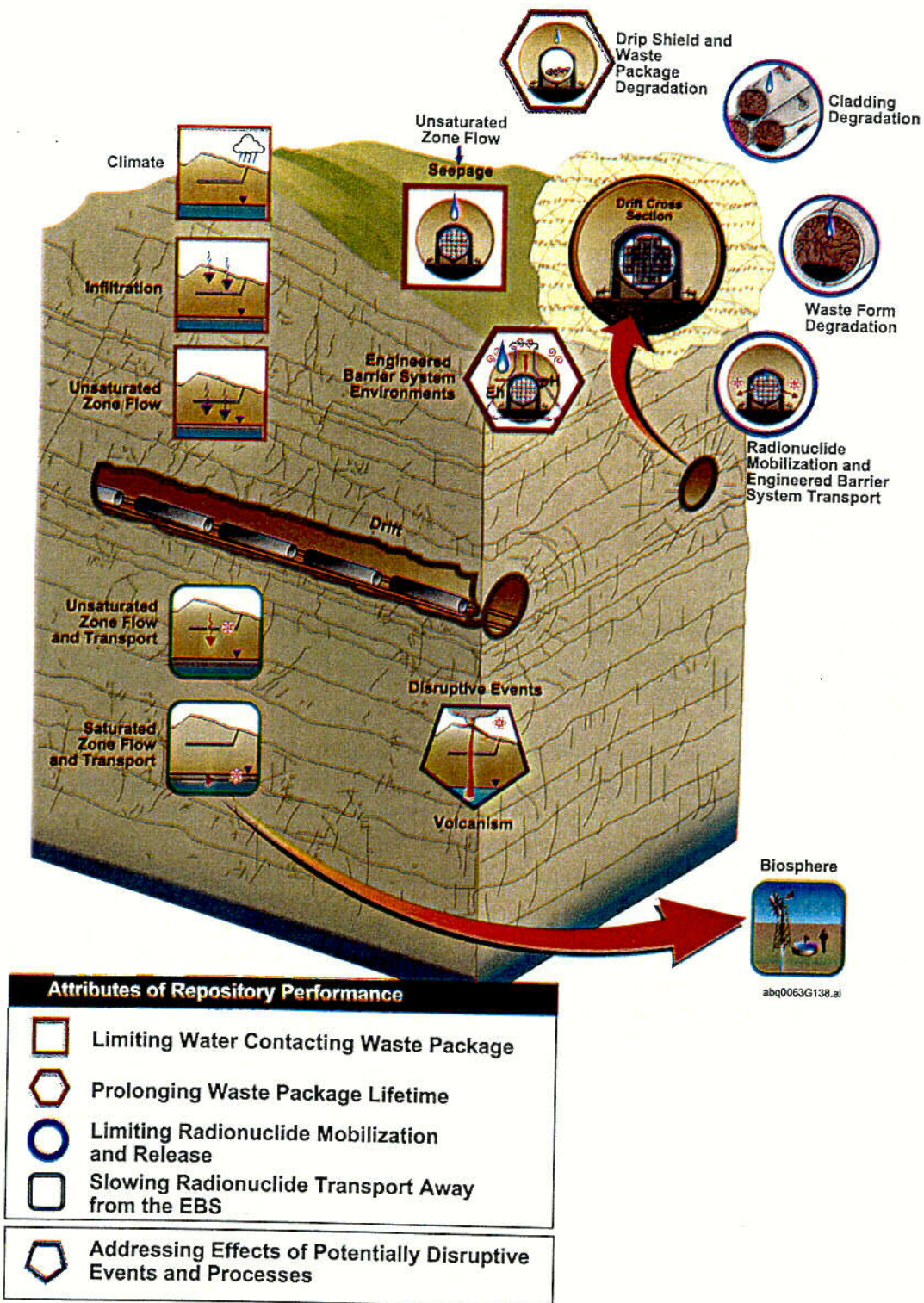
Mountain, and an ambient (i.e., not thermally perturbed) seepage submodel that uses detailed numerical calculations to support parameter distributions used in a simplified TSPA abstraction (CRWMS M&O 2000 [143665], Section 3).

The model components and factors related to limiting the amount of water contacting the waste package, the first attribute of repository performance, include climate, infiltration, UZ flow, mountain-scale and drift-scale coupled processes (including thermal hydrology), seepage (into the drift and through degraded drip shields), in-drift geochemical environment, and degradation of the drip shield. Together, these components define the temporal and spatial distribution of water flow through the unsaturated tuffs above the repository at Yucca Mountain and the temporal and spatial distribution of water seeps onto the waste packages. There could be short- or long-term (thousands to tens of thousands of years) climate variations. In addition, the thermal regime generated by the decay of the radioactive wastes can mobilize connate water over the first hundreds to thousands of years. For these reasons, the amount of water flowing in the rock and seeping onto the waste packages is expected to vary with time (CRWMS M&O 2000 [143665], Section 3.3).

The model components related to long waste package lifetime, the second attribute of repository performance, include all the above components plus waste package degradation. Together, these components define the spatial and temporal distribution of the times when waste packages are expected to breach. These thermal, hydrologic, mechanical, and geochemical processes acting on the surface of the waste packages are the most important environmental factors affecting the waste package corrosion rate.

The model components related to slow mobilization and release of radionuclides from the EBS, the third performance attribute, include all the above components plus coupled processes within the package (including seepage through the package), waste form degradation (including cladding degradation for CSNF), radionuclide mobilization (including dissolved concentration limits and colloid associated concentrations), and radionuclide transport through the EBS. Together, these components lead to a determination of the spatial and temporal distribution of the mass of radioactive wastes released from the waste packages. (CRWMS M&O 2000 [143665], Section 3).

The model components related to transport away from the EBS (i.e., through the natural barriers and biosphere), the fourth attribute of repository performance, include all the above components plus radionuclide transport through the UZ and SZ, dilution from pumping, and radionuclide transport in the biosphere. Together, these components determine the spatial and temporal variation of radionuclide concentrations in groundwater. The groundwater concentration ultimately yields the mass of radionuclides that may be ingested or inhaled by individuals exposed to that groundwater, which in turn causes a level of radiological dose or risk associated with that potential exposure. Radionuclide transport may occur by advection (radionuclide movement which occurs with the bulk movement of the groundwater) or diffusion (radionuclide movement which occurs because of a concentration gradient). The concentration depends on the mass release rate of the radionuclides and the volumetric flow of water along the different pathways in the different components.



NOTE: Shown are the individual component models and submodels that together must be analyzed in evaluating the behavior of the Yucca Mountain repository system. These components comprise the individual building blocks of the TSPA analysis. The components are correlated to the four attributes of repository performance.

Figure 6-22. Major Components of the Total System Performance Assessment Model

C20

Each of the above attributes of repository performance and TSPA model components are used to describe the nominal behavior of the Yucca Mountain repository system. In addition, other Features, Events, and Processes (FEPs) can occur that could alter the behavior of the system. However, these FEPs have a sufficiently low probability of occurring over the period of interest that they are usually not considered in the nominal behavior. They may essentially be classified as unanticipated processes and events. An example of such a disruptive event is igneous activity (see Section 6.3.9).

The following sections (Sections 6.3.1 through 6.3.9) address the conceptualization of nine component models and submodels that were developed for the TSPA-SR model (eight for the nominal scenario, plus one for the disruptive scenario that utilizes all of the other eight) and the implementation of these components into the performance assessment analyses. Each component of the TSPA-SR model is described in four subsections:

- Overview
- Inputs to the Performance Assessment Model
- Implementation in the Performance Assessment Model
- Results and Verification.

A general overview of each component model is given, then the inputs to each component model and the details of the component model implementation into the TSPA-SR model are described. Attachment I provides a description of the GoldSim graphical elements that are shown in the implementation subsections. Results from a median value simulation are presented for each component model (where appropriate), and those results are verified by checking them against the results expected from the AMR(s) that developed the component model.

6.3.1 Unsaturated Zone Flow

Unsaturated zone flow at Yucca Mountain affects repository performance in several ways. Some of the more important effects include the amount of liquid seeping into emplacement drifts, transport time for radionuclides traveling from breached packages to the water table, and the timing and degree of geochemical effects resulting from the decay heat of the packages.

Four components of UZ flow are considered in the TSPA: climate, infiltration, mountain-scale unsaturated zone flow, and seepage into repository emplacement drifts. These components include processes at several scales. At the global scale is climate, including changes in solar heating caused by changes in the earth's orbit and inclination, and formation of ice sheets during glacial periods. There are also important regional-scale climate effects, such as the "rain shadow" caused by the Sierra Nevada mountain range and the proximity of the polar jet stream, that make climate variations at Yucca Mountain different from the global average. Infiltration and flow through the mountain, or mountain-scale UZ flow, are modeled at the scale of the site. These two site-scale models includes effects of surface topography and subsurface hydrogeologic layering. At the drift scale, a seepage model (CRWMS M&O 2000 [142004]) was developed to evaluate the interaction of percolating water with an emplacement drift (approximately 5.5 m in diameter) and the amount of water that seeps into the drift. Processes at the scale of individual fractures, in particular those affecting fracture-matrix coupling (fluid flow between fractures and the porous rock matrix) are important both to seepage and mountain-scale

flow. Processes within individual fractures are not modeled explicitly, but are represented by parameters in the dual-continuum flow models. Some of the important processes for unsaturated zone flow are pictured in Figure 6-23. The following subsections summarize the climate, infiltration, seepage, and UZ flow models and their implementation into the TSPA model.

A much more complete description of the conceptual models described here is given in TSPA-SR Technical Document (CRWMS M&O 2000 [143665]).

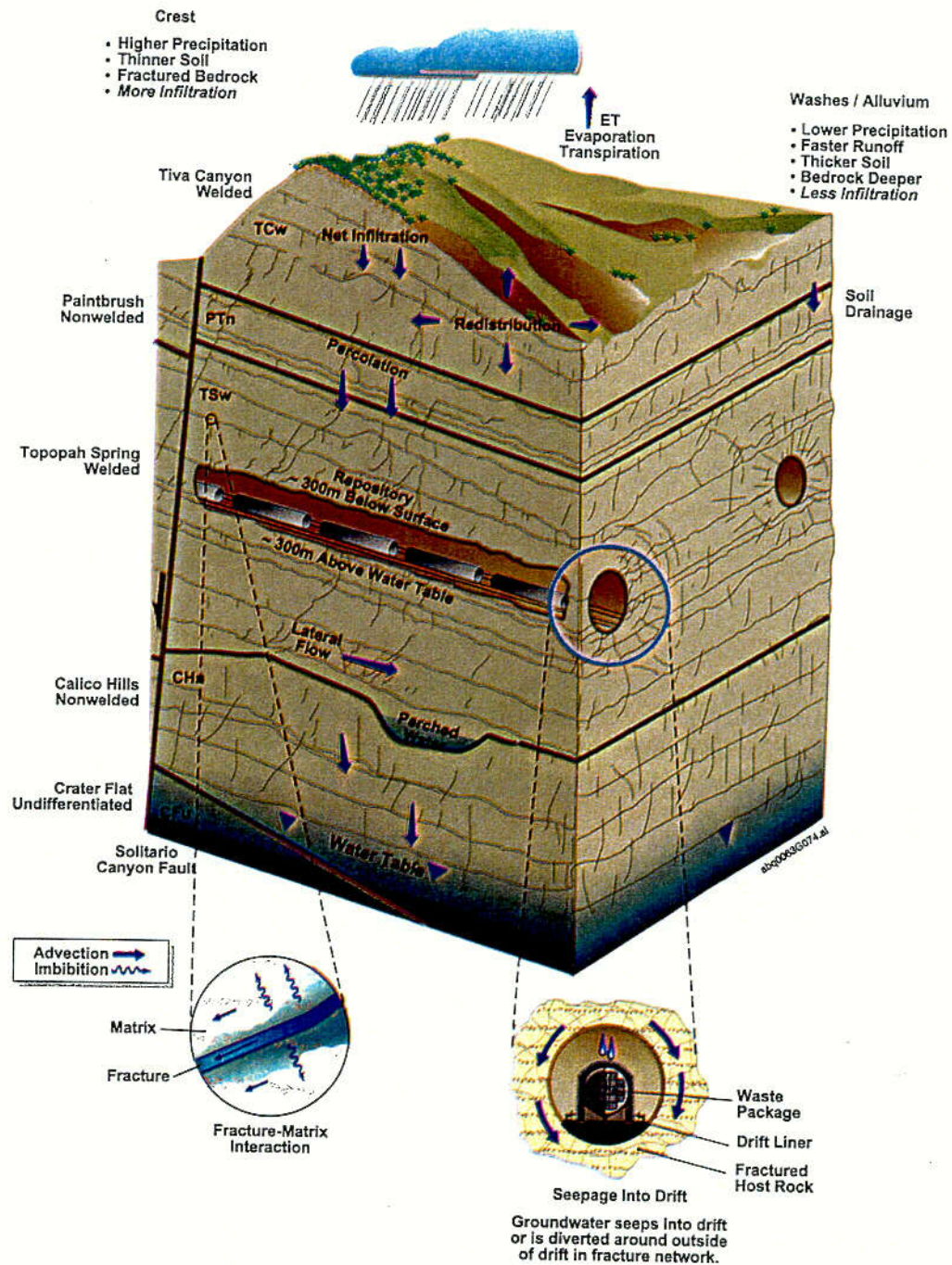


Figure 6-23. Conceptual Drawing of Unsaturated Zone Flow Processes at Different Scales

6.3.1.1 Climate and Infiltration

Overview

Analysis of past climatic data, such as mean annual and seasonal precipitation, and mean annual and seasonal air temperature, was used to estimate the nature of future climates at Yucca Mountain. Forecasting the timing of future climate change requires identification of a past climate sequence believed to be part of a cycle that will repeat itself in the future (see 5.3.1.1, assumptions 1 through 4). In the base-case TSPA-SR model the future climate at Yucca Mountain over the 10,000-year regulatory period is treated as a sequence of three distinct states: present-day or modern, monsoon, and glacial-transition. Each climate state is defined in terms of climate analogs, which are present-day sites with climates like those projected for Yucca Mountain in the future. The monsoon climate is somewhat warmer than present with a potential to be significantly wetter; in particular, having more summer rain. The glacial-transition climate is cooler than present-day and possibly significantly wetter, with relatively cool, dry summers and cool, wet winters (CRWMS M&O 2000 [145774], Section 3.5.1.4). In order to capture the uncertainty in future climate, upper-bound and lower-bound analogs have been defined for each future climate state, with the upper bound representing wetter conditions and the lower bound representing drier conditions, *Total System Performance Assessment For The Site Recommendation* (CRWMS M&O 2000 [143665], Table 3.2-1).

Since climate is a large-scale phenomenon, no spatial variability of climate is included in the Yucca Mountain TSPA-SR model. Temporal variability is included as a sequence of climate states, as described above. The TSPA base case does not include uncertainty in climate durations. However, many uncertainties do exist that may affect the timing of the three climate states. Nevertheless, the uncertainty in the time of climate change can be neglected in the TSPA because it has little impact on the dose results. In the current TSPA model, the waste packages are so robust that there are no failures for over 10,000 years, which makes climate-change uncertainties of a few hundred years, or even a few thousand years, insignificant. In the TSPA for the Viability Assessment, effects of uncertainty in climate-change time were investigated and found to be unimportant (DOE 1998 [100550], Volume 3, Section 5.1.1).

Net infiltration is the penetration of water through the ground surface to a depth where it can no longer be withdrawn by evaporation or transpiration by plants. Once water has entered bedrock or has penetrated below the root zone in soil, it has infiltrated. The conceptual model used for infiltration calculations is based on evidence from field studies at Yucca Mountain, combined with established concepts in soil physics and hydrology. The overall framework of the conceptual model is provided by the hydrologic cycle, including processes on the surface and just below the surface that affect net infiltration (see Section 3.2.2 of *Total System Performance Assessment For The Site Recommendation*, CRWMS M&O 2000 [143665]).

In order to represent infiltration uncertainty in TSPA simulations, three infiltration “maps” (spatially distributed net infiltration rates over the surface of Yucca Mountain) were generated for each of the three climate states. They are termed the low-, medium-, and high-infiltration cases. For present-day climate, the medium-infiltration case was developed using the best estimates for precipitation, temperature, etc.; the high-infiltration case was developed by including precipitation data from one of the wetter nearby meteorological stations (on Rainier

Mesa); and the low-infiltration case was developed by selectively choosing low infiltrations for each spatial location from a set of infiltration simulations. For future climates, the low-infiltration cases were simulated using the lower-bound climate analogs, the high-infiltration cases were simulated using the upper-bound climate analogs, and the medium-infiltration cases were developed from the low- and high-infiltration maps by averaging them at each spatial location.

In order to include the three infiltration cases for each climate state into TSPA simulations, it is necessary to estimate their relative probability or likelihood. The probabilities were derived by means of a detailed analysis of infiltration uncertainty using the Monte Carlo method. The uncertainty analysis focused on 12 key input parameters, for which uncertainty distributions were developed. The key parameters include precipitation, bedrock and soil hydrologic properties, and potential evapotranspiration. The infiltration model was run 100 times, with each realization having different sampled values of the 12 key parameters. The glacial-transition climate was used for the analysis, because that climate state is in effect most of the time, and it is in effect at later times when radionuclide releases are more likely. Probabilities for the three infiltration cases were assigned in such a way as to make the log mean and standard deviation of the three-point discrete distribution (i.e., the distribution consisting of the three infiltration cases with defined probabilities) equal to the log mean and standard deviation of the distribution from the Monte Carlo simulation. Log values were used in deriving the weighting factors because the distribution has a more normal shape in log space than in linear space (CRWMS M&O 2000 [145774], Sections 3.5.2.6 and 3.5.3.2).

Inputs to the TSPA model

The inputs to the TSPA climate model are listed in Table 6-1. The inputs consist of the duration of each climate state forecasted to occur during the next 10,000 years, from the present day climate to a warmer and wetter monsoonal climate, and then to a cooler and wetter glacial-transition climate. The climate abstraction AMR does provide ranges to represent the uncertainty in the length of the climate analog period (USGS 2000 [136368], Section 7); however, the upper values of those ranges were used in the TSPA-SR model for the reasons discussed above in the Overview section. Also, note that the climate discussions in the climate AMR are limited to 10,000 years in the future. In the TSPA-SR model, when longer periods are modeled, the glacial-transition climate is simply extended throughout the additional period (up to 1,000,000 years).

Table 6-1. Climate State Durations Used in the TSPA Model

Parameter Name	Description	Parameter Value	Reference AMR
Climate_State	Present-day climate	Duration of 600 years	ANL-NBS-GS-000008, Future Climate Analysis, Section 6.6.1 (USGS 2000 [136368])
Climate_State	Monsoonal Climate	Duration of 1,400 years	ANL-NBS-GS-000008, Future Climate Analysis, Section 6.6.1 (USGS 2000 [136368])
Climate_State	Glacial-transition	remainder of simulation	ANL-NBS-GS-000008, Future Climate Analysis, Section 6.6.1 (USGS 2000 [136368])

DTN: GS000308315121.003 [151139]

The weighting factors or probabilities for the lower, medium, and high infiltration cases were calculated in the *AMR Analysis Of Infiltration Uncertainty* (CRWMS M&O 2000 [143244], Section 6.3). The calculated weighting factors are given in Table 6-2. These factors are applied regardless of the climate state, i.e., the same infiltration probabilities apply in each of the three climate states—present day, monsoon, or glacial transition. Note that for the median value case analyzed in this TSPA-SR Model document, the median value infiltration map is the medium case.

Table 6-2. Infiltration Case Weighting Factors Used in the TSPA Model

Parameter Name	Description	Parameter Value (probability)	Reference AMR
Infiltration_Scenario	Low infiltration case (index = 1)	0.17	ANL-NBS-HS-000027, Analysis Of Infiltration Uncertainty, Section 6.3, Table 2 (CRWMS M&O 2000 [143244], Table 6-2)
Infiltration_Scenario	Medium infiltration case (index = 2)	0.48	ANL-NBS-HS-000027, Analysis Of Infiltration Uncertainty, Section 6.3, Table 2 (CRWMS M&O 2000 [143244], Table 6-2)
Infiltration_Scenario	High infiltration case (index = 3)	0.35	ANL-NBS-HS-000027, Analysis Of Infiltration Uncertainty, Section 6.3, Table 2 (CRWMS M&O 2000 [143244], Table 6-2)

DTN: SN0003T0503100.001 [149556]

Implementation

The climate model is implemented in the TSPA model using a single selector element (switch). The selector element chooses a climate state based on elapsed time since waste emplacement in the repository. If the elapsed time is less than 600 years, then the selector state is equal to 1, which corresponds to the present-day climate. If the elapsed time is less than 2,000 years, but greater than or equal to 600 years, then the selector state changes to 2, which corresponds to a monsoonal climate state. For times greater than or equal to 2,000 years, the selector state changes to 3, which corresponds to a glacial-transition climate state. Figure 6-24 shows the selector element, *Climate_State*, used to implement climate state in the TSPA-SR model.

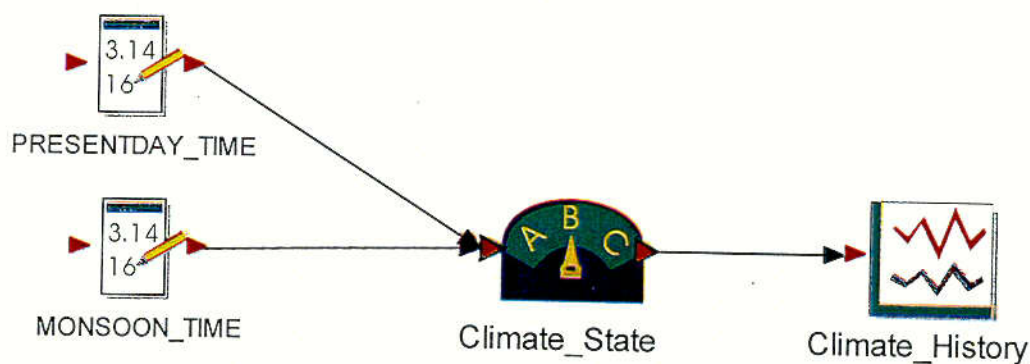
The TSPA implementation of the weighting factors for the lower, medium, and high infiltration cases is simply a stochastic element that is defined as a discrete distribution, *Infiltration_Scenario*, as shown in Figure 6-25.

Results and Verification

To show that the climate model is implemented correctly, a 10,000-year expected value simulation was run. Figure 6-26 shows the time history output from the climate selector over the 10,000 year simulation time.

The time history result shown in Figure 6-26 for the climate state selector shows that for the first 600 years the selector state is 1, which corresponds to the present-day climate state as defined in the switch. At 600 years, the selector state changes from 1 to 2, which corresponds to a monsoonal climate state. At 2,000 years, the selector state changes from 2 to 3, which indicates a glacial-transition climate state. This result is the desired result as discussed above in the overview section, and in the *Future Climate Analysis* AMR (USGS 2000 [136368], Section 7). Thus, the climate state selector is working correctly. The climate selector does not receive input from any other models.

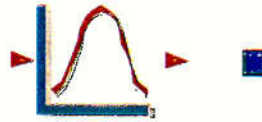
The weighting factors for the lower, medium, and high infiltration cases are implemented simply as a stochastic element that is defined as a discrete distribution, and therefore, there is no calculation or results. Figure 6-25 showed a graph of the discrete probability distribution function as defined in GoldSim, *Infiltration_Scenario*, which corresponds to the weighting factors given in Table 6-2 above and in the AMR *Analysis Of Infiltration Uncertainty* (CRWMS M&O 2000 [143244], Table 7-1). Thus, the infiltration case weighting factors are implemented correctly. The infiltration case weighting factors do not receive input from any other models. In the TSPA-SR Model, these three infiltration cases (corresponding to maps of spatially variable infiltration rates across the surface of the mountain) are used primarily to select the correct 3-D UZ flow field (Section 6.3.6) and the correct thermohydrology tables (Section 6.3.2.1) and seepage tables (Section 6.3.1.2). In fact, the parameter *Infiltration_Scenario*, links to 137 other parameters in the Total System Model.



NOTE: See Attachment I for Explanation of the Symbols.

Figure 6-24. A Graphical Illustration of the TSPA Model Implementation of the Climate Model

C 22



Infiltration_Scenario

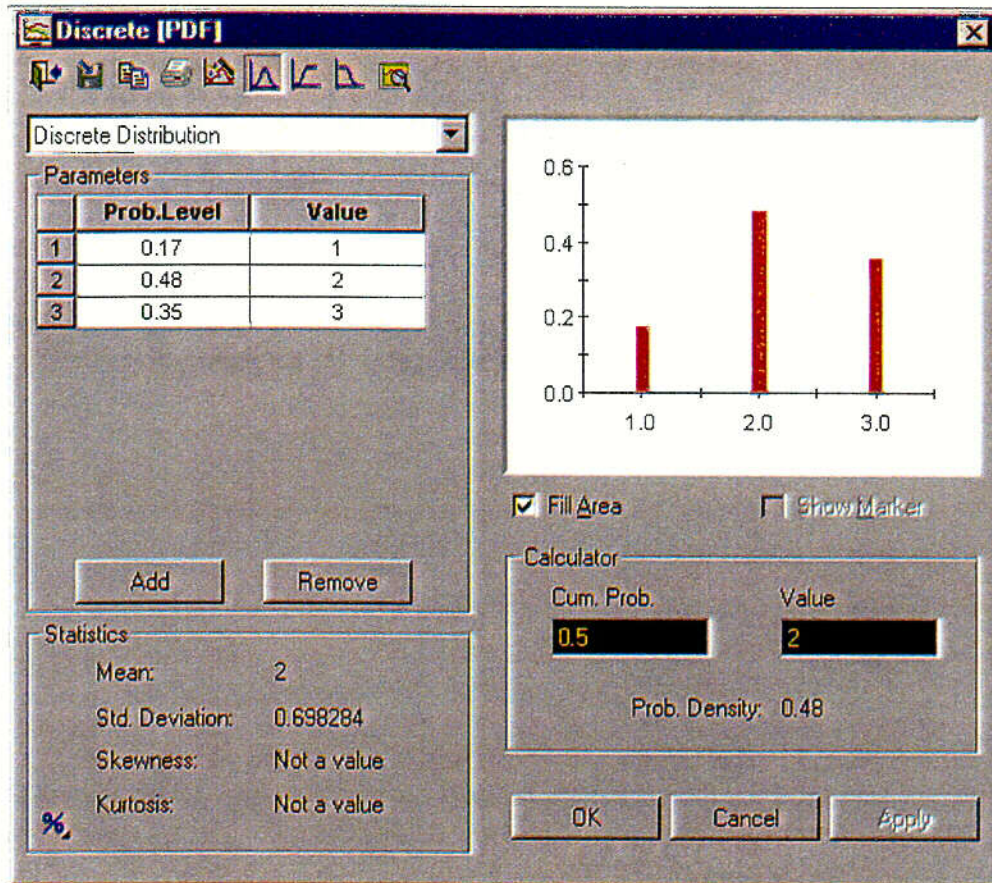


Figure 6-25. TSPA Implementation of the Infiltration Rate Map Weighting Factors

C23

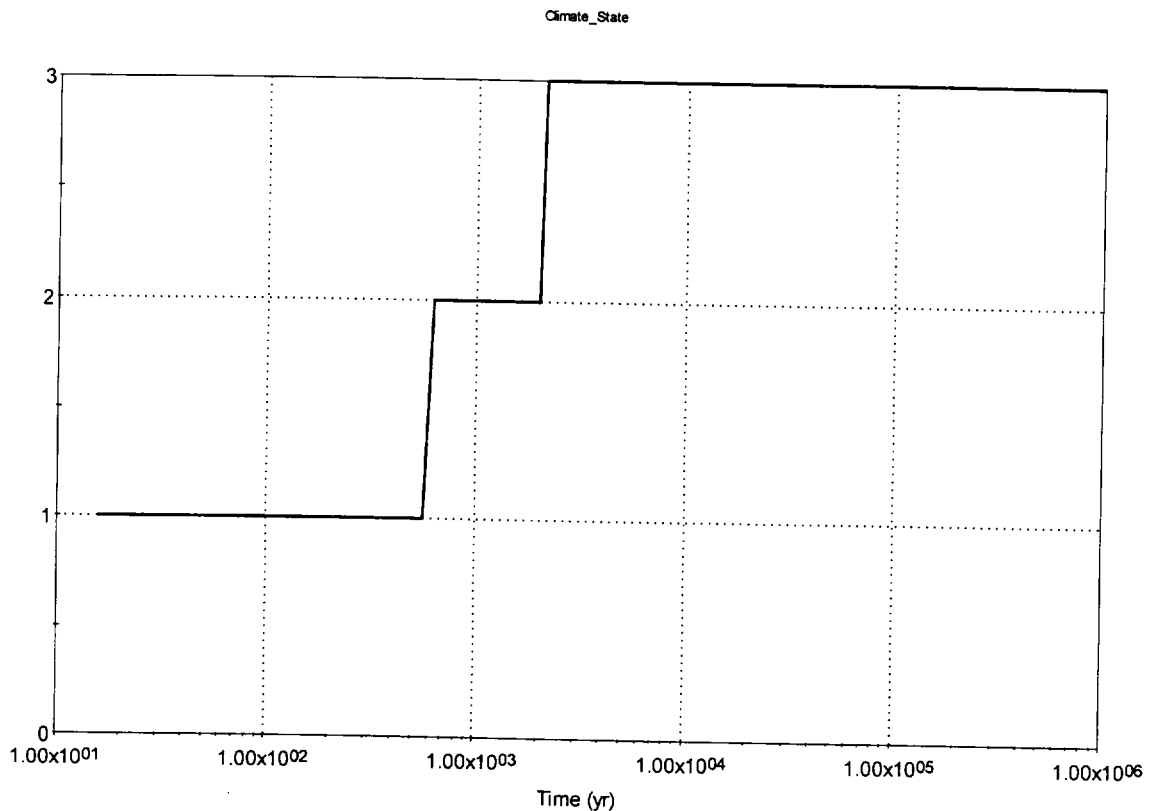


Figure 6-26. Result of a Simulation of the Climate State Model

6.3.1.2 Seepage into Drifts

Overview

Seepage into the repository drifts is an important factor in total system performance due to its potential to contribute to the degradation of the engineered barrier system. The function of the seepage portion of the TSPA-SR model is to calculate the seepage fractions (the fraction of waste packages experiencing seepage) and the seepage flows (the amount of seepage onto a dripshield and potentially into a waste package). This information is then used by the model to calculate waste form degradation and engineered barrier system (EBS) transport. A probabilistic approach was used to calculate drift seepage due to both spatial and temporal variability and inherent uncertainty in the flux of water from the geologic material overlying the repository into the repository drifts.

For the TSPA-SR model, the repository was divided into 610 spatial locations for the no-backfill case or 623 spatial locations for the backfill case (CRWMS M&O 2000 [149860], Section 6.2). However, for computational efficiency, within GoldSim the waste packages are separated into five "infiltration bins," based on the infiltrations at the 610 or 623 locations. The calculation of seepage into drifts is a function of the percolation flux at each spatial location, but then the seepage results are averaged over the five infiltration bins, as described in the remainder of this section. Glacial-transition infiltration is used to determine the categorization into bins because

the glacial-transition climate is in effect during most of a TSPA-SR simulation, and during later times when radionuclide releases are more likely. Monsoon and present day climates, on the other hand, are only in effect at early times in the simulations. For a complete discussion of the three climate states, see Section 6.3.1.1 Climate and Infiltration.

The basis for selection of the infiltration bins is discussed here and summarized in Table 6-3. Three sets of seepage distributions are defined for the seepage abstraction: a lower-bound (minimum) case, a most-likely (peak) case, and an upper-bound (maximum) case (CRWMS M&O 2000 [142004], Section 6.4). Each of those cases has a percolation-flux threshold, below which there is no seepage. The thresholds are 3.4 mm/year for the upper-bound case, 9.9 mm/year for the most likely case, and 97.9 mm/year for the lower bound case (see Table 6-4). Note that a lower threshold implies more seepage, which is why the upper-bound case has the lowest threshold. The first two bin boundaries (3 mm/year and 10 mm/year) were rounded from the upper-bound and most-likely seepage thresholds. Few of the 610 or 623 spatial locations within the repository are in areas where the percolation flux is greater than the 97.9-mm/yr threshold. Therefore, the lower-bound seepage threshold was not used for defining bin boundaries. Instead, the remaining two bin boundaries (20 mm/yr and 60 mm/yr) were primarily chosen to differentiate between the three infiltration cases: low, medium, and high. Complete differentiation is not possible since the infiltration distributions for the low, medium, and high cases overlap considerably.

Table 6-3. Basis for Selection of Infiltration Bins

Infiltration Bin Number	Infiltration Bin Boundaries (flux in mm/year)	Based on Seepage Threshold	Overlap of distribution of waste packages in the bins for low, medium, and high infiltration cases ** Higher proportion of waste packages * Lower Proportion of waste packages		
			Low	Medium	High
1	0-3	Yes (3.4 mm/year upper boundary)	**	*	
2	3-10	Yes (9.9 mm/year most likely boundary)	**	*	*
3	10-20	No		**	*
4	20-60	No		**	**
5	>60	No		*	**

In summary, infiltration bins 1 through 5 were specified based on percolation flux values of 0-3 mm/year, 3-10 mm/year, 10-20 mm/year, 20-60 mm/year, and > 60 mm/year, respectively (see Table 6-3). For these bin definitions, all percolation flux data for realizations with low infiltration fall within the first two bins (i.e., between 0 and 10 mm/year). Percolation flux data for realizations with medium infiltration fall predominately in the third and fourth bins but some fall within the other three bins as well. Percolation flux data for realizations with high infiltration fall mostly in the fourth and fifth bins but some also occur in the second and third bins (CRWMS M&O 2000 [149860], Table 5). A complete discussion of how the spatial locations and bins were used in the calculation of seepage into drifts can be found in the Implementation Section and in Attachment II.

The calculation of drift seepage is also a function of the waste package type. Although the fuels have several different waste package configurations, the number of configurations included in the model was limited for computational efficiency by modeling two basic waste package types: a representative waste package for CSNF and a representative waste package for Co-Disposed (CDSP) DSNF and DHLW glass (see Section 6.3.4.1 Radionuclide Inventory). The distinction in types was made for the seepage calculations because the two types of waste have separate percolation flux data due to their differences in heat output.

Inputs to the TSPA-SR model

Within the TSPA-SR model, calculation of seepage into the drifts is performed using the external program seepdll (model element Seepage, see Figure 6-27). This program requires nine input parameters plus the percolation flux versus time data for each waste package type, infiltration scenario, and spatial location. Seepdll also requires a listing of the names of the files containing the percolation flux data.

The nine input parameters for seepdll are:

- The seepage fraction, f_s
- The mean seep flow rate for locations with seepage, μ_{Q_s}
- The standard deviation of the seep flow rate for locations with seepage, σ_{Q_s}
- The flow-focusing factor, F
- Two random seeds
- The seepage uncertainty factor, R
- The infiltration scenario
- The backfill case.

The first three input parameters (f_s , μ_{Q_s} , and σ_{Q_s}) are functions of the percolation flux, q . The seepage fraction defines the probability that seepage flow occurs at a waste-package location. The seep flow rate, Q_s , is the volumetric flow rate of seepage in a drift segment. These three input parameters are uncertain and are represented in the TSPA-SR model as triangular distributions as described in the supporting AMR, *Abstraction of Drift Seepage* (CRWMS M&O 2000 [142004], Section 6.4). Because these three parameters are a function of the percolation flux, q , their uncertainty distributions are also a function of the percolation flux. As discussed in CRWMS M&O 2000 [142004], Sections 6.2.3 and 6.4, a triangular distribution represents the most significant features of the uncertainty in f_s , μ_{Q_s} , and σ_{Q_s} . The minimum, peak, and maximum values for the distributions as a function of q are provided in Table 6-4. These distributions are not directly included in the TSPA-SR model as model elements but rather are contained in files that are external to the model and are read directly by seepdll.

Table 6-4. Uncertainty in Seepage Fraction, Mean Seep Flow Rate, and Seep Flow Rate Standard Deviation as a Function of Percolation Flux

q (mm/yr)	Minimum Value			Peak Value			Maximum Value		
	fs	Mean Qs (m3/yr)	Std.Dev. Qs (m3/yr)	fs	Mean Qs (m3/yr)	Std.Dev. Qs (m3/yr)	fs	Mean Qs (m3/yr)	Std.Dev. Qs (m3/yr)
3.4	0	0	0	0	0	0	0	0	0
5	0	0	0	0	0	0	1.97×10^{-3}	3.21×10^{-3}	3.16×10^{-3}
9.9	0	0	0	0	0	0	3.00×10^{-2}	1.30×10^{-2}	1.39×10^{-2}
14.6	0	0	0	2.45×10^{-3}	7.95×10^{-3}	7.09×10^{-3}	5.75×10^{-2}	2.26×10^{-2}	2.45×10^{-2}
73.2	0	0	0	0.250	0.106	0.198	0.744	0.404	0.409
97.9	0	0	0	0.292	0.354	0.366	0.779	0.917	0.733
213	4.91×10^{-3}	0.284	0.188	0.487	1.51	1.15	0.944	3.31	2.24
500	6.01×10^{-2}	0.992	1.05	0.925	5.50	4.48	0.999	13.0	5.74
549.2	6.96×10^{-2}	1.11	1.20	1	6.19	5.05	1	14.6	6.33
5383.4	1	13.0	15.7	1	73.4	61.1	1	177	65.2

Source: DTN: SN9912T0511599.002 [146902], Excel spreadsheet Seep-sr.xls.

The remaining six input parameters are directly included in the TSPA-SR model as model elements. The flow-focusing factor, the two random seeds and seepage uncertainty are found in the drift seepage portion of the model (see Figure 6-27). The infiltration scenario is found in the Climate and Infiltration portion of the model (see Section 6.3.1.1), and the backfill case is found in the Simulation Settings portion of the model (see Section 6.4). In addition to the discussion below, Table 6-5 provides a brief description, the value, the reference AMR, and the DTN for each of these parameters.

Table 6-5. SEEPDLL Input Parameters Directly Implemented in GoldSim

Parameter Name	Description	Parameter Value	Reference AMR	DTN
Flow_Focus_Low	Flow focusing factor for low infiltration scenario, lower bound of log uniform distribution	1	CRWMS M&O 2000 [142004], Section 6.3.3.2	SN9912T0511599.002 [146902]
Flow_Focus_Low	Flow focusing factor for low infiltration scenario, upper bound of log uniform distribution	47.3	CRWMS M&O 2000 [142004], Section 6.3.3.2	SN9912T0511599.002 [146902]
Flow_Focus_Mean	Flow focusing factor for medium infiltration scenario, lower bound of log uniform distribution	1	CRWMS M&O 2000 [142004], Section 6.3.3.2	SN9912T0511599.002 [146902]
Flow_Focus_Mean	Flow focusing factor for medium infiltration scenario, upper bound of log uniform distribution	22.4	CRWMS M&O 2000 [142004], Section 6.3.3.2	SN9912T0511599.002 [146902]

Table 6-5. SEEPDLL Input Parameters Directly Implemented in GoldSim (Continued)

Parameter Name	Description	Parameter Value	Reference AMR	DTN
Flow_Focus_High	Flow focusing factor for high infiltration scenario, lower bound for log uniform distribution	1	CRWMS M&O 2000 [142004], Section 6.3.3.2	SN9912T0511599.002 [146902]
Flow_Focus_High	Flow focusing factor for high infiltration scenario, upper bound for log uniform distribution	9.7	CRWMS M&O 2000 [142004], Section 6.3.3.2	SN9912T0511599.002 [146902]
Seep_Uncertainty	Seepage uncertainty lower bound for uniform distribution	0	NA – not data	NA – not data
Seep_Uncertainty	Seepage uncertainty upper bound for uniform distribution	1	NA – not data	NA – not data
Random_Seed_1	Random number passed from GoldSim to seepdll. Used to set the random seed used in seepdll.	Uniform distribution Min = 1 Max = 231-1	NA – not data	NA – not data
Random_Seed_2	Random number passed from GoldSim to seepdll. Used to set the random seed used in seepdll.	Uniform distribution Min = 1 Max = 231-1	NA – not data	NA – not data
Infiltration_Scenario	Stochastic distribution of different infiltration scenarios: low, medium and high	See Section 6.3.1.1	See Section 6.3.1.1	See Section 6.3.1.1
Backfill_Case	Flag for backfill case	See Section 6.4	See Section 6.4	See Section 6.4

The flow focusing factor, F , takes into account the focusing of flow that occurs on intermediate scales (tens of meters) in a heterogeneous system. The estimate of flow focusing is based on the “active-fracture” conceptual flow model (Liu et al. 1998 [105729]) and is discussed in the supporting AMR (CRWMS M&O 2000 [142004], Section 6.3.3). Flow focusing (i.e., the channeling of flow into discrete fractures or fracture sets) in the unsaturated zone may affect seepage into the drifts and result in higher percolation fluxes in some locations, thereby increasing the amount of seepage in those areas. This is in contrast to homogeneous flow that results in an even distribution of percolation fluxes and seepage. Application of F has the effect of reducing the seepage fraction and increasing the seep flow rate at seepage locations from values that would have been obtained without focusing (CRWMS M&O 2000 [142004], Section 6.3.3.2).

The flow-focusing factor is uncertain and is represented by a log-uniform distribution. Separate distributions for F are provided for the low, medium, and high infiltration cases CRWMS M&O 2000 [142004], Section 6.3.3.2. For all infiltration cases, the minimum value for

the distribution is 1. The maximum values are 47.3, 22.4, and 9.7 for the low, medium, and high infiltration rates, respectively (DTN: SN9912T0511599.002 [146902]).

The seepage uncertainty, R , is the random number used to evaluate the triangular distributions for f_s , μ_{Q_s} , and σ_{Q_s} . R is represented by a uniform distribution varying from 0 to 1. Note that a DTN is not required for this parameter because it does not meet the QARD definition of data. For this reason, no DTN is given for this parameter in Table 6–5. The infiltration scenario (discussed in Section 6.3.1.1) is used by seepdll to determine which percolation flux histories and flow-focusing factor to use for the seepage calculations.

The parameters Random_Seed_1 and Random_Seed_2 are used by seepdll to determine the random number r , which is used to represent the spatial variability in seepage (see the Implementation section). They are uniform distributions varying between 1 and $2^{31}-1$ (the maximum 32-bit integer). These parameters also do not meet the QARD definition of data. Therefore, DTNs are not required for them.

The percolation flux at the drift wall is highly perturbed due to both the capillary barrier formed by the drift opening and by thermal dry-out. Therefore, the flux some distance above the drift is preferable. The flux at 5 m above the drift was used in the seepage model. This distance is great enough to avoid the capillary-barrier perturbation and most of the thermal dryout, but is close enough to the drift that there is significant drainage of thermally mobilized water.

Percolation flux versus time histories are available for the 623 locations (backfill case) or 610 locations (no backfill case) within the repository at a distance of 5m above the drift. The percolation flux time histories are taken from DTN: SN9912T0511599.002 [146902]. These data are separated by waste package type to account for the differences in the two types of packages. Thermal effects on seepage are accounted for by using the flux time histories from the thermal-hydrology abstraction (CRWMS M&O 2000 [149860] Section 6.3) as the input into the seepage abstraction. Only the fracture component of the percolation flux was taken from the thermal-hydrology model because the seepage model includes only fracture flow (capillary forces are strong enough to prevent matrix flow from seeping into drifts). Although flux time history data are available at numerous locations, seepdll averages the seepage calculations across all locations within a bin; the spatial information is not used by the downstream models.

The percolation flux history data are separated by infiltration scenario. The low, medium, and high infiltration scenarios have flux data in bins 1 and 2, all five bins, and bins 2 through 5, respectively. The total number of percolation flux histories used by the seepage model is 22, 11 for each waste package type.

Implementation

The flow focusing factor is determined within GoldSim from four model elements: *Flow_Focus_Low*, *Flow_Focus_Mean*, *Flow_Focus_High*, and *Flow_Focus* (see Figure 6–27). The first three elements contain the distributions of the flow-focusing factor for the low, medium, and high infiltration scenarios, respectively. The fourth element is a selector switch that determines which flow-focusing factor will be used in a realization based on the infiltration scenario. For example, if the infiltration scenario is 1 (i.e., low infiltration), the sampled value

from *Flow_Focus_Low* will be used for the flow focusing factor in the seepage calculations. Recall that the flow focusing factor is used to account for focusing of flow above the drifts due to flow channeling in fractures. Therefore, seepdll (1) increases the percolation flux by the flow focusing factor: $q' = Fq$ and (2) reduces the seepage fraction by the flow focusing factor: $f_s' = f_s/F$ (CRWMS M&O 2000 [142004], Section 6.3.3.2).

As discussed in the input section, the input parameters f_s , μ_{Q_s} , and σ_{Q_s} are represented by triangular distributions as functions of the percolation flux. These distributions are not directly included in the TSPA-SR model as model elements but rather are implemented as a set of 1-D look-up tables contained in files external to the model and read directly by seepdll. At each timestep, seepdll (1) reads the percolation flux, q , from the appropriate history data-set based on the infiltration scenario for the realization and the waste package type, (2) multiplies that flux by the flow focusing factor, F , to get the flux, q' , and (3) looks up the values of f_s , μ_{Q_s} , and σ_{Q_s} for that modified flux. If the values for these three parameters are needed for a q' other than one included in the tables, seepdll uses linear interpolation to determine the parameter values.

The triangular distributions for f_s , μ_{Q_s} , and σ_{Q_s} are correlated because the underlying uncertainty for all three parameters is due to the uncertainty in hydrologic properties of the fractures around the drifts. The input parameter seepage uncertainty, R , provides the random number used to evaluate the triangular distributions for seepage fraction, mean seep flow, and seep flow standard deviation. Because the seepage uncertainty is determined only once during a realization, the same random number is used to sample the triangular distributions for every timestep. Seepage uncertainty is generated by GoldSim using the stochastic element *Seep_Uncertainty* (see Figure 6-27).

A second random number, r , is sampled internally by seepdll. This random number is used to represent the spatial variability in seepage and is regenerated each time the program begins to process a new location. In order to produce a unique, reproducible random number (r) for each realization, two random seeds, *Random_Seed_1* and *Random_Seed_2*, are passed to seepdll. The distributions for two random seeds (see Figure 6-27) are generated in GoldSim and accessed by seepdll. The values of *Random_Seed_1* and *Random_Seed_2* are used to set the random seed in seepdll (see Attachment II). Passing the random seeds from GoldSim ensures that each realization has a unique pair of reproducible seeds, which in turn means the spatial variability has 1246 or 1220 (backfill and no backfill cases, respectively) separate values in each realization (one for each of the spatial locations times the two fuel types).

The function of the sampled mean seep flow rate and seep flow rate standard deviation is to determine the range and shape of a beta distribution. That beta distribution is then sampled to determine the seepage flow if the location was previously determined to have seepage. Determination of whether a location has seepage or not is discussed in the following paragraph. The beta distribution is assigned a minimum value of zero, since seepage flow cannot be less than zero. As long as a large value is used for the maximum in the beta distribution, the particular value chosen will not have a significant effect on the sampled value. Thus, the maximum value was set equal to the sampled mean seep flow rate plus ten times the sampled value for the seep flow rate standard deviation. The sampled values for the mean seep flow rate and seep flow rate standard deviation are also used to determine the shape of the beta distribution. When the standard deviation is small compared to the mean, the beta distribution is

similar to a normal distribution. When the standard deviation is near the mean, the beta distribution is highly skewed and becomes more like an exponential distribution. The seepage flow is determined by randomly sampling from the beta distribution using the random number, r , that is internally generated by seepdll.

The following steps briefly summarize how seepdll calculates seepage flow and the fraction of waste packages that see seepage (see Attachment II for specific details on the calculations performed by seepdll).

- 1) A random number, R , uniformly distributed between 0 and 1, is generated by GoldSim element *Seep_Uncertainty*. This random number is used to represent the uncertainty in seepage due to the uncertainty in hydrologic properties around the drifts.
- 2) The flow focusing factor, F , is generated by GoldSim element *Flow_Focus* for the appropriate infiltration scenario.
- 3) For each location in the repository, the following steps are followed for each waste package type:
 - a) A random number, r , uniformly distributed between 0 and 1, is sampled internally by seepdll. This random number is used to represent the spatial variability in seepage and is regenerated each time the program begins to process a new location.
 - b) The flux is read from the appropriate history file.
 - c) The flux is multiplied by the flow focusing factor, $q' = Fq$.
 - d) The seepage fraction, f_s , is sampled from its triangular distribution using the random number R .
 - e) The seepage fraction is divided by the flow focusing factor, $f'_s = f_s/F$.
 - f) If the random number r is greater than or equal to the modified seepage fraction ($r \geq f'_s$), then the flow rate at that location for that time and waste package type is assigned a value of zero.
 - g) If the random number r is less than the modified seepage fraction ($r < f'_s$), then that location for that time and waste package type will have seepage and the seepage flow is determined as follows:
 - i) The random number r is re-scaled to $r' = r/f'_s$ so that r' is between 0 and 1.
 - ii) The mean seep flow rate, μ_{Qs} , and seep flow rate standard deviation, σ_{Qs} , are sampled from their triangular distributions using random number R .
 - iii) The beta distribution is developed using μ_{Qs} and σ_{Qs} .

- iv) The beta distribution is sampled for the seepage flow using random number r' .
- h) Repeat steps b through g for each time step.
- 4) Once step 3 has been completed for each location at each time for each waste package type, the following calculations are performed:
 - a) The seepage flow at each location is characterized. Locations can have:
 - i) zero seepage flow at all times (these are locations that never see seepage)
 - ii) non-zero seepage flow at some times (these are location that intermittently see seepage)
 - iii) non-zero seepage flow at all times (these are locations that always see seepage).

Note that the term “intermittent” does not necessarily imply that seepage flow turns on and off repeatedly, but only that flow takes place part of the time.

- b) For each bin at each time, an areal-weighted average of the seepage flow for all locations with the same seepage history (i.e., intermittent or always) is calculated for each waste package type.
- c) For each bin, the fraction of locations that see the different seepage histories (i.e., never, intermittent, or always) is calculated for each waste package type.

The results from step 4b are fed from seepdll to GoldSim and stored in container *Seepage_Flux_multi* (see Figure 6–27) which is used for multiple realizations. The contents of this container are graphically illustrated in Figure 6–28. As shown in this figure, seepdll outputs a set of 1-D tables for always and intermittent seepage into bins 1 through 5 for both waste package types. A total of 20 time versus seepage flow tables are output by seepdll. An analogous second set of look-up tables under backfill and no backfill conditions for median values of time versus seepage flow are contained in *Seepage_Flux_median* (see Figure 6–27), and are not output from seepdll, but are fixed. The median values in these tables were obtained by running the seepage model as a stand-alone GoldSim model for 300 realizations for both the backfill and no backfill case. The median curves were then extracted and placed into the look-up tables for the TSPA-SR model. The 20 median value time versus seepage tables for each case (backfill and no backfill) are depicted in Figure 6–29 and Figure 6–30. The selector switches in the *Seepage_Flux* container (see Figure 6–31) determine which set of tables values are used based on input from *Simulation_Settings* (see Section 6.4).

The seepdll results from step 4c are stored by GoldSim in container *Seepage_Fraction* (see Figure 6–27). The contents of this container are graphically illustrated in Figure 6–32. Seepdll outputs multiple realization data on the fraction of waste packages that always see seepage (*SeepFrac_Al_multi*) and intermittently see seepage (*SeepFrac_In_multi*). The fraction of waste packages that never see seepage (*SeepFrac_ND_multi*) is calculated as one minus the fractions

that always and intermittently see seepage. Each of these data elements contains the fraction of both CSNF and CDSP waste packages in each infiltration bin that see the respective seepage.

Seepage fractions for backfill and no backfill median value cases are contained in the *Median_Seep_Fractions* container (see Figure 6–33). The seepage fractions for *SeepFrac_Al_median_bf*, *SeepFrac_In_median_bf*, *SeepFrac_Al_median_nbf*, and *SeepFrac_In_median_nbf* were obtained by running the seepage model as a stand-alone GoldSim model for 300 realizations. The seepage fraction values for *SeepFrac_Al_median* and *SeepFrac_In_median* are set equal to either the backfill or no backfill median seepage fraction values based on the value of *Backfill_Case*. The *SeepFrac_ND_median* is then calculated as one minus the fraction that always and intermittently see seepage.

Either the multiple realization values or the median seepage fraction values are chosen by the *SeepFrac_Always*, *SeepFrac_Intermittent*, and *SeepFrac_ND* elements depending on case input from *Simulation_Settings* (see Section 6.4).

Results and Verification

The verification of correct functioning of links, calculations, and selector switches as well as the results is demonstrated in the following paragraphs.

The drift seepage abstraction defines distributions for the flow focusing factor in the three infiltration scenarios: *Flow_Focus_Low*, *Flow_Focus_Mean*, and *Flow_Focus_High*. The *Flow_Focus* switch receives infiltration scenario data from the Climate and Infiltration portion of the model and determines the flow-focusing factor appropriate to the scenario. To verify the distributions in the model are correct, they were compared to the values provided in the abstraction and were found to be identical. Verification of the proper selection of the flow-focusing factor is demonstrated by the following analysis.

The switch *Flow_Focus* is directed to choose the flow-focusing factor based on the following logic statements:

```
If Infiltration_Scenario==1 then Flow_Focus_Low
else if Infiltration_Scenario==2 then Flow_Focus_Mean
else Flow_Focus_High
```

Table 6–6 shows the seepdll input parameters generated by GoldSim. Included in this table is the seepdll input value of 2 for *Infiltration_Scenario*. This indicates that the correct flow-focusing factor chosen by the switch should be taken from the distribution for *Flow_Focus_Mean* and should have a value of 4.73286.

Table 6-6. SEEPDLL Input Parameters Generated by Median Value, One Million-Year Simulation

Seepdll Input Parameters Generated By GoldSim	Median Value Simulation Results
Infiltration_Scenario	2
Random_Seed_1	1.07374 e+009
Random_Seed_2	1.07374 e+009
Flow_Focus	4.73286
Seep_Uncertainty	0.5

The input data listed in Table 6-6 were verified to have been accessed by seepdll from GoldSim by verifying the links between seepdll and GoldSim. Verification of the transfer of the information produced by seepdll to the *Seepage_Fraction* container and the 20 table elements in the *Seepage_Flux_median* container was performed in the same manner. The links between the elements within the *Seepage_Fraction* container have also been verified to be correct.

Recall that seepage flux values are either taken from the *Seepage_Flux_median* container or the *Seepage_Flux_multi* container, depending on whether a median-value or multiple-realization case is being run.. The switch selectors contained in the *Seepage_Flux* container select the seepage flux values from the appropriate container based on the logic statements below and the fact that *Median_Value_Run* = 1 and *Backfill_Case* = 0 (see *Simulation_Settings*, Section 6.4) for this median value simulation. For example, switch *SeepFlux_In_CSNF_3* contains the following logic:

```

If      Median_Value_Run==0 then SeepFlux_In_CSNF_3_multi
Elseif  Median_Value_Run==1 and Backfill_Case==0 then
        SeepFlux_In_CSNF_3_median_nbf
else    SeepFlux_In_CSNF_3_median_bf

```

Verification that the correct selections were made by the switches (see Figure 6-31) is demonstrated by the fact that the switches selected values from the tables in the *Seepage_Flux_median* container (see Figure 6-29) for time = 1E6 years, which is appropriate for this median value, million-year simulation.

The median value simulation results (the values actually selected by the switches) with their corresponding selector switch names are shown in Table 6-7. The median value tables within the *Seepage_Flux_median* container (from which the switches selected the values) are listed by name along with their corresponding values for time = 1E6 years in Table 6-7. A comparison of the values in Table 6-7 shows that they are identical and are therefore correct. The median value simulation results show that there are no waste packages that always see seepage and that most of the waste packages do not see any seepage the median case.

Table 6-7. *Seepage_Flux_Switch* Input Parameters Generated by the Median Value, No Backfill Simulation at One Million Years

Selector Switch Name	Median Value No Backfill Simulation Results m ³ /yr]	Seepage_Flux_median Container	
		Table Name	Value at t=1E6 yrs [m ³ /yr]
SeepFlux_AI_CS NF_1	0	SeepFlux_AI_CS NF_1_median	0
SeepFlux_AI_CS NF_2	0	SeepFlux_AI_CS NF_2_median	0
SeepFlux_AI_CS NF_3	0	SeepFlux_AI_CS NF_3_median	0
SeepFlux_AI_CS NF_4	0.48208	SeepFlux_AI_CS NF_4_median	0.48208
SeepFlux_AI_CS NF_5	0	SeepFlux_AI_CS NF_5_median	0
SeepFlux_In_CS NF_1	0	SeepFlux_In_CS NF_1_median	0
SeepFlux_In_CS NF_2	0.00978	SeepFlux_In_CS NF_2_median	0.00978
SeepFlux_In_CS NF_3	0.11349	SeepFlux_In_CS NF_3_median	0.11349
SeepFlux_In_CS NF_4	0.96564	SeepFlux_In_CS NF_4_median	0.96564
SeepFlux_In_CS NF_5	0	SeepFlux_In_CS NF_5_median	0
SeepFlux_AI_CDSP_1	0	SeepFlux_AI_CDSP_1_median	0
SeepFlux_AI_CDSP_2	0	SeepFlux_AI_CDSP_2_median	0
SeepFlux_AI_CDSP_3	0	SeepFlux_AI_CDSP_3_median	0
SeepFlux_AI_CDSP_4	0.53622	SeepFlux_AI_CDSP_4_median	0.53622
SeepFlux_AI_CDSP_5	0	SeepFlux_AI_CDSP_5_median	0
SeepFlux_In_CDSP_1	0	SeepFlux_In_CDSP_1_median	0
SeepFlux_In_CDSP_2	0.01018	SeepFlux_In_CDSP_2_median	0.01018
SeepFlux_In_CDSP_3	0.10770	SeepFlux_In_CDSP_3_median	0.10770
SeepFlux_In_CDSP_4	1.02400	SeepFlux_In_CDSP_4_median	1.02400
SeepFlux_In_CDSP_5	0	SeepFlux_In_CDSP_5_median	0

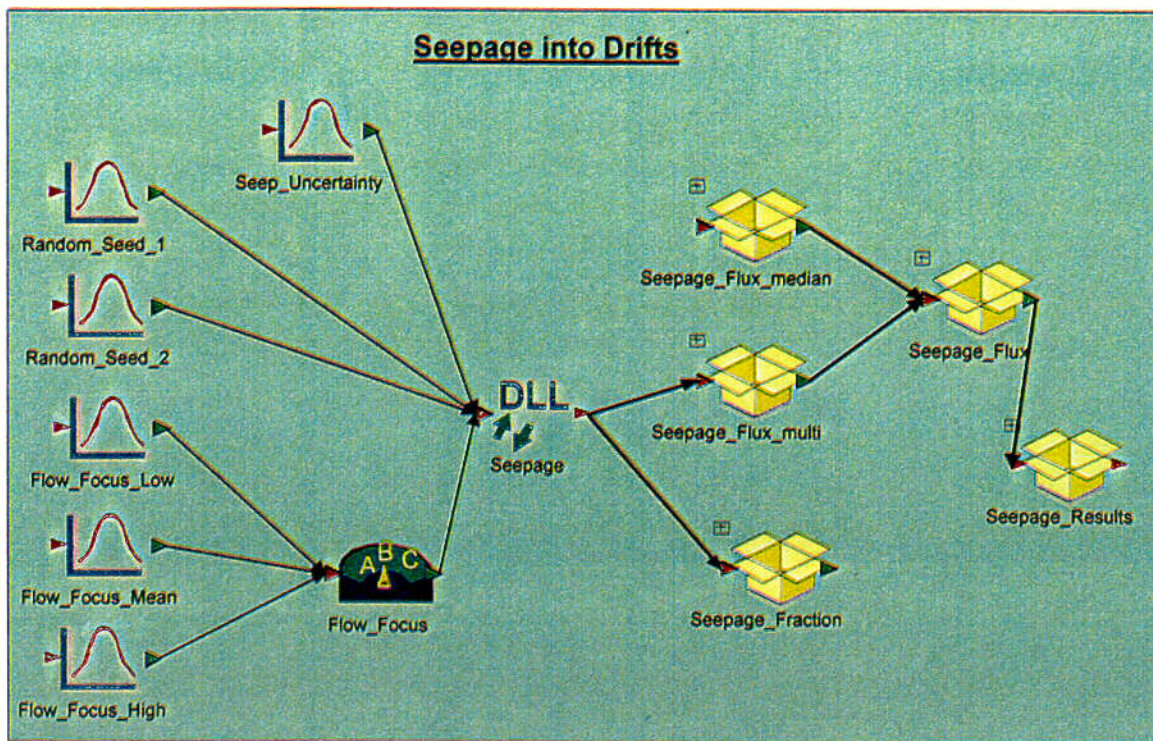
The elements *SeepFrac_Always*, *SeepFrac_Intermittent*, and *SeepFrac_ND*, as mentioned previously, select seepage fraction from the seepdll output for multiple realizations or the median case based on data supplied by *Median_Value_Run* and *Backfill_Case*, which are located in *Simulation_Settings*. In this example *Median_Value_Run* equals 1 and *Backfill_Case* equals 0, which means the values for the no backfill, median case should be used. The inputs for each of the elements were examined and contain the correct no backfill, median case links from *SeepFrac_AI_multi*, *SeepFrac_In_multi*, *SeepFrac_ND_multi*, *SeepFrac_AI_median*, *SeepFrac_In_median*, *SeepFrac_ND_median* for always dripping, intermittent, and no drip conditions in each of the five bins for both types of fuel. The outputs from *SeepFrac_Always*, *SeepFrac_Intermittent*, and *SeepFrac_ND* were also verified to correctly link to *Seepage_Fraction* for each of the five infiltration bins for both types of fuel. For validation and verification of seepdll and its subroutines, refer to Attachment II.

The contents of the *Seepage_Results* container consists of 20 sets of time versus seepage flux data: one for each of the five bins and both types of fuel in always dripping and intermittent conditions. The analysis of the data sets is as follows:

As shown in Table 6-8, several of the data sets are empty. This result is expected and correct as the corresponding seepage flux values (see Table 6-7) for these data sets are zero. Figure 6-34 below is an example of intermittent seepage results and Figure 6-35 is an example of always seeps results.

Table 6-8. Seepage Time History Results of Median Value, No Backfill, One Million-Year Simulation

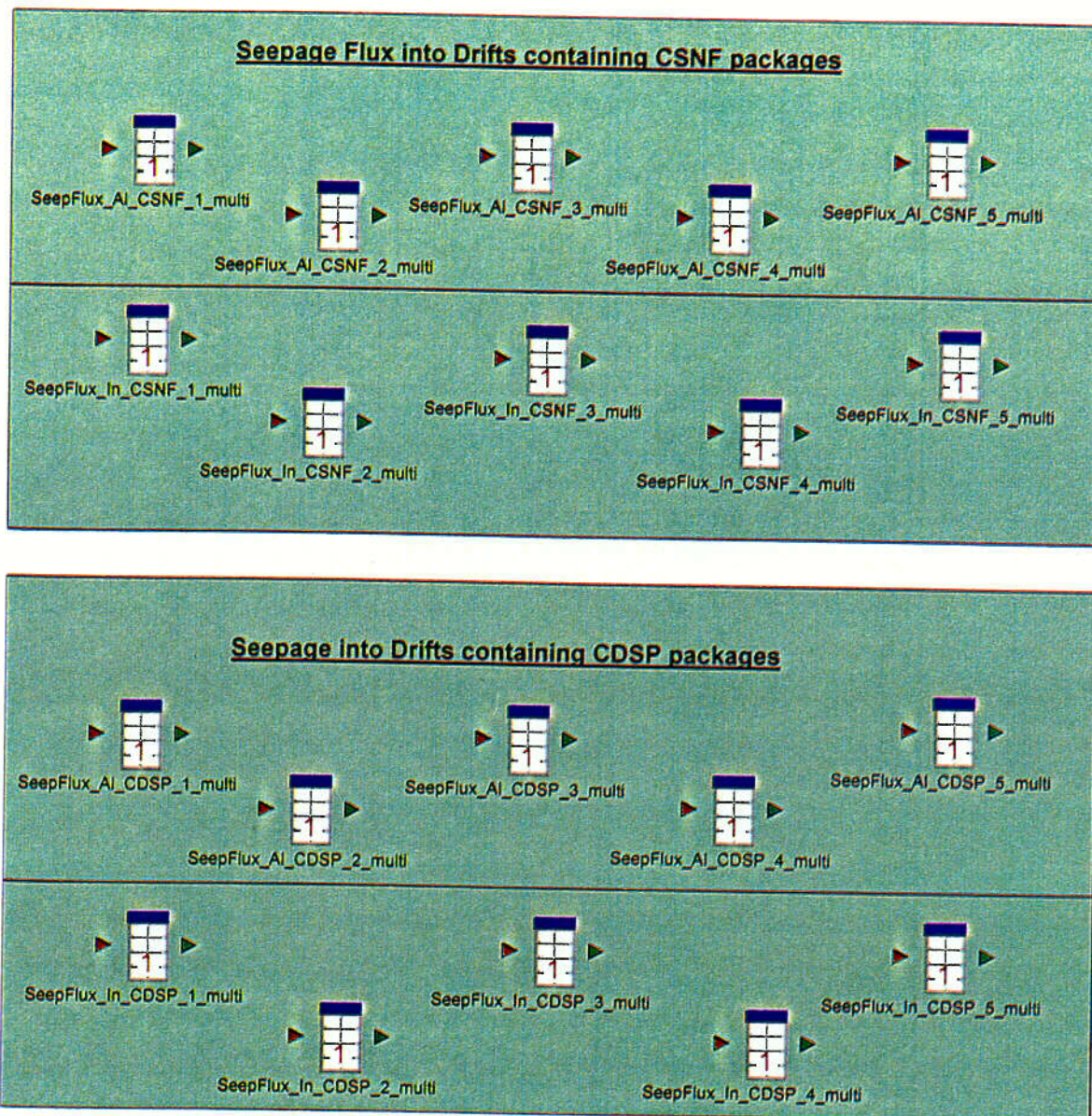
Seepage_Results Time History Result Name	Result Summary
CSNF_AI_Bin1	None
CSNF_AI_Bin2	None
CSNF_AI_Bin3	None
CSNF_AI_Bin4	Always seeping
CSNF_AI_Bin5	None
CSNF_In_Bin1	None
CSNF_In_Bin2	Intermittent seepage
CSNF_In_Bin3	Intermittent seepage
CSNF_In_Bin4	Intermittent seepage
CSNF_In_Bin5	None
CDSP_AI_Bin1	None
CDSP_AI_Bin2	None
CDSP_AI_Bin3	None
CDSP_AI_Bin4	Always seeping
CDSP_AI_Bin5	None
CDSP_In_Bin1	None
CDSP_In_Bin2	Intermittent seepage
CDSP_In_Bin3	Intermittent seepage
CDSP_In_Bin4	Intermittent seepage
CDSP_In_Bin5	None



NOTE: See Attachment I for explanation of the symbols.

Figure 6-27. Diagram of the GoldSim Seepage Model

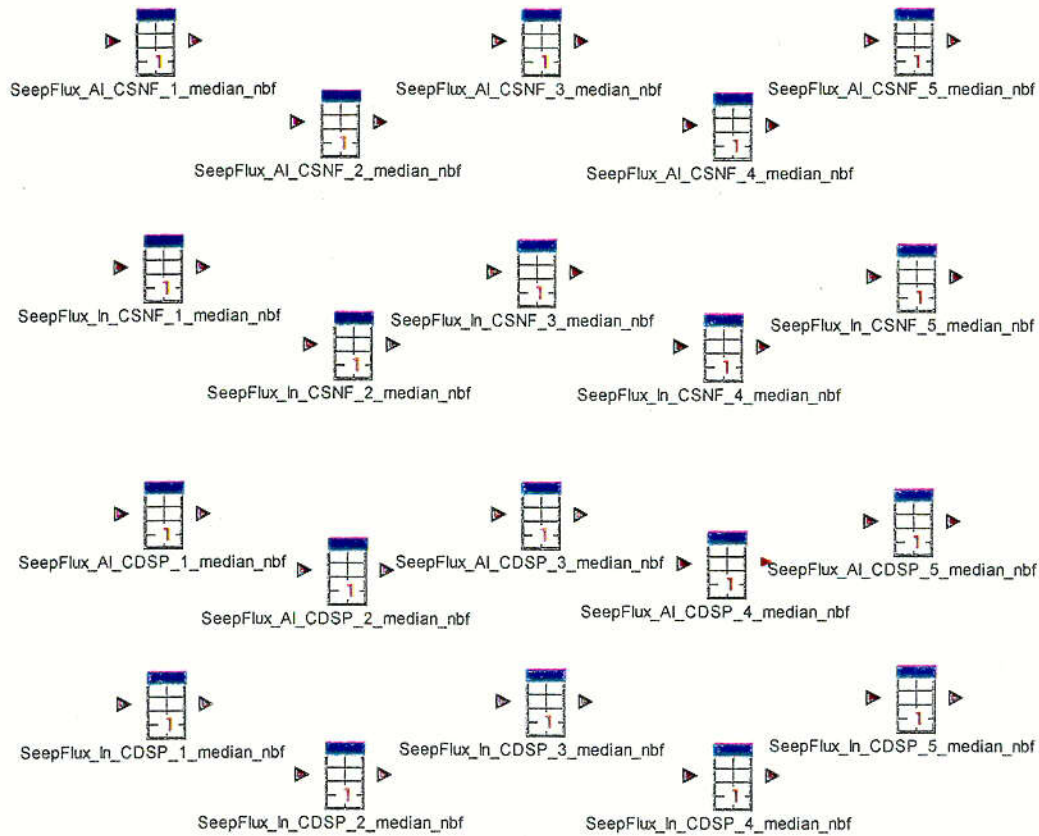
C24



NOTE: See Attachment I for explanation of the symbols.

Figure 6-28. Illustration of the Contents of the *Seepage_Flux_multi* Container Showing Tables Containing Time-Varying Seepage Flow for Always and Intermittent Seepage in Each Infiltration Bin for CSNF and CDSP Waste Packages

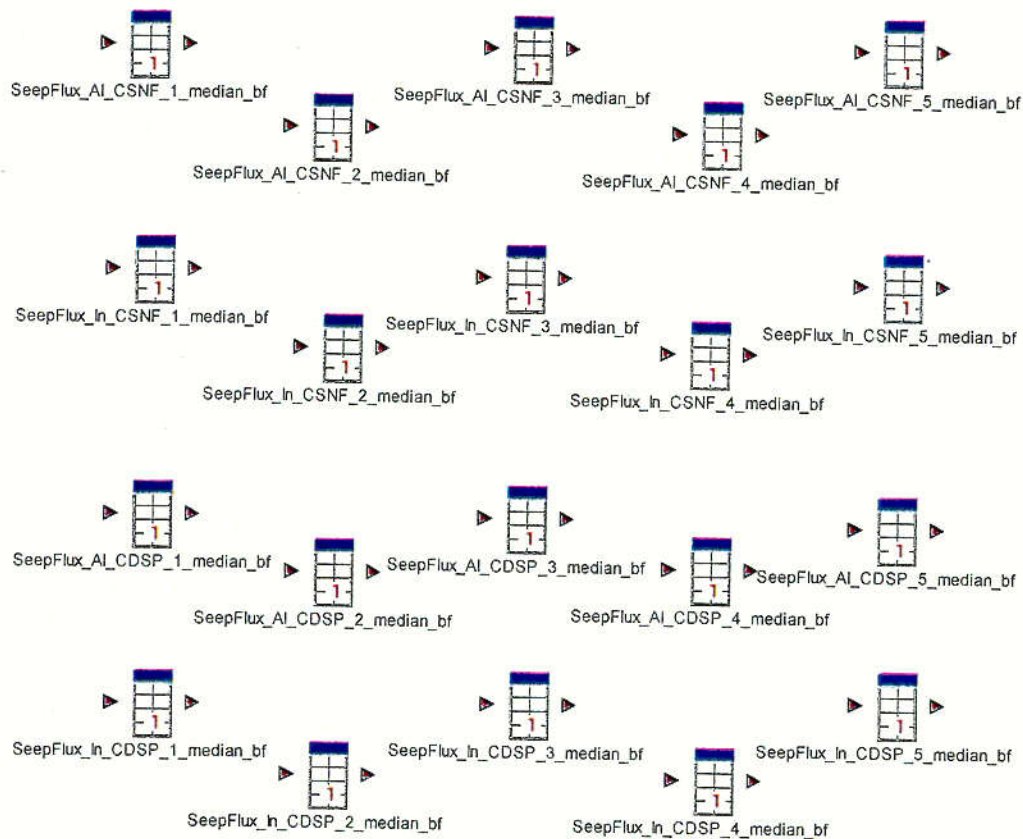
C25



NOTE: See Attachment I for explanation of the symbols.

Figure 6-29. The Contents Of The *No_Backfill* Container Showing Tables Containing Median-Value Time-Varying Seepage Flow for Always and Intermittent Seepage in Each Infiltration Bin for CSNF and CDSP Waste Packages

C26



NOTE: See Attachment I for explanation of the symbols.

Figure 6-30. The Contents of the *Backfill* Container Showing Tables Containing Median-Value Time-Varying Seepage Flow for Always and Intermittent Seepage in Each Infiltration Bin for CSNF and CDSP Waste Packages

C27

Selector Switches in Seepage_Flux Container

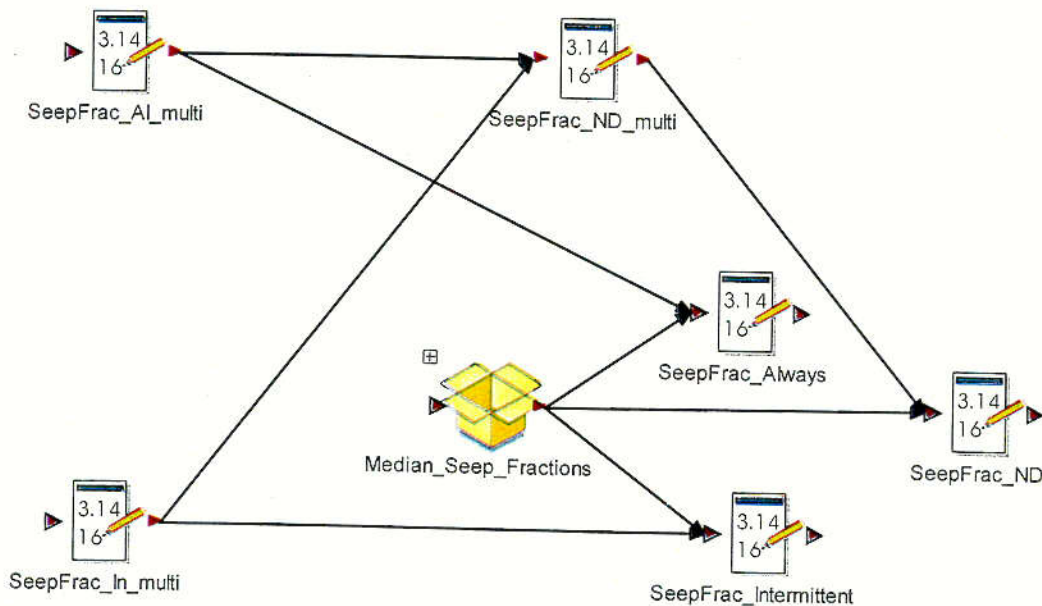


NOTE: See Attachment I for explanation of the symbols.

Figure 6-31. The Selector Switches In the *Seepage_Flux* Container that are Used to Determine Whether Values are Chosen from *Seepage_Flux_median* or *Seepage_Flux_multi* Look-Up Tables

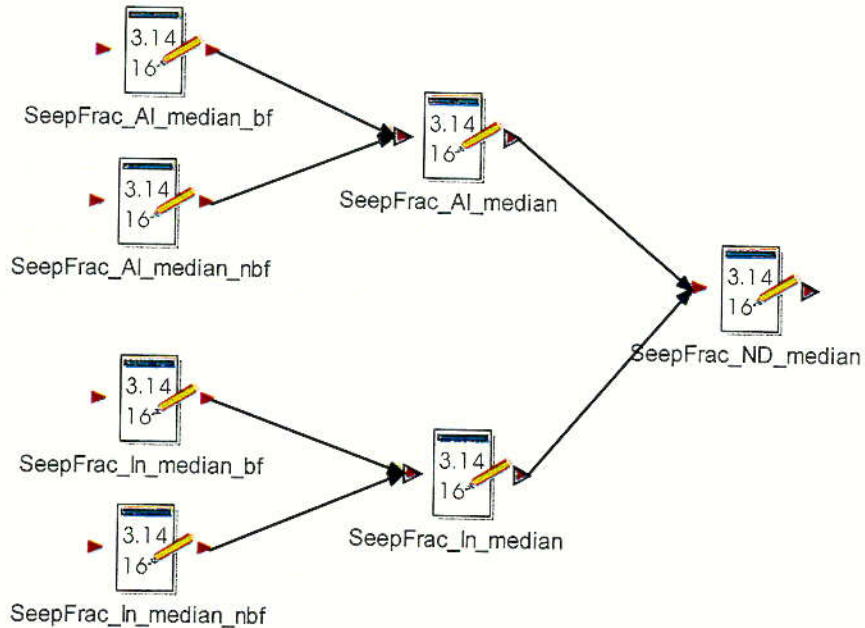
C28

Fraction of Packages Seeing Drips



NOTE: See Attachment I for explanation of the symbols.

Figure 6-32. The Contents of the *Seepage_Fraction* Container Showing Data Elements Containing the Fraction of CDSP and CSNF Waste Packages that Always, Intermittently, and Never See Seepage in Each of the Infiltration Bins



NOTE: See Attachment I for explanation of the symbols.

Figure 6-33. The Contents of the *Median_Seep_Fractions* Container Showing Data Elements Containing the Fraction of CDSP and CSNF Waste Packages that Always, Intermittently, and Never See Seepage in Each of the Infiltration Bins for Backfill and No Backfill Median Value Cases

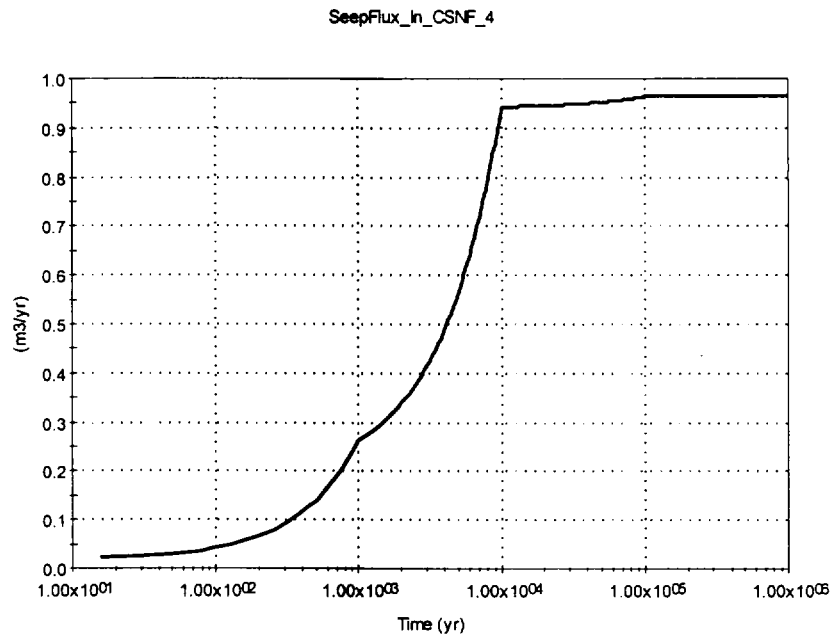


Figure 6-34. Intermittent Seepage for Bin 4 Containing CSNF

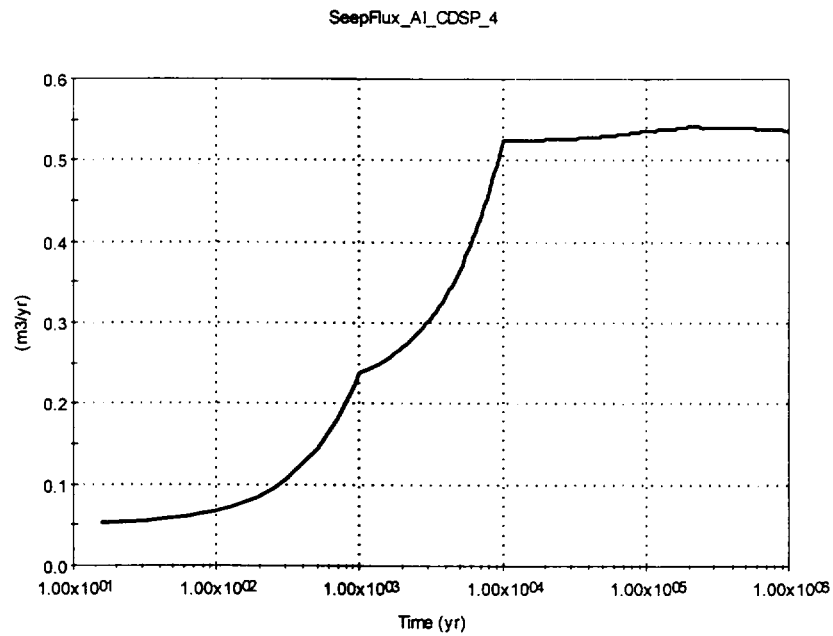


Figure 6-35. Always Seeping Conditions for Bin 4 Containing CDSP

6.3.1.3 Mountain-Scale Unsaturated Zone Flow

Overview

Unsaturated zone flow is the percolation of groundwater through rocks above the water table. The consideration of mountain-scale UZ flow is important to the overall modeling of total system performance because the movement of water in the UZ controls the transport of radionuclides from the repository to the water table.

The mountain-scale UZ flow model uses a dual-permeability conceptual flow model that captures the effects of fast flow paths and allows for weak fracture-matrix coupling. Flow is modeled in two interacting continua (fracture and matrix), with each continuum assigned its own spatially variable hydrologic properties, such as permeability and porosity. In general, the fractures are modeled as a highly permeable continuum having low porosity, while the matrix is modeled as a much less permeable continuum having higher porosity. Fracture-matrix interaction is represented with an active-fracture model, in which only a portion of the fractures is actively flowing under unsaturated conditions (CRWMS M&O 2000 [145774], Section 3.3.4). Major faults are included in the model explicitly. In fault zones, fracture density and permeability are higher than in the rest of the model, which enables them to act as preferential flow paths in parts of the model.

Wetter conditions in the past suggest that more groundwater flowed beneath Yucca Mountain than flows under modern conditions. Several studies have shown that the water table has risen at most 115 m (380 ft) in the past (CRWMS M&O 2000 [123913], Section 6.2). For monsoon and glacial-transition climates in the TSPA simulations, the water table is conservatively set to an elevation of 850 m (2790 ft) above sea level, which is approximately 120 m (390 ft) higher than the present-day water table under the potential repository (CRWMS M&O 2000 [145774], Section 3.7.5.2).

The mountain-scale UZ flow model is a steady-state, isothermal model. Thermal effects can be neglected because flow is strongly perturbed by heat only near the emplacement drifts and at early times (CRWMS M&O 2000 [145774], Sections 1.2.3, 3.3.12, 3.10, and 3.12). Short-term episodic transients can be neglected because of the buffering effect of the Paintbrush nonwelded hydrogeologic unit above the potential repository (CRWMS M&O 2000 [145774], Sections 1.2.4, 3.3.6, 3.3.7, and 3.7.3.1). Long-term transients due to climate change are expected to be important to calculations of potential-repository performance, and those are included in the TSPA by approximating mountain-scale UZ flow with a sequence of steady states. With this approximation, the UZ flow fields can be calculated with the steady-state model and then the UZ transport model can simply switch from one flow field to another at climate-change times (Section 6.3.6).

The three-dimensional, mountain-scale flow model for the unsaturated zone (CRWMS M&O 2000 [145774], Section 3.7) was used in calculating mountain-scale UZ flow for this TSPA. Three-dimensional modeling is needed primarily because of flow characteristics below the potential repository, where significant lateral flow is believed to occur as a result of low-permeability zeolitic layers and perched water. The direct use of the three-dimensional, mountain-scale flow model eliminates the need to test simplified abstractions against more

complex process models. The models were tested directly against site data as part of the calibration procedure (CRWMS M&O 2000 [145774], Sections 3.6-3.8). The following paragraphs summarize the most important features of the mountain-scale UZ flow model.

The numerical discretization of the mountain-scale flow model is illustrated in Figure 6-36. Figure 6-36a shows an east-west cross section through the geologic framework model (CRWMS M&O 2000 [145774], Figure 3.4-8). The cross section has been chosen to intersect three drill holes, named SD-6, SD-12, and UZ#16. The stratigraphy and important hydrogeologic properties are known at the locations of the drill holes; at other locations, they are inferred. The stratigraphic division into hydrogeologic units is shown, including offsets for four major faults. The nomenclature for identifying hydrogeologic units will not be explained here, but it can be found in CRWMS M&O 2000 [145774], Section 3.2.2. Figure 6-36b shows the same cross section as it is represented in the mountain-scale flow model (CRWMS M&O 2000 [145774], Figure 3.4-8). In the model, the stratigraphy is discretized and simplified to a certain extent (e.g., by making the Ghost Dance fault vertical rather than slightly inclined). The second cross section shows the designators used for the hydrogeologic units within the UZ flow model (e.g., the repository host units are tsw34 [middle nonlithophysal], tsw35 [lower lithophysal], and tsw36 [lower nonlithophysal]). Figure 6-36c shows the model discretization as seen from above.

In the UZ flow model, spatial variability is included by use of a three-dimensional model that incorporates the appropriate geometry, geology, and hydrostratigraphy. Temporal variability is included by using different UZ flow simulations for different climate states. The primary change in going from one climate to another is in the use of a different infiltration map for the surface boundary condition. In addition, the water table elevation is higher for future climates.

The uncertainty regarding the appropriate level of net infiltration, discussed in Section 6.3.1.1, was carried forward through the mountain-scale flow model. Sensitivity analyses have shown that infiltration is the quantity that has the greatest impact on UZ flow and transport and that other uncertainties have little impact on repository performance (e.g., DOE 1998 [100550], Volume 3, Section 5.1.3). Although there is a considerable amount of data for calibrating the mountain-scale flow model, the hydrologic properties are not fully constrained, and it is possible to develop calibrated mountain-scale flow models for all three infiltration cases (CRWMS M&O 2000 [145774], Section 3.6). Additional calibrated models were developed with a different treatment of the flow in the vicinity of the perched water between the potential repository level and the water table (CRWMS M&O 2000 [145774], Section 3.7.3.3). However, the alternative perched-water treatment did not lead to greatly different radionuclide transport times from the potential repository to the water table; consequently, only the more conservative of the two perched-water models (perched-water model #1) was used for TSPA simulations (CRWMS M&O 2000 [145774], Section 3.7.5.3).

UZ flow calibration was done only for the present-day climate, because there is not sufficient information about paleohydrology to be able to calibrate flow for monsoon and glacial-transition climates. Thus, the flow for future climates is simulated using the same calibrated hydrologic properties and only changing the infiltration boundary condition at the surface. The three calibrated property sets (low-infiltration, medium-infiltration, and high-infiltration) times three climate states lead to a total of nine mountain-scale UZ flow fields in the TSPA.

The probabilities for the three infiltration cases apply also to the UZ flow fields derived from those infiltration cases. Because the flow fields represent a large quantity of three-dimensional information, they are not easily summarized. Additional description and visualization of the flow fields can be found in Section 3.7.4 of the TSPA-SR Technical Document (CRWMS M&O 2000 [143665]), *Unsaturated Zone Flow and Transport Model Process Model Report* (CRWMS M&O 2000 [145774], Section 3.7); *UZ Flow Models and Submodels* (CRWMS M&O 2000 [122797], Sections 6.6 and 6.7); and *Analysis of Base-Case Particle Tracking Results of the Base-Case Flow Fields (ID:UO160)* (CRWMS M&O 2000 [134732], Section 6.2).

Inputs to the TSPA model

The nine flow fields are the only inputs to the TSPA-SR model for UZ flow. Those fields are contained in the *.ini files listed in Table 6-9 and found in DTN: SN9910T0581699.002 [126110]. The flow field files are used during the UZ transport calculation (see Section 6.3.6). Several other internal parameters are used within TSPA-SR model to select the correct flow field for a given infiltration and climate state.

Table 6-9. List of Input Parameters used from TSPA-SR Model to Select the Flow Fields used in the UZ Transport Calculations and the Names and Source for the Flow Field Files

Parameter/Files	Value/Description	Notes/Source
Infiltration_Scenario	1 for low infiltration 2 for medium infiltration 3 for high infiltration	Internal GoldSim code parameter to determine the infiltration scenario for a realization (see Section 6.3.1.1).
Climate_State	1 for present climate (0 to 600 yrs) 2 for monsoon climate (600 to 2000 yrs) 3 for glacial transition climate (> 2000 yrs)	Internal GoldSim code parameter to specify the climate states through time for a realization (see Section 6.3.1.1).
Findex_PresentDay	If infiltration_scenario == 1 then 100 Else if infiltration_scenario == 2 then 200 Else 300	Infiltration index equal to 100 times infiltration scenario parameter. 100 is low, 200 is medium and 300 is high.
FlowField_Index	Findex_PresentDay+ (Climate_State-1)*1000	Internal GoldSim code parameter for selection of correct flow field in UZ flow and transport 0100 low infiltration, present climate 1100 low infiltration, monsoon climate 2100 low infiltration, glacial-transition climate 0200 medium infiltration, present climate 1200 medium infiltration, monsoon climate 2200 medium infiltration, glacial-transition climate 0300 high infiltration, present climate 1300 high infiltration, monsoon climate 2300 high infiltration, glacial-transition climate.
ff0100.ini ff1100.ini ff2100.ini ff0200.ini ff1200.ini ff2200.ini ff0300.ini ff1300.ini ff2300.ini	Flow field files for use in FEHM UZ transport calculations (see Section 6.3.6.1)	DTN SN9910T0581699.002 [126110] Note that the different files correspond to assumed infiltration and climate states in the model with index values described above.

Implementation

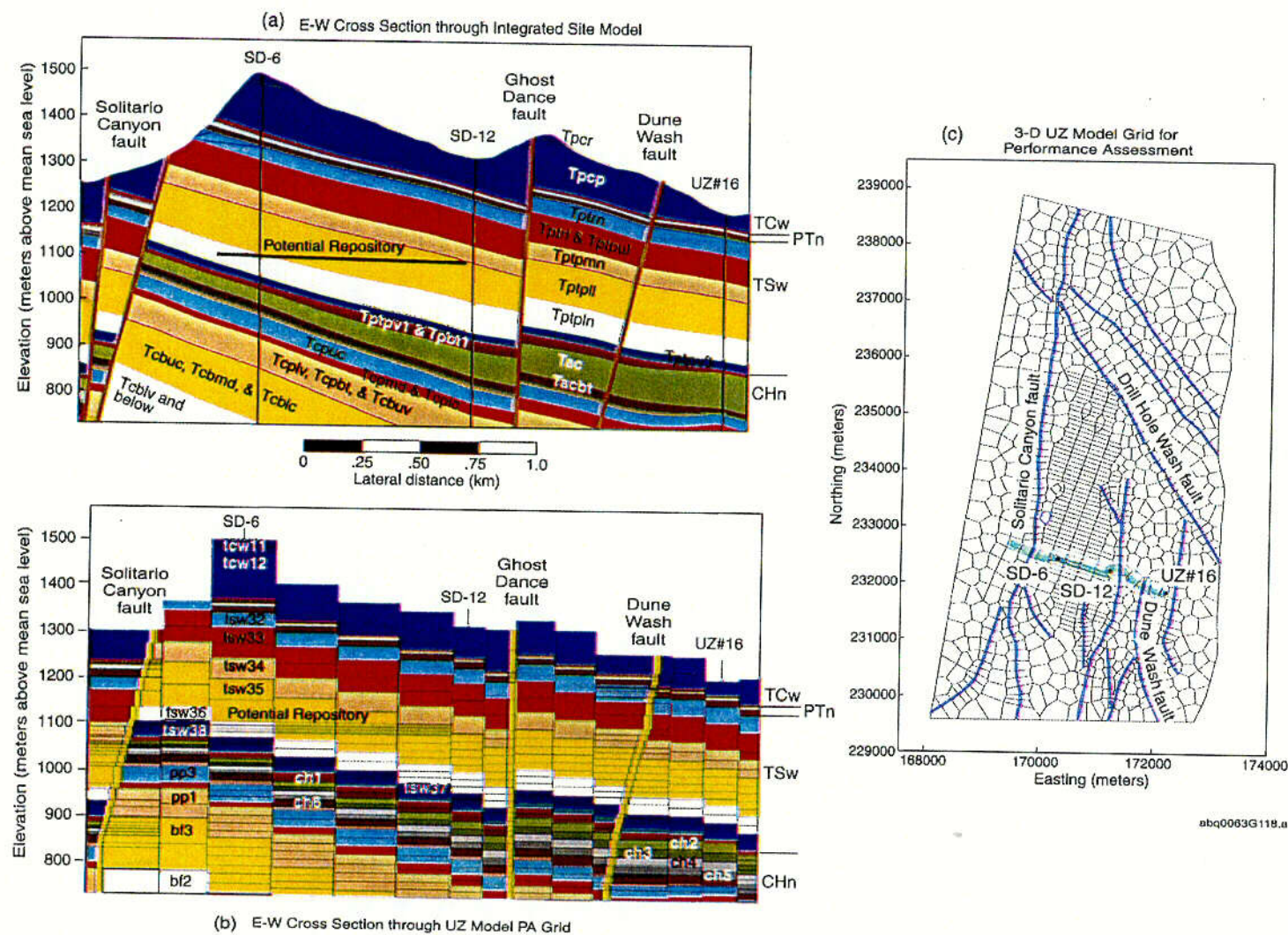
Three-dimensional steady state flow fields from the process-level UZ flow model are used directly in the total system model with no abstraction; therefore, the implementation in the TSPA-SR model was fairly simple—although some postprocessing was required (see Attachment VI). The computer program FEHM (LANL 1999 [146971]; Zyvoloski et al. 1997 [100528]), coupled directly to GoldSim code, is used for UZ transport in the total system model (see Section 6.3.6). At run time, FEHM, in the form of a Dynamically Linked Library (DLL), is called by GoldSim code at each timestep. FEHM requires input files describing the UZ properties, 3-D UZ grid geometry, and the UZ flow fields and uses that information to perform radionuclide transport via particle tracking. The UZ flow component of the total system model is used in conjunction with the UZ transport component. For more information on UZ transport and for a description of the associated 3-D UZ property and geometry files read by FEHM, see Section 6.3.6 and Attachment VI.

As described in Table 6-9, two internal inputs are required from GoldSim code—index parameters for selecting the flow fields to be used during a realization. The index *Findex_PresentDay* consists of unique values for each infiltration scenario. This index is then used by the index *FlowField_Index* to generate the numbers used by GoldSim code to select the appropriate flow field files for each realization. These latter numbers (e.g., 2300 for high infiltration case, glacial-transition climate) are a function of both the infiltration scenario and climate state. For each realization, three flow fields are used; one for each of the three climate states. Table 6-9 lists the parameters that define, and the values for, the flow field indices (see Notes in Table 6-9). *FlowField_Index* is one of several parameters passed to the FEHM external DLL, as shown in Figure 6-37, and then used by FEHM to select the appropriate flow field on which to transport radionuclide particles. Each simulation includes three climate changes (Section 6.3.1.1). At each climate change, there is a corresponding change in the flow field used for the UZ transport calculations, i.e., a different *.ini file from Table 6-9. With each climate change there is also a potential change in the water table at the base of UZ, i.e., different sink points in the FEHM 3-D grid where the mass is collected and sent back to GoldSim code. This water table rise is built into the format of the *.ini files. Attachment VI of this document gives more detail on how the nine UZ flow fields, generated by the TOUGH2 computer code, were made compatible with the FEHM particle tracker.

Results and Verification

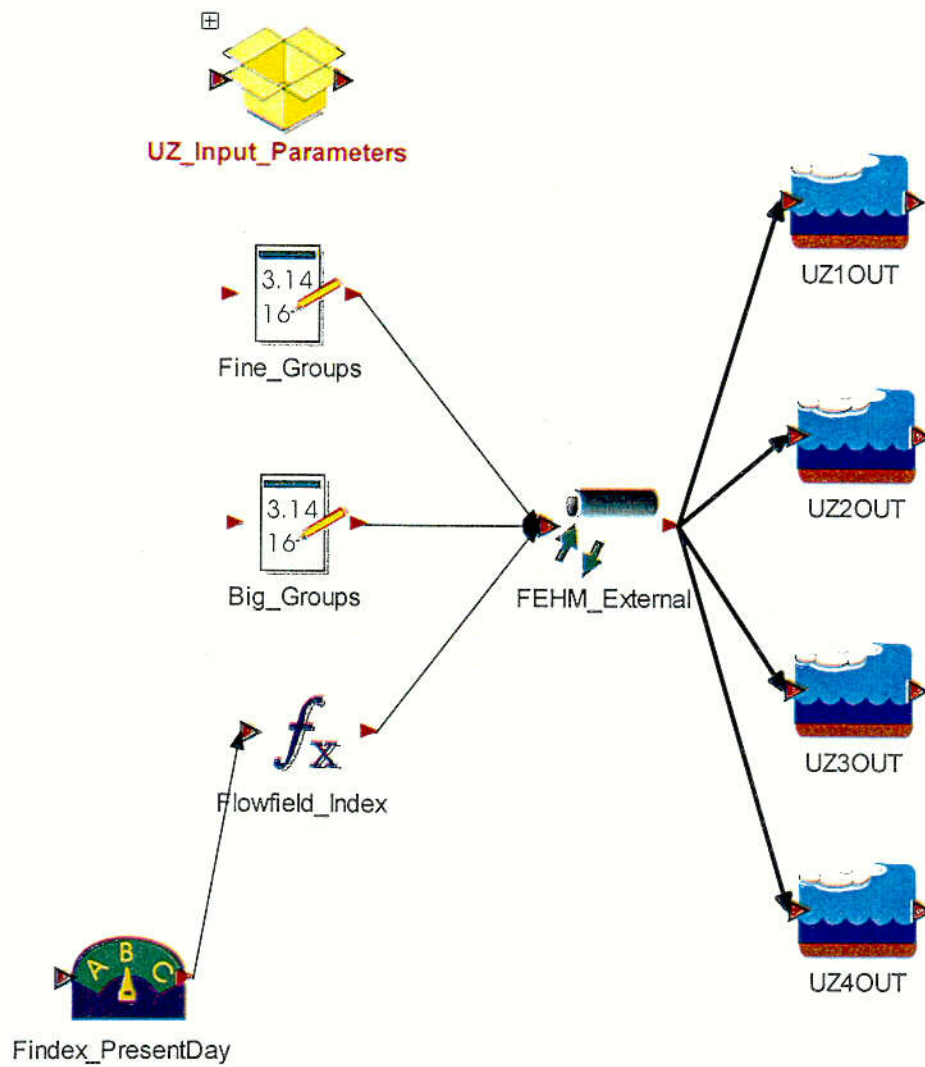
The only effect on the TSPA model from UZ flow is through the effect on the UZ transport. It is not possible to isolate the effects of the UZ flow from the UZ transport in the total system results, although CRWMS M&O 2000 [134732], Section 6.2 provides breakthrough curves for Tc and Np to demonstrate the effect of climate state and infiltration scenario on travel times in the unsaturated zone.

The nine UZ flow fields are used as inputs to the TSPA-SR model. The validation of the flow fields is discussed in CRWMS M&O 2000 [122797], Section 6.8. No further validation is required.



Source: Adapted from CRWMS M&O 2000 [145774], Figure 3.4-8.

Figure 6-36. Stratigraphy and Mesh for Mountain-Scale Flow Model



NOTE: See Attachment I for Explanation of the Symbols

Figure 6-37. A Graphical Illustration of the TSPA Model Implementation of the UZ Flow Model

C31

6.3.2 Near Field Environment

The Commercial Spent Nuclear Fuel (CSNF) and Co-Disposed Spent Fuel (CDSP) waste packages will be placed into drifts in a potential geologic repository at Yucca Mountain. The emplacement of heat generating waste packages in the drift will have an effect on the thermodynamic environment immediately surrounding the emplaced wastes and in the near-field host rock. The Near Field Environment (NFE) component in the TSPA-SR model simulates the changes in environmental conditions which affect the chemical composition of gas, water, colloids, and solids within the emplacement drifts under the thermally perturbed conditions of the repository heating environment. Thermal changes in the NFE, caused by radioactive decay within the waste packages, will result in substantial changes in the temperature, relative humidity, liquid saturation, rate of water evaporation, percolation flux in the near-field host rock, and liquid volume flow rates in-drift. As will be elaborated upon in subsequent sections of this document, how the drift thermodynamic and chemical environment changes with time is important to repository performance in that the changes help determine degradation rates of the engineered barrier components, quantities and species of mobilized radionuclides, and transport of radionuclides through the drift and into the unsaturated zone.

The TSPA-SR model provides a NFE component that simulates temporal and spatial fluctuations in the quantities described above. The TSPA-SR model uses as input averaged quantities of temperature, liquid saturation, relative humidity, evaporation rate, and volume flow rate. The averaged quantities are based on a division of the potential repository footprint into infiltration rate bins based on the glacial-transition climate state (which begins 2,000 years after waste emplacement) (see Section 6.3.4.1 for a detailed discussion of the repository environments). The bin averages are computed for repository locations with similar infiltration rates (e.g., 3-10 mm/yr). Consequently, if most of the locations for a given range of infiltration happen to represent repository edge like conditions, this will be represented in the average applied in the TSPA model since it represents the dominant processes that may be occurring at similar infiltration rates. If for a different infiltration range the locations are primarily repository center, this will also be represented in the averages associated with that infiltration rate bin. The averaging relationships and bases for infiltration rate binning of the thermal hydrologic (TH) data were developed for each bin in the AMR *Abstraction of NFE Drift Thermodynamic Environment and Percolation Flux* (CRWMS M&O 2000 [149860] Section 6.2). This AMR provided the qualitative and quantitative description of the potential thermal hydrologic variability and an assessment of the uncertainty in the thermal hydrologic data based on three different infiltration flux characterizations and hydrologic property sets (e.g., low, mean, and high infiltration flux cases). The abstracted quantities described in the abstraction AMR and used by the TSPA-SR model were specified to preserve and highlight the variability and uncertainty in the thermal hydrologic system.

The AMR *Multiscale Thermohydrologic Model* (CRWMS M&O 2000 [149862]) describes a process-level model that determined environmental conditions for a number of waste package locations using relationships derived from four multiscale thermal hydrologic submodels. The multiscale TH model takes into account host rock variability, proximity to repository edges, infiltration rate variability, climate state transitions, and varying thermal outputs associated with different waste package types. Additionally, three different infiltration flux scenarios were applied in the process-level model so that the uncertainty in the TH processes based on

infiltration rate uncertainty is quantified in subsequent abstractions and ultimately in the TSPA model. The multiscale TH model results in a comprehensive set of variables that are used to characterize the thermodynamic environment of both the emplacement drift components and the surrounding host rock. The TSPA-SR model specifically applies the following variables from the process model: waste package temperature, drip shield temperature, drift wall temperature, invert temperature, waste package relative humidity, drip shield relative humidity, invert relative humidity, invert liquid saturation, drip shield evaporation rate, invert evaporation rate, percolation flux at 5m, volume flow at the invert, and the temperature at the top of the drip shield. The AMR *Abstraction of NFE Drift Thermodynamic Environment and Percolation Flux* (CRWMS M&O 2000 [149860]) abstracted appropriate relationships from the process model data generated by the multiscale thermal hydrologic model. The abstracted relationships were used to simulate NFE conditions in the TSPA-SR model through a division of the repository footprint into infiltration rate bins.

The emplacement of spent nuclear fuel into the Yucca Mountain geologic repository will have significant effects on the environmental conditions within the mountain. Heat emanating from the waste packages will elevate both waste package and surrounding host rock temperatures to 96°C and above (CRWMS M&O 2000 [149860], Table 6 and Figure 35). Elevated temperatures in-drift cause a corresponding decrease in the relative humidity surrounding the engineered barrier components. Elevated host rock temperatures will cause water percolating near the emplacement drifts and residing in the host rock pores to evaporate and redistribute by vapor flow into cooler regions where condensation can occur. Enhanced fracture flows result as heat driven waters are redistributed to other locations by gravity. Some dry-out forms around the emplacement drifts as fracture waters shed near and in-between pillars. Capillary flow redistributes moisture in the matrix towards the drier regions. Seeping fracture water and matrix pore water containing dissolved minerals will leave mineral deposits in the matrix and fracture voids as it evaporates. Since the porosity of the matrix is larger than the fracture, relative changes in fracture properties due to precipitation or dissolution reactions can be greater than the changes in the matrix. As time progresses, radioactive decay decreases and the temperature within the near field environment decreases such that evaporation rates decrease. The relative humidity and percolation flux into the drifts will increase as temperature decreases. The percolation flux above the crown of the drift increases at late times not only due to decreases in temperature but also (primarily) due to future climate change to glacial transitional climate. Seepage water will dissolve the accumulated deposits in the drift, causing a change in the chemical nature of the water. An increase in the ionic strength will increase the corrosivity of the seeping water and accelerate the waste package degradation process. Each of the thermal hydrologic and coupled thermal-hydrologic-chemical processes just described are included in the process-level models and maintained in subsequent abstractions. The abstraction data are applied directly to the total system model so that a heat driven evolution of the NFE influences repository performance. The abstracted thermal-hydrologic inputs applied in the TSPA model are described in detail in Section 6.3.2.1. The abstracted thermal-hydrologic-chemical inputs applied in the TSPA model are described in detail in Section 6.3.2.2.

6.3.2.1 Thermal Hydrology

Overview

Radioactive decay is an exothermic process, as such the waste packages emplaced in the potential repository drifts will thermally perturb the surrounding engineered barrier system and geologic system including the pore fluids in the host rock fractures and matrix. It is expected that the decay of the spent nuclear fuel deposited in the Yucca Mountain Repository will result in thermal fluctuations over many thousands of years after waste emplacement. Thermal fluctuations will vary for different locations throughout the repository footprint (e.g., waste packages residing near repository edges or in high infiltration zones). Heat released during radioactive decay will be conducted through the waste package inner and outer containing layers, elevating the temperature of the waste package outer surface. Heat emanating from the waste package surface will increase the temperature of the drift components and host rock near to or exceeding the boiling temperature of water as described above. The duration and extent of repository heat driven changes in properties used to characterize the engineered barrier system and NFE depend on how heat and mass transfer is modeled in the surrounding host rock. Consistent with the unsaturated zone flow model used by TSPA, the thermal hydrology process-level models also use the active fracture dual permeability conceptual flow model. The basis for using this conceptual flow model in the thermal hydrology process models is in comparison with the measured thermal results obtained from a number of different field thermal tests. The resulting changes in temperature will affect water percolation above the crown of the drift, the relative humidity, evaporation rates, and the liquid saturation within the near field environment.

The AMR *Multiscale Thermohydrologic Model* (CRWMS M&O 2000 [149862]) used an ensemble of models to simulate the environmental conditions within the repository under thermally perturbed conditions. The models were used to account for different thermal hydrologic processes initiated as a result of a thermal perturbation. They were also used to characterize a variety of different input processes and conditions. The TH process-level analysis subdivided the repository footprint into 610 spatial locations for the no backfill case and 623 spatial locations for the backfill repository design (CRWMS M&O 2000 [149862], Section 6). The potential repository environment was determined at each location. The percolation flux at each location was among the variables evaluated. Using the percolation flux at these specific locations, the spatial locations and corresponding process model data were assigned to one of five groups, called infiltration bins (CRWMS M&O 2000 [149860], Section 5.1.1). The abstraction of the process-level model data places repository location environments (e.g., 610 locations for no backfill) into predefined infiltration rate bins (5 total) based on the percolation flux Table 6-10. The process-level data in each bin are either averaged into a single representative curve or are applied directly as a location dependent variable.

Table 6-10. Five Infiltration Rate Bins Based Upon Percolation Flux as Defined by Thermal Hydrology Calculations

BIN Number	Infiltration Rate
1	0-3 mm/yr
2	3-10 mm/yr
3	10-20 mm/yr
4	20-60 mm/yr
5	60+ mm/yr

Source: CRWMS M&O 2000 [149860]

The AMR *Abstraction of NFE Drift Thermodynamic Environment and Percolation Flux* (CRWMS M&O 2000 [149860]) used the multiscale TH model results as inputs to develop the NFE relationships used as inputs in the TSPA-SR model. The abstraction of the TH process model data requires a time-history description of the variables that characterize how heat influences the in-drift components and the surrounding host rock. The time-history data from the multiscale analysis were grouped by infiltration rate bins and averaged, accounting for variability and uncertainty in the TH results (CRWMS M&O 2000 [149860], Section 6.4). Also, due to the importance of the variability in waste package failure times, the full suite of spatial location dependent results described above were used in the both the corrosion and seepage models (see Section 6.3.3 Waste Package Degradation and Section 6.3.1.2 Seepage into Drifts). The drip shield and waste package environmental inputs are representative of a variety of different repository locations as determined by the multiscale TH model. That is, each of the individual components that make up the infiltration rate bin averaged values (for temperature and relative humidity) are used instead of the averaged values themselves. This provides reasonable variability of inputs to the corrosion models. The TSPA-SR model applied the abstraction results for two different repository designs. The base case repository design required a TH abstraction from a process-level model without backfill emplacement in the repository drifts. This abstraction resulted in a set of time-histories used to describe the influence of the no backfill repository on the in-drift thermodynamic and near-field environment. Additionally, a TH abstraction from a process-level model including backfill was also required. This abstraction resulted in a different set of time-histories used to describe the influence of a backfilled repository on the in-drift thermodynamic and near-field environment.

For more information regarding the development of the process model and an abstraction of the NFE conditions, the reader is referred to the AMRs: *MultiScale Thermohydrologic* CRWMS M&O 2000 [149862]) and *Abstraction of NFE Drift Thermodynamic Environment and Percolation Flux* (CRWMS M&O 2000 [149860]).

Inputs to the TSPA Model

The TSPA-SR model used the abstracted time-history data tables submitted to the technical data management system (TDMS) with a description of the data in the AMR *Abstraction of NFE Drift Thermodynamic Environment and Percolation Flux* (CRWMS M&O 2000 [149860] DTN: SN0001T0872799.006 [147198] (with backfill case) and SN0007T0872799.014 [152545] (without backfill case)). The infiltration rate bin averaged data tables represented the temporal variations in temperature, relative humidity, evaporation rate, liquid saturation, and percolation

flux. These data tables were directly incorporated into the TSPA-SR model on an infiltration rate bin basis. Percolation flux versus time histories are available for the 623 locations within the repository at a distances of 5m above the drift. These data are separated by waste package type to account for the differences in the two types of packages and are used as the input into the seepage abstraction (Section 6.3.1.2). These data files are read directly by the SEEPAGE DLL, and do not correspond with parameters within the TSPA-SR model file (Section 6.3.2.1). Table 6-11 presents the TSPA-SR model parameters or seepage input files with the corresponding AMR reference file.

Table 6-11. Input Parameters for the Thermal Hydrology Calculations

TSPA Parameter ^a	Description	Reference File ^b
TEMP_LOW_CSNF_WP_1	Average CSNF Waste Package Surface Temperature in Bin 1, Low Infiltration Flux Scenario	RIP_Tavg_csnf_d0010500_bin0-3_low
TEMP_LOW_CSNF_WP_1_NOBF		RIP_Tavg_csnf_d1050100_bin0-3_low
TEMP_LOW_CSNF_WP_2	Average CSNF Waste Package Surface Temperature in Bin 2, Low Infiltration Flux Scenario	RIP_Tavg_csnf_d0010500_bin3-10_low
TEMP_LOW_CSNF_WP_2_NOBF		RIP_Tavg_csnf_d1050100_bin3-10_low
TEMP_LOW_CSNF_WP_3	Average CSNF Waste Package Surface Temperature in Bin 3, Low Infiltration Flux Scenario	RIP_Tavg_csnf_d0010500_bin10-20_low
TEMP_LOW_CSNF_WP_3_NOBF		RIP_Tavg_csnf_d1050100_bin10-20_low
TEMP_LOW_CSNF_WP_4	Average CSNF Waste Package Surface Temperature in Bin 4, Low Infiltration Flux Scenario	RIP_Tavg_csnf_d0010500_bin20-60_low
TEMP_LOW_CSNF_WP_4_NOBF		RIP_Tavg_csnf_d1050100_bin20-60_low
TEMP_LOW_CSNF_WP_5	Average CSNF Waste Package Surface Temperature in Bin 5, Low Infiltration Flux Scenario	RIP_Tavg_csnf_d0010500_bin60_low
TEMP_LOW_CSNF_WP_5_NOBF		RIP_Tavg_csnf_d1050100_bin60_low
TEMP_MEAN_CSNF_WP_1	Average CSNF Waste Package Surface Temperature in Bin 1, Mean Infiltration Flux Scenario	RIP_Tavg_csnf_d0010500_bin0-3_mean
TEMP_MEAN_CSNF_WP_1_NOBF		RIP_Tavg_csnf_d1050100_bin0-3_mean
TEMP_MEAN_CSNF_WP_2	Average CSNF Waste Package Surface Temperature in Bin 2, Mean Infiltration Flux Scenario	RIP_Tavg_csnf_d0010500_bin3-10_mean
TEMP_MEAN_CSNF_WP_2_NOBF		RIP_Tavg_csnf_d1050100_bin3-10_mean
TEMP_MEAN_CSNF_WP_3	Average CSNF Waste Package Surface Temperature in Bin 3, Mean Infiltration Flux Scenario	RIP_Tavg_csnf_d0010500_bin10-20_mean
TEMP_MEAN_CSNF_WP_3_NOBF		RIP_Tavg_csnf_d1050100_bin10-20_mean
TEMP_MEAN_CSNF_WP_4	Average CSNF Waste Package Surface Temperature in Bin 4, Mean Flux Infiltration Scenario	RIP_Tavg_csnf_d0010500_bin20-60_mean
TEMP_MEAN_CSNF_WP_4_NOBF		RIP_Tavg_csnf_d1050100_bin20-60_mean
TEMP_MEAN_CSNF_WP_5	Average CSNF Waste Package Surface Temperature in Bin 5, Mean Infiltration Flux Scenario	RIP_Tavg_csnf_d0010500_bin60_mean
TEMP_MEAN_CSNF_WP_5_NOBF		RIP_Tavg_csnf_d1050100_bin60_mean
TEMP_HIGH_CSNF_WP_1	Average CSNF Waste Package Surface Temperature in Bin 1, High Infiltration Flux Scenario	RIP_Tavg_csnf_d0010500_bin0-3_high
TEMP_HIGH_CSNF_WP_1_NOBF		RIP_Tavg_csnf_d1050100_bin0-3_high
TEMP_HIGH_CSNF_WP_2	Average CSNF Waste Package Surface Temperature in Bin 2, High Infiltration Flux Scenario	RIP_Tavg_csnf_d0010500_bin3-10_high
TEMP_HIGH_CSNF_WP_2_NOBF		RIP_Tavg_csnf_d1050100_bin3-10_high
TEMP_HIGH_CSNF_WP_3	Average CSNF Waste Package Surface Temperature in Bin 3, High Infiltration Flux Scenario	RIP_Tavg_csnf_d0010500_bin10-20_high
TEMP_HIGH_CSNF_WP_3_NOBF		RIP_Tavg_csnf_d1050100_bin10-20_high
TEMP_HIGH_CSNF_WP_4	Average CSNF Waste Package Surface Temperature in Bin 4, High Infiltration Flux Scenario	RIP_Tavg_csnf_d0010500_bin20-60_high
TEMP_HIGH_CSNF_WP_4_NOBF		RIP_Tavg_csnf_d1050100_bin20-60_high

Table 6-11. Input Parameters for the Thermal Hydrology Calculations (Continued)

TSPA Parameter ^a	Description	Reference File ^b
TEMP_HIGH_CSINF_WP_5	Average CSNF Waste Package Surface Temperature in Bin 5, High Infiltration Flux Scenario	RIP_Tavg_csnf_d0010500_bin60_high
TEMP_HIGH_CSINF_WP_5_NOBF		RIP_Tavg_csnf_d1050100_bin60_high
TEMP_LOW_CDSP_WP_1	Average CDSP Waste Package Surface Temperature in Bin 1, Low Infiltration Flux Scenario	RIP_Tavg_hlw_d0010500_bin0-3_low
TEMP_LOW_CDSP_WP_1_NOBF		RIP_Tavg_hlw_d1050100_bin0-3_low
TEMP_LOW_CDSP_WP_2	Average CDSP Waste Package Surface Temperature in Bin 2, Low Infiltration Flux Scenario	RIP_Tavg_hlw_d0010500_bin3-10_low
TEMP_LOW_CDSP_WP_2_NOBF		RIP_Tavg_hlw_d1050100_bin3-10_low
TEMP_LOW_CDSP_WP_3	Average CDSP Waste Package Surface Temperature in Bin 3, Low Infiltration Flux Scenario	RIP_Tavg_hlw_d0010500_bin10-20_low
TEMP_LOW_CDSP_WP_3_NOBF		RIP_Tavg_hlw_d1050100_bin10-20_low
TEMP_LOW_CDSP_WP_4	Average CDSP Waste Package Surface Temperature in Bin 4, Low Infiltration Flux Scenario	RIP_Tavg_hlw_d0010500_bin20-60_low
TEMP_LOW_CDSP_WP_4_NOBF		RIP_Tavg_hlw_d1050100_bin20-60_low
TEMP_LOW_CDSP_WP_5	Average CDSP Waste Package Surface Temperature in Bin 5, Low Infiltration Flux Scenario	RIP_Tavg_hlw_d0010500_bin60_low
TEMP_LOW_CDSP_WP_5_NOBF		RIP_Tavg_hlw_d1050100_bin60_low
TEMP_MEAN_CDSP_WP_1	Average CDSP Waste Package Surface Temperature in Bin 1, Mean Infiltration Flux Scenario	RIP_Tavg_hlw_d0010500_bin0-3_mean
TEMP_MEAN_CDSP_WP_1_NOBF		RIP_Tavg_hlw_d1050100_bin0-3_mean
TEMP_MEAN_CDSP_WP_2	Average CDSP Waste Package Surface Temperature in Bin 2, Mean Infiltration Flux Scenario	RIP_Tavg_hlw_d0010500_bin3-10_mean
TEMP_MEAN_CDSP_WP_2_NOBF		RIP_Tavg_hlw_d1050100_bin3-10_mean
TEMP_MEAN_CDSP_WP_3	Average CDSP Waste Package Surface Temperature in Bin 3, Mean Infiltration Flux Scenario	RIP_Tavg_hlw_d0010500_bin10-20_mean
TEMP_MEAN_CDSP_WP_3_NOBF		RIP_Tavg_hlw_d1050100_bin10-20_mean
TEMP_MEAN_CDSP_WP_4	Average CDSP Waste Package Surface Temperature in Bin 4, Mean Infiltration Flux Scenario	RIP_Tavg_hlw_d0010500_bin20-60_mean
TEMP_MEAN_CDSP_WP_4_NOBF		RIP_Tavg_hlw_d1050100_bin20-60_mean
TEMP_MEAN_CDSP_WP_5	Average CDSP Waste Package Surface Temperature in Bin 5, Mean Infiltration Flux Scenario	RIP_Tavg_hlw_d0010500_bin60_mean
TEMP_MEAN_CDSP_WP_5_NOBF		RIP_Tavg_hlw_d1050100_bin60_mean
TEMP_HIGH_CDSP_WP_1	Average CDSP Waste Package Surface Temperature in Bin 1, High Infiltration Flux Scenario	RIP_Tavg_hlw_d0010500_bin0-3_high
TEMP_HIGH_CDSP_WP_1_NOBF		RIP_Tavg_hlw_d1050100_bin0-3_high
TEMP_HIGH_CDSP_WP_2	Average CDSP Waste Package Surface Temperature in Bin 2, High Infiltration Flux Scenario	RIP_Tavg_hlw_d0010500_bin3-10_high
TEMP_HIGH_CDSP_WP_2_NOBF		RIP_Tavg_hlw_d1050100_bin3-10_high
TEMP_HIGH_CDSP_WP_3	Average CDSP Waste Package Surface Temperature in Bin 3, High Infiltration Flux Scenario	RIP_Tavg_hlw_d0010500_bin10-20_high
TEMP_HIGH_CDSP_WP_3_NOBF		RIP_Tavg_hlw_d1050100_bin10-20_high
TEMP_HIGH_CDSP_WP_4	Average CDSP Waste Package Surface Temperature in Bin 4, High Infiltration Flux Scenario	RIP_Tavg_hlw_d0010500_bin20-60_high
TEMP_HIGH_CDSP_WP_4_NOBF		RIP_Tavg_hlw_d1050100_bin20-60_high
TEMP_HIGH_CDSP_WP_5	Average CDSP Waste Package Surface Temperature in Bin 5, High Infiltration Flux Scenario	RIP_Tavg_hlw_d0010500_bin60_high
TEMP_HIGH_CDSP_WP_5_NOBF		RIP_Tavg_hlw_d1050100_bin60_high
TEMP_LOW_CSINF_INV_1	Average CSNF Invert Temperature in Bin 1, Low Infiltration Flux Scenario	RIP_Tinvavg_csnf_d0010500_bin0-3_low
TEMP_LOW_CSINF_INV1_NOBF		RIP_Tinvavg_csnf_d1050100_bin0-3_low
TEMP_LOW_CSINF_INV_2	Average CSNF Invert Temperature in Bin 2, Low Infiltration Flux Scenario	RIP_Tinvavg_csnf_d0010500_bin3-10_low
TEMP_LOW_CSINF_INV2_NOBF		RIP_Tinvavg_csnf_d1050100_bin3-10_low
TEMP_LOW_CSINF_INV_3	Average CSNF Invert Temperature in Bin 3, Low Infiltration Flux Scenario	RIP_Tinvavg_csnf_d0010500_bin10-20_low
TEMP_LOW_CSINF_INV3_NOBF		RIP_Tinvavg_csnf_d1050100_bin10-20_low

Table 6-11. Input Parameters for the Thermal Hydrology Calculations (Continued)

TSPA Parameter ^a	Description	Reference File ^b
TEMP_LOW_CSNF_INV_4	Average CSNF Invert Temperature in Bin 4, Low Infiltration Flux Scenario	RIP_Tinvavg_csnf_d0010500_bin20-60_low
TEMP_LOW_CSNF_INV4_NOBF		RIP_Tinvavg_csnf_d1050100_bin20-60_low
TEMP_LOW_CSNF_INV_5	Average CSNF Invert Temperature in Bin 5, Low Infiltration Flux Scenario	RIP_Tinvavg_csnf_d0010500_bin-60_low
TEMP_LOW_CSNF_INV5_NOBF		RIP_Tinvavg_csnf_d1050100_bin-60_low
TEMP_MEAN_CSNF_INV_1	Average CSNF Invert Temperature in Bin 1, Mean Infiltration Flux Scenario	RIP_Tinvavg_csnf_d0010500_bin0-3_mean
TEMP_MEAN_CSNF_INV1_NOBF		RIP_Tinvavg_csnf_d1050100_bin0-3_mean
TEMP_MEAN_CSNF_INV_2	Average CSNF Invert Temperature in Bin 2, Mean Infiltration Flux Scenario	RIP_Tinvavg_csnf_d0010500_bin3-10_mean
TEMP_MEAN_CSNF_INV2_NOBF		RIP_Tinvavg_csnf_d1050100_bin3-10_mean
TEMP_MEAN_CSNF_INV_3	Average CSNF Invert Temperature in Bin 3, Mean Infiltration Flux Scenario	RIP_Tinvavg_csnf_d0010500_bin10-20_mean
TEMP_MEAN_CSNF_INV3_NOBF		RIP_Tinvavg_csnf_d1050100_bin10-20_mean
TEMP_MEAN_CSNF_INV_4	Average CSNF Invert Temperature in Bin 4, Mean Infiltration Flux Scenario	RIP_Tinvavg_csnf_d0010500_bin20-60_mean
TEMP_MEAN_CSNF_INV4_NOBF		RIP_Tinvavg_csnf_d1050100_bin20-60_mean
TEMP_MEAN_CSNF_INV_5	Average CSNF Invert Temperature in Bin 5, Mean Infiltration Flux Scenario	RIP_Tinvavg_csnf_d0010500_bin-60_mean
TEMP_MEAN_CSNF_INV5_NOBF		RIP_Tinvavg_csnf_d1050100_bin-60_mean
TEMP_HIGH_CSNF_INV_1	Average CSNF Invert Temperature in Bin 1, High Infiltration Flux Scenario	RIP_Tinvavg_csnf_d0010500_bin0-3_high
TEMP_HIGH_CSNF_INV1_NOBF		RIP_Tinvavg_csnf_d1050100_bin0-3_high
TEMP_HIGH_CSNF_INV_2	Average CSNF Invert Temperature in Bin 2, High Infiltration Flux Scenario	RIP_Tinvavg_csnf_d0010500_bin3-10_high
TEMP_HIGH_CSNF_INV2_NOBF		RIP_Tinvavg_csnf_d1050100_bin3-10_high
TEMP_HIGH_CSNF_INV_3	Average CSNF Invert Temperature in Bin 3, High Infiltration Flux Scenario	RIP_Tinvavg_csnf_d0010500_bin10-20_high
TEMP_HIGH_CSNF_INV3_NOBF		RIP_Tinvavg_csnf_d1050100_bin10-20_high
TEMP_HIGH_CSNF_INV_4	Average CSNF Invert Temperature in Bin 4, High Infiltration Flux Scenario	RIP_Tinvavg_csnf_d0010500_bin20-60_high
TEMP_HIGH_CSNF_INV4_NOBF		RIP_Tinvavg_csnf_d1050100_bin20-60_high
TEMP_HIGH_CSNF_INV_5	Average CSNF Invert Temperature in Bin 5, High Infiltration Flux Scenario	RIP_Tinvavg_csnf_d0010500_bin-60_high
TEMP_HIGH_CSNF_INV5_NOBF		RIP_Tinvavg_csnf_d1050100_bin-60_high
TEMP_LOW_CDSP_INV_1	Average CDSP Invert Temperature in Bin 1, Low Infiltration Flux Scenario	RIP_Tinvavg_hlw_d0010500_bin0-3_low
TEMP_LOW_CDSP_INV1_NOBF		RIP_Tinvavg_hlw_d1050100_bin0-3_low
TEMP_LOW_CDSP_INV_2	Average CDSP Invert Temperature in Bin 2, Low Infiltration Flux Scenario	RIP_Tinvavg_hlw_d0010500_bin3-10_low
TEMP_LOW_CDSP_INV2_NOBF		RIP_Tinvavg_hlw_d1050100_bin3-10_low
TEMP_LOW_CDSP_INV_3	Average CDSP Invert Temperature in Bin 3, Low Infiltration Flux Scenario	RIP_Tinvavg_hlw_d0010500_bin10-20_low
TEMP_LOW_CDSP_INV3_NOBF		RIP_Tinvavg_hlw_d1050100_bin10-20_low
TEMP_LOW_CDSP_INV_4	Average CDSP Invert Temperature in Bin 4, Low Infiltration Flux Scenario	RIP_Tinvavg_hlw_d0010500_bin20-60_low
TEMP_LOW_CDSP_INV4_NOBF		RIP_Tinvavg_hlw_d1050100_bin20-60_low
TEMP_LOW_CDSP_INV_5	Average CDSP Invert Temperature in Bin 5, Low Infiltration Flux Scenario	RIP_Tinvavg_hlw_d0010500_bin-60_low
TEMP_LOW_CDSP_INV5_NOBF		RIP_Tinvavg_hlw_d1050100_bin-60_low
TEMP_MEAN_CDSP_INV_1	Average CDSP Invert Temperature in Bin 1, Mean Infiltration Flux Scenario	RIP_Tinvavg_hlw_d0010500_bin0-3_mean
TEMP_MEAN_CDSP_INV1_NOBF		RIP_Tinvavg_hlw_d1050100_bin0-3_mean
TEMP_MEAN_CDSP_INV_2	Average CDSP Invert Temperature in Bin 2, Mean Infiltration Flux Scenario	RIP_Tinvavg_hlw_d0010500_bin3-10_mean
TEMP_MEAN_CDSP_INV2_NOBF		RIP_Tinvavg_hlw_d1050100_bin3-10_mean
TEMP_MEAN_CDSP_INV_3	Average CDSP Invert Temperature in Bin 3, Mean Infiltration Flux Scenario	RIP_Tinvavg_hlw_d0010500_bin10-20_mean
TEMP_MEAN_CDSP_INV3_NOBF		RIP_Tinvavg_hlw_d1050100_bin10-20_mean
TEMP_MEAN_CDSP_INV_4	Average CDSP Invert Temperature in Bin 4, Mean Infiltration Flux Scenario	RIP_Tinvavg_hlw_d0010500_bin20-60_mean
TEMP_MEAN_CDSP_INV4_NOBF		RIP_Tinvavg_hlw_d1050100_bin20-60_mean
TEMP_MEAN_CDSP_INV_5	Average CDSP Invert Temperature in Bin 5, Mean Infiltration Flux Scenario	RIP_Tinvavg_hlw_d0010500_bin-60_mean
TEMP_MEAN_CDSP_INV5_NOBF		RIP_Tinvavg_hlw_d1050100_bin-60_mean

Table 6-11. Input Parameters for the Thermal Hydrology Calculations (Continued)

TSPA Parameter ^a	Description	Reference File ^b
TEMP_HIGH_CDSP_INV_1	Average CDSP Invert Temperature in Bin 1, High Infiltration Flux Scenario	RIP_Tinvavg_hlw_d0010500_bin0-3_high
TEMP_HIGH_CDSP_INV1_NOBF		RIP_Tinvavg_hlw_d1050100_bin0-3_high
TEMP_HIGH_CDSP_INV_2	Average CDSP Invert Temperature in Bin 2, High Infiltration Flux Scenario	RIP_Tinvavg_hlw_d0010500_bin3-10_high
TEMP_HIGH_CDSP_INV2_NOBF		RIP_Tinvavg_hlw_d1050100_bin3-10_high
TEMP_HIGH_CDSP_INV_3	Average CDSP Invert Temperature in Bin 3, High Infiltration Flux Scenario	RIP_Tinvavg_hlw_d0010500_bin10-20_high
TEMP_HIGH_CDSP_INV3_NOBF		RIP_Tinvavg_hlw_d1050100_bin10-20_high
TEMP_HIGH_CDSP_INV_4	Average CDSP Invert Temperature in Bin 4, High Infiltration Flux Scenario	RIP_Tinvavg_hlw_d0010500_bin20-60_high
TEMP_HIGH_CDSP_INV4_NOBF		RIP_Tinvavg_hlw_d1050100_bin20-60_high
TEMP_HIGH_CDSP_INV_5	Average CDSP Invert Temperature in Bin 5, High Infiltration Flux Scenario	RIP_Tinvavg_hlw_d0010500_bin60_high
TEMP_HIGH_CDSP_INV5_NOBF		RIP_Tinvavg_hlw_d1050100_bin60_high
RH_LOW_CSNF_INV_1	Average CSNF Invert Relative Humidity in Bin 1, Low Infiltration Flux Scenario	RIP_RHinvavg_csnf_d0010500_bin0-3_low
RH_LOW_CSNF_BIN1_NOBF		RIP_RHinvavg_csnf_d1050100_bin0-3_low
RH_LOW_CSNF_INV_2	Average CSNF Invert Relative Humidity in Bin 2, Low Infiltration Flux Scenario	RIP_RHinvavg_csnf_d0010500_bin3-10_low
RH_LOW_CSNF_BIN2_NOBF		RIP_RHinvavg_csnf_d1050100_bin3-10_low
RH_LOW_CSNF_INV_3	Average CSNF Invert Relative Humidity in Bin 3, Low Infiltration Flux Scenario	RIP_RHinvavg_csnf_d0010500_bin10-20_low
RH_LOW_CSNF_BIN3_NOBF		RIP_RHinvavg_csnf_d1050100_bin10-20_low
RH_LOW_CSNF_INV_4	Average CSNF Invert Relative Humidity in Bin 4, Low Infiltration Flux Scenario	RIP_RHinvavg_csnf_d0010500_bin20-60_low
RH_LOW_CSNF_BIN4_NOBF		RIP_RHinvavg_csnf_d1050100_bin20-60_low
RH_LOW_CSNF_INV_5	Average CSNF Invert Relative Humidity in Bin 5, Low Infiltration Flux Scenario	RIP_RHinvavg_csnf_d0010500_bin60_low
RH_LOW_CSNF_BIN5_NOBF		RIP_RHinvavg_csnf_d1050100_bin60_low
RH_MEAN_CSNF_INV_1	Average CSNF Invert Relative Humidity in Bin 1, Mean Infiltration Flux Scenario	RIP_RHinvavg_csnf_d0010500_bin0-3_mean
RH_MEAN_CSNF_BIN1_NOBF		RIP_RHinvavg_csnf_d1050100_bin0-3_mean
RH_MEAN_CSNF_INV_2	Average CSNF Invert Relative Humidity in Bin 2, Mean Infiltration Flux Scenario	RIP_RHinvavg_csnf_d0010500_bin3-10_mean
RH_MEAN_CSNF_BIN2_NOBF		RIP_RHinvavg_csnf_d1050100_bin3-10_mean
RH_MEAN_CSNF_INV_3	Average CSNF Invert Relative Humidity in Bin 3, Mean Infiltration Flux Scenario	RIP_RHinvavg_csnf_d0010500_bin10-20_mean
RH_MEAN_CSNF_BIN3_NOBF		RIP_RHinvavg_csnf_d1050100_bin10-20_mean
RH_MEAN_CSNF_INV_4	Average CSNF Invert Relative Humidity in Bin 4, Mean Infiltration Flux Scenario	RIP_RHinvavg_csnf_d0010500_bin20-60_mean
RH_MEAN_CSNF_BIN4_NOBF		RIP_RHinvavg_csnf_d1050100_bin20-60_mean
RH_MEAN_CSNF_INV_5	Average CSNF Invert Relative Humidity in Bin 5, Mean Infiltration Flux Scenario	RIP_RHinvavg_csnf_d0010500_bin60_mean
RH_MEAN_CSNF_BIN5_NOBF		RIP_RHinvavg_csnf_d1050100_bin60_mean
RH_HIGH_CSNF_INV_1	Average CSNF Invert Relative Humidity in Bin 1, High Infiltration Flux Scenario	RIP_RHinvavg_csnf_d0010500_bin0-3_high
RH_HIGH_CSNF_BIN1_NOBF		RIP_RHinvavg_csnf_d1050100_bin0-3_high
RH_HIGH_CSNF_INV_2	Average CSNF Invert Relative Humidity in Bin 2, High Infiltration Flux Scenario	RIP_RHinvavg_csnf_d0010500_bin3-10_high
RH_HIGH_CSNF_BIN2_NOBF		RIP_RHinvavg_csnf_d1050100_bin3-10_high
RH_HIGH_CSNF_INV_3	Average CSNF Invert Relative Humidity in Bin 3, High Infiltration Flux Scenario	RIP_RHinvavg_csnf_d0010500_bin10-20_high
RH_HIGH_CSNF_BIN3_NOBF		RIP_RHinvavg_csnf_d1050100_bin10-20_high
RH_HIGH_CSNF_INV_4	Average CSNF Invert Relative Humidity in Bin 4, High Infiltration Flux Scenario	RIP_RHinvavg_csnf_d0010500_bin20-60_high
RH_HIGH_CSNF_BIN4_NOBF		RIP_RHinvavg_csnf_d1050100_bin20-60_high
RH_HIGH_CSNF_INV_5	Average CSNF Invert Relative Humidity in Bin 5, High Infiltration Flux Scenario	RIP_RHinvavg_csnf_d0010500_bin60_high
RH_HIGH_CSNF_BIN5_NOBF		RIP_RHinvavg_csnf_d1050100_bin60_high

Table 6-11. Input Parameters for the Thermal Hydrology Calculations (Continued)

TSPA Parameter ^a	Description	Reference File ^b
RH_LOW_CDSP_INV_1	Average CDSP Invert Relative Humidity in Bin 1, Low Infiltration Flux Scenario	RIP_RHinvavg_hlw_d0010500_bin0-3_low
RH_LOW_CDSP_BIN1_NOBF		RIP_RHinvavg_hlw_d1050100_bin0-3_low
RH_LOW_CDSP_INV_2	Average CDSP Invert Relative Humidity in Bin 2, Low Infiltration Flux Scenario	RIP_RHinvavg_hlw_d0010500_bin3-10_low
RH_LOW_CDSP_BIN2_NOBF		RIP_RHinvavg_hlw_d1050100_bin3-10_low
RH_LOW_CDSP_INV_3	Average CDSP Invert Relative Humidity in Bin 3, Low Infiltration Flux Scenario	RIP_RHinvavg_hlw_d0010500_bin10-20_low
RH_LOW_CDSP_BIN3_NOBF		RIP_RHinvavg_hlw_d1050100_bin10-20_low
RH_LOW_CDSP_INV_4	Average CDSP Invert Relative Humidity in Bin 4, Low Infiltration Flux Scenario	RIP_RHinvavg_hlw_d0010500_bin20-60_low
RH_LOW_CDSP_BIN4_NOBF		RIP_RHinvavg_hlw_d1050100_bin20-60_low
RH_LOW_CDSP_INV_5	Average CDSP Invert Relative Humidity in Bin 5, Low Infiltration Flux Scenario	RIP_RHinvavg_hlw_d0010500_bin-60_low
RH_LOW_CDSP_BIN5_NOBF		RIP_RHinvavg_hlw_d1050100_bin-60_low
RH_MEAN_CDSP_INV_1	Average CDSP Invert Relative Humidity in Bin 1, Mean Infiltration Flux Scenario	RIP_RHinvavg_hlw_d0010500_bin0-3_mean
RH_MEAN_CDSP_BIN1_NOBF		RIP_RHinvavg_hlw_d1050100_bin0-3_mean
RH_MEAN_CDSP_INV_2	Average CDSP Invert Relative Humidity in Bin 2, Mean Infiltration Flux Scenario	RIP_RHinvavg_hlw_d0010500_bin3-10_mean
RH_MEAN_CDSP_BIN2_NOBF		RIP_RHinvavg_hlw_d1050100_bin3-10_mean
RH_MEAN_CDSP_INV_3	Average CDSP Invert Relative Humidity in Bin 3, Mean Infiltration Flux Scenario	RIP_RHinvavg_hlw_d0010500_bin10-20_mean
RH_MEAN_CDSP_BIN3_NOBF		RIP_RHinvavg_hlw_d1050100_bin10-20_mean
RH_MEAN_CDSP_INV_4	Average CDSP Invert Relative Humidity in Bin 4, Mean Infiltration Flux Scenario	RIP_RHinvavg_hlw_d0010500_bin20-60_mean
RH_MEAN_CDSP_BIN4_NOBF		RIP_RHinvavg_hlw_d1050100_bin20-60_mean
RH_MEAN_CDSP_INV_5	Average CDSP Invert Relative Humidity in Bin 5, Mean Infiltration Flux Scenario	RIP_RHinvavg_hlw_d0010500_bin-60_mean
RH_MEAN_CDSP_BIN5_NOBF		RIP_RHinvavg_hlw_d1050100_bin-60_mean
RH_HIGH_CDSP_INV_1	Average CDSP Invert Relative Humidity in Bin 1, High Infiltration Flux Scenario	RIP_RHinvavg_hlw_d0010500_bin0-3_high
RH_HIGH_CDSP_BIN1_NOBF		RIP_RHinvavg_hlw_d1050100_bin0-3_high
RH_HIGH_CDSP_INV_2	Average CDSP Invert Relative Humidity in Bin 2, High Infiltration Flux Scenario	RIP_RHinvavg_hlw_d0010500_bin3-10_high
RH_HIGH_CDSP_BIN2_NOBF		RIP_RHinvavg_hlw_d1050100_bin3-10_high
RH_HIGH_CDSP_INV_3	Average CDSP Invert Relative Humidity in Bin 3, High Infiltration Flux Scenario	RIP_RHinvavg_hlw_d0010500_bin10-20_high
RH_HIGH_CDSP_BIN3_NOBF		RIP_RHinvavg_hlw_d1050100_bin10-20_high
RH_HIGH_CDSP_INV_4	Average CDSP Invert Relative Humidity in Bin 4, High Infiltration Flux Scenario	RIP_RHinvavg_hlw_d0010500_bin20-60_high
RH_HIGH_CDSP_BIN4_NOBF		RIP_RHinvavg_hlw_d1050100_bin20-60_high
RH_HIGH_CDSP_INV_5	Average CDSP Invert Relative Humidity in Bin 5, High Infiltration Flux Scenario	RIP_RHinvavg_hlw_d0010500_bin-60_high
RH_HIGH_CDSP_BIN5_NOBF		RIP_RHinvavg_hlw_d1050100_bin-60_high
QEVAP_LOW_CS NF_INV_1	Average CSNF Invert Evaporation Rate in Bin 1, Low Infiltration Flux Scenario	RIP_Qevap_invavg_csnf_d0010500_bin0-3_low
QEVAP_LOW_CS NF_BIN1_NOBF		RIP_Qevap_invavg_csnf_d1050100_bin0-3_low
QEVAP_LOW_CS NF_INV_2	Average CSNF Invert Evaporation Rate in Bin 2, Low Infiltration Flux Scenario	RIP_Qevap_invavg_csnf_d0010500_bin3-10_low
QEVAP_LOW_CS NF_BIN2_NOBF		RIP_Qevap_invavg_csnf_d1050100_bin3-10_low
QEVAP_LOW_CS NF_INV_3	Average CSNF Invert Evaporation Rate in Bin 3, Low Infiltration Flux Scenario	RIP_Qevap_invavg_csnf_d0010500_bin10-20_low
QEVAP_LOW_CS NF_BIN3_NOBF		RIP_Qevap_invavg_csnf_d1050100_bin10-20_low
QEVAP_LOW_CS NF_INV_4	Average CSNF Invert Evaporation Rate in Bin 4, Low Infiltration Flux Scenario	RIP_Qevap_invavg_csnf_d0010500_bin20-60_low
QEVAP_LOW_CS NF_BIN4_NOBF		RIP_Qevap_invavg_csnf_d1050100_bin20-60_low

Table 6-11. Input Parameters for the Thermal Hydrology Calculations (Continued)

TSPA Parameter ^a	Description	Reference File ^b
QEVAP_LOW_CSNF_INV_5	Average CSNF Invert Evaporation Rate in Bin 5, Low Infiltration Flux Scenario	RIP_Qevap_invavg_csnf_d0010500_bin-60_low
QEVAP_LOW_CSNF_BIN5_NOBF		RIP_Qevap_invavg_csnf_d1050100_bin-60_low
QEVAP_MEAN_CSNF_INV_1	Average CSNF Invert Evaporation Rate in Bin 1, Mean Infiltration Flux Scenario	RIP_Qevap_invavg_csnf_d0010500_bin0-3_mean
QEVAP_MEAN_CSNF_BIN1_NOBF		RIP_Qevap_invavg_csnf_d1050100_bin0-3_mean
QEVAP_MEAN_CSNF_INV_2	Average CSNF Invert Evaporation Rate in Bin 2, Mean Infiltration Flux Scenario	RIP_Qevap_invavg_csnf_d0010500_bin3-10_mean
QEVAP_MEAN_CSNF_BIN2_NOBF		RIP_Qevap_invavg_csnf_d1050100_bin3-10_mean
QEVAP_MEAN_CSNF_INV_3	Average CSNF Invert Evaporation Rate in Bin 3, Mean Infiltration Flux Scenario	RIP_Qevap_invavg_csnf_d0010500_bin10-20_mean
QEVAP_MEAN_CSNF_BIN3_NOBF		RIP_Qevap_invavg_csnf_d1050100_bin10-20_mean
QEVAP_MEAN_CSNF_INV_4	Average CSNF Invert Evaporation Rate in Bin 4, Mean Infiltration Flux Scenario	RIP_Qevap_invavg_csnf_d0010500_bin20-60_mean
QEVAP_MEAN_CSNF_BIN4_NOBF		RIP_Qevap_invavg_csnf_d1050100_bin20-60_mean
QEVAP_MEAN_CSNF_INV_5	Average CSNF Invert Evaporation Rate in Bin 5, Mean Infiltration Flux Scenario	RIP_Qevap_invavg_csnf_d0010500_bin-60_mean
QEVAP_MEAN_CSNF_BIN5_NOBF		RIP_Qevap_invavg_csnf_d1050100_bin-60_mean
QEVAP_HIGH_CSNF_INV_1	Average CSNF Invert Evaporation Rate in Bin 1, High Infiltration Flux Scenario	RIP_Qevap_invavg_csnf_d0010500_bin0-3_high
QEVAP_HIGH_CSNF_BIN1_NOBF		RIP_Qevap_invavg_csnf_d1050100_bin0-3_high
QEVAP_HIGH_CSNF_INV_2	Average CSNF Invert Evaporation Rate in Bin 2, High Infiltration Flux Scenario	RIP_Qevap_invavg_csnf_d0010500_bin3-10_high
QEVAP_HIGH_CSNF_BIN2_NOBF		RIP_Qevap_invavg_csnf_d1050100_bin3-10_high
QEVAP_HIGH_CSNF_INV_3	Average CSNF Invert Evaporation Rate in Bin 3, High Infiltration Flux Scenario	RIP_Qevap_invavg_csnf_d0010500_bin10-20_high
QEVAP_HIGH_CSNF_BIN3_NOBF		RIP_Qevap_invavg_csnf_d1050100_bin10-20_high
QEVAP_HIGH_CSNF_INV_4	Average CSNF Invert Evaporation Rate in Bin 4, High Infiltration Flux Scenario	RIP_Qevap_invavg_csnf_d0010500_bin20-60_high
QEVAP_HIGH_CSNF_BIN4_NOBF		RIP_Qevap_invavg_csnf_d1050100_bin20-60_high
QEVAP_HIGH_CSNF_INV_5	Average CSNF Invert Evaporation Rate in Bin 5, High Infiltration Flux Scenario	RIP_Qevap_invavg_csnf_d0010500_bin-60_high
QEVAP_HIGH_CSNF_BIN5_NOBF		RIP_Qevap_invavg_csnf_d1050100_bin-60_high
QEVAP_LOW_CDSP_INV_1	Average CDSP Invert Evaporation Rate in Bin 1, Low Infiltration Flux Scenario	RIP_Qevap_invavg_hlw_d0010500_bin0-3_low
QEVAP_LOW_CDSP_BIN1_NOBF		RIP_Qevap_invavg_hlw_d1050100_bin0-3_low
QEVAP_LOW_CDSP_INV_2	Average CDSP Invert Evaporation Rate in Bin 2, Low Infiltration Flux Scenario	RIP_Qevap_invavg_hlw_d0010500_bin3-10_low
QEVAP_LOW_CDSP_BIN2_NOBF		RIP_Qevap_invavg_hlw_d1050100_bin3-10_low

Table 6-11. Input Parameters for the Thermal Hydrology Calculations (Continued)

TSPA Parameter ^a	Description	Reference File ^b
QEVAP_LOW_CDSP_INV_3	Average CDSP Invert Evaporation Rate in Bin 3, Low Infiltration Flux Scenario	RIP_Qevap_invavg_hlw_d0010500_bin10-20_low
QEVAP_LOW_CDSP_BIN3_NOBF		RIP_Qevap_invavg_hlw_d1050100_bin10-20_low
QEVAP_LOW_CDSP_INV_4	Average CDSP Invert Evaporation Rate in Bin 4, Low Infiltration Flux Scenario	RIP_Qevap_invavg_hlw_d0010500_bin20-60_low
QEVAP_LOW_CDSP_BIN4_NOBF		RIP_Qevap_invavg_hlw_d1050100_bin20-60_low
QEVAP_LOW_CDSP_INV_5	Average CDSP Invert Evaporation Rate in Bin 5, Low Infiltration Flux Scenario	RIP_Qevap_invavg_hlw_d0010500_bin-60_low
QEVAP_LOW_CDSP_BIN5_NOBF		RIP_Qevap_invavg_hlw_d1050100_bin-60_low
QEVAP_MEAN_CDSP_INV_1	Average CDSP Invert Evaporation Rate in Bin 1, Mean Infiltration Flux Scenario	RIP_Qevap_invavg_hlw_d0010500_bin0-3_mean
QEVAP_MEAN_CDSP_BIN1_NOBF		RIP_Qevap_invavg_hlw_d1050100_bin0-3_mean
QEVAP_MEAN_CDSP_INV_2	Average CDSP Invert Evaporation Rate in Bin 2, Mean Infiltration Flux Scenario	RIP_Qevap_invavg_hlw_d0010500_bin3-10_mean
QEVAP_MEAN_CDSP_BIN2_NOBF		RIP_Qevap_invavg_hlw_d1050100_bin3-10_mean
QEVAP_MEAN_CDSP_INV_3	Average CDSP Invert Evaporation Rate in Bin 3, Mean Infiltration Flux Scenario	RIP_Qevap_invavg_hlw_d0010500_bin10-20_mean
QEVAP_MEAN_CDSP_BIN3_NOBF		RIP_Qevap_invavg_hlw_d1050100_bin10-20_mean
QEVAP_MEAN_CDSP_INV_4	Average CDSP Invert Evaporation Rate in Bin 4, Mean Infiltration Flux Scenario	RIP_Qevap_invavg_hlw_d0010500_bin20-60_mean
QEVAP_MEAN_CDSP_BIN4_NOBF		RIP_Qevap_invavg_hlw_d1050100_bin20-60_mean
QEVAP_MEAN_CDSP_INV_5	Average CDSP Invert Evaporation Rate in Bin 5, Mean Infiltration Flux Scenario	RIP_Qevap_invavg_hlw_d0010500_bin-60_mean
QEVAP_MEAN_CDSP_BIN5_NOBF		RIP_Qevap_invavg_hlw_d1050100_bin-60_mean
QEVAP_HIGH_CDSP_INV_1	Average CDSP Invert Evaporation Rate in Bin 1, High Infiltration Flux Scenario	RIP_Qevap_invavg_hlw_d0010500_bin0-3_high
QEVAP_HIGH_CDSP_BIN1_NOBF		RIP_Qevap_invavg_hlw_d1050100_bin0-3_high
QEVAP_HIGH_CDSP_INV_2	Average CDSP Invert Evaporation Rate in Bin 2, High Infiltration Flux Scenario	RIP_Qevap_invavg_hlw_d0010500_bin3-10_high
QEVAP_HIGH_CDSP_BIN2_NOBF		RIP_Qevap_invavg_hlw_d1050100_bin3-10_high
QEVAP_HIGH_CDSP_INV_3	Average CDSP Invert Evaporation Rate in Bin 3, High Infiltration Flux Scenario	RIP_Qevap_invavg_hlw_d0010500_bin10-20_high
QEVAP_HIGH_CDSP_BIN3_NOBF		RIP_Qevap_invavg_hlw_d1050100_bin10-20_high
QEVAP_HIGH_CDSP_INV_4	Average CDSP Invert Evaporation Rate in Bin 4, High Infiltration Flux Scenario	RIP_Qevap_invavg_hlw_d0010500_bin20-60_high
QEVAP_HIGH_CDSP_BIN4_NOBF		RIP_Qevap_invavg_hlw_d1050100_bin20-60_high
QEVAP_HIGH_CDSP_INV_5	Average CDSP Invert Evaporation Rate in Bin 5, High Infiltration Flux Scenario	RIP_Qevap_invavg_hlw_d0010500_bin-60_high
QEVAP_HIGH_CDSP_BIN5_NOBF		RIP_Qevap_invavg_hlw_d1050100_bin-60_high

Table 6-11. Input Parameters for the Thermal Hydrology Calculations (Continued)

TSPA Parameter ^a	Description	Reference File ^b
SAT_LOW_CSNF_1	Average CSNF Invert Liquid Saturation in Bin 1, Low Infiltration Flux Scenario	RIP_SLavg_csnf_d0010500_bin0-3_low
SAT_LOW_CSNF_BIN1_NOBF		RIP_SLavg_csnf_d1050100_bin0-3_low
SAT_LOW_CSNF_2	Average CSNF Invert Liquid Saturation in Bin 2, Low Infiltration Flux Scenario	RIP_SLavg_csnf_d0010500_bin3-10_low
SAT_LOW_CSNF_BIN2_NOBF		RIP_SLavg_csnf_d1050100_bin3-10_low
SAT_LOW_CSNF_3	Average CSNF Invert Liquid Saturation in Bin 3, Low Infiltration Flux Scenario	RIP_SLavg_csnf_d0010500_bin10-20_low
SAT_LOW_CSNF_BIN3_NOBF		RIP_SLavg_csnf_d1050100_bin10-20_low
SAT_LOW_CSNF_4	Average CSNF Invert Liquid Saturation in Bin 4, Low Infiltration Flux Scenario	RIP_SLavg_csnf_d0010500_bin20-60_low
SAT_LOW_CSNF_BIN4_NOBF		RIP_SLavg_csnf_d1050100_bin20-60_low
SAT_LOW_CSNF_5	Average CSNF Invert Liquid Saturation in Bin 5, Low Infiltration Flux Scenario	RIP_SLavg_csnf_d0010500_bin-60_low
SAT_LOW_CSNF_BIN5_NOBF		RIP_SLavg_csnf_d1050100_bin-60_low
SAT_MEAN_CSNF_1	Average CSNF Invert Liquid Saturation in Bin 1, Mean Infiltration Flux Scenario	RIP_SLavg_csnf_d0010500_bin0-3_mean
SAT_MEAN_CSNF_BIN1_NOBF		RIP_SLavg_csnf_d1050100_bin0-3_mean
SAT_MEAN_CSNF_2	Average CSNF Invert Liquid Saturation in Bin 2, Mean Infiltration Flux Scenario	RIP_SLavg_csnf_d0010500_bin3-10_mean
SAT_MEAN_CSNF_BIN2_NOBF		RIP_SLavg_csnf_d1050100_bin3-10_mean
SAT_MEAN_CSNF_3	Average CSNF Invert Liquid Saturation in Bin 3, Mean Infiltration Flux Scenario	RIP_SLavg_csnf_d0010500_bin10-20_mean
SAT_MEAN_CSNF_BIN3_NOBF		RIP_SLavg_csnf_d1050100_bin10-20_mean
SAT_MEAN_CSNF_4	Average CSNF Invert Liquid Saturation in Bin 4, Mean Infiltration Flux Scenario	RIP_SLavg_csnf_d0010500_bin20-60_mean
SAT_MEAN_CSNF_BIN4_NOBF		RIP_SLavg_csnf_d1050100_bin20-60_mean
SAT_MEAN_CSNF_5	Average CSNF Invert Liquid Saturation in Bin 5, Mean Infiltration Flux Scenario	RIP_SLavg_csnf_d0010500_bin-60_mean
SAT_MEAN_CSNF_BIN5_NOBF		RIP_SLavg_csnf_d1050100_bin-60_mean
SAT_HIGH_CSNF_1	Average CSNF Invert Liquid Saturation in Bin 1, High Infiltration Flux Scenario	RIP_SLavg_csnf_d0010500_bin0-3_high
SAT_HIGH_CSNF_BIN1_NOBF		RIP_SLavg_csnf_d1050100_bin0-3_high
SAT_HIGH_CSNF_2	Average CSNF Invert Liquid Saturation in Bin 2, High Infiltration Flux Scenario	RIP_SLavg_csnf_d0010500_bin3-10_high
SAT_HIGH_CSNF_BIN2_NOBF		RIP_SLavg_csnf_d1050100_bin3-10_high
SAT_HIGH_CSNF_3	Average CSNF Invert Liquid Saturation in Bin 3, High Infiltration Flux Scenario	RIP_SLavg_csnf_d0010500_bin10-20_high
SAT_HIGH_CSNF_BIN3_NOBF		RIP_SLavg_csnf_d1050100_bin10-20_high
SAT_HIGH_CSNF_4	Average CSNF Invert Liquid Saturation in Bin 4, High Infiltration Flux Scenario	RIP_SLavg_csnf_d0010500_bin20-60_high
SAT_HIGH_CSNF_BIN4_NOBF		RIP_SLavg_csnf_d1050100_bin20-60_high
SAT_HIGH_CSNF_5	Average CSNF Invert Liquid Saturation in Bin 5, High Infiltration Flux Scenario	RIP_SLavg_csnf_d0010500_bin-60_high
SAT_HIGH_CSNF_BIN5_NOBF		RIP_SLavg_csnf_d1050100_bin-60_high
SAT_LOW_CDSP_1	Average CDSP Invert Liquid Saturation in Bin 1, Low Infiltration Flux Scenario	RIP_SLavg_hlw_d0010500_bin0-3_low
SAT_LOW_CDSP_BIN1_NOBF		RIP_SLavg_hlw_d1050100_bin0-3_low
SAT_LOW_CDSP_2	Average CDSP Invert Liquid Saturation in Bin 2, Low Infiltration Flux Scenario	RIP_SLavg_hlw_d0010500_bin3-10_low
SAT_LOW_CDSP_BIN2_NOBF		RIP_SLavg_hlw_d1050100_bin3-10_low
SAT_LOW_CDSP_3	Average CDSP Invert Liquid Saturation in Bin 3, Low Infiltration Flux Scenario	RIP_SLavg_hlw_d0010500_bin10-20_low
SAT_LOW_CDSP_BIN3_NOBF		RIP_SLavg_hlw_d1050100_bin10-20_low
SAT_LOW_CDSP_4	Average CDSP Invert Liquid Saturation in Bin 4, Low Infiltration Flux Scenario	RIP_SLavg_hlw_d0010500_bin20-60_low
SAT_LOW_CDSP_BIN4_NOBF		RIP_SLavg_hlw_d1050100_bin20-60_low
SAT_LOW_CDSP_5	Average CDSP Invert Liquid Saturation in Bin 5, Low Infiltration Flux Scenario	RIP_SLavg_hlw_d0010500_bin-60_low
SAT_LOW_CDSP_BIN5_NOBF		RIP_SLavg_hlw_d1050100_bin-60_low
SAT_MEAN_CDSP_1	Average CDSP Invert Liquid Saturation in Bin 1, Mean Infiltration Flux Scenario	RIP_SLavg_hlw_d0010500_bin0-3_mean
SAT_MEAN_CDSP_BIN1_NOBF		RIP_SLavg_hlw_d1050100_bin0-3_mean

Table 6-11. Input Parameters for the Thermal Hydrology Calculations (Continued)

TSPA Parameter ^a	Description	Reference File ^b
SAT_MEAN_CDSP_2	Average CDSP Invert Liquid Saturation in Bin 2, Mean Infiltration Flux Scenario	RIP_SLavg_hlw_d0010500_bin3-10_mean
SAT_MEAN_CDSP_BIN2_NOBF		RIP_SLavg_hlw_d1050100_bin3-10_mean
SAT_MEAN_CDSP_3	Average CDSP Invert Liquid Saturation in Bin 3, Mean Infiltration Flux Scenario	RIP_SLavg_hlw_d0010500_bin10-20_mean
SAT_MEAN_CDSP_BIN3_NOBF		RIP_SLavg_hlw_d1050100_bin10-20_mean
SAT_MEAN_CDSP_4	Average CDSP Invert Liquid Saturation in Bin 4, Mean Infiltration Flux Scenario	RIP_SLavg_hlw_d0010500_bin20-60_mean
SAT_MEAN_CDSP_BIN4_NOBF		RIP_SLavg_hlw_d1050100_bin20-60_mean
SAT_MEAN_CDSP_5	Average CDSP Invert Liquid Saturation in Bin 5, Mean Infiltration Flux Scenario	RIP_SLavg_hlw_d0010500_bin-60_mean
SAT_MEAN_CDSP_BIN5_NOBF		RIP_SLavg_hlw_d1050100_bin-60_mean
SAT_HIGH_CDSP_1	Average CDSP Invert Liquid Saturation in Bin 1, High Infiltration Flux Scenario	RIP_SLavg_hlw_d0010500_bin0-3_high
SAT_HIGH_CDSP_BIN1_NOBF		RIP_SLavg_hlw_d1050100_bin0-3_high
SAT_HIGH_CDSP_2	Average CDSP Invert Liquid Saturation in Bin 2, High Infiltration Flux Scenario	RIP_SLavg_hlw_d0010500_bin3-10_high
SAT_HIGH_CDSP_BIN2_NOBF		RIP_SLavg_hlw_d1050100_bin3-10_high
SAT_HIGH_CDSP_3	Average CDSP Invert Liquid Saturation in Bin 3, High Infiltration Flux Scenario	RIP_SLavg_hlw_d0010500_bin10-20_high
SAT_HIGH_CDSP_BIN3_NOBF		RIP_SLavg_hlw_d1050100_bin10-20_high
SAT_HIGH_CDSP_4	Average CDSP Invert Liquid Saturation in Bin 4, High Infiltration Flux Scenario	RIP_SLavg_hlw_d0010500_bin20-60_high
SAT_HIGH_CDSP_BIN4_NOBF		RIP_SLavg_hlw_d1050100_bin20-60_high
SAT_HIGH_CDSP_5	Average CDSP Invert Liquid Saturation in Bin 5, High Infiltration Flux Scenario	RIP_SLavg_hlw_d0010500_bin-60_high
SAT_HIGH_CDSP_BIN5_NOBF		RIP_SLavg_hlw_d1050100_bin-60_high
QFLUX_LOW_CS NF_INV_1	Average CSNF Invert Liquid Volume Flow Rate in Bin 1, Low Infiltration Flux Scenario	RIP_qpercinvavg_csnf_d0010500_bin0-3_low
QFLUX_LOW_CS NF_INV1_NOBF		RIP_qpercinvavg_ABS_csnf_d1050100_bin0-3_low
QFLUX_LOW_CS NF_INV_2	Average CSNF Invert Liquid Volume Flow Rate in Bin 2, Low Infiltration Flux Scenario	RIP_qpercinvavg_csnf_d0010500_bin3-10_low
QFLUX_LOW_CS NF_INV2_NOBF		RIP_qpercinvavg_ABS_csnf_d1050100_bin3-10_low
QFLUX_LOW_CS NF_INV_3	Average CSNF Invert Liquid Volume Flow Rate in Bin 3, Low Infiltration Flux Scenario	RIP_qpercinvavg_csnf_d0010500_bin10-20_low
QFLUX_LOW_CS NF_INV3_NOBF		RIP_qpercinvavg_ABS_csnf_d1050100_bin10-20_low
QFLUX_LOW_CS NF_INV_4	Average CSNF Invert Liquid Volume Flow Rate in Bin 4, Low Infiltration Flux Scenario	RIP_qpercinvavg_csnf_d0010500_bin20-60_low
QFLUX_LOW_CS NF_INV4_NOBF		RIP_qpercinvavg_ABS_csnf_d1050100_bin20-60_low
QFLUX_LOW_CS NF_INV_5	Average CSNF Invert Liquid Volume Flow Rate in Bin 5, Low Infiltration Flux Scenario	RIP_qpercinvavg_csnf_d0010500_bin-60_low
QFLUX_LOW_CS NF_INV5_NOBF		RIP_qpercinvavg_ABS_csnf_d1050100_bin-60_low
QFLUX_MEAN_CS NF_INV_1	Average CSNF Invert Liquid Volume Flow Rate in Bin 1, Mean Infiltration Flux Scenario	RIP_qpercinvavg_csnf_d0010500_bin0-3_mean
QFLUX_MEAN_CS NF_INV1_NOBF		RIP_qpercinvavg_ABS_csnf_d1050100_bin0-3_mean
QFLUX_MEAN_CS NF_INV_2	Average CSNF Invert Liquid Volume Flow Rate in Bin 2, Mean Infiltration Flux Scenario	RIP_qpercinvavg_csnf_d0010500_bin3-10_mean
QFLUX_MEAN_CS NF_INV2_NOBF		RIP_qpercinvavg_ABS_csnf_d1050100_bin3-10_mean
QFLUX_MEAN_CS NF_INV_3	Average CSNF Invert Liquid Volume Flow Rate in Bin 3, Mean Infiltration Flux Scenario	RIP_qpercinvavg_csnf_d0010500_bin10-20_mean
QFLUX_MEAN_CS NF_INV3_NOBF		RIP_qpercinvavg_ABS_csnf_d1050100_bin10-20_mean

Table 6-11. Input Parameters for the Thermal Hydrology Calculations (Continued)

TSPA Parameter ^a	Description	Reference File ^b
QFLUX_MEAN_CSNF_INV_4	Average CSNF Invert Liquid Volume Flow Rate in Bin 4, Mean Infiltration Flux Scenario	RIP_qpercinvavg_csnf_d0010500_bin20-60_mean
QFLUX_MEAN_CSNF_INV4_NOBF		RIP_qpercinvavg_ABS_csnf_d1050100_bin20-60_mean
QFLUX_MEAN_CSNF_INV_5	Average CSNF Invert Liquid Volume Flow Rate in Bin 5, Mean Infiltration Flux Scenario	RIP_qpercinvavg_csnf_d0010500_bin-60_mean
QFLUX_MEAN_CSNF_INV5_NOBF		RIP_qpercinvavg_ABS_csnf_d1050100_bin-60_mean
QFLUX_HIGH_CSNF_INV_1	Average CSNF Invert Liquid Volume Flow Rate in Bin 1, High Infiltration Flux Scenario	RIP_qpercinvavg_csnf_d0010500_bin0-3_high
QFLUX_HIGH_CSNF_INV1_NOBF		RIP_qpercinvavg_ABS_csnf_d1050100_bin0-3_high
QFLUX_HIGH_CSNF_INV_2	Average CSNF Invert Liquid Volume Flow Rate in Bin 2, High Infiltration Flux Scenario	RIP_qpercinvavg_csnf_d0010500_bin3-10_high
QFLUX_HIGH_CSNF_INV2_NOBF		RIP_qpercinvavg_ABS_csnf_d1050100_bin3-10_high
QFLUX_HIGH_CSNF_INV_3	Average CSNF Invert Liquid Volume Flow Rate in Bin 3, High Infiltration Flux Scenario	RIP_qpercinvavg_csnf_d0010500_bin10-20_high
QFLUX_HIGH_CSNF_INV3_NOBF		RIP_qpercinvavg_ABS_csnf_d1050100_bin10-20_high
QFLUX_HIGH_CSNF_INV_4	Average CSNF Invert Liquid Volume Flow Rate in Bin 4, High Infiltration Flux Scenario	RIP_qpercinvavg_csnf_d0010500_bin20-60_high
QFLUX_HIGH_CSNF_INV4_NOBF		RIP_qpercinvavg_ABS_csnf_d1050100_bin20-60_high
QFLUX_HIGH_CSNF_INV_5	Average CSNF Invert Liquid Volume Flow Rate in Bin 5, High Infiltration Flux Scenario	RIP_qpercinvavg_csnf_d0010500_bin-60_high
QFLUX_HIGH_CSNF_INV5_NOBF		RIP_qpercinvavg_ABS_csnf_d1050100_bin-60_high
QFLUX_LOW_CDSP_INV_1	Average CDSP Invert Liquid Volume Flow Rate in Bin 1, Low Infiltration Flux Scenario	RIP_qpercinvavg_hlw_d0010500_bin0-3_low
QFLUX_LOW_CDSP_INV1_NOBF		RIP_qpercinvavg_ABS_hlw_d1050100_bin0-3_low
QFLUX_LOW_CDSP_INV_2	Average CDSP Invert Liquid Volume Flow Rate in Bin 2, Low Infiltration Flux Scenario	RIP_qpercinvavg_hlw_d0010500_bin3-10_low
QFLUX_LOW_CDSP_INV2_NOBF		RIP_qpercinvavg_ABS_hlw_d1050100_bin3-10_low
QFLUX_LOW_CDSP_INV_3	Average CDSP Invert Liquid Volume Flow Rate in Bin 3, Low Infiltration Flux Scenario	RIP_qpercinvavg_hlw_d0010500_bin10-20_low
QFLUX_LOW_CDSP_INV3_NOBF		RIP_qpercinvavg_ABS_hlw_d1050100_bin10-20_low
QFLUX_LOW_CDSP_INV_4	Average CDSP Invert Liquid Volume Flow Rate in Bin 4, Low Infiltration Flux Scenario	RIP_qpercinvavg_hlw_d0010500_bin20-60_low
QFLUX_LOW_CDSP_INV4_NOBF		RIP_qpercinvavg_ABS_hlw_d1050100_bin20-60_low
QFLUX_LOW_CDSP_INV_5	Average CDSP Invert Liquid Volume Flow Rate in Bin 5, Low Infiltration Flux Scenario	RIP_qpercinvavg_hlw_d0010500_bin-60_low
QFLUX_LOW_CDSP_INV5_NOBF		RIP_qpercinvavg_ABS_hlw_d1050100_bin-60_low
QFLUX_MEAN_CDSP_INV_1	Average CDSP Invert Liquid Volume Flow Rate in Bin 1, Mean Infiltration Flux Scenario	RIP_qpercinvavg_hlw_d0010500_bin0-3_mean
QFLUX_MEAN_CDSP_INV1_NOBF		RIP_qpercinvavg_ABS_hlw_d1050100_bin0-3_mean
QFLUX_MEAN_CDSP_INV_2	Average CDSP Invert Liquid Volume Flow Rate in Bin 2, Mean Infiltration Flux Scenario	RIP_qpercinvavg_hlw_d0010500_bin3-10_mean
QFLUX_MEAN_CDSP_INV2_NOBF		RIP_qpercinvavg_ABS_hlw_d1050100_bin3-10_mean

Table 6-11. Input Parameters for the Thermal Hydrology Calculations (Continued)

TSPA Parameter ^a	Description	Reference File ^b
QFLUX_MEAN_CDSP_INV_3	Average CDSP Invert Liquid Volume Flow Rate in Bin 3, Mean Infiltration Flux Scenario	RIP_qpercinvavg_hlw_d0010500_bin10-20_mean
QFLUX_MEAN_CDSP_INV3_NOBF		RIP_qpercinvavg_ABS_hlw_d1050100_bin10-20_mean
QFLUX_MEAN_CDSP_INV_4	Average CDSP Invert Liquid Volume Flow Rate in Bin 4, Mean Infiltration Flux Scenario	RIP_qpercinvavg_hlw_d0010500_bin20-60_mean
QFLUX_MEAN_CDSP_INV4_NOBF		RIP_qpercinvavg_ABS_hlw_d1050100_bin20-60_mean
QFLUX_MEAN_CDSP_INV_5	Average CDSP Invert Liquid Volume Flow Rate in Bin 5, Mean Infiltration Flux Scenario	RIP_qpercinvavg_hlw_d0010500_bin60_mean
QFLUX_MEAN_CDSP_INV5_NOBF		RIP_qpercinvavg_ABS_hlw_d1050100_bin60_mean
QFLUX_HIGH_CDSP_INV_1	Average CDSP Invert Liquid Volume Flow Rate in Bin 1, High Infiltration Flux Scenario	RIP_qpercinvavg_hlw_d0010500_bin0-3_high
QFLUX_HIGH_CDSP_INV1_NOBF		RIP_qpercinvavg_ABS_hlw_d1050100_bin0-3_high
QFLUX_HIGH_CDSP_INV_2	Average CDSP Invert Liquid Volume Flow Rate in Bin 2, High Infiltration Flux Scenario	RIP_qpercinvavg_hlw_d0010500_bin3-10_high
QFLUX_HIGH_CDSP_INV2_NOBF		RIP_qpercinvavg_ABS_hlw_d1050100_bin3-10_high
QFLUX_HIGH_CDSP_INV_3	Average CDSP Invert Liquid Volume Flow Rate in Bin 3, High Infiltration Flux Scenario	RIP_qpercinvavg_hlw_d0010500_bin10-20_high
QFLUX_HIGH_CDSP_INV3_NOBF		RIP_qpercinvavg_ABS_hlw_d1050100_bin10-20_high
QFLUX_HIGH_CDSP_INV_4	Average CDSP Invert Liquid Volume Flow Rate in Bin 4, High Infiltration Flux Scenario	RIP_qpercinvavg_hlw_d0010500_bin20-60_high
QFLUX_HIGH_CDSP_INV4_NOBF		RIP_qpercinvavg_ABS_hlw_d1050100_bin20-60_high
QFLUX_HIGH_CDSP_INV_5	Average CDSP Invert Liquid Volume Flow Rate in Bin 5, High Infiltration Flux Scenario	RIP_qpercinvavg_hlw_d0010500_bin60_high
QFLUX_HIGH_CDSP_INV5_NOBF		RIP_qpercinvavg_ABS_hlw_d1050100_bin60_high
CSNF_bf_high_pf_bin2.dat (seepage DLL input file)	Percolation Flux 5 m above drift for CSNF BIN2 spatial locations, High Infiltration Flux Scenario, Backfill Case	RIP_csnf_qperc_d0010500_bin3-10_high
CSNF_bf_high_pf_bin3.dat (seepage DLL input file)	Percolation Flux 5 m above drift for CSNF BIN3 spatial locations, High Infiltration Flux Scenario, Backfill Case	RIP_csnf_qperc_d0010500_bin10-20_high
CSNF_bf_high_pf_bin4.dat (seepage DLL input file)	Percolation Flux 5 m above drift for CSNF BIN4 spatial locations, High Infiltration Flux Scenario, Backfill Case	RIP_csnf_qperc_d0010500_bin20-60_high
CSNF_bf_high_pf_bin5.dat (seepage DLL input file)	Percolation Flux 5 m above drift for CSNF BIN5 spatial locations, High Infiltration Flux Scenario, Backfill Case	RIP_csnf_qperc_d0010500_bin60_high
CSNF_bf_low_pf_bin1.dat (seepage DLL input file)	Percolation Flux 5 m above drift for CSNF BIN1 spatial locations, Low Infiltration Flux Scenario, Backfill Case	RIP_csnf_qperc_d0010500_bin0-3_low
CSNF_bf_low_pf_bin2.dat (seepage DLL input file)	Percolation Flux 5 m above drift for CSNF BIN2 spatial locations, Low Infiltration Flux Scenario, Backfill Case	RIP_csnf_qperc_d0010500_bin3-10_low
CSNF_bf_mean_pf_bin1.dat (seepage DLL input file)	Percolation Flux 5 m above drift for CSNF BIN1 spatial locations, Mean Infiltration Flux Scenario, Backfill Case	RIP_csnf_qperc_d0010500_bin0-3_mean
CSNF_bf_mean_pf_bin2.dat (seepage DLL input file)	Percolation Flux 5 m above drift for CSNF BIN2 spatial locations, Mean Infiltration Flux Scenario, Backfill Case	RIP_csnf_qperc_d0010500_bin3-10_mean

Table 6-11. Input Parameters for the Thermal Hydrology Calculations (Continued)

TSPA Parameter^a	Description	Reference File^b
CSNF_bf_mean_pf_bin3.dat (seepage DLL input file)	Percolation Flux 5 m above drift for CSNF BIN3 spatial locations, Mean Infiltration Flux Scenario, Backfill Case	RIP_csnf_qperc_d0010500_bin10-20_mean
CSNF_bf_mean_pf_bin4.dat (seepage DLL input file)	Percolation Flux 5 m above drift for CSNF BIN4 spatial locations, Mean Infiltration Flux Scenario, Backfill Case	RIP_csnf_qperc_d0010500_bin20-60_mean
CSNF_bf_mean_pf_bin5.dat (seepage DLL input file)	Percolation Flux 5 m above drift for CSNF BIN5 spatial locations, Mean Infiltration Flux Scenario, Backfill Case	RIP_csnf_qperc_d0010500_bin-60_mean
CSNF_nbf_high_pf_bin2.dat (seepage DLL input file)	Percolation Flux 5 m above drift for CSNF BIN2 spatial locations, High Infiltration Flux Scenario, No Backfill Case	RIP_csnf_qperc_d1050100_bin3-10_high
CSNF_nbf_high_pf_bin3.dat (seepage DLL input file)	Percolation Flux 5 m above drift for CSNF BIN3 spatial locations, High Infiltration Flux Scenario, No Backfill Case	RIP_csnf_qperc_d1050100_bin10-20_high
CSNF_nbf_high_pf_bin4.dat (seepage DLL input file)	Percolation Flux 5 m above drift for CSNF BIN4 spatial locations, High Infiltration Flux Scenario, No Backfill Case	RIP_csnf_qperc_d1050100_bin20-60_high
CSNF_nbf_high_pf_bin5.dat (seepage DLL input file)	Percolation Flux 5 m above drift for CSNF BIN5 spatial locations, High Infiltration Flux Scenario, No Backfill Case	RIP_csnf_qperc_d1050100_bin-60_high
CSNF_nbf_low_pf_bin1.dat (seepage DLL input file)	Percolation Flux 5 m above drift for CSNF BIN1 spatial locations, Low Infiltration Flux Scenario, No Backfill Case	RIP_csnf_qperc_d1050100_bin0-3_low
CSNF_nbf_low_pf_bin2.dat (seepage DLL input file)	Percolation Flux 5 m above drift for CSNF BIN2 spatial locations, Low Infiltration Flux Scenario, No Backfill Case	RIP_csnf_qperc_d1050100_bin3-10_low
CSNF_nbf_mean_pf_bin1.dat (seepage DLL input file)	Percolation Flux 5 m above drift for CSNF BIN1 spatial locations, Mean Infiltration Flux Scenario, No Backfill Case	RIP_csnf_qperc_d1050100_bin0-3_mean
CSNF_nbf_mean_pf_bin2.dat (seepage DLL input file)	Percolation Flux 5 m above drift for CSNF BIN2 spatial locations, Mean Infiltration Flux Scenario, No Backfill Case	RIP_csnf_qperc_d1050100_bin3-10_mean
CSNF_nbf_mean_pf_bin3.dat (seepage DLL input file)	Percolation Flux 5 m above drift for CSNF BIN3 spatial locations, Mean Infiltration Flux Scenario, No Backfill Case	RIP_csnf_qperc_d1050100_bin10-20_mean
CSNF_nbf_mean_pf_bin4.dat (seepage DLL input file)	Percolation Flux 5 m above drift for CSNF BIN4 spatial locations, Mean Infiltration Flux Scenario, No Backfill Case	RIP_csnf_qperc_d1050100_bin20-60_mean
CSNF_nbf_mean_pf_bin5.dat (seepage DLL input file)	Percolation Flux 5 m above drift for CSNF BIN5 spatial locations, Mean Infiltration Flux Scenario, No Backfill Case	RIP_csnf_qperc_d1050100_bin-60_mean
HLW_bf_high_pf_bin2.dat (seepage DLL input file)	Percolation Flux 5 m above drift for HLW BIN2 spatial locations, High Infiltration Flux Scenario, Backfill Case	RIP_hlw_qperc_d0010500_bin3-10_high

Table 6-11. Input Parameters for the Thermal Hydrology Calculations (Continued)

TSPA Parameter^a	Description	Reference File^b
HLW_bf_high_pf_bin3.dat (seepage DLL input file)	Percolation Flux 5 m above drift for HLW BIN3 spatial locations, High Infiltration Flux Scenario, Backfill Case	RIP_hlw_qperc_d0010500_bin10-20_high
HLW_bf_high_pf_bin4.dat (seepage DLL input file)	Percolation Flux 5 m above drift for HLW BIN4 spatial locations, High Infiltration Flux Scenario, Backfill Case	RIP_hlw_qperc_d0010500_bin20-60_high
HLW_bf_high_pf_bin5.dat (seepage DLL input file)	Percolation Flux 5 m above drift for HLW BIN5 spatial locations, High Infiltration Flux Scenario, Backfill Case	RIP_hlw_qperc_d0010500_bin-60_high
HLW_bf_low_pf_bin1.dat (seepage DLL input file)	Percolation Flux 5 m above drift for HLW BIN1 spatial locations, Low Infiltration Flux Scenario, Backfill Case	RIP_hlw_qperc_d0010500_bin0-3_low
HLW_bf_low_pf_bin2.dat (seepage DLL input file)	Percolation Flux 5 m above drift for HLW BIN2 spatial locations, Low Infiltration Flux Scenario, Backfill Case	RIP_hlw_qperc_d0010500_bin3-10_low
HLW_bf_mean_pf_bin1.dat (seepage DLL input file)	Percolation Flux 5 m above drift for HLW BIN1 spatial locations, Mean Infiltration Flux Scenario, Backfill Case	RIP_hlw_qperc_d0010500_bin0-3_mean
HLW_bf_mean_pf_bin2.dat (seepage DLL input file)	Percolation Flux 5 m above drift for HLW BIN2 spatial locations, Mean Infiltration Flux Scenario, Backfill Case	RIP_hlw_qperc_d0010500_bin3-10_mean
HLW_bf_mean_pf_bin3.dat (seepage DLL input file)	Percolation Flux 5 m above drift for HLW BIN3 spatial locations, Mean Infiltration Flux Scenario, Backfill Case	RIP_hlw_qperc_d0010500_bin10-20_mean
HLW_bf_mean_pf_bin4.dat (seepage DLL input file)	Percolation Flux 5 m above drift for HLW BIN4 spatial locations, Mean Infiltration Flux Scenario, Backfill Case	RIP_hlw_qperc_d0010500_bin20-60_mean
HLW_bf_mean_pf_bin5.dat (seepage DLL input file)	Percolation Flux 5 m above drift for HLW BIN5 spatial locations, Mean Infiltration Flux Scenario, Backfill Case	RIP_hlw_qperc_d0010500_bin-60_mean
HLW_nbf_high_pf_bin2.dat (seepage DLL input file)	Percolation Flux 5 m above drift for HLW BIN2 spatial locations, High Infiltration Flux Scenario, No Backfill Case	RIP_hlw_qperc_d1050100_bin3-10_high
HLW_nbf_high_pf_bin3.dat (seepage DLL input file)	Percolation Flux 5 m above drift for HLW BIN3 spatial locations, High Infiltration Flux Scenario, No Backfill Case	RIP_hlw_qperc_d1050100_bin10-20_high
HLW_nbf_high_pf_bin4.dat (seepage DLL input file)	Percolation Flux 5 m above drift for HLW BIN4 spatial locations, High Infiltration Flux Scenario, No Backfill Case	RIP_hlw_qperc_d1050100_bin20-60_high
HLW_nbf_high_pf_bin5.dat (seepage DLL input file)	Percolation Flux 5 m above drift for HLW BIN5 spatial locations, High Infiltration Flux Scenario, No Backfill Case	RIP_hlw_qperc_d1050100_bin-60_high
HLW_nbf_low_pf_bin1.dat (seepage DLL input file)	Percolation Flux 5 m above drift for HLW BIN1 spatial locations, Low Infiltration Flux Scenario, No Backfill Case	RIP_hlw_qperc_d1050100_bin0-3_low
HLW_nbf_low_pf_bin2.dat (seepage DLL input file)	Percolation Flux 5 m above drift for HLW BIN2 spatial locations, Low Infiltration Flux Scenario, No Backfill Case	RIP_hlw_qperc_d1050100_bin3-10_low
HLW_nbf_mean_pf_bin1.dat (seepage DLL input file)	Percolation Flux 5 m above drift for HLW BIN1 spatial locations, Mean Infiltration Flux Scenario, No Backfill Case	RIP_hlw_qperc_d1050100_bin0-3_mean
HLW_nbf_mean_pf_bin2.dat (seepage DLL input file)	Percolation Flux 5 m above drift for HLW BIN2 spatial locations, Mean Infiltration Flux Scenario, No Backfill Case	RIP_hlw_qperc_d1050100_bin3-10_mean
HLW_nbf_mean_pf_bin3.dat (seepage DLL input file)	Percolation Flux 5 m above drift for HLW BIN3 spatial locations, Mean Infiltration Flux Scenario, No Backfill Case	RIP_hlw_qperc_d1050100_bin10-20_mean

Table 6-11. Input Parameters for the Thermal Hydrology Calculations (Continued)

TSPA Parameter ^a	Description	Reference File ^b
HLW_nbf_mean_pf_bin4.dat (seepage DLL input file)	Percolation Flux 5 m above drift for HLW BIN4 spatial locations, Mean Infiltration Flux Scenario, No Backfill Case	RIP_hlw_qperc_d1050100_bin20-60_mean
HLW_nbf_mean_pf_bin5.dat (seepage DLL input file)	Percolation Flux 5 m above drift for HLW BIN5 spatial locations, Mean Infiltration Flux Scenario, No Backfill Case	RIP_hlw_qperc_d1050100_bin-60_mean

DTN: SN0001T0872799.006 [147198]; SN0007T0872799.014 [152545]

NOTES: ^aNOBF in the parameter name denotes a no backfill case data set;

^bCRWMS M&O 2000 [149860]

Implementation

The TSPA-SR abstraction of the multiscale thermal hydrologic model data generated parameters describing the temporal fluctuations in the waste package surface temperature, invert temperature, invert relative humidity, invert liquid evaporation rates, invert liquid saturation, and invert liquid volume flow rate. For each design option, backfill or no backfill, thirty data sets were generated for each of these six parameters. They were generated for each infiltration rate bin (e.g., 5 bins), including each infiltration flux scenario (e.g., low, mean, and high) and each waste package type (e.g., CSNF, CDSP). It is noted that within a given infiltration flux scenario (e.g., the mean infiltration flux case), the same thermal hydrology results (for that flux case) were used for all three seepage state environments: Always Drips, Intermittent Drips, and No Drips. The data files applied to the total system model are obtained from the abstraction AMR (CRWMS M&O 2000 [149860], Section 7) and are listed in Table 6-11. The electronic data files were used as received from the TDMS. Figure 6-38 shows the organization of the TSPA-SR TH Model component. A model parameter called '*Backfill_Case*' is used to determine which set of thermal hydrologic data will be used for a given simulation. A value of 1 indicates a backfill design option, a value of 0 indicates the no backfill design option will be simulated.

Figure 6-39 and Figure 6-40 illustrate the organization and selection of the appropriate surface temperature time history for the CSNF waste packages in each infiltration bin. The temperature parameters include temperature profiles for the waste package surface and invert temperature, as well as the maximum waste package temperatures obtained for each infiltration rate bin in each infiltration flux scenario. Figure 6-39 shows the separation of each waste package type. Figure 6-40 illustrates the selection of the appropriate CSNF waste package surface temperature profile for the model calculations. There is one input profile per infiltration rate bin for each of the three infiltration flux scenarios. The model selects the correct profile for each infiltration rate bin based on the infiltration scenario, low, mean, or high, determined at the initiation of the simulation (see Section 6.3.1.1 Climate and Infiltration).

The TSPA-SR parameter *TEMP_MEAN_CSNF_WP* combines the mean infiltration flux case surface temperature profiles for CSNF waste packages in each of the five infiltration bins (*TEMP_MEAN_CSNF_WP_1*, *TEMP_MEAN_CSNF_WP_2*, *TEMP_MEAN_CSNF_WP_3*, *TEMP_MEAN_CSNF_WP_4*, and *TEMP_MEAN_CSNF_WP_5*) into one vector. *TEMP_LOW_CSNF_WP* and *TEMP_HIGH_CSNF_WP* are analogous vectors for the low and high infiltration flux scenarios, respectively. Additionally, *TEMP_MEAN_CSNF_WP_NOBF*,

TEMP_LOW_CSNF_WP_NOBF, and *TEMP_HIGH_CSNF_WP_NOBF* are use for the no backfill temperature profiles. The selector switch *TEMP_CSNF_WP* selects the appropriate vector and retains these values for use by the other model components referencing the CSNF waste package surface temperatures. The data from all of the vectors; *TEMP_LOW_CSNF_WP*, *TEMP_MEAN_CSNF_WP*, *TEMP_HIGH_CSNF_WP*, *TEMP_MEAN_CSNF_WP_NOBF*, *TEMP_LOW_CSNF_WP_NOBF*, or *TEMP_HIGH_CSNF_WP_NOBF*, are retained based on the infiltration flux scenario assigned at the initiation of the model simulation. If the value assigned to the parameter *Infiltration_Scenario* (from the Infiltration Model component described in Section 6.3.1.1 Climate and Infiltration) equals 1, and the *Backfill_Case* selector equals 1, then the backfill design and low infiltration scenario applies and the selector switch chooses *TEMP_LOW_CSNF_WP* to represent the average surface temperatures of the CSNF waste packages. If the value assigned to *Infiltration_Scenario* is 2 and the *Backfill_Case* selector equals 0, then *TEMP_MEAN_CSNF_WP_NOBF* is selected. The combined logic for the of the infiltration scenario and design option selectors is used to select the remaining thermal hydrologic temperature profiles (*Infiltration_Scenario* = 1, *Backfill_Case* = 0, *TEMP_LOW_CSNF_WP_NOBF*; *Infiltration_Scenario* = 2, *Backfill_Case* = 0, *TEMP_MEAN_CSNF_WP_NOBF*; *Infiltration_Scenario* = 3, *Backfill_Case* = 0, *TEMP_HIGH_CSNF_WP_NOBF*; *Infiltration_Scenario*=1, *Backfill_Case*=1, *TEMP_LOW_CSNF_WP*; *Infiltration_Scenario* = 2, *Backfill_Case* = 1, *TEMP_MEAN_CSNF_WP*, *Infiltration_Scenario* = 3, *Backfill_Case* = 1, *TEMP_HIGH_CSNF_WP*).

The peak CSNF waste package surface temperature for each infiltration bin was extracted from the abstraction input data. There are thirty temporal profiles for the average CSNF waste package surface temperature; one profile for each infiltration rate bin included in an infiltration flux scenario for both backfill and no backfill design options. There are also thirty maximum CSNF surface temperatures profiles. Unlike the previous cases (e.g., average waste package surface temperature) where a profile implied a time history curve for a particular bin, only the maximum temperature (at the time the maximum occurs) will be recorded in any given realization. Five selector switches were added to the TSPA-SR model to pass the peak temperature to other components of the TSPA-SR model (i.e., see Section 6.3.4.3 Cladding Degradation Model). These selector switches are; *Peak_Temp_CSNF_1*, *Peak_Temp_CSNF_2*, *Peak_Temp_CSNF_3*, *Peak_Temp_CSNF_4*, and *Peak_Temp_CSNF_5*. Each selector switch reads the current value assigned to the TSPA-SR model parameters *Infiltration_Scenario* (see Section 6.3.1.1 Climate and Infiltration) and *Backfill_Case*. Based on these values the five selector switches record and pass the appropriate temperature, encoded into the switch criteria, to other TSPA-SR model components.

The implementation for the CDSP waste package surface temperatures is very similar. The organization and logic are identical, but the parameter names contain the CDSP identifier instead of the CSNF identifier. Also, the appropriate CDSP raw data source files are used for each infiltration rate bin, infiltration flux scenario, and repository design option. The CDSP does not include peak waste package surface temperatures, as this is only necessary for CSNF as it is used for cladding degradation (see Section 6.3.4.3).

The TSPA-SR model routine for selecting temporal profiles for invert temperature, invert relative humidity, invert evaporation rate, invert liquid saturation, and invert liquid volume flow

rate are similar as well. For a selected waste package type and infiltration flux scenario, the five (bin) data tables included in the infiltration flux scenario are combined into one vector for the backfill design and one vector for the no backfill design. The TSPA-SR model selects the appropriate vector based on the infiltration scenario and backfill design option selected at the initiation of a simulation.

Figure 6-41 through Figure 6-58 illustrate the input profiles from the thermal hydrology abstraction AMR for the six NFE parameters (surface temperature of the waste package, invert temperatures, RH of the invert, invert evaporation, invert saturation, and invert flux) for the CSNF waste packages and the no backfill design option.

Results and Verification

The results of the NFE TH Model component of the TSPA-SR model consist of twelve time history plots. There are time history plots for each package type, CSNF and CDSP, for each of the six NFE conditions: waste package surface temperature, invert temperature, invert relative humidity, invert evaporation rate, invert liquid saturation, and invert volume flow rate. Each of the twelve temporal profiles contains the time history data for all five infiltration rate bins. The data set selected for plotting the time histories internally selected by the TSPA model for the median value case for each parameter depends on the infiltration flux scenario and backfill design option assigned at the initiation of the simulation. For the median value case, the mean infiltration flux scenario and no backfill design option are selected. The time history profiles are displayed to demonstrate that the correct abstraction data are contained within the total system model. The time histories for each of the six parameters are shown for the CSNF waste packages in Figure 6-59 through Figure 6-64. A comparison between the appropriate input data set, depicted in Figure 6-41 through Figure 6-58 and Figure 6-59 through Figure 6-64 shows that the TSPA-SR model results mimic the input data. The data from the input source and TSPA-SR model are plotted at different time intervals. The TSPA-SR model interpolates between two source data points when an input data point is not available for a model time step; however, the input data match the model data when a time point in the input data matches a time point in the source data.

The implementation of the TSPA-SR TH Model component uses as input the data sets generated in the abstraction AMR developed to represent the average temporal profiles of the six NFE parameters:

- Waste package surface temperature
- Invert temperature
- Invert relative humidity
- Invert evaporation rate
- Invert liquid saturation
- Invert flux.

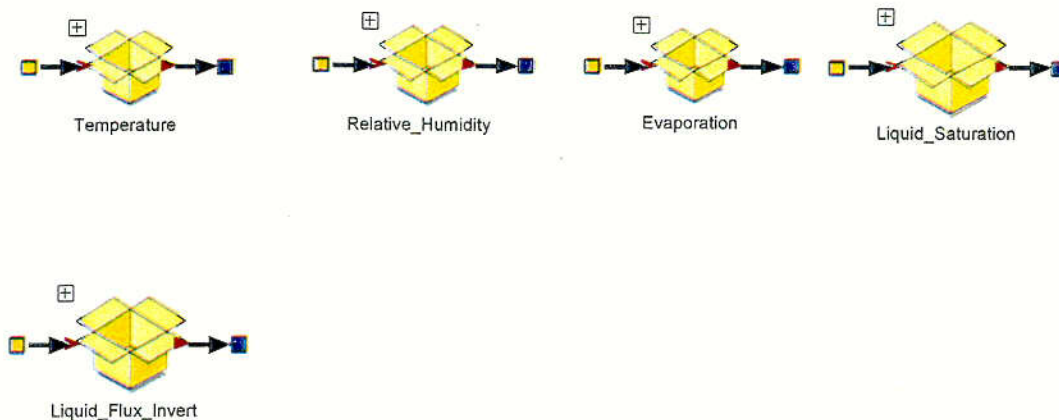
The objective of this total system model component is to select the appropriate data sets for the given model options (e.g., backfill or no backfill and infiltration scenario) and pass the appropriate data onto other model components; thus there are no calculations in this component.

The implemented logic for selecting the correct data set is the same for all six NFE parameters and both waste package types. The verification of one selection process is presented below, that for the CSNF waste package surface temperature.

The TSPA-SR TH Model component contains six vectors that define the temporal profile of CSNF waste package surface temperatures, *TEMP_MEAN_CSNF_WP*, *TEMP_LOW_CSNF_WP*, *TEMP_HIGH_CSNF_WP*, *TEMP_MEAN_CSNF_WP_NOBF*, *TEMP_LOW_CSNF_WP_NOBF*, and *TEMP_HIGH_CSNF_WP_NOBF*. The model chooses the appropriate vector based on the infiltration scenario and backfill design option selected at the initiation of the model. Neither the infiltration scenario, nor the design option, changes over the course of simulating one realization, so the data from only one vector will be chosen for any given realization. However, for a probabilistic simulation, containing multiple realizations, the design option is constant for all realizations, whereas the infiltration scenario can vary for each realization. The selector switch that chooses the appropriate TH vector is *TEMP_CSNF_WP* (see Figure 6-39). For the median value simulation, the value assigned to the parameter *Infiltration_Scenario* equals 2, the mean infiltration case, and the parameter *Backfill_Case* equals 0, no backfill design option. The selector switch, *TEMP_CSNF_WP* assigns the values contained in the vector *TEMP_MEAN_CSNF_WP_NOBF* to represent the temporal profile for the CSNF waste package surface temperature in bins 1 through 5.

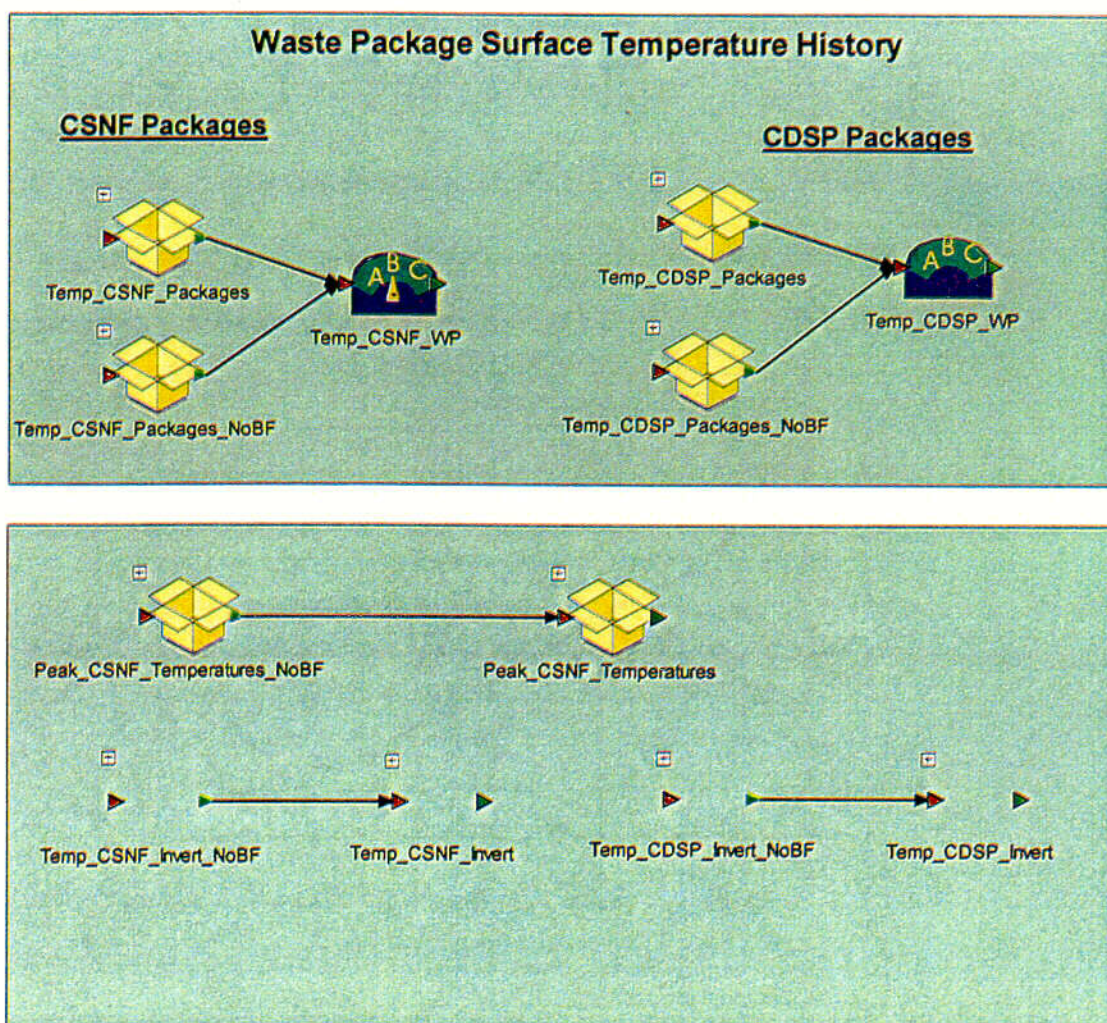
Figure 6-65 plots the data assigned to *TEMP_CSNF_WP* for the median value simulation and the input data from the *TEMP_MEAN_CSNF_WP_NOBF* vector. The plotted markers show the data from the input vector *TEMP_MEAN_CSNF_WP_NOBF*. The plotted line is the TSPA-SR model time history output of the variable *TEMP_CSNF_WP*. Note that the two curves plot the same data and therefore the implemented logic selects the appropriate input table for the waste package surface temperature profiles.

The model results match the expected output, verifying that the model logic implemented in the TSPA-SR TH Model component is correct. Furthermore, the value assigned to the parameter *Infiltration_Scenario* was correctly passed from the TSPA-SR Infiltration Model component to the TSPA-SR TH Model component.



\\TSPA_Model\\Engineered_Barrier_System\\NFE\\ThermoHydrology\\

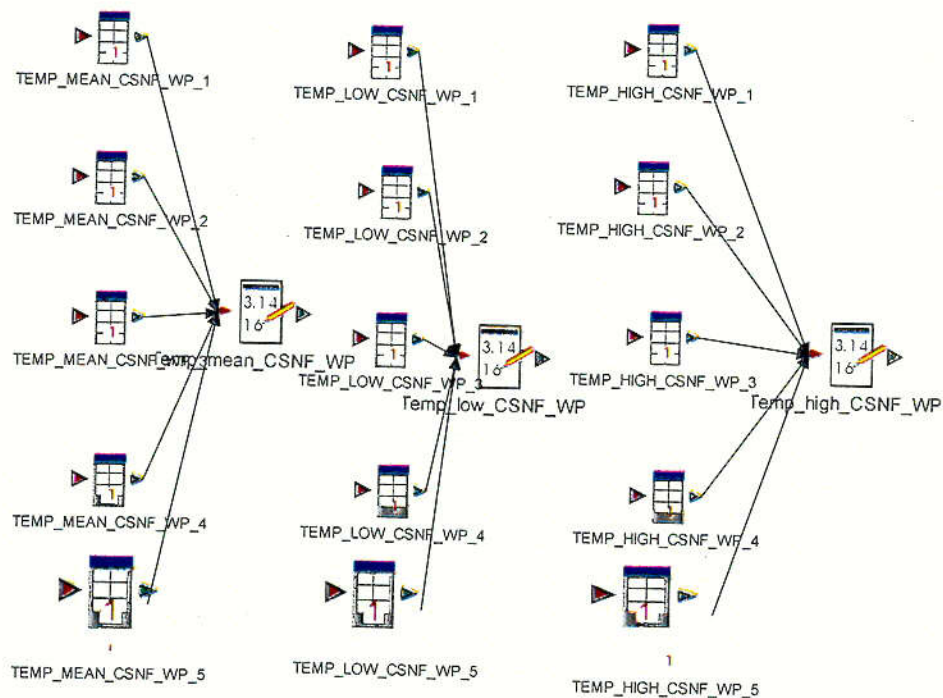
Figure 6-38. The TSPA-SR Model Organization for TH Implementation



\\TSPA_Model\\Engineered_Barrier_System\\NFE\\ThermoHydrology\\Temperature\\

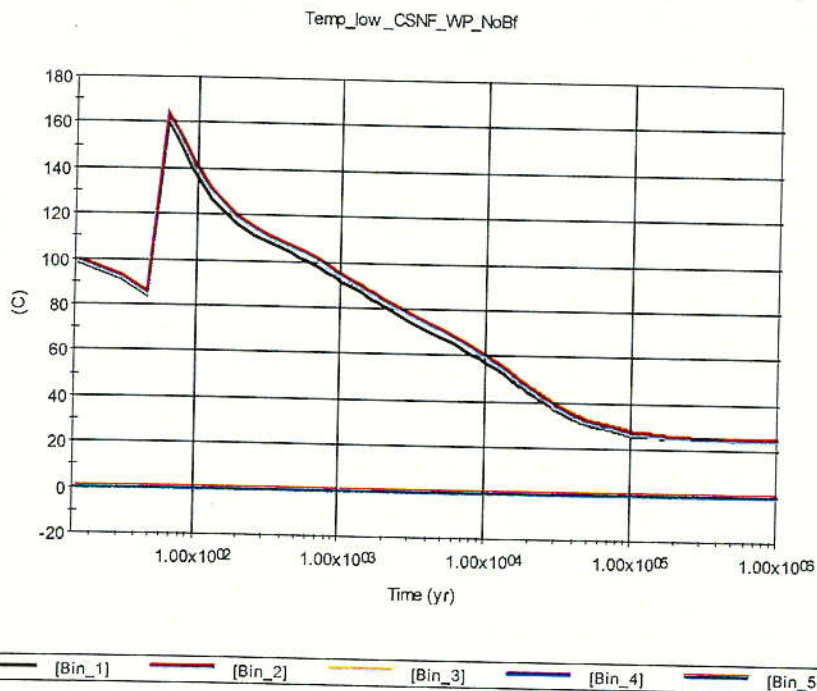
NOTE: NoBF indicates a no backfill data set.

Figure 6-39. Graphical Representation of the Temperature Profiles for the TH Model



\\TSPA_Model\\Engineered_Barrier_System\\NFE\\ThermoHydrology\\Temperature\\Temp_CSNF_Packages

Figure 6-40. Illustration of the CSNF Waste Package Surface Temperature Implementation



NOTE: Infiltration Bins 3-5 contain no data as they do not exist during low infiltration scenarios.

Figure 6-41. CSNF Waste Package Surface Temperature, Low Infiltration, No Backfill Design

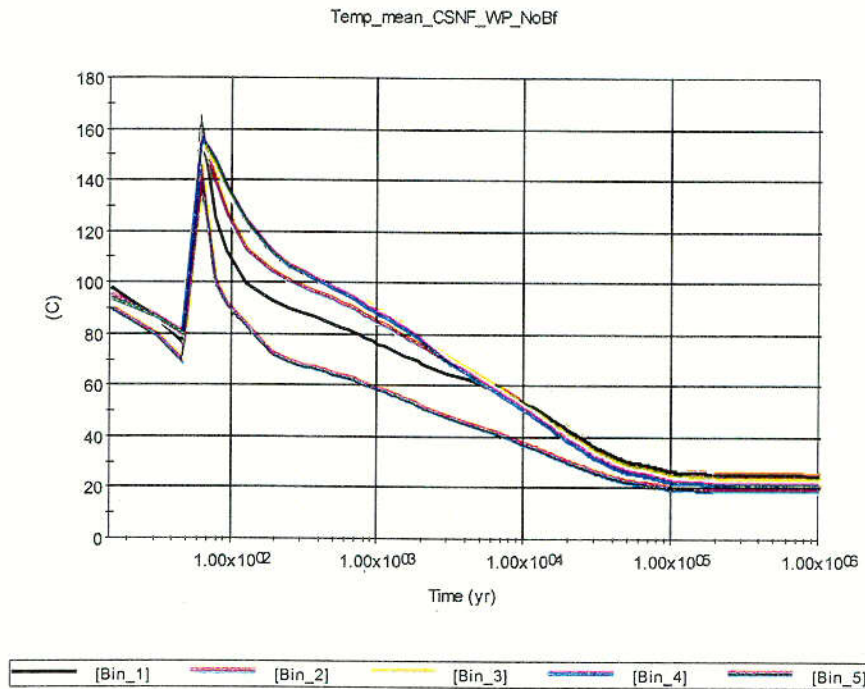


Figure 6-42. CSNF Waste Package Surface Temperature, Mean Infiltration, No Backfill Design

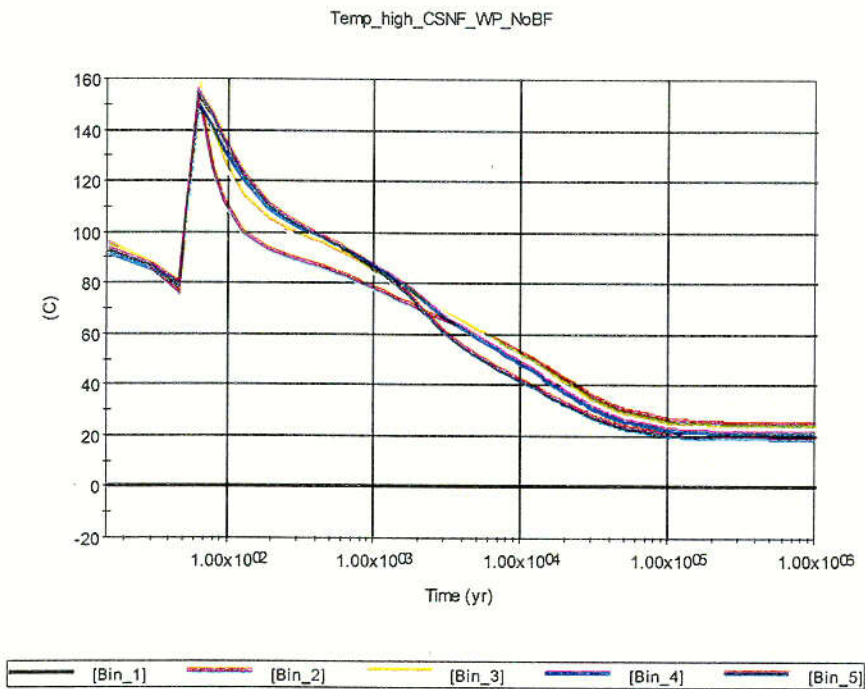
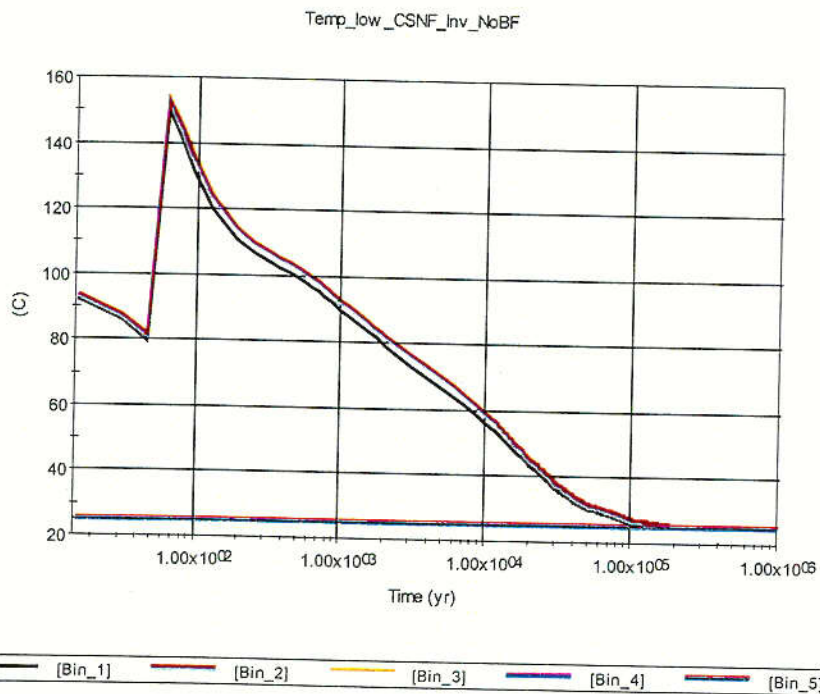


Figure 6-43. CSNF Waste Package Surface Temperature, High Infiltration, No Backfill Design

C34



NOTE: Bins 3-5 have no data as they do not exist during low infiltration scenarios.

Figure 6-44. CSNF Invert Temperatures, Low Infiltration, No Backfill Design

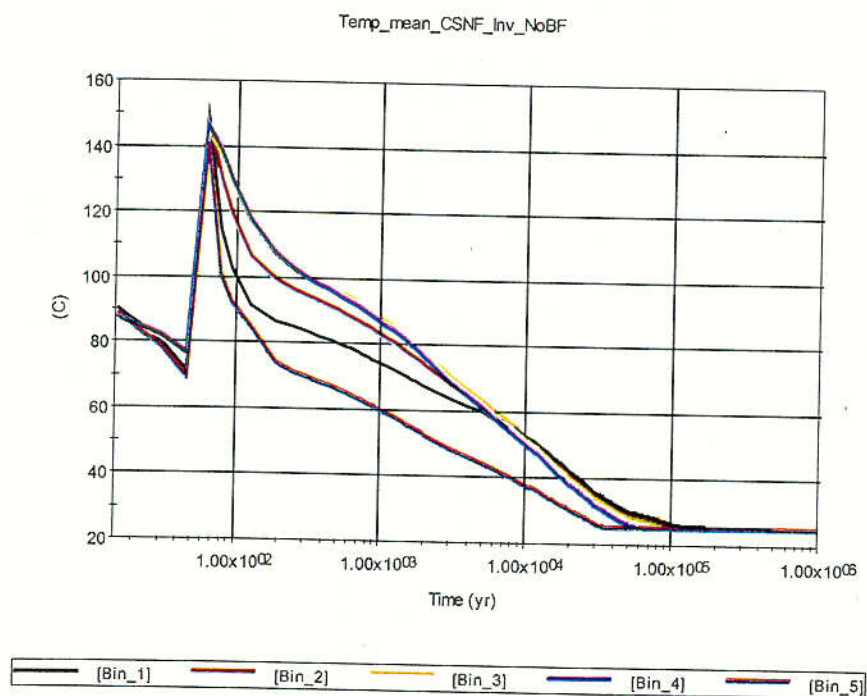
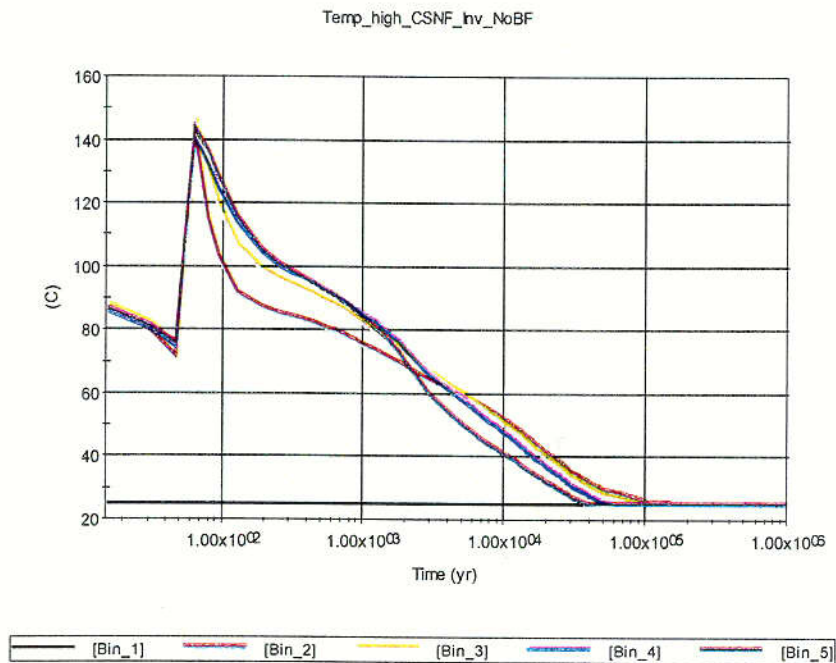


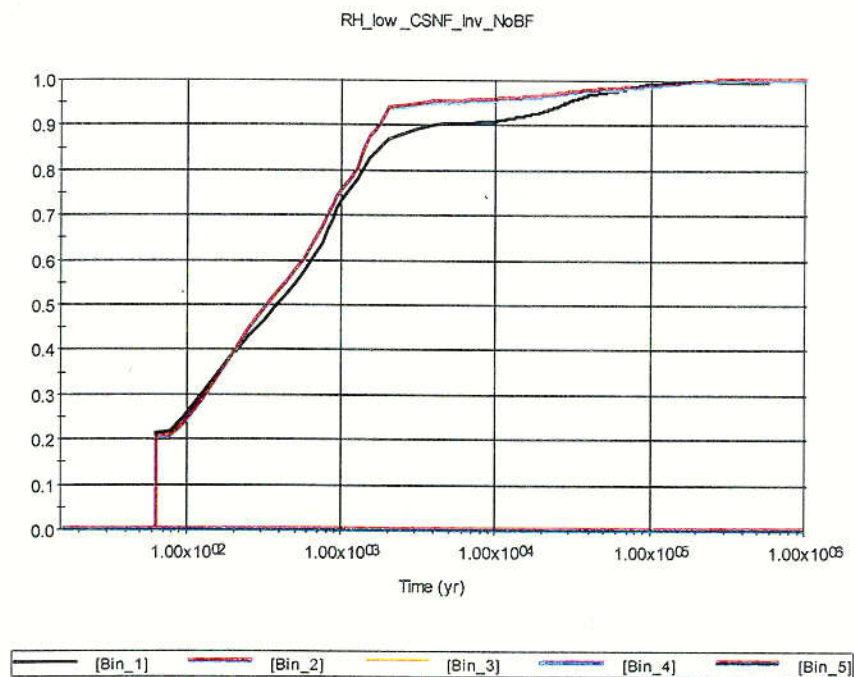
Figure 6-45. CSNF Invert Temperatures, Mean Infiltration, No Backfill Design

C35



NOTE: Bin1 has no data as it does not exist during high infiltration scenarios.

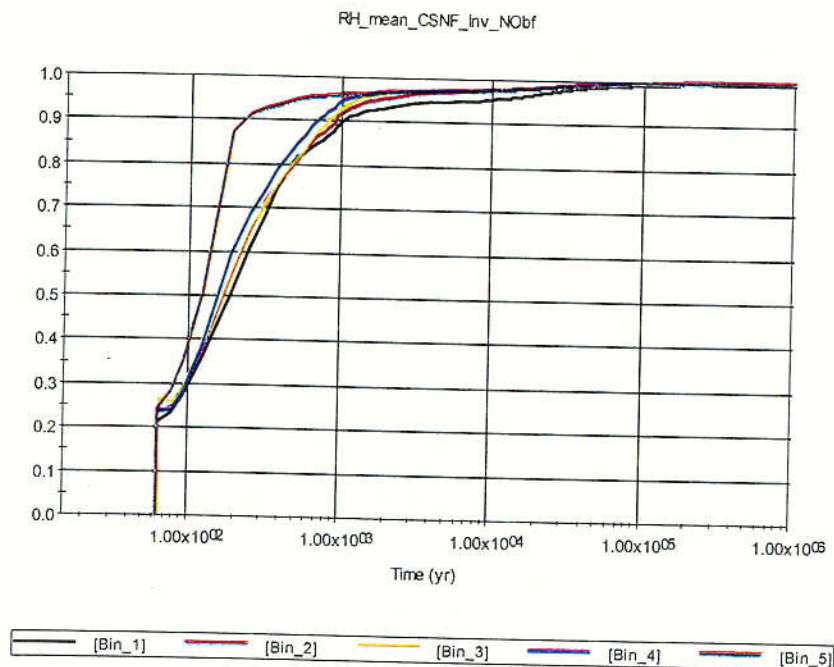
Figure 6-46. CSNF Invert Temperatures, High Infiltration, No Backfill Design



NOTE: Bins 3-5 have no data as they do not exist during low infiltration scenarios. Additionally, RH values are below 0 before 50 years and do not plot on this scale. The first non-negative RH in the TSPA model occurs at the time step at 62.5 years.

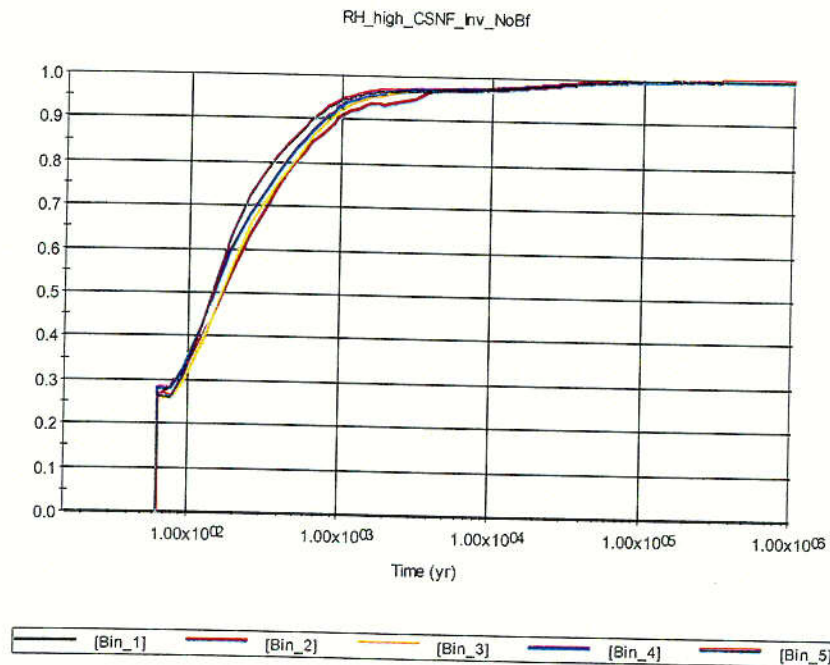
Figure 6-47. CSNF Invert Relative Humidities, Low Infiltration, No Backfill Design

C36.



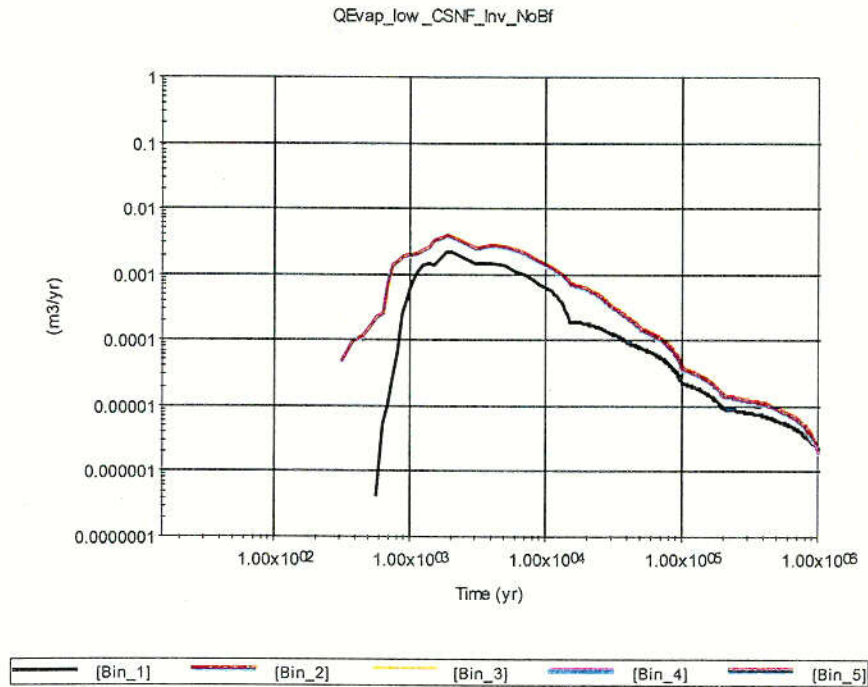
NOTE: RH values are below 0 before 50 years and do not plot on this scale. The first non-negative RH in the TSPA model occurs at the time step at 62.5 years.

Figure 6-48. CSNF Invert Relative Humidities, Mean Infiltration, No Backfill Design



NOTE: Bin1 has no data as it does not exist during high infiltration scenarios. Additionally, RH values are below 0 before 50 years and do not plot on this scale. The first non-negative RH in the TSPA model occurs at the time step at 62.5 years.

Figure 6-49. CSNF Invert Relative Humidities, High Infiltration, No Backfill Design



NOTE: Bins 3-5 have no data as they do not exist during low infiltration scenarios.

Figure 6-50. CSNF Invert Evaporation Flux, Low Infiltration, No Backfill Design

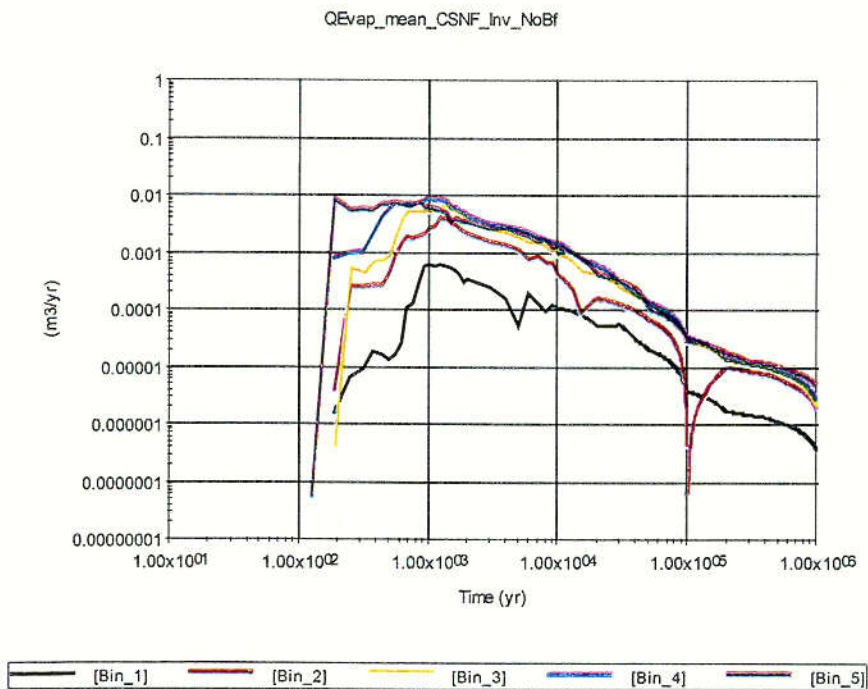
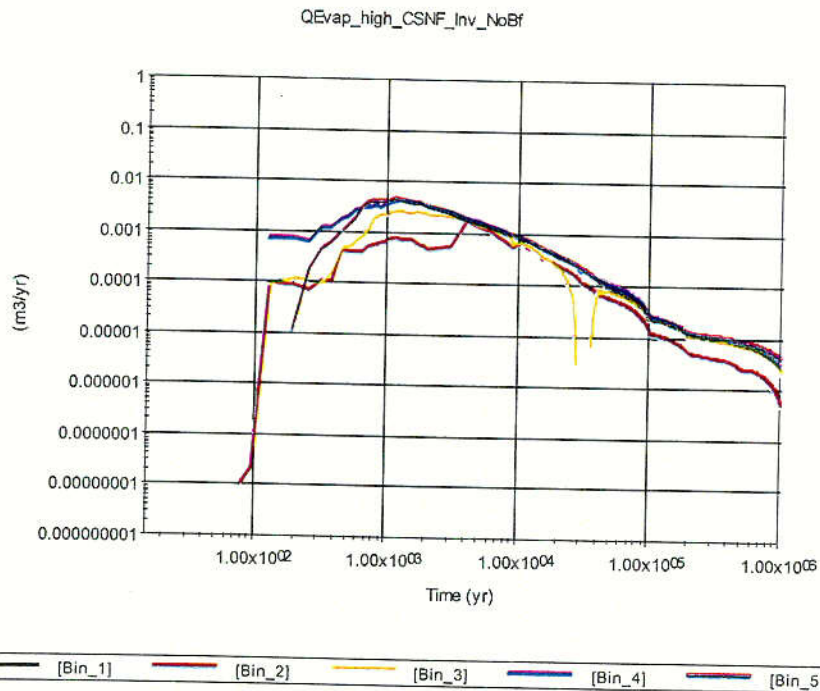


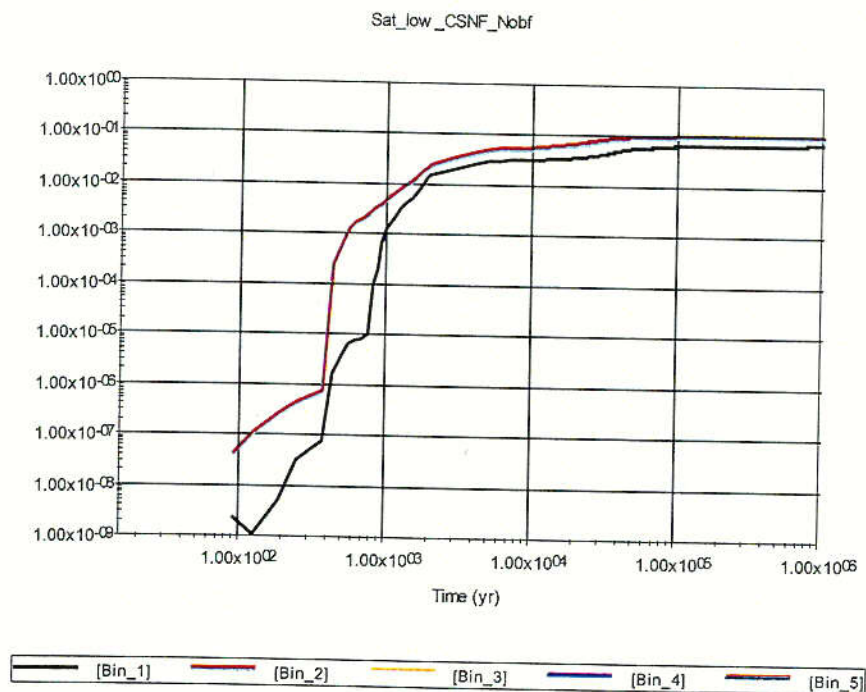
Figure 6-51. CSNF Invert Evaporation Flux, Mean Infiltration, No Backfill Design

C38



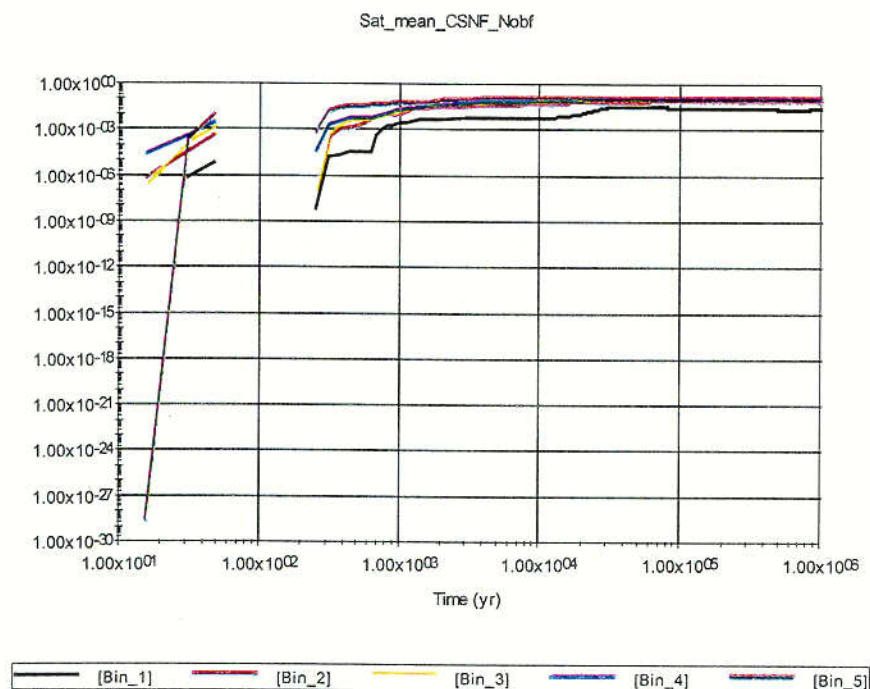
NOTE: Bin 1 has no data as it does not exist during high infiltration scenarios. Gaps in the curves correspond to values equal to zero (zero values are not plotted on a log axis).

Figure 6-52. CSNF Invert Evaporation Flux, High Infiltration, No Backfill Design



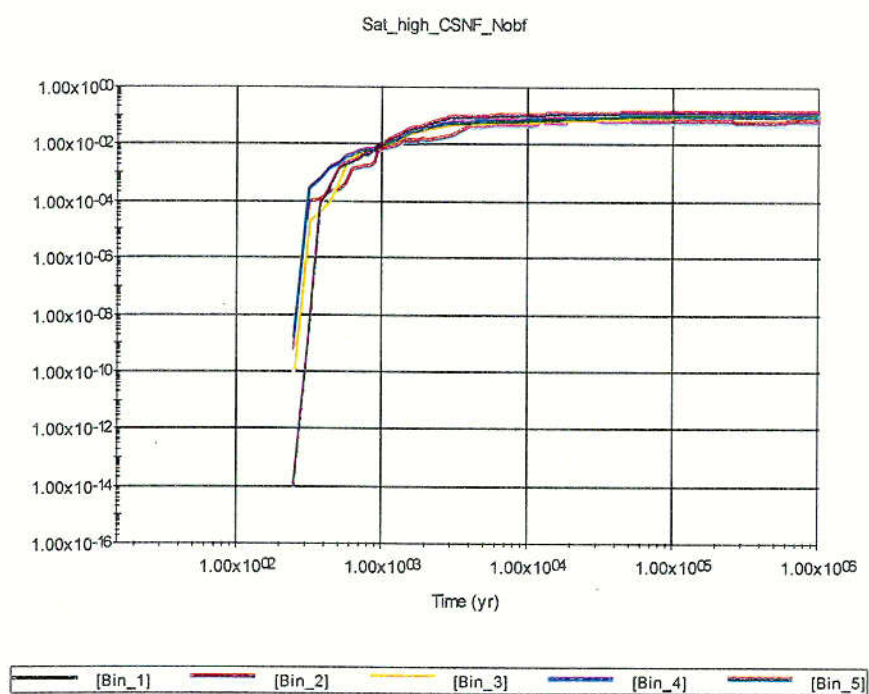
NOTE: Bins 3-5 have no data as they do not exist during low infiltration scenarios.

Figure 6-53. CSNF Invert Saturation, Low Infiltration, No Backfill Design



NOTE: Gaps in the curves correspond to values equal to zero (zero values are not plotted on a log axis).

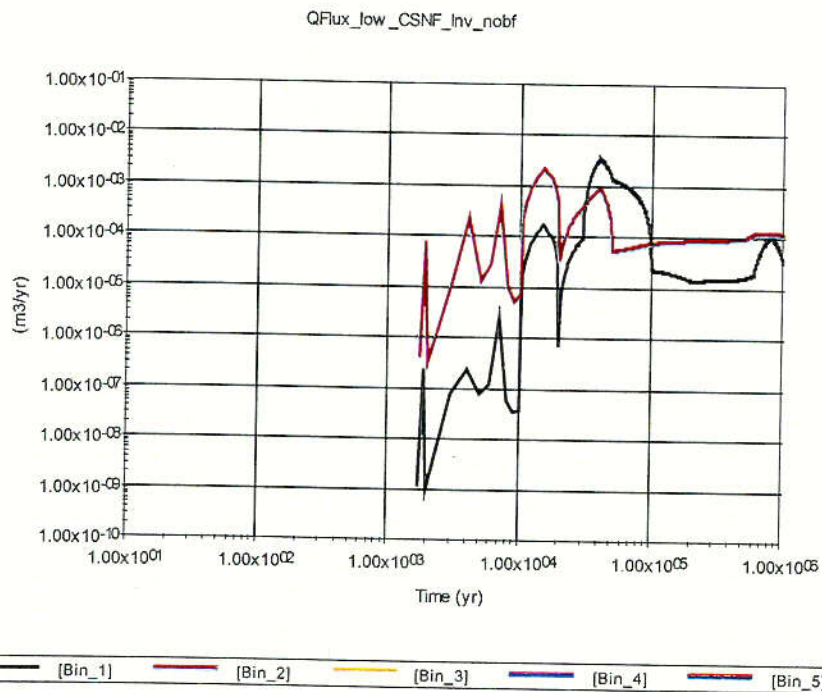
Figure 6-54. CSNF Invert Saturation, Mean Infiltration, No Backfill Design



NOTE: Bin 1 has no data as it does not exist during high infiltration scenarios.

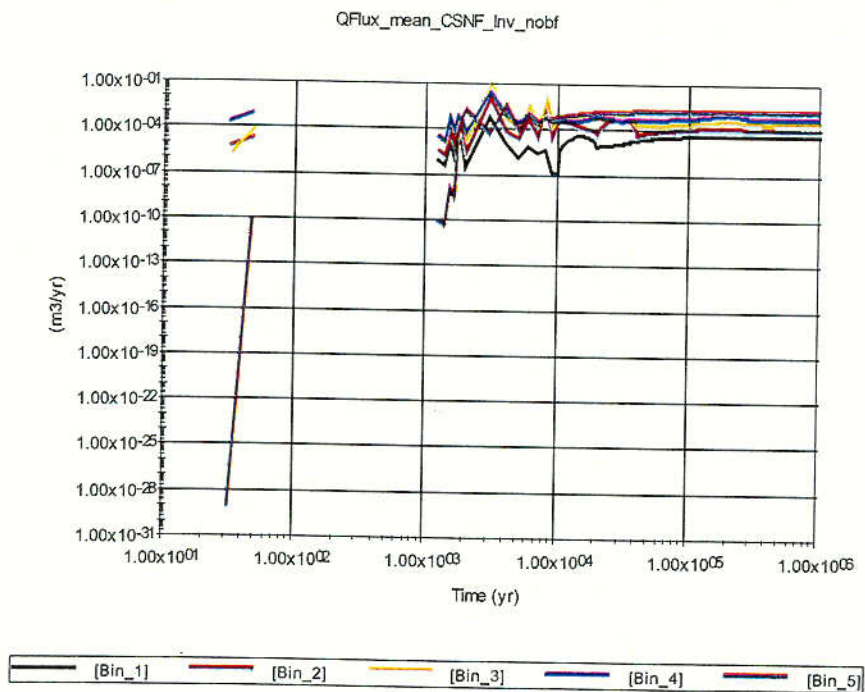
Figure 6-55. CSNF Invert Saturation, High Infiltration, No Backfill Design

C40



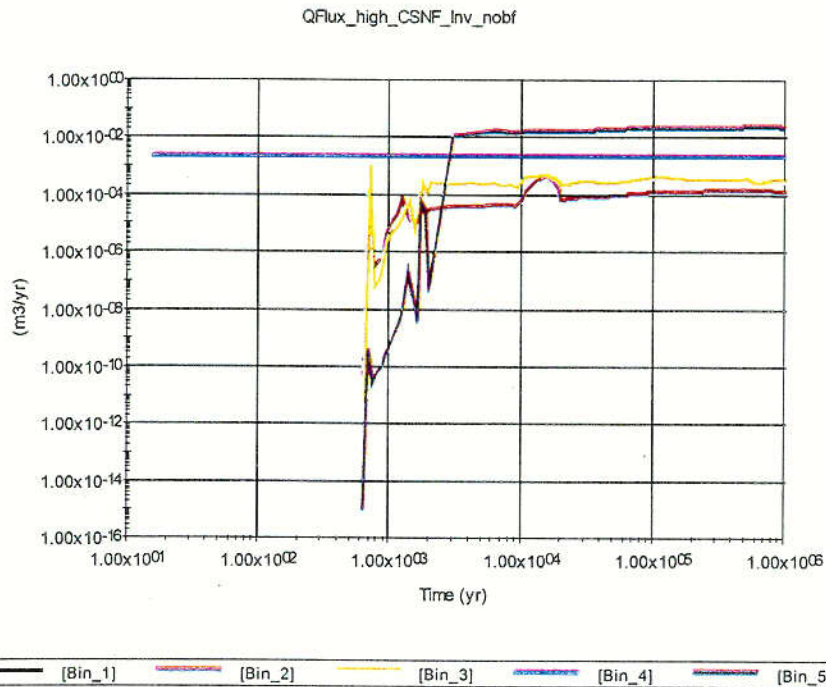
NOTE: Bins 3-5 have no data as they do not exist during low infiltration scenarios.

Figure 6-56. CSNF Invert Flux, Low Infiltration, No Backfill Design



NOTE: Gaps in the curves correspond to values equal to zero (zero values are not plotted on a log axis).

Figure 6-57. CSNF Invert Flux, Mean Infiltration, No Backfill Design



NOTE: Bin 1 has no data as it does not exist during high infiltration scenarios, additionally, BIN 4 displays the 1e6 year value for Invert Qflux due to an error in the model file. This error has no impact on the results as the packages don't fail until after 10,000 years, at which time the Qflux invert is near a steady state value.

Figure 6-58. CSNF Invert Flux, High Infiltration, No Backfill Design

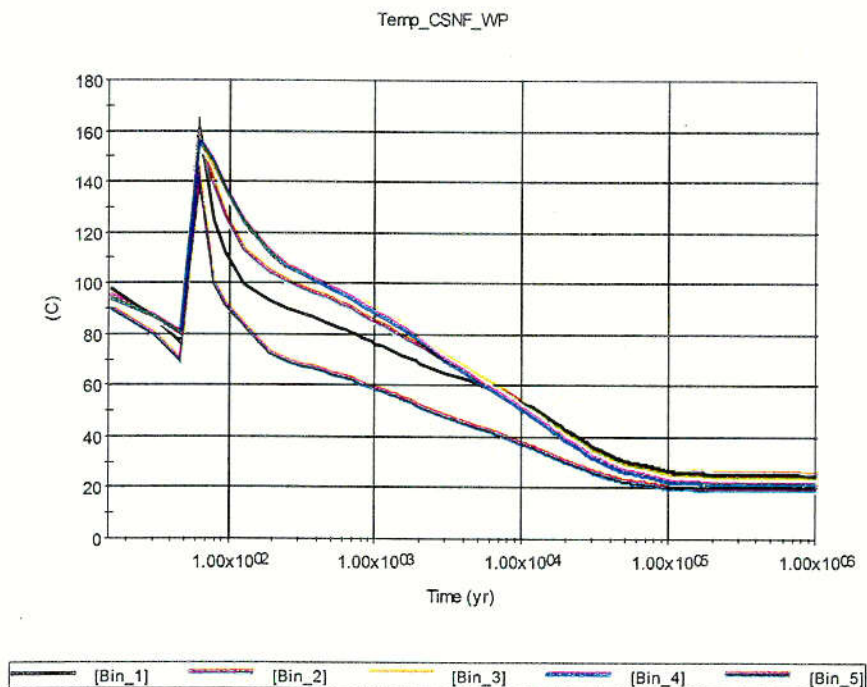


Figure 6-59. CSNF Waste Package Surface Temperature Profile for the Median Value Simulation

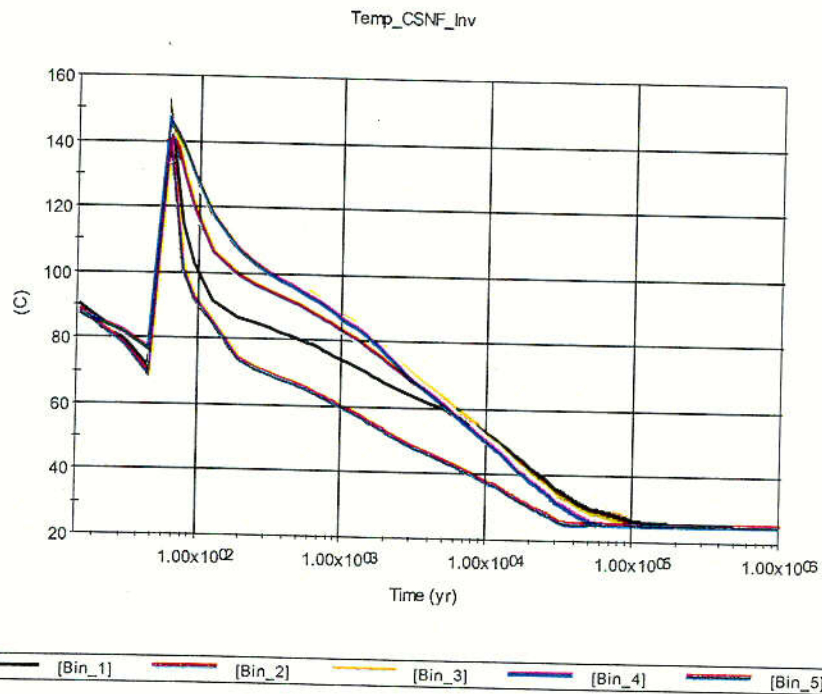


Figure 6-60. CSNF Invert Temperature Profiles for the Median Value Simulation

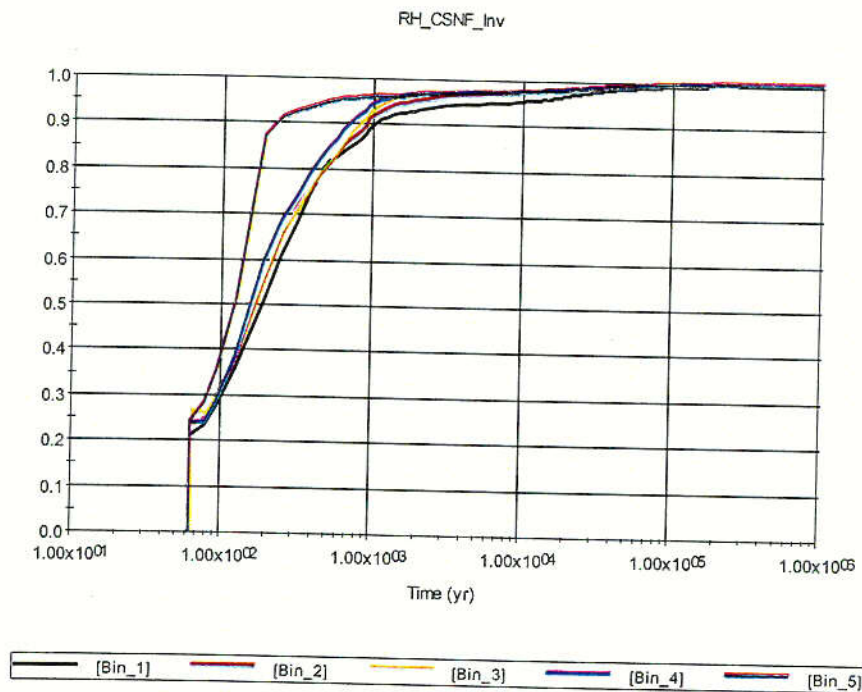


Figure 6-61. CSNF Invert Relative Humidity Profiles for the Median Value Simulation

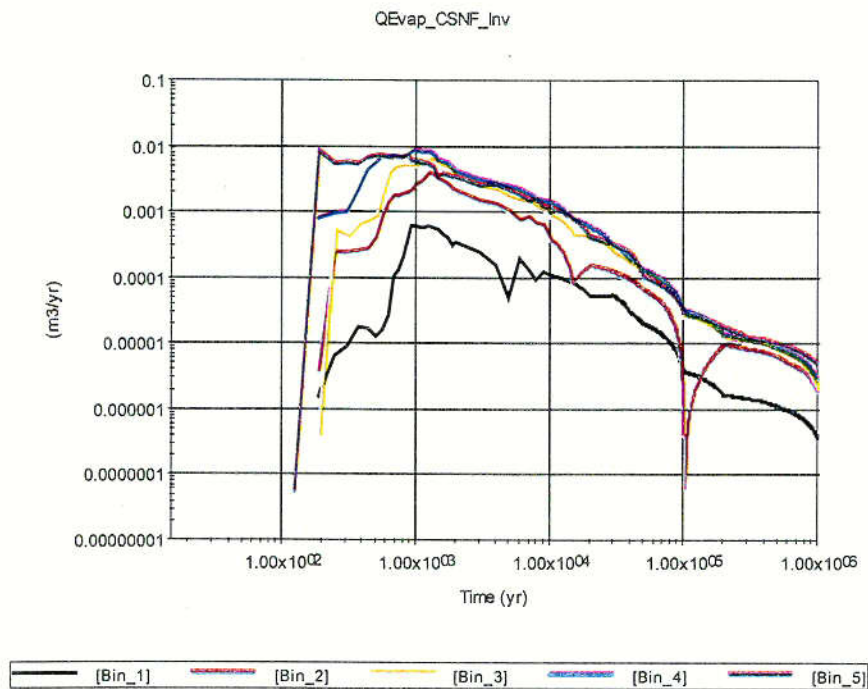
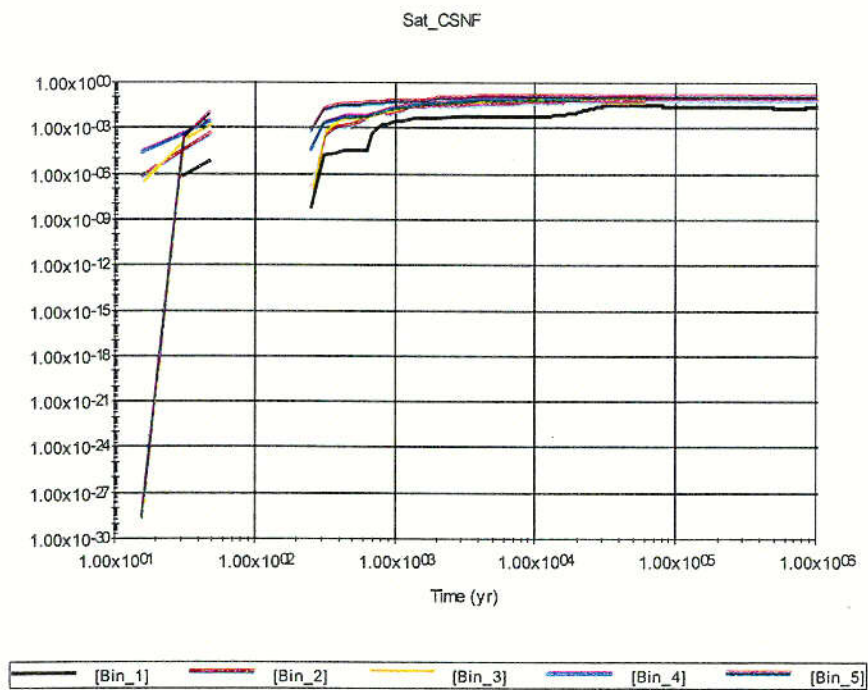


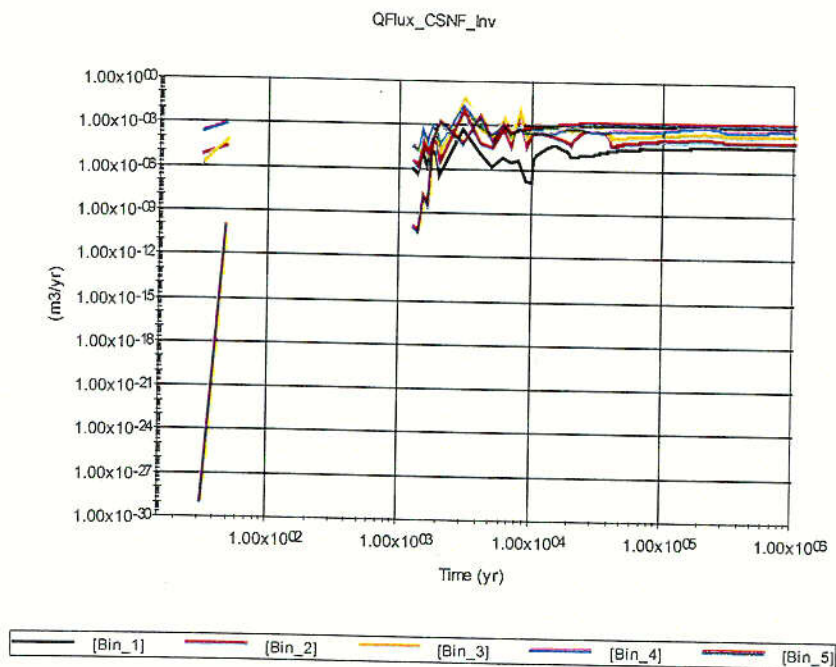
Figure 6-62. CSNF Invert Evaporation Rate Profiles for the Median Value Simulation



NOTE: Gaps in the curves correspond to values equal to zero (zero values are not plotted on a log axis).

Figure 6-63. CSNF Invert Liquid Saturation Profiles for the Median Value Simulation

c44.



NOTE: Gaps in the curves correspond to values equal to zero (zero values are not plotted on a log axis).

Figure 6-64. CSNF Invert Liquid Flux Profiles for the Median Value Simulation

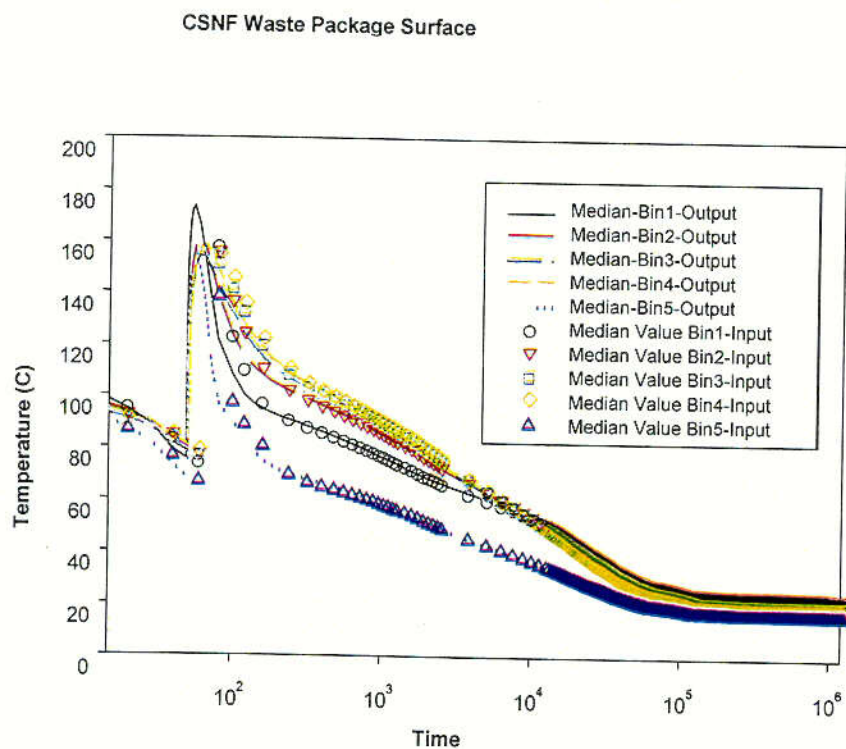


Figure 6-65. Comparison of the Median Value Simulation Model Results and the Predicted Results: CSNF Waste Package Surface Temperature

C45:

6.3.2.2 In-drift Geochemical Environment

Overview

The objective of the in-drift chemistry model is to model those processes that govern salt precipitation, dissolution, and resulting water composition in the Engineered Barrier System (EBS). Vaporization of water in the drift will affect the quantity, migration, and composition of liquid water in the repository, especially during the first several thousand years when the drift temperature is high. Vaporization causes brine formation and salt and mineral precipitation which will affect the composition of water in the drift. The resulting pH and concentrations of dissolved solids are key parameters in determining drip shield and waste package corrosion rates (refer to Section 6.3.3, Waste Package Degradation). In addition, these parameters may affect spent fuel dissolution rates and radionuclide transport in the geosphere. For these reasons, the chemical composition of water in the drift over time and the interaction of precipitated salts and minerals may affect the chemical environment within the drift and, possibly, repository performance.

As the drift temperature falls, the relative humidity rises. Eventually, the average rate at which incoming water enters the drift will exceed the evaporation rate, and the result will be an evaporated water composition within the drift that is no longer controlled by the relative humidity and the solubilities of the soluble salts. As a result, the evaporated water composition within the drift will become more dilute over time as the temperatures fall. The end point of the conceptual model is when temperature and relative humidity within the drift reach ambient conditions. When ambient conditions are achieved, the incoming seepage and water chemistry within the drift are no longer markedly altered by evaporative processes (CRWMS M&O 2000 [127818], Section 6.2).

The *In-Drift Precipitates/Salts Analysis* AMR (CRWMS M&O 2000 [127818], Section 6.4) developed two submodels that are intended to provide a continuous precipitates/salts model for the two regimes expected to occur in the drifts for all simulation times. The low relative humidity model describes the regime in which relative humidity is low ($50 \leq RH \leq 85$) and the solubility of soluble salts controls the water chemistry. Incoming seepage water evaporates, concentrating the water solution and precipitating salts.

The high relative humidity model describes the regime where the relative humidity is high (> 85 percent) and the steady state water composition is controlled by chemical equilibrium and the ratio of the rates of evaporation and seepage. In this regime, the ratio of the rates of evaporation and seepage is always less than one.

The modeling period of the potential repository is divided into a set of time periods in which the inputs are abstracted to representative constant values. These abstracted time periods have been defined as:

- Period 1, pre-closure, 0 – 50 years after waste emplacement
- Period 2, boiling period, 50 – 1,000 years after waste emplacement

- Period 3, transitional cool-down, 1,000 – 2,000 years after waste emplacement
- Period 4, extended cool-down, 2,000 – 100,000 years after waste emplacement (CRWMS M&O 2000 [151708], Table 1).

For times greater than 100,000 years (referred to as period 5), period 3 conditions are assumed (see Section 5.2, assumption 3). The important independent variables to the in-drift chemistry model are:

- Incoming seepage composition (C_i^s)
- Relative humidity (RH)
- Temperature (T)
- Relative evaporation rate (R^{es}), which is the evaporation flux divided by the incoming seepage flux
- Volume fraction of carbon dioxide (f_{CO_2}).

The outputs of the in-drift chemistry model that are important to TSPA-SR are:

- pH
- Ionic strength.

The combinations of potential values of these inputs are unlimited. Therefore, the results from a subset of these combinations were obtained to define the response surface for interpolating results for all potential input values and combinations of input values. The input variables were limited to a small number of values, which included their approximate minimum and maximum potential values. Temperature was varied among the values 25°C, 45°C, 75°C, and 95°C. The volume fraction of carbon dioxide was varied among the values 10^{-1} , 10^{-3} , and 10^{-6} . The entire relative humidity range from 0 percent to 100 percent was covered for < 50.3 percent, with several discrete values between 50.3 percent and 85.0 percent, and for > 85 percent. The relative evaporation flux range from 0 to 1 was covered with the values 0, 0.1, 0.5, 0.9, 0.99, 0.999, and 1 (CRWMS M&O 2000 [127818], Section 7.2). Incoming seepage composition values and volume fractions of carbon dioxide in the ambient gas were obtained from the time period abstractions described above.

Sets of pH and ionic strength results from the model were generated for values of the input variables. The results are summarized in Table 6-12 and in lookup tables presented in Table 6-13, Table 6-14, and Table 6-15, which constitute response surfaces. For the given input variable values of a given abstracted time increment, the steady state pH and ionic strength can be obtained or interpolated from these tables.

Inputs to the TSPA Model

The output values required from the in-drift chemistry model are the values for pH and ionic strength for a given set of inputs intended to encompass the likely conditions that could occur. The output values are summarized in a set of lookup tables presented in Table 6-13, Table 6-14, and Table 6-15. The outputs for “dry” conditions (i.e., when *RH* is less than 50 percent) are the *I_bound_a*, *I_bound_b*, *I_bound_c*, *pH_bound_a*, *pH_bound_b*, and *pH_bound_c* parameters listed in Table 6-12.

Table 6-12. Input Parameters to the In-Drift Chemistry Model

Parameter Name	Description	Parameter Value	Reference
<i>I_bound_a</i>	Log of ionic strength in invert for <i>RH</i> less than 50% for abstracted period 2	1.392 [”]	CRWMS M&O 2000 [151708], Table 2
<i>I_bound_b</i>	Log of ionic strength in invert for <i>RH</i> less than 50% for abstracted periods 3 and 5	1.388 [”]	CRWMS M&O 2000 [151708], Table 3
<i>I_bound_c</i>	Log of ionic strength in invert for <i>RH</i> less than 50% for abstracted period 4	1.386 [”]	CRWMS M&O 2000 [151708], Table 4
<i>I_drip_case2a</i>	Log of ionic strength in invert when <i>RH</i> is greater than or equal to 50% and less than or equal to 85%, for abstracted period 2	See Table 6-12	CRWMS M&O 2000 [151708], Table 2
<i>I_drip_case2b</i>	Log of ionic strength in invert when relative humidity is greater than or equal to 50% and less than or equal to 85%, for abstracted periods 3 and 5	See Table 6-13	CRWMS M&O 2000 [151708], Table 3
<i>I_drip_case2c</i>	Log of ionic strength in invert when relative humidity is greater than or equal to 50% and less than or equal to 85%, for abstracted period 4	See Table 6-14	CRWMS M&O 2000 [151708], Table 4
<i>I_drip_case3a</i>	Log of ionic strength in invert when <i>RH</i> is greater than 85%, for abstracted period 2	See Table 6-12	CRWMS M&O 2000 [151708], Table 2
<i>I_drip_case3b</i>	Log of ionic strength in invert when <i>RH</i> is greater than 85%, for abstracted periods 3 and 5	See Table 6-13	CRWMS M&O 2000 [151708], Table 3
<i>I_drip_case3c</i>	Log of ionic strength in invert when <i>RH</i> is greater than 85%, for abstracted period 4	See Table 6-14	CRWMS M&O 2000 [151708], Table 4
<i>pH_bound_a</i>	pH for <i>RH</i> less than 50% for abstracted period 2	9.4 [”]	CRWMS M&O 2000 [151708], Table 2
<i>pH_bound_b</i>	pH for <i>RH</i> less than 50% for abstracted periods 3 and 5	7.64 [”]	CRWMS M&O 2000 [151708], Table 3

Table 6-12. Input Parameters to the In-Drift Chemistry Model (Continued)

Parameter Name	Description	Parameter Value	Reference
pH_bound_c	pH for RH less than 50% for abstracted period 4	7.02 ^{**}	CRWMS M&O 2000 [151708], Table 4
pH_drip_case2	pH in invert when RH is greater than or equal to 50% and less than or equal to 85%, for abstracted periods 2, 3, 4 and 5	See Table 6-12, Table 6-13, and Table 6-14	CRWMS M&O 2000 [151708], Table 2, Table 3, and Table 4
pH_drip_case3a	pH in invert when RH is greater than 85%, for abstracted period 2	See Table 6-12	CRWMS M&O 2000 [151708], Table 2
pH_drip_case3b	pH in invert when RH is greater than 85%, for abstracted periods 3 and 5	See Table 6-13	CRWMS M&O 2000 [151708], Table 3
pH_drip_case3c	pH in invert when RH is greater than 85%, for abstracted period 4	See Table 6-14	CRWMS M&O 2000 [151708], Table 4

DTN: MO0002SPALOO46.010 [149168]

NOTES: Abstracted time periods: period 1 is pre-closure, 0 - 50 years; period 2 is boiling period, 50 - 1,000 years; period 3 is transitional cool-down, 1,000 - 2,000 years; period 4 is extended cool-down, 2,000 - 100,000 years; and period 5 is defined the same as period 3 for times greater than 100,000 years.

** GoldSim requires numeric input even under 'dry' conditions (RH<50.3 percent). For these conditions the values for RH=50.3 percent are used.

Table 6-13. Lookup Table for In-Drift pH and Ionic Strength for Time Period

Input Parameters			Precipitates/Salts Model Output	
RH (%)	T (°C)	1-R ^{es}	pH	Log I (molal)
< 50.3%	nf ^a	nf	na ^b	na
50.3%	nf	nf	9.40	1.392
51.0%	nf	nf	9.40	1.384
53.1%	nf	nf	9.40	1.332
55.2%	nf	nf	9.40	1.286
60.5%	nf	nf	9.40	1.060
65.7%	nf	nf	9.40	0.770
71.0%	nf	nf	9.40	0.606
76.2%	nf	nf	9.40	0.560
81.5%	nf	nf	9.40	0.612
85.0%	nf	nf	9.40	0.671
> 85%	nf	> or = 1	8.58	-2.222
> 85%	nf	0.9	8.62	-2.155
> 85%	nf	0.5	8.87	-1.921
> 85%	nf	0.1	9.21	-1.244

Table 6-13. Lookup Table for In-Drift pH and Ionic Strength for Time Period (Continued)

Input Parameters			Precipitates/Salts Model Output	
RH (%)	T (°C)	1-R**	pH	Log I (molal)
> 85%	nf	0.01	9.28	-0.423
> 85%	nf	0.001	9.41	0.483
> 85%	nf	< 0.001	9.40	0.694

DTN: MO0002SPALOO46.010 [149168]

NOTES: ^a Not a function of this parameter

^b Not applicable (dry conditions)

Table 6-14. Lookup Table for In-Drift p and Ionic Strength for Time Periods 3 and 5

Input Parameters			Precipitates/Salts Model Output	
RH (%)	T (°C)	1-R**	pH	Log I (molal)
< 50.3%	nf ^a	nf	na ^b	na
50.3%	nf	nf	7.64	1.388
51.0%	nf	nf	7.64	1.380
53.1%	nf	nf	7.64	1.324
55.2%	nf	nf	7.64	1.276
60.5%	nf	nf	7.64	1.041
65.7%	nf	nf	7.64	0.752
71.0%	nf	nf	7.64	0.592
76.2%	nf	nf	7.64	0.549
81.5%	nf	nf	7.64	0.598
85.0%	nf	nf	7.64	0.656
> 85%	nf	> or = 1	7.72	-1.987
> 85%	nf	0.9	7.71	-1.943
> 85%	nf	0.5	7.64	-1.703
> 85%	nf	0.1	7.45	-1.023
> 85%	nf	0.01	7.58	-0.180
> 85%	nf	0.001	7.64	0.671
> 85%	nf	< 0.001	7.64	0.656

DTN: MO0002SPALOO46.010 [149168]

NOTES: ^a Not a function of this parameter

^b Not applicable (dry conditions)

Table 6-15. Lookup Table for In-Drift pH and Ionic Strength for Time Period 4

Input Parameters			Precipitates/Salts Model Output	
RH (%)	T (°C)	1-R ^{es}	pH	Log I (molal)
< 50.3%	nf ^a	nf	na ^b	na
50.3%	nf	nf	7.02	1.386
51.0%	nf	nf	7.02	1.377
53.1%	nf	nf	7.02	1.320
55.2%	nf	nf	7.02	1.270
60.5%	nf	nf	7.02	1.034
65.7%	nf	nf	7.02	0.745
71.0%	nf	nf	7.02	0.588
76.2%	nf	nf	7.02	0.545
81.5%	nf	nf	7.02	0.593
85.0%	nf	nf	7.02	0.650
> 85%	75	> or = 1	7.19	-1.917
> 85%	75	0.9	7.18	-1.879
> 85%	75	0.5	7.14	-1.666
RH (%)	T (°C)	1-R ^{es}	pH	Log I (molal)
> 85%	75	0.1	6.97	-1.007
> 85%	75	0.01	7.02	-0.161
> 85%	75	0.001	7.02	0.677
> 85%	75	< 0.001	7.02	0.650
> 85%	50	> or = 1	7.22	-1.866
> 85%	50	0.9	7.22	-1.833
> 85%	50	0.5	7.18	-1.636
> 85%	50	0.1	7.03	-1.002
> 85%	50	0.01	6.95	-0.128
> 85%	50	0.001	6.86	0.688
> 85%	50	< 0.001	7.02	0.650
> 85%	25	> or = 1	7.05	-1.866
> 85%	25	0.9	7.09	-1.821
> 85%	25	0.5	7.23	-1.592
> 85%	25	0.1	7.11	-0.991
> 85%	25	0.01	6.99	-0.108
> 85%	25	0.001	6.78	0.708
> 85%	25	< 0.001	7.02	0.650

DTN: MO0002SPAL0046.010 [149168]

NOTES: ^a Not a function of this parameter

^b Not applicable (dry conditions)

Implementation

This subsection describes the implementation of the in-drift chemistry model into the TSPA-SR Model. The majority of the in-drift chemistry calculations are performed in each bin (e.g., CSNF Infiltration Bin 1) in the model. Figure 6-66 provides an illustration of how the bin-level

chemistry in the invert is modeled. However, in-drift chemistry conditions that are not dependent on bin-level parameters (e.g., pH and ionic strength for $RH < 50$ percent, pH for $50 \text{ percent} \leq RH \leq 85 \text{ percent}$) are calculated at the EBS level of the model (see Figure 6-67, Figure 6-68, and Figure 6-69).

At the bin level the function *Q_ratio* calculates the ratio of evaporative flow to seepage flow. Evaporative flow and seepage flow (parameter names *QEvap_CSNF_Inv* and *QFlux_CSNF_Inv*) are calculated in the NFE Thermal Hydrology portion of the TSPA-SR model (refer to Section 6.3.2.1, Thermal Hydrology). The pH and ionic strength are selected based on the *one_minus_Q_ratio* parameter for abstracted time periods 2 and 3, and the *one_minus_Q_ratio* parameter and invert temperature for abstracted time period 4 when the relative humidity is greater than 85 percent (relative humidity in the invert is calculated in the Thermal Hydrology portion of the TSPA-SR model, refer to Section 6.3.2.1, Thermal Hydrology).

At the EBS level the log of invert ionic strength and the invert pH are defined for relative humidities of less than 50 percent. Switch *Ionic_Str_invert_bound* selects a value from *I_bound_a*, *I_bound_b*, and *I_bound_c* based on the abstracted time period.

```
If      Etime <= 1000 {yr} then I_bound_a
Elseif  Etime > 1000 {yr} and Etime <= 2000 {yr} then I_bound_b
Elseif  Etime > 2000 {yr} and Etime <= 100000 {yr} then I_bound_c
else    I_bound_c
```

Switch *pH_invert_bound* selects a value from *pH_bound_a*, *pH_bound_b*, and *pH_bound_c* based on the abstracted time period.

```
If      Etime <= 1000 {yr} then pH_bound_a
Elseif  Etime > 1000 {yr} and Etime <= 2000 {yr} then pH_bound_b
Elseif  Etime > 2000 {yr} and Etime <= 100000 {yr} then pH_bound_c
else    pH_bound_c
```

The invert pH for relative humidities between 50 percent and 85 percent (inclusive) is also defined at the EBS level by switch *pH_drip_case2*.

```
If      Etime <= 1000 {yr} then 9.4
Elseif  Etime > 1000 {yr} and Etime <= 2000 {yr} then 7.64
Elseif  Etime > 2000 {yr} and Etime <= 100000 {yr} then 7.02
else    7.64
```

The logic for determining the ionic strength and pH in the invert is contained within the containers *Ionic_Strength_Invert* and *pH*, respectively. The ionic strength and pH of the invert have been calculated in the AMR *In-Drift Precipitates/Salts Analysis* (CRWMS M&O 2000 [127818]) and calculation *Precipitates/Salts Model Results for THC Abstraction*, (CRWMS M&O 2000 [151708]). Lookup tables have been developed in that calculation to give the ionic strength and pH in the invert under specific conditions during each abstracted time period. The following paragraphs describe in detail how this has been implemented in the TSPA-SR model.

Invert Ionic Strength—The ionic strength in the invert is determined based primarily on the relative humidity and the abstracted time period. Figure 6-70 shows the contents of container *Ionic_Strength_Invert*. This logic shows how the ionic strength in the invert is selected using Table 6-13, Table 6-14, and Table 6-15. When the relative humidity in the invert is greater than or equal to 50 percent and less than or equal to 85 percent, the 1-D tables *I_drip_case2a*, *I_drip_case2b*, and *I_drip_case2c* are used to select the ionic strength of the invert. The 1-D table *I_drip_case2a* is used for abstracted time period 2, the 1-D Table *I_drip_case2b* is used for abstracted time periods 3 and 5, and the 1-D table *I_drip_case2c* is used for abstracted time period 4. The 1-D table *I_drip_case3a* is used to determine the ionic strength of the invert when the relative humidity is greater than 85 percent for abstracted periods 2 and the 1-D table *I_drip_case3b* is used for abstracted time periods 3 and 5. The 2-D table *I_drip_case3c* is used to determine the ionic strength in the invert when the relative humidity is greater than 85 percent during abstracted time period 4; ionic strength is selected based on invert temperature and the *one_minus_Q_ratio* parameter. The selector elements (switches) *I_drip_case2* and *I_drip_case3* select the appropriate tables based on the abstracted time period for their respective relative humidity ranges.

Figure 6-68 shows the contents of container *Ionic_Strength_Invert*. This logic shows how the ionic strength in the invert for *RH* < 50 percent is selected using data from Table 6-12. The selector *Ionic_Str_Invert_bound* uses the value of *I_bound_a*, *I_bound_b*, or *I_bound_c* for abstracted time periods 2, 3 or 5, and 4, respectively.

The selector element *Ionic_Str_Invert* selects the ionic strength in the invert from *I_drip_case2*, *I_drip_case3*, or *Ionic_Str_Invert_bound* based on relative humidity. Note that the ionic strength values in Table 6-12, Table 6-13, Table 6-14, and Table 6-15 and hence, all the *I_drip_case* table elements) are logs of the ionic strength. Therefore, the inverse log operation is performed to give ionic strength.

Invert pH—Like ionic strength, the pH in the invert is primarily defined by the relative humidity in the invert and by the abstracted time period. Figure 6-71 shows the logic for determining the pH of the invert when the relative humidity is greater than or equal to 50 percent. The selector element *pH_Invert* selects the pH based on the relative humidity in the invert. If the relative humidity is less than 50 percent, the selector element *pH_invert_bound* (shown in Figure 6-69) is selected. The pH is then selected from table *pH_bound_a*, *pH_bound_b*, or *pH_bound_c* based upon the abstracted time period. If the relative humidity is greater than or equal to 50 percent and less than or equal to 85 percent, *pH_Invert* selects *pH_drip_case2*, which is shown in Figure 6-69. As can be seen in Table 6-13, Table 6-14, and Table 6-15 for relative humidity conditions between 50 percent and 85 percent, the pH does not vary with relative humidity, only with the abstract time period. Therefore, the pH for relative humidity conditions between 50 percent and 85 percent can simply be selected by the selector element *pH_drip_case2* based on the abstracted time period.

If the relative humidity is greater than 85 percent, *pH_Invert* selects *pH_drip_case3*. Table *pH_drip_case3a* is used when in abstracted time period 2; the pH is determined based on the *one_minus_Q_ratio* parameter. Similarly, Table *pH_drip_case3b* is used when in abstracted time periods 3 and 5; the pH is determined based on the *one_minus_Q_ratio* parameter. When the relative humidity is greater than 85 percent and while in abstracted time period 4, the

two-dimensional table *pH_drip_case3c* is used to determine the pH invert. The pH in the invert is determined from table *pH_drip_case3c* based on the *one_minus_Q_ratio* parameter and the temperature of the invert.

Results and Verification

The determination of the ionic strength and pH in the invert at a particular time step can be checked using the appropriate lookup table to verify the correct implementation of the model in the TSPA-SR model. The ionic strength and pH will be checked at the following timesteps: 1,000 years, 2,000 years, and 100,000 years. This will verify that the correct ionic strength and pH are selected for abstracted time periods 2, 3, and 4 (abstracted time period 5 uses the same conditions as abstracted time period 3).

Invert Ionic Strength—GoldSim gives a value of 4.9431 for the ionic strength in the invert (Bin 4, CSNF) at 1,000 years, which is during abstracted time period 2. To check the ionic strength calculation, Table 6-13 is used. To use Table 6-13, the relative humidity, invert seepage flux, and invert evaporation flux are needed. The thermal hydrology model shows that the relative humidity in the invert (*RH_CS NF_Inv*) at 1,000 years is 0.94602 or 94.602 percent. The seepage flux (*QFlux_CS NF_Inv*) is 0.0 m³/year and the evaporative flux (*QEvap_CS NF_Inv*) is 0.008704 m³/year. When the seepage flux equals 0.0 m³/year the *Q_ratio* is set equal to 1.0. Hence one minus the evaporative flux to seepage flux ratio gives 0.0. Table 6-13 shows that at this relative humidity and $1-R^{es}$, the log of the ionic strength is 0.694. Taking the inverse log of 0.694 gives 4.9431, which is the result calculated in GoldSim.

Table 6-14 is used to verify the ionic strength calculation during abstracted time period 3. GoldSim shows that the ionic strength in the invert at 2,000 years is 4.529. To use Table 6-14 the relative humidity, invert seepage flux, and invert evaporation flux are needed. The relative humidity in the invert (*RH_CS NF_Inv*) at 2,000 years is 0.96983 or 96.983 percent. The seepage flux (*QFlux_CS NF_Inv*) is 4.8769E-05 m³/year and the evaporative flux (*QEvap_CS NF_Inv*) is 0.0042728 m³/year. So one minus the evaporative flux to seepage flux ratio gives -86.614. Table 6-14 shows that at this relative humidity and $1-R^{es}$, the log of the ionic strength is 0.656. The inverse log of 0.656 gives an ionic strength of 4.529; the same result as given in GoldSim.

For abstracted time period 4, the ionic strength calculated by the GoldSim model at 100,000 years (Bin 4, CSNF) is 0.014466. This result can be checked using Table 6-15. To use this table, the relative humidity and the invert temperature are needed as well as the invert seepage flux and evaporative flux. The relative humidity passed from the thermal hydrology model (*RH_CS NF_Inv*) is 0.99831 (99.831 percent) in Bin 4 at 100,000 years, and the temperature (*Temp_CS NF_Inv*) is 25°C. The seepage flux (*QFlux_CS NF_Inv*) passed from the thermal hydrology model 5.6523E-04 m³/year and the evaporative flux is 3.3093E-05 m³/year. So one minus the evaporative flux to seepage flux ratio gives 0.94145. Using this value along with the temperature and relative humidity, Table 6-15 shows that the value lies between -1.866 and -1.821. Interpolation between these two values gives the log of the ionic strength as -1.8396. Taking the inverse log of -1.8396 gives 0.014466, which is the result calculated in the TSPA-SR model. This verifies that the in-drift ionic strength model is implemented correctly, and that the thermal hydrology inputs are correctly transferred.

Invert pH—GoldSim gives a value of 9.4 for the pH in the invert (Bin 4, CSNF) at 1,000 years, which is during abstracted period 2. To check the pH calculation, Table 6-13 is used. The thermal hydrology model shows that the relative humidity in the invert (RH_CSNF_Inv) at 1,000 years is 0.94602 or 94.602 percent. One minus the evaporative flux to seepage flux ratio for period 2 is as given above. Table 6-13 shows that at this relative humidity, the pH is 9.4, which is the result calculated in GoldSim.

Table 6-14 is used to verify the pH calculation during abstracted time period 3. GoldSim shows that the pH in the invert at 2,000 years is 7.64. To use Table 6-14, the relative humidity, seepage flux, and evaporation flux are needed. The relative humidity in the invert (RH_CSNF_Inv) at 2,000 years is 0.96983 or 96.983 percent. The seepage flux ($QFlux_CSNF_Inv$) is $4.8769E-05$ m³/year and the evaporative flux ($QEvap_CSNF_Inv$) is 0.0042728 m³/year. So one minus the evaporative flux to seepage flux ratio gives -86.614 . Table 6-14 shows that at this relative humidity and $1-R^{es}$ the pH is 7.64, which is the same result as given in GoldSim.

For abstracted time period 4, the pH that is calculated by the GoldSim model at 100,000 years (Bin 4, CSNF) is 7.0734. This result can be checked using Table 6-15. To use this table, the relative humidity and temperature in the invert are needed as well as the seepage flux and evaporative flux. The relative humidity passed from the thermal hydrology model (RH_CSNF_Inv) is 0.99831 (99.831 percent) in Bin 4 at 100,000 years, and the temperature ($Temp_CSNF_Inv$) is 25°C. The seepage flux ($QFlux_CSNF_Inv$) passed from the thermal hydrology model $5.6523E-04$ m³/year and the evaporative flux is $3.3093E-05$ m³/year. So one minus the evaporative flux to seepage flux ratio gives 0.94145. Using this value along with the temperature and relative humidity, Table 6-15 shows that the value lies between 7.05 and 7.09. Interpolation between these two values gives the pH as 7.0734, which is the result calculated in the TSPA-SR model. This verifies that the in-drift pH model is implemented correctly, and that the thermal hydrology inputs are correctly transferred.

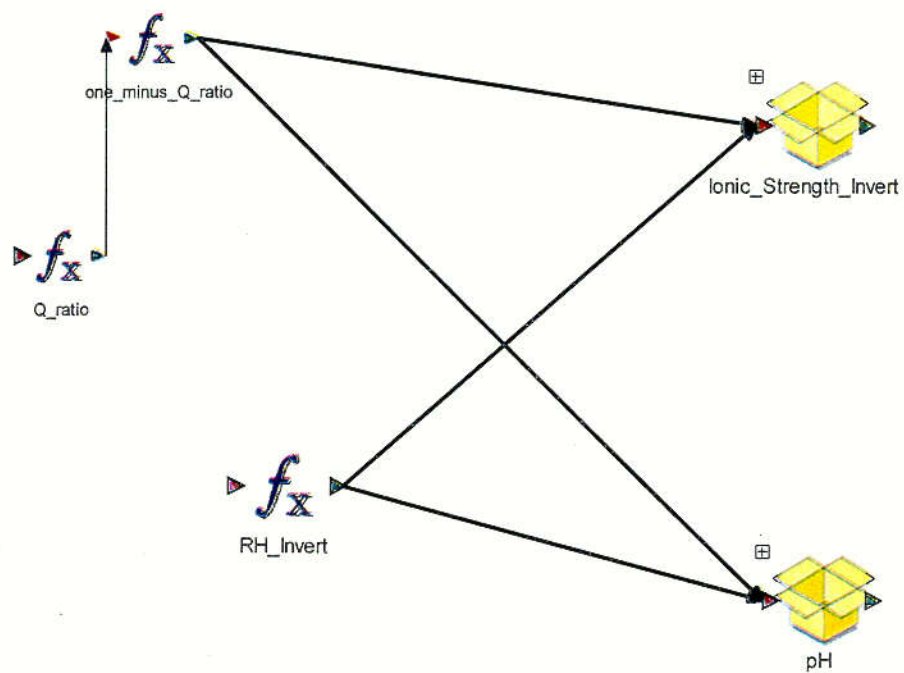


Figure 6-66. A Graphical Illustration of the Bin-Level In-Drift Chemistry Model

C46

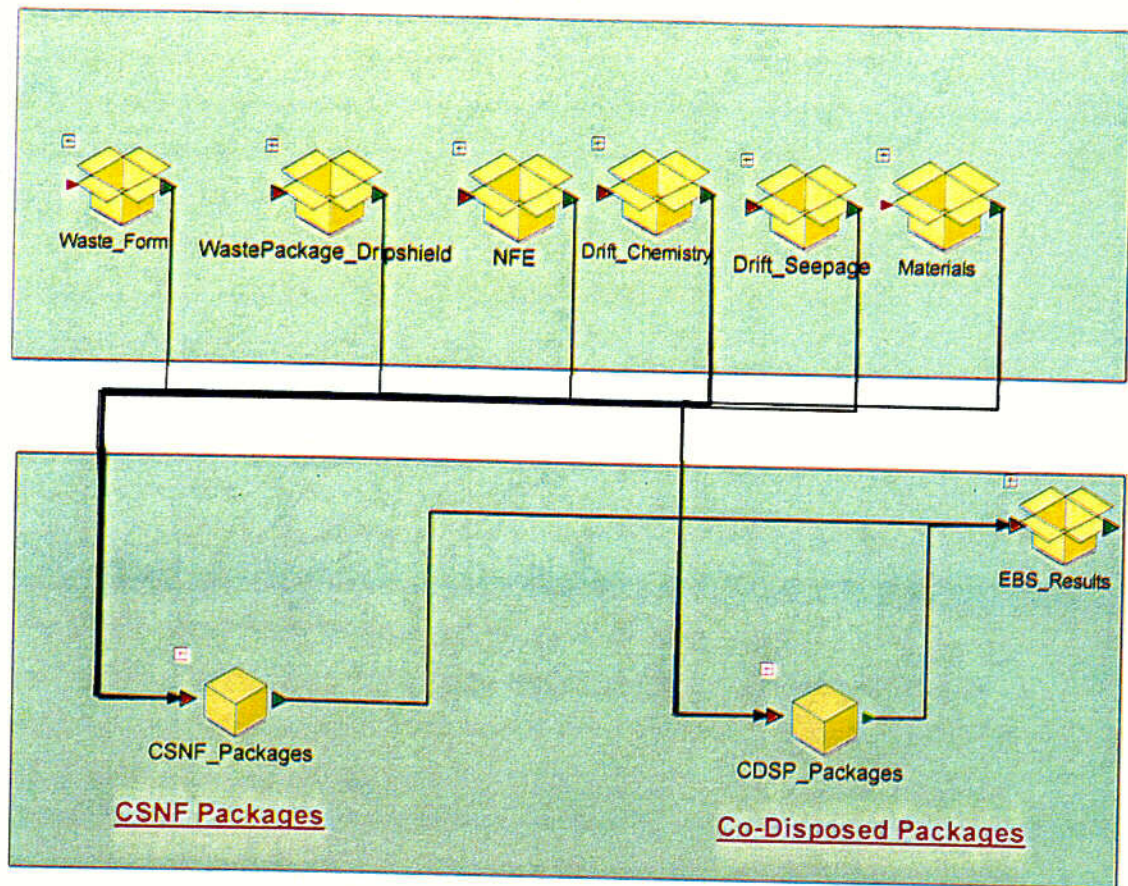


Figure 6-67. A Graphical Illustration of In-Drift Chemistry at the EBS Level of the Model

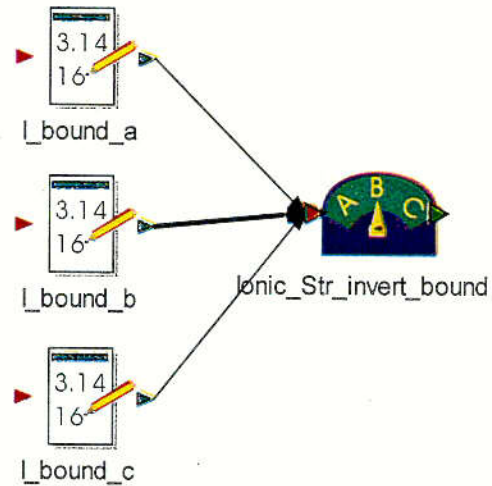


Figure 6-68. Illustration of Selection of In-drift Ionic Strength for Relative Humidities Less Than 50 percent (Ionic_Str_invert_bound)

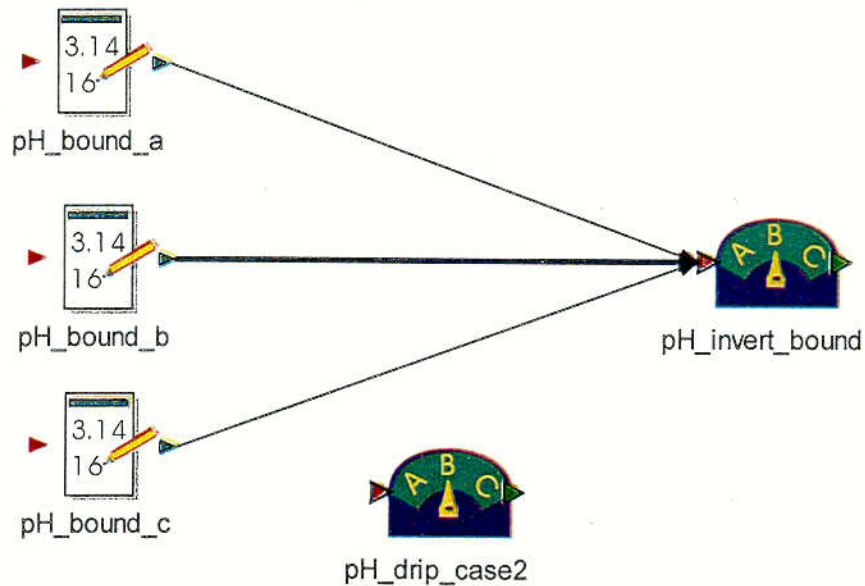


Figure 6-69. Illustration of Selection of In-drift pH for Relative Humidities Less Than 50 percent (pH_invert_bound) and Relative Humidities Between 50 and 85 percent (pH_drip_case2)

c48

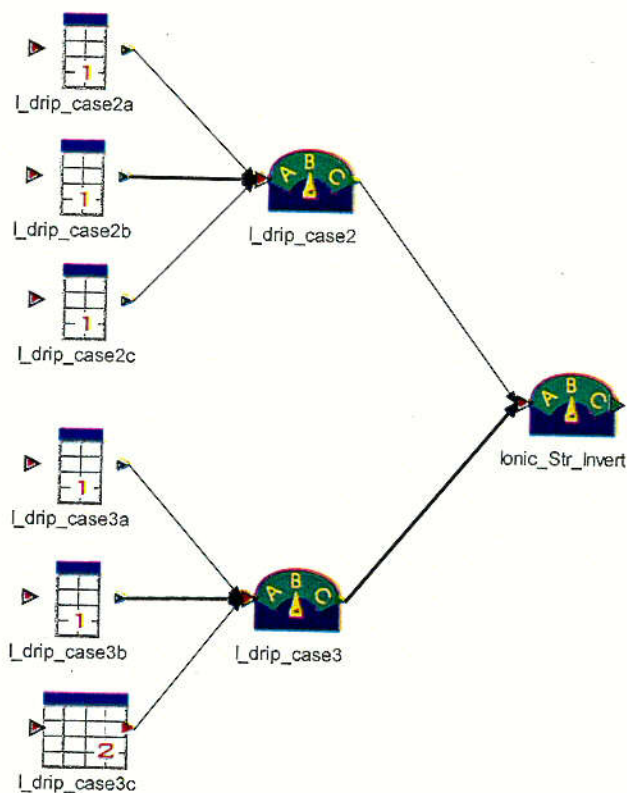


Figure 6-70. Model Logic for Determining the Ionic Strength of the Invert when the Relative Humidity is Greater than or Equal to 50 Percent

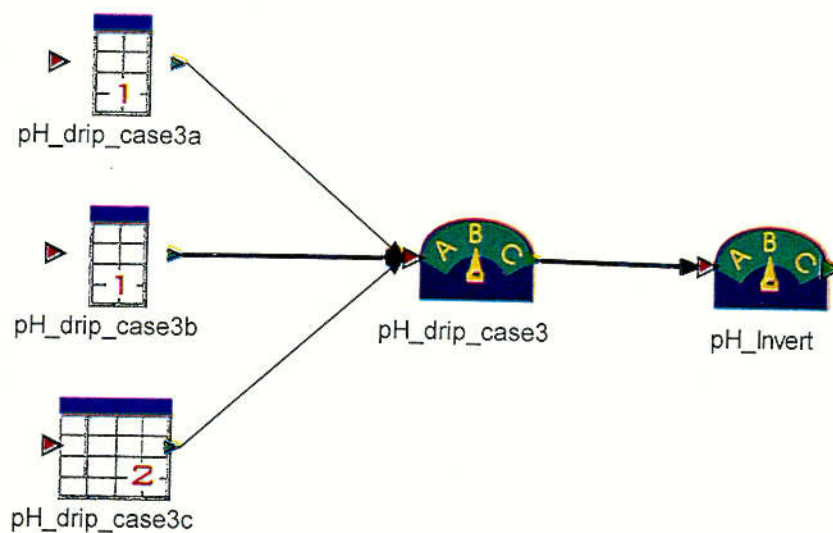


Figure 6-71. Model Logic for Determining the pH of the Invert When the Relative Humidity is Greater than or Equal to 50 Percent

C49

6.3.3 Waste Package Degradation

Overview

The engineered barriers, consisting of the drift, the drip shield, and the corrosion-resistant waste package outer barrier, are designed to contain the waste materials and delay the release of radionuclides to the environment. Waste package has two major design functions; 1) waste containment (i.e., complete isolation of waste from the environment until the package fails) and 2) after failure limited release of waste materials (i.e., radionuclide) from the failed waste package. The primary design function of the drip shield is to provide protection of the underlying waste package until the waste package fails, and after the waste package fails, it works together with the waste package (by limiting advective water flow into the package) to limit the waste material release from the failed waste package to the environment. Computer simulations incorporating the potential corrosion scenarios were run to analyze the effectiveness of the waste packages and drip shields to potentially contribute to limiting the release of waste material (CRWMS M&O 2000 [151566]). This section describes the coupling of the waste package degradation simulation software into the TSPA-SR model and presents the results of the median value simulation as they pertain to waste package degradation.

The engineered barrier simulations model the degradation of the drip shield and the waste packages. The drip shield surface area is determined based on the assumption that the drip shield is composed of three parts; two vertical parallelepipeds and one horizontal parallelepiped, each 15 mm thick (CRWMS M&O 2000 [151566], Section 5.1). The surface area of the modeled waste package is determined based on the "Single CRM 21-PWR Waste Package" (CRWMS M&O 2000 [151566], Section 5.1). The current waste package design consists of a 20 mm thick Alloy 22 outer barrier encompassing a 50 mm thick 316 Nuclear Grade stainless steel inner shell. No performance credit is taken for the 316 Nuclear Grade stainless steel inner shell (CRWMS M&O 2000 [151853]). The waste package has one Alloy 22 lid on one end of the waste package outer barrier and two Alloy 22 lids (one 10 mm thick inner lid and one 25 mm thick outer lid) on the closure end of the waste package outer barrier. All welds used in waste package fabrication are completely stress-annealed with the exception of the closure welds on the closure lids. In order to best model the dual Alloy 22 lid design for the waste package outer barrier, the 20 mm Alloy 22 outer barrier is modeled as being composed of two layers; one 25 mm thick and one 10 mm thick. The model parameters are chosen in such a way that the 25 mm thick layer behaves like a 10 mm layer except for the region of that layer that comprises the closure-lid area. For example, the general corrosion rates applied to the 25 mm layer are 2.5 times greater than those for Alloy 22 except for the lid region for which general corrosion rates appropriate for Alloy 22 are used (CRWMS M&O 2000 [151566], Section 6.2). In the waste package degradation simulations, waste package failure is defined to be the time of first penetration of the inner layer of the outer barrier, i.e., the 10 mm inner layer.(CRWMS M&O 2000 [151566], Section 6.2).

The degradation of the drip shields and waste packages is simulated with the Waste Package Degradation (WAPDEG) software. A discussion of the WAPDEG software and the GoldSim implementation parameters relevant to modeling waste package degradation are reported in the AMR *WAPDEG Analysis of Waste Package and Drip Shield Degradation* (CRWMS M&O 2000 [151566]). The TSPA-SR waste package degradation analysis using the WAPDEG code simulates the behavior of four hundred waste packages (CRWMS M&O 2000 [151566]),

Section 6.3.3). Effects of spatial and temporal variations in the exposure conditions over the repository were modeled explicitly incorporating relevant exposure condition histories into the analysis. The exposure condition parameters that were considered to vary over the proposed repository area are relative humidity and temperature at the waste package surface, seepage into the emplacement drift, and the chemistry of the seepage water. In addition, potentially variable corrosion processes within a single waste package were represented by sub-dividing each waste package surface into "patches" and stochastically populating the corrosion model parameter values (e.g., corrosion rates) over the patches.

The simulation software, WAPDEG 4.0, is a FORTRAN program compiled as a Dynamic Link Library (DLL). The WAPDEG code was specifically designed to calculate drip shield and waste package failure profiles in a manner consistent with the information requirements of the TSPA-SR model (CRWMS M&O 2000 [151566], Section 3.1.3). Abstracted corrosion relationships containing variability and uncertainty were derived from process level analyses and are incorporated into the WAPDEG code. The corrosion mechanisms simulated are (CRWMS M&O 2000 [151566], Section 6.2):

- General corrosion of the Alloy 22 waste package outer barrier under humid-air and aqueous conditions
- General corrosion of the Titanium Grade 7 drip shield under humid-air and aqueous conditions
- Localized corrosion of the waste package outer barrier
- Stress corrosion cracking and manufacturing defects in the waste package outer barrier closure-lid welds
- Enhanced general corrosion of the waste package outer barrier due to microbiologically induced corrosion
- Enhanced general corrosion of the waste package closure welds due to aging and phase instability
- Inside-out corrosion of the waste package outer barrier once failure of the waste package has occurred.

General corrosion of the drip shield and waste package outer barrier is initiated once the relative humidity of the surface exceeds a specified critical relative humidity threshold (CRWMS M&O 2000 [151566], Section 6.3.8). The critical relative humidity is a function of temperature, and decreases as temperature increases. General corrosion occurs in the presence or absence of seepage drips. General corrosion continues as long as the relative humidity exceeds the critical threshold. In the TSPA-SR model, variability in the general corrosion rate across the waste package or drip shield surface is represented by allowing the general corrosion rate applied to a given patch on a given waste package or drip shield to differ from the general corrosion rate applied to a different patch on the same waste package or drip shield.

Localized corrosion of the drip shield and waste package outer barrier occurs only under aqueous conditions and is initiated once the corrosion potential exceeds the critical potential (CRWMS M&O 2000 [151566], Section 6.2). The difference between the corrosion potential and the critical potential is a function of pH. If localized corrosion occurs, it continues as long as the corrosion potential exceeds the critical threshold. In the TSPA-SR model, localized corrosion can potentially occur at several locations, referred to as pits, on each patch.

Stress corrosion cracking (SCC) processes can lead to crack penetration of the waste package outer barrier closure welds (CRWMS M&O 2000 [151566], Section 4.1.9 page 25). SCC requires the presence of tensile stress, a corrosive environment, and material susceptible to SCC. Cracks can initiate from microscopic defects, such as surface roughness, grain boundary junctions, or from pre-existing manufacturing defects, such as inclusions or weld flaws. The crack growth rate is a function of the stress intensity factor at the crack tip, which is directly related to the stress at the crack location. In the TSPA-SR model, stress corrosion cracking can potentially occur at several locations, referred to as cracks, on each patch.

Microbiologically Induced Corrosion (MIC) of the waste package outer barrier is initiated once the relative humidity exceeds 90 percent (CRWMS M&O 2000 [151566], Section 4.1.10). MIC continues as long as the relative humidity exceeds 90 percent. Effect of MIC is implemented as an enhancement factor that increases the general corrosion rate by a multiplication factor uniformly distributed between 1 to 2 (CRWMS M&O 2000 [151566], Section 4.1.10 Table 13). In the TSPA-SR implementation, the MIC is assumed conservatively when the relative humidity exceeds the relative humidity threshold for corrosion initiation, and the enhancement factor is applied.

Effects of aging and phase instability of the waste package outer barrier closure welds occurs due exposures to high temperature conditions CRWMS M&O 2000 [151566]. Aging and phase instability are implemented as an enhancement factor which increases the general corrosion rate by a multiplication factor uniformly distributed between 1 to 2.5 (CRWMS M&O 2000 [151566], Section 4.1.11, Table 14).

The relative humidity affects the corrosion rates of the drip shield and waste packages. The relative humidity and temperature profiles are inputs from the Thermal Hydrology (TH) Model component of the TSPA-SR model (see Section 6.3.2 Thermal Hydrology) and the TH AMR describing the environmental conditions in the Near-Field Environment, *Abstraction of Near-Field Environment Thermodynamic Environment and Percolation Flux* (CRWMS M&O 2000 [149860], Section 6.3.2 and 6.3.3). The pH of the seepage water inside the drift and inside a failed waste package are calculated using the same equations used to calculate in-drift pH (see Section 6.3.2.2 In-Drift Geochemical Environment) and in-package pH (see Section 6.3.4.2 In-Package Chemistry). For more information regarding the calculation of the temporal profiles for the environmental conditions inputs to the WAPDEG software, refer *WAPDEG Analysis of Waste Package and Drip Shield Degradation* (CRWMS M&O 2000 [151566], Attachment I).

The WAPDEG analysis provides, as output, the cumulative probability of waste package failure by the failure modes considered as a function of time (CRWMS M&O 2000 [151566], Section 6.4). The analysis also provides the average number of penetrations (patches, pits, and cracks) per failed drip shield and waste package as a function of time. The initial release of

unbound radionuclides (gap fraction) and the maximum release rate of radionuclides to the unsaturated zone is limited by the failure openings in the waste package. Once a waste package has failed, material entering or leaving the waste package can do so only through the failed areas. The TSPA-SR model tracks the average area failed in a waste package and hence can appropriately calculate the quantity of material entering and leaving failed packages.

There are four DLLs that the TSPA-SR model uses for simulating degradation of the drip shields and waste packages. WAPDEG is one of the four DLLs called by the waste package degradation component. There are three other FORTRAN subroutines which were all compiled as DLLs and incorporated in the TSPA-SR model. The additional software subroutines are GVP, MFD, and SCCD. Each of these subroutines interface with the TSPA-SR model and WAPDEG, providing WAPDEG with pertinent information (e.g., CDFs and data tables) for waste package degradation calculations. The TSPA-SR model supplies inputs to each of the DLLs, allows the DLLs to perform their operations, and then receives the DLL output for use in the WAPDEG computations.

The GVP DLL (Gaussian Variance Partitioning) is a FORTRAN subroutine compiled as a DLL. The code takes an input distribution containing both uncertainty and variability and solves it into one distribution that characterizes variability at a given uncertainty level. For more information on the GVP DLL the reader is referred to *GVP Software Routine Report* (CRWMS M&O 2000 [152496]).

The MFD DLL (Manufacturing Defects) is a FORTRAN subroutine compiled as a DLL. The code calculates two cumulative probability distributions, one for the number of manufacturing defects per waste package and one for the size of manufacturing defects in the closure weld of the waste packages given the probability of non-detection and the fraction of surface breaking flaws. The outputs of the MFD DLL are a file containing the cumulative distribution function (CDF) table for the number of defects in a weld, a file containing the CDF table for defect sizes, and one output argument, containing the probability of at least one crack occurring on a waste package. For more information on the MFD DLL the reader is referred to *MFD Software Routine Report* (CRWMS M&O 2000 [152497]).

The SCCD DLL (Stress Corrosion Cracking Dissolution) is a FORTRAN subroutine compiled as a DLL. The code calculates the hoop stress and stress intensity factor versus depth curves for the waste package outer barrier closure lid weld regions. The outputs of the SCCD DLL are a file in WAPDEG table format for the hoop stress versus depth at the specified number of angles and a file in WAPDEG table format for the stress intensity factor versus depth at the specified number of angles. For more information on the SCCD DLL the reader is referred to *SCCD Software Routine Report* (CRWMS M&O 2000 [152499]).

For more information regarding the input distributions and other calculations pertaining to waste package degradation, the reader is referred to the AMR *WAPDEG Analysis of Waste Package and Drip Shield Degradation* (CRWMS M&O 2000 [151566], Section 6.0) and its full compliment of feed calculations and reports.

Inputs to the TSPA Model

The inputs to the Waste Package Degradation component of the TSPA-SR model are all developed for use in the TSPA-SR model. All of the inputs, unless otherwise stated, are outputs from the analysis *WAPDEG Analysis of Waste Package and Drip Shield Degradation* (CRWMS M&O 2000 [151566]). The output from the reference report is tracked in the TDMS with DTN: MO0010MWDWAP01.009 [153127]. The inputs to the TSPA-SR model include the text files tracked with DTN: MO0010MWDWAP01.009 [153127] as well as the case18-19.gsm which is included. The parameter names and values in the GoldSim file case18-19.gsm are tracked by DTN: MO0010MWDWAP01.009 [153127] and are identical to those in the TSPA-SR model. (A search using the GoldSim "Find" command will ease the TDMS user's search for data verification.)

The GVP DLL is called six times in each TSPA-SR realization. Each call resolves one general corrosion rate cumulative input distribution containing variability and uncertainty into one cumulative distribution containing variability only. Other than the model parameters U , qu , L , $index1$, and $index2$ there are no data inputs into the GVP DLL (Table 6-16). The parameter U is the fraction of the original distributions' variance that is due to uncertainty. The fraction is itself uncertain and is randomly selected by GoldSim from a uniform distribution between 0 and 1 (CRWMS M&O 2000 [151566], Section 6.3.7). The parameter qu is the cumulative probability used to sample the median corrosion rate of the variability distribution from the uncertainty distribution. The probability is also uncertain and is randomly selected by GoldSim from a uniform distribution between 0 and 1 (CRWMS M&O 2000 [151566], Section 6.3.7). (A numeral from 1 to 6 was added to each parameter name to distinguish these parameters by the appropriate call to the GVP subroutine.) The parameter L is a model logic flag used to determine whether or not the natural logarithm of the CDF values should be taken ($L > 0 = \text{YES}$) (CRWMS M&O 2000 [151566], Section 6.3.7). The parameters $index1$ and $index2$ are cross-reference indices instructing the GVP DLL which files to use as its input and which files to use for its output, respectively (CRWMS M&O 2000 [151566], Table 1-4). That is, the value assigned to $index1$ is the line number in the wd4dll.wap file containing the input filename.

Table 6-16. Input Parameters for the GVP Calculation

TSPA Parameter	Description	Parameter Value
GVP1 = U_GVP_GA22SR00 GVP2 = U_GVP_GTi7SR00 GVP3 = U_GVP_22x2P5_CDF GVP4 = U_GVP_NDTi GVP5 = U_GVP_GA22x0P5_CDF_1 GVP6 = U_GVP_GA22x0P5	Gaussian Variance Partitioning parameter for the fraction of the original distributions' variance	Uniform 0 to 1
GVP1 = qu_GVP_GA22SR00 GVP2 = qu_GVP_GTi7SR00 GVP3 = qu_GVP_22x2P5_CDF GVP4 = qu_GVP_NDTi GVP5 = qu_GVP_GA22x0P5_CDF_1 GVP6 = qu_GVP_GA22x0P5	Gaussian Variance Partitioning parameter for the cumulative probability used to sample the median of the variability distribution from the uncertainty distribution	Uniform 0 to 1

Table 6-16. Input Parameters for the GVP Calculation (Continued)

TSPA Parameter	Description	Parameter Value
L	Switch to determine if the natural log of the CDF should be taken (if L>0, yes, otherwise no)	-1 (no)
Index1	Index number that is used be the GVP dll to call the correct input file for each GVP dll.	GVP1 = 19 GVP2 = 20 GVP3 = 18 GVP4 = 20 GVP5 = 18 GVP6 = 21
Index2	Index number that is used be the GVP dll to call the correct output file for each GVP dll	GVP1 = 2 GVP2 = 3 GVP3 = 1 GVP4 = 6 GVP5 = 22 GVP6 = 10

DTN: MO0010MWDWAP01.009 [153127]

The MFD DLL is called twice in one TSPA-SR realization, once for assessing defects in the weld securing the waste package outer barrier extended closure lid and once for the weld securing the outer barrier flat closure lid. Table 6-17 presents the input parameters used by the MFD routine. In addition to these parameters there are two additional parameters incorporated into the MFD component of the TSPA-SR model. These parameters are *fileFlaws* and *fileSize*. The parameter *fileFlaws* is a cross-reference index (see Table 6-17) that instructs the MFD DLL to which file to write the CDF table of the number of defects per waste package. The parameter *fileSize* is the cross-reference index instructing the MFD DLL to which filename to write the CDF table for the defect sizes (CRWMS M&O 2000 [151566], Section 6.3.11.1).

Table 6-17. Input Parameters for the MFD Calculation

TSPA Parameter	Description	Parameter Value	Reference
Thickness	The lid thickness in mm	Inner Lid = 10 mm Outer Lid = 25 mm	CRWMS M&O 2000 [151566], Table 4
lid_radius	The lid radius for both lids in m	0.76 m	CRWMS M&O 2000 [151566], Table 4
b_ML	The location parameter of the non-detection probability for the inner lid	Uniform Distribution Min=1.6, Max=5.0	CRWMS M&O 2000 [151566], Table 4
b_OL	The location parameter of the non-detection probability for the outer lid	Uniform Distribution Min=1.6, Max=5.0	CRWMS M&O 2000 [151566], Table 4
v_ML	The scale parameter of the non-detection probability for the inner lid.	Uniform Distribution Min=1.0, Max=3.0	CRWMS M&O 2000 [151566], Table 4

Table 6-17. Input Parameters for the MFD Calculation (Continued)

TSPA Parameter	Description	Parameter Value	Reference
v_OL	The scale parameter of the non-detection probability for the outer lid.	Uniform Distribution Min=1.0, Max=3.0	CRWMS M&O 2000 [151566], Table 4
psi_ML	The fraction of surface breaking defects in the inner lid	Uniform Distribution Min=0.3481, Max=0.3632	CRWMS M&O 2000 [151566], Table 4 (psi_middle)
psi_OL	The fraction of surface breaking defects in the outer lid	Uniform Distribution Min=0.3481, Max=0.3632	CRWMS M&O 2000 [151566], Table 4 (psi_outer)

DTN: MO0010MWDWAP01.009 [153127]

The SCCD DLL is called twice in one TSPA-SR realization, once for assessing the hoop stress and hoop stress intensity factor for the inner lid and once for the outer lid. Table 6-18 presents the input parameters used by the SCCD DLL subroutine. In addition to these parameters there are three additional parameters incorporated into the SCCD component of the TSPA-SR model. These parameters are *idxinp*, *idxkin* and *idxstr*. The parameter *idxinp* is a cross-reference index (Table 6-18) which instructs the SCCD DLL which file to use as its input. The parameters *idxkin* and *idxstr* are the cross-reference indices which instruct the SCCD DLL which files to use for its outputs.

Table 6-18. Input Parameters for the SCCD Calculation

TSPA Parameter	Description	Parameter Value	Source
z_ML	Uncertain deviation from median yield strength range for inner lid	Truncated Triangle Distribution Mean = 0, Min=-3, Max = 3	CRWMS M&O 2000 [151566], Table 10
z_OL	Uncertain deviation from median yield strength range for inner lid	Truncated Triangle Distribution Mean = 0, Min=-3, Max = 3	CRWMS M&O 2000 [151566], Table 10
sinf	Sine of fracture angle	Inner lid=0.608873 Outer lid=1	CRWMS M&O 2000 [151566], page 24
A1_ML A1_OL	Zero order regression coefficient from model abstraction for stress vs. depth at zero degrees	Inner lid (ML)=-437.721 Outer lid (OL)=-356.268	CRWMS M&O 2000 [151566], Table 8(A0)
A2_ML A2_OL	First order regression coefficient from model abstraction for stress vs. depth at zero degrees	Inner lid (ML)=176.967 Outer lid (OL)=37.1808	CRWMS M&O 2000 [151566], Table 8 (A1)
A3_ML A3_OL	Second order regression coefficient from model abstraction for stress vs. depth at zero degrees	Inner lid (ML)=-15.6061 Outer lid (OL)=1.43639	CRWMS M&O 2000 [151566], Table 8 (A2)

Table 6-18. Input Parameters for the SCCD Calculation (Continued)

TSPA Parameter	Description	Parameter Value	Source
A4_ML A4_OL	Third order regression coefficient from model abstraction for stress vs. depth at zero degrees	Inner lid (ML)=0.367099 Outer lid (OL)=-0.065282	CRWMS M&O 2000 [151566], Table 8 (A3)
nangle	The number of angles in the range zero to pi radians to compute tables of stress and KI versus depth	5	CRWMS M&O 2000 [151566], Section 6.3.12.1
YS_ML YS_OL	Expected yield strength in Mpa	322.3	CRWMS M&O 2000 [151566], Table 10 (YS)
fys_ML fys_OL	Fraction yield strength range	0.3	CRWMS M&O 2000 [151566], Table 10 (amp)
amp_ML amp_OL	Angular amplitude for the equation of angular variation of stress in MPa	17.2369	CRWMS M&O 2000 [151566], Equation 6
Stress_ThreshMLF ac	Fraction of expected yield stress for assigning stress threshold in the inner lid	Uniform Distribution Min = 0.2, Max = 0.3	CRWMS M&O 2000 [151566], Table 11
Stress_ThreshOLF ac	Fraction of expected yield stress for assigning stress threshold in the outer lid	Uniform Distribution Min = 0.2, Max = 0.3	CRWMS M&O 2000 [151566], Table 11
nob	Crack growth exponent for slip dissolution in the outer barrier	Uniform Distribution Min=3.0, Max = 3.36	CRWMS M&O 2000 [151566], Sec 4.1.9
nib	Crack growth exponent for slip dissolution in the inner barrier	Uniform Distribution Min=3.0, Max = 3.36	CRWMS M&O 2000 [151566], Sec 4.1.9
idxinp	K table index	ML = 15 OL = 14	CRWMS M&O 2000 [151566], Table 7
idxkin	Stress Intensity CDF Index	ML = 7 OL = 4	CRWMS M&O 2000 [151566], Sec 6.3.2
idxstr	Stress Index	ML = 8 OL = 5	CRWMS M&O 2000 [151566], Sec 6.3.2
ASCCib	Crack growth pre-exponent for slip dissolution in the middle barrier from SCCD component	$7.8 \times 10^{-2} (nib/4)^{3.6}$ $(4.1 \times 10^{-14})^{(nib/4)} \times$ 3.1558149×10^7	CRWMS M&O 2000 [151566], Equation 12 & 13; Sec. 4.1.9
ASCCob	Crack growth pre-exponent for slip dissolution in the outer barrier from SCCD component	$7.8 \times 10^{-2} (nob/4)^{3.6}$ $(4.1 \times 10^{-14})^{(nob/4)} \times$ 3.1558149×10^7	CRWMS M&O 2000 [151566], Equation 12 & 13; Sec 4.1.9

DTN: MO0010MWDWAP01.009 [153127]

The WAPDEG DLL is called once in each TSPA-SR realization to calculate the degradation profiles for the drip shields and waste packages. The DLL requires 1,040 input parameters to simulate the degradation of the drip shield and waste packages. Some of these inputs tell the WAPDEG DLL which degradation models to use while others are values of degradation model parameters. These inputs are stored in the TSPA-SR input deck, within a data element named *WAPDEG_Inputs*. The TSPA-SR model furnishes the input deck with 45 of 1,040 input parameters. These 45 parameters are a combination of input data, DLL output, cross-reference

indices, and sampled variance shares. There are 28 stochastic distributions *VarShar_1* to *VarShar_26* used to determine the partitioning of the variance of a variability distribution between waste package to waste package variability and patch-to-patch variability on a given waste package. The partitioning fractions of the variability are uncertain and are randomly sampled from a uniform distribution between 0 and 1 (CRWMS M&O 2000 [151566], Section 6.3.17). The WAPDEG routine performs a stochastic calculation and a random seed is necessary. The random seed is the parameter *WDSeed* and is a uniform distribution between 1 and $2^{31}-1$, the maximum positive 32-bit integer (CRWMS M&O 2000 [151566], Section 6.1.1). The parameter *hist_index* is a cross-reference index that instructs the WAPDEG DLL which thermal hydrology file to use as input (backfill or no backfill design options, see Section 6.3.2.1 Thermal Hydrology).

Table 6-19 provides the cross-reference list for the input and output files used or generated by the GVP, MFD, SCCD, and WAPDEG DLLs. Each file is assigned an index number identifying the proper files to be used, passed, and referenced between the TSPA-SR model and the associated waste package degradation DLLs. A GVP, MFD, or SCCD DLL output file is generally a WAPDEG DLL input.

Table 6-19. File Description and Index Cross-Reference for TSPA-SR DLL Inputs and Outputs

File Name	Description	File Index
WDdA22x2p5.cdf	GVP output general corrosion rate distribution for the waste package outer barrier outer layer for aqueous and humid-air conditions	1
WDdA22SR00.cdf	GVP output general corrosion rate distribution for the waste package outer barrier inner layer for aqueous and humid-air conditions	2
WDdT7SR00.cdf	GVP output general corrosion rate distribution for the drip shield for aqueous conditions	3
WDKISCCO.fil	SCCD output stress intensity versus depth at nangle angles for the waste package outer lid	4
WDStressO.fil	SCCD output stress versus depth at nangle angles for the waste package outer lid	5
WDndT7SR00.cdf	GVP output general corrosion rate distribution for the drip shield for humid-air conditions	6
WDKISCCM.fil	SCCD output stress intensity versus depth at nangle angles for the waste package inner lid	7
WDStressM.fil	SCCD output stress versus depth at nangle angles for the waste package inner lid	8
WDRHcrit.fil	Look-up table identifying the relative humidity threshold and the temperature to which it applies	9
WDdA22x0p5.cdf	GVP output general corrosion rate distribution for the waste package outer barrier inner layer for in-package conditions	10
WDMFDNDO.cdf	MFD output cumulative distribution for the number of manufacturing defect flaws in the outer lid.	11
WDMFDSizeO.cdf	MFD output cumulative distribution for the length of the defect flaws in the outer lid	12
WDHLW_high_bin2.ou	Data set tabulating the environmental condition profiles (backfill design option)	13
WDKlinO.fil	SCCD input table of stress intensity versus depth for the waste package outer lid	14

Table 6-19. File Description and Index Cross-Reference for TSPA-SR DLL Inputs and Outputs (Continued)

File Name	Description	File Index
WDKlinM.fil	SCCD input table of stress intensity versus depth for the waste package inner lid	15
WDMFDNDM.cdf	MFD output cumulative distribution for the number of manufacturing defect flaws in the inner lid.	16
WDMFDSizeM.cdf	MFD output cumulative distribution for the length of the defect flaws in the inner lid	17
WDgA22x2p5.cdf	GVP input general corrosion rate distribution for the waste package outer barrier outer layer for aqueous, humid-air and in-package conditions	18
WDgA22SR00.cdf	GVP input general corrosion rate distribution provided for the waste package outer barrier for aqueous, humid-air, and in-package conditions	19
WDgTi7Sr00.cdf	GVP input general corrosion rate distribution provided for the drip shield for aqueous and humid-air conditions	20
WDgA22x0p5.cdf	GVP input general corrosion rate distribution for the waste package outer barrier inner layer for aqueous, humid-air and in-package conditions	21
WDiA22x2p5.cdf	GVP output general corrosion rate distribution for the waste package outer barrier outer layer for in-package conditions	22
WDHLW_nbf_high_bin2.ou	Data set tabulating the environmental condition profiles (no backfill design option)	23

Source: WD4DLL.WAP. See CRWMS M&O 2000 [151566], Section 6.1.2 and DTN: MO0010MWDAP01.009 [153127]

The analysis of the drip shield and waste package degradation requires that specific parameters describing the geometry of the drip shield and waste packages and the size and number of perforations be defined (see EBS Transport Section 6.3.5). Table 6-20 lists these required inputs.

Table 6-20. Inputs to the Waste Package Degradation Model Component

TSPA Parameter	Description	Parameter Value	Source
Thick_WP_Lid1	Thickness of external lid of a waste package lid in mm	25 mm	CRWMS M&O 2000 [151566], Table 4
Thick_WP_Lid2	Thickness of flat lid of a waste package lid in mm	10 mm	CRWMS M&O 2000 [151566], Table 4
DS_Total_Length	Length of the drip shield in mm	4775 mm	CRWMS M&O 2000 [151566], Table 1
Number_DS_Patches	The number of simulated patches on the drip shield	500	CRWMS M&O 2000 [151566], (Section 5.1)
Number_WP_Patches	The number of simulated patches on a waste package	1000	CRWMS M&O 2000 [151566], (Section 5.1)

DTN: MO0010MWDWAP01.009 [153127]

All of the WAPDEG input to the TSPA-SR model, with the exception of the data in Table 6-20 and the WAPDEG modifications stated in Section 5 are tracked by DTN: MO0010MWDWAP01.009 [153127]. This DTN captures the entire WAPDEG code as it is implemented in GoldSim, the four DLLs, the cumulative distributions as well as the input data.

Implementation

At the initiation of each realization, the TSPA-SR model assigns an appropriate value to every stochastic variable in the model. This value will remain constant for the duration of the a realization. The 29 stochastic parameters (that are direct inputs to WAPDEG DLL) identified in Table 6-21 will be assigned an appropriate value, within the specified distribution. After each stochastic variable is assigned, a call to each DLL will be initiated. The TSPA-SR model initializes the DLL and passes the required inputs in a format that it can receive. If the required inputs are derived from stochastic parameters, the TSPA-SR model will pass the assigned value from that distribution to the DLL.

Table 6-21. Input Parameters for the WAPDEG Calculations

TSPA Parameter	Description	Parameter Value
NumPak	Number of waste packages to simulate in WAPDEG calculations	400
hist_index	History table index number	13
WDSeed	WAPDEG input random seed	Uniform Distribution Min=1, Max= $2^{31}-1$
VarShar_1	WAPDEG Variance input: A22OBND	Uniform Distribution Min=0.0, Max=1.0
VarShar_2	WAPDEG Variance input: A22IBND	Uniform Distribution Min=0.0, Max=1.0
VarShar_3	WAPDEG Variance input: A22OBND	Uniform Distribution Min=0.0, Max=1.0
VarShar_4	WAPDEG Variance input: A22OBND	Uniform Distribution Min=0.0, Max=1.0
VarShar_5	WAPDEG Variance input: A22OBND	Uniform Distribution Min=0.0, Max=1.0
VarShar_6	WAPDEG Variance input: A22OBND	Uniform Distribution Min=0.0, Max=1.0
VarShar_7	WAPDEG Variance input: A22OBND	Uniform Distribution Min=0.0, Max=1.0
VarShar_8	WAPDEG Variance input: A22OBND	Uniform Distribution Min=0.0, Max=1.0
VarShar_9	WAPDEG Variance input: A22OBND	Uniform Distribution Min=0.0, Max=1.0
VarShar_10	WAPDEG Variance input: A22OBND	Uniform Distribution Min=0.0, Max=1.0
VarShar_11	WAPDEG Variance input: A22OBND	Uniform Distribution Min=0.0, Max=1.0
VarShar_12	WAPDEG Variance input: A22OBND	Uniform Distribution Min=0.0, Max=1.0
VarShar_13	WAPDEG Variance input: A22OBND	Uniform Distribution Min=0.0, Max=1.0
VarShar_14	WAPDEG Variance input: A22OBND	Uniform Distribution Min=0.0, Max=1.0
VarShar_15	WAPDEG Variance input: A22OBND	Uniform Distribution Min=0.0, Max=1.0

Table 6-21. Input Parameters for the WAPDEG Calculations (Continued)

TSPA Parameter	Description	Parameter Value
VarShar_16	WAPDEG Variance input: A22OBND	Uniform Distribution Min=0.0, Max=1.0
VarShar_17	WAPDEG Variance input: A22OBND	Uniform Distribution Min=0.0, Max=1.0
VarShar_18	WAPDEG Variance input: A22OBND	Uniform Distribution Min=0.0, Max=1.0
VarShar_19	WAPDEG Variance input: A22OBND	Uniform Distribution Min=0.0, Max=1.0
VarShar_20	WAPDEG Variance input: A22OBND	Uniform Distribution Min=0.0, Max=1.0
VarShar_21	WAPDEG Variance input: A22OBND	Uniform Distribution Min=0.0, Max=1.0
VarShar_22	WAPDEG Variance input: A22OBND	Uniform Distribution Min=0.0, Max=1.0
VarShar_23	WAPDEG Variance input: A22OBND	Uniform Distribution Min=0.0, Max=1.0
VarShar_24	WAPDEG Variance input: A22OBND	Uniform Distribution Min=0.0, Max=1.0
VarShar_25	WAPDEG Variance input: A22OBND	Uniform Distribution Min=0.0, Max=1.0
VarShar_26	WAPDEG Variance input: A22OBND	Uniform Distribution Min=0.0, Max=1.0
Nob	Crack growth exponent for slip dissolution in the outer barrier from SCCD component	Uniform Distribution Min=3.0, Max = 3.36
Nib	Crack growth exponent for slip dissolution in the inner barrier from SCCD component	Uniform Distribution Min=3.0, Max = 3.36
ASCCob	Crack growth pre-exponent for slip dissolution in the outer barrier from SCCD component	$7.8 \times 10^{-2} (\text{nob}/4)^{3.6} (4.1 \times 10^{-14})^{(\text{nob}/4)} \times 3.1558149 \times 10^7$
ASCCib	Crack growth pre-exponent for slip dissolution in the inner barrier from SCCD component	$7.8 \times 10^{-2} (\text{nib}/4)^{3.6} (4.1 \times 10^{-14})^{(\text{nib}/4)} \times 3.1558149 \times 10^7$
SCCD_Middle_Lid. Stress_ThreshML	Stress threshold for inner lid from SCCD component	YS*Stress_ThreshMLFac
SCCD_Outer_Lid. Stress_ThreshOL	Stress threshold for outer lid from SCCD component	YS*Stress_ThreshOLFac
GVP_CDF_Dist_1. Median	GVP.dll output for the median corrosion rate variability of WDdA22SR00.cdf	GVP.dll calculated output
GVP_CDF_Dist_2. Median	GVP.dll output for the median corrosion rate variability of WDdTi7Sr00.cdf	GVP.dll calculated output
GVP_CDF_Dist_3. Median	GVP.dll output for the median corrosion rate variability of WDdA22x2p5.cdf	GVP.dll calculated output
GVP_CDF_Dist_4. Median	GVP.dll output for the median corrosion rate variability of WdndTi7SR00.cdf	GVP.dll calculated output
GVP_CDF_Dist_5. Median	GVP.dll output for the median corrosion rate variability of WDiA22x2p5.cdf	GVP.dll calculated output
GVP_CDF_Dist_6. Median	GVP.dll output for the median corrosion rate variability of WDgA22x0p5.cdf	GVP.dll calculated output

Table 6-21. Input Parameters for the WAPDEG Calculations (Continued)

TSPA Parameter	Description	Parameter Value
SCCD_Outer_Lid.Output1	SCCD.dll output for the deviate of a stochastic parameter	SCCD.dll calculated output
SCCD_Middle_Lid.Output1	SCCD.dll output for the deviate of a stochastic parameter	SCCD.dll calculated output
MFD_Outer_Lid.FlawnProb	MFD.dll output for the probability that a defect is in the outer lid	MFD.dll calculated output
MFD_Middle_Lid.FlawnProb	MFD.dll output for the probability that a defect is in the inner lid	MFD.dll calculated output

Figure 6-72 through Figure 6-80 illustrate the interface between the TSPA-SR model and the waste package degradation DLLs. Figure 6-72 shows the interface between the TSPA-SR model and the WAPDEG DLL. Note that all of the WAPDEG inputs are fed into one input deck, *WAPDEG_Inputs*. This data table contains all 1,040 WAPDEG input parameters, including the 45 fed to WAPDEG from the TSPA-SR model. Table 6-21 presents the complete list of TSPA-SR input parameters used by the WAPDEG DLL. The TSPA-SR inputs to the WAPDEG model are written to the input deck, which WAPDEG references for each simulation. Because a number of the input parameters fed from the TSPA-SR model to the WAPDEG code are values extracted from a specified distribution, the WAPDEG results should vary when multiple realizations are run.

Figure 6-73 illustrates the TSPA-SR calls to the GVP DLL. The six containers each contain one external call to the GVP DLL. The six calls are made to resolve the provided distributions, associated with indexes 18, 19, 20 and 21, into the distributions used by WAPDEG, associated with indexes 1, 2, 3, 10, 22, and 6 see Table 6-19 and Table 6-22. One call is made for each of the six output distributions, hence the six localized containers shown in Figure 6-73. The contents within the six containers are identical, with the exception of the file index values.

Figure 6-74 shows the arrangement inside the first of the six localized groups in Figure 6-73. The input parameters for the GVP DLL are *U*, *qu*, *L*, *Index1*, and *Index2*. These five parameters feed into the TSPA-SR model element *Inputs*. *Inputs* is a vector containing the five input values for the GVP DLL. The external element, *GVP_Module_GA22SR00_CDF* calls the GVP DLL and passes it the values from *Inputs*. The GVP routine is performed on the appropriate general corrosion cumulative distribution, with the supplied inputs. The results are written in a text file, and the DLL returns the median corrosion rate of the variability distribution, *GVP_CDF_Dist1.median*, to the TSPA-SR model. The value assigned to *GVP_CDF_Dist1.median* is then passed to the vector *WAPDEG_Inputs*.

The routine for the remaining GVP calls is identical. Since the input distributions and the values assigned to the stochastic parameters *U* and *qu* could be different, the GVP DLL could return unique responses for each call. Two stochastic parameters are used for each of the six GVP DLL calls.

Figure 6-75 illustrates the two calls to the MFD DLL, one for the calculation of manufacturing defects in the waste package outer middle inner lid and one for the outer lid. The contents of both MFD groups are identical, with only the lid thickness, *thickness*, and the values referencing

the proper file indexes being different. Figure 6-76 shows the TSPA-SR interface with the MFD DLL called for the middle lid. The TSPA-SR input parameters *thickness*, *lid_radius*, *b*, *v*, *psi*, *fileFlaws*, and *fileSize* were described in Table 6-17. These are the inputs for the MFD DLL. The TSPA-SR model assigns a value to each stochastic and passes all of the inputs to the MFD DLL through the external element *MFD_mod*. Three stochastic parameters are used for each of the two MFD DLL calls. The MFD DLL calculates a cumulative distribution for the number of manufacturing defects expected and the expected defect sizes and writes the distributions to text files. The DLL also calculates the probability of having at least one defect occurring and passes this result back to the TSPA-SR model. The TSPA-SR model receives the value passed from the MFD DLL and assigns the value to the parameter *MFD_Middle_Lid.FlawProb*. The value assigned to *MFD_Middle_Lid.FlawProb* is then passed to the WAPDEG input deck within the TSPA-SR model, where it will be used as a WAPDEG DLL input.

Using the appropriate values for the lid thickness and file index identifiers, the implementation of the outer lid MFD calculation is identical to that discussed above.

Figure 6-77 shows the two calls to the SCCD DLL for the calculation of the hoop stress versus depth and hoop stress intensity versus depth for the middle and outer lids. Figure 6-78 shows the interface between the TSPA-SR model and the SCCD DLL. With the exception of *s*, the input parameters to the SCCD DLL are constants and are described in Table 6-18. At the initiation of the simulation a value, representative of its defined distribution, is assigned to *s*. The TSPA-SR model passes this value along with the values for the other 12 input parameters to the SCCD DLL through the external element, *SCCDdll*. The DLL receives the parameters, locates the proper input tables, based on the values assigned to *idxinp* (Table 6-18) and the cross reference index of Table 6-19, calculates the proper tables to be used by the WAPDEG DLL and writes them to the proper text files identified by index numbers in Table 6-19. The SCCD DLL passes the value assigned to *s* back to the TSPA-SR model, indicating that it is performed its operations. The TSPA-SR model receives the value and stores it as the parameter, *SCCD_Middle_Lid.Output1*. The TSPA-SR model then sends this value to the vector *WAPDEG_Inputs*. The model then calculates a value for the stress corrosion threshold, *Stress_ThreshML* based on the equation in Table 6-18 and the values assigned to the stochastics *Stress_ThreshMLFac* and *YS*. The calculated value is passed to the WAPDEG input deck. The routine for the outer lid is nearly identical, with the only differences being the indices identifying the proper inputs and outputs listed in Table 6-18 and Table 6-19.

The slip dissolution model component of the waste package degradation is shown in Figure 6-79. At the initiation of the simulation, the TSPA-SR model assigns values to the stochastic parameters *nib* and *nob*. The values are used to calculate *ASCCib* and *ASCCob*, respectively. The calculation is based on the equation listed in Table 6-21. The results of the calculation are passed to the element *WAPDEG_Inputs* where they are used by the WAPDEG DLL. Because the input tables, the values for the slip dissolution parameters, and the stochastic parameter *s* could be different for the each lid type, the outputs for the SCCD DLL are likely to be different.

Figure 6-72, the parameters *num_pak*, *WDSeed*, and *hist_index* are fed directly into the WAPDEG input deck, *WAPDEG_Inputs*. These values represent the number of waste packages to be simulated in each WAPDEG calculation, the random number seed for initializing stochastic parameters within the WAPDEG DLL, and a file index identifying the file which contains the

environmental conditions which affect the WAPDEG calculations (the index is cross referenced to Table 6-19).

The remaining input parameters assigned in the TSPA-SR model and passed to the WAPDEG input deck are shown in Figure 6-80. Each distribution is a variance sharing parameter. Variance sharing partitions the variance of a variability distribution between waste package to waste package variability and patch-to-patch variability on a given waste package. At the initiation of each model simulation, a value is assigned to each of the 28 variance sharing parameters. These 28 values are passed to the WAPDEG DLL through the *WAPDEG_Inputs* table element.

Once the supporting DLLs have run and have returned values to the TSPA-SR model, the WAPDEG DLL is called by the TSPA-SR model through the external element *WAPDEG_External*. Before calling WAPDEG, the TSPA-SR model writes the values assigned to the 45 WAPDEG inputs it has received (see Table 6-21), assigned, or calculated to the vector. WAPDEG reads input values from the 2000 line input vector, including the 45 from the TSPA-SR model, and calculates a temporal profile for the failure of drip shields and waste packages. These profiles are sent to the TSPA-SR model and stored in the tables *DS_Failure*, *WP_Failure_lower* and *WP_Failure_upper*, respectively. These curves are used to determine the fraction of the drip shields that have failed and the fraction of waste packages that have failed in any bin environment at any given time. The temporal profiles can be viewed by double clicking on the time history icon labeled *DS_FailureGRF*, *WP_FailureGRF* and *Combined*.

A first breach curve smoothing/correction algorithm was implemented in the waste package degradation module used in the TSPA-SR Model. This algorithm was necessitated by the fact that the waste package degradation module and the TSPA-SR Model evaluate the fraction of waste packages failed using different time steps. The waste package degradation module uses the time steps contained within the thermal hydrology file *WDHLW_nbf_high_bin2.ou* while the TSPA-SR Model uses 500-year time steps. A "Master Time Grid" was developed by recording each unique time listed in each of the 14 thermal hydrology time history files contained in the *WDHLW_nbf_high_bin2.ou* file. These 98 unique time points are stored in a GoldSim data element labeled *Time_Grid* within the waste package degradation module. The fraction of waste packages failed at each time listed in the *Time_Grid* element are determined. Linear interpolation is performed to determine the fraction of waste packages failed at times in between the times listed in the *Time_Grid* element. This results in the average interpolated failure rate between the WAPDEG time steps being used at the TSPA-SR Model time steps.

At each TSPA-SR time step, *ETime*, the TSPA-SR Model time, is compared to the times listed in the *Time_Grid* data element. The upper and lower bounding times from the *Time_Grid* data element are determined such that *ETime* is between these bounds. This is accomplished through the GoldSim selectors *WD_Time_lower* and *WD_Time_upper*, i.e., *WD_Time_lower* is equal to the lower bounding time and *WD_Time_upper* is equal to the upper bounding time. The fraction of waste packages failed at *WD_Time_lower* is determined using the GoldSim 1-D table *WP_Failure_lower* and the fraction of waste packages failed at *WD_Time_upper* is determined using the GoldSim 1-D table *WP_Failure_upper*. The GoldSim function element *WP_Failure_CDF* performs linear interpolation to find the fraction of waste packages failed at *Etime*.

WAPDEG also returns a data set, *Failure_Openings*, containing the temporal profiles for several failure parameters. These results are cross-referenced for identification purposes in Table 6-22.

Table 6-22. Cross-Reference Table for WAPDEG Results Tabulated in *Failure_Openings*

Column Number	Contents
1	Average number of patch failures (per failed drip shield) on the drip shield top
2	Average number of pit failures (per failed drip shield) on the drip shield top
3	Average number of crack failures (per failed drip shield) on the drip shield top
4	Average number of patch failures (per failed drip shield) on the drip shield side
5	Average number of pit failures (per failed drip shield) on the drip shield side
6	Average number of crack failures (per failed drip shield) on the drip shield side
7	The cumulative number of first patch failures on the drip shield (top and side)
8	The cumulative number of first pit failures on the drip shield (top and side)
9	The cumulative number of first crack failures on the drip shield (top and side)
10	Average number of patch failures (per failed waste package) on the waste package layer 1 top
11	Average number of pit failures (per failed waste package) on the waste package layer 1 top
12	Average number of crack failures (per failed waste package) on the waste package layer 1 top
13	Average number of patch failures (per failed waste package) on the waste package layer 1 side
14	Average number of pit failures (per failed waste package) on the waste package layer 1 side
15	Average number of crack failures (per failed waste package) on the waste package layer 1 side
16	Average number of patch failures (per failed waste package) on the waste package layer 1 bottom
17	Average number of pit failures (per failed waste package) on the waste package layer 1 bottom
18	Average number of crack failures (per failed waste package) on the waste package layer 1 bottom
19	The cumulative number of first patch failures on the waste package layer 1 (top, side, and bottom)
20	The cumulative number of first pit failures on the waste package layer 1 (top, side, and bottom)
21	The cumulative number of first crack failures on the waste package layer 1 (top, side, and bottom)
22	Average number of patch failures (per failed waste package) on the waste package layer 2 top
23	Average number of pit failures (per failed waste package) on the waste package layer 2 top
24	Average number of crack failures (per failed waste package) on the waste package layer 2 top
25	Average number of patch failures (per failed waste package) on the waste package layer 2 side
26	Average number of pit failures (per failed waste package) on the waste package layer 2 side
27	Average number of crack failures (per failed waste package) on the waste package layer 2 side
28	Average number of patch failures (per failed waste package) on the waste package layer 2 bottom
29	Average number of pit failures (per failed waste package) on the waste package layer 2 bottom
30	Average number of crack failures (per failed waste package) on the waste package layer 2 bottom
31	The cumulative number of first patch failures on the waste package layer 2 (top, side, and bottom)
32	The cumulative number of first pit failures on the waste package layer 2 (top, side, and bottom)
33	The cumulative number of first crack failures on the waste package layer 2 (top, side, and bottom)

Source: CRWMS M&O 2000 [151566], Section 6.3.2 Table 15

The data table *Failure_Openings* can be analyzed to ensure appropriate results are being calculated. Several expressions and time histories have been stored in the *GRF_Functions* (see Figure 6-72) container for results analysis. A description of the calculations and associated histories is presented in Table 6-23.

Table 6-23. List of WAPDEG Results for Performance Analysis

TSPA Parameter	Description	Calculation (Failure_Openings Column Number)	Associated Time History
DS_PatchFailures	Avg number of patch failures on the drip shield	1+4	DS_PatchGRF
DS_PitFailures	Avg number of pit failures on the drip shield	2+5	DS_PitGRF
DS_Cracks	Avg number of crack failures on the drip shield	3+6	DS_CracksGRF
DS_1 st _Patch	The cumulative number of first patch failures on the drip shield (top and side)	7	DS_1 st _PatchGRF
DS_1 st _Pit	The cumulative number of first pit failures on the drip shield (top and side)	8	DS_1 st _PitGRF
DS_1 st _Crack	The cumulative number of first crack failures on the drip shield (top and side)	9	DS_1 st _CrackGRF
WP_Outer_Patch	Avg number of patch failures on the waste package outer barrier	10+13+16	WP_Outer_PatchGRF
WP_Outer_Pits	Avg number of pit failures on the waste package outer barrier	11+14+17	WP_Outer_PitGRF
WP_Outer_Cracks	Avg number of crack failures on the waste package outer barrier	12+15+18	WP_Outer_CrackGRF
WPOB_1 st _patch	The cumulative number of first patch failures on the waste package layer 1 (top, side, and bottom)	19	WPOB_1 st _patchGRF
WPOB_1 st _Pit	The cumulative number of first pit failures on the waste package layer 1 (top, side, and bottom)	20	WPOB_1 st _PitGRF
WPOB_1 st _crack	The cumulative number of first crack failures on the waste package layer 1 (top, side, and bottom)	21	WPOB_1 st _crackGRF
WP_Inner_PatchFailures	Avg number of patch failures on the waste package inner barrier	22+25+28	WP_Inner_PatchGRF
WP_Inner_Pits	Avg number of pit failures on the waste package inner barrier	23+26+29	WP_Inner_PitGRF
WP_Inner_Cracks	Avg number of crack failures on the waste package inner barrier	24+27+30	WP_Inner_CracksGRF
WPIB_1 st _Patch	The cumulative number of first patch failures on the waste package layer 2 (top, side, and bottom)	31	WPIB_1 st _PatchGRF
WPIB_1 st _Pit	The cumulative number of first pit failures on the waste package layer 2 (top, side, and bottom)	32	WPIB_1 st _PitGRF
WPIB_1 st _Crack	The cumulative number of first crack failures on the waste package layer 2 (top, side, and bottom)	33	WPIB_1 st _CrackGRF

The waste package failure conditions are used throughout the TSPA-SR model. The output from WAPDEG effects the quantity of water which can enter and leave a waste package (e.g., *Waste_Form* cell, see Section 6.3.5). The flux through the waste package is a fraction of the flux through the drip shield scaled to the fraction of the waste package surface area which has opened from patches. The fraction of the drip shield that is open with time is calculated by taking the (average) total number of patches per drip shield (output from the WAPDEG dll) divided by the total number of patches possible per drip shield (500) (*DS_Frac_Patch*). The fraction of a failed waste package surface area open for advective flux is calculated by taking the (average) total number of pathes per failed waste package for top, side, and waste package lids (output from the WAPDEG dll) multiplied by the length of a patch divided by the total length of the waste package. The total area of the waste package open for diffusive release is defined by the sum of the average number of cracks, pits, and patches per waste package output from the WAPDEG dll, multiplied by their respective areas. This total area is used per package for diffusive releases (see Section 6.3.5 EBS Transport). Table 6-24 presents a list of TSPA-SR parameters which are not inputs to the waste package degradation component model, but are relevent to waste package degradation calculations and are used by other model components.

Table 6-24. Supplemental TSPA-SR Parameters for Drip Shield and Waste Package Degradation Calculations

Description	TSPA Parameter	Calculation
Surface area of a CSNF waste package in m ²	WP_SA_CSNF	$(2 \pi \text{Radius_CSNF} * \text{Length_CSNF}) + (2 \pi \text{Radius_CSNF}^2)$
Surface area of a CDSP waste package in m ²	WP_SA_CDSP	$(2 \pi \text{Radius_CDSP} * \text{Length_CDSP}) + (2 \pi \text{Radius_CDSP}^2)$
Area of a patch on a CDSP waste package in m ²	WP_Patch_Area_CDSP	WP_SA_CDSP/Number_WP_Patches
Axial length of a CDSP patch	L_WP_Patch_CDSP	sqrt(WP_Patch_Area_CDSP)
Area of a patch on a CSNF waste package in m ²	WP_Patch_Area_CSNF	WP_SA_CSNF/Number_WP_Patches
Axial length of a CSNF patch	L_WP_Patch_CSNF	sqrt(WP_Patch_Area_CSNF)
Axial length of a WP pit	L_WP_Pit	sqrt(WP_Pit_Area)
Number of patch openings on the top of the drip shield	DS_Top_Patch_Failures	if DS_Failure <=0 then 0 Else Failure Opening.Column 1
Fraction of the drip shield which is open from patches	DS_Frac_Patch	DS_Top_Patch_Failures / Number_DS_Packages
Axial length of pit openings on the top of the drip shield	DS_Top_Pit_Failures	if DS_Failure <=0 then 0 Else Failure Opening.Column 2*L_WP_Pit
Fraction of the drip shield which is open from pits	DS_Frac_Pit	DS_Top_Pit_Failures / DS_Total_Length
Total patch area on a CSNF waste package in m ²	WP_Total_Patch_Area_CSNF	if WP_Failure <=0 then 0 Else (Failure Opening.Column 22+ Failure Opening.Column 25+ Failure Opening.Column 28) *WP_Patch_Area_CSNF

Table 6-24. Supplemental TSPA-SR Parameters for Drip Shield and Waste Package Degradation Calculations (Continued)

Description	TSPA Parameter	Calculation
Total patch area on a CDSP waste package in m ²	WP_Total_Patch_Area_CDSP	if WP_Failure <=0 then 0 Else (Failure Opening.Column 22+ Failure Opening.Column 25+ Failure Opening.Column 28) *WP_Patch_Area_CDSP
Total pit area on a waste package in m ²	WP_Total_Pit_Area	if WP_Failure <=0 then 0 Else (Failure Opening.Column 23+ Failure Opening.Column 26+ Failure Opening.Column 29) *WP_Pit_Area
Total crack area on a waste package in m ²	WP_Total_Crack_Area	if WP_Failure <=0 then 0 Else (Failure Opening.Column 24+ Failure Opening.Column 27+ Failure Opening.Column 30) *WP_Crack_Area
Total patch length on a CSNF waste package in m	WP_Total_Patch_Length_CSNF	if WP_Failure <=0 then 0 Else (Failure Opening.Column 22+ Failure Opening.Column 25+ Failure Opening.Column 28) *L_WP_Patch_CSNF
Fraction of surface area open as patches on a CSNF package	WP_Frac_Patch_CSNF	WP_Total_Patch_Length_CSNF/Length_CSNF
Length of waste package open from pits in m	WP_Total_Pit_Length	if WP_Failure <=0 then 0 Else (Failure Opening.Column 23+ Failure Opening.Column 26+ Failure Opening.Column 29) *L_WP_Pit
Fraction of CSNF waste package which is open from pits	WP_Frac_Pit_CSNF	WP_Total_Pit_Length/Length_CSNF
Fraction of CDSP waste package which is open from pits	WP_Frac_Pit_CDSP	WP_Total_Pit_Length/Length_CDSP
Total patch length on a CDSP waste package in m	WP_Total_Patch_Length_CDSP	if WP_Failure <=0 then 0 Else (Failure Opening.Column 22+ Failure Opening.Column 25+ Failure Opening.Column 28) *L_WP_Patch_CDSP
Fraction of surface area open as patches on a CDSP packages	WP_Frac_Patch	WP_Total_Patch_Length_CDSP/Length_CDSP

Results and Verification

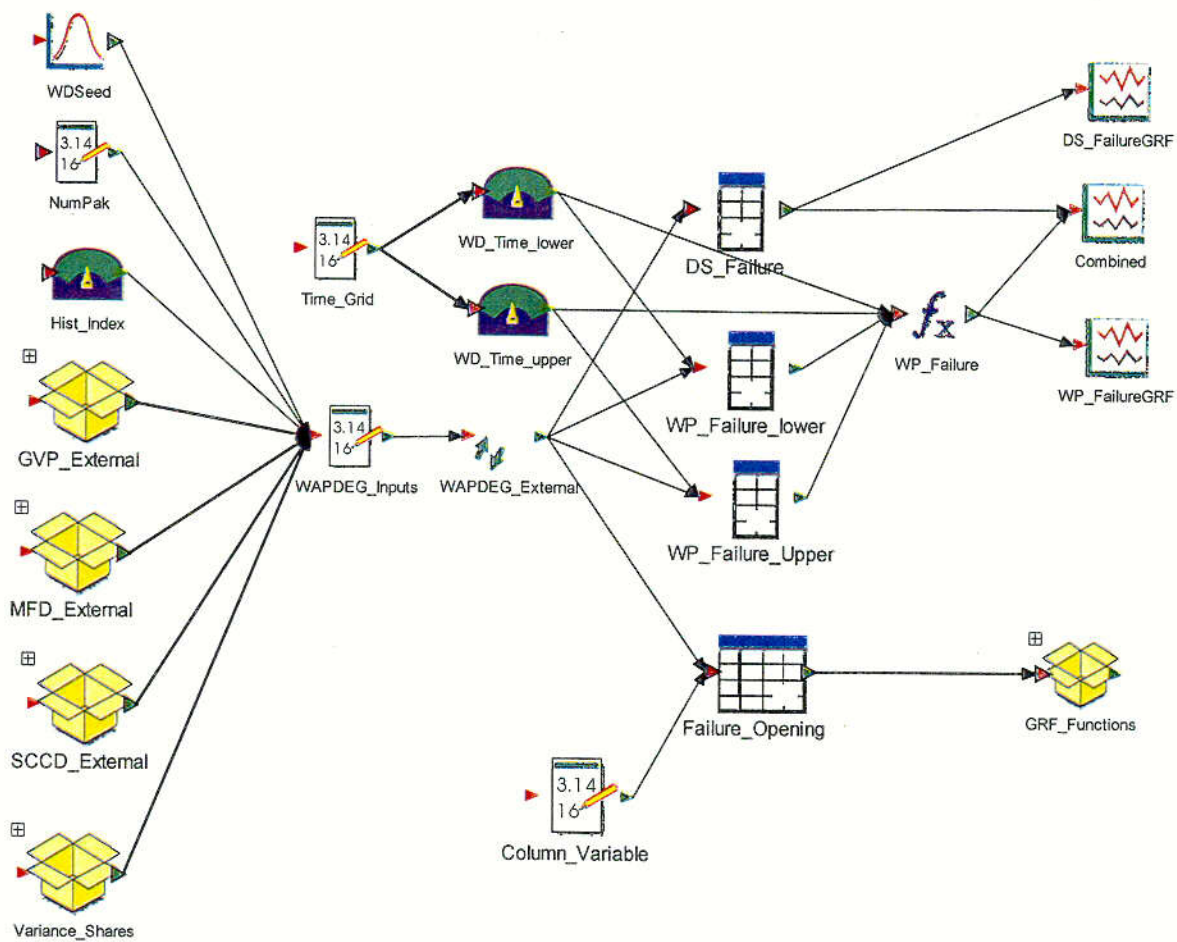
The drip shield and waste package failure curves for the median value simulation are shown in Figure 6-81.

The curves represent the fraction of the drip shield and waste packages that have failed. According to the graph the drip shield first begins to fail at *Etime* = 21,500 years. By the time *Etime* reaches 99,000 years, the drip shield is 100 percent failed. The first waste package is breached by 40,500 years. By 300,000 years the waste packages are completely failed.

Figure 6-82 shows the average number of patches, pits and cracks per failed waste package appearing on a drip shield and on a waste package barrier. Note that the first patch, pit, or crack

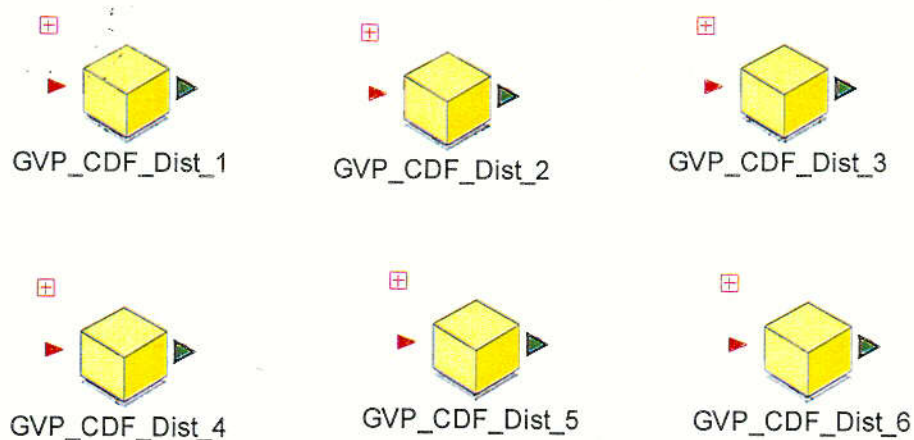
failure on both the drip shield and waste package barrier correspond to the initial failure curve. The total number of failed waste packages, is defined as a package with a patch on the inner barrier or a crack penetrating the inner barrier. The average number of patches on failed waste packages is the ratio of the total number of inner patch failures divided by the total number of failed waste packages.

Figure 6-83 shows the number of failed waste packages inside the three infiltration bin environments, *Always_Drips*, *Intermittent_Drips*, and *No_Drips* inside bin 4 for the median value simulation. Note that the failure of waste packages in the *No_Drips* environment precedes failures in the *Always Drips* environment. Because the greatest number of packages occurs in the *No_Drips* environment, the fraction failed multiplied by the total number of packages approaches a whole number quicker, thus packages fail sooner.



\\TSPA_Model\\Engineered_Barrier_System\\WastePackage_Dripshield\\WP_Degradation\\

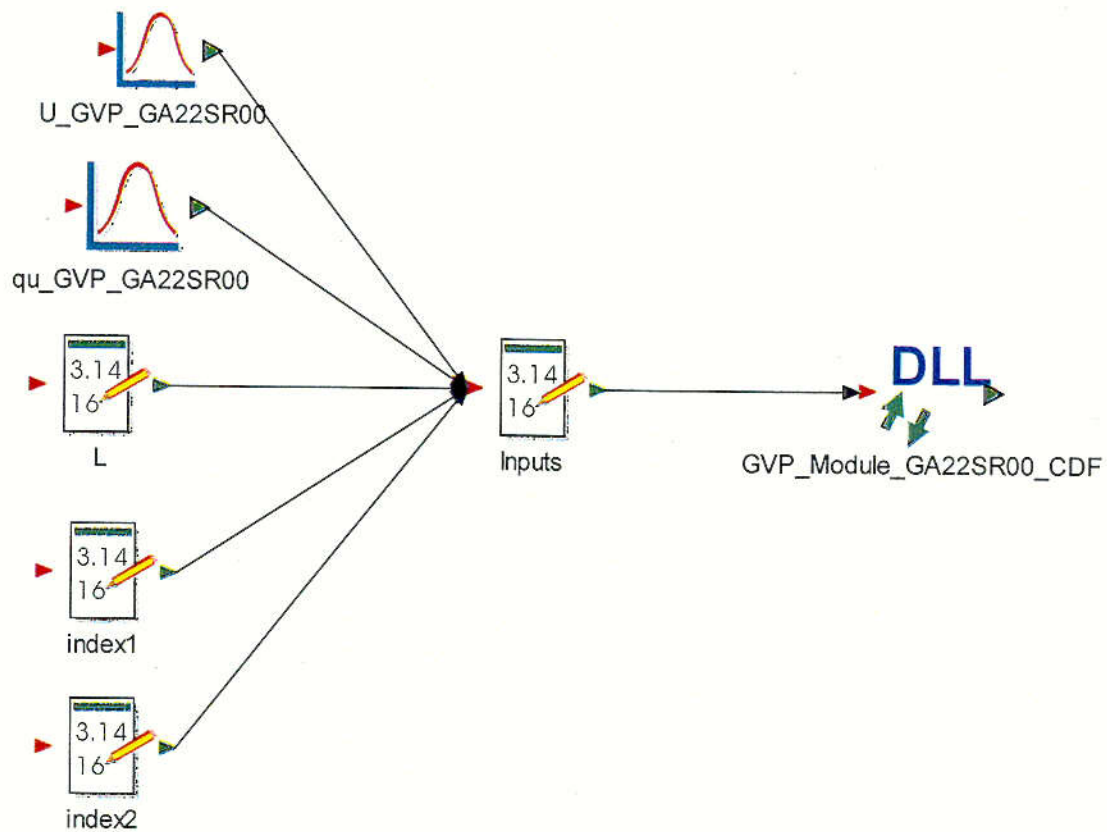
Figure 6-72.. The Waste Package Degradation Component of the TSPA-SR Model



\\TSPA_Model\\Engineered_Barrier_System\\WastePackage_Dripshield\\WP_Degradation\\GVP_External\\

Figure 6-73. Illustration of the Six GVP DLL Calls from the TSPA-SR Model

C50



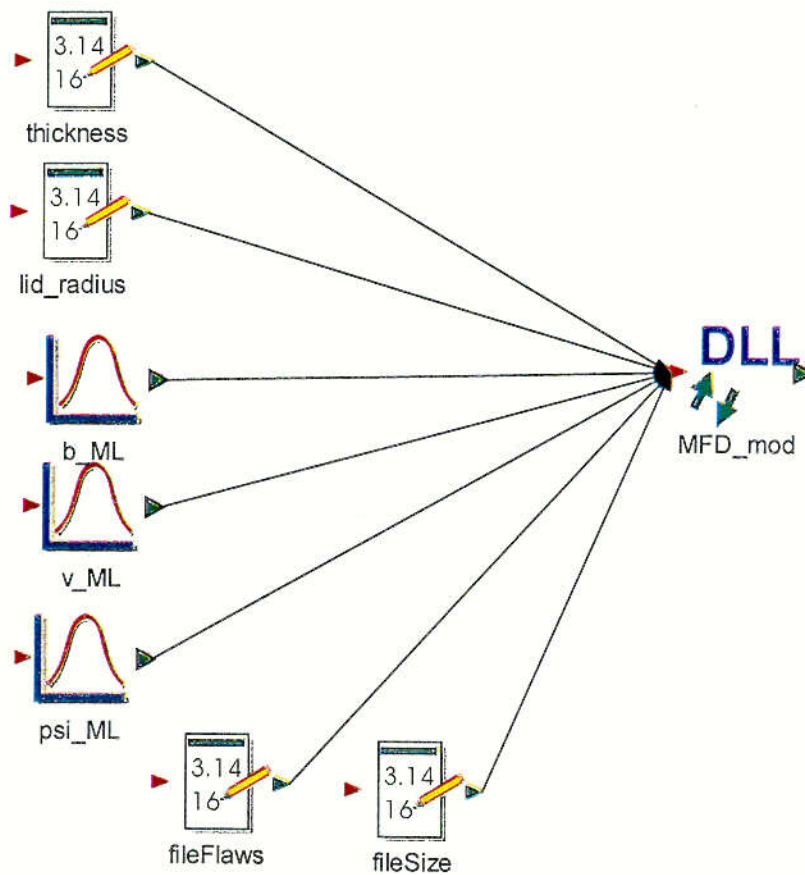
\\TSPA_Model\\Engineered_Barrier_System\\WastePackage_Dripshield\\WP_Degradation\\GVP_External\\GVP_CDF_Dist_1\\

Figure 6-74. Illustration of the TSPA-SR / GVP.dll Interface



\\TSPA_Model\\Engineered_Barrier_System\\WastePackage_Dripshield\\WP_Degradation\\MFD_External\\

Figure 6-75. Two Calls to MFD.dll



\\TSPA_Model\\Engineered_Barrier_System\\WastePackage_Dripshield\\WP_Degradation\\MFD_External\\MFD_Middle_Lid\\

Figure 6-76. TSPA-SR / MFD.dll Interface

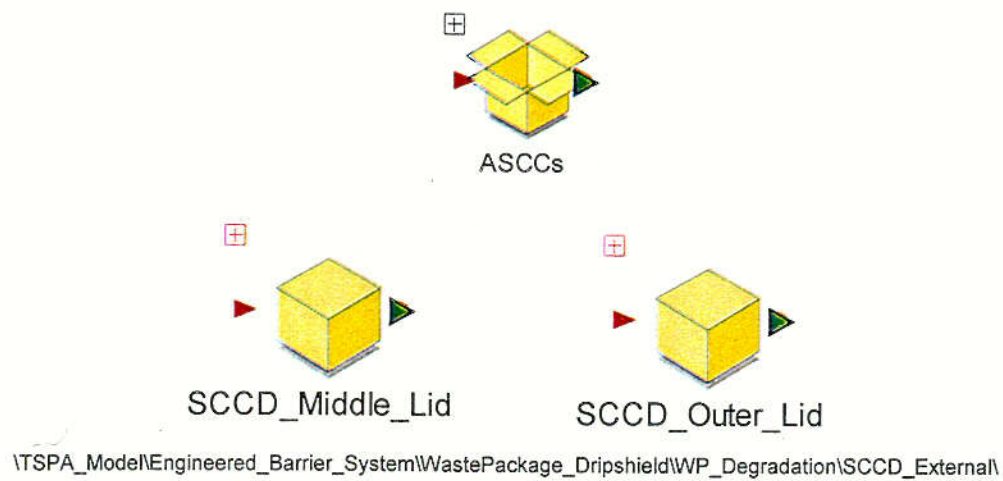
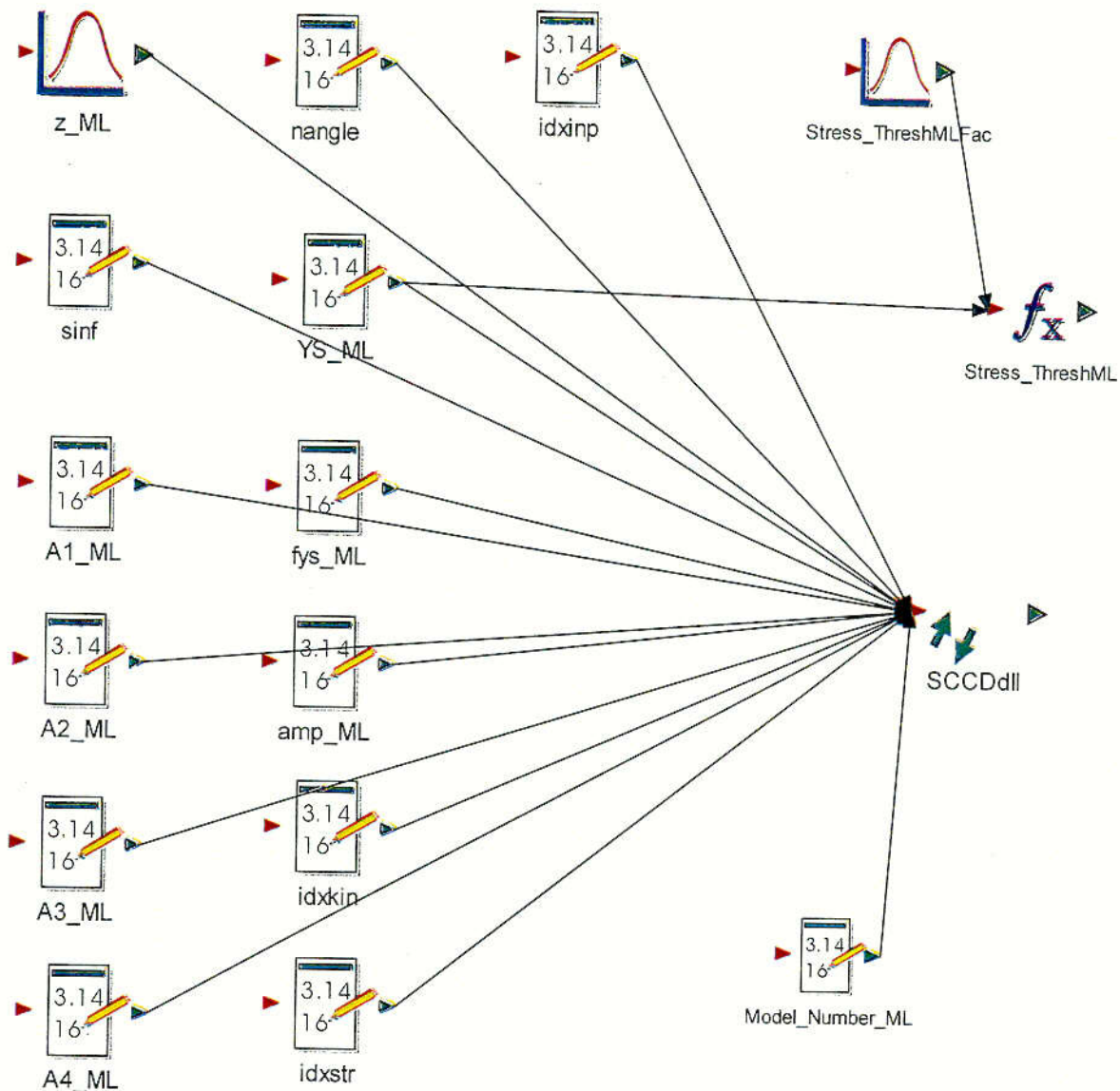


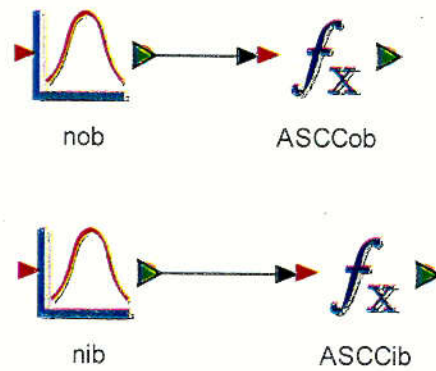
Figure 6-77. Illustration of the Two Calls to the SCCD.dll

C52



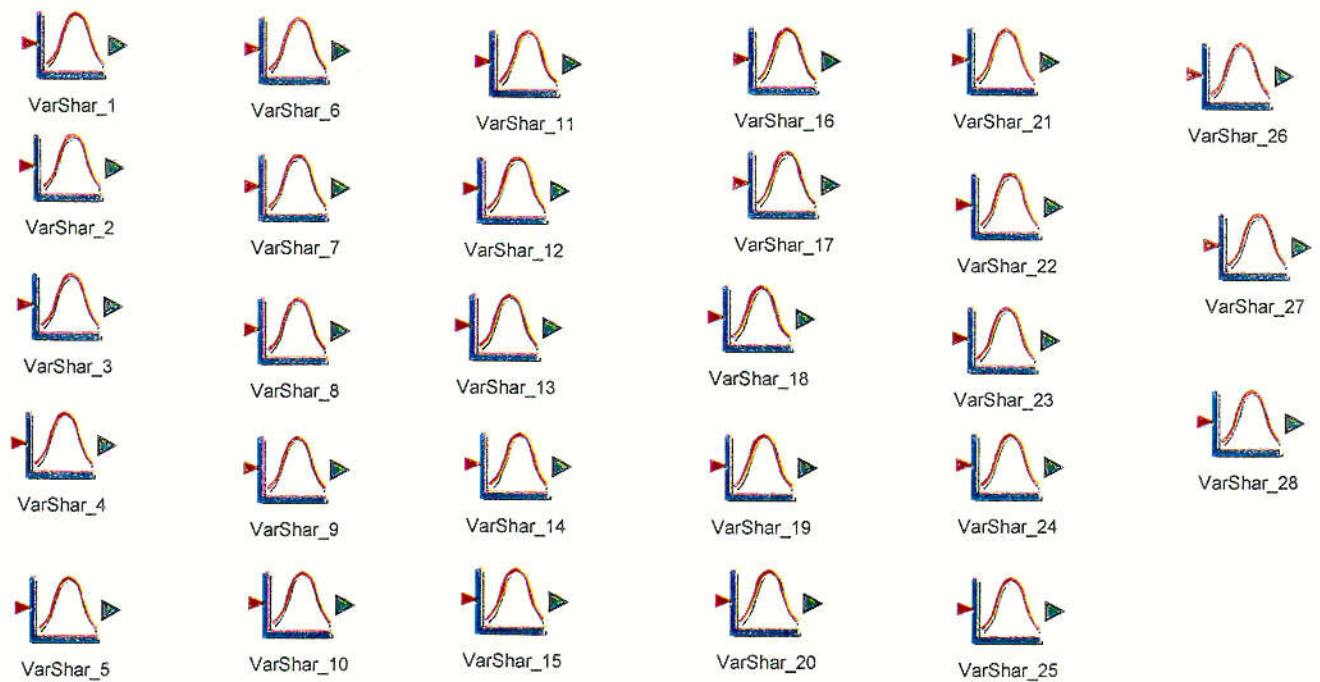
\\TSPA_Model\\Engineered_Barrier_System\\WastePackage_Dripshield\\WP_Degradation\\SCCD_External\\SCCD_Middle_Lid\\

Figure 6-78. Illustration of the TSPA-SR / SCCD.dll Interface



\\TSPA_Model\\Engineered_Barrier_System\\WastePackage_Dripshield\\WP_Degradation\\SCCD_External\\ASCCs\\

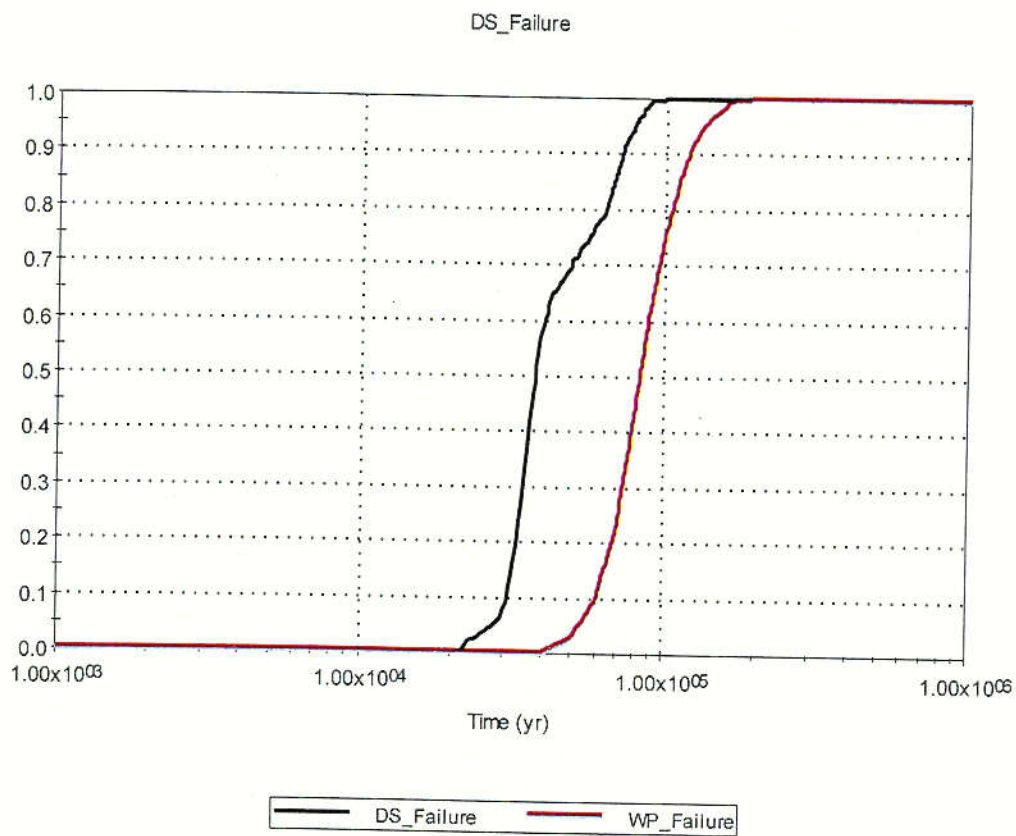
Figure 6-79. Illustration of the Slip Dissolution Component in the SCCD Component



\\TSPA_Model\\Engineered_Barrier_System\\WastePackage_Dripshield\\WP_Degradation\\Variance_Shares\\

Figure 6-80. Graphical Illustration of the Input Variance Sharing Distribution for the WAPDEG DLL

C54



\\TSPA_Model\\Engineered_Barrier_System\\WastePackage_Dripshield\\WP_Degradation\\

Figure 6-81. Drip Shield and Waste Package Failure Curves for the Median Value Simulation

C55

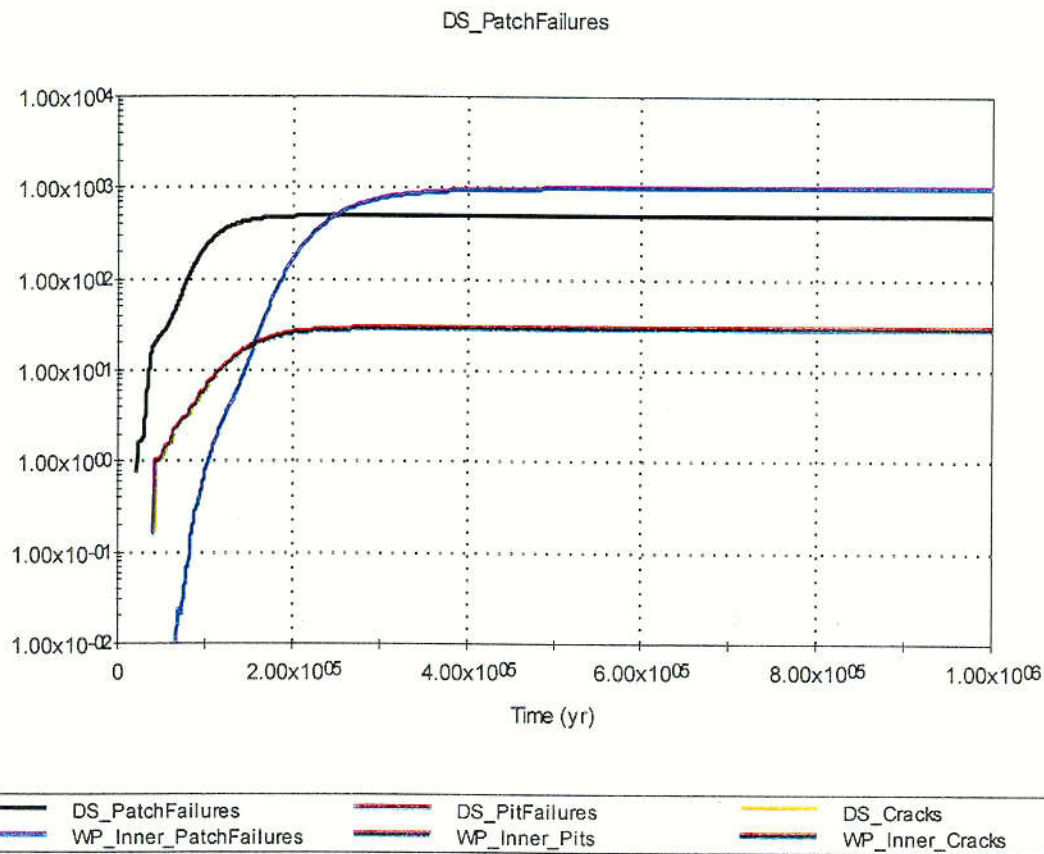


Figure 6-82. Time History of the Evolution of Patch, Pit, and Crack Formations on the Drip Shield and Waste Packages for the Median Value Simulation

C56

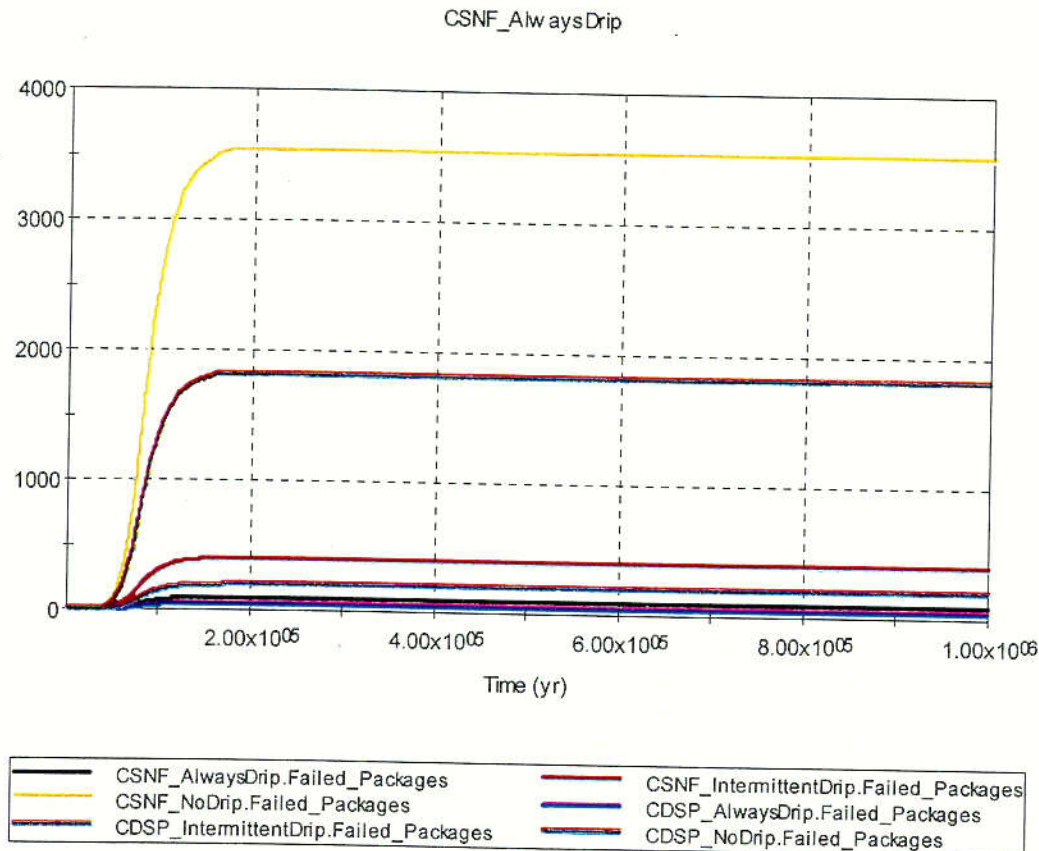


Figure 6-83. Time History of the Number of Failed Packages in Each Bin 4 Environment for the Median Value Simulation

6.3.4 Waste Form Degradation and Mobilization

The purpose of the waste form degradation model is to evaluate the rate of degradation of commercial spent nuclear fuel cladding, commercial and DOE spent fuel matrix, and high-level waste glass rods. Additionally, evaluation of the rate of mobilization of radioisotopes, and the migration of radioisotopes through remaining portions of the waste package is conducted within the waste form degradation components of the TSPA-SR model. Figure 6-84 shows the major components and inputs of the waste degradation model.

The commercial spent nuclear fuel (CSNF), high level waste (HLW), and DOE spent nuclear fuel (DSNF) waste emplaced in the repository will initially be contained in and protected by the waste packages. After degradation and failure of the waste packages, spent nuclear fuel assemblies and high-level radioactive waste glass rods will be exposed to the drift environment including air, water-vapor and, possibly, dripping water. After waste package failure, radionuclides are not available for release and transport until three things have occurred:

1. Failure of the fuel cladding for CSNF
2. Degradation of the spent nuclear fuel matrix or high-level waste glass matrix

3. Mobilization of radionuclides into aqueous solution, aqueous colloidal suspension, (interaction with particles 0.001 to 1 micron in size through sorption and other chemical mechanisms).

Mobile radionuclides are transported out of the degraded waste package and through the engineered barrier system to the unsaturated zone. Transport occurs through one of two mechanisms:

1. Movement of dissolved or colloidal material because of random molecular, or thermal, motion along continuous water pathways within the waste package (diffusive transport) (See Section 6.3.5 EBS Transport)
2. Movement of dissolved or colloidal material because of the bulk flow of a fluid, which in this case is water, through the waste form and waste package (advective transport) (See Section 6.3.5 EBS Transport).

Waste form degradation and radionuclide mobilization depend on the initial waste form type and amount, the initial design of the system and the environmental conditions occurring in the drift environment. Thermal history and package lifetime determine the temperature of the waste forms when they are exposed to degrading processes. Composition of the gas phase and aqueous chemistry of incoming water, along with the waste temperature, control the rates of waste form degradation and the nature of mobilized products available for transport.

The engineered barrier system is comprised of all components of the repository within the drifts. The analysis of transport of radionuclides within the engineered barrier system requires definition of numerous parameters and models. This transport is influenced by waste package degradation; waste form degradation, including cladding degradation; the thermal-hydrologic and chemical environment; and design of the engineered barrier system. Radionuclides released from the engineered barrier system enter the natural system for transport through the unsaturated and saturated zones to the accessible environment where overall repository performance is measured (engineered barrier system transport is discussed in Section 6.3.5, UZ transport is discussed in Section 6.3.6, and SZ transport is discussed in Section 6.3.7).

The subsections that follow present the waste form degradation and mobilization models that were developed for implementation into the TSPA-SR Model. These models are:

- Radionuclide inventory
- In-package chemistry
- Cladding degradation/Unzipping Rate
- Dissolution rate/Degradation Rate of DSNF and HLW Glass
- Dissolved concentration limits
- Colloids.

The following subsections summarize these models and their implementation into the TSPA-SR model.

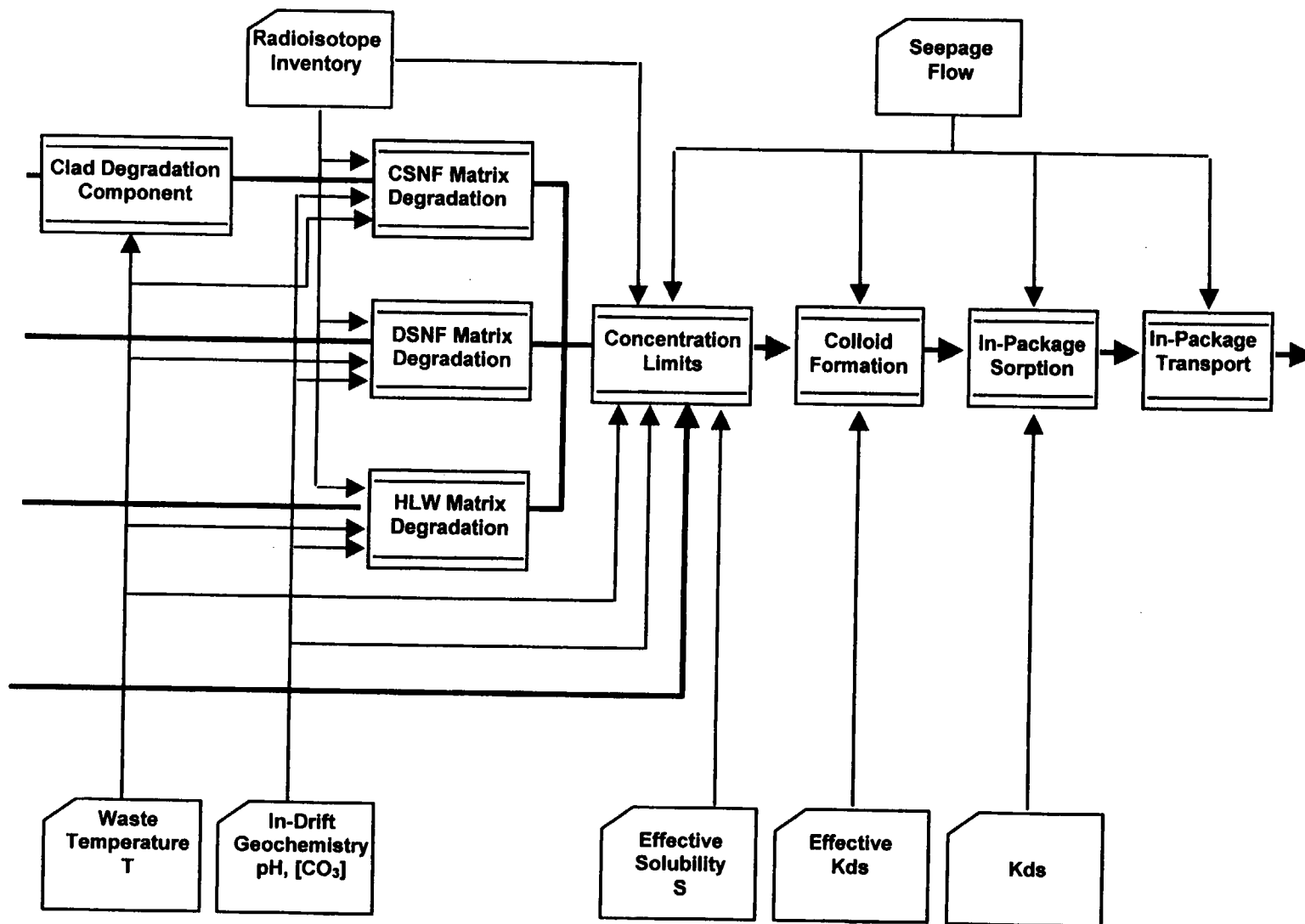


Figure 6-84. Major Components and Inputs of the Waste Degradation Model

6.3.4.1 Radionuclide Inventory

Overview

The TSPA-SR models two basic waste package types, a representative waste package for commercial spent nuclear fuel (CSNF) and a representative waste package for co-disposal fuel (CDSP) combining DOE-owned spent nuclear fuel (DSNF) and DOE-owned high level waste (DHLW) glass. The base case repository design can accommodate a total waste inventory of 70,000 metric tons of heavy metal (MTHM) (Attachment 1, (Stroupe, E.P. 2000 [142632])). As designed, approximately 63,000 MTHM of the total inventory is within 7,860 CSNF waste packages (Attachment I, Section 3.4.1, CRWMS M&O 2000 [136383]), which are comprised of five different waste package configurations CRWMS M&O 2000 [136383], Table I-1. The additional 7,000 MTHM of the total inventory is in 3,910 CDSP waste packages (Attachment I, Section 3.5.1, CRWMS M&O 2000 [136383]) comprised of five different waste package configurations CRWMS M&O 2000 [136383], Table I-1. The radionuclide inventory for a representative CSNF and a representative CDSP waste package can be derived by averaging the radionuclide inventories in each of the five CSNF and five CDSP waste package configurations over the number of packages per configuration (CRWMS M&O 2000 [136383], Table I-1). In the TSPA model these two basic inventory groups (CSNF and CDSP) are further discretized in five subgroups based on infiltration and three sub-subgroups based on seepage (see Section 6.3.1.2), for a total of $2 \times 5 \times 3 = 30$ distinct source term groups in GoldSim code⁷. Each of these 30 source term groups represents many of the 11,770 ($= 3910 + 7860$) packages distributed over the entire repository area. For example, if the packages were evenly distributed over the 30 groups, there would be $11,770/30$ or about 392 packages represented by each of the groups. However, as shown below in Figure 6-87 and 6-88 of this section, the groups are unevenly divided based first on infiltration and then seepage.

The number of radionuclides modeled in TSPA-SR model is slightly different based on the scenario. There are three distinct cases for radionuclide transport and dose: (1) groundwater release via either the nominal scenario or igneous intrusion, (2) atmospheric release via igneous eruption, and (3) groundwater release via human intrusion.

The nominal and indirect volcanic release scenarios both involve the process of moving radionuclides to the biosphere via a groundwater transport mechanism. The nominal scenario includes all those features, events, and process (FEPs) with an occurrence probability of 1.0 during the first 10,000 years. This encompasses all the natural physical-chemical processes such as fluid flow and mass transport, as well as other processes that do not occur continuously with time but that would occur at some time during the first 10,000 years. Examples of these latter processes include climate change and seismicity. The indirect volcanic release scenario (Section 6.3.9.2) is an intrusive igneous event in the repository (e.g., intrusion of a magmatic dike) that is assumed to cause total disintegration of a certain number of waste packages. This allows the entire waste form to be exposed and available for contact with groundwater (see Section 3.10 of *Total System Performance Assessment For the Site Recommendation*, (CRWMS

⁷ There are actually 31 separate source term groups because stainless-steel-clad CSNF is put into its own separate group. However, it has no subgroups because it is put in the always drip, infiltration bin 4 environment for the high and medium infiltration cases and into the no drip, infiltration bin 1 environment for the low infiltration case.

M&O 2000 [143665]) and subsequent transport of radionuclides through the unsaturated and saturated zones.

The direct volcanic release scenario (Section 6.3.9.1) is a violent volcanic eruption that ejects the radionuclides contained within the waste packages directly into the atmosphere and surrounding environment. Transport of the radionuclides to the biosphere is via the atmosphere and deposition of ash in the biosphere. The individual dose resulting from this scenario comes from a number of biosphere pathways, but primarily via the inhalation pathway (see Section 3.10 of *Total System Performance Assessment For the Site Recommendation* (CRWMS M&O 2000 [143665])).

The human intrusion scenario (Section 6.3.9.3) is a stylized groundwater release scenario in which surface water penetrates the repository through a borehole left by drilling. The scenario assumes that the drilling equipment penetrates only one waste package and its contents are contacted by the surface water, which then seeps through a highly permeable pathway, created by the borehole, from the unsaturated zone into the saturated zone (see Section 4.4 of *Total System Performance Assessment For the Site Recommendation* (CRWMS M&O 2000 [143665])). This scenario complies with the EPA Human-Intrusion Standard outlined in proposed EPA 40 CFR Part 197 (Subparts 197.25, 197.26) and proposed NRC 10 CFR Part 63 (64 FR 8640 [101680]) Section 113(d).

Besides the radionuclides required to compute dose for the above three scenario classes, two additional radionuclides from the inventory are included to evaluate compliance with the groundwater protection requirements in proposed EPA 40 CFR Part 197 (EPA 1999 [143799] Subpart 197.35) and proposed NRC 10 CFR Part 63 (64 FR 8640 [101680] Sections 113(b) and 115). These two are ^{232}Th and ^{228}Ra , which are necessary to compute the activity of radium in the groundwater.

Inputs to the TSPA Model

The output from the supporting AMR, *Inventory Abstraction* [136383] consists of a definition of the total number of packages, 7,860 CSNF and 3,910 CDSP (CRWMS M&O 2000 [136383], Table I-1), and a weighted average for the radionuclide inventory calculated over all of the waste package configurations for each waste package type (CSNF and CDSP). It is used as input data for the TSPA model and is shown in Table 6-25. Table 6-26 lists the decay rates for these radionuclides and Table 6-27 lists their specific activities.

Table 6-25. Inventory for 1,000,000-Year Nominal Igneous Groundwater Release Scenarios[†]

RN Species	Mass per CSNF Package (g)	DOE-SNF Mass per Co-Disposal Package (g)	HLW Mass per Co-Disposal Package (g)
Ac-227	3.09E-06	1.05E-04	4.36E-04
Am-241	1.90E+04	1.13E+02	6.03E+01
Am-243	1.29E+03	1.68E+00	1.55E+00
C-14	1.37E+00	6.63E-01	7.11E-03
Cs-137	5.34E+03	5.52E+02	4.04E+02

Table 6-25. Inventory for 1,000,000-Year Nominal Igneous Groundwater Release Scenarios[†]
(Continued)

RN Species	Mass per CSNF Package (g)	DOE-SNF Mass per Co-Disposal Package (g)	HLW Mass per Co-Disposal Package (g)
I-129	1.80E+03	8.08E+01	4.41E+01
Np-237	4.74E+03	4.26E+02	1.78E+02
Pa-231	9.87E-03	3.02E-01	7.44E-01
Pb-210	0.00E+00	1.38E-08	1.31E-07
Pu-238	1.51E+03	8.79E+01	5.69E+01
Pu-239	4.38E+04	2.13E+03	3.52E+03
Pu-240	2.09E+04	4.55E+02	3.39E+02
Pu-242	5.41E+03	1.15E+01	6.25E+00
Ra-226	0.00E+00	2.21E-06	1.52E-05
Ra-228	0.00E+00	6.46E-06	6.51E-06
Sr-90	2.24E+03	3.01E+02	2.67E+02
Tc-99	7.68E+03	4.53E+02	7.01E+02
Th-229	0.00E+00	2.46E-02	3.79E-03
Th-230	1.84E-01	1.75E-02	7.00E-03
Th-232	0.00E+00	1.38E+04	1.59E+04
U-232	1.01E-02	1.37E-01	7.64E-04
U-233	7.00E-02	1.98E+02	1.02E+01
U-234	1.83E+03	2.77E+02	3.39E+01
U-235	6.28E+04	1.74E+04	1.56E+03
U-236	3.92E+04	5.27E+03	3.65E+01
U-238	7.92E+06	4.67E+05	7.86E+05

NOTE: [†] From the *Inventory Abstraction AMR* (CRWMS M&O 2000 [136383], Tables I-2, I-3, and I-4) and from the Input Transmittal 00306 [150559], DTN: SN0005T0810599.012 [152110]

Table 6-26. Decay Rates for the Radionuclides[†]

RN Species	Decay Rate (1/yr)
Ac-227	0.031839558
Am-241	0.001603765
Am-243	9.40498e-05
C-14	0.000121286
Cs-137	0.022876145
I-129	4.07734e-08
Np-237	3.23901e-07
Pa-231	2.13276e-05
Pb-210	0.030670229
Pu-238	0.007900013
Pu-239	2.87494e-05
Pu-240	0.000106034

Table 6-26. Decay Rates for the Radionuclides[†] (Continued)

RN Species	Decay Rate (1/yr)
Pu-242	1.84348e-06
Ra-226	0.000433488
Ra-228	0.120338052
Sr-90	0.023819491
Tc-99	3.25421e-06
Th-229	8.77401e-05
Th-230	9.19293e-06
Th-232	4.95105e-11
U-232	0.010060191
U-233	4.35942e-06
U-234	2.82917e-06
U-235	9.84584e-10
U-236	2.96217e-08
U-238	1.55414e-10

[†]DTN: MO0004SPADEC00.002 [151063]

Table 6-27. Specific Activities for the Radionuclides[†]

RN Species	Specific Activity (Ci/g)
Ac-227	72.341
Am-241	3.4322
Am-243	0.19962
C-14	4.4681
Cs-137	86.121
I-129	0.00016302
Np-237	0.00070487
Pa-231	0.047618
Pb-210	75.326
Pu-238	17.12
Pu-239	0.062041
Pu-240	0.22787
Pu-242	0.0039289
Ra-226	0.98927
Ra-228	272.22
Sr-90	136.5
Tc-99	0.016953
Th-229	0.19761
Th-230	0.020614
Th-232	1.1007e-7

Table 6-27. Specific Activities for the Radionuclides[†] (Continued)

RN Species	Specific Activity (Ci/g)
U-232	22.365
U-233	0.0096498
U-234	0.0062357
U-235	2.1609e-6
U-236	6.4736e-5
U-238	3.3679e-7

NOTE: [†] Computed in GoldSim based on the decay rate, the atomic weight, and Avogadro's number.

Figure 6-85 is a graphical representation in GoldSim of the fuel inventory model. Depending on the waste-form type, the initial inventory listed in Table 6-25 may be further categorized into a gap or free fraction and a bound fraction. For example, some fission gases and waste form particulates from partially degraded CSNF waste forms are assumed to be released into the gap between the fuel pellets and the cladding and are available for release immediately after waste package and cladding failure (*Gap_Inventory*). The remainder of the radionuclide inventory is bound to the waste form matrix (*Bound_Inventory*). Thus, the *CSNF_Bound_Inventory* is equal to the *CSNF_Inventory* minus the *Gap_Inventory*. The *Gap_Inventory* is determined by the *Gap_Fraction* (fraction of fuel in the gap). The *Gap_Fraction* of each radionuclide species is sampled from a stochastic distribution (*Gap_Distribution*) that is uniform between 0 and 0.004 (CRWMS M&O 2000 [147210] Section 6.5). Two radionuclides, Cs-137 and I-129, have an additional component added to their *Gap_Fraction* value. This is *FGR* (or fission gas release), as illustrated in Figure 6-85. *FGR* has a fixed value of 0.042. For I-129 this value is added directly to the sampled value of *Gap_Distribution* to give the I-129 value of *Gap_Fraction*. For Cs-137, *FGR*/3 is added to the sampled value of *Gap_Distribution*, to give the I-129 value of *Gap_Fraction*. After these modifications for Cs-137 and I-129, the *Gap_Fraction* vector is then multiplied by the *CSNF_Inventory* vector to derive the *Gap_Inventory* vector.

DOE-owned SNF (DSNF) also has a gap fraction (DOE 1999 [107790]; DTN: MO0004SPAFRE00.003 [151062]), called *Free_Fraction* in the GoldSim model. It is equal to a constant value of 0.001 for all radionuclides. Thus, 0.001 times the *DSNF_Inventory* vector yields the *DSNF_Free_Inventory* vector and the *DSNF_Bound_Inventory* is equal to the *DSNF_Inventory* minus the *DSNF_Free_Inventory*.

HLW Glass is not considered to have a gap fraction inventory.

Implementation

The *Inventory Abstraction* AMR (CRWMS M&O 2000 [136383], Sections 7.1 and 7.2) establishes the following initial sets of radionuclides to be used in evaluating the various scenarios discussed earlier:

1. Sixteen radionuclides for the 10,000-year nominal and igneous groundwater release scenarios: Ac-227, Am-241, Am-243, C-14, I-129, Np-237, Pu-238, Pu-239, Pu-240, Tc-99, Th-229, U-232, U-233, U-234, U-236, and U-238.
2. Twenty-one radionuclides for the 1,000,000-year nominal and igneous groundwater release scenarios: the 10,000-year nominal/indirect set, plus Pa-231, Pb-210, Pu-242, Ra-226, and Th-230.
3. Twelve radionuclides for the 10,000-year eruptive volcanic release scenario: Ac-227, Am-241, Am-243, Cs-137, Pa-231, Pu-238, Pu-239, Pu-240, Sr-90, Th-229, U-232, and U-233.
4. Seventeen radionuclides for the 1,000,000-year eruptive volcanic release scenario: the 10,000-year direct set, plus Np-237, Pb-210, Pu-242, Ra-226, and Th-230.
5. Eighteen radionuclides for the 10,000-year human intrusion groundwater release scenario: the 10,000-year nominal/indirect set, plus Cs-137 and Sr-90.

For the TSPA-SR model the above sets of nuclides based on 10,000 years were also considered valid out to 100,000 years, so that any simulations carried out to 100,000 years or less used the 10,000-year groups of radionuclides, i.e., groups 1, 3, and 5.

Disposition of the Radionuclides in the Component Models (EBS Transport, UZ Transport, SZ Transport, and Biosphere) for the Nominal and Igneous Groundwater Release Scenarios

In this section we show tables of the disposition of the radionuclides in the various component *transport* models for the nominal and igneous groundwater release scenarios discussed above. The basis for the set of radionuclides modeled in the TSPA-SR is the *Inventory Abstraction* AMR (CRWMS M&O 2000 [136383]), mentioned above. This AMR used a selection method based on potential dose rate and sorption to reduce the potential set of modeled radionuclides from hundreds to 26 for the nominal and igneous groundwater release scenarios. Specifically the hundreds of radionuclides initially present in the waste form are divided into three groups based on their sorption affinity (high, medium, or low) for the host rocks. Out of each group only those radionuclides are retained which would account for 95 percent of the dose. As documented in the following discussion, the resulting combined set of radionuclides from all three groups has been modified slightly for inclusion into various component TSPA-SR models.

Table 6-28 indicates the disposition in the transport models over the 1,000,000-year time frame. A slightly smaller subset was transported for the 10,000-year to 100,000-year time frame; this omitted set is indicated by asterisks in Table 6-28. For the groundwater release scenarios, the list of 21 radionuclides in item #2 above is modified as follows: Th-232 and Ra-228 are added in order to compute groundwater protection requirements; U-235 is added because it must be transported to compute the Pa-231 and Ac-227 doses, U-232 is deleted because of short half-life. This brings the total considered to 23 radionuclides. In addition, each Pu and Am species is split into two species, an irreversibly sorbed species and a reversibly sorbed/solute species.⁸ Since there are 6 of these Pu/Am species, this increase the total to 29 species tracked in the EBS. Also, it was shown that the daughter of irreversibly bound Am-241 (i.e., irreversibly bound Np-237) may also be important to dose, so it was tracked as a separate species, bringing the total species tracked for the groundwater release scenarios to 30. (Other irreversibly bound decay products, not already considered, were found to be negligible in their contribution to dose.⁹).

The following additional generalizations can be made:

- In order to reduce computational requirements, secular equilibrium between parent and daughter was assumed for parent nuclides that had a considerably longer half-life than their decay products. Secular equilibrium was assumed for Ac-227 with Pa-231, for Pb-210 with Ra-226, for Ra-226 with Th-230, and for Ra-228 with Th-232. This assumption reduces the number of radionuclides tracked through the UZ and SZ by 4. From the original 30 tracked in the EBS, this yields 26 tracked in the UZ and SZ.
- Transport of radionuclides in the SZ is accomplished with two models, a 3-D and a 1-D model. The 3-D model is used wherever possible, but since it does not allow for chain decay and ingrowth, it can in general only be used for the top parents in a chain. However, using a method called "inventory boosting", the 3-D model was also used for the first generation daughter in each decay chain. Specifically, for each timestep the amount of radionuclide mass injected into the 3-D SZ model over the duration of that timestep is boosted by the mass of the parent that could possibly decay during the remaining time of the simulation. For example, for Pu-239, this is equal to (in terms of GoldSim code-defined variables):

$$\text{UZ1OUT.Water_to_SZ_External[Am243]} * (239/243) * (1 - \exp(-\text{Decay_Rate.Decay_Rate[Am243]} * \text{Run_Time} - \text{ETime})))$$

⁸ Irreversibly sorbed species were only generated in the HLW/DSNF inventory. Reversibly sorbed species were generated in both HLW/DSNF and CSNF inventory.

⁹ The irreversible colloids are assumed to represent a closed system in which no radionuclide mass is added or subtracted (except through decay and ingrowth) during travel from the waste package to the accessible environment. In other words, daughters of parent radionuclides sorbed irreversibly onto colloids are also assumed to be bound within the colloids for the duration of their travel through the system. For ²⁴²Pu_{irr}, ²⁴⁰Pu_{irr}, and ²³⁹Pu_{irr}, the combined dose of their daughters and grandchildren within the colloid is several orders of magnitude less than the dose of the parent during the travel time within the natural barriers, based on decay rates, specific activities, and BDCFs. (This assumes the travel time is about 75,000 years or less for irreversible colloids). Thus, for these three species, it is not necessary to consider the transport of their irreversibly bound decay products. ²³⁸Pu_{irr} decays so quickly that its daughter products have a negligible effect on dose.

Table 6-28. Disposition of Radionuclides for 1,000,000-Year Nominal and Igneous Groundwater Release Scenarios

Radionuclide	Disposition in EBS Cells Model and 3-D UZ FEHM Model	Disposition in SZ Models (3-D SZ_Convolute and 1-D Pipe)	Disposition in Biosphere
Fission Products (simple decay, no ingrowth of daughters)			
C-14	transport solute	3-D transport of nonsorbing solute	dose from 3-D
Sr-90	exclude (short half-life)	exclude (short half-life)	exclude
Tc-99	transport solute	3-D transport of Tc	dose from 3-D
I-129	transport solute	3-D transport of I	dose from 3-D
Cs-137	exclude (short half-life)	exclude (short half-life)	exclude
U-232	exclude (short half-life)	exclude (short half-life)	exclude
Actinium Series			
Am-243	transport irreversible colloid Am-243 _{irr} (decay to Pu-239 _{irr}) transport reversible colloid & solute (decay to Pu-239)	3-D transport of irr. coll. 3-D transport of Am/Pu rev. coll.	dose from 3-D
Pu-239	transport irreversible colloid Pu-239 _{irr} (simple decay) transport reversible colloid & solute (decay to U-235)	3-D transport of irr. coll., boosted by the maximum decay (over the remaining simulation time) of the Am-243 _{irr} mass at the UZ/SZ interface 3-D transport of Am/Pu rev. coll., boosted by the maximum decay (over the remaining simulation time) of the Am-243 _{rev/sol} mass at the UZ/SZ interface	dose from 3-D
U-235	transport solute (decay to Pa-231)	1-D transport only (solute)	dose not computed
Pa-231	transport reversible colloid & solute (simple decay) no irreversible colloid (initial inventory too small)	1-D transport only (reversible colloid & solute)	dose from 1-D
Ac-227	not transported	not transported	dose from 1-D, secular equilibrium with Pa-231
Neptunium Series			
Am-241 [†]	transport irreversible colloid Am-241 _{irr} (decay to Np-237 _{irr}) transport reversible colloid & solute (decay to Np-237)	3-D transport of irr. coll. 3-D transport of Am/Pu rev. coll.	dose from 3-D
Np-237	transport irreversible colloid, Np-237 _{irr} (simple decay) transport solute (decay to U-233)	3-D transport of irr. coll., boosted by the maximum decay (over the remaining simulation time) of the Am-241 _{irr} mass at the UZ/SZ interface 3-D transport of Np solute, boosted by the maximum decay (over the remaining simulation time) of the Am-241 _{rev/sol} mass at the UZ/SZ interface	dose from 3-D

Table 6-28. Disposition of Radionuclides for 1,000,000-Year Nominal and Igneous Groundwater Release Scenarios (Continued)

Radionuclide	Disposition in EBS Cells Model and 3-D UZ FEHM Model	Disposition in SZ Models (3-D SZ_Convolute and 1-D Pipe)	Disposition in Biosphere
U-233	transport solute (decay to Th-229)	1-D transport only (solute)	dose from 1-D
Th-229	transport reversible colloid & solute (simple decay)	1-D transport only (reversible colloid & solute)	dose from 1-D
Thorium Series			
Pu-240	transport irreversible colloid Pu-240 _{irr} (simple decay) transport reversible colloid & solute (decay to U-236)	3-D transport of irr. coll. 3-D transport of Am/Pu rev. coll.	dose from 3-D
U-236	transport solute (simple decay)	3-D transport of U-236 solute, boosted by the maximum decay (over the remaining simulation time) of the Pu-240 _{rev/sol} mass at the UZ/SZ interface	dose from 3-D
Th-232	transport reversible colloid & solute (simple decay)	1-D transport only (reversible colloid & solute)	dose not computed; concentration from 1-D
Ra-228	not transported	not transported	dose not computed; concentration from 1-D, secular equilibrium with Th-232
Uranium Series			
Pu-242	transport irreversible colloid Pu-242 _{irr} (simple decay) transport reversible colloid & solute (decay to U-238)	3-D transport of irr. coll. 3-D transport of Am/Pu rev. coll.	dose from 3-D
Pu-238 [†]	transport irreversible colloid Pu-238 _{irr} (simple decay) transport reversible colloid and solute (decay to U-234)	3-D transport of irr. coll. 3-D transport of Am/Pu rev. coll.	dose from 3-D
U-238	transport solute (decay to U-234)	3-D transport of U-238 solute, boosted by the maximum decay (over the remaining simulation time) of the Pu-242 _{rev/sol} mass at the UZ/SZ interface	dose from 3-D
U-234	transport solute (decay to Th-230)	3-D transport of U-234 solute, boosted by the maximum decay (over the remaining simulation time) of the U-238 mass at the UZ/SZ interface	dose from 3-D
Th-230 [†]	transport reversible colloid & solute (simple decay)	1-D transport only (reversible colloid & solute)	dose from 1-D
Ra-226	not transported	not transported	dose from 1-D, secular equilibrium with Th-230

Table 6-28. Disposition of Radionuclides for 1,000,000-Year Nominal and Igneous Groundwater Release Scenarios (Continued)

Radionuclide	Disposition in EBS Cells Model and 3-D UZ FEHM Model	Disposition in SZ Models (3-D SZ_Convolute and 1-D Pipe)	Disposition in Biosphere
Pb-210	not transported	not transported	dose from 1-D, secular equilibrium with Ra-226

[†] These radionuclides are not transported through the UZ and SZ for any simulations with a time span of 100,000 years or less. In particular, they are not tracked for any of the 100,000-year analyses in Chapters 4 and 5 of *Total System Performance Assessment For The Site Recommendation* (CRWMS M&O 2000 [143665]). Leaving out these species in the 100,000-years-or-less time frame has been found to have a negligible effect on the dose rate. (Actually, the irreversibly sorbed Am-241 and Pu-238 are transported because of their possibly short travel time, but their solute and reversibly sorbed species are not.) The 1,000,000-year base case GoldSim input file for the entire list of species in this table is named SR00_042nm6.gsm DTN: MO0011MWDNM601.021 [153126]). The 100,000-year base case GoldSim input file for the reduced set of radionuclides (i.e., without Th-230, Am-241, and Pu-238) is named SR00_047nm5.gsm (DTN: MO0008MWDNM501.005 [151714]).

The 3-D SZ model with inventory boosting was used for 13 unique parents and first generation daughters, but because of the splitting of the 7 Pu/Am/Np species into reversible and irreversible colloid components, this brings the total to 20 radionuclides transported through the 3-D SZ model. For the 3-D SZ model, breakthrough curves were developed for 8 elements/species; a nonsorbing solute (e.g., C-14), Tc, I, U, Np, an irreversible colloid, an Am/Pu reversible colloid (modeled with Am K_{ds}/K_{cs}), and a Cs/Sr reversible colloid. These 8 breakthrough curves were sufficient to model the transport of all 20 of the aforementioned species. The 3-D model does allow for simple decay, i.e., no ingrowth of a daughter, and this is assumed in the following tables, though not explicitly indicated in the third column under the heading "Disposition in SZ model."

For 6 granddaughters, a 1-D model with full chain decay and ingrowth is used to give the mass flux and concentration at 20 km needed to compute dose. Based on all of the previous considerations, the number of radionuclides transported through each of the models for the groundwater release scenarios is: 30 through the EBS, 26 through the UZ, 20 through the 3-D SZ, and 6 through the 1-D SZ. (Actually, because of the architecture of the GoldSim model, all radionuclides are transported through the 1-D model, but it is only used to compute the dose of 6 of these radionuclides).

- In the UZ and SZ transport models, all colloids were transported with the same K_d and K_c values based on the values for Am waste-form colloids as described in *Waste Form Colloid-Associated Concentrations Limits: Abstraction and Summary* (CRWMS M&O 2000 [125156], Table 1). However, in the EBS transport model, Am and Th were tracked with the Am K_{ds}/K_{cs} while Pu and Pa were modeled with the Pu K_{ds}/K_{cs} , again as described in *Waste Form Colloid-Associated Concentrations Limits: Abstraction and Summary* (CRWMS M&O 2000 [125156], Table 1).

Disposition of the Radionuclides in the Component Models (EBS Transport, UZ Transport, SZ Transport, and Biosphere) for the Human Intrusion Groundwater Release Scenario

Table 6-29 shows the disposition of the radionuclides in the various transport models for the human intrusion scenario. No simulations for this scenario were carried beyond 100,000 years. The primary differences between this scenario and the nominal and intrusion scenarios are:

- Sr-90 and Cs-137 are added to the list of transported radionuclides because of their possibly very short travel time through the borehole in the UZ.
- Th-232 and Ra-228, required for the groundwater protection regulations, need not be tracked in the human intrusion scenario.

The reversibly sorbed colloidal forms of Am, Pu, Th, and Pa are transported in the EBS and SZ, but not in the UZ. (Irreversibly sorbed and dissolved Am and Pu are tracked in the UZ borehole, and dissolved Th and Pa are tracked in the UZ borehole.)

Disposition of the Radionuclides in the Eruptive Igneous Scenario Component Models (ASHPLUME and Biosphere)

Table 6-30 lists the radionuclides transported in ASHPLUME for the eruptive igneous scenario, plus the subset of these transported nuclides that are used to compute dose for the 10,000-year to 100,000-year time frame. As discussed above, the 10,000-year radionuclide screening arguments in the *Inventory Abstraction* AMR (CRWMS M&O 2000 [136383], Section 1) are strictly only valid for 10,000 years but were applied to 100,000-year simulations using the TSPA model. Although no simulations for igneous eruption were carried out beyond 100,000 years to 1,000,000 years, if they had been, it would have been appropriate to add the five additional radionuclides listed above: Np-237, Pb-210, Pu-242, Ra-226, and Th-230.

Division of the Inventory into Groups Based on Infiltration and Seepage

The repository horizon is discretized into five noncontiguous areal regions (or bins) based upon infiltration rates and thermal-hydrologic response (see Sections 6.3.1.2 and 6.3.2.1). These regions form the basis for the degree of areal heterogeneity in the near field models, such as the waste package degradation model, the waste form degradation and mobilization model, and the EBS transport model. The basis for the discretization in these TSPA models is the discretization in the multi-scale thermal-hydrologic model (see Section 3.3.3 of *Total System Performance Assessment For The Site Recommendation* CRWMS M&O 2000 [143665] and CRWMS M&O 2000 [139610] *Multiscale Thermohydrologic Model*). In particular, there are approximately 800 grid blocks in the mountain-scale portion of the multi-scale T-H model, which are further subdivided into 2 waste packages per grid block (an average CSNF and average CDSP package), yielding about 1600 different histories for waste package temperature, relative humidity in the drift, invert liquid saturation, and percolation flux 5 m above the drift crown. These histories are grouped into five regions based on the histogram of percolation at 5 m above the drift crown during the glacial transition climate. This then determines the fraction of the repository area associated with each of the five infiltration/percolation bins. The fraction

Table 6-29. Disposition of Radionuclides for 10,000- to 100,000-Year Human Intrusion Groundwater Release Scenarios

Radionuclide	Disposition in EBS Cells Model	Disposition in 1-D UZ Borehole Pipe Model	Disposition in SZ Models (3-D SZ Convolute and 1-D Pipe)	Disposition in Biosphere
Fission Products (simple decay, no ingrowth of daughters)				
C-14	Transport solute	transport solute	3-D transport of nonsorbing solute	dose from 3-D
Sr-90	Transport solute	transport solute	3-D transport of Cs/Sr coll.	dose from 3-D
Tc-99	Transport solute	transport solute	3-D transport of Tc	dose from 3-D
I-129	Transport solute	transport solute	3-D transport of I	dose from 3-D
Cs-137	Transport solute	transport solute	3-D transport of Cs/Sr coll.	dose from 3-D
U-232	Exclude (short half-life)	exclude (short half-life)	exclude (short half-life)	exclude
Actinium Series				
Am-243	Transport irreversible colloid Am-243 _{irr} (decay to Pu-239 _{irr}) Transport reversible colloid & solute (decay to Pu-239)	transport irreversible colloid Am-243 _{irr} (decay to Pu-239 _{irr}) transport solute (decay to Pu-239)	3-D transport of irr. coll. 3-D transport of Am/Pu rev. coll.	dose from 3-D
Pu-239	Transport irreversible colloid Pu-239 _{irr} (simple decay) Transport reversible colloid & solute (decay to U-235)	transport irreversible colloid Pu-239 _{irr} (simple decay) transport solute (decay to U-235)	3-D transport of irr. coll., boosted by the maximum decay (over the remaining simulation time) of the Am-243 _{irr} mass at the UZ/SZ interface 3-D transport of Am/Pu rev. coll., boosted by the maximum decay (over the remaining simulation time) of the Am-243 _{rev/sol} mass at the UZ/SZ interface	dose from 3-D
U-235	Transport solute (decay to Pa-231)	transport solute (decay to Pa-231)	1-D transport only (solute)	dose not computed
Pa-231	Transport reversible colloid & solute (simple decay) No irreversible colloid (initial inventory too small)	transport solute (simple decay) no irreversible colloid (initial inventory too small)	1-D transport only (reversible colloid & solute)	dose from 1-D
Ac-227	Not transported	not transported	not transported	dose from 1-D, secular equilibrium with Pa-231
Neptunium Series				
Am-241	Transport irreversible colloid Am-241 _{irr} (decay to Np-237 _{irr}) Transport reversible colloid & solute (decay to Np-237)	transport irreversible colloid Am-241 _{irr} (decay to Np-237 _{irr}) transport solute (decay to Np-237)	3-D transport of irr. coll. 3-D transport of Am/Pu rev. coll.	dose from 3-D

Table 6-29. Disposition of Radionuclides for 10,000- to 100,000-Year Human Intrusion Groundwater Release Scenarios (Continued)

Radionuclide	Disposition in EBS Cells Model	Disposition in 1-D UZ Borehole Pipe Model	Disposition in SZ Models (3-D SZ_Convolute and 1-D Pipe)	Disposition in Biosphere
Np-237	Transport irreversible colloid, Np-237 _{irr} (simple decay) Transport solute (decay to U-233)	transport irreversible colloid, Np-237 _{irr} (simple decay) transport solute (decay to U-233)	3-D transport of irr. coll., boosted by the maximum decay (over the remaining simulation time) of the Am-241 _{irr} mass at the UZ/SZ interface 3-D transport of Np solute	dose from 3-D
U-233	Transport solute (decay to Th-229)	transport solute (decay to Th-229)	1-D transport only (solute)	dose from 1-D
Th-229	transport reversible colloid & solute (simple decay)	transport solute (simple decay)	1-D transport only (reversible colloid & solute)	dose from 1-D
Thorium Series				
Pu-240	transport irreversible colloid Pu-240 _{irr} (simple decay) transport reversible colloid & solute (decay to U-236)	transport irreversible colloid Pu-240 _{irr} (simple decay) transport solute (decay to U-236)	3-D transport of irr. coll. 3-D transport of Am/Pu rev. coll.	dose from 3-D
U-236	transport solute (simple decay)	transport solute (simple decay)	3-D transport of U-236 solute, boosted by the maximum decay (over the remaining simulation time) of the Pu-240 _{rev/sol} mass at the UZ/SZ interface	dose from 3-D
Th-232	exclude	Exclude	exclude	exclude
Ra-228	exclude	Exclude	exclude	exclude
Uranium Series				
Pu-242	transport irreversible colloid Pu-242 _{irr} (simple decay) transport reversible colloid & solute (decay to U-238)	transport irreversible colloid Pu-242 _{irr} (simple decay) transport solute (decay to U-238)	3-D transport of irr. coll. 3-D transport of Am/Pu rev. coll.	dose from 3-D
Pu-238	transport irreversible colloid Pu-238 _{irr} (simple decay) transport reversible colloid and solute (decay to U-234)	transport irreversible colloid Pu-238 _{irr} (simple decay) transport solute (decay to U-234)	3-D transport of irr. coll. 3-D transport of Am/Pu rev. coll.	dose from 3-D
U-238	transport solute (decay to U-234)	transport solute (decay to U-234)	3-D transport of U-238 solute, boosted by the maximum decay (over the remaining simulation time) of the Pu-242 _{rev/sol} mass at the UZ/SZ interface	dose from 3-D

Table 6-29. Disposition of Radionuclides for 10,000- to 100,000-Year Human Intrusion Groundwater Release Scenarios (Continued)

Radionuclide	Disposition in EBS Cells Model	Disposition in 1-D UZ Borehole Pipe Model	Disposition in SZ Models (3-D SZ_Convolute and 1-D Pipe)	Disposition in Biosphere
U-234	transport solute (decay to Th-230)	transport solute (decay to Th-230)	3-D transport of U-234 solute, boosted by the maximum decay (over the remaining simulation time) of the U-238 mass at the UZ/SZ interface	dose from 3-D
Th-230	excluded	Excluded	excluded	excluded
Ra-226	excluded	excluded	excluded	excluded
Pb-210	excluded	Excluded	excluded	excluded

Table 6-30. Disposition of Radionuclides for 10,000-Year to 100,000-Year Eruptive Release Scenario

Radionuclide	Disposition in ASHPLUME Transport Model	Disposition in Biosphere
Fission Products		
C-14	Transport	Exclude
Sr-90	Transport	Include
Tc-99	Transport	Exclude
I-129	Transport	Exclude
Cs-137	Transport	Include
U-232	Transport	Include
Actinium Series		
Am-243	Transport	Include
Pu-239	Transport	Include
U-235	Transport	Exclude
Pa-231	Transport	Include
Ac-227	Transport	Include
Neptunium Series		
Am-241	Transport	Include
Np-237	Transport	Exclude
U-233	Transport	Include
Th-229	Transport	Include
Thorium Series		
Pu-240	Transport	Include
U-236	Transport	Exclude
Th-232	Exclude	Exclude
Ra-228	Exclude	Exclude
Uranium Series		
Pu-242	Transport	Exclude
Pu-238	Transport	Include
U-238	Transport	Exclude
U-234	Transport	Exclude
Th-230	Transport	Exclude
Ra-226	Transport	Exclude
Pb-210	Transport	Exclude

of CSNF and CDSP inventory in each of these five regions of the repository is a function of the area of the region or bin (see Figure 6-86). The infiltration bin size varies with infiltration scenario (there are three infiltration scenarios), thus the fraction of packages in each of the five bins must vary with infiltration scenario (see Table 6-31 and Table 6-32).

Each of the 10 bins (5 percolation/infiltration bins \times 2 inventory bins) is further divided into three sub-bins based upon seepage rates. The distinction amongst these 3 sub-bins is: “always dripping” conditions, “sometimes dripping” conditions, or “never dripping” conditions. The same logic described above for bin segregation of the waste packages based on infiltration, is

used to subdivide the number of packages in each bin within each seepage zone based upon the seepage fraction. The final result is 30 waste-package/waste-form groups in TSPA model, each having different release rates. CSNF packages containing stainless steel clad fuel are removed from the total number of packages by multiplying the fraction of stainless steel clad fuel by the total number of packages. That quantity of SS-clad packages is then assigned to the always drip bin 4 environment for the medium and high infiltration cases and the no drip bin 1 environment for the low infiltration case. The final result of segregating the SS-clad CSNF packages is a total of 31 source term groups in GoldSim.

Input parameters that are used to calculate the distribution of waste packages into groups are shown in Table 6-31 and Table 6-32.

Table 6-31. Various TSPA Model Input Parameters used for Dividing the Waste Inventory into Groups Based on Infiltration

Parameter Name	Description	Parameter Value
Total_CSNF_Packages	Total number of CSNF waste packages in the repository	7860
Total_CDSP_Packages	Total number of CDSP waste packages in the repository	3910
Frac_CSNF_Pkgs_SS	Fraction of CSNF waste packages that contain stainless-steel clad fuel	0.0349
FractionArea_Bin1	Areal fraction of the repository corresponding to infiltration bin 1	see row "Bin 1" in Table 6-3
FractionArea_Bin2	Areal fraction of the repository corresponding to infiltration bin 2	see row "Bin 2" in Table 6-3
FractionArea_Bin3	Areal fraction of the repository corresponding to infiltration bin 3	see row "Bin 3" in Table 6-3
FractionArea_Bin4	Areal fraction of the repository corresponding to infiltration bin 4	see row "Bin 4" in Table 6-3
FractionArea_Bin5	Areal fraction of the repository corresponding to infiltration bin 5	see row "Bin 5" in Table 6-3

Table 6-32. Fraction of Waste Packages in the Five Infiltration Bins as a Function of the Infiltration Scenario

Infiltration bin	Low infiltration (1)	Medium infiltration (2)	High infiltration (3)
Bin 1	0.5907	0.01607	0.0
Bin 2	0.4030	0.13154	0.0123
Bin 3	0.0	0.32120	0.1340
Bin 4	0.0	0.52850	0.5480
Bin 5	0.0	0.00269	0.3057

Waste packages are parsed in the model first by infiltration bin, then by dripping environment. The parsing by infiltration bin occurs in the *Num_Packages* container located in \TSPA_Model\Engineered_Barrier_System\WastePackage_Dripshield\ (see Figure 6-86).

Data elements, *Total_CSNF_Packages* and *Total_CDSP_Packages* define the number of waste packages of each type in the repository. The fraction of CSNF waste packages that contain stainless-steel clad fuel is defined in data element *Frac_CSNF_Pkgs_SS*. The number of CSNF waste packages containing stainless-steel clad fuel is calculated by *Num_CSNF_Pkgs_SS*, where *Total_CSNF_Packages* is multiplied by *Frac_CSNF_Pkgs_SS* and the result rounded to the nearest whole number. The number of CSNF packages without stainless-steel clad fuel is then calculated by *Tot_CSNF_Pkgs_Mod*, which subtracts *Num_CSNF_Pkgs_SS* from *Total_CSNF_Packages*.

The areal fraction of the repository that corresponds to the infiltration bins under each infiltration scenario are given by the set of one-dimensional look-up tables, *FractionArea_Bin1*, *FractionArea_Bin2*, *FractionArea_Bin3*, *FractionArea_Bin4*, and *FractionArea_Bin5*. The independent variable for each look-up table is the *Infiltration_Scenario*. Hence, each of the tables return the areal fraction associated with each bin for the given infiltration scenario. These values are passed to the data element *Fractional_Area*, which is defined as a vector dimensioned by infiltration bin (e.g., *Bin_1*, *Bin_2*, *Bin_3*, *Bin_4*, *Bin_5*) and located inside the *Package_Calculation* container (see Figure 6-87).

The number of waste packages for each fuel type (*Frac_CSNF_WP* and *Frac_CDSP_WP*) within each bin is calculated by multiplying the *Fractional_Area* by the *Tot_CSNF_Pkgs_Mod* for CSNF WPs and by the *Total_CDSP_Packages* for CDSP WPs and rounding the results to the nearest whole number. In the process of rounding it is possible that the total number of CSNF or CDSP waste packages may be increased or decreased. To ensure that all the packages are placed in one of the five bins, the bin with the largest fractional area is selected to receive the remaining packages that may have been missed due to rounding (*Max_Bin* identifies the bin with the largest fractional area by applying the *maxv* function to the *Fractional_Area* vector).

The potential difference for CSNF packages is calculated in *CSNF_Package_Difference* (Figure 6-87) by subtracting the sum of the packages calculated in *Frac_CSNF_WP* from *Tot_CSNF_Pkgs_Mod*. Likewise, the potential difference for CDSP packages is calculated in *CDSP_Package_Difference* by subtracting the sum of the packages calculated in *Frac_CDSP_WP* from *Tot_CDSP_Pkgs*. The data elements *CSNF_Pkg_Adjust* and *CDSP_Pkg_Adjust* are used to associate any package difference with the infiltration bin that has the largest areal fraction as illustrated in Table 6-33.

Table 6-33. Contents of the Data Element *CSNF_Pkg_Adjust*

Vector Location	Function
Bin_1	if(Fractional_Area.Fractional_Area[Bin_1]==Max_Bin,CSNF_Package_Difference,0)
Bin_2	if(Fractional_Area.Fractional_Area[Bin_2]==Max_Bin,CSNF_Package_Difference,0)
Bin_3	if(Fractional_Area.Fractional_Area[Bin_3]==Max_Bin,CSNF_Package_Difference,0)
Bin_4	if(Fractional_Area.Fractional_Area[Bin_4]==Max_Bin,CSNF_Package_Difference,0)
Bin_5	if(Fractional_Area.Fractional_Area[Bin_5]==Max_Bin,CSNF_Package_Difference,0)

The data elements *Frac_CSNF_WP* and *CSNF_Package_Adjust* are then added together to yield the number of CSNF waste packages (*Num_CSNF_WP*) in each bin (Figure 6-86). Similarly,

data elements *Frac_CDSP_WP* and *CDSP_Package_Difference* are added together to yield the number of CDSP waste packages (*Num_CDSP_WP*) in each bin.

Each of the bins is further divided into three sub-bins based upon seepage rates (“always dripping” conditions, “sometimes dripping” conditions, or “never dripping” conditions). The parsing of the waste packages among the dripping environments in a given infiltration bin is performed in the *Number_Packages* container located within each infiltration bin container. Within this container the number of packages in the bin (for example, CSNF Infiltration Bin 4) are specified in data element *Num_Packages* (see Figure 6-88). An IF-statement

if(Switch_Zone2 == 1, CSNF_WP_BIN4, Num_CSNF_WP.Num_CSNF_WP[Bin_4])

determines if a disruptive event with Zone 2 packages is being evaluated, in which case the number of packages is specified by the package calculation in the *Disruptive_Events* container (Switch_Zone2 == 1) (see Section 6.3.9). If a disruptive event with Zone 2 packages is not being evaluated the number of packages in the bin is specified from either *Num_CSNF_WP* or *Num_CDSP_WP* described earlier (see Figure 6-86).

The data element *Seepage_Fraction* (Figure 6-88) contains the global seepage fractions for the three dripping environments (Always_Seep, Sometimes_Seep, No_Seep). The number of packages in each dripping environment is calculated in data element *Frac_Pkgs* by multiplying the number of packages in the bin *Num_Packages* by *Seepage_Fraction* and rounding the results. As in the calculation to determine the number of waste packages in each bin, rounding the number of packages in each environment may cause an increase or decrease in the total number of packages in the bin. This potential difference is calculated by *Num_Pkgs_Difference* by subtracting the sum of the packages calculated in *Frac_Pkgs* from *Num_Packages*. Following this, the data element *Num_Pkgs_Adjust* (see Table 6-34) associates any package difference with the seepage environment that has the largest number of packages as identified by *Max_Fraction*.

Table 6-34. Contents of the Data Element *Num_Pkgs_Adjust*

Vector Location	Function
Always_Seep	if(Seepage_Fraction.Seepage_Fraction[Always_Seep]= Max_Fraction, Num_Pkgs_Difference,0)
Sometimes_Seep	if(Seepage_Fraction.Seepage_Fraction[Sometimes_Seep] Max_Fraction, Num_Pkgs_Difference,0)
No_Seep	if(Seepage_Fraction.Seepage_Fraction[No_Seep] = Max_Fraction, Num_Pkgs_Difference,0)

The data elements *Frac_Pkgs* and *Num_Pkgs_Adjust* are then added together to yield the number of waste packages in each dripping environment, adjusted for potential rounding errors.

Results and Verification

The calculations for parsing the waste packages among the infiltration bins and dripping environments is verified by the hand-calculation shown in Figure 6-89. The first part of the hand-calculation determines the number of waste packages in each infiltration bin. The second part of the hand-calculation determines the number of waste packages in each dripping

environment for CSNF in infiltration bin 4. As shown in the Figure 6-89, the hand-calculation results match the GoldSim model results.

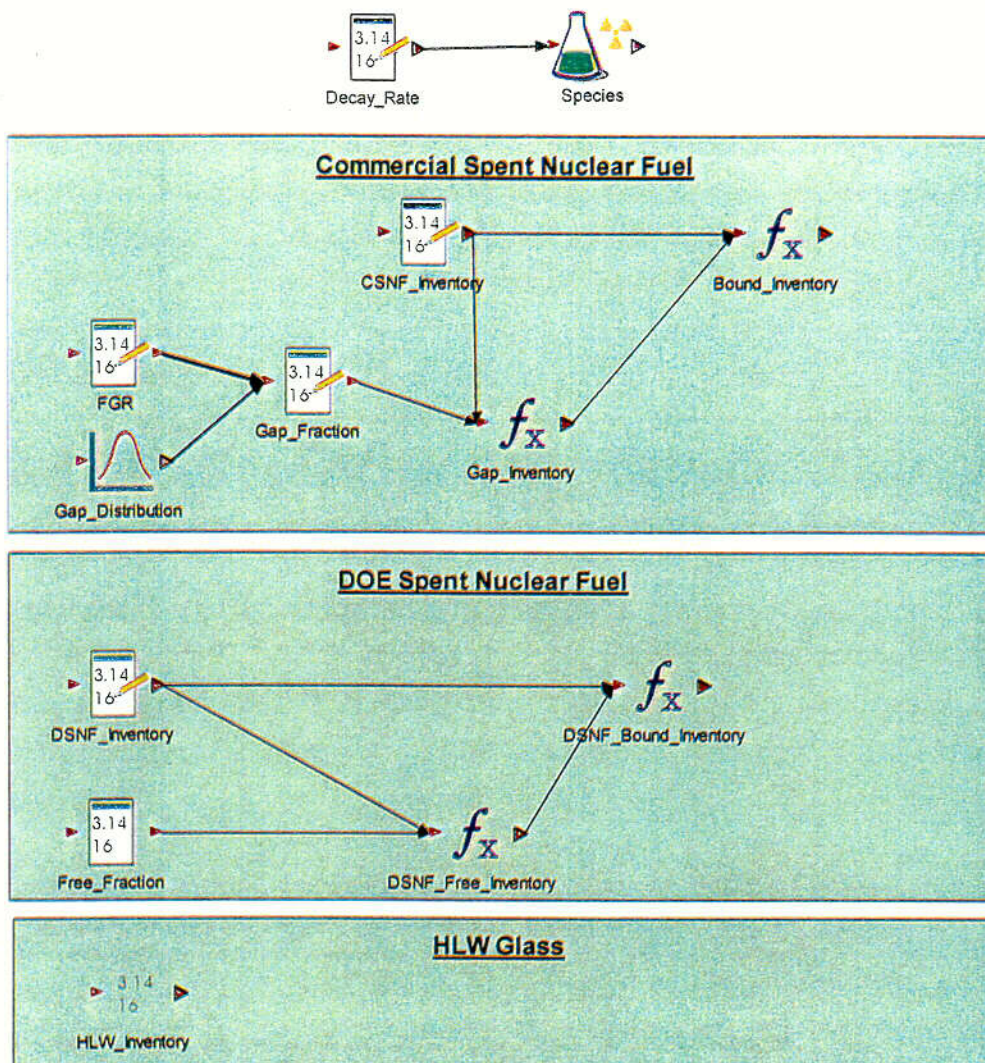


Figure 6-85. Graphical Representation of the Three Different Fuel Inventories as Implemented in GoldSim

C58

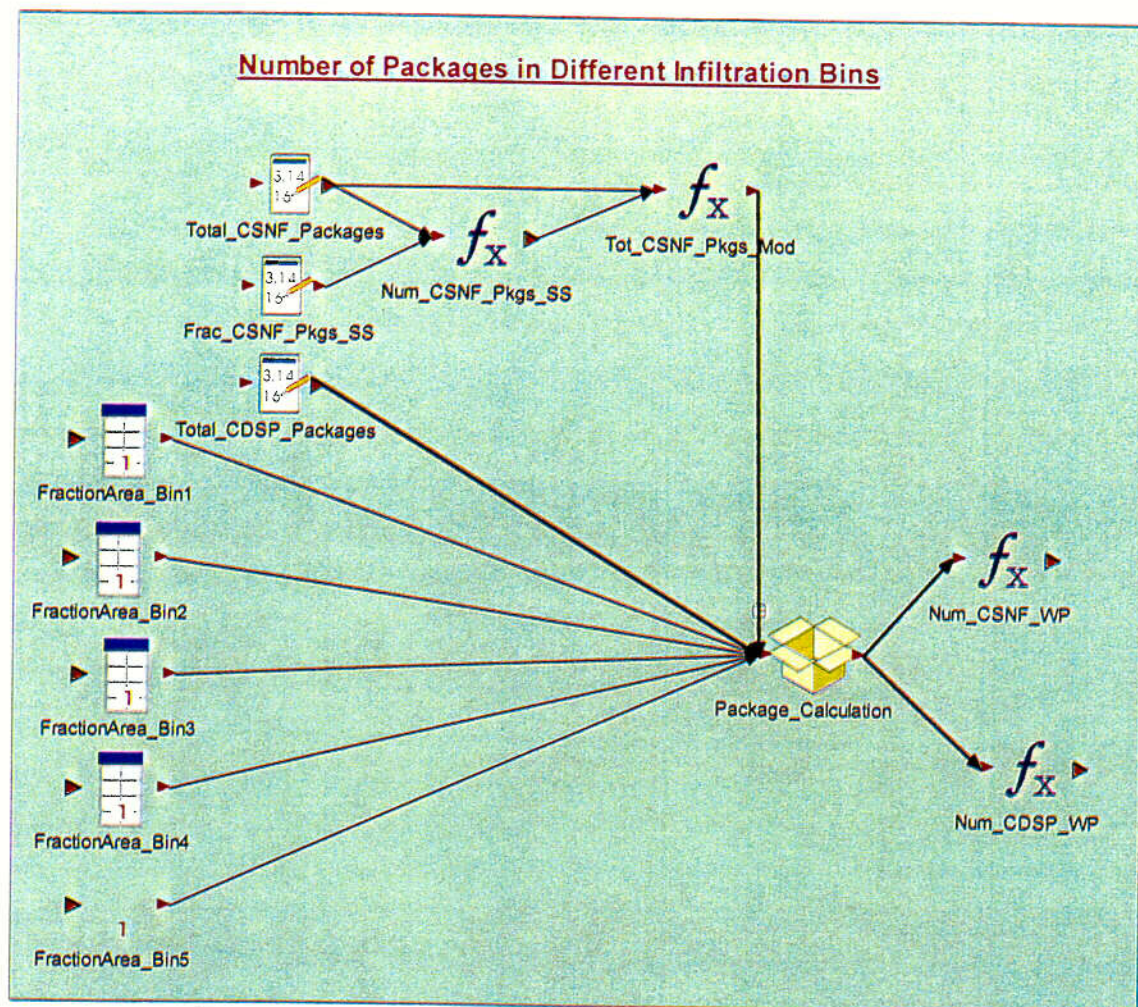
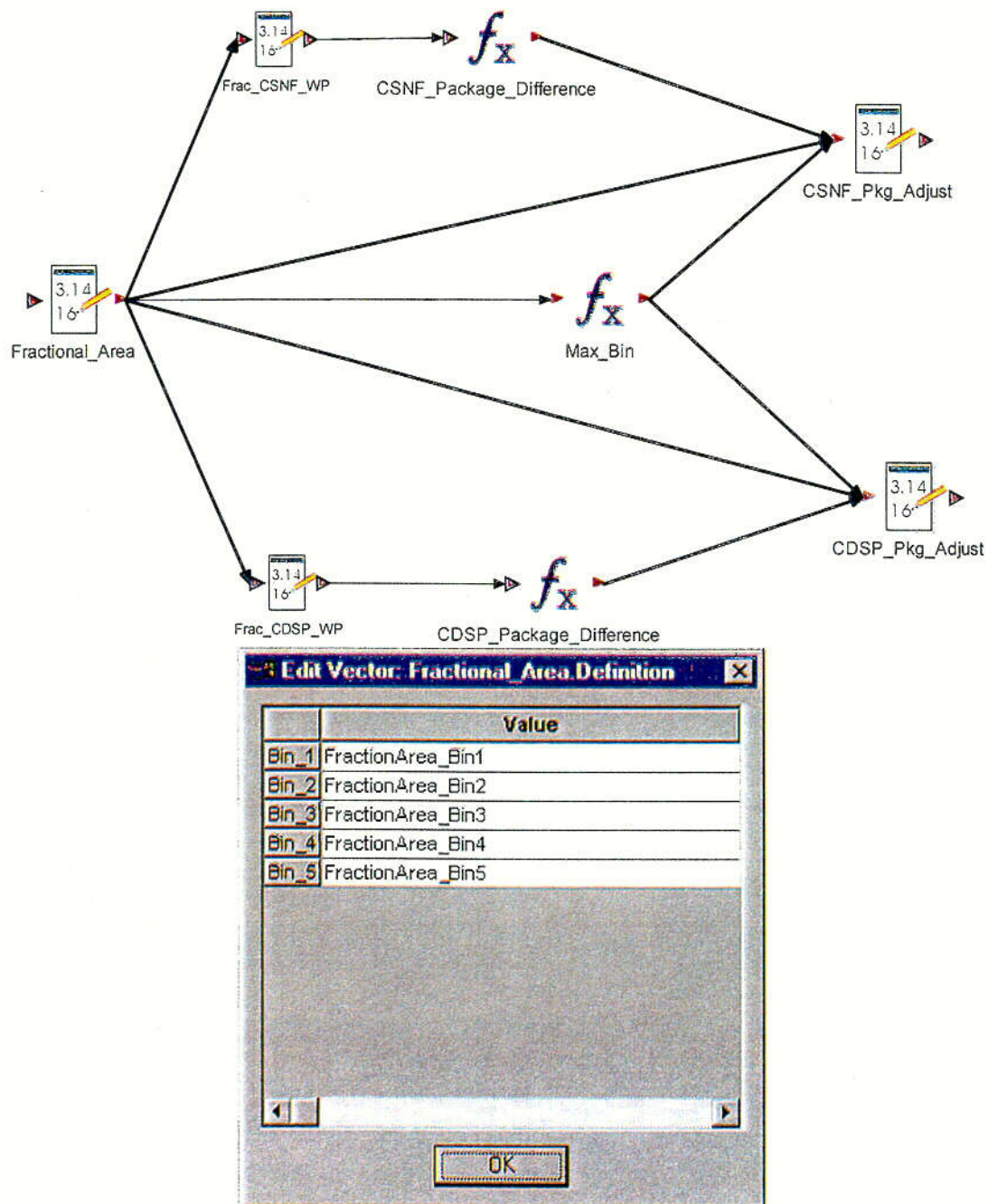


Figure 6-86. Graphical Representation of the Calculation of Fraction of CSNF and CDSP Waste Packages in Each Bin from the GoldSim container *Num_Packages* in the *WastePackage_Dripshield* container

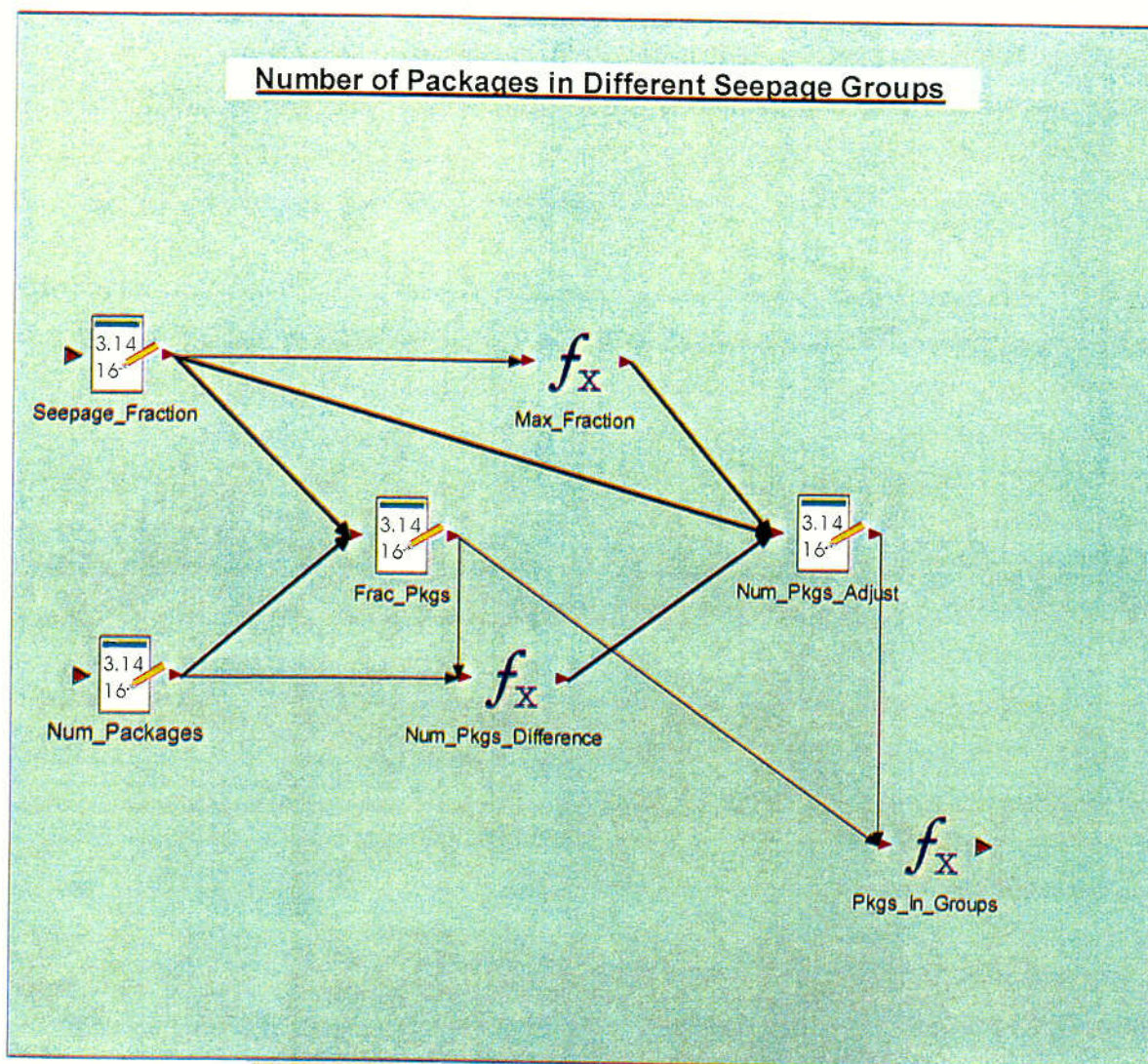
C59



NOTE: Represents the *Package_Calculation* subcontainer seen in Figure 6-88

Figure 6-87. Illustration of the Adjustment for Round-off Error in the Calculation of Number of CSNF and CDSP Waste Packages in Each Infiltration Bin

C60



Edit Vector: Seepage_Fraction Definition

	Value
Always_Seep	SeepFrac_Always.SeepFrac_Always[bin_1,CSNF]
Sometimes_Seep	SeepFrac_Intermittent.SeepFrac_Intermittent[bin_1,CSNF]
No_Seep	SeepFrac_ND.SeepFrac_ND[bin_1,CSNF]

OK

Figure 6-88. Graphical Representation for the Calculation of Number of Waste Packages in Each Seepage Group

Hand-Calculation for # of Waste Packages in Each Infiltration Bin

	Input/Calculated	GoldSim
total CSNF pkgs	7860	7860
total CDSP pkgs	3910	3910
fraction of CSNF with SS-clad fuel	0.0349	0.0349
# CSNF pkgs w/ SS-clad fuel (rounded)	274.314 274	— 274
# of CSNF pkgs w/o SS-clad fuel	7586	7586

Infiltration Bin	FractionalArea	# of CSNF pkgs (calculated)	# of CSNF pkgs (rounded)	# of CSNF pkgs (GoldSim)	# of CDSP pkgs (calculated)	# of CDSP pkgs (rounded)	# of CDSP pkgs (GoldSim)
Bin 1	0.01607	121.9070	122	122	62.8337	63	63
Bin 2	0.13154	997.8624	998	998	514.3214	514	514
Bin 3	0.32120	2436.6232	2437	2437	1255.8920	1256	1256
Bin 4	0.52850	4009.2010	4009	4009	2066.4350	2066	2066
Bin 5	0.00269	20.4063	20	20	10.5179	11	11
total			7586	7586		3910	3910

	calculated	Goldsim
CSNF pkg difference	0	0
CDSP pkg difference	0	0
max bin	0.52850	0.52850

Infiltration Bin	# of CSNF pkgs (calculated)	# of CSNF pkgs (GoldSim)	# of CDSP pkgs (calculated)	# of CDSP pkgs (GoldSim)
Bin 1	122	122	63	63
Bin 2	998	998	514	514
Bin 3	2437	2437	1256	1256
Bin 4	4009	4009	2066	2066
Bin 5	20	20	11	11
total	7586	7586	3910	3910

Hand-Calculation for # of CSNF Bin 4 Waste Packages in Each Dripping Environment

	calculated	GoldSim
# of CSNF Bin 4 pkgs	4009	4009

dripping environment	seepage fraction	# of pkgs (calculated)	# of pkgs (rounded)	# of pkgs (GoldSim)
Always Seep	0.024169	96.883521	97	97
SomeTimes Seep	0.096677	387.578093	388	388
No Seep	0.87915	3524.51235	3525	3525

	calculated	Goldsim
pkg difference	-1	-1
max fraction	0.87915	0.87915

dripping environment	# of pkgs (calculated)	# of pkgs (GoldSim)
Always Seep	97	97
SomeTimes Seep	388	388
No Seep	3524	3524
total	4009	4009

Figure 6-89. Verification of GoldSim Calculations for the Number of Waste Packages Present within Infiltration Bins and Seepage (Dripping Environment) Groups

6.3.4.2 In-Package Chemistry

Overview

The in-package chemistry component in the TSPA-SR couples the seepage rate of water into the package, the degradation rate of the waste package components, and the cladding coverage or glass dissolution rate to the resulting effluent chemistry. The water chemistry parameters of interest include: hydronium ion activity, redox potential, ionic strength, total aqueous carbonate, fluorine, and chloride concentrations (CRWMS M&O 2000 [129287], Section 4.1.2). These parameters are used in the TSPA because they influence the principle factors of degradation of the CSNF cladding and matrix, HLW degradation, radionuclide solubility, and colloid availability and stability.

The fluid chemistry inside the package (in-package chemistry) is dependent upon the initial chemistry of the water entering the breached package and the volume of water flowing through the package. The in-package chemistry model current at the time this document was prepared assumes a fully flooded container for the volume of water present in the container at all times (CRWMS M&O 2000 [111880], Section 5.1). In addition, the in-package chemistry is dependent upon the degradation rates of the contents of the package. Two representative waste packages were modeled, a CSNF package and a DSNF/HLW codisposal package. In both cases, there is an inner stainless steel disposal container, but the basket materials and waste forms are different and influence the fluid chemistry at least for short time periods (CRWMS M&O 2000 [111880], Section 6.1.1).

Direct use of a complex equilibrium code within the TSPA-SR calculation was not practical due to run-time constraints; rather, a limited number of simulations were run with the complex equilibrium/kinetic code, for a variety of input conditions and degradation rates of the contents (CRWMS M&O 2000 [111880], Section 6.2). Regression equations were then developed for use directly in the TSPA-SR calculations as explained below (CRWMS M&O 2000 [129287], Section 6).

At the process level, the in-package chemistry was modeled using the EQ3/6 software package and the results were presented in the Analysis and Modeling Report (AMR) *Summary of In-Package Chemistry for Waste Forms* (CRWMS M&O 2000 [111880]).

The J-13 well water composition was used as water entering the failed waste package. This composition was chosen because it is thought to represent a composition in equilibrium with the Yucca Mountain host rock mineralogy (CRWMS M&O 2000 [111880], Section 5.2). No attempts were made to simulate the early-stage, high-temperature phenomena such as evaporation and concentration since the waste package is not envisioned to fail until the thermal period has passed.

The in-package chemical reaction calculations used three input fluid fluxes of 1.5, 15 and 150 L/year (CRWMS M&O 2000 [111880], Section 6.2). The temperature of the simulations was set at 25°C to represent the conditions that will occur several thousand years after waste package emplacement, when the original thermal pulse has passed and temperatures have returned to near ambient levels. The partial pressure of carbon dioxide and oxygen were set to

$10^{-3.0}$ and $10^{-0.7}$ bar, respectively (CRWMS M&O 2000 [111880], Section 5.6). The latter represents equilibrium with oxygen at atmospheric levels. Measurements of J-13 well water indicated that the carbon dioxide partial pressure is somewhat higher than atmospheric levels (CRWMS M&O 2000 [111880], Section 5.6).

The physical model of liquid flow through the waste package involved use of the solid-centered flow-through mode in EQ3/6; in this mode, an increment of aqueous feed solution is added to the waste package system and a like amount of solution is removed at each time step. Each breached waste package is modeled as a continually stirred, constant fluid volume reactor (CRWMS M&O 2000 [111880], Section 4). The simplest approach to estimating the nature and extent of chemical reaction within the waste package was to assume that the volume is perfectly mixed.

In-drift solutions seeping into a breached waste package would encounter a number of kinetically reactive solids whose reaction rates are only known within orders of magnitude. Fluids intruding into waste packages containing CSNF would encounter UO_2 fuel wrapped in zircaloy cladding, Al alloy, 316 stainless steel, and A516 low carbon steel (CRWMS M&O 2000 [111880], Section 6.1.1). A range of degradation rates was used for each. Dissolution of the fuel, and release of radioisotopes, occurs only after degradation of some of the cladding. General corrosion of cladding is likely to be insignificant under the geochemical conditions expected inside reacting waste packages. Uncertainty in the initial failures, localized corrosion, mechanical damage, and other degradation mechanisms are addressed in the cladding degradation AMRs and were not available when the in-package calculations were started, so a range of clad damage and CSNF fuel exposure was investigated (100 percent, 20 percent, and 1 percent). The waste package configuration used for the codisposal packages (CDSP) calculation was that of the Fast Flux Test Facility (FFTF) DSNF with five DHLW glass logs (CRWMS M&O 2000 [111880], Section 6.1.1).

In order to simulate a range of possible chemistries several independent parameters were perturbed from their baseline values in the EQ6 process model(s) simulations. These parameters included water flux through the waste package, waste package component corrosion rates (kinetic constants), cladding coverage (for CSNF packages), and HLWG dissolution rates (for DSNF packages) (CRWMS M&O 2000 [111880], Section 6.2). The waste package component corrosion rates refer to the degradation of the steel and/or components in the waste package (CRWMS M&O 2000 [111880], Section 6.2). The results of the process model(s) were time-dependent values of aqueous chemistry (CRWMS M&O 2000 [111880], Sections 6.2 and 6.3). The basis of the abstraction was use of the time dependent chemistry and the values of the independent variables used as EQ3/6 input.

The results of the EQ6 simulations were abstracted and incorporated into the TSPA-SR model. The abstraction of the EQ3/6 results simplified the detailed complex time dependant chemistry into blocks of time where conservative assumptions were used to bound the chemistry. A series of abstracted multi-dimensional response surfaces, model equations, and stochastic distributions were directly implemented in the TSPA-SR code to calculate in-package chemical conditions. Each chemical condition is assigned an appropriate relationship based on the abstracted relationships in the feed AMR *In-Package Chemistry Abstraction* (CRWMS M&O 2000 [129287]).

The abstracted in-package pH for CSNF waste packages is a function of time, seepage flux through the waste package, cladding coverage, and the waste package corrosion rate. For CDSP waste packages, which do not contain cladding, the pH is dependent on the dissolution rate of the HLW glass.

The time discretization for the in-package chemistry abstraction was based on changes in the solution pH. Changes in pH are indicative of changes in bulk fluid chemistry, and as such, pH functions as an indicator variable for the aqueous chemistry (CRWMS M&O 2000 [129287], Section 5.2). Therefore, based on the pH-time histories from the process model outputs a coarse time discretization was identified for the post breach period.

The simulated in-package pH, from the process level analysis, changed rapidly during the first 1,000 years following waste package breach, reaching its minimum value during this phase. This is likely to be due to the dissolution of carbon steel and the coincident production of protons which lowers the pH (CRWMS M&O 2000 [129287], Section 6.1). Once the dissolution of carbon steel diminishes, the pH increases. After 1,000 years the in-package pH maintained pseudo-steady state conditions. This trend in pH was observed for both the CSNF and CDSP waste packages. Consequently, the pH analysis was divided into two time frames, early and late. The early phase corresponds to the first 1,000 years after a waste package is breached. The late phase corresponds to time beyond 1,000 years after breach. Hereafter in the discussion of in-package chemistry, all time references will be the time elapsed since package breach, unless otherwise stated.

The in-package pH is a function of the water flux through the package, the waste package corrosion rate and the cladding coverage or glass dissolution rate. For CSNF packages, pH calculations using EQ6 were performed for three water flux rates, 0.0015 m³/year, 0.015 m³/year, and 0.15 m³/year, three cladding coverage fractions, 0.01, 0.2, and 0.99, and two waste package corrosion rates, low and high (CRWMS M&O 2000 [129287], Section 6.1.1). Similarly, CDSP pH calculations were performed for the same three water flux rates and the same corrosion rates. Since CDSP waste packages do not have cladding, pH equations based on cladding coverage fractions are inappropriate. The analogous relationship for CDSP pH calculations is the dissolution rate of the waste form glass in which the radionuclides are bound.

Three-dimensional response surfaces establishing the pH boundary limits were determined using the extreme values for one input condition, the waste package corrosion rate (CRWMS M&O 2000 [129287], Section 6.1.1 and 6.1.2). EQ6 simulation results were plotted in three-dimensional space and the pH response surfaces were modeled as a planar surface. Data regression was performed using the equation of a plane (Equation 6-1).

$$z = y_0 + ax + by \quad (\text{Eq. 6-1})$$

For each time phase (early and late) and each package type (CSNF and CDSP) one pH surface was generated for a low waste package corrosion rate scenario and one pH surface was generated for a high waste package corrosion rate scenario. These surfaces constitute the boundaries of the range of in-package pH values. The actual waste package corrosion rate is randomly sampled from the range bounded by these low and high values.

Both total carbonate and redox potential (Eh) are pH dependent and may be calculated directly from the abstracted pH value (CRWMS M&O 2000 [129287], Sections 6.2 and 6.3,). The chemical parameters of fluoride (F) and ionic strength (I) were set to ranges where maximum and minimum concentrations were provided (CRWMS M&O 2000 [129287], Section 6.4). The remaining parameters, chloride (Cl) (CRWMS M&O 2000 [129287], Section 6.4), pO_2 , and pCO_2 (CRWMS M&O 2000 [129287], Section 6.5) were constants.

The carbonate concentration was calculated from equilibrium mass action equations. The carbonate concentration is a function of CO_2 partial pressure and pH. If a constant CO_2 partial pressure ($P_{CO_2} = 0.001$ atm) is assumed, the equation is reduced to a function of pH.

For more details regarding on the development and abstraction of the in-package chemistry relationships, the reader is referred to the *AMR In-Package Chemistry Abstraction* (CRWMS M&O 2000 [129287]).

Inputs to the TSPA Model

There are eight pH response surfaces that were abstracted in the *AMR In-Package Chemistry Abstraction* (CRWMS M&O 2000 [129287], Sections 6.1.1 and 6.1.2). Table 6-35 summarizes the conditions of each response surface.

Table 6-35. Response Surface Characteristics

Response Surface Number	Time Period	Waste Package Corrosion Rate	Package Type	Boundary with other surface
1	Early	Low	CSNF	2
2	Early	High	CSNF	1
3	Late	Low	CSNF	4
4	Late	High	CSNF	3
5	Early	Low	CDSP	6
6	Early	High	CDSP	5
7	Late	Low	CDSP	8
8	Late	High	CDSP	7

In the referenced AMR (CRWMS M&O 2000 [129287]), the EQ6 data for each response surface, output from the *AMR Summary of In-Package Chemistry for Waste Forms* (CRWMS M&O 2000 [111880]), were plotted in three-dimensional space and a plane fit to the data (CRWMS M&O 2000 [129287], Section 6.1). The regressed equations are summarized in Table 6-36 and Table 6-37. The response surfaces generated from the EQ6 simulations provide the boundaries of the pH calculation in the TSPA-SR model.

Table 6-36. pH Response Surface Parameters for CSNF Waste Packages

$z = y_0 + ax + by$					
TSPA Parameter	Response Surface	y_0	a	b	Reference
pH_CSNF_data.early_low	1	3.4916	-1.0918	0.4571	CRWMS M&O 2000 [129287], Table 6
pH_CSNF_data.early_high	2	3.3977	-0.7468	0.3515	CRWMS M&O 2000 [129287], Table 6
pH_CSNF_data.late_low	3	6.0668	-0.5395	4.0479	CRWMS M&O 2000 [129287], Table 6
pH_CSNF_data.late_high	4	6.0913	-0.3057	1.2913	CRWMS M&O 2000 [129287], Table 6

DTN: MO9911SPACDP37.001 [139569]

NOTE: z = pH, x = \log_{10} (cladding coverage), y = water flux (m^3/year)

Table 6-37. pH Response Surface Parameters for CDSP Waste Packages

$z = y_0 + ax + by$					
TSPA Parameter	Response Surface	y_0	a	b	Reference
pH_CDSP_data.early_low	5	5.1257	2.6692	0.0764	CRWMS M&O 2000 [129287], Table 12
pH_CDSP_data.early_high	6	4.7324	0.7307	0.0837	CRWMS M&O 2000 [129287], Table 12
pH_CDSP_data.late_low	7	8.4247	-3.4173	0.1403	CRWMS M&O 2000 [129287], Table 12
pH_CDSP_data.late_high	8	9.2554	-3.1280	-0.0418	CRWMS M&O 2000 [129287], Table 12

DTN: MO9911SPACDP37.001 [139569]

NOTE: z = pH, x =water flux (m^3/year), y = relative glass dissolution rate

For CSNF waste packages, the cladding coverage parameter, x , is calculated in the Cladding Degradation Model component of the TSPA-SR model (see Section 6.3.4.3 Cladding Degradation Model). The localized water flux rate parameter, y , is calculated in the EBS Flow and Transport component of the TSPA-SR model (see Section 6.3.5.1 EBS Flow and Transport Pathways). These parameters are used to calculate the boundaries for the localized in-package pH at each time step.

For CDSP waste packages, the localized relative glass dissolution rate, y , is a constant value. The localized water flux rate parameter, x , is calculated in the EBS Flow and Transport component of the TSPA-SR model (see Section 6.3.5.1 EBS Flow and Transport Pathways). These parameters are used to calculate the localized in-package pH at each time step.

Table 6-38 provides the other TSPA-SR In-Package Chemistry Model component input parameters and the associated value/relationship for each.

Table 6-38. Input Parameters for In-Package Chemistry Calculations

TSPA Parameter	Description	Parameter Value	Reference
Rel_diss_rate	Glass dissolution rate for CDSP packages	1	Data developed was applicable to CDSP packages and no glass composition correction is needed.
Ionic_Str_CSNF_early	Ionic strength in CSNF waste packages at early times in mol/kg	Beta Distribution Min=2.757E-03 Max=2.922E-03 Mean=2.821E-03 Std Dev=5.1716E-05	CRWMS M&O 2000 [129287], Table 16
Ionic_Str_CSNF_late	Ionic strength in CSNF waste packages at late times in mol/kg	Beta Distribution Min=2.827E-03 Max=3.943E-01 Mean=9.484E-02 Std Dev=0.13026125	CRWMS M&O 2000 [129287], Table 17
Ionic_Str_CDSP_early	Ionic strength in CDSP waste packages at early times in mol/kg	Beta Distribution Min=2.537E-03 Max=3.479E-03 Mean=3.179E-03 Std Dev=2.764E-04	CRWMS M&O 2000 [129287], Table 18
Ionic_Str_CDSP_late	Ionic strength in CDSP waste packages at early times in mol/kg	Beta Distribution Min=7.860E-03 Max=1.353 Mean=3.384E-01 Std Dev=4.764E-01	CRWMS M&O 2000 [129287], Table 19
Cl	Chloride ion concentration in mol/kg	2.014E-04	CRWMS M&O 2000 [129287], Section 6.4.2
log_fO2	Log Oxygen Fugacity	-0.7	CRWMS M&O 2000 [129287], Table 20
log_fCO2	Log Carbon Dioxide Fugacity	-3.0	CRWMS M&O 2000 [129287], Table 20
Total_CO3	Total Carbonate Concentration in mol/kg	$10^{-4.47} + 10^{-10.82}/10^{-\text{pH}} + 10^{-21.15}/10^{-2\text{pH}}$	CRWMS M&O 2000 [129287], Table 14

DTN: MO9911SPACDP37.001 [139569]

Implementation

This section describes the TSPA-SR model implementation of the in-package chemistry calculations, using the abstracted relationships.

The pH of the environmental fluid within a breached waste package is a function of the magnitude and chemistry of the seepage flux, the cladding coverage/glass dissolution rate, and the corrosion rate. The cladding coverage/glass dissolution rate is specific to the package type, CSNF or CDSP; therefore, pH calculations must be performed separately for each package type. The seepage flux varies spatially within the repository and thus the pH will also vary spatially within the repository. To account for the spatial variability, the TSPA-SR model is partitioned into five groups called bins. Each bin is distinguished by the quantity of water seeping into the drift. Bin 1 has the least amount of seeping water (0-3 mm/year) and bin 5 has the most (>60 mm/year). Due to spatial placement, each waste package in a bin may not always be exposed to the dripping water. Therefore, each bin is further divided into three subgroups, called environments. Each environment is distinguished by the duration of waste package exposure to the percolating water. The environments are Always Drip, Intermittent Drip, and Never Drip.

Because the waste package exposure to seepage water is different in each environment, the seepage flux varies in each environment; therefore, the in-package pH will also vary within each environment. The pH must be calculated locally within each of these environments.

The CSNF and CDSP waste packages have different radionuclide contents and package configurations. It is expected that the pH calculation for each package type is specific to the package type, as indicated by the set of pH response surfaces. Figure 6-90 shows the separation of CSNF and CDSP components for model calculations.

The following discussion details the model implementation for calculating the pH within CSNF waste packages. The TSPA-SR model uses the same model relationships to calculate the pH within each CSNF environment. Although the pH response surface model equations are the same, the input values correspond to the specific conditions within each environment; hence, the calculated results will be specific to each environment.

The pH calculation for CSNF packages is graphically depicted in Figure 6-91 through Figure 6-95. Figure 6-91 illustrates the separation of the waste packages into bins, accounting for the spatial variability within the repository. Figure 6-92 illustrates the further subgrouping into environments within one of the five bins. This subdivision is based on the duration of seepage exposure a waste package receives in a specified bin. Figure 6-93 graphically illustrates the localized calculation of model parameters within one environment. Figure 6-94 shows the localized pH calculation inside one environment. Figure 6-95 graphically illustrates the pH calculation within the identified environment.

At the initiation of the simulation, the code assigns a value to every stochastic distribution in the model. If the expected value simulation is run, the assigned value is the distribution mean, otherwise it is randomly selected from the distribution range. Once a value has been assigned to each of the stochastic parameters, these values are used throughout the remainder of the simulation.

The in-package pH is calculated within each of environments using local conditions. The following scenario illustrates the calculation of the pH inside one CSNF bin environment.

At any time, the seepage flux rate, *QFlux_WP*, and fraction of cladding coverage, *Fuel_Exposed*, within each environment are known or calculated (see Section 6.3.5.1 EBS Flow and Transport Pathways and Section 6.3.4.3 Cladding Degradation Model). When waste packages are failed the *Fuel_Exposed* parameter is equal to the *Avg_Clad_Failed* parameter from the previous time step. This is done to allow GoldSim to handle the feedback between cladding and pH (i.e., cladding failure is a function of pH and pH is a function of cladding failure). Before any waste packages fail the parameter *Avg_Clad_Failed* is set equal to 1.0 to prevent divide-by-zero errors. For CSNF waste packages, the model uses the values of *QFlux_WP* and *Fuel_Exposed* and the pH response surface equations, identified in a matrix format, *pH_CSNF_data*, to calculate the inner package pH boundaries for the CSNF environment. At early times, the pH response surface equation corresponding to the early time, low waste package corrosion rate, Response Surface Number 1, is used to calculate a pH for the low degradation rate bound, *pH_CSNF_early_low_b*. The model then uses the same seepage flux rate and cladding coverage values in the equation for Response Surface Number 2 to calculate the early time, high

degradation rate bound, *pH_CSNF_early_high_b*. Once calculated, these values define the pH range for early times. Due to the dependence of pH on the seepage flux rate, *QFlux_WP*, the potential to calculate a pH value beyond the pH scale is possible when *QFlux_WP* is large. The selector switches *pH_CSNF_early_high* and *pH_CSNF_early_low* prevent the calculation of pHs beyond the bounds of the in-package chemistry model due to large flux rates. If the water flux rate exceeds the appropriate limit specified in Table 6-39 during the early time phase, the pH is bounded at 8.1, the pH of the J-13 well water. If the water flux rate does not exceed the specified limit, the pH is bounded by the range defined by *pH_CSNF_early_low_b* and *pH_CSNF_early_high_b*. To account for variability and uncertainty in the pH behavior, the calculation of the early time pH, *pH_CSNF_early*, uses a uniform random number, *pH_random*, to calculate a random pH from within the pH range bounded by *pH_CSNF_early_low* and *pH_CSNF_early_high*. The result is an environment specific, randomly chosen in-package pH for early times. The pH is stored as a value in the model parameter *pH_CSNF_early*.

Table 6-39. Bounding Waste Package Flux Rates for pH Calculations

TSPA Parameter	Qflux_WP (m ³ /year)
pH_CSNF_early_high	5.3
pH_CSNF_early_low	5.3
pH_CSNF_late_high	0.15
pH_CSNF_late_low	0.15
pH_CDSP_early_high	1.1
pH_CDSP_early_low	1.1
pH_CDSP_late_high	0.36
pH_CDSP_late_low	0.36

A similar procedure is used to calculate the late phase in-package pH using the CSNF pH response surfaces for time periods beyond 1,000 years after breach. The resulting value is *pH_CSNF_late*.

The localized CSNF in-package pH for the current timestep will be *pH_CSNF_early* or *pH_CSNF_late*. A selector switch, *pH_CSNF*, assigns the appropriate pH value based on the elapsed time since the package was first breached, *Avg_Pkg_Failtime* (see Section 6.3.3 Waste Package Degradation). If no waste packages have been breached the in-package pH is set equal to 5.0. If, at a given time step, the elapsed time since a waste package has breached is less than or equal to 1,000 years, the in-package pH, *pH_CSNF*, equals the value assigned to *pH_CSNF_early*, otherwise it equals the value assigned to *pH_CSNF_late*. The value assigned to *pH_CSNF* will be used when the in-package pH is referenced in other environment specific calculations (i.e., total carbonate in the seepage water, solubility of U, Am and Np, colloid formation, and the CSNF degradation rate).

Identical model calculations are used to calculate the in-package pH of the CSNF waste packages in all three environments, in bins 1 through 5, and the stainless steel bin. The model inputs, *Avg_Pkg_Failtime*, *Avg_Clad_Failed* and *QFlux_WP* are environment specific parameters and thus all environments can have different pH histories.

The procedure for calculating the in-package pH of CSDP waste packages is similar. The calculations use the appropriate local conditions for each CDSP environment. The CDSP packages do not have a cladding coverage term because these packages do not have cladding. The analogous term for the CDSP packages is the relative dissolution rate of the glass within the package, *rel_diss_rate*. In the TSPA-SR model the relative dissolution rate is set as a constant equal to one. The abstracted relationships were developed for the type of glass used in the CDSP waste forms and is therefore appropriate for use without any glass dissolution rate modifications. Using the appropriate pH response surfaces, the in-package pH of the CDSP packages is calculated at each time step for each of the CDSP waste package environments. The value assigned to *pH_CDSP* will be used when the in-package pH is referenced in other environment specific calculations.

Once the pH is calculated for each environment in each bin, the total carbonate in the package is calculated. The carbonate ion concentration is specific to each dripping environment in the model. Because the carbonate only affects the dissolution rate of the CSNF waste package, the carbonate concentration uses the appropriate *pH_CSNF* value in the model calculation. The calculation of *Total_CO3* in a bin environment uses the environment specific *pH_CSNF*. Total carbonate is calculated using the relationship in Table 6-38. The graphical representation is presented as Figure 6-94.

The function in the expression element, *Total_CO3*, is directly from the AMR *In-Package Chemistry Abstraction* (CRWMS M&O 2000 [129287], Section 6.2, Table 14). The value assigned to *Total_CO3* will be used when the total carbonate ion concentration is referenced for the CSNF waste form degradation rate calculation.

The ionic strength inside a waste package has been defined for two phases, an early phase and a late phase. The early phase ionic strength applies when the elapsed time since waste package breach, *Avg_Pkg_Failtime*, is less than or equal to 1,000 years. The late phase applies for all other times. Due to dependence on waste package failure times, the ionic strength switch must be locally implemented within each of the 30 environments. The calculation for one environment is described next.

The AMR *In-Package Chemistry Abstraction* calculated ionic strength values for each waste package scenario at both the early and late phases (CRWMS M&O 2000 [129287], Section 6.4.1 pp. 35-38). In the TSPA model the ionic strength is represented by a stochastic distribution, *Ionic_Str_CSNF_early* or *Ionic_Str_CSNF_late*, which mimics the AMR results. The stochastic parameters are defined globally so that every bin environment will use the same ionic strength value for appropriate calculations; however, the switch from early phase to late phase values is defined locally so the ionic strength shifts correlate with package failures. Figure 6-96 shows the global definition of the ionic strength parameters; Figure 6-97 shows the local switch that selects the ionic strength at the bin-environment level. Table 6-38 summarizes the input data and how it was incorporated into the TSPA model.

The TSPA model selects which variable is used, the early phase ionic strength or the late phase ionic strength, based on the time elapsed since first breach, *Avg_Pkg_Failtime* (discussed later in this section). The selector switch that evaluates the *Avg_Pkg_Failtime* condition is called *Ionic_Str_CSNF* within each CSNF bin environment and *Ionic_Str_CDSP* within each CDSP bin

environment. If the time elapsed since first breach is less than 1,000 years, the value of *Ionic_Str_CSNF* and *Ionic_Str_CDSP* equal the early phase ionic strengths, *Ionic_Str_CSNF_early* and *Ionic_Str_CDSP_early*, respectively. Otherwise, *Ionic_Str_CSNF_late* or *Ionic_Str_CDSP_late* are used as appropriate. The value of *Ionic_Str_CSNF* and *Ionic_Str_CDSP* are referenced in colloid formation calculations (see Section 6.3.4.6 Colloids).

During multiple realizations the model will select one value from the appropriate distribution for each of the four ionic strength variables listed in Table 6-37, *Ionic_Str_CSNF_early*, *Ionic_Str_CSNF_late*, *Ionic_Str_CDSP_early* and *Ionic_Str_CDSP_late*. When evaluated for multiple realizations the assigned values mimic the appropriate distribution for the realization suite. The assigned values are held constant during one realization.

The chloride concentration, Cl, is defined as a constant value equal to 2.014×10^{-4} mol/kg but is not used in any TSPA-SR model calculations.

The fugacities of carbon dioxide and oxygen are defined globally. These parameters are defined as constants. The AMR *In-Package Chemistry Abstraction* stipulates that the log values for the fugacity of oxygen should be -0.7 and the log value for the fugacity of carbon dioxide should be -3.0 (CRWMS M&O 2000 [129287], Table 20). The TSPA model representation is shown in Figure 6-96. The value -3.0 is assigned to the parameter *log_fCO2*. The expressions *fCO2* and *fO2* convert the log values into the anti-log equivalent which are used in the remainder of the model simulation.

The elapsed time since packages have failed is critical to the in-package chemistry calculations. The elapsed time since package failure is calculated in the Waste Package Degradation component of the TSPA-SR model. The implementation is shown in Figure 6-98.

The average package fail time is the average time that has elapsed from the first package failure to all other package failures and is calculated in each bin environment. Although each bin environment uses the same waste package degradation curve, *WP_Failure*, to determine the number of failed packages in a bin environment, the number of actual failed packages will be different for each bin environment. The WAPDEG DLL returns a curve that represents the fraction of waste packages that have failed at any given time. Each bin environment uses this curve to determine the number of its packages that have failed. Because the number of packages in each bin environment is different, the number of failed packages in each bin environment will also be different. Take for example two hypothetical bin environments, Bin 1 contains 1,000 waste packages and Bin 2 contains 10 waste packages. Each bin environment uses the same hypothetical failure curve. According to this curve the first failures occur at time t and accounts for 0.1 percent of the packages. Thus at time t , one package has failed in Bin 1 and 0.01 packages have failed in Bin 2. Since 0.01 is not a full package, Bin 2 is assigned zero package failures. At time t_2 , four percent of the packages fail. At t_2 40 packages in Bin 1 have failed and 0.4 in Bin 2 have failed. Again zero failures are assigned to Bin 2. At time t_n , ten percent of the packages have failed. Thus 100 packages in Bin 1 have failed and one package in Bin 2 finally fails. Thus although the model uses the same failure curve, it is possible that bin failures are realized at different times in different bin environments.

The average package failure time is calculated using feedback links that the TSPA-SR model uses to indicate that the value for the previous timestep is supposed to be used. The logic for calculating the average package failure time is shown below:

$$\text{if}(\text{CSNF_IntermittentDrip.Failed_Packages} > 0, \\ (\text{AvgPkg_FailTime_PrevTime} + \text{MasterClock.Timestep_Length}) * (\text{Failed_Pkgs_PrevTime} / \text{CSNF_IntermittentDrip.Failed_Packages}), 0\{\text{year}\})$$

Where *Failed_Pkgs_PrevTime* is the number of packages that were failed at the previous time step, *AvgPkg_FailTime_PrevTime* is the average package fail time recorded at the previous time step, and *MasterClock.Timestep_Length* is the time elapsed in between the current and previous time step. At the time step corresponding to the first package failure, *Failed_Pkgs_PrevTime* and *AvgPkg_FailTime_PrevTime* equal zero. The time step is *t* years. Thus the result is $(0+t)*(0/1)$ which equals zero years (no time has elapsed since the last package has failed because this is the first package to fail). At the next time step four more hypothetical packages have failed. Thus the equation result is $(0+t)*(1/5)$ which equals $0.2t$ years. At the next time step 2 additional packages have failed, thus the equation result becomes $(0.2t+t)*(5/7)=6t/7=0.857t$ years. If no packages fail in the next time step *AvgPkg_FailTime* will equal $(0.857t+t)*(7/7)=1.857t$ years. The average package fail time is a moving average. The average package fail time is calculated as a local parameter and is used by the in-package chemistry section to calculate the pH and ionic strength inside a failed waste package.

Table 6-40 and Table 6-41 summarize the TSPA model parameters which affect the in-package chemistry calculations. Table 6-40 tabulates all of the TSPA model parameters that are not inputs, but are necessary to implement the model correctly.

Table 6-40. Parameter Details for Supplemental TSPA-SR Parameters

TSPA Parameter	Description	Parameter Value/Other Inputs	Applicability
pH_Random	Random Number Generator	Uniform (Min=0.0, Max=1.0)	Global
Clad_Factor	Multiplier for the contribution of cladding term for pH calculations	If the number of failed packages in the bin environment equals 0 then 0, else 1.	Local to CSNF Environment
pH_CSNF_early_low_b	Calculation of the lower pH bound for early time in CSNF packages	pH_CSNF_data.early_low (Response Surface 1), Avg_Clad_Failed, QFlux_WP	Local to CSNF Environment
pH_CSNF_early_high_b	Calculation of the upper pH bound for early time in CSNF packages	pH_CSNF_data.early_high (Response Surface 2), Avg_Clad_Failed, QFlux_WP	Local to CSNF Environment
pH_CSNF_late_low_b	Calculation of the lower pH bound for late time in CSNF packages	pH_CSNF_data.late_low (Response Surface 3), Avg_Clad_Failed, QFlux_WP	Local to CSNF Environment
pH_CSNF_late_high_b	Calculation of the upper pH bound for late time in CSNF packages	pH_CSNF_data.late_high (Response Surface 4), Avg_Clad_Failed, QFlux_WP	Local to CSNF Environment
pH_CDSP_early_low_b	Calculation of the lower pH bound for early time in CDSP packages	pH_CDSP_data.early_low (Response Surface 5), rel_diss_rate, QFlux_WP	Local to CDSP Environment

Table 6-40. Parameter Details for Supplemental TSPA-SR Parameters (Continued)

TSPA Parameter	Description	Parameter Value/Other Inputs	Applicability
pH_CDSP_early_high_b	Calculation of the upper pH bound for early time in CDSP packages	pH_CDSP_data.early_high (Response Surface 6), rel_diss_rate, QFlux_WP	Local to CDSP Environment
pH_CDSP_late_low_b	Calculation of the lower pH bound for late time in CDSP packages	pH_CDSP_data.late_low (Response Surface 7), rel_diss_rate, QFlux_WP	Local to CDSP Environment
pH_CDSP_late_high_b	Calculation of the upper pH bound for late time in CDSP packages	pH_CDSP_data.late_high (Response Surface 8), rel_diss_rate, QFlux_WP	Local to CDSP Environment
pH_CSNF_early_high	Determine whether to use the pH bound of 8.1 or the value of pH_CSNF_early_high_b	pH_CSNF_early_high_b OR 8.1 depending on QFlux_WP	Local to CSNF Environment
pH_CSNF_early_low	Determine whether to use the pH bound of 8.1 or the value of pH_CSNF_early_low_b	pH_CSNF_early_low_b OR 8.1 depending on QFlux_WP	Local to CSNF Environment
pH_CSNF_late_high	Determine whether to use the pH bound of 8.1 or the value of pH_CSNF_late_high_b	pH_CSNF_late_high_b OR 8.1 depending on QFlux_WP	Local to CSNF Environment
pH_CSNF_late_low	Determine whether to use the pH bound of 8.1 or the value of pH_CSNF_late_low_b	pH_CSNF_late_low_b OR 8.1 depending on QFlux_WP	Local to CSNF Environment
pH_CDSP_early_high	Determine whether to use the pH bound of 8.1 or the value of pH_CDSP_early_high_b	pH_CDSP_early_high_b OR 8.1 depending on QFlux_WP	Local to CDSP Environment
pH_CDSP_early_low	Determine whether to use the pH bound of 8.1 or the value of pH_CDSP_early_low_b	pH_CDSP_early_low_b OR 8.1 depending on QFlux_WP	Local to CDSP Environment
pH_CDSP_late_high	Determine whether to use the pH bound of 8.1 or the value of pH_CDSP_late_high_b	pH_CDSP_late_high_b OR 8.1 depending on QFlux_WP	Local to CDSP Environment
pH_CDSP_late_low	Determine whether to use the pH bound of 8.1 or the value of pH_CDSP_late_low_b	pH_CDSP_late_low_b OR 8.1 depending on QFlux_WP	Local to CDSP Environment
Fuel_Exposed	Calculate cladding coverage for model calculations	if((Etime = 0 {year}) OR (~Avg_Clad_Failed<=0),1 Else ~Avg_Clad_Failed	Local to CSNF Environment
pH_CSNF_early	Random pH for CSNF packages, early time step	pH_CSNF_early_low + pH_Random*(pH_CSNF_early_high - pH_CSNF_early_low)	Local to CSNF Environment

Table 6-40. Parameter Details for Supplemental TSPA-SR Parameters (Continued)

TSPA Parameter	Description	Parameter Value/Other Inputs	Applicability
pH_CSNF_late	Random pH for CSNF packages, late time step	$\text{pH_CSNF_late_low} + \text{pH_Random} * (\text{pH_CSNF_late_high} - \text{pH_CSNF_late_low})$	Local to CSNF Environment
pH_CSNF	Time related switch for using early or late pH in CSNF packages	If Avg_Pkg_Failtime < 1000 year, pH_CSNF_early Else pH_CSNF_late	Local to CSNF Environment
pH_CDSP_early	Random pH for CDSP packages, early time step	$\text{pH_CDSP_early_low} + \text{pH_Random} * (\text{pH_CDSP_early_high} - \text{pH_CDSP_early_low})$	Local to CDSP Environment
pH_CDSP_late	Random pH for CDSP packages, late time step	$\text{pH_CDSP_late_low} + \text{pH_Random} * (\text{pH_CDSP_late_high} - \text{pH_CDSP_late_low})$	Local to CDSP Environment
pH_CDSP	Time related switch for using early or late pH in CDSP packages	If Avg_Pkg_Failtime < 1000 year, pH_CDSP_early Else pH_CDSP_late	Local to CDSP Environment
Ionic_Str_CSNF	Time related switch for using early or late ionic strength distributions in CSNF packages	If Avg_Pkg_Failtime < 1000 year, Ionic_Str_CSNF_early Else Ionic_Str_CSNF_late	Local to CSNF Environment
Ionic_Str_CDSP	Time related switch for using early or late ionic strength distributions in CDSP packages	If Avg_Pkg_Failtime < 1000 year, Ionic_Str_CDSP_early Else Ionic_Str_CDSP_late	Local to CDSP Environment
fCO2	Convert CO ₂ fugacity log values to CO ₂ fugacity values	$10^{\text{log_fCO2}}$	Global
fO2	Convert O ₂ fugacity log values to CO ₂ fugacity values	$10^{\text{log_fO2}}$	Global

Table 6-41. Other TSPA-SR Model Parameters with In-Package Chemistry Component Impacts

Description	TSPA Parameter	TSPA Model Reference	Applicability
Average elapsed time of package failures	Avg_Pkg_Failtime	Section 6.3.3 Waste Package Degradation	Local to Environment
CSNF waste package cladding coverage	Avg_Clad_Failed	Section 6.3.4.3 Cladding Degradation Model	Local to CSNF Environment
Seepage flux through waste package	QFlux_WP	Section 6.3.5.1 EBS Flow and Transport Pathways	Local to Environment
Parameter for assessment of initial perforations	Gap_Distribution	Section 6.3.1.1 Radionuclide Inventory	Global
Parameter for assessment of initial perforations	Total_Initial_Perforation	Section 6.3.4.3 Cladding Degradation Model	Local to Environment

Table 6-41 tabulates the TSPA model parameters which are not inputs, but are other TSPA model parameters calculated in other sections of the model and used during the in-package chemistry calculations.

Results and Verification

The TSPA-SR model calculates pH time histories for each of the two waste package types in each of the bin environments. The results are a time-dependant profile for each specific environment. The environment-specific time histories for the inner-package pH of the CSNF and CDSP waste packages in bin 4 are shown in Figure 6-99 and Figure 6-100. These temporal profiles are results from the base-case median value simulation. Note that in Figure 6-99 and Figure 6-100 the x-axis corresponds to the time since the initiation of the simulation and not the time since waste package breach. The time histories show a jump in pH corresponding to a change in the time phase from early to late. Prior to this time, the pH results correspond to the early phase equations, beyond this time the results correspond to the late phase equations.

The pH in the waste package remains constant until the waste packages begin to fail. In the median value simulation the CSNF waste packages begin to fail at 42,500 years in the Bin 4 Always Drip environment, 41,000 years in the Bin 4 Intermittent Drip environment, and 40,500 years in the Bin 4 No Drip environment. Prior to failure the pH is equal to the predefined value of 5.0. Once the waste packages begin failing, the pH is subject to change. In the early time, the pH inside the waste packages in each CSNF bin 4 environment is 3.44446. At early times, the dissolution of carbon steel and coincident production of protons causes the solution to be acidic. After 1,000 years, the late phase, the carbon steel is exhausted and the pH increases. Figure 6-99 shows the pH histories for CSNF waste packages in Bin 4. The solid black line represents the Always Drip environment in Bin 4, the red line represents the Intermittent Drip environment and the blue line the No Drip environment.

The calculated pHs for the CSNF waste packages in Bin 4 environments have a minimum pH equal to 3.446 and a maximum pH equal to 8.1. The reported minimum pH for CSNF waste packages is 3.4179, the reported averages range from 6.0356 to 7.3336 (CRWMS M&O 2000 [129287], Section 6.1.1). The TSPA-SR model calculations are within the calculated range of the abstracted data, even though the flux values exceed the flux data used in the pH abstraction.

The pH of the CDSP waste packages is shown in Figure 6-100. In the median value simulation the CDSP waste packages begin to fail at 44,500 years in the Bin 4 Always Drip environment, 41,500 years in the Bin 4 Intermittent Drip environment, and 40,500 years in the Bin 4 No Drip environment. The solid black line represents the Always Drip environment in Bin 4, the red line represents the Intermittent Drip environment and the blue line the No Drip environment. The early time phase shows no change in pH under the calculated conditions and it can be stated that the Q_{Flux_WP} contribution is negligible at early times after package failure. The switch from the early phase to the late phase is readily apparent in Figure 6-100. The increase in pH at 46,500 years, 43,000 years, and 43,000 years in the Always Drip, Intermittent Drip, and No Drip bin environments, respectively, is a result in the time phase calculation change. After the time switch the pH in the Always Drip and Intermittent Drip environments are constant, then begin to decline until the flux through the waste package exceeds the limits in Table 6-39 at which point the pH stabilizes to the bounding limit, 8.1.

The total carbonate is a function of pH and is used exclusively for waste form degradation calculations for the CSNF waste packages. The calculated time histories for the median value simulation total carbonate concentrations are presented in Figure 6-101.

The carbon dioxide fugacity, oxygen fugacity, and chloride ion concentration are globally defined as constants (see Table 6-38). These values do not change over time.

In the TSPA-SR model the ionic strength is a function of package failure and is implemented as a set of stochastic parameters inside each bin environment. The ionic strength is scheduled to change 1,000 years after package failure. The time history results for the three CSNF bin 4 environments for the base case median value simulation is presented in Figure 6-102. Note that the x-axis represents the absolute time, the elapsed simulation time and not the time since first breach. The ionic strength is initially 0.00281 molal. Once the TSPA-SR parameter *Avg_Pkg_Failtime* exceeds 1,000 years in each environment, the environment specific ionic strength switches to the late phase ionic strength 0.0150 molal. The value of *Avg_Pkg_Failtime* exceeds 1,000 years on the 44,000 year time step for the Always Drip and No Drip CSNF Bin 4 environment, on the 43,500 year time step for the Intermittent Drip CSNF Bin 4 environment, and on the 43,000 year time step for the No Drip time step.

The in-package pHs for the three environments in bin 4 were calculated manually to verify the model computations. Comparisons were performed for the median value simulation. Two time steps for each bin were selected to verify the pH calculations, one in the early phase and one in the late phase. The *Avg_Pkg_Failtime* parameter for each environment was extracted from the waste package degradation component to determine the early and late phases. The data were evaluated and found to have only one or two time steps within the first 1,000 years after breach. The later value of these time steps was selected for verification of the early time phase calculations. The required data for the identified time step was recorded and tabulated. For the late phase calculations the model results calculated at time equals 200,000 years were extracted and documented. The recorded values were used for the hand calculations comparisons performed to verify the model calculations. The appropriate *Avg_Clad_Failed* and *QFlux_WP* parameters were identified for the CSNF waste packages. The appropriate *rel_diss_rate* and *QFlux_WP* parameters were identified for the CDSP waste packages. The pH bounds were calculated using the applicable Response Surface equations from Table 6-36 and Table 6-37. The results are presented in Table 6-42.

Table 6-42 shows that the pH results for each environment in bin 4 are between the boundaries calculated using the Response Surface equations. Furthermore, for the median value simulation, the value of *pH_random* is 0.5, the mean of the uniform distribution between 0 and 1. The difference between the two bounding pHs is multiplied by *pH_random* and added to the lower of the two values is the calculated pH. This value equals the value reported by the model for the median value simulation. Thus the pH calculations are implemented correctly in the TSPA-SR model.

Table 6-42. pH Calculation Verification for the Median Value Simulation

TSPA Parameter	Time Phase	Response Surface	Fuel Exposed/ Rel Diss Rate	Qflux_WP (m ³ /year)	Calculated pH Bound	Calculated pH	Observed pH
pH_CSNF Always Drip (t=43,500 years)	Early	1	1	0	3.4916	3.4447	3.4447
	Early	2	1	0	3.3977		
pH_CSNF Intermittent Drip (t=42,000 years)	Early	1	1	0	3.4916	3.4447	3.4447
	Early	2	1	0	3.3977		
pH_CSNF No Drip (t=42,000 years)	Early	1	1	0	3.4916	3.4447	3.4447
	Early	2	1	0	3.3977		
pH_CSNF Always Drip (t=200,000 years)	Late	3	0.1739	0.4694	8.3768	8.1	8.1
	Late	4	0.1739	0.4694	6.9297		
pH_CSNF Intermittent Drip (t=200,000 years)	Late	3	0.2471	0.9382	10.1919	8.1	8.1
	Late	4	0.2471	0.9382	7.4883		
pH_CSNF No Drip (t=200,000 years)	Late	3	0.0708	0	6.6872	6.5650	6.5650
	Late	4	0.0708	0	6.4429		
pH_CDSP Always Drip (t=98,000 years)	Early	5	1	0.007857	5.2231	8.8636	8.8636
	Early	6	1	0.007857	4.8218		
pH_CDSP Intermittent Drip (t=100,000 years)	Early	5	1	0.018713	5.2520	8.8281	8.8281
	Early	6	1	0.018713	4.8298		
pH_CDSP No Drip (t=98,000 years)	Early	5	1	0	5.2021	8.8893	8.8893
	Early	6	1	0	4.8161		
pH_CDSP Always Drip (t=200,000 years)	Late	7	1	0.526657	6.7653	8.1	8.1
	Late	8	1	0.526657	7.5662		
pH_CDSP Intermittent Drip(t=200,000 years)	Late	7	1	0.997207	5.1572	8.1	8.1
	Late	8	1	0.997207	6.0943		
pH_CDSP No Drip (t=200,000 years)	Late	7	1	0	8.5650	8.8893	8.8893
	Late	8	1	0	9.2136		

The median value simulation results verify that the calculated pH values throughout the entire time history are within the bounds stated in the feed AMR, *In-Package Chemistry Abstraction* (CRWMS M&O 2000 [129287]). Furthermore, since the hand calculations using the extracted values for the *Avg_Clad_Failed* and *QFlux_WP* from the actual source components within the

TSPA-SR model, equaled the model results, it is verified that the model sends and receives parameter values accurately between the different model components.

The total carbonate concentration is a function of pH and varies over time. The total carbonate concentration profile for the expected value simulation in CSNF bin 4 is presented in Figure 6-101. The equation for calculating the total carbonate concentration, $Total_CO_3$, (see Table 6-38) was taken directly from the AMR, *In-Package Chemistry Abstraction* (CRWMS M&O 2000 [129287], Section 6.2, Table 14). To verify that the calculation is implemented correctly, the total carbonate concentration for each environment in bin 4 was manually calculated. The pH in each environment for one time step, $t=100,000$ years, was identified for the median value simulation. The total carbonate concentration is calculated for each environment in each case for the appropriate time step and compared to the model result. Table 6-43 presents the results of this analysis.

Table 6-43. Total Carbonate Concentration Calculation Verification for the Median Value Simulation

Location	Observed pH	Calculated CO_3 Concentration (molal)	Model CO_3 Concentration (molal)
Always Drip	6.7284	0.04253	0.04253
Intermittent Drip	6.7445	0.04414	0.04414
Never Drip	6.7107	0.04084	0.04084

The calculated values using the pH extracted from the TSPA-SR model at time step 100,000 years equal the model results reported for this time step. This verifies that the model implementation is correct and furthermore, this verifies that the software sends and receives values properly between the model components.

The values assigned to the carbon dioxide fugacity, fCO_2 , oxygen fugacity, fO_2 , and chloride concentration, Cl , are constants.

The in-package ionic strength parameters are stochastic parameters that are applicable at two different time phases. The switch from the early phase to the late phase must be verified. The differentiation of the early phase and late phase is the environment specific time since waste package failure. The ionic strength should switch from the early phase values to the late phase values 1,000 years after the average package fails. In the median value simulation, the CDSP No Drip environment in bin 4 was chosen to verify the switch implementation. The switch logic is the same for the other bin environments and will behave similarly.

An evaluation of the *CDSP_NoDrip* source term reveals that packages in this environment begin to fail at $t=40,500$ years. At $t=42,000$ years the value of *Avg_Pkg_Failtime* equals 777.8 years and 1045.4 years at $t=42,500$ years. Thus at time steps before and including 42,000 years, up to 1,000 years after packages begin failing, the selector switch *Ionic_Str_CDSP* should equal the value assigned to *Ionic_Str_CDSP_early*. The value assigned to *Ionic_Str_CDSP_early* equals 0.003263 molal. The value of *Ionic_Str_CDSP* at $t=42,000$ years equals 0.003263. At all time steps after 42,000 years the value assigned to *Ionic_Str_CDSP* equals the value assigned to *Ionic_Str_CDSP_late*. For the median value simulation this value is 0.03376. A review of the

data set plotted for the time history for the selector switch *Ionic_Str_CSNF* shown in Figure 6-102 verifies that the selector switch is working properly and the correct ionic strength is being reported.

Figure 6-103 shows a plot of failed waste packages, previous time-step average waste package failure time, and average waste package failure time for the CSNF Bin 4 Intermittent Drip environment. As seen in the figure, a single waste package fails at 41,000 years (note that *Failed_Pkgs_PrevTime* is equal to *CSNF_IntermittentDrip.Failed_Packages*); at this time the *AvgPkg_Failtime* and *AvgPkg_FailTime_PrevTime* are both equal to 0 years. At the next time step (41,500 years) no further packages fail, the *AvgPkg_FailTime_PrevTime* is equal to 0 years (value of *AvgPkg_Failtime* at the previous timestep) and *AvgPkg_Failtime* is equal to 500 years (sum of *AvgPkg_Failtime* and the *MasterClock.Timestep_Length* (500 years)) multiplied by the value of *Failed_Pkgs_PrevTime* from the previous timestep (1 package) divided by the number of failed packages at the current timestep (*CSNF_IntermittentDrip.Failed_Packages*). When another package fails at 42,000 years, the sum of sum of *AvgPkg_Failtime* and the *MasterClock.Timestep_Length* (1,000 years) multiplied by *Failed_Pkgs_PrevTime* divided by *CSNF_IntermittentDrip.Failed_Packages* (1/2) is equal to 500 years.

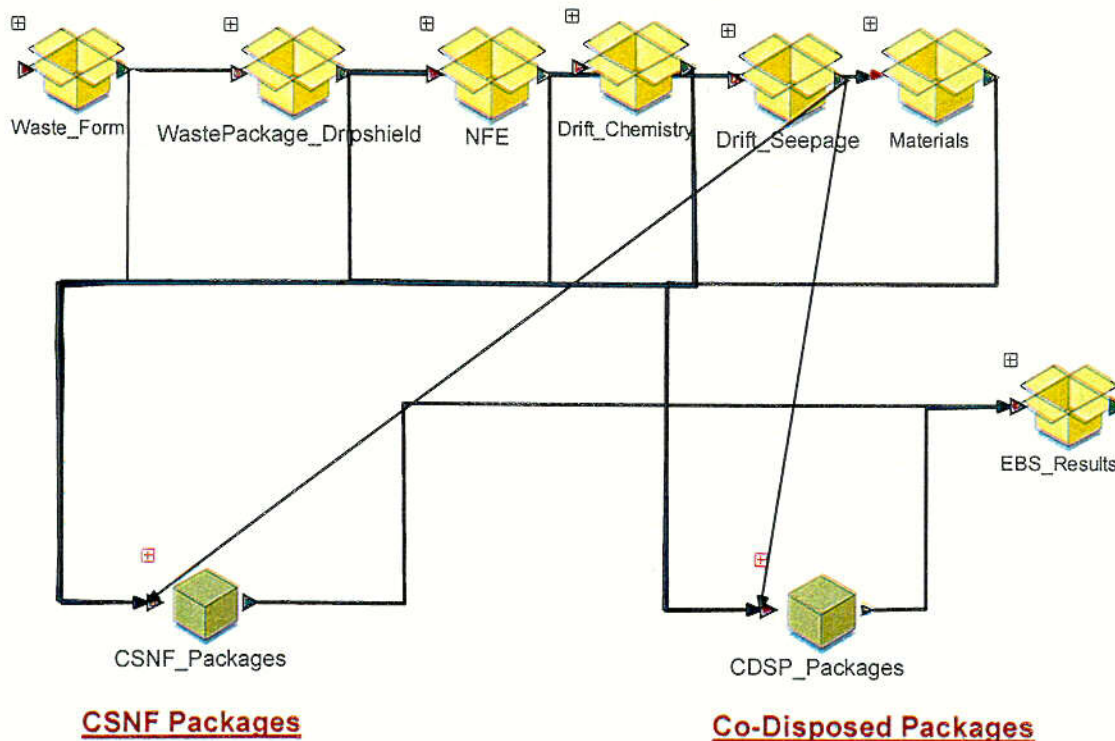


Figure 6-90. Separation of CSNF and CDSP Waste Packages for the pH Calculations

C62

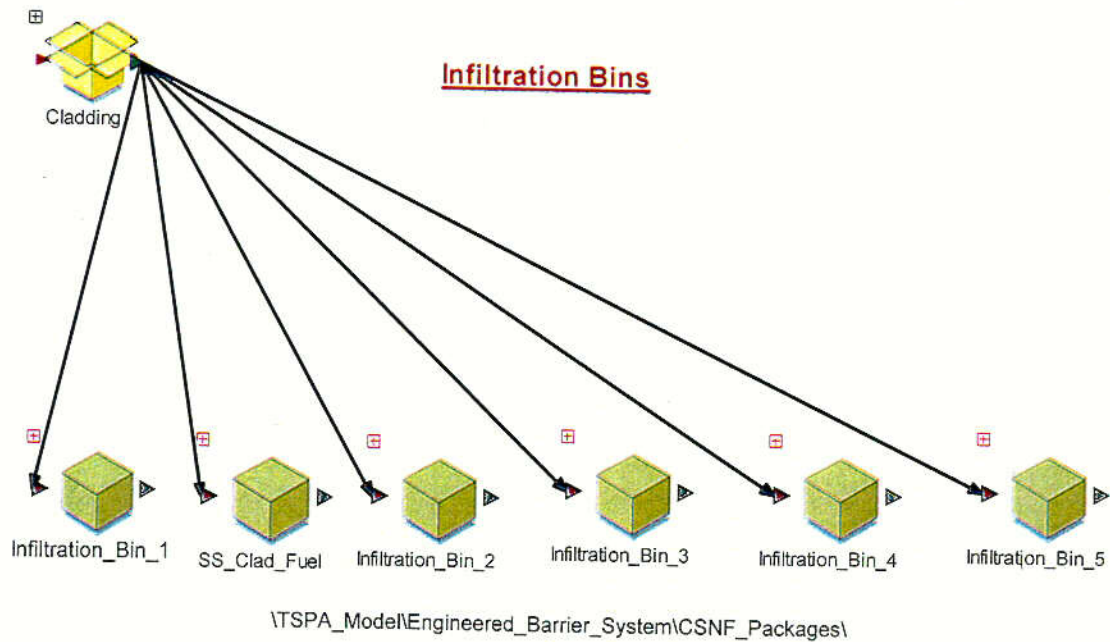


Figure 6-91. Grouping of Waste Package by Bins

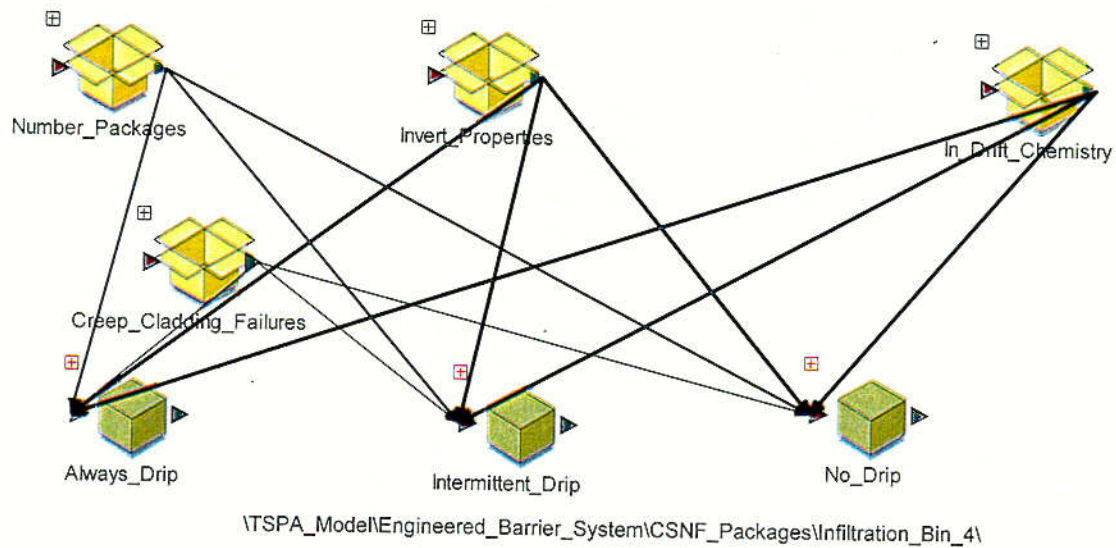
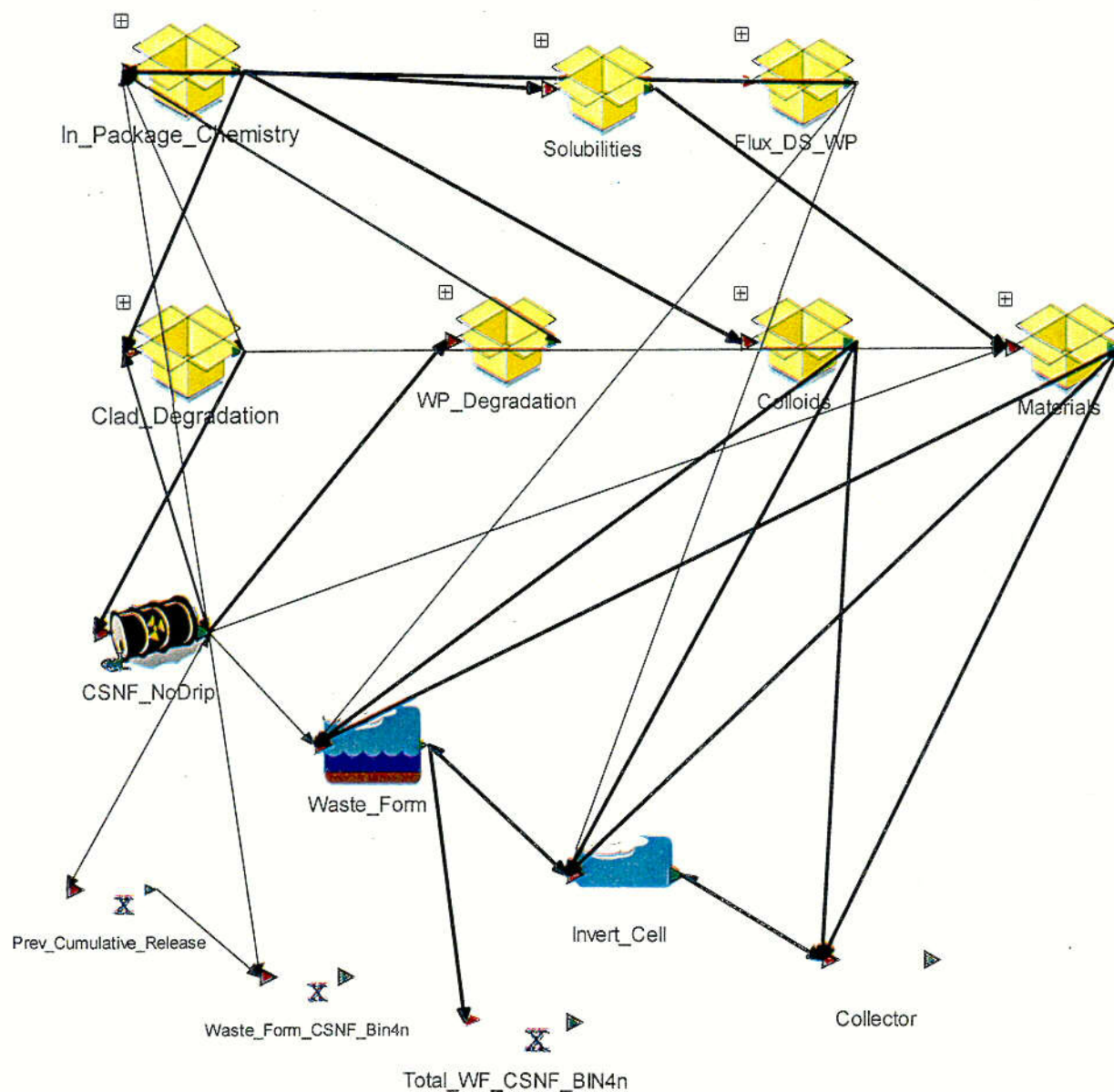


Figure 6-92. Grouping of Waste Packages by Environments within a Bin

C63.



\\TSPA_Model\\Engineered_Barrier_System\\CSNF_Packages\\Infiltration_Bin_4\\Intermittent_Drip\\

Figure 6-93. Calculations within One Bin Environment

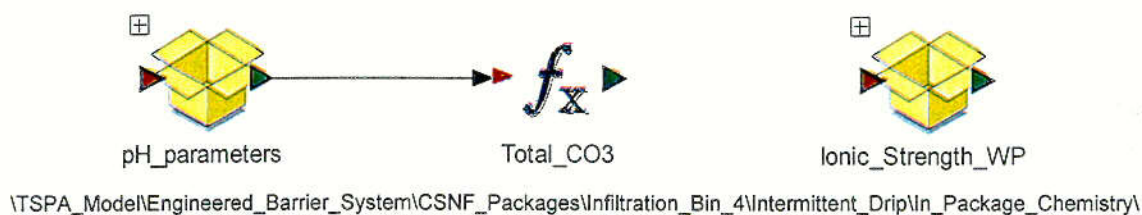
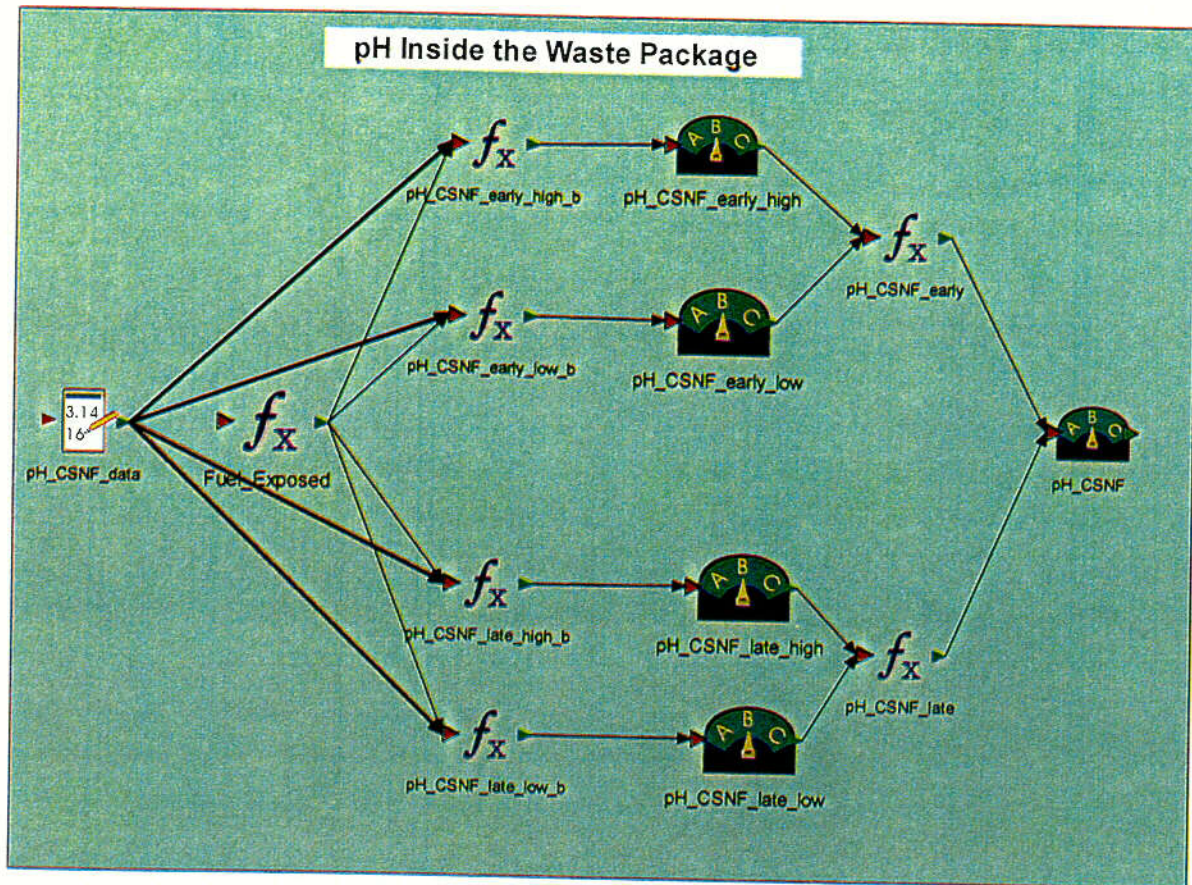


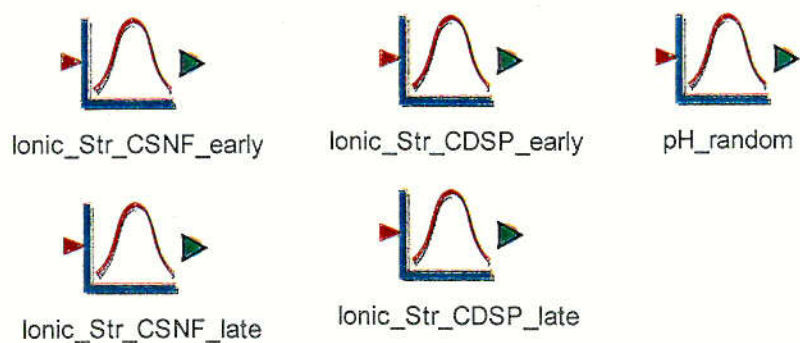
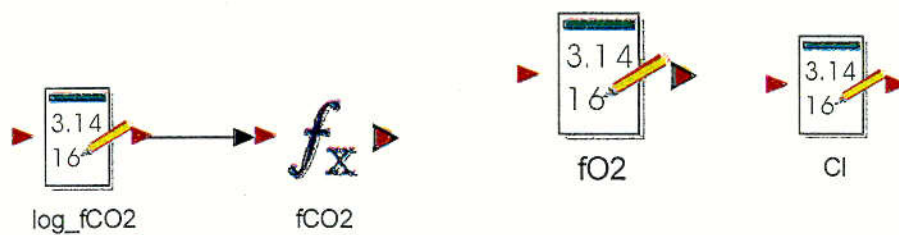
Figure 6-94. Organization of the In-Package Chemistry Calculations



\\TSPA_Model\\Engineered_Barrier_System\\CSNF_Packages\\Infiltration_Bin_4\\Intermittent_Drip\\In_Package_Chemistry\\pH_parameters\\

Figure 6-95. Illustration of the pH Calculation within One Bin Environment

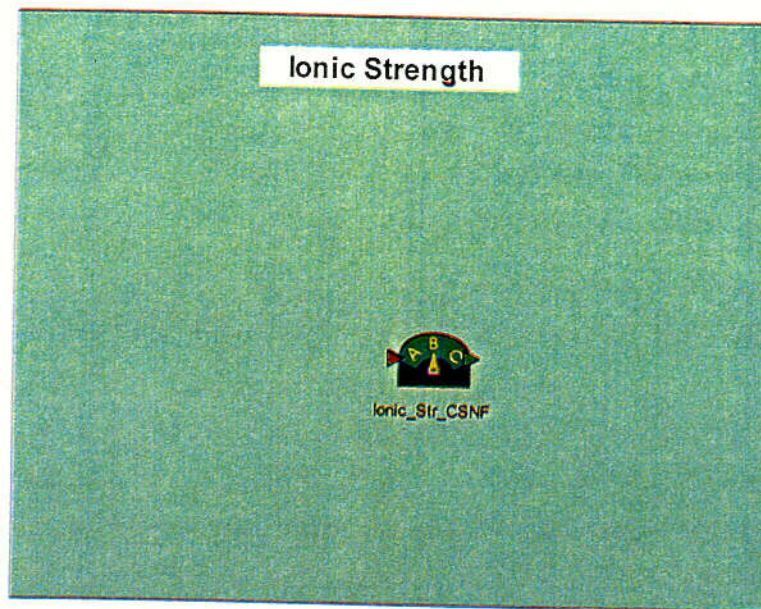
C65



\\TSPA_Model\\Engineered_Barrier_System\\Waste_Form\\In_Package_Chemistry\\

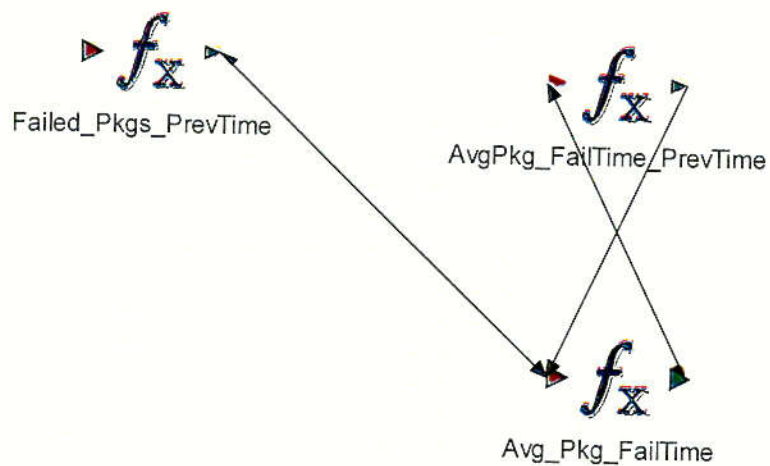
Figure 6-96. Globally Defined In-Package Chemistry Parameters

C66



\\TSPA_Model\\Engineered_Barrier_System\\CSNF_Packages\\Infiltration_Bin_4\\Intermittent_Drip\\In_Package_Chemistry\\Ionic_Stren

Figure 6-97. Locally Defined In-Package Ionic Strength



\\TSPA_Model\\Engineered_Barrier_System\\CSNF_Packages\\Infiltration_Bin_4\\Intermittent_Drip\\WP_Degradation\\

Figure 6-98. Average Package Failure Time Calculation

C67.

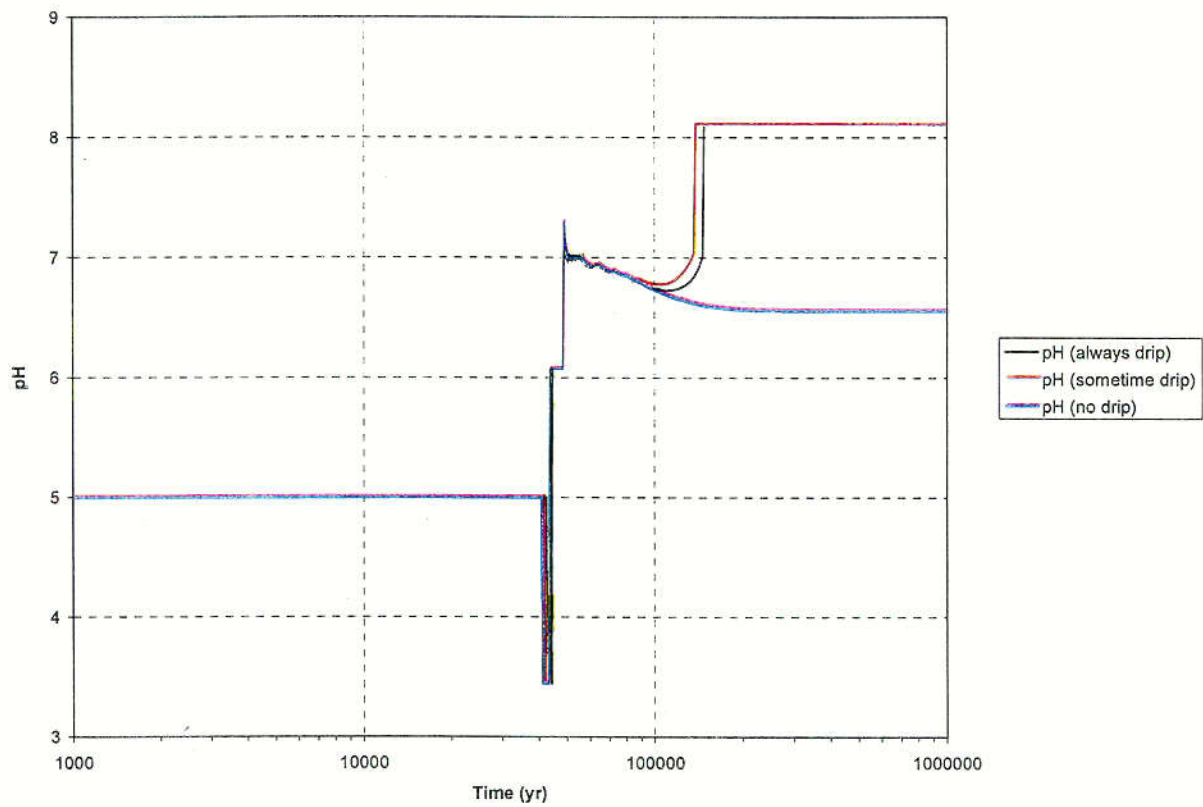


Figure 6-99. Temporal Profile of the In-Package pH of a CSNF Waste Package in Bin 4

C68

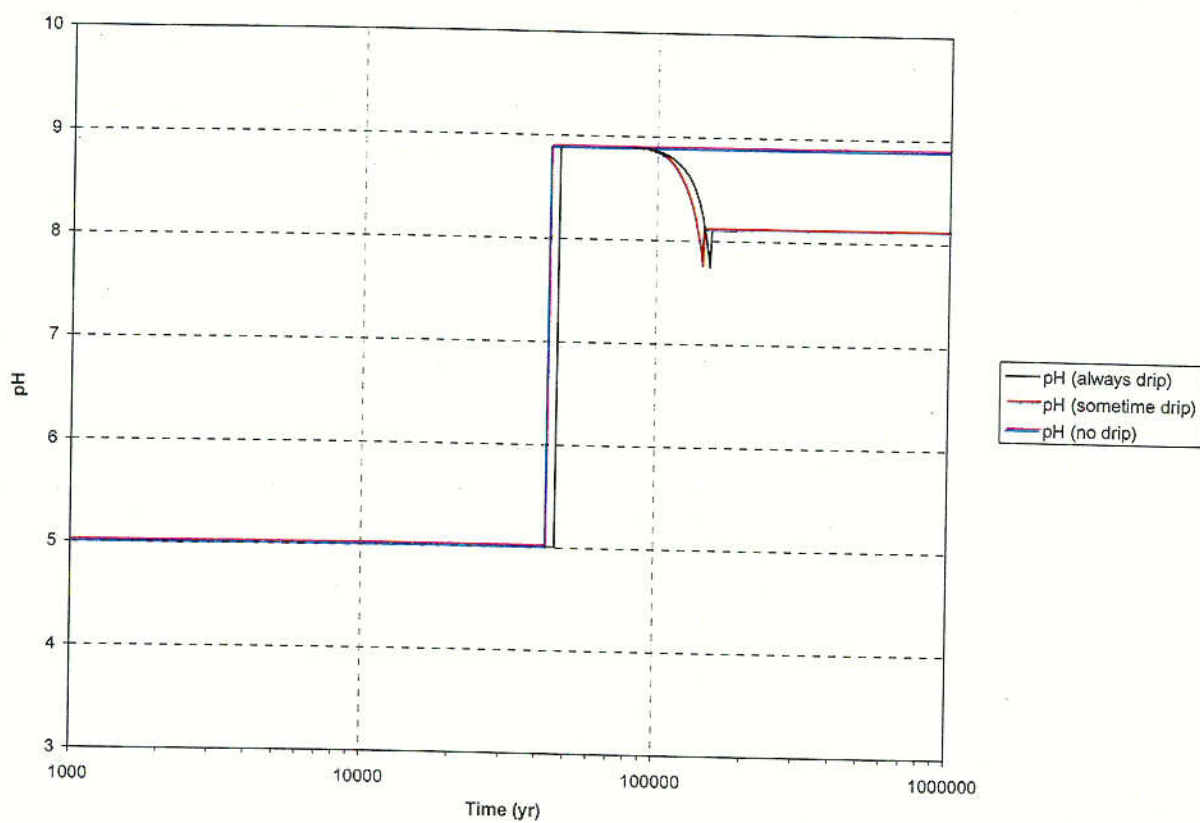


Figure 6-100. Temporal Profile of In-Package pH of a CDSP Waste Package in Bin 4

c69

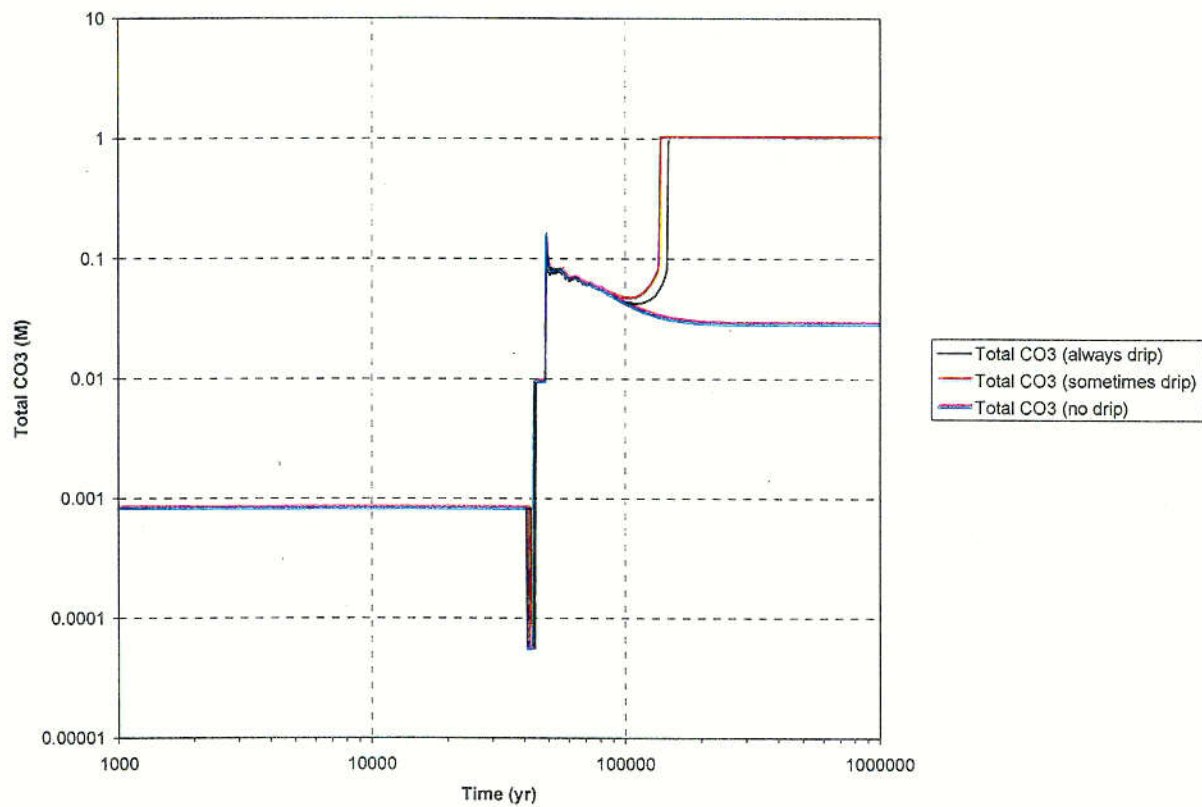


Figure 6-101. Temporal Profile of the Total Carbonate within a CSNF Waste Package in Bin 4

C70

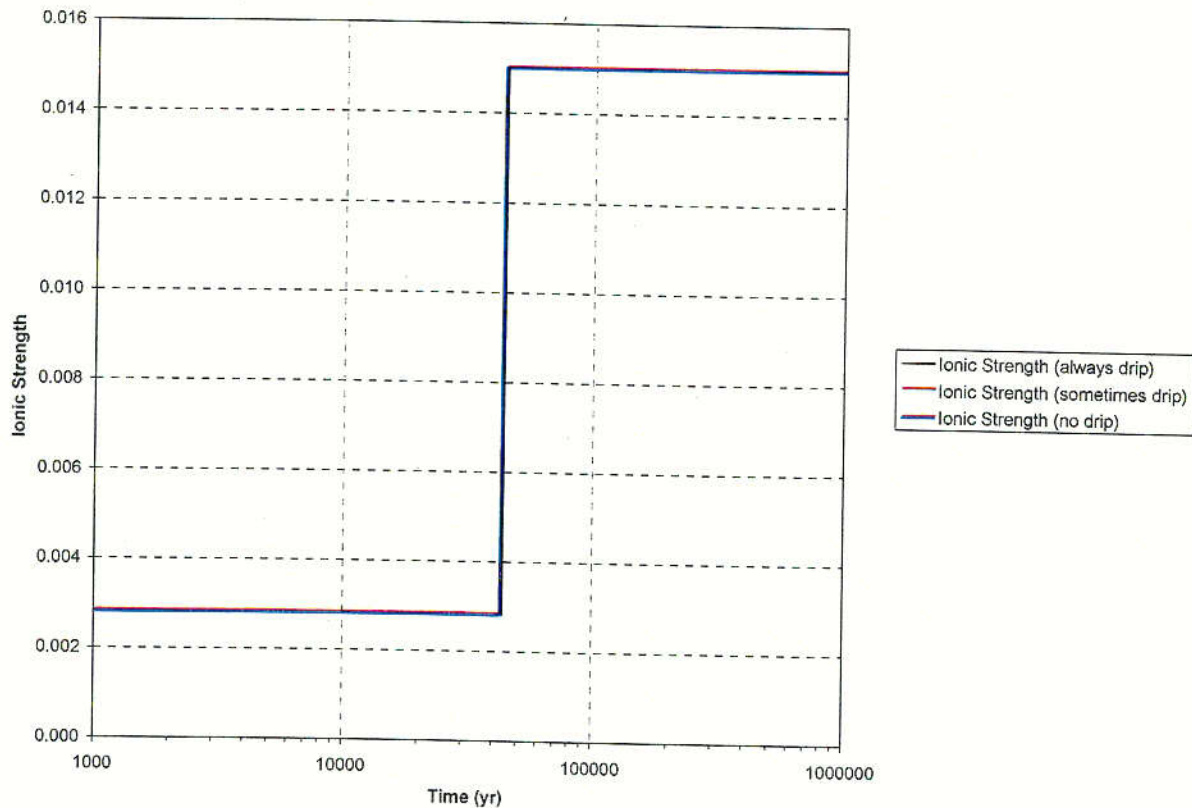


Figure 6-102. Temporal Profile of the Ionic Strength Inside a CSNF Waste Package in Bin 4

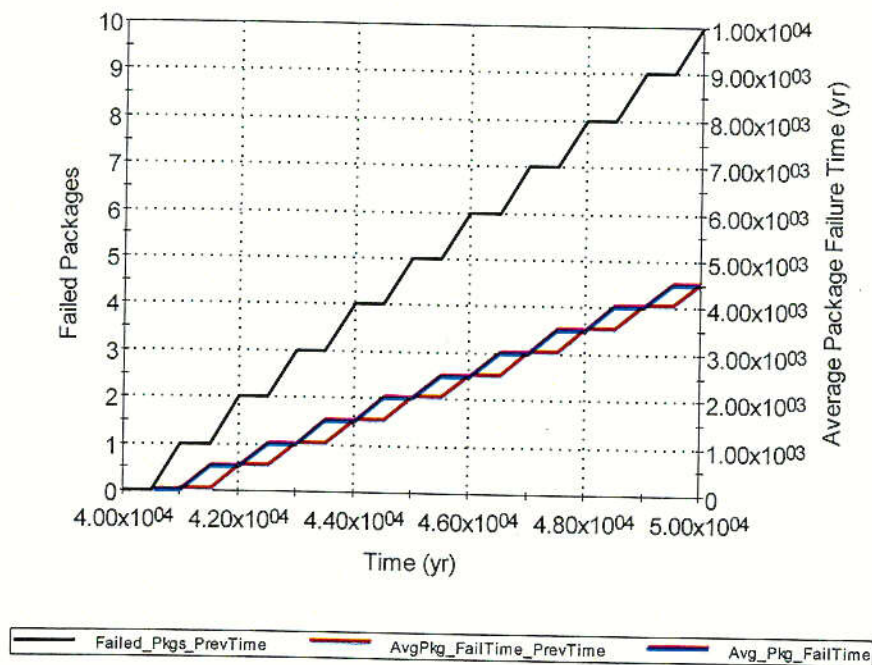


Figure 6-103. Temporal Profile of the Package Failures and Average Package Failure Time (CSNF, Bin 4, Intermittent Drip)

6.3.4.3 Cladding Degradation Model

Overview

This overview section is largely based on the *Clad Degradation—Summary and Abstraction* AMR (CRWMS M&O 2000 [147210]). Commercial Spent Nuclear Fuel (CSNF) is composed of a uranium dioxide matrix that is enriched in ^{235}U , and formed into pellets. The fuel pellets are encased in a thin corrosion resistant protective cladding to form fuel rods. Most CSNF cladding is made of a zirconium alloy known as Zircaloy, which is highly resistant to corrosion. Some of the earlier commercial fuels were fabricated with stainless steel cladding, but because of the superior corrosion resistance and neutronic properties of Zircaloy, all U.S. commercial reactors today use fuels with Zircaloy cladding.

The TSPA cladding degradation model estimates the degradation of CSNF cladding in the repository environment as a function of time. The TSPA-SR CSNF cladding degradation model consists of two basic phases, cladding perforation and cladding unzipping. Cladding perforation is the formation of small cracks or holes in the cladding from various sources ranging from failures during reactor operation to cladding creep rupture during repository storage. Perforation permits the fuel inside the cladding to begin to react with moisture or air and leads to the cladding unzipping phase. In the unzipping phase, the cladding is torn open by the formation of secondary mineral phases on the fuel, the pellets are sufficiently degraded and radionuclides are available for release.

The cladding degradation model defines three main mechanisms for cladding perforation: 1) initial failures during reactor operation, dry storage handling, or transportation, 2) failures from creep strain and stress corrosion cracking (SCC), and 3) failure from corrosion after waste package breach. In addition, a seismic event failure mechanism has been included for cladding failures that are expected to occur in a severe earthquake.

Some of the fuel rods will have failed before emplacement in the repository. The TSPA abstraction for initial (juvenile) cladding failures is represented in the TSPA model by a triangular distribution. Cladding failures due to creep and SCC can occur during dry storage, during transportation, or after emplacement in the repository if the cladding temperature is high enough. Cladding failure due to creep and SCC are represented in the TSPA model as a triangular distribution with the minimum, most likely, and maximum values that are based upon the peak waste package surface temperature experienced after emplacement prior to waste package failure.

If the local environment in a cladding pit or crevice becomes sufficiently reducing, and if a sufficient concentration of oxidizing ions is present and buffer compounds are not present, corrosion will occur. Such corrosion could lead to perforated cladding. Zirconium is known to be susceptible to corrosion by fluorides. Cladding corrosion is modeled as localized corrosion that requires a flux of water to enter the waste package to continually introduce more fluorides. The abstraction for localized corrosion after waste package breach is in terms of a rate of rod perforations proportional to the volume of water that has entered the waste package. The local corrosion uncertainty is expressed in the model as a log-uniform distribution that varies by two orders of magnitude.

Cladding unzipping is assumed to start at waste package failure. Fuel in unbreached waste packages is not subject to alteration because the internal environment is inert. Similarly, fuel rods with intact cladding will not allow alteration because the fuel is contained and protected by the cladding. Cladding damage may exist at the time of emplacement, or it may occur in the repository. Under wet/humid air conditions, the fuel matrix is assumed to react at the intrinsic dissolution rate and precipitate locally as metaschoepite. This secondary phase isolates most of the fuel from the moisture but the fuel in the split cladding region continues to react, increasing volume, and forcing the split further along the cladding. Such alteration results in significant volume expansion, so the cladding breach will eventually propagate from its original location to the ends of the rod. The time it takes a rod to unzip is the unzipping velocity multiplied by one-half the length of a CSNF rod. It is conservatively assumed that a perforation occurs in the center of a fuel rod and propagates in both directions to the ends of the rod. The unzipping velocity is treated as a multiple of the intrinsic dissolution rate. The cladding degradation abstraction provides an optimistic, a nominal, and a conservative estimate of the ratio of the unzipping velocity to the intrinsic dissolution rate. These estimates are used to define a triangular distribution that is multiplied by the intrinsic dissolution rate to determine the unzipping velocity. Unzipping occurs only after the waste package has failed and the inner cladding barrier is breached.

A seismic analysis has shown that a severe earthquake (a once in a million years event) would fail most of the fuel rods, but a more moderate frequency event would fail no rods. Within the TSPA-SR model, a seismic event is included as part of the cladding model, and when this event occurs, all the cladding is assumed to fail. The event frequency is 1.1×10^{-6} events per year. (CRWMS M&O 2000 [147210], Section 6.4.1)

Stainless steel clad CSNF fuel is modeled separately. The TSPA model does not take any cladding credit for stainless steel clad fuel which accounts for 1.1 percent of the total commercial spent fuel to be placed into the repository. The stainless steel cladding is assumed to be perforated when the waste package fails, and is therefore immediately available for unzipping upon waste package failure. (CRWMS M&O 2000 [147210], Section 6.7)

Inputs to the TSPA Model

The data inputs to the TSPA model for cladding degradation are listed in Table 6-44. A detailed discussion on the TSPA cladding degradation model can be found in *Clad Degradation-Summary and Abstraction* (CRWMS M&O 2000 [147210]).

Table 6-44. Data Inputs to the TSPA Model for Cladding Degradation

Parameter Name	Description	Parameter Value	Reference AMR
Initial_Rod_Failures	Initial cladding failures (%)	Triangular (0.0155, 0.0948, 1.29)	CRWMS M&O 2000 [147210], Sections 6.1 & 7
Creep_Used_Bin1 Creep_Used_Bin2 Creep_Used_Bin3 Creep_Used_Bin4 Creep_Used_Bin5	Fraction of cladding perforated due to creep and SCC (based on peak WP temp. in each bin)	Triangular (Creep_Min, Creep_Mean, Creep_Max)	CRWMS M&O 2000 [147210], Section 6.2.4

Table 6-44. Data Inputs to the TSPA Model for Cladding Degradation (Continued)

Parameter Name	Description	Parameter Value	Reference AMR
Creep_Min, Creep_Mean, Creep_Max	Min., max., and most likely creep failure fractions (function of peak WP temperature)	See Table 6-2	CRWMS M&O 2000 [147210] Section 6.2.4, Table 5
LC_uncert	Localized corrosion rate uncertainty	Log-uniform (0.1-10)	CRWMS M&O 2000 [147210] Section 6.3 and Attachment I
LC_Flux_Term	Volume of seepage in a WP to fail all cladding via corrosion	2424 m ³	CRWMS M&O 2000 [147210] Sections 6.3 & 7
CF_Int_Diss_Velocity	Conversion factor for the intrinsic dissolution velocity	2.190E-5 (cm/yr)/((mg/m ²)/day)	CRWMS M&O 2000 [147210] Attachment I, Line 75
Length_Rod	Spent fuel rod length	3.66 m	CRWMS M&O 2000 [147210] Attachment I
a0	Dissolution rate parameter	pH > 7 = 4.69 pH ≤ 7 = 7.13	CRWMS M&O 2000 [147210] Section 6.6.2, Table 8 & Attachment I
a1	Dissolution rate parameter	-1085	CRWMS M&O 2000 [147210] Section 6.6.2, Table 8 & Attachment I
a2	Dissolution rate parameter	pH > 7 = -0.12 pH ≤ 7 = 0	CRWMS M&O 2000 [147210] Section 6.6.2, Table 8 & Attachment I
a3	Dissolution rate parameter	-0.32	CRWMS M&O 2000 [147210] Section 6.6.2, Table 8 & Attachment I
a4	Dissolution rate parameter	pH > 7 = 0 pH ≤ 7 = -0.41	CRWMS M&O 2000 [147210] Section 6.6.2, Table 8 & Attachment I
Uncert_a0	Uncertainty term for dissolution rate parameter a0	Uniform (-1,1)	CRWMS M&O 2000 [147210] Attachment I
Unzip_uncert	Unzipping velocity uncertainty	Triangular (1, 40, 240)	CRWMS M&O 2000 [147210] Sections 6.6.1, 7 and Attachment I
SS_Fraction	Fraction of fuel (in those packages that contain stainless steel clad fuel) that is stainless steel clad	0.329	CRWMS M&O 2000 [147210] Section 6.7
Frac_CSNF_Pkgs_SS	Fraction of CSNF packages that contains stainless steel clad fuel	0.0349	CRWMS M&O 2000 [147210] Section 6.7
Seismic_Clad_Event	Frequency of a very severe seismic event that would fail all cladding	1.1E-06 yr ⁻¹	CRWMS M&O 2000 [147210] Section 6.4.1

DTN: MO0004SPACLD07.043 [151368]

Implementation

Commercial spent nuclear fuel cladding is modeled as degrading in two distinct steps: (1) perforation of the cladding through the formation of small cracks or holes, and (2) unzipping (splitting) of the cladding. The mechanisms for cladding perforation that are modeled in the TSPA are the following:

- Initial failures due to reactor operation, dry storage handling, and transportation
- Creep and stress corrosion cracking
- Localized corrosion
- Stainless steel cladding failures
- Failures due to a very severe seismic event.

The sum of the failed cladding due to initial failures and due to creep and SCC defines the inventory immediately available for unzipping when the waste package fails. Those waste packages that also contain stainless steel clad fuel will have additional initial failures because no credit is taken for stainless steel cladding (i.e., stainless steel cladding is assumed to be perforated when the waste package fails).

Unzipping occurs when the fuel matrix is exposed to wet/humid air conditions, which causes the fuel matrix to alter to form a different mineral phase. If alteration results in significant volume expansion, the cladding breach will propagate (unzip) from its original location to the ends of the rods. The unzipping time is a function of temperature, pH, and in-package chemistry (in-package chemistry is discussed in Section 6.3.4.2) (CRWMS M&O 2000 [147210], Section 6.6). To determine the inventory of radionuclides that is available for release, it is necessary to have a means for predicting the fraction of breached waste packages, the fraction of fuel rods with cladding breaches, and the speed of propagation of a split.

An overview of the implementation of the TSPA cladding degradation model is illustrated in Figure 6-104. The container *Clad* holds the containers that determine localized corrosion of the cladding after waste package failure and the dissolution rate of the fuel matrix. These containers are shown in Figures 6-105, 6-106, and Figure 6-107 show the global cladding parameters that are common to all the cladding model logic (i.e., they are the same for all bins).

Initial Cladding Failures. The condition of the CSNF cladding as it is received at the repository site establishes the initial boundary condition for the subsequent analysis of degradation of the cladding in the repository. It defines the fraction of fuel rods that are perforated before emplacement in the repository and thus the fraction immediately available for cladding unzipping when the waste package fails. The cladding degradation abstraction AMR provides an abstraction for the initial cladding failures that occur due to reactor operation, dry storage handling, and transportation. This abstraction defines the single initial failure percentage for the fuel rods in a waste package for all five bins or groups of waste packages defined in the TSPA. The initial cladding failure percentage is defined as a triangular distribution with the minimum equal to 0.0155, the best estimate equal to 0.0948, and the maximum equal to 1.285 percent (CRWMS M&O 2000 [147210], Section 6.1). This stochastic element is shown in Figure 6-107 as Initial_Rod_Failures.

Creep and SCC Failures. Cladding failures due to creep and SCC can occur during dry storage, during transportation, or after emplacement in the repository if the cladding temperature is high enough. The cladding degradation AMR provides an abstraction for cladding failures due to creep and SCC (CRWMS M&O 2000 [147210], Section 6.2). This abstraction uses the peak waste package surface temperature to define a triangular distribution for the fraction of rod perforated due to creep and SCC. The peak waste package temperature in each repository bin is used to define the triangular distribution for the fraction of rods perforated per waste package for that bin using Table 6-45.

Table 6-45. Fraction of Rods Perforated from Creep as a Function of Peak Waste Package Surface Temperature

Peak Waste Package Surface Temperature (C)	Lower limit	Mean Failure Fraction	Upper Limit
≤177	0.0105	0.0244	0.1942
227	0.0105	0.0244	0.1949
252	0.0105	0.0258	0.2057
262	0.0105	0.0267	0.2156
277	0.0106	0.0339	0.2479
292	0.0120	0.0604	0.3264
297	0.0133	0.0783	0.3628
302	0.0173	0.0987	0.4080
312	0.0370	0.1622	0.5052
327	0.1067	0.3019	0.6379
352	0.3424	0.5567	0.8227
377	0.5920	0.7789	0.9553
402	0.7986	0.9302	0.9970
≥412	0.8720	0.9658	0.9985

DTN: MO0004SPACLD07.043 [151368]

The one-dimensional tables illustrated in Figure 6-108 specify the fraction of cladding that experiences creep failure as a function of the peak waste package surface temperature (see Table 6-45). During each realization, the peak waste package temperature is used to define the minimum, mean, and maximum values of the triangular distribution that describes cladding creep failures (*Creep_Used_Bin4*). The peak waste package temperature is determined in the Thermohydrology model, refer to Section 6.3.2.1. The function *Creep_Failure* is an error trapping function for preventing the fraction of cladding failed from exceeding one.

Localized Corrosion. Localized corrosion of cladding by numerous mechanisms including radiolysis, microbial induced corrosion, or fluoride present in Yucca Mountain groundwater is modeled as a cladding perforation mechanism in the TSPA. The resulting model is that the fraction of fuel rods failed by fluoride corrosion starts at zero when the waste package is breached. After breach, the fraction of cladding failed is proportional to the volume of water that has entered the package, reaching one when 2424 m³ of water has entered the waste package. An alternative description is that the fraction of fuel rods that fail in a given year is the volume of water that enters the waste package during that year divided by 2424 m³ (CRWMS M&O 2000 [147210], Section 6.3). The uncertainty range is a factor of ten (10) in either direction, and is defined in the model as a log-uniform distribution ranging from 0.1 to 10. This analysis makes

the rod failure fraction linearly dependent on the water ingress rate (percent failed = $0.0413 \times \text{m}^3 \text{ water in the waste package}$). The water ingress into the waste package increases with time as additional patches open. Water ingress also depends on the location of the waste package group because of different drip rates in different repository regions.

Figure 6-109 shows the TSPA model implementation of local corrosion of cladding within the cladding degradation model. The element *LC_Rate* divides the seepage rate entering the waste package, *QFlux_WP_Clad*, by the volume of water required to fail all fuel rods in a waste package by localized corrosion, *LC_Flux_Term* (2424 m³). Uncertainty in the localized corrosion rate is expressed by a log-uniform distribution that ranges from 0.1 to 10 (*LC_Uncert* is shown in Figure 6-107). Thus, *LC_Slope* gives the fraction of rods failed per year due to localized corrosion at the seepage rate defined by *QFlux_WP_Clad*.

The quantity element *LC_Fraction* is used to accumulate the total fraction of fuel rods that have failed due to localized corrosion. This is done using the consequence generator, *LC_Consequence*, which will add to *LC_Fraction* the fraction of cladding that has failed due to localized corrosion during each timestep. The fraction of cladding failed due to localized corrosion during each timestep is calculated in *LC_Fraction_Added* by multiplying the fraction of rods failed per year by the timestep length.

The calculation for determining the seepage rate entering the waste package, *QFlux_WP_Clad*, is based upon the seepage rate that would occur at one million years. It was necessary to use the million-year value due to the way GoldSim code simulates the start of inner barrier failure (i.e., cladding). In the TSPA SR model cladding does not begin to fail until after the waste package (i.e., the outer barrier) has been breached. When the outer barrier fails, GoldSim code evaluates the inner barrier failure at a time beginning at zero years. The inner barrier failure curve (*Clad_Fraction_Perforated* is described in the unzipping discussion below) is a function of the localized corrosion rate. When the outer barrier fails as the default GoldSim code would start the calculation for the inner barrier local corrosion rate with the seepage rate into the package that corresponds to time zero (i.e., the time at which the repository is closed). The seepage rate at time zero may be much different than at the time when the waste packages begin failing. Inspection of the seepage flux time histories show that the seepage flux reaches a quasi-steady state by the time when the waste packages start to fail out to a million years. Therefore, the seepage rate at one million years was used to define the seepage rate into the waste packages for the localized corrosion of cladding calculations.

Stainless Steel Clad Fuel. The commercial spent nuclear fuel waste packages that contain stainless steel clad fuel are modeled as a separate group within the total system model. It is expected that 3.49 percent of the CSNF waste packages will contain 32.9 percent stainless steel clad fuel (CRWMS M&O 2000 [147210], Section 6.7). Since the number of waste packages containing stainless steel cladding is small relative to the total number of waste packages, they are not distributed among the five different percolation bins. Instead they are assigned to the bin that covers the largest fraction of the repository. For the mean and high infiltration cases, all waste packages with stainless steel clad fuel assemblies are assigned to the fourth percolation bin of the repository, while for the low infiltration case they are assigned to the first percolation bin. To further simplify the model, all CSNF waste packages that contain stainless steel clad fuel are assigned to the "always dripping" group. This means that these waste packages will have both

advective and diffusive releases to the invert below them, once a waste package fails due to pits or patches.

Within these waste packages, the assumption is that all the stainless steel clad fuel (32.9 percent) is perforated, and thus immediately available for unzipping upon waste package failure. This is implemented by adding the fraction of stainless steel clad fuel, *SS_Fraction*, to the fraction of Zircaloy cladding that is initially perforated. This essentially results in a larger percentage of the fuel in each of these waste packages with initial cladding perforations and thus available for unzipping immediately after waste package failure. Other than this difference, the radionuclide release from these packages through the entire engineered barrier system is modeled like the remaining commercial spent nuclear fuel packages.

Seismic Cladding Event. The clad degradation abstraction indicates that the seismic analysis shows that most fuel rods would fail from a very severe earthquake (once in a million years event), but no rods would fail for more moderate frequency events (CRWMS M&O 2000 [147210], Section 6.4.1). Thus, the seismic failures have been implemented into the TSPA-SR model as a disruptive event. An event generator, *Seismic_Clad_Event*, has been defined to represent a very severe earthquake. The frequency of occurrence is 1.1×10^{-6} (CRWMS M&O 2000 [147210], Section 6.4.1), and the event will cause all the CSNF cladding to fail and therefore be immediately available for unzipping when the waste package fails.

Dissolution Rate. The intrinsic dissolution rate is used in the unzipping calculations to determine the reaction rate velocity. The dissolution rate of CSNF is based on local chemical (in-package) conditions; specifically, pH, temperature, $P(\text{CO}_3)$, and $P(\text{O}_2)$. Refer to Figure 6-110 for the TSPA model implementation of the CSNF intrinsic dissolution rate. The intrinsic dissolution rate, *Log_CSNF_Diss_Rate*, (in $\text{mg}/\text{m}^2\text{-d}$) is defined by the following equation 6-2 (CRWMS M&O 2000 [147210], Section 6.6.2):

$$\text{Log}_{10}(\text{rate}) = a_0 + a_1 / T_k + a_2 * P\text{CO}_3 + a_3 * P\text{O}_2 + a_4 * \text{pH} \quad (\text{Eq. 6-2})$$

Where T_k is the waste package temperature in Kelvin, $P\text{CO}_3$ is $-\log_{10}$ (molar concentration of CO_3), $P\text{O}_2$ is $-\log_{10}$ (partial pressure in atmospheres of O_2), and pH is the pH inside the CSNF waste packages. The coefficients for Equation 6-2 are a function of pH; they are summarized in Table 6-46.

Table 6-46. CSNF Intrinsic Dissolution Rate Equation Coefficients as a Function of pH

In-package pH	Intrinsic Dissolution Rate Coefficients				
	a_0	a_1	a_2	a_3	a_4
pH>7	4.69	-1085	-0.12	-0.32	0
pH≤7	7.13	-1085	0	-0.32	-0.41

DTN: MO0004SPACLD07.043 [151368]

An uncertainty term (*Uncert_a0*) is added to a_0 that is defined as a uniform distribution with a minimum equal to -1 and a maximum equal to 1. Waste package temperature and in-package chemistry change with time, so the intrinsic dissolution rate and therefore the unzipping rate are evaluated during each timestep in a realization.

The values for PCO_3 , PO_2 , and pH are calculated in the in-package chemistry model (parameter names: *Total_CO3*, *fO2*, and *pH_CSNF*) and are described in Section 6.3.4.2. The waste package temperature is determined in the Thermohydrology model, Section 6.3.2.1, and passed to the function *Temp_WP*.

Unzipping. At any time, each fuel rod can be classified as intact, unzipping, or exhausted. Intact fuel rods are those that are protected from alteration and include all fuel rods in intact waste packages and all fuel rods with intact cladding in breached waste packages. Those fuel rods that are in breached waste packages and have breached cladding, but are not yet fully unzipped are said to be unzipping. Those fuel rods that have unzipped all the way to the ends of the fuel rod are exhausted.

The intrinsic dissolution velocity, *Intrinsic_Diss_Velocity*, is found by multiplying the CSNF dissolution rate (*CSNF_Diss_Rate*) by the conversion factor 2.190×10^{-5} cm/yr/(mg/m²-day) to give the unzipping velocity in cm/yr. (CRWMS M&O 2000 [147210], Attachment I, Line 75). The cladding degradation abstraction provides an optimistic, a nominal, and a conservative estimate of the ratio of the unzipping velocity to the intrinsic dissolution rate (CRWMS M&O 2000 [147210], Section 6.6.1). These estimates are used to define a triangular distribution (minimum = 1, best estimate = 40, and maximum = 240) that is multiplied by the intrinsic dissolution rate to determine the unzipping velocity. The unzipping rate, *Unzip_Rate*, is then determined by dividing the unzipping velocity by one-half the fuel rod length. One-half the rod length is used because it is conservatively assumed that each rod perforation begins at the center of the rod and propagates to the ends of the rod. The unzipping rate is used to define the source inventory matrix degradation rate. The TSPA-SR model implementation of cladding unzipping is shown in the lower portion of Figure 6-111.

The total fraction of initially failed rods is the fraction of initially failed rods plus those that experience creep and SCC failure (*Total_Initial_Perforation* = *Initial_Rod_Failures* + *Creep_Failure*). The fraction of cladding perforated (*Clad_Fraction_Perforated*) at any time is determined by adding the total fraction of fuel rods that have failed due to local corrosion (*LC_Fraction*) to the total fraction of initial perforations. The fraction of perforated cladding is used to define the fraction of the inner barrier that has failed (in the CSNF source properties).

Average Fuel Exposed. Fuel that has corroded can have an affect on the in-package chemistry, specifically on the in-package pH. The pH within the package is a function of the fraction of the fuel that is exposed within a failed CSNF waste package (see Section 6.3.4.2). Waste packages are grouped according to the percolation flux ranges and the dripping conditions to which they are exposed. This approach requires calculating an average fuel exposure within a group, since waste packages fail at different times and with different fractions of cladding failures. The methodology for calculating this average cladding fraction is described below. See Figure 6-112 for an illustration of the implementation of this calculation. Refer to Section 6.3.4.2 for the discussion of in-package chemistry.

The amount of radionuclides that are exposed or available for dissolution and transport out of the package is calculated from the fraction of cladding failed at any point in time. A long lived radionuclide like ²³⁸U is chosen as the representative species for doing this calculation to ensure the species is not completely decayed for the duration of the calculation. The total amount of

^{238}U within the group is calculated by multiplying the inventory per package by the total number of packages in the group. Plutonium 242 decays via alpha emission into ^{238}U (Section 6.3.4.1). This addition (in-growth) to the ^{238}U inventory must be determined when calculating the total ^{238}U inventory (*Total_Inventory*). The container *Ingrowth_from_Pu242* contains logic, shown in Figure 6-113, for adding the ingrowth of ^{238}U from the decay of ^{242}Pu . Radioactive decay of ^{238}U and the in-growth of ^{238}U from the decay of ^{242}Pu are factored into the expression *Total_Inventory* to calculate the total amount of ^{238}U at any point in time.

The amount of ^{238}U within the failed waste packages is calculated in the next expression *Failed_Inventory*. This is the amount of ^{238}U that will be exposed once the cladding protection is lost (e.g. (# of failed waste packages)*(total inventory ^{238}U per package)/(# waste packages per group)). The ratio between the amount of ^{238}U that is exposed due to both package and cladding failures to the amount of ^{238}U contained within the failed packages gives the average cladding failed at any point in time. This is calculated using the expression *Avg_Clad_Failed* and is used as input for calculating the pH within the failed waste packages.

Results and Verification

The cladding degradation AMR defines three main mechanisms for cladding perforation: 1) initial failures that are a result of reactor operation, dry storage handling, and transportation, 2) failures from creep strain and stress corrosion cracking (SCC), and 3) failure from corrosion after waste package breach. Table 6-47 shows GoldSim results for the first 100,000 years for the fraction of cladding that has perforated for a median value, one million year simulation in Bin 4 under intermittent dripping conditions. To verify that these results are correct, the three mechanisms for cladding perforation can be summed (using the median values).

The median value (50th percentile) of the triangular distribution (0.0155, 0.0948, 1.29%) that determines the initial cladding failures is 0.417 percent (0.00417). The fraction of cladding that fails due to creep is defined by a triangular distribution that is a function of peak waste package temperature. The peak waste package surface temperature in Bin 4 (*Peak_Temp_CS NF_4*) given in the model is 156.76°C. Table 6-45 (linearly interpolated between points) is used to define the creep failure distribution (triangular) with the minimum equal to 0.0105, the mean equal to 0.0244, and the maximum equal to 0.1942. Therefore, the median value of this triangular distribution is 0.069. The fraction of cladding failed due to localized corrosion is determined by dividing the total seepage into the waste package by 2424 m³. The first two columns of Table 6-48 give the seepage rate time histories into the waste package (*QFlux_WP_Clad*), and the third column was added to give the cumulative seepage into the waste package. At 100,000 years, 93.13 m³ of water has seeped into the waste package, and so the fraction of cladding that would have failed due to localized corrosion is 0.038. Therefore, the total fraction of cladding perforated at 100,000 years is 0.11, which agrees with the GoldSim model result shown in Table 6-47. This verifies that the fraction of cladding perforated is correctly calculated, and that the peak waste package surface temperature and the seepage rate into the waste package are correctly passed to the cladding model.

Table 6-47. GoldSim Results for the Fraction of Cladding that has Perforated in Bin 4 (Intermittent Dripping) Versus Time for a Median Value Simulation

Time (yr)	Cladding Fraction Perforated (Bin 4)
0 – 65,500	0.073489
100,000	0.11191

DTN: MO0009MWDMED01.020 [152838]

Table 6-48. Cumulative Seepage into CSNF Waste Package (Bin 4, Intermittent Drip)

Time (yr)	Seepage Flux into the WP (m ³ /yr)	Total Seepage in WP (m ³)
56500	0	0
65500	4.07E-06	0.0020364
66000	1.56E-05	0.0098344
66500	2.77E-05	0.0236664
67000	4.02E-05	0.0437594
67500	5.31E-05	0.0703304
68000	6.68E-05	0.1037134
68500	7.88E-05	0.1430974
69000	8.24E-05	0.1842979
69500	8.61E-05	0.2273544
70000	8.98E-05	0.2722569
70500	8.92E-05	0.3168619
71000	8.84E-05	0.3610784
71500	8.75E-05	0.4048149
72000	8.79E-05	0.4487534
72500	8.87E-05	0.4930794
73000	8.93E-05	0.5377399
73500	0.00010073	0.5881049
74000	0.00012783	0.6520199
74500	0.00015646	0.7302499
75000	0.00018649	0.8234949
75500	0.00020734	0.9271649
76000	0.00022908	1.0417049
76500	0.0002517	1.1675549
77000	0.00028494	1.3100249
77500	0.0003289	1.4744749
78000	0.00037477	1.6618599
78500	0.00042253	1.8731249
79000	0.00043954	2.0928949
79500	0.0004548	2.3202949
80000	0.00047027	2.5554299
80500	0.00051824	2.8145499
81000	0.00065156	3.1403299

Table 6-48. Cumulative Seepage into CSNF Waste Package (Bin 4, Intermittent Drip) (Continued)

Time (yr)	Seepage Flux into the WP (m ³ /yr)	Total Seepage in WP (m ³)
81500	0.00079091	3.5357849
82000	0.00093632	4.0039449
82500	0.0010573	4.5325949
83000	0.0011564	5.1107949
83500	0.0012591	5.7403449
84000	0.0013654	6.4230449
84500	0.0015053	7.1756949
85000	0.0016626	8.0069949
85500	0.0018251	8.9195449
86000	0.0019929	9.9159949
86500	0.0021816	11.0067949
87000	0.0023807	12.1971449
87500	0.0025862	13.4902449
88000	0.0027982	14.8893449
88500	0.0029614	16.3700449
89000	0.0031129	17.9264949
89500	0.003268	19.5604949
90000	0.0034268	21.2738949
90500	0.0036199	23.0838449
91000	0.003833	25.0003449
91500	0.0040516	27.0261449
92000	0.0042756	29.1639449
92500	0.0045315	31.4296949
93000	0.0048237	33.8415449
93500	0.0051235	36.4032949
94000	0.0054308	39.1186949
94500	0.0057788	42.0080949
95000	0.0062945	45.1553449
95500	0.0068235	48.5670949
96000	0.007366	52.2500949
96500	0.0079219	56.2110449
97000	0.0085622	60.4921449
97500	0.0092389	65.1115949
98000	0.0099318	70.0774949
98500	0.010641	75.3979949
99000	0.011304	81.0499949
99500	0.011817	86.9584949
100000	0.01234	93.1284949

DTN: MO0009MWDMED01.020 [152838]

Figure 6-114 shows the cladding unzipping rate in Bin 4 (intermittent drip). To verify that the unzipping rate is calculated correctly, the unzipping rate at 100,000 years will be calculated and compared to the TSPA model result. Table 6-49 shows the TSPA model results for the intrinsic dissolution rate and the unzipping rate in Bin 4, intermittent drip, for several time steps.

Table 6-49. TSPA Model Results for the CSNF Cladding Intrinsic Dissolution Rate and Unzipping Rate in Bin 4, Intermittent Drip

Simulation Time (years)	Intrinsic Dissolution Rate (mg/m ² /day) (CSNF Diss Rate)	Unzipping Rate (fraction/yr ⁻¹) (Unzip Rate)
40500	18.092	0.0001849
60500	2.7855	2.846E-05
80500	2.8878	2.915E-05
100000	2.9492	3.014E-05

DTN: MO0009MWDMED01.020 [152838]

The intrinsic dissolution rate is first calculated using Equation 6-2, with the coefficients given in Table 6-44. Since this is a median value calculation, the uncertainty term that is added to a_0 is zero (uniform -1,1). Table 6-50 gives in-package chemistry and thermohydrology values used in the cladding model for several time steps. The time history values at 100,000 years are: $pH_{CSNF} = 6.7445$, $Temp_{WP} = 22.407$ C (=295.567 K), $Total_{CO_3} = 0.044138$, and $fO_2 = 0.1995$. Note that for pH values less than or equal to 7, $a_2 = 0$, so the third term in Equation-1 becomes zero. Also note that PO_2 is $-\log_{10}(fO_2)$. The result calculated for the log intrinsic dissolution rate = 0.46983, or an intrinsic dissolution rate of 2.95 mg/m²/day.

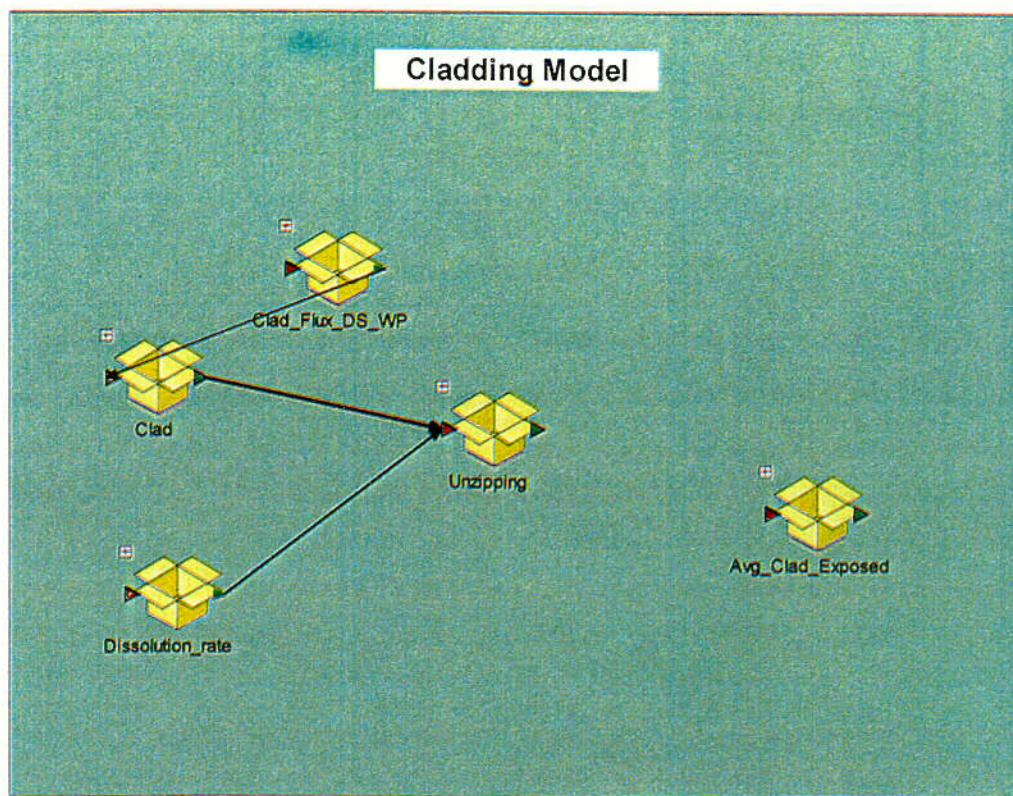
Table 6-50. TSPA Model Results for the In-package Chemistry and Thermohydrology Values Used in the Cladding Unzipping Rate Verification Calculation

Simulation Time (years)	pH_{CSNF}	$Temp_{WP}$ (C)	$Total_{CO_3}$	Fo_2
40500	5.0	28.364 C	0.00082821	0.1995
60500	6.8978	25.502 C	0.062808	0.1995
80500	6.8128	23.935 C	0.051654	0.1995
100000	6.7445	22.407 C	0.044138	0.1995

DTN: MO0009MWDMED01.020 [152838]

The intrinsic dissolution velocity is found by multiplying the intrinsic dissolution rate by the conversion factor 2.190×10^{-5} (cm/yr)/((mg/m²)/day), $CF_{Int_Diss_Velocity}$, to obtain 6.4605×10^{-5} cm/yr. or 2.047×10^{-14} m/s. The unzipping velocity is defined as a multiple of the intrinsic dissolution velocity. This multiple, $Unzip_uncert$, is defined as a triangular distribution with a minimum equal to 1, a mean equal to 40, and a maximum equal to 240. The median value (50th percentile) for this distribution is 85.4, so the unzipping velocity is $1.748E-12$ m/s. The unzipping rate (at 100,000 years) is calculated by dividing the unzipping velocity by one-half length of the fuel rod; this gives an unzipping rate of 9.55×10^{-13} s⁻¹ or 3.014×10^{-5} yr⁻¹. This verifies that the cladding unzipping rate is correctly calculated in the TSPA model, and that the in-package chemistry and thermohydrology links are correctly passing values to the cladding model.

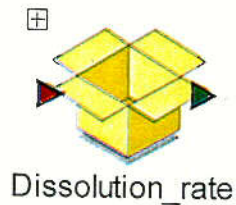
Figure 6-115 shows a time history plot of the average fraction of fuel exposed in Bin 4 (intermittent drip) for a median value simulation. This TSPA model calculation was not from an abstraction AMR, rather this calculation was implemented using the GoldSim code's ability to track the amount of exposed and unexposed mass. The result of this calculation is used in the in-package chemistry model for determining in-package pH (see Section 6.3.4.2).



\\TSPA_Model\\Engineered_Barrier_System\\CSNF_Packages\\SS_Clad_Fuel\\Clad_Degradation\\

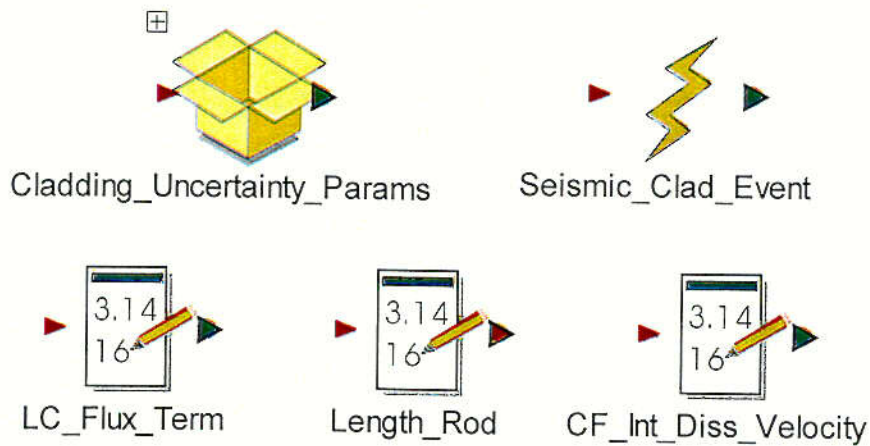
Figure 6-104. Overview of the TSPA Cladding Degradation Model

C72



\\TSPA_Model\\Engineered_Barrier_System\\CSNF_Packages\\SS_Clad_Fuel\\Clad_Degradation\\Clad\\

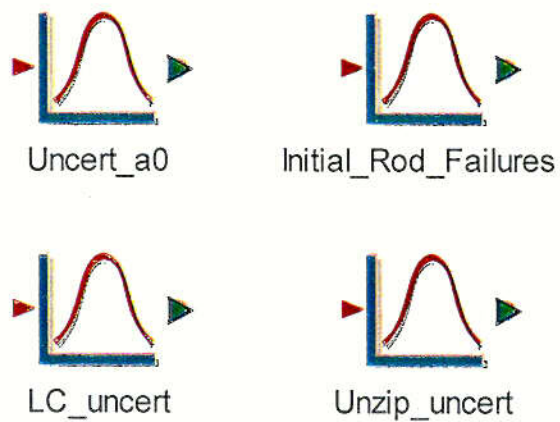
Figure 6-105. The Clad Container Includes the Containers for the Determining Localized Corrosion of the Cladding and the Intrinsic Dissolution Rate of the Fuel Matrix



\\TSPA_Model\\Engineered_Barrier_System\\CSNF_Packages\\Cladding\\

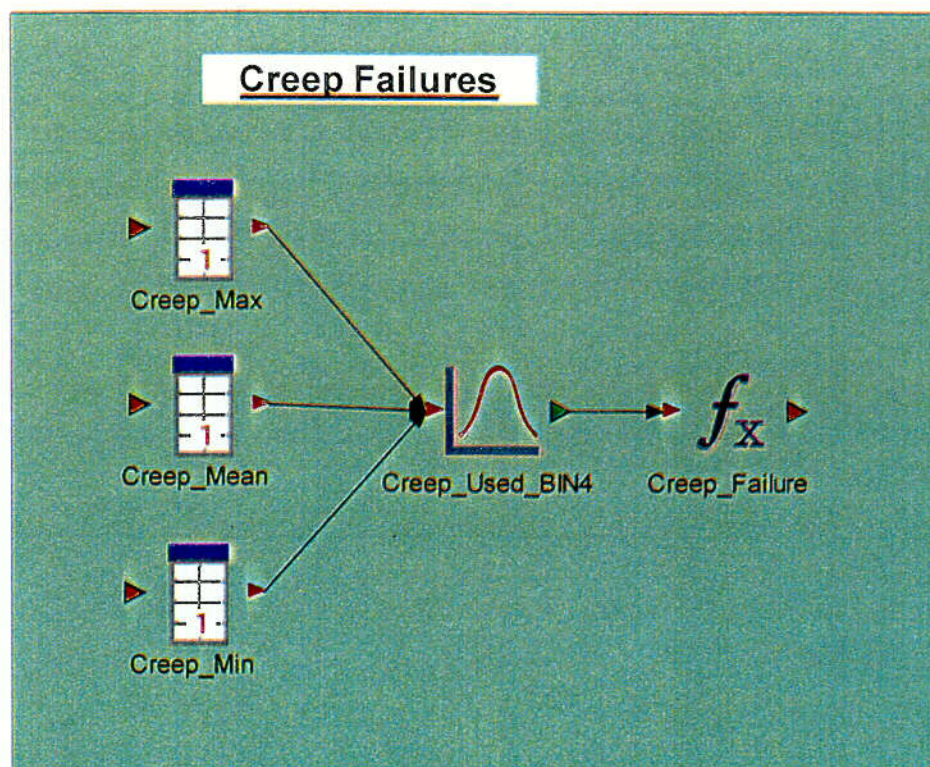
Figure 6-106. Cladding Model Parameters that are Defined Globally in the TSPA-SR Model

C73



\\TSPA_Model\\Engineered_Barrier_System\\CSNF_Packages\\Cladding\\Cladding_Uncertainty_Params\\

Figure 6-107. Global Parameters within the *Cladding_Uncertainty_Params* Container

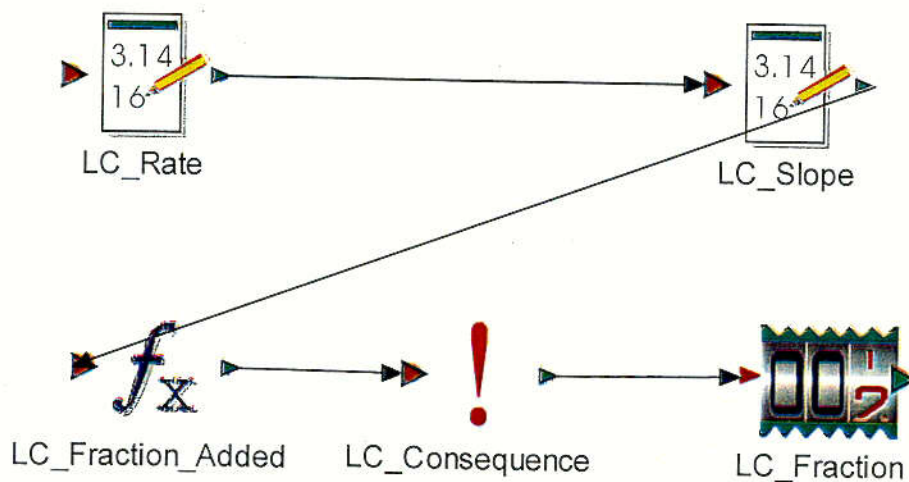


\\TSPA_Model\\Engineered_Barrier_System\\CSNF_Packages\\Infiltration_Bin_4\\Creep_Cladding_Failures\\

Figure 6-108. TSPA-SR Model Implementation of Creep and SCC Failures

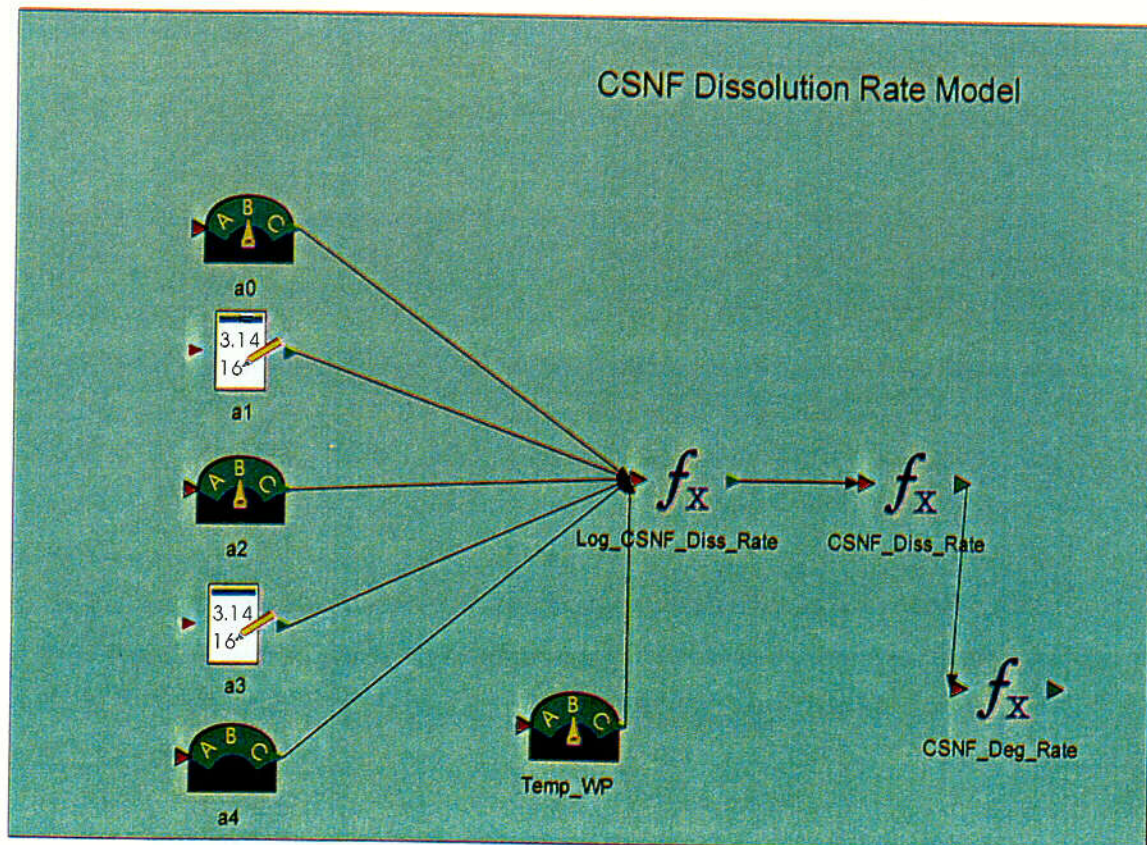
C74

Local Corrosion



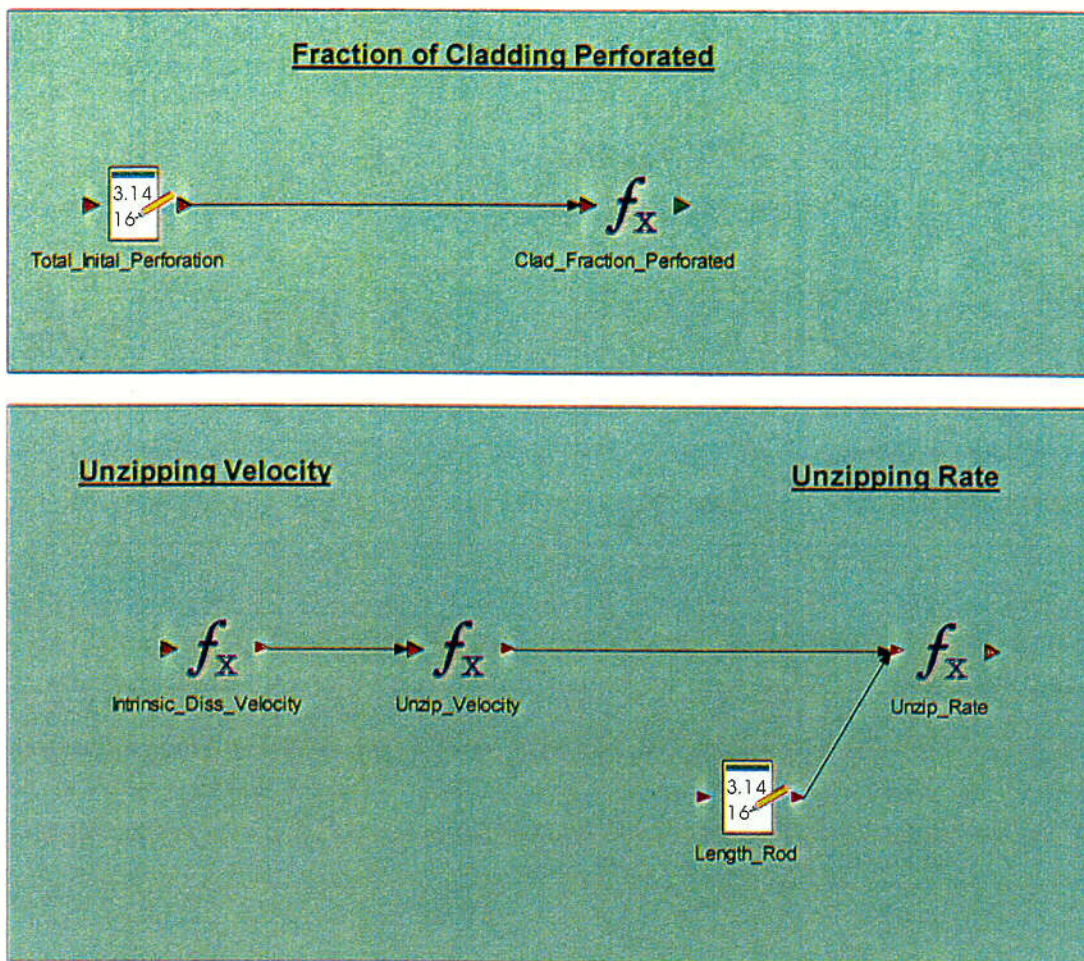
\\TSPA_Model\\Engineered_Barrier_System\\CSNF_Packages\\SS_Clad_Fuel\\Clad_Degradation\\Clad\\Local_Corrosion\\

Figure 6-109. TSPA Model Implementation of Local Cladding Corrosion



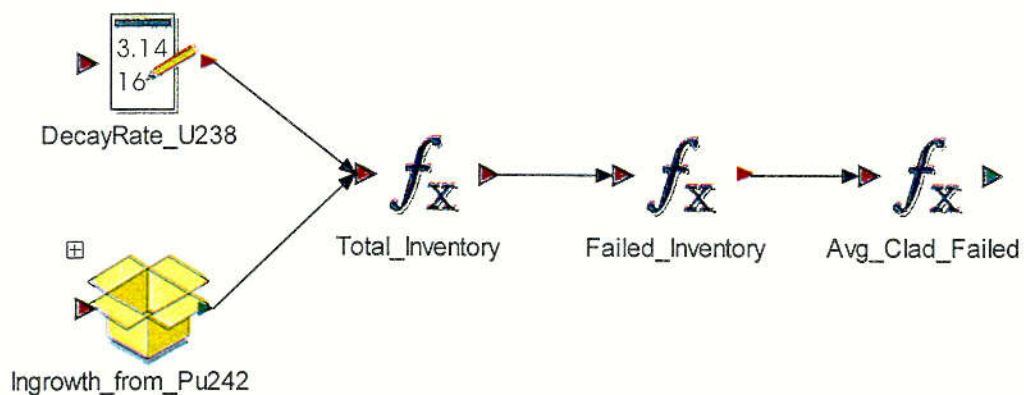
\\TSPA_Model\\Engineered_Barrier_System\\CSNF_Packages\\SS_Clad_Fuel\\Clad_Degradation\\Dissolution_rate\\

Figure 6-110. TSPA Model Implementation of CSNF Cladding Dissolution Rate



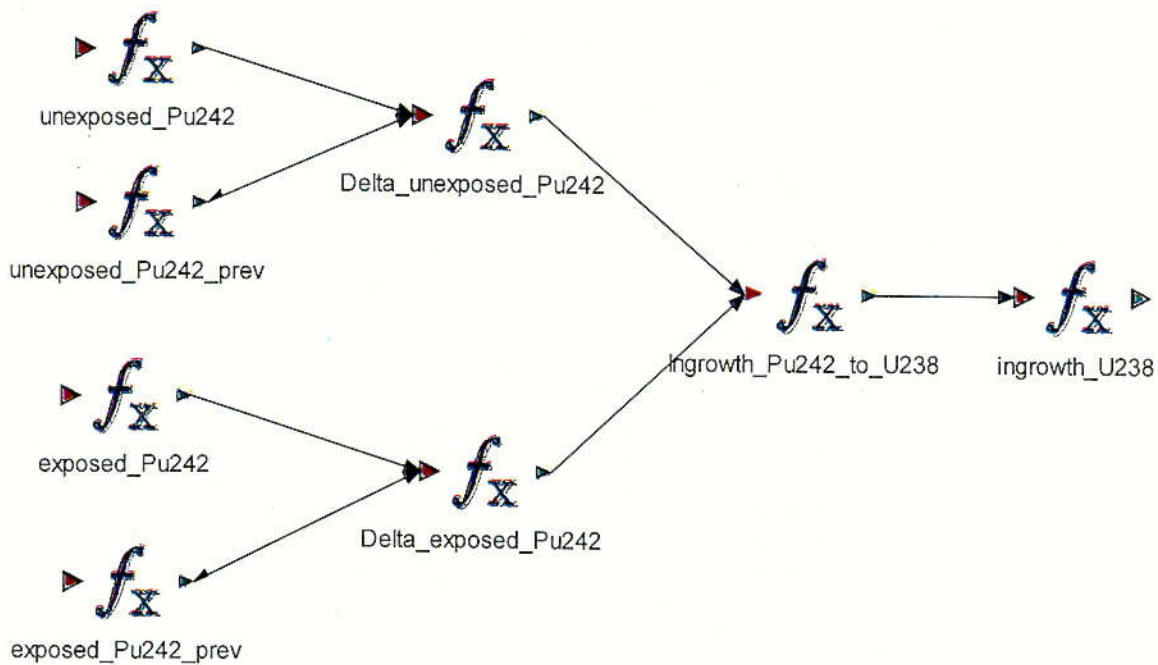
\\TSPA_Model\\Engineered_Barrier_System\\CSNF_Packages\\SS_Clad_Fuel\\Clad_Degradation\\Unzipping

Figure 6-111. TSPA Model Implementation of the CSNF Cladding Unzipping



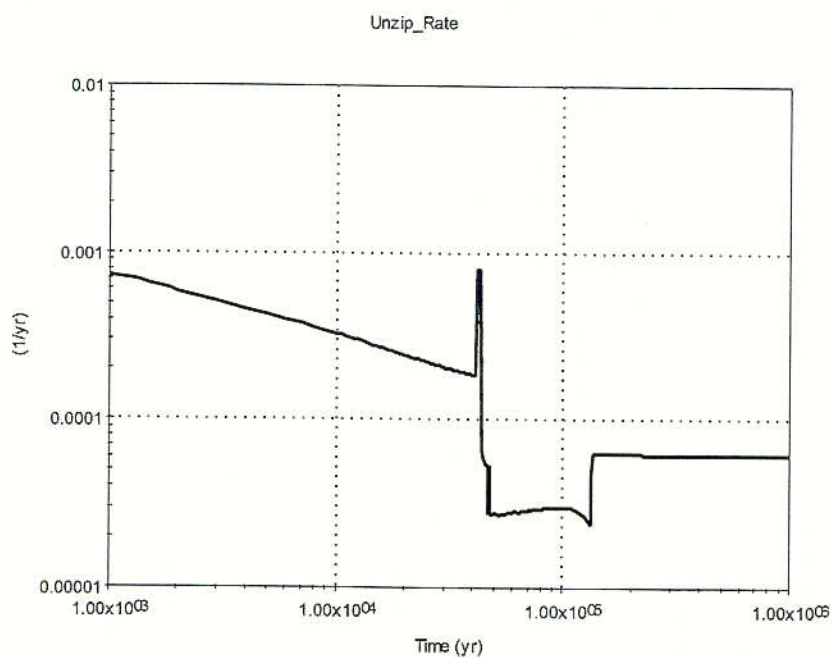
\\TSPA_Model\\Engineered_Barrier_System\\CSNF_Packages\\SS_Clad_Fuel\\Clad_Degradation\\Avg_Clad_Exposed\\

Figure 6-112. An Illustration of Implementation of the Calculation of the Average Amount of Failed CSNF Cladding



\\TSPA_Model\\Engineered_Barrier_System\\CSNF_Packages\\SS_Clad_Fuel\\Clad_Degradation\\Avg_Clad_Exposed\\Ingrowth_from_Pu242\\

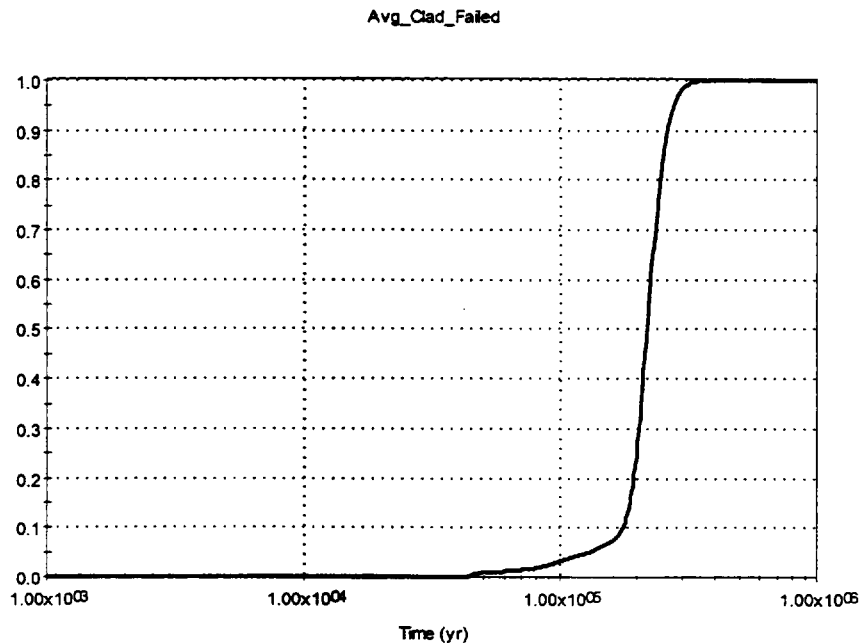
Figure 6-113. Calculation of the In-growth of ^{238}U from the Decay of ^{242}Pu ; used in Calculating Average Cladding Exposed



\\TSPA_Model\\Engineered_Barrier_System\\CSNF_Packages\\Infiltration_Bin_4\\Intermittent_Drip\\Clad_Degradation\\Unzipping\\

Figure 6-114. CSNF Unzipping Rate, Bin 4, Intermittent Seepage

C77



\\TSPA_Model\Engineered_Barrier_System\CSNF_Packages\Infiltration_Bin_4\Intermittent_Drip\Clad_Degradation\Avg_Clad_Exposed\

Figure 6-115. Time History of the Average Fuel Exposed for Bin 4, Intermittent Drip (Median Value Simulation)

6.3.4.4 Dissolution Rate Model

Overview

The co-disposed spent fuel packages (CDSP) contain a combination of DOE spent nuclear fuel (DSNF) and high-level waste (HLW) material (CRWMS M&O 2000[136383], Attachment 1). Both DSNF and HLW will be packaged differently for storage in the proposed repository: the radionuclides for DSNF will be bound in a variety of solidifying matrices (e.g., Uranium metal) (CRWMS M&O 2000 [144164], Section 6.3.1 through 6.3.12), while the radionuclides in the HLW will be bound in a glass matrix (CRWMS M&O 2000 [143420], Section 7, p. 44 Paragraph 1). As the infiltrating water seeps through the drift and comes in contact with the CDSP waste package, it will slowly dissolve the bounding material and lead to the release of radionuclides.

For TSPA-SR model, it is conservatively assumed that the entire surface of both the HLW and DSNF waste forms is exposed to the near-field environment as soon as the waste package is breached. Once exposed, the waste form is assumed to be covered by a “thin” film of water, and alteration/dissolution processes are initiated (CRWMS M&O 2000 [143420], Section 6.3.2 p. 38). In a failed waste package containing HLW material, water seeping into the package will dissolve the glass matrix releasing the bound radionuclides. Since the release of radionuclides from the glass matrix will depend on the prior dissolution of the glass, the dissolution rate of the glass imposes an upper bound on the radionuclide release rate. The *Defense High Level Waste*

Glass Degradation AMR (CRWMS M&O 2000 [143420]) provides model relationships used to calculate the dissolution rate of waste glass when contacted by water. The release rate of a particular radionuclide is the product of the glass dissolution rate, the mass fraction of the radionuclide in the glass and the surface area of the glass contacted by water (CRWMS M&O 2000 [143420], Section 6.1).

The model for HLW glass dissolution is based on the rate expression for aqueous dissolution of waste glass. The parameter values for the rate expression are based on several waste glass compositions (CRWMS M&O 2000 [143420], Section 7, p. 41). The rate expression to calculate the dissolution rate (DR) of waste glass in an aqueous solution for the TSPA-SR analysis is given by Equation 6-3 (CRWMS M&O 2000 [143420], Section 7, Equation 17).

$$DR = S_{im} \cdot k_{eff} \cdot 10^{\eta \cdot pH} \cdot \exp(-E_a/RT) \quad (\text{Eq. 6-3})$$

where

- DR = the dissolution rate of the glass (mass/time)
- S_{im} = the surface area of glass immersed in water (area)
- k_{eff} = the effective dissolution rate constant (mass/area•time)
- η = the pH dependence coefficient (dimensionless)
- E_a = the effective activation energy (kJ/mol)
- R = the Universal gas constant (8.314×10^{-3} kJ/mol•K)
- T = the absolute temperature (Kelvin)
- pH = the local pH in the environment (dimensionless)

The dissolution rate of some waste glasses have a “V” shaped pH dependence such that lower rates occur near neutral pH conditions and higher rates occur near lower and higher pH conditions (CRWMS M&O 2000 [143420], Section 6.2.1, p. 16). This pH dependence is probably the result of different reactions or reaction mechanisms being predominant at low pH and high pH values (CRWMS M&O 2000 [143420], Section 6.2.1, p. 13).

To simulate the pH dependent dissolution rate, different parameter values were required to solve Equation 6-3. Values for S_{im} , pH, and T depend on the exposure conditions while the parameter values for η , E_a , and k_{eff} were selected from a limited database based on glass composition. The values of η and E_a were taken from Knauss et al. (1990 [101701]) based on a single-pass flow-through tests for a simple five-component analogue glass (CSG), while the values for k_{eff} were based on the results from the short-term Product Consistency Tests (CRWMS M&O 2000 [143420], Section 6.2.1, p. 17). The test results from other waste glasses were also used to corroborate these parameter values. The available evidence indicates that the rates calculated with the selected parameter values will bound the forward dissolution rates for the full range of waste glass compositions (CRWMS M&O 2000 [143420], Section 6.2.1.2, p. 21 and Section 6.2.1.3, p. 22). This bounding approach is adopted in TSPA-SR model to accommodate uncertainties in the database and rate expressions (CRWMS M&O 2000 [143420], Section 6.1.1, p. 13). Since the dissolution rate does not directly depend on the volume of water that is in contact with the glass or whether the contact is static or dynamic, the calculated rate expression provides an upper bound for the glass dissolution under all three water contact modes: humid air, dripping water, and immersion (CRWMS M&O 2000 [143420], Section 6.1.1, p. 13). For a

detailed discussion on the analysis of the glass dissolution rate, the reader is referred to the *Defense High Level Waste Glass Degradation* AMR (CRWMS M&O 2000 [143420], Section 5.0, paragraphs 5 and 6).

The dissolution rate of DSNF is conservatively assumed to be a constant value, resulting in complete dissolution of the fuel in a single time step (CRWMS M&O 2000 [144164], Section 7.2.1, p. 26). This value is multiplied by a specific surface area to calculate the matrix degradation rate. For detailed analyses, refer to *DSNF and Other Waste Form Degradation Abstraction* AMR (CRWMS M&O 2000 [144164]).

Inputs to the TSPA Model

Data reported in the *Defense High Level Waste Glass Degradation* AMR (CRWMS M&O 2000 [143420]) were measured in tasks conducted at Argonne National Laboratory (ANL). In addition some data were taken from the literature and some from unpublished data taken from scientific notebooks on file at ANL. The specific surface area of the glass log was calculated by dividing the surface area by its weight for each glass log considered and then taking the mean from the range of calculated values. The parameter values for the low pH and high pH legs are presented in Table 6-51.

Table 6-51. Parameter Values for the HLW Glass Dissolution Rate Calculation

Description	TSPA Parameter	Parameter Value	Reference/DTN
Logarithm of k_{eff} at high pH (g/m ² /day)	Log_Keff_high	Uniform Distribution Min = 6.4, Max = 7.4	CRWMS M&O 2000 [143420], Table 7, p. 43 DTN: MO0007RIB00091.000 [151712]
pH dependence coefficient at high pH	mew_high	Uniform Distribution Min = 0.3, Max = 0.5	CRWMS M&O 2000 [143420], Table 7, p. 43 DTN: MO0007RIB00091.000 [151712]
Effective activation energy at high pH (kJ/mol)	Ea_high	Uniform Distribution Min = 70, Max = 90	CRWMS M&O 2000 [143420], Table 7, p. 43 DTN: MO0007RIB00091.000 [151712]
Logarithm of k_{eff} at low pH (g/m ² /day)	Log_Keff_low	Uniform Distribution Min = 8, Max = 10	CRWMS M&O 2000 [143420], Table 7, p. 43 DTN: MO0007RIB00091.000 [151712]
pH dependence coefficient at low pH	Mew_low	Uniform Distribution Min = -0.7, Max = -0.5	CRWMS M&O 2000 [143420], Table 7, p. 43 DTN: MO0007RIB00091.000 [151712]
Effective activation energy at low pH (kJ/mol)	Ea_low	Uniform Distribution Min = 43, Max = 73	CRWMS M&O 2000 [143420], Table 7, p. 43 DTN: MO0007RIB00091.000 [151712]
Specific surface area of glass immersed in water	Surface_Area_Glass	5.63e-05 m ² /g	CRWMS M&O 2000 [143420], Table 7, p. 43 and Section 6.1.2, p. 15
Relative humidity threshold for CDSP matrix degradation	Dissolution_Threshold	5%	CRWMS M&O 2000 [143420], Section 5, p. 11 Conservative Assumption
Universal Gas Constant	R	8.31451 (kg m ²)/(s ² mol K)	Weast 1979 [102865]

The DSNF dissolution rate is conservatively assumed equal to the rate for U-Metal Based fuel, $1.75\text{E}+06 \text{ mg/m}^2/\text{day}$ (CRWMS M&O 2000 [144164], Table 1, p. 29). The exposed surface area is equal to $7.0\text{e}-5 \text{ m}^2/\text{g}$.

Implementation

Equation 6-3 was incorporated into the TSPA-SR model for the calculation of the HLW glass dissolution rate. The glass dissolution rate calculation is a function of five variables, k_{eff} , η , pH, E_a , and T , and two constants, S_{im} and R . Due to the "V"-shaped pH dependence of the glass dissolution rate, two conditions for these parameters were implemented, a low pH case and a high pH case.

Equation 6-3 shows the implementation of k_{eff} , η , and E_a for both cases. Due to uncertainty in parameter values, they are represented as stochastic elements with uniform distribution. The six distributions in Table 6-51 and Figure 6-116 represent the range of values for $\log k_{\text{eff}}$, η , and E_a for both the high and low pH cases. The other two variables presented in Equation 6-3, pH and T , are computed locally within the model. The illustration of a local calculation is presented in Figure 6-116 through Figure 6-119. The two parameters, *exponent_high* and *exponent_low*, shown in Figure 6-118, are calculated at the bin level in the bin container *Glass_Dissolution*, shown in Figure 6-117. Figure 6-119 shows the implementation to calculate the in-package pH at the environment level.

The TSPA-SR model calculates the dissolution rates for both the high and low pH cases simultaneously, and the corresponding model functions and parameters are distinguished by either a "high" or "low" identifier. At the initiation of the simulation, the code assigns a value to each of the stochastic distributions, *log_Keff_high*, *mew_high*, *Ea_high*, *log_Keff_low*, *mew_low*, and *Ea_low* (Table 6-51), based upon the type of simulation chosen. When a median value simulation is chosen, the median values for these parameters are selected from the range of values defined for that distribution but when evaluated for multiple realizations, the values are randomly sampled from the assigned distribution using latin-hypercube sampling method. It should be noted that the assigned value for each stochastic parameter does not change during the course of a single realization. Since the stochastic parameters for rate calculation are defined globally within the model, and thus remain unchanged for a given realization, the only difference between rate calculation results among the fifteen modeled CDSP bin environments will be due to the differences in the local pH and local temperatures. Once a value has been assigned to each of the input distributions, the model converts these values into the appropriate form as necessary. For example, the values assigned to *log_Keff_high* and *log_Keff_low* values are converted to scalar values, *Keff_high* and *Keff_low*, by taking the anti-log.

The two functions, *exponent_high* and *exponent_low*, compute the exponential term, $\exp(-E_a/RT)$, in Equation 6-3. These calculations are dependent on the stochastic variables *Ea_high* or *Ea_low* and the temperature of the waste package, *TEMP_CDSP_WP*, which is calculated in the TSPA-SR Thermohydrology Model component (see Section 6.3.2.1). Since the temperature of the CDSP waste package is a function of time, *Ea_high* and *Ea_low* will vary over time. The specific surface area of the glass, *Surface_area_glass*, is defined as a constant equal to $0.0000563 \text{ m}^2/\text{g}$ (Table 6-51).

Once the preliminary calculations are completed at the bin level, the dissolution rate is calculated at the environment level within each bin. The dissolution rate for HLW glass for both the high and low pH cases are computed by the model functions *Glass_Deg_Rate_high* and *Glass_Deg_Rate_low*, respectively. Both calculations use the same pH value, *pH_CDSP*, which is calculated in the TSPA-SR In-Package Chemistry Model component (see Section 6.3.4.2 In-Package Chemistry). Once both dissolution rates have been calculated, the model compares the high pH and low pH dissolution rates. The expression, *Glass_Deg_Rate*, conservatively extracts the larger of the two rates with one exception that if the relative humidity of invert, derived from the Thermal Hydrology model component (See Section 6.3.2.1), is less than the relative humidity threshold, *Dissolution_Threshold*, then the degradation rate is set to zero. The parameter *Glass_Deg_Rate* represents Equation 6-3. In the *Defense High Level Waste Glass Degradation* AMR (CRWMS M&O 2000 [143420]) the relative humidity threshold for initiation of glass dissolution is assumed to be 80% (CRWMS M&O 2000 [143420], Section 5, p. 11), but in the TSPA model this threshold value is conservatively assumed to be 5%. This change is also warranted to avoid sharp variation in calculated dissolution rates at later times and to avoid instability in the model parameters that depend on the dissolution rate at early times.

Table 6-52 and Table 6-53 summarize the TSPA-SR model parameters that affect the glass dissolution rate calculations. Table 6-52 tabulates all of the TSPA-SR model parameters that are not inputs, but are necessary to implement the model within GoldSim code. Table 6-52 tabulates the TSPA-SR model parameters which are not inputs, but are TSPA-SR model parameters calculated in other sections of the model and used during the rate calculations. Note that some expressions in the table under Parameter Values/Other Inputs reference bin 1. These parameters vary between the five different bins used within the model to account for the spatial variability of the percolation flux values. References to bin 1 are presented here for illustrative purposes only.

Table 6-52. Parameter Details for Supplemental HLW Glass Dissolution Calculations

Description	TSPA Parameter	Parameter Value/Other Inputs	Applicability
Convert Log_Keff value to scalar at high pH	Keff_high	$10^{(\log_Keff_high)}$	Localized to Environment
Calculate exponential term in rate equation at high pH	Exponent_high	$\text{Exp}(-Ea_high/(R*Temp_CDSP_WP.Temp_CDSP_WP[Bin_1]))$	Localized to Environment
Calculate glass degradation rate at high pH	Glass_Deg_Rate_high	$\text{Surface_area_glass} * Keff_high * 10^{(mew_high * pH_CDSP)} * \text{exponent_high}$	Localized to Environment
Convert Log_Keff value to scalar at low pH	Keff_Low	$10^{(\log_Keff_low)}$	Localized to Environment
Calculate exponential term in rate equation at low pH	Exponent_low	$\text{Exp}(-Ea_low/(R*Temp_CDSP_WP.Temp_CDSP_WP[Bin_1]))$	Localized to Environment
Calculate glass degradation rate at low pH	Glass_Deg_Rate_low	$\text{Surface_area_glass} * Keff_low * 10^{(mew_low * pH_CDSP)} * \text{exponent_low}$	Localized to Environment
Assign glass dissolution rate	Glass_Deg_Rate	$\text{If}(RH_Invert > \text{Dissolution_Threshold}, \max(\text{Glass_Deg_Rate_high}, \text{Glass_Deg_Rate_low}), 1e-30\{1/yr\})$	Localized to Environment

Table 6-53. Other TSPA-SR Model Parameters with HLW Glass Dissolution Impacts

Description	TSPA Parameter	TSPA Model Reference	Applicability
Average waste package temperature in Bin	Temp_CDSP_WP	Thermohydrology (see Section 6.3.2.1)	Localized to Bin
In-package pH of CDSP waste packages	pH_CDSP	In-Package Chemistry Model (see Section 6.3.4.2)	Localized to Environment

Results and Verification

The results of modeling the dissolution of the waste forms contained within the CDSP packages in the TSPA-SR model are discussed in this section. Figure 6-120 illustrates the glass degradation rate for the median value simulation representing all three seepage environments (always drip, intermittent drip, and no drip) for Bin 4. It should be noted that although the glass degradation rate is being calculated at each time step, matrix degradation is not actually initiated until the waste package is breached. Once the waste package is breached, the matrix degrades at the rate calculated in each timestep.

From Figure 6-120 it is observed that the glass degradation rate is very high initially and declines gradually with time. This is a direct result of the temperature influence on the rate equation because the temperature in the CDSP waste packages start to peak typically within first hundred years from the time of emplacement and then steadily decline approaching ambient conditions. The matrix degradation rates are also observed to be the same for all three environments at early times. This is attributed to the presence of similar temperature and in-package pH profiles for all three environments at early times. In the median value simulation, the waste packages in all three environments for Bin 4 start to fail after around 40,000 years. Immediately after the packages begin failing, the seeping water is exposed to the waste form leading to the changes in the in-package chemistry and pH (see Section 6.3.4.2 In-Package Chemistry). The observed changes in the in-package pH correspond to the changes in the *Glass_Deg_Rate* and hence it can be concluded that the glass dissolution rate is largely pH dependent (temperature effects are minimal as the repository temperatures are near ambient conditions after 40,000 years). Furthermore, the waste package surface temperatures are defined per bin and are not environment specific and thus any observed degradation rate differences within the environments must be due to differences in the pH inside the waste packages.

For the simulation period prior to the first waste package failure, the pH in the waste package is set equal to the value of 5.0 (see Section 6.3.4.2). The pH inside the waste package begins to change once the waste packages are breached and water seeps into the waste package. Differences in the seepage flux through the waste package leads to differences in pH that result in different glass degradation rates being calculated. In the median value simulation, under no-drip environment for Bin 4, the pH increases up to a value of 8.8893 after 43,000 years, while for the always- and intermittent-drip environments the pH increases to a maximum value of 8.8893 but drops to a constant value of 8.1 after 156,000 years and 144,000 years respectively. Note that the observed pH values of up to four decimal places are computed by the model and have not been rounded off even though such precise values are difficult to measure by instruments.

The purpose of providing these values is to only verify the model results and to show the calculated values.

The degradation rate of DSNF matrix is defined with a constant value, calculated by taking the product of the dissolution rate (*DSNF_Diss_Rate*) and the specific surface area (*DSNF_Surface_Area*), resulting in a matrix degradation rate of 44.71 per year.

The TSPA-SR HLW Glass Dissolution Rate Model component calculations reference two input parameters from other model components, *TEMP_CDSP_WP* and *pH_CDSP*. The functions, *exponent_high* and *exponent_low*, both use the surface temperature of a CDSP waste package, *TEMP_CDSP_WP*, to calculate the exponential term in the glass dissolution rate equation. To verify that these functions receive the correct values from the TSPA-SR Thermohydrology Model component and calculate the results properly, the time histories for the end calculation were saved and compared to results obtained from manual computation. The results from the timestep corresponding to 100,000 year for the median value simulation are presented in Table 6-54.

In Table 6-54 the values for the pH and temperature were extracted from the In-Package Chemistry and Thermal Hydrology components of the TSPA-SR model, respectively. Since the results of the hand calculation and model calculation are equivalent (considering roundoff errors), it is verified that Equation 6-3 is properly implemented in the Glass Dissolution Rate component of the TSPA-SR model. Furthermore, it is verified that the model sends and receives the correct values between the In-Package Chemistry component and the Glass Dissolution Rate component and between the Thermohydrology component and the Glass Dissolution Rate component.

Table 6-54. Verification of HLW Glass Dissolution Rate Calculation for the Median Value Simulation

TSPA Parameter	Bin	Environment	Conditions @ 100,000 years	Calculated value	Observed value
Glass_Deg_Rate_high	4	Always Drip	pH = 8.8573 T = 295.461 K Ea = 80 kJ/mol $\eta = 0.4$ $K_{eff} = 10^{6.9} \text{ g/m}^2\text{d}$	4.0953E-06 yr-1	4.1035E-06 yr ⁻¹
Glass_Deg_Rate_high	4	Intermittent Drip	pH = 8.8281 T = 295.461 K Ea = 80 kJ/mol $\eta = 0.4$ $K_{eff} = 10^{6.9} \text{ g/m}^2\text{d}$	3.9866E-07 yr-1	3.9943E-07 yr ⁻¹
Glass_Deg_Rate_high	4	Never Drip	pH = 8.8893 T = 295.461 K Ea = 80 kJ/mol $\eta = 0.4$ $K_{eff} = 10^{6.9} \text{ g/m}^2\text{d}$	4.2177E-06 yr-1	4.2261E-06 yr ⁻¹

Table 6-54. Verification of HLW Glass Dissolution Rate Calculation for the Median Value Simulation (Continued)

TSPA Parameter	Bin	Environment	Conditions @ 100,000 years	Calculated value	Observed value
Glass_Deg_Rate_low	4	Always Drip	pH = 8.8573 T = 295.461 K Ea = 58 kJ/mol $\eta = -0.6$ $K_{eff} = 10^9 \text{ g/m}^2\text{d}$	5.5527E-09 yr ⁻¹	5.5604E-09 yr ⁻¹
Glass_Deg_Rate_low	4	Intermittent Drip	pH = 8.8281 T = 295.461 K Ea = 58 kJ/mol $\eta = -0.6$ $K_{eff} = 10^9 \text{ g/m}^2\text{d}$	5.7813E-09 yr ⁻¹	5.7899E-09 yr ⁻¹
Glass_Deg_Rate_low	4	Never Drip	pH = 8.8893 T = 295.461 K Ea = 58 kJ/mol $\eta = -0.6$ $K_{eff} = 10^9 \text{ g/m}^2\text{d}$	5.3126E-09 yr ⁻¹	5.3202E-09 yr ⁻¹

Within the TSPA-SR model, glass dissolution rates are calculated separately using parameters defined for both low and high pH conditions (Table 6-51). Using a conservative approach, the greater of the two rates calculated is selected for all the subsequent calculations. Verification of the correct functioning of the selector switch, *Glass_Deg_Rate*, can be done graphically. A plot of both *Glass_Deg_Rate_high* and *Glass_Deg_Rate_low* together with *Glass_Deg_Rate* shows the overlap of the calculation results. Figure 6-121 shows this relationship for the Always Drip environment in bin 4 for the median value simulation. It can be seen that at early times the low pH degradation rate exceeds the high pH degradation rate and the resulting value for *Glass_Deg_Rate* equals the *Glass_Deg_Rate_low* values. During this phase the pH in the waste package is acidic and the low pH curve is expected to dominate. At later times, the packages fail and the inner package pH increases. During this phase the pH in the waste package becomes basic and the high pH curve is expected to dominate: the calculated dissolution rate corresponding to the *Glass_Deg_Rate_high* becomes greater than the *Glass_Deg_Rate_low*. As a result, the curve for the HLW glass dissolution rate (*Glass_Deg_Rate*) that was initially tracking the curve for *Glass_Deg_Rate_low* starts tracking the curve for *Glass_Deg_Rate_high*. Thus it is concluded that the selector switch, *Glass_Deg_Rate*, functions properly and the entire implementation works as expected.

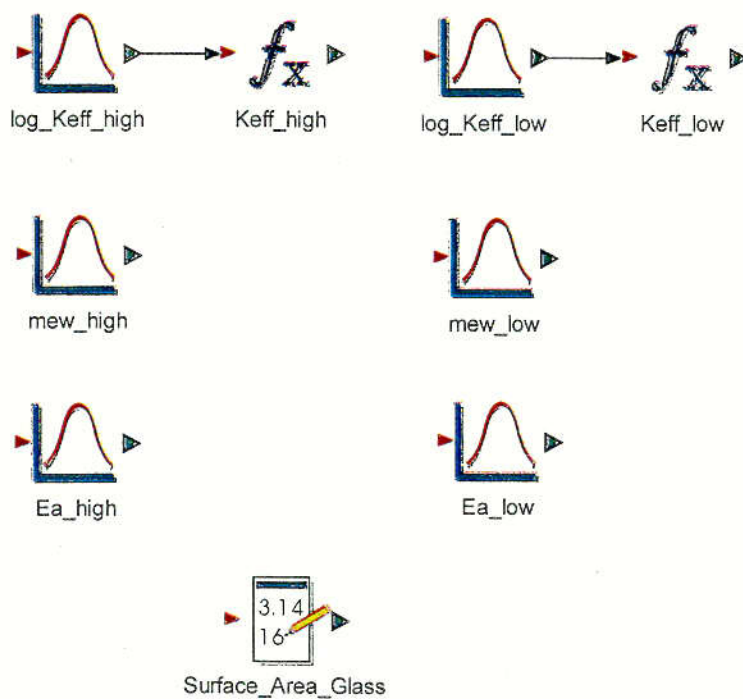


Figure 6-116. Illustration of the HLW Glass Dissolution Rate Parameters

Infiltration Bin

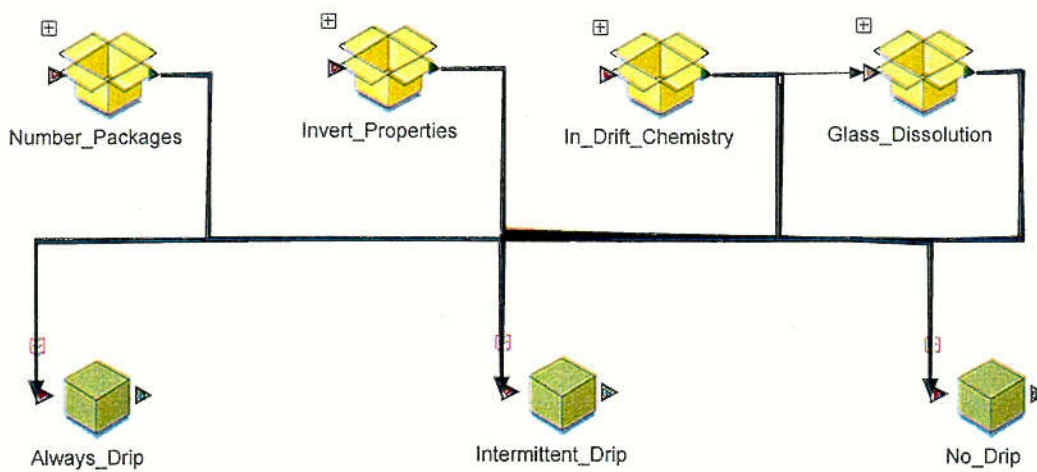


Figure 6-117. Representation of the HLW Glass Dissolution Rate Calculation

C78

► f_x ►
DSNF_Deg_Rate

► f_x ►
exponent_high

► f_x ►
exponent_low

Figure 6-118. Illustration of the Exponential Term Calculation for the HLW Glass Dissolution Rate and DSNF Degradation Rate

Glass Dissolution Rate Model

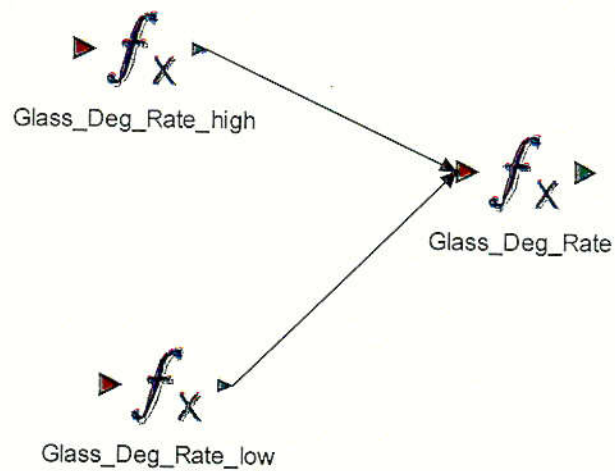


Figure 6-119. Illustration of the HLW Glass Dissolution Rate Calculation

C79

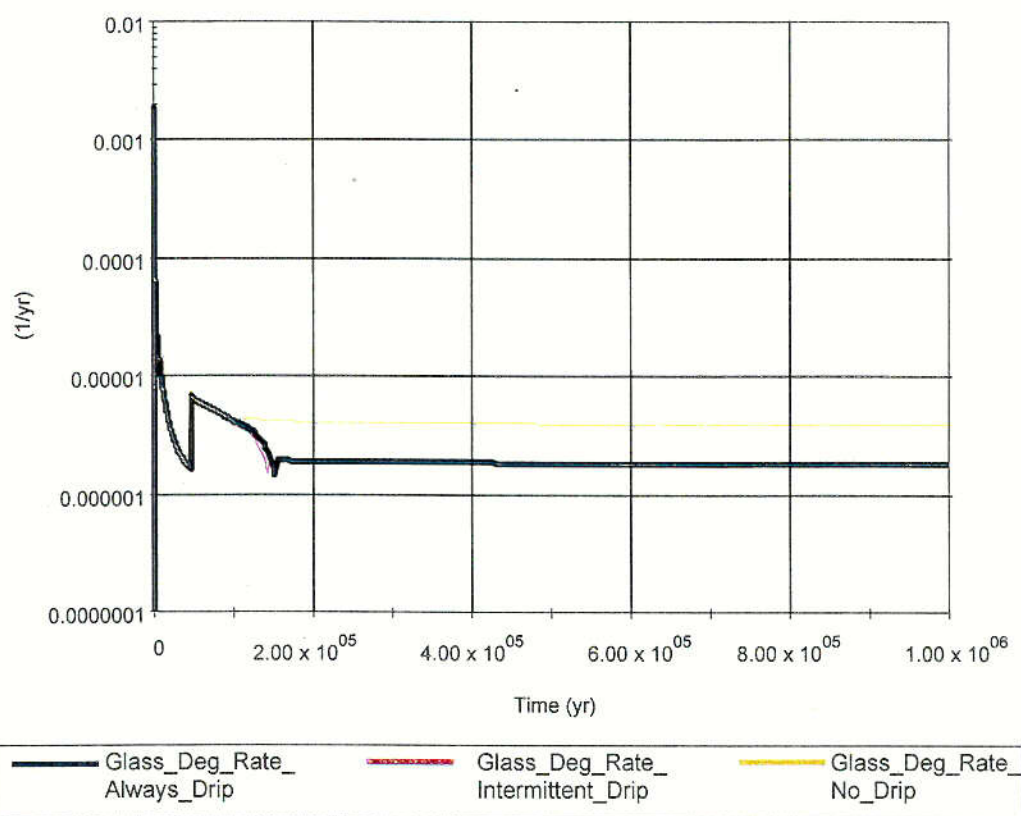


Figure 6-120. Temporal Profile of the HLW Glass Dissolution Rate in Bin 4

C80

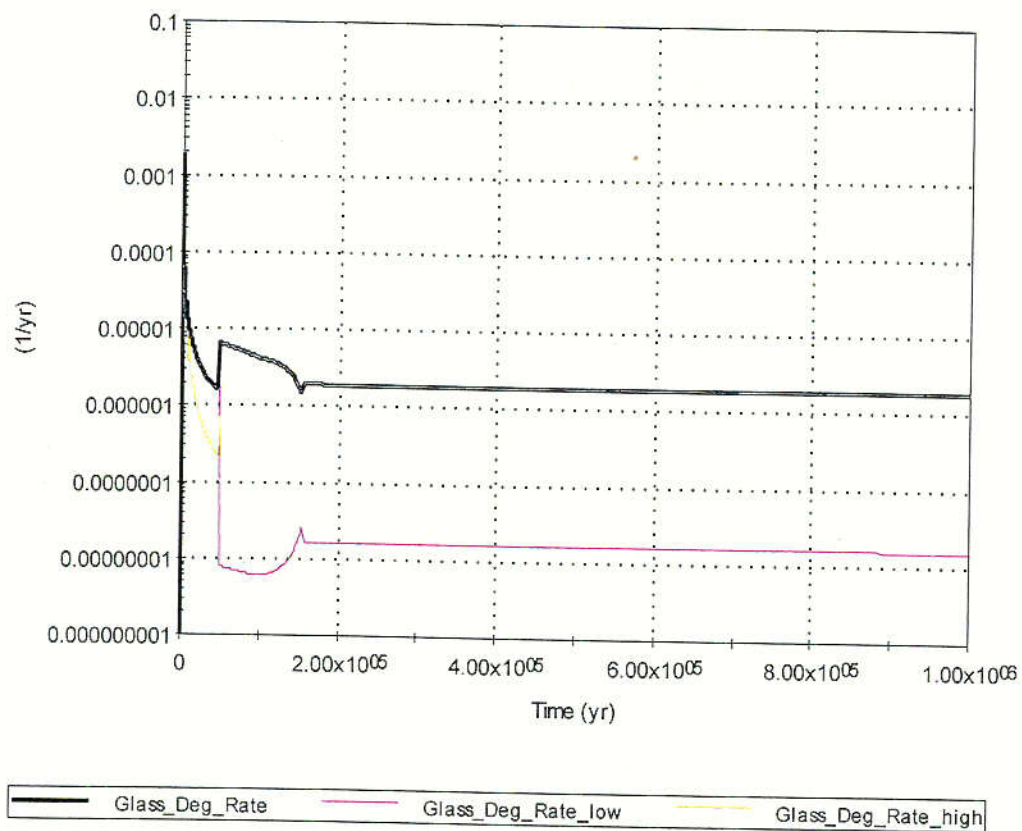


Figure 6-121. Glass Degradation Rate Comparison Using Parameters Defined for Both Low and High pH Conditions with the Model Output

C81.

6.3.4.5 Dissolved Concentration Limits

Overview

Infiltrating water seeping into the repository drift and onto the waste package can eventually corrode the waste package. Once the waste package is breached, water will seep through the openings and degrade the waste form leading to the release of radionuclides. Radionuclides that migrate through the engineered barrier system can also move through the unsaturated and saturated zones and can end up in the biosphere.

The mobilization of radionuclides from a breached waste package will be constrained by the chemical inventory in the waste package and the solubility of the radionuclide in the fluid (CRWMS M&O 2000 [143569], Section 6.1.1, p. 14). The aqueous concentration of each element mobilized from the waste package cannot exceed the solubility limit of that element, unless suspended colloids are included, nor can it exceed the amount originally present in the inventory. From the investigations conducted on the solubility of selected elements, solubility limits were abstracted into a form that can be implemented in the TSPA-SR model. The abstracted relationships incorporated in the model are reported in the *Summary of Dissolved Concentration Limits* AMR (CRWMS M&O 2000 [143569]).

Solubility limits were modeled using a geochemical modeling package, EQ3/6. This software is capable of calculating solubility limits under different environmental conditions, such as at different temperatures, pHs, Ehs, and CO₂ fugacity values. Finally, a regression analysis of the solubility data and key parameters was performed to abstract deterministic functions to represent solubility limits for each element in the TSPA-SR model. When the solubility limit of the solubility-controlling mineral phase for an element was found to be independent of the environmental conditions, then stochastic distributions or constants representing the elemental solubility limit were implemented in the TSPA-SR model.

The solubility limits of 21 radioactive elements were investigated for the TSPA-SR model (CRWMS M&O 2000 [143569], Section 6). The investigation was performed for the solubility-controlling mineral under the proposed repository conditions and for the regulatory time scale of the proposed repository (CRWMS M&O 2000 [143569], Section 6.1.2). Solubility limits are incorporated into the TSPA-SR model as functions, stochastic distributions, or constants. For more details on the development and abstraction of the solubility relationships, the reader is referred to the *Summary of Dissolved Concentration Limits* AMR (CRWMS M&O 2000 [143569]).

Inputs to the TSPA Model

The solubility limits defined within the TSPA-SR model are taken directly from the *Summary of Dissolved Concentration Limits* AMR (CRWMS M&O 2000 [143569], Section 7, Table 18 and 19) that are tracked by the DTN: MO0004SPASOL10.002 [151713]. Table 6-55 summarizes the solubility relationships for the elements investigated for the TSPA-SR model. Note that the solubility of Carbon (C), Chlorine (Cl), Cesium (Cs), Iodine (I), Strontium (Sr), and Technetium (Tc) are arbitrarily set equal to 1 mol/L (a conservative upper bound), as it is assumed that no

solubility controlling solids can exist for these elements under the repository conditions (CRWMS M&O 2000 [143569], Section 5).

Table 6-55. Solubility Limits for the Elements Considered in the TSPA-SR Model

Description	TSPA Parameter	Parameter Value	Reference/DTN
Logarithm of Ac, Cm, and Sm Solubility in mg/L	Not in model	$A+B \cdot pH + C \cdot pH^2 + D \cdot \log f_{CO_2} + E \cdot (\log f_{CO_2})^2 + G \cdot pH^2 \cdot \log f_{CO_2} + H \cdot pH \cdot (\log f_{CO_2})^2$	CRWMS M&O 2000 [143569], Table 18 DTN: MO0004SPASOL10.002 [151713]
Am Solubility in mg/L	Solubility_Am	$10^{(A+B \cdot pH + C \cdot pH^2 + D \cdot \log f_{CO_2} + E \cdot (\log f_{CO_2})^2 + G \cdot pH^2 \cdot \log f_{CO_2} + H \cdot pH \cdot (\log f_{CO_2})^2)}$	CRWMS M&O 2000 [143569], Table 18 DTN: MO0004SPASOL10.002 [151713]
C Solubility in mg/L	Solubility_C	1.2E04	CRWMS M&O 2000 [143569], Table 19 DTN: MO0004SPASOL10.002 [151713]
Cl Solubility in mg/L	Not in model	3.54E04	CRWMS M&O 2000 [143569], Table 19 DTN: MO0004SPASOL10.002 [151713]
Cs Solubility in mg/L	Solubility_Cs	1.33E05	CRWMS M&O 2000 [143569], Table 19 DTN: MO0004SPASOL10.002 [151713]
I Solubility in mg/L	Solubility_I	1.27E05	CRWMS M&O 2000 [143569], Table 19 DTN: MO0004SPASOL10.002 [151713]
Nb Solubility in mg/L	Not in model	9.29E-03	CRWMS M&O 2000 [143569], Table 19 DTN: MO0004SPASOL10.002 [151713]
Logarithm of Ni Solubility in mg/L	Not in model	Log-Uniform Distribution Min=-1.08, Max=5.25	CRWMS M&O 2000 [143569], Table 19 DTN: MO0004SPASOL10.002 [151713]
Np Solubility in mg/L	Solubility_Np	$7.538E-8 + 1.086 \times 10^{(8-pH)}$	CRWMS M&O 2000 [143569], Table 18 DTN: MO0004SPASOL10.002 [151713]
Logarithm of Pa Solubility in mg/L	Solubility_Paa	Log-Uniform Distribution Min=-4.64, Max=0.36	CRWMS M&O 2000 [143569], Table 19 DTN: MO0004SPASOL10.002 [151713]
Logarithm of Pb Solubility in mg/L	Not in Model	Log-Uniform Distribution Min=-4.68, Max=0.32	CRWMS M&O 2000 [143569], Table 19 DTN: MO0004SPASOL10.002 [151713]
Logarithm of Pu Solubility in mg/L	Solubility_Pua	Log-Uniform Distribution Min=-4.62, Max=1.68	CRWMS M&O 2000 [143569], Table 19 DTN: MO0004SPASOL10.002 [151713]

Table 6-55. Solubility Limits for the Elements Considered in the TSPA-SR Model (Continued)

Description	TSPA Parameter	Parameter Value	Reference/DTN
Ra Solubility in mg/L	Not in Model	0.52	CRWMS M&O 2000 [143569], Table 19 DTN: MO0004SPASOL10.002 [151713]
Sn Solubility in mg/L	Not in Model	5.934E-03	CRWMS M&O 2000 [143569], Table 19 DTN: MO0004SPASOL10.002 [151713]
Sr Solubility in mg/L	Solubility_Sr	8.76E04	CRWMS M&O 2000 [143569], Table 19 DTN: MO0004SPASOL10.002 [151713]
Tc Solubility in mg/L	Solubility_Tc	9.89E04	CRWMS M&O 2000 [143569], Table 19 DTN: MO0004SPASOL10.002 [151713]
Th Solubility in mg/L	Solubility_Th	2.32	CRWMS M&O 2000 [143569], Table 19 DTN: MO0004SPASOL10.002 [151713]
Logarithm of U Solubility in mg/L. This equation is not applicable for temperatures above 90°C	Log_Sol_U_a	$7.9946 - 2.6963\text{pH} + 0.4292\text{pH}^2 - 1.6286\log f_{\text{CO}_2} + 0.0095T + 0.4161\text{pH} \times \log f_{\text{CO}_2} - 0.0051\text{pH} \times T - 0.0022\log f_{\text{CO}_2} \times T$	CRWMS M&O 2000 [143569], Table 18 DTN: MO0004SPASOL10.002 [151713]
Zr Solubility in mg/L	Not in model	6.20E-05	CRWMS M&O 2000 [143569], Table 18 DTN: MO0004SPASOL10.002 [151713]

In Table 6-55, pH is the local pH inside the waste package, f_{CO_2} is the fugacity of CO_2 within the waste package in bar, T is the temperature of the waste package in Kelvin, and coefficients A through H are constants. The values of coefficients for Am are listed in Table 6-56 (values for Ac, Cm, and Sm are not shown).

Table 6-56. Coefficients for the Am Solubility Function

Coefficient	Value
A	58.0335
B	-18.9422
C	1.4744
D	-6.0032
E	-0.7005
G	0.1162
H	0.1146

DTN: MO0004SPASOL10.002 [151713]

NOTE: CRWMS M&O 2000 [143569], Table 18

Implementation

The aqueous concentration of radionuclides from a breached waste package cannot exceed the elemental solubility limit (CRWMS M&O 2000 [143569], Section 6.1.1). Hence, if multiple isotopes of a radionuclide are present in the aqueous phase, the sum of the concentrations of all the isotopes cannot exceed the elemental solubility limit. The TSPA-SR model accounts for this upper bound on solubility by ensuring that each isotope is identified with a proper name and isotope identifier.

Solubility limits for elements defined using distributions and constants (see Table 6-54) are referenced in the model at a global level (i.e., accessible to all bins) as they are not affected by any environmental parameters implemented here. The elements that come under this category are: Pu, Pa, Tc, C, I, Sr, Cs, and Th. Figure 6-122 shows the organization of these parameters within the TSPA-SR model at a global level.

Solubility limits of U, Np, and Am, as implemented in the model, depend on environmental parameters, such as temperature, pH, and CO₂ fugacity. As both temperature and pH are expected to vary spatially within the repository at any given time (see Section 6.3.2.1 Thermal Hydrology and Section 6.3.4.2 In-Package Chemistry), the solubility limits of U, Np and Am are defined local to each environment (always drip, intermittent drip, and no drip) in the model. The pH within the waste package is dependent on (a) the seepage flux that enters the waste package and (b) the relative glass dissolution rate (for CDSP packages) or the fraction of cladding exposed (for CSNF packages) (see Section 6.3.4.2 In-Package Chemistry). The temperature of the waste package is defined per bin and not localized to each environment. Since the temperature is a function of the infiltration scenario, waste form type (CSNF or CDSP), and time, all temperature dependent parameters will vary with time. The in-package CO₂ fugacity is a constant and defined globally. The solubility limits for U, Np and Am are calculated in each of the fifteen bin environments for each waste form type. Figure 6-123 shows a representation of the solubility limit calculations in an environment.

The solubility equation for Uranium, derived in the feed AMR (CRWMS M&O 2000 [143569]), and defined by the parameter *log_Sol_U_a* is not valid for temperatures above 90°C. For times when the waste package temperatures are greater than 90°C, Uranium solubility is calculated by the parameter *log_Sol_U_b*, which is based on the local pH and water temperature set equal to 90°C. The parameter, *Solubility_U*, compares the temperature passed from the Thermal Hydrology Component (see Section 6.3.2.1); if the temperature exceeds 90°C, it returns the calculated value of *log_Sol_U_b*, otherwise it returns the calculated value of *log_Sol_U_a*. The appropriate local conditions, such as, the pH (e.g., *pH_CSNF*), temperature (e.g., *Temp_CSNF_WP.Temp_CSNF_WP[Bin_4]*), and *f*_{CO2} (*fCO2*) are also used. The solubility of Uranium in the invert is calculated using the same model logic with the appropriate parameters for invert conditions, *pH_Invert* and *Temp_CSNF_Inv* or *Temp_CDSP_Inv*. The solubility of Uranium in the invert is also a local parameter and is calculated in the TSPA-SR model container *Invert_Solubilities* within each bin environment.

The expression element *Solubility_Np* in Figure 6-123 calculates the localized Neptunium solubility limit. The calculation uses the function identified in Table 6-55. The TSPA-SR model uses the appropriate localized pH (*pH_CSNF* or *pH_CDSP*), for the calculation at each time step.

The solubility of Neptunium in the invert is calculated in the TSPA-SR model container *Invert_Solubilities* within each bin environment using the appropriate local parameter, *pH_Invert*.

The expression element *Solubility_Am* in Figure 6-123 calculates the localized Americium solubility limit. The calculation uses the function identified in Table 6-55 and the coefficient values listed in Table 6-56. The calculation uses the appropriate localized pH (*pH_CSNF* or *pH_CDSP*), for the calculation at each time step. The solubility of Americium in the invert is calculated using the same model logic with the appropriate parameters for invert conditions, *pH_Invert*. The solubility of Americium in the invert is a local parameter and is calculated in the TSPA-SR model container *Invert_Solubilities* within each bin environment.

The solubility limits of U, Np, and Am, are calculated the same way for every environment in each of the five bins for both CSNF and CDSP waste packages. Although the parameters *Solubility_U*, *Solubility_Np* and *Solubility_Am* are defined globally, as illustrated in Figure 6-129, these parameters are just place-holders to define the *Water* element (and element solubilities) globally as required within the GoldSim code. The default value of -1 mg/L is assigned to these parameters to designate infinite solubility. These values are never used for calculation purposes as these are replaced at the local level, where solubility limit calculations are performed, using the conditions specific to each environment.

Tables 6-57 and 6-58 summarize the TSPA-SR model parameters that affect the solubility limit calculations. Table 6-57 tabulates all of the TSPA-SR model parameters that although are not direct inputs to the solubility calculations are necessary to implement the model correctly.

Table 6-57. Supplemental TSPA-SR Model Parameters for Solubility Limit Calculations

Description	TSPA Parameter	Parameter Value [†]	Applicability
Converts Solubility_Pua into a solubility in mg/L	Solubility_Pu	$10^{\text{Solubility_Pua}}$	Global
Converts Solubility_Paa into a solubility in mg/L	Solubility_Pa	$10^{\text{Solubility_Paa}}$	Global
Global default for solubility implementation	Solubility_U	-1 mg/L	Global
Global default for solubility implementation	Solubility_Np	-1 mg/L	Global
Global default for solubility implementation	Solubility_Am	-1 mg/L	Global
Log of the Uranium solubility in a CSNF waste package above 90°C in mg/L	Log_Sol_U_b	$7.9946 - 2.6963 * \text{pH_CSNF} + 0.4292 * \text{pH_CSNF}^2 - 1.6286 * \log(\text{fCO2}) + 0.0095 * (90\{\text{C}\}/1\{\text{K}\}) + 0.4161 * \text{pH_CSNF} * \log(\text{fCO2}) - 0.0051 * \text{pH_CSNF} * (90\{\text{C}\}/1\{\text{K}\}) - 0.0022 * \log(\text{fCO2}) * (90\{\text{C}\}/1\{\text{K}\})$	Localized to CSNF Environment

Table 6-57. Supplemental TSPA-SR Model Parameters for Solubility Limit Calculations (Continued)

Description	TSPA Parameter	Parameter Value [†]	Applicability
Log of the Uranium solubility in a CDSP waste package above 90°C in mg/L	Log_Sol_U_b	$7.9946 - 2.6963 * pH_CDSP + 0.4292 * pH_CDSP^2 - 1.6286 * \log(fCO_2) + 0.0095 * (90\{C\}/1\{K\}) + 0.4161 * pH_CDSP * \log(fCO_2) - 0.0051 * pH_CDSP * (90\{C\}/1\{K\}) - 0.0022 * \log(fCO_2) * (90\{C\}/1\{K\})$	Localized to CDSP Environment
Converts log_sol_U_a or log_Sol_U_b in a CSNF environment into a solubility in mg/L	Solubility_U	$if(Temp_CSNF_WP.Temp_CSNF_WP[Bin_1]>90\{C\}, (10^{\log_Sol_U_b}\{mg/l\}), (10^{\log_Sol_U_a}\{mg/l\}))$	Localized to CSNF Environment
Converts log_sol_U_a or log_Sol_U_b in a CDSP environment into a solubility in mg/L	Solubility_U	$if(Temp_CDSP_WP.Temp_CDSP_WP[Bin_1]>90\{C\}, (10^{\log_Sol_U_b}\{mg/l\}), (10^{\log_Sol_U_a}\{mg/l\}))$	Localized to CDSP Environment
Log of the Uranium solubility in the Invert of a CSNF waste package in mg/l	Log_Sol_U_Invert_a	$7.9946 - 2.6963 * pH_Invert + 0.4292 * pH_Invert^2 - 1.6286 * \log(fCO_2) + 0.0095 * (Temp_CSNF_Inv.Temp_CSNF_Inv[Bin_1]/1\{K\}) + 0.4161 * pH_Invert * \log(fCO_2) - 0.0051 * pH_Invert * (Temp_CSNF_Inv.Temp_CSNF_Inv[Bin_1]/1\{K\}) - 0.0022 * \log(fCO_2) * (Temp_CSNF_Inv.Temp_CSNF_Inv[Bin_1]/1\{K\})$	Localized to CSNF Environment
Log of the Uranium solubility in the Invert of a CDSP waste package in mg/l	Log_Sol_U_Invert_a	$7.9946 - 2.6963 * pH_Invert + 0.4292 * pH_Invert^2 - 1.6286 * \log(fCO_2) + 0.0095 * (Temp_CDSP_Inv.Temp_CDSP_Inv[Bin_1]/1\{K\}) + 0.4161 * pH_Invert * \log(fCO_2) - 0.0051 * pH_Invert * (Temp_CDSP_Inv.Temp_CDSP_Inv[Bin_1]/1\{K\}) - 0.0022 * \log(fCO_2) * (Temp_CDSP_Inv.Temp_CDSP_Inv[Bin_1]/1\{K\})$	Localized to CDSP Environment
Log of the Uranium solubility in the invert of a CSNF waste package above an invert temperature of 90°C in mg/L	Log_Sol_U_Invert_b	$7.9946 - 2.6963 * pH_Invert + 0.4292 * pH_Invert^2 - 1.6286 * \log(fCO_2) + 0.0095 * (90\{C\}/1\{K\}) + 0.4161 * pH_Invert * \log(fCO_2) - 0.0051 * pH_Invert * (90\{C\}/1\{K\}) - 0.0022 * \log(fCO_2) * (90\{C\}/1\{K\})$	Localized to a CSNF Environment
Log of the Uranium solubility in the invert of a CDSP waste package above an invert temperature of 90°C in mg/L	Log_Sol_U_Invert_b	$7.9946 - 2.6963 * pH_Invert + 0.4292 * pH_Invert^2 - 1.6286 * \log(fCO_2) + 0.0095 * (90\{C\}/1\{K\}) + 0.4161 * pH_Invert * \log(fCO_2) - 0.0051 * pH_Invert * (90\{C\}/1\{K\}) - 0.0022 * \log(fCO_2) * (90\{C\}/1\{K\})$	Localized to CDSP Environment

Table 6-57. Supplemental TSPA-SR Model Parameters for Solubility Limit Calculations (Continued)

Description	TSPA Parameter	Parameter Value [†]	Applicability
Solubility of Uranium in the invert of a CSNF waste package in mg/L	Solubility_U_Invert	$\text{if}(\text{Temp_CSNF_Inv.Temp_CSNF_Inv}[\text{Bin_1}] > 90\{^{\circ}\text{C}\}, (10^{\log_{\text{Sol_U_Invert_b}}\{\text{mg/l}\}}, (10^{\log_{\text{Sol_U_Invert_a}}\{\text{mg/l}\}}))$	Localized to CSNF Environment
Solubility of Uranium in the invert of a CDSP waste package in mg/L	Solubility_U_Invert	$\text{if}(\text{Temp_CDSP_Inv.Temp_CDSP_Inv}[\text{Bin_1}] > 90\{^{\circ}\text{C}\}, (10^{\log_{\text{Sol_U_Invert_b}}\{\text{mg/l}\}}, (10^{\log_{\text{Sol_U_Invert_a}}\{\text{mg/l}\}}))$	Localized to CDSP Environment
Solubility of Np in a CSNF waste package in mg/l	Solubility_Np	$(7.538\text{e-}8 + 1.086 \cdot 10^{(8-\text{pH_CSNF})})\{\text{mg/l}\}$	Localized to CSNF Environment
Solubility of Np in a CDSP waste package in mg/l	Solubility_Np	$(7.538\text{e-}8 + 1.086 \cdot 10^{(8-\text{pH_CDSP})})\{\text{mg/l}\}$	Localized to CDSP Environment
Solubility of Np in the invert of a CSNF waste package in mg/l	Solubility_Np_Invert	$(7.538\text{e-}8 + 1.086 \cdot 10^{(8-\text{pH_Invert})})\{\text{mg/l}\}$	Localized to CSNF Environment
Solubility of Np in the invert of a CDSP waste package in mg/l	Solubility_Np_Invert	$(7.538\text{e-}8 + 1.086 \cdot 10^{(8-\text{pH_Invert})})\{\text{mg/l}\}$	Localized to CDSP Environment
Solubility of Am in a CSNF waste package in mg/l	Solubility_Am	$(10^{(58.0335 + (-18.9422 \cdot \text{pH_CSNF}) + (1.4744 \cdot \text{pH_CSNF}^2) + (-6.0032 \cdot \log(\text{fCO}_2)) + (-0.7005 \cdot \log(\text{fCO}_2)^2) + (0.1162 \cdot \text{pH_CSNF}^2 \cdot \log(\text{fCO}_2)) + (0.1146 \cdot \text{pH_CSNF} \cdot \log(\text{fCO}_2)^2))})\{\text{mg/l}\}$	Localized to CSNF Environment
Solubility of Am in a CDSP waste package in mg/l	Solubility_Am	$(10^{(58.0335 + (-18.9422 \cdot \text{pH_CDSP}) + (1.4744 \cdot \text{pH_CDSP}^2) + (-6.0032 \cdot \log(\text{fCO}_2)) + (-0.7005 \cdot \log(\text{fCO}_2)^2) + (0.1162 \cdot \text{pH_CDSP}^2 \cdot \log(\text{fCO}_2)) + (0.1146 \cdot \text{pH_CDSP} \cdot \log(\text{fCO}_2)^2))})\{\text{mg/l}\}$	Localized to CDSP Environment
Solubility of Am in the invert of a CSNF waste package in mg/l	Solubility_Am_Invert	$(10^{(58.0335 + (-18.9422 \cdot \text{pH_Invert}) + (1.4744 \cdot \text{pH_Invert}^2) + (-6.0032 \cdot \log(\text{fCO}_2)) + (-0.7005 \cdot \log(\text{fCO}_2)^2) + (0.1162 \cdot \text{pH_Invert}^2 \cdot \log(\text{fCO}_2)) + (0.1146 \cdot \text{pH_Invert} \cdot \log(\text{fCO}_2)^2))})\{\text{mg/l}\}$	Localized to CSNF Environment
Solubility of Am in the invert of a CDSP waste package in mg/l	Solubility_Am_Invert	$(10^{(58.0335 + (-18.9422 \cdot \text{pH_Invert}) + (1.4744 \cdot \text{pH_Invert}^2) + (-6.0032 \cdot \log(\text{fCO}_2)) + (-0.7005 \cdot \log(\text{fCO}_2)^2) + (0.1162 \cdot \text{pH_Invert}^2 \cdot \log(\text{fCO}_2)) + (0.1146 \cdot \text{pH_Invert} \cdot \log(\text{fCO}_2)^2))})\{\text{mg/l}\}$	Localized to CDSP Environment

NOTE: [†] Temperature conversion from °C to °K is done internally by GoldSim

Table 6-58 tabulates the TSPA-SR model parameters that are calculated in other sections of the model and used during the solubility limit calculations.

Table 6-58. Other TSPA-SR Model Parameters with Solubility Limit Calculation Impacts

Description	TSPA Parameter	TSPA Model Reference	Applicability
Average CSNF waste package temperature in Bin	Temp_CSNF_WP	Thermohydrology (see Section 6.3.2.1)	Localized to CSNF Bin
In-package pH of CDSP waste packages	PH_CSNF	In-Package Chemistry Model (see Section 6.3.4.2)	Localized to CSNF Environment
Average CDSP waste package temperature in Bin	Temp_CDSP_WP	Thermohydrology (see Section 7.3.2.1)	Localized to CDSP Bin
In-package pH of CDSP waste packages	PH_CDSP	In-Package Chemistry Model (see Section 6.3.4.2)	Localized to CDSP Environment
Carbon dioxide fugacity	FCO2	In-Package Chemistry Model (see Section 6.3.4.2)	Global

Results and Verification

At the initiation of each simulation a value for each stochastic parameter defined in the model is sampled and used throughout the model for that realization. For the median value simulation, the values assigned to *Solubility_Paa* and *Solubility_Pua* are the mean of the distributions, 0.007244 mg/L and 0.0338844 mg/L, respectively. The solubility limits of Tc, Th, C, I, Sr, and Cs are defined globally as constant values in the model (Table 6-59).

Table 6-59. Solubility Limits for Tc, Th, C, I, Sr, and Cs

TSPA Parameter	Assigned Value (mg/L)	Simulation Value (mg/L)
Solubility_Tc	9.89E+04	98900
Solubility_Th	2.32	2.32
Solubility_C	1.2E+04	12000
Solubility_I	1.27E+05	127000
Solubility_Sr	8.76E+04	87600
Solubility_Cs	1.33E+05	133000

Figure 6-124 shows the calculated solubility limits for the three radionuclide elements, U, Np, and Am, for both the CSNF waste package and the invert for the Always Drip environment in Bin 4. The abstracted solubility relationships were determined for a pH range between 5 and 9 for Uranium, 4.5 to 8.5 for Neptunium, and 5 to 12 for Americium. It was later determined that the solubility calculated with pH values below these ranges can deviate from the values calculated using EQ3/6. For example, a calculation of Uranium solubility limit at pH = 3.6 showed that the solubility limit of Uranium increases at low pH values using the abstracted relationships. This value was found to be about 50 percent higher than the simulated solubility limit predicted using EQ3/6 (CRWMS M&O 2000 [143569], Section 6.3.6, p. 26). Thus it

should be noted that the calculation for the Uranium solubility in the model at low pH is conservative. Similarly, calculation of Np solubility at low pH (between 3.6 and 4.0) was also conducted using the abstracted relationship and compared to the value predicted by EQ3/6. The abstracted relationship underestimated the Np solubility limit by about 10% at low pH values (CRWMS M&O 2000 [143569], Section 6.4.6, p. 32). A low pH impact analysis was not reported for Americium.

In the median value simulation the CSNF waste packages within the Always Drip environment in Bin 4 have first package failure around 42,000 years. The calculated solubility limits before 42,000 years are unimportant as no mass is exposed to seeping water until the inner barrier of the package fails. Once the packages fail, dissolution of the waste form occurs eventually leading to the release of radionuclides. As the dissolution of waste form occurs, the pH within the packages change leading to changes in solubility limits for Uranium, Neptunium, and Americium. The sharp changes in the calculated solubility limits are directly correlated to sharp changes in the in-package pH (see Section 6.3.4.2 In-Package Chemistry). This is because the temperature dependence on the Uranium solubility limit has little effect once the packages have failed; at times beyond 50,000 years the thermal changes in the repository are minor and the conditions within the repository are near ambient (see Section 6.3.2.1 Thermal Hydrology). Furthermore, none of the variability in the solubility limits can be attributed to changes in CO₂ fugacity since it is held constant in all the simulations.

The invert solubility limits are calculated using the same abstracted relationships as discussed for the waste package except that the local pH and temperatures for the invert conditions are used. The pH in the invert does not fluctuate as much as the waste package pH and therefore the solubility limit profiles for the invert show minor changes. Comparing the solubility limits between the waste package and invert, it is observed that higher solubility limits exist for the waste package at times immediately following package failure. Thus more mass can be carried out of the waste package to the invert. Upon reaching invert, conditions of relatively low solubility limits may be encountered, resulting in precipitation of some species from the solution.

The solubility limits for Uranium, Neptunium, and Americium inside a CDSP waste package and invert are compared in Figure 6-125. In the median value simulation for Bin 4, Always Drip environment, the waste packages begin to fail around 44,000 years. As a result, the pH changes significantly and the calculated solubility limits change. Similar to the CSNF calculations, the changes in solubility limits beyond 40,000 years are largely due to the changes in pH only.

The implementation of the solubility of U, Np, and Am, can be verified through manual calculations. The solubility at a certain time step, $t = 100,000$ years, was randomly selected for the computation. This computation compared the expected results with the calculated results for both the waste package types in the Always Drip environment in Bin 4. The median values for the simulated pH (pH_{CSNF} , pH_{CDSP} , and pH_{Invert}) and temperature ($Temp_{CSNF_WP}$, $Temp_{CSNF_WP}[Bin_4]$, $Temp_{CDSP_WP}$, $Temp_{CSNF_WP}[Bin_4]$, $Temp_{CSNF_Inv}$, $Temp_{CSNF_Inv}[Bin_4]$ and $Temp_{CDSP_Inv}$, $Temp_{CDSP_Inv}[Bin_4]$) inside each waste package and invert environment located in Bin 4 were extracted from the appropriate model components and tabulated for $t=100,000$ years. These values and the globally defined CO₂ fugacity were used to calculate the solubility of U, Np, and Am as defined by the appropriate equations in Table 6-55 and Table 6-56. The results are compared in Table 6-60.

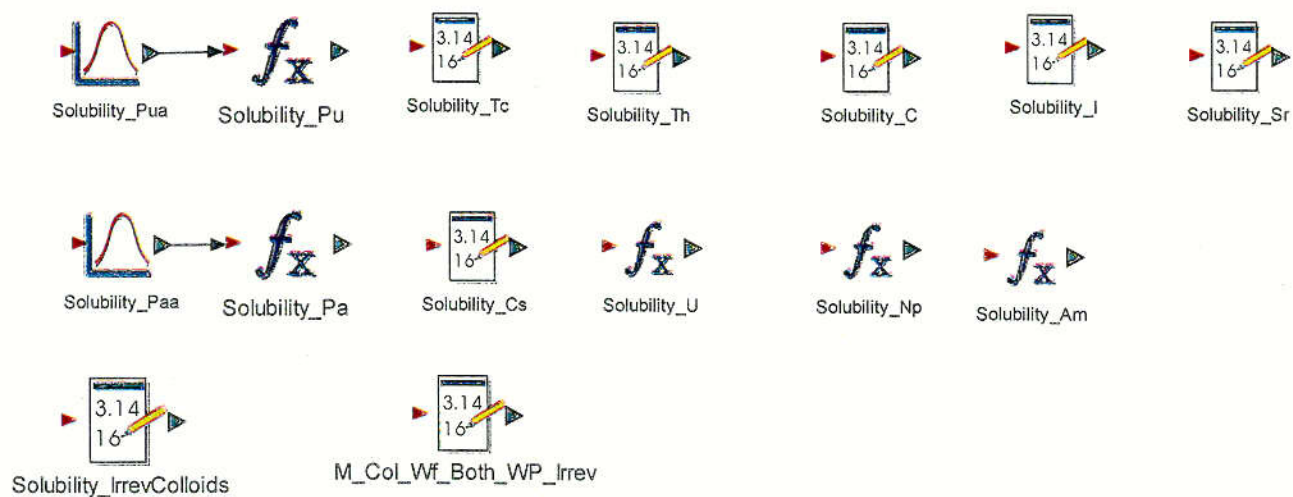
The model calculated results for the solubility of U, Np, and Am are nearly identical, within roundoff error, to the values calculated manually using the equations described in the *Summary of Dissolved Concentration Limits* AMR (CRWMS M&O [143569]). This verifies that the solubility implementation for U, Np, and Am is correct. Furthermore, the agreement between the calculated values and the model results verify that the model correctly sends and receives parameter values (i.e., the temperature, pH, and carbon dioxide fugacity) between components.

Table 6-60. Verification of the TSPA-SR Model Solubility Limit Calculations for U, Am, and Np

TSPA Parameter	Location	pH	Temperature (K)	CO ₂ Fugacity (atm)	Manual Calculation	Model Value
Solubility_U	CSNF, Bin 4, Always Drip	6.7436	295.56	0.001	2.4630	2.4634
Solubility_U	CDSP, Bin 4, Always Drip	8.8573	295.46	0.001	1056.1	1056.2
Solubility_U_Invert	CSNF, Bin 4, Always Drip	7.0734	298.15	0.001	3.1439	3.1440
Solubility_U_Invert	CDSP, Bin 4, Always Drip	7.0732	298.15	0.001	3.1431	3.1430
Solubility_Np	CSNF, Bin 4, Always Drip	6.7436	Not Applicable	Not Applicable	19.599	19.598
Solubility_Np	CDSP, Bin 4, Always Drip	8.8573	Not Applicable	Not Applicable	0.1508	0.1508
Solubility_Np_Invert	CSNF, Bin 4, Always Drip	7.0734	Not Applicable	Not Applicable	9.1713	9.1709
Solubility_Np_Invert	CDSP, Bin 4, Always Drip	7.0732	Not Applicable	Not Applicable	9.1755	9.1757
Solubility_Am	CSNF, Bin 4, Always Drip	6.7436	Not Applicable	0.001	1.4203	1.4200
Solubility_Am	CDSP, Bin 4, Always Drip	8.8573	Not Applicable	0.001	0.2619	0.2620
Solubility_Am_Invert	CSNF, Bin 4, Always Drip	7.0734	Not Applicable	0.001	0.2374	0.2374
Solubility_Am_Invert	CDSP, Bin 4, Always Drip	7.0732	Not Applicable	0.001	0.2376	0.2376

The solubility limits of Pu and Pa are also implemented properly. The median value simulation results for the solubility limits of Pu and Pa are 0.0338844 mg/L and 0.00724436 mg/L, respectively, which match the distribution means built into the uniform distributions for Pu ($10^{-1.47}$ mg/L = 0.033884415 mg/L) and Pa ($10^{-2.14}$ mg/L = 0.007244359 mg/L).

Solubility



Uranium, Neptunium and Americium Solubility are defined local to every drip group

Figure 6-122. Illustration of the Globally Defined Solubility Limits in the TSPA-SR Model

Solubility

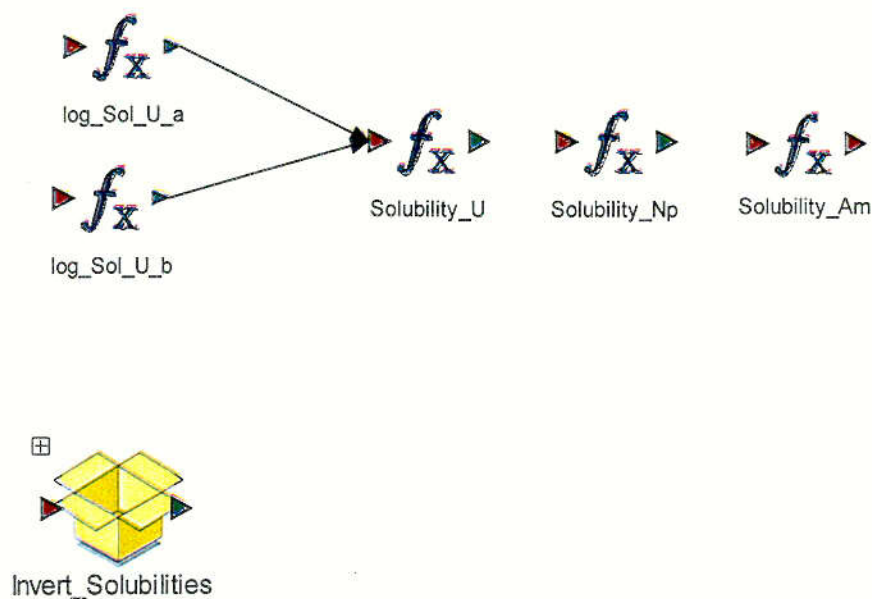


Figure 6-123. Graphical Representation of the Localized Solubility Limit Calculations for an Environment

C82

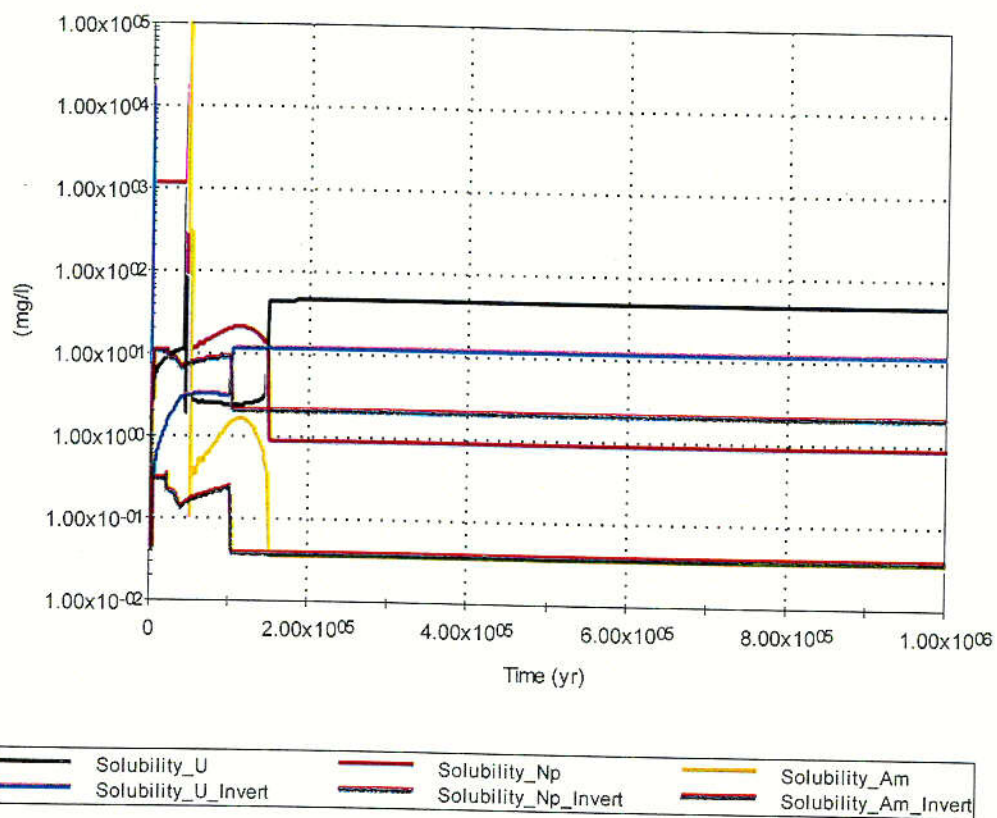


Figure 6-124. Calculated Solubility Limits of the Selected Radionuclides for the Median Value Simulation, Bin 4 Always Drip Environment: CSNF Waste Packages and Invert

C83.

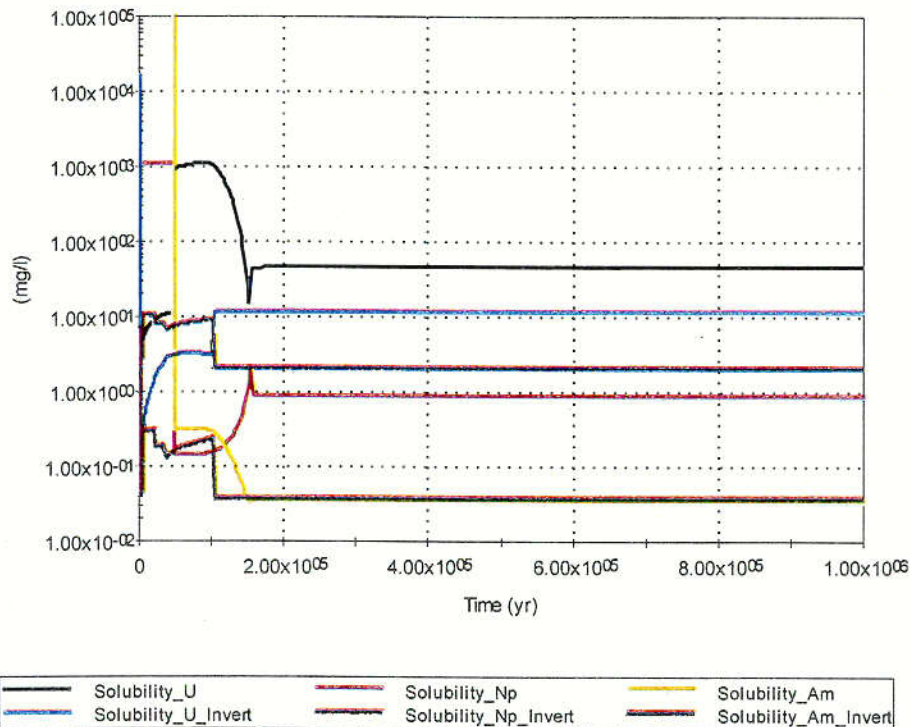


Figure 6-125. Calculated Solubility Limits of the Selected Radionuclides for the Median Value Simulation, Bin 4 Always Drip Environment: CDSP Waste Packages and Invert

6.3.4.6 Colloids

Overview

Colloid-facilitated mobilization and transport of radionuclides in the engineered barrier system (EBS) is modeled for plutonium, americium, and their daughter products. Several types of colloids are expected to be generated within the Yucca Mountain repository system (CRWMS M&O 2000 [125156], Section 6.1.1.3). Of these, three types are modeled within the TSPA-SR model colloids derived from DOE High Level Waste (HLW) glass, naturally occurring groundwater colloids, and colloids derived from the degradation of the steel components of the EBS (iron-(hydr)oxides)(CRWMS M&O 2000 [125156], Section 6.1.1).

Radionuclides from HLW, within CDSP waste packages, will be initially bound in a glass matrix. As seepage water percolates through the drift and into a failed CDSP waste package, it will slowly degrade the glass matrix. As the glass matrix degrades, smectite colloids will be produced. These clay colloids derived from the degradation of HLW glass wastes will have plutonium and americium radionuclides entrained (engulfed) within colloid (CRWMS M&O 2000 [125156], Section 6.1.1.1). The entrained plutonium has been determined to behave 'irreversibly' (i.e., they do not release radionuclides through dissolution or degradation), and the mass of a radionuclide initially bound within the irreversible colloid will be permanently locked within the colloid throughout its transport toward the accessible environment. All irreversible colloids produced will also act as sites for the reversible sorption of additional radionuclides

C84

species (CRWMS M&O 2000 [125156], Section 6.2.1.3). No irreversible waste form colloids will be produced from the degradation of CSNF wastes (CRWMS M&O 2000 [125156]).

Iron-(hydr)oxide and naturally occurring groundwater colloids occur in infiltrating waters for both CSNF and CDSP waste packages. Radionuclides released during waste form degradation of DSNF, HLW, and CSNF are expected to reversibly sorb to colloids suspended within the infiltrating waters. For CDSP packages the total mass of colloids available for *reversible* sorption is comprised of iron-(hydr)oxides from the degradation of EBS steel materials, naturally occurring colloids, and waste form colloids containing irreversibly bound radionuclides. For CSNF packages the total mass of colloids available for *reversible* sorption are only those which occur in the infiltrating waters, i.e., naturally occurring ground water and corrosion product colloids (CRWMS M&O 2000 [125156], Section 6.4.1).

The stability of colloids and consequently, the mobility of sorbed or bound plutonium, is defined as a function of the ionic strength and pH of the waste package waters (CRWMS M&O 2000 [125156], Section 6.3.3.1). In other words, the abundance of mobile colloids (stability) is strongly dependent upon the water chemistry. Conditional tests are performed to determine the final concentration of Pu entrained in or sorbed onto irreversible and reversible colloids. The process logic developed for accessing colloidal stability and mass concentrations detailed in the flow charts shown in Figure 6-126 through Figure 6-128.

The concentration of americium *bound irreversibly* in waste form colloids is determined as a function of the mass fraction of Am to Pu in the HLW itself (CRWMS M&O 2000 [125156], Section 6.2.1.1). By using the total concentration of Pu bound irreversibly and the ratio of Am to Pu in the source term, the total concentration of Am *bound irreversibly* can be calculated. All *reversibly sorbed* species are calculated based on the total mass of colloids available for reversible sorption within the waste form cell (i.e., waste form, iron-(hydr)oxide, and ground water colloids) and the species distribution coefficient, Kd (CRWMS M&O 2000 [125156], Section 6.1.3).

For a detailed analysis of the colloids and colloid formation, the reader is referred to *AMR Waste Form Colloid-Associated Concentration Limits: Abstraction and Summary* (CRWMS M&O 2000 [125156]).

Inputs to the TSPA Model

Table 6-61 lists the input parameters for the colloid model for irreversible Pu waste form iron-hydr(oxide), and ground water colloids. All data are qualified except DTN: MO0003SPAHLO12.004 [147952] and MO0003SPAION02.003 [147951], and taken primarily *Colloid-Associated Concentration Limits: Abstraction and Summary* Section 4.1 (CRWMS M&O 2000 [125156]).

Table 6-61. Input Parameters for the Colloid Model Calculations

Parameter Description	TSPA Parameter*	Parameter Value	Source/DTN
Highest observed mass of both types of waste form colloids per unit volume of water in mg/l	M_Col_Wf_Both_Max	5.0	Section 4.1 CRWMS M&O 2000 [125156] DTN: LL991109851021.095 [142902]
Lowest observed concentration of radionuclide associated waste form colloids; for Pu only in mol/l	CPu_Col_Wf_Irrev_Min	1e-11	Section 4.1 CRWMS M&O 2000 [125156] DTN: MO0003SPALOW12.001 [147953]
Highest observed concentration of radionuclide associated waste form colloids; for Pu only in mol/l	CPu_Col_Wf_Irrev_Max	6e-8	Section 4.1 CRWMS M&O 2000 [125156] DTN: LL991109851021.095 [142902]
Ionic strength below which colloids are stable (mol/l)	I_lo_thresh_Col	0.01	Section 4.1 CRWMS M&O 2000 [125156] DTN: MO0003SPAION02.003 [147951]
Ionic strength above which colloids are unstable (mol/l)	I_hi_thresh_Col	0.05	Section 4.1 CRWMS M&O 2000 [125156] DTN: MO0003SPAION02.003 [147951]
Lowest observed mass of iron-hydroxide colloids per unit volume of water in mg/l	M_Col_FeOX_Min	1e-3	Section 4.1 CRWMS M&O 2000 [125156] DTN: MO0003SPAHIG12.002 [147949]
Highest observed mass of iron-hydroxide colloids per unit volume of water in mg/l	M_Col_FeOX_Max	1	Section 4.1 CRWMS M&O 2000 [125156] DTN: MO0003SPAHIG12.002 [147949]
Lowest observed mass of groundwater colloids per unit volume of water in mg/l	M_Col_GW_Min	3e-6	Section 4.1 CRWMS M&O 2000 [125156] DTN: MO0003SPAHLO12.004 [147952]
Highest observed mass of groundwater colloids per unit volume of water in mg/l	M_Col_GW_Max	3e-2	Section 4.1 CRWMS M&O 2000 [125156] DTN: MO0003SPAHLO12.004 [147952]
Distribution coefficient for reversible sorption of Pu onto waste form colloids in ml/g	Kd_Wf_Coll_Pu	Log-Normal Distribution Geometric Mean=1e4 S.D. = 10	Section 4.1 CRWMS M&O 2000 [125156] DTN: MO0004SPAKDS42.005 [148810]

Table 6-61. Input Parameters for the Colloid Model Calculations (Continued)

Parameter Description	TSPA Parameter*	Parameter Value	Source/DTN
Distribution coefficient for reversible sorption of Am onto waste form colloids in ml/g	Kd_Wf_Coll_Am	Log-Normal Distribution Geometric Mean=1e5 S.D. = 10	Section 4.1 CRWMS M&O 2000 [125156] DTN: MO0004SPAKDS42.005 [148810]
Distribution coefficient for reversible sorption of Pu onto Iron Oxy hydroxide colloids in ml/g	Kd_Fe_Coll_Pu	Log-Normal Distribution Geometric Mean=1e4 S.D. = 10	Section 4.1 CRWMS M&O 2000 [125156] DTN: MO0004SPAKDS42.005 [148810]
Distribution coefficient for reversible sorption of Am onto Iron Oxy hydroxide colloids in ml/g	Kd_Fe_Coll_Am	Log-Normal Distribution Geometric Mean=1e4 S.D. = 10	Section 4.1 CRWMS M&O 2000 [125156] DTN: MO0004SPAKDS42.005 [148810]
Distribution coefficient for reversible sorption of Pu onto groundwater colloids in ml/g	Kd_Gw_Coll_Pu	Log-Normal Distribution Geometric Mean=1e3 S.D. = 10	Section 4.1 CRWMS M&O 2000 [125156] DTN: MO0004SPAKDS42.005 [148810]
Distribution coefficient for reversible sorption of Am onto groundwater colloids in ml/g	Kd_Gw_Coll_Am	Log-Normal Distribution Geometric Mean=1e3 S.D. = 10	Section 4.1 CRWMS M&O 2000 [125156] DTN: MO0004SPAKDS42.005 [148810]

Implementation

The colloid flow chart logic in Figure 6-126 through Figure 6-128 is implemented in the TSPA-SR model to calculate the concentration of Pu irreversibly bound in waste form colloids and the mass concentration of reversible colloids available for sorption of radionuclides. In addition, the following assumptions concerning colloids were used:

1. The irreversible colloids represent a closed system in which no radionuclide mass is added or subtracted (except through decay and ingrowth) during travel from the waste package to the accessible environment. Transport of irreversible colloids and their daughter products are handled in three separate ways (from the perspective of decay):
 - a. For $^{242}\text{Pu}_{\text{irr}}$, $^{240}\text{Pu}_{\text{irr}}$, $^{239}\text{Pu}_{\text{irr}}$, and $^{238}\text{Pu}_{\text{irr}}$ the combined dose of the daughters and granddaughters within the colloid is several orders of magnitude less than the dose of the parent during the travel time within the natural barriers. (This assumes the travel time is about 75,000 years or less for irreversible colloids). No decay to irreversible daughter products for these species, only decay with ingrowth to dissolved daughter species.

- b. $^{243}\text{Am}_{\text{irr}}$ is decayed to $^{239}\text{Pu}_{\text{irr}}$, but the daughters of $^{239}\text{Pu}_{\text{irr}}$ are dissolved species.
 - c. $^{241}\text{Am}_{\text{irr}}$ is decayed to its irreversible daughter ($^{237}\text{Np}_{\text{irr}}$) that is irreversibly bound within the colloid.
- 2. Irreversible colloids are created as the HLW glass degrades and contain a known initial mass of the parent radionuclide but no initial mass of the daughter products.
- 3. For calculational purposes no reversible colloids are present until the maximum concentration of irreversible colloids is satisfied in a given time step.
- 4. There are no irreversible CSNF colloids (CRWMS M&O 2000 [125156], Section 7).
- 5. There are only naturally occurring smectites and iron-(hydr)oxide colloids available for CSNF radionuclides to reversibly attach.
- 6. Attachment of Pu and Am to colloids is both irreversible and reversible. The reversible portion is based on the total mass of all colloids present or entering the package.
- 7. Th and Pa are both transported as reversibly attached to colloids
- 8. When colloids enter the EBS cells, their stability (based on ionic strength and pH) is determined on the basis of the chemistry of the invert cell. If coagulation is indicated, then the irreversible colloidal species (e.g., $^{241}\text{Am}_{\text{irr}}$ and $^{237}\text{Np}_{\text{irr}}$ daughter) are precipitated against a "solubility" limit computed from the colloid stability.
- 9. Radionuclides irreversibly bound to colloids are assigned to the colloids according to their isotopic mass fraction at the time of formation of the colloids.
- 10. The Kc equilibrium model, which combines radionuclide distribution coefficients and constant colloid mass concentration, will be used for the transport of radionuclides reversibly bound to colloids in unsaturated zone (UZ) and saturated zone (SZ) transport calculations.

The input data is globally defined in the *Materials* container in the *Engineered_Barrier_System* and is illustrated in Figure 6-129.

Calculation of Pu and Am Concentration Bound in Irreversible Colloids from HLW Waste. Figure 6-130 illustrates the TSPA-SR implementation of the calculation of Pu irreversibly bound to waste form colloids generated from the degradation of the HLW waste form. The model logic implemented in the TSPA-SR model mimics the logic depicted in the flow charts in Figure 6-126. The colloid calculations reference local conditions for ionic strength and pH (see Section 6.3.4.2, In-package Chemistry) and must be calculated within each bin environment. The calculation of waste form colloids is performed in the waste form and invert cells for CDSP waste packages only. The implementation for the HLW waste form colloid calculations for CDSP waste packages is discussed next.

The logic implemented in the selector switch *CPu_Col_Wf_Irrev_a* calculates the concentration of Pu colloids generated in a given time step according to the logic in Figure 6-126. The calculation compares the ionic strength of the seepage water in the package, *Ionic_Str_CDSP* to the threshold values, *I_hi_thresh_Col* and *I_lo_thresh_Col*. Based on the result of the comparison the value of *CPu_Col_Wf_Irrev_a* equals the value of the input parameters *CPu_Col_Wf_Irrev_Min*, or *CPu_Col_Wf_Irrev_Max*, or the result of the calculation (see Equation 6-4) (CRWMS M&O 2000 [125156], Equation 6-4):

$$(-1.25\text{e-}6 * (\text{Ionic_Str_CDSP}) + 7.25\text{e-}8) \text{ \{mol/l\}} \quad (\text{Eq. 6-4})$$

The expression element *CPu_Col_Wf_Irrev_b* implements the colloid stability criteria depicted in Figure 6-126. If the ionic strength, *Ionic_Str_CDSP*, is greater than or equal to the in-package pH, *pH_CDSP* divided by 200 (CRWMS M&O 2000 [125156], Section 6.3.3.1), the colloids are unstable and the value of *CPu_Col_Wf_Irrev_b* equals the value of *CPu_Col_Wf_Irrev_Min*, otherwise the colloids are stable and the value of *CPu_Col_Wf_Irrev_b* equals the value of *CPu_Col_Wf_Irrev_a* (CRWMS M&O 2000 [125156], Section 6.3.3.1).

The model parameter *M_Col_Wf_Both_WP_Rev* calculates the mobile mass of waste-form colloids with reversibly or irreversibly attached Pu (CRWMS M&O 2000 [125156], Section 6.3.3.1). The implemented expression is shown in Figure 6-130. This mass is used to calculate the reversible mass for sorbtion of radionuclides for transport. This value is used in the *Waste_Form* Cell: *M_Col_Wf_Both_WP_Rev * Vol_Water* is the total mass of colloids available for reversible transport of sorbing radionuclides. The parameter *Solubility_IrrevColloids* calculates the mobile radionuclide concentration of the colloidal species (note that, in the strict sense, this is *not* "solubility;" in this document, however, solubility is used in a general sense to describe concentrations of mobile colloidal radionuclides as well as dissolved concentrations of radionuclides). It is equal to the value of *CPu_Col_Wf_Irrev_b* times the average atomic weight of Pu (239 (g/mol)). The atomic weight of ²³⁹Pu is used to approximate the total solubility of the irreversible colloids in the waste form water volume. The colloids (Ic species in TSPA model) will compete for the solubility limit in the waste form cell and must have the same solubility defined. The other parameters in Figure 6-130 are used to calculate the mass of Pu colloids generated. The model parameter *M_Col_Wf_Both_WP_Irrev* calculates the solubility of the *Col* species, a model species added to track the mass of colloids generated in the waste form cell. Fundamentally, the generation of irreversible colloidal mass is a function of the rate at which the waste form glass degrades and the amount of spallation of colloidal particles. The maximum irreversible colloidal abundance is given as a concentration limit as a function of the water chemistry in the waste form cell, and it is not based upon the available waste form material. Since we do not know how much of the waste form will be irreversible colloidal material prior to the model run, irreversible colloid mass cannot be added to the inventory at the expense of their soluble species, rather this mass must be calculated from the maximum concentration available based on the waste form water chemistry for each CDSP BIN and environment in the TSPA-SR model. *M_Col_Wf_Both_WP_Irrev* is calculated as the concentration of colloids generated from the HLW waste form degradation, *CPu_Col_Wf_Irrev_a* divided by the maximum amount of colloids that can be generated, *CPu_Col_Wf_Irrev_Max*, multiplied by the maximum mass of both types of waste form colloids per unit volume of water, *M_Col_Wf_Both_Max*. This maximum concentration is used as the solubility limit of the species 'Col' in the waste form cell. The mass of 'Col' transported from the waste form cell to the invert is then used as the total mass

of irreversible colloids in the waste form cell per time step. This is used to calculate the mass fraction of each irreversible colloid (see below).

The Plutonium based colloidal species are *Ic234*, *Ic237*, *Ic238*, *Ic239*, and *Ic240*. The Americium based colloidal species are *Ic241* and *Ic243*. The model parameters *Pu_wf_cell*, *Pu_Species*, *Pu_Total*, and *Pu_Mole_Fraction* are used to calculate the mass fraction of each Pu species to the total Pu available in the waste form at each time step. The calculation converts the mass of each species into a mole quantity, sums the total number of moles and calculates the mole fraction of each Pu species. The mole fractions are then used to calculate the maximum concentrations of each individual Pu species irreversibly attached to the colloids, *CPu_Col_Wf_Irrev_Pu238*, *CPu_Col_Wf_Irrev_Pu239*, *CPu_Col_Wf_Irrev_Pu240*, and *CPu_Col_Wf_Irrev_Pu242*, as a function of the total calculated concentration of irreversibly bound Pu (*CPu_Col_Wf_Irrev_a*) and fraction of the species to the total available Pu mass in the waste form cell (*Pu_Mole_Fraction*).

The concentration of Am bound irreversibly in waste form colloids is calculated in the TSPA-SR model as depicted in Figure 6-131. It is assumed that for a given concentration of Pu irreversibly bound an amount of Am will be also be bound irreversibly in proportion to the mole fraction of Am/Pu that is released from the source term at each time step (CRWMS M&O 2000 [125156], Section 6.2.1.1). Figure 6-131 illustrates the calculation of the concentration of Am irreversibly bound in colloids in the waste form cell. The parameters *Am_Wf_cell*, *Am_Species*, *Am_Total*, *Am_Mol_Fraction* are analogous to those used in the Pu parameter calculations and are used to distribute the entrained masses of Am species entrained by the colloids. The expression element *CAM_Col_Wf_Irrev* calculates the concentration of Am irreversibly entrained within the colloids. The value of *CAM_Col_Wf_Irrev* equals the concentration of Pu irreversibly bound to the colloids (*CPu_Col_Wf_Irrev_a*) multiplied by the ratio of Am to Pu mass in the waste form. The parameters *CAM_Col_Wf_Irrev_Am241* and *CAM_Col_Wf_Irrev_Am243* are the species specific concentrations on the colloids ($Am_Mole_Fraction(Species) * CAM_Col_Wf_Irrev_a * Species\ molecular\ weight\ \{g/mol\}$).

Stable colloids are available for transport from the waste form to the invert. The mass of colloids in the invert is bounded on the upper end by the mass of colloids generated in the waste form. Deviations in chemical conditions in the invert could cause the colloids to become unstable within the invert. The *In_Invert_Wf_Colloids* container contains parameters that implement the logic to capture the deviations in colloid stability that may arise due to changes in chemical conditions from the waste form cell to the invert cell. The model logic for calculating *CPu_Col_Wf_Irrev_Invert_b*, *M_Col_Wf_Both_Invert*, and *Solubility_IrrevColloid_Invert* is analogous to the waste form parameter calculation logic except the invert conditions, *ionic_str_invert* and *pH_Invert* (see Section 6.3.2.2 In-drift Geochemical Environment) are used in the conditional statements instead of the waste form conditions, *Ionic_Str_CDSP* and *pH_CDSP*. The solubility of the irreversible colloid species is redefined for the invert cell based on the invert calculated stabilities for the colloidal particles.

Calculation of Iron-(hydr)oxide Colloids. The mass of iron-(hydr)oxide colloids available for reversible sorption in the waste form cell is conducted in accordance with the logic outlined in the flow chart depicted in Figure 6-127. The colloid calculations reference local conditions for ionic strength and pH and must be calculated within each bin environment. The concentration of

iron-(hydr)oxide colloids is calculated within the waste form and invert for both CDSP and CSNF waste packages. The model logic for each calculation is identical, but the calculations use the appropriate local conditions for each waste package type.

The iron-(hydr)oxide colloid calculations are implemented using conditional expression elements which test the logic conditions in the flow chart (Figure 6-127). These expression elements are *Condition_A_WP*, *Condition_B_WP*, *Condition_C_WP*, *Condition_D_WP*, and *Condition_E_WP*. Figure 6-132 shows the model implementation.

The parameter *Condition_A_WP* tests to determine whether or not the ionic strength, *Ionic_Str_CDSP*, is within the threshold range, *I_lo_thresh_Col* and *I_hi_thresh_Col*. If the ionic strength at the given time step is within this range, the value of *Condition_A_WP* equals 1, otherwise it equals 0 (note that 1 and 0 correspond to switches representing “yes” and “no”). The parameter *Condition_B_WP* tests to see whether or not the colloids are within the stability range based on the chemical conditions within the waste package. The stability criteria are functions of ionic strength, *Ionic_Str_CDSP*, and pH, *pH_CDSP*, constrained by Equation 6-5 and Equation 6-6 (CRWMS M&O 2000 [125156], Section 6.3.3.2):

$$ST_{\text{coll,FeOX,pHhi}} = -0.02 * pH_CDSP + 0.17 \quad (\text{Eq. 6-5})$$

and

$$ST_{\text{coll,FeOX,pHlo}} = +0.02 * pH_CDSP - 0.17 \quad (\text{Eq. 6-6})$$

If the value of *Ionic_Str_CDSP* is greater than either of the calculated values, for the given time step, the value of *Condition_B_WP* equals 1, otherwise it equals 0. *Condition_C_WP* tests one other stability condition. If the value of *Ionic_Str_CDSP* is below the minimum ionic strength threshold, *I_lo_thresh_Col*, and the value of *pH_CDSP* is between 8 and 9, inclusive, the colloids are unstable and the value of *Condition_C_WP* equals 1, otherwise it equals 0. *Condition_D_WP* combines an IF statement and the two conditional statements *Condition_A_WP* and *Condition_B_WP* to test the first two conditions in Figure 6-127. If *Ionic_Str_CDSP* is greater than *I_hi_thresh_Col* or *Condition_A_WP* and *Condition_B_WP* both equal 1 then the colloids formed are unstable and *Condition_D_WP* equals 1; otherwise it equals 0. The final conditional parameter, *Condition_E_WP*, equals 1 if either *Condition_C_WP* or *Condition_D_WP* equal 1; otherwise it equals 0. If *Condition_E_WP* equals 1, the iron-(hydr)oxide colloids are unstable and the mass of iron-(hydr)oxide colloids per unit volume of water, *M_Col_FeOX_WP*, equals the minimum expected mass concentration of iron-(hydr)oxide colloids, *M_Col_FeOx_Min*. If *Condition_E_WP* equals 0, the iron-(hydr)oxide colloids are stable and the mass of iron-(hydr)oxide colloids per unit volume of water, *M_Col_FeOX_WP* equals the maximum expected mass concentration of iron-(hydr)oxide colloids, *M_Col_FeOx_Max*.

The chemical conditions in the invert may be different than the chemical conditions in the waste package. Thus the mass of colloidal particles in the invert may be different than the mass of colloidal particles in the waste package. The mass concentration of colloidal particles in the invert, *M_Col_FeOX_Invert*, is calculated the same way *M_Col_FeOX_WP* is calculated except the ionic strength and pH conditions reference the invert conditions, *Ionic_Str_Invert* and

pH_Invert and not the waste package conditions. Figure 6-133 shows the graphical illustration of the invert calculation.

Calculation of Naturally Occurring Ground Water Colloids. The calculation of the mass concentration of ground water colloids available for reversible sorption in the waste form cell is conducted in accordance with the logic outlined in the flow chart depicted in Figure 6-129. The colloid calculations reference local conditions for ionic strength and pH and must be calculated within each bin environment. The calculation of groundwater colloids is calculated within the waste form and invert for both CDSP and CSNF waste packages. The model logic for each calculation is identical, but the calculations use the appropriate local conditions for each waste package type. The implementation for the groundwater colloid calculations for CDSP waste packages is discussed next. The implementation is illustrated in Figure 6-134.

According to the AMR *Waste Form Colloid-Associated Concentration Limits: Abstraction and Summary* (CRWMS M&O 2000 [125156]) the stability function $ST_{coll,gw}$ equals

$$10^{[A \cdot \log(Ionic_Str_CDSP) + B]} \quad (Eq. 6-7)$$

where

$$A = \frac{\log(M_{coll,gw,max}) - \log(M_{coll,gw,min})}{\log(I_{lo_thresh,coll,gw}) - \log(I_{hi_thresh,coll,gw})}, \text{ and}$$

$$B = \frac{[\log(M_{coll,gw,min}) \times \log(I_{lo_thresh,coll,gw})] - [\log(M_{coll,gw,max}) \times \log(I_{hi_thresh,coll,gw})]}{\log(I_{lo_thresh,coll,gw}) - \log(I_{hi_thresh,coll,gw})}$$

which represents the equation for a line in log-log space.

The model parameter $M_Col_GW_A_WP$ calculates the first term in Equation 6-6 using the appropriate time step values for $M_Col_GW_Max$, $M_Col_GW_Min$, $I_{lo_thresh_Col}$, $I_{hi_thresh_Col}$, and $Ionic_Str_CDSP$. The model parameter $M_Col_GW_B_WP$ calculates the “B” term using the appropriate time step values for $M_Col_GW_Max$, $M_Col_GW_Min$, $I_{lo_thresh_Col}$, and $I_{hi_thresh_Col}$. The parameter $M_Col_GW_C_WP$ calculates Equation 6-6. The selector switch $M_Col_GW_WP_a$ implements the model logic in Figure 6-129. If the value of $Ionic_Str_CDSP$ is greater than the ionic strength threshold, $I_{hi_thresh_Col}$, then the value of $M_Col_GW_WP_a$ equals $M_Col_GW_Min$. If the value of $Ionic_Str_CDSP$ is between, $I_{hi_thresh_Col}$ and $I_{lo_thresh_Col}$ then the value of $M_Col_GW_WP_a$ equals the result of Eq. 4, $M_Col_GW_C_WP$. Otherwise it equals $M_Col_GW_Max$. The selector switch $M_Col_GW_WP$ implements the stability criteria illustrated in Figure 6-129. If the value of $Ionic_Str_CDSP$ is greater than or equal to $I_{hi_thresh_Col}$ or $pH_CDSP/200$ (CRWMS M&O 2000 [125156], Section 6.3.3.3, p. 62) then the colloids are unstable and the value of $M_Col_GW_WP$ equals the value of $M_Col_GW_Min$, otherwise it equals the value of $M_Col_GW_WP_a$.

The TSPA-SR model implementation for calculating groundwater colloids in the invert is identical to the calculation of groundwater colloids in the waste form; however, the calculations

use the appropriate parameters for the invert chemistry, *Ionic_Str_Invert* and *pH_Invert* in the conditional statements instead of the waste form chemistry parameters. The implementation is illustrated in Figure 6-135.

Irreversible Colloid Mass in the Waste Form Cell. In the TSPA-SR model a species' irreversible mass is tracked separately from the soluble mass. The soluble mass of each isotope is available for transport as a dissolved species or by reversible sorption onto colloids. The irreversible mass of each species behaves as a non-sorbing species. Its mass is tracked separately to isolate it from the constraints placed on the soluble portion. Additionally, the irreversible mass of each species is tracked separately to accurately pass the irreversible mass to the UZ model (FEHM) (see Section 6.3.6 Unsaturated Zone Transport). In the TSPA-SR model additional species were added to the master species list for each of the irreversible colloids. These species are given the prefix of 'Ic' and their atomic number, e.g., *Ic243* for irreversible ²⁴³Am. The mass of irreversible colloids released from the source term to the waste form cell is controlled by the mass of waste form exposed, the glass matrix dissolution rate, *Glass_Deg_Rate*, for HLW (see Section 6.3.4.4 Dissolution Rate Model) and the calculated concentration of irreversible colloids produced. The total soluble mass of Pu and Am released from the waste form glass is modified to remove the fraction that is bound irreversibly as colloids.

The total concentration of Pu (or Am) bound irreversibly within waste form colloids, *CPu_Col_Wf_Irrev_a*, is controlled by the logic outlined in the flow chart depicted in Figure 6-126 as discussed previously. The soluble mass of Pu and Am must be adjusted in the waste form cell to remove the fraction of Pu and Am bound irreversibly; the mass fraction bound irreversibly must be known. As the amount of irreversible colloids is not known prior to the model run, it cannot be added to the source term at the expense of soluble Pu and Am. The colloid model for TSPA-SR, yields a concentration of colloids as a function of the water chemistry. The mass release of Pu and Am bound in irreversible colloids must be calculated and removed from the soluble Pu and Am available in the waste form cell. This mass is not readily available, thus a method was devised to 'simulate' the release of colloidal mass from the waste form cell to the invert cell. This simulated flux was used to calculate the amount of Pu and Am to remove from the soluble mass and add to the Pu and Am irreversible colloidal mass in the waste form cell. Again, the mass of colloid is not known, given that the concentration of colloids is known (calculated), by creating a species called "Col" with an unlimited inventory and setting the solubility of Col in the waste form cell to the calculated concentration, the flux from the waste form cell to the invert of Col in g/yr is equal to the total flux of colloids from the waste form at a given calculated concentration of irreversible colloids produced. Specifically, a "fictitious" species, *Col*, is added to the species list. This species is tracked solely to be used to calculate the irreversible species mass in the waste form cell. *Col* is given a high abundance in the HLW inventory so that the source term will continuously release it at the rate of the HLW glass matrix dissolution, *Glass_Deg_Rate*. Given that there is always more mass of *Col* available in the source term than the combined mass of the Pu and Am species, at any time in the waste form cell, the abundance of *Col* will exceed the abundance of Pu and Am. This allows us to define the species *Col* a solubility limit equal to *M_Col_Wf_Both_WP_Irrev*, the total mobile colloid mass, where the concentration of the irreversibly bound species is defined by the parameter *CPu_Col_Wf_Irrev_a*. Due to an extremely high abundance of *Col* in the waste form cell the mass flux of *Col* from the waste form cell to the drift cell will always be solubility

limited when advective processes are dominating. When there is no advection, the species *Col* is allowed to diffuse with the other radionuclide species. The mass flux of *Col* from the waste form cell is controlled by the concentration of irreversible colloids produced from the source term, *CPu_Col_Wf_Irrev_a*. Given the flux of *Col* from the waste form cell in grams of colloid per year, *Colloid_MassFlux*, the following relationship (Equation 6-8) is used to calculate the mass of Pu (or Am) as irreversible colloids:

$$\left(\frac{CPu_col_wf_irrev_a \left(\frac{g(Pu)}{l} \right)}{M_col_wf_both_WP_a \left(\frac{g(Colloid)}{l} \right)} \right) Colloid_MassFlux \left(\frac{g(colloid)}{yr} \right) \cdot timestep_length(yr) \text{ (Eq. 6-8)}$$

For each irreversible colloid species (e.g., *Ic240*), the concentration (e.g., *CPu_col_wf_irrev_a_Pu240*) is used in Equation 6-7 to calculate the mass of the Pu (or Am) isotope bound irreversibly in colloids. This mass is then removed (subtracted) from the total mass of the species in the waste form cell. This process is preformed in the TSPA-SR model for the irreversible Pu species as depicted in Figure 6-136.

For each radionuclide the cumulative mass exposed from the source term is tracked by GoldSim for every time step. The cumulative mass of ²⁴⁰Pu released from the “AlwaysDrip” source element, *CDSP_AlwaysDrip.Cumulative_to_Waste_Form[Pu240]*, is tracked and recorded as output. Similar output is tracked for each radionuclide for each source term. The parameters *Prev_Pu238_exposed*, *Prev_Pu239_exposed*, *Prev_Pu240_exposed*, *Prev_Pu242_exposed*, *Prev_Am241_exposed*, and *Prev_Am243_exposed* are the cumulative masses of each radionuclide released from the source into the waste form from the previous time step and are stored in the *Previous_Mass_Exposed* container in Figure 6-136. The data elements *Prev_Pu_Exposed* and *Prev_Am_Exposed* combine the data for the Pu and Am isotopes into a species specific vector tracking the previous masses exposed. The mass of each isotope irreversibly bound in the HLW waste form colloid is calculated at each time step in the species specific expression elements, *Mass_Pu238_Irrev*, *Mass_Pu239_Irrev*, *Mass_Pu240_Irrev*, *Mass_Pu242_Irrev*, *Mass_Am241_Irrev*, and *Mass_Am243_Irrev* using Equation 6-7. Each expression element compares the mass of each species released from the waste form at each time step and takes the lesser of the two values. Based on experimental evidence, most of the mass released from the waste form will initially occur as engulfed radionuclides in colloids. Therefore, for calculational purposes, *Mass_in_Pathway*, will first be bound in irreversible colloids. Once the calculated mass in the pathway exceeds the maximum mass irreversibly bound in waste form colloids the maximum mass irreversibly bound in waste form colloids is saturated and the remaining mass is available for reversible sorption and solubilization. The vector parameter *Mod_Source* tracks the impact of colloid generation on the formation of each ‘Ic’ species and the decrease of each isotope species. *Mod_Source* adds the mass of an irreversibly bound radionuclide (i.e., *Mass_Pu238_Irrev*) to the irreversible colloid species (i.e., *Ic238*) and subtracts this same amount from the radionuclide species (i.e., *Pu238*). The consequence element is the implemented mechanism to change the inventory in the source element by the values in the *Mod_Source* vector. The *Mod_Source* vector is added to the waste form cell as a discrete event that occurs at each time step. This allows the waste form cell mass to be adjusted each time step to fractionate the species mass between soluble and irreversible species.

Reversible Colloid Mass Flux from the Waste Form Cell. For each colloid type (waste form, iron-(hydr)oxide, and ground water) a solid species element was defined. Figure 6-137 illustrates this implementation. Each solid element has specific Kd values for each reversibly sorbed radionuclide species. In the *Waste_Form* cell each solid element is defined as a suspended material and allowed to interact with the dissolved radionuclide mass. For each colloid type, a mass of the material is needed to calculate the mass fraction of a dissolved radionuclide species reversibly sorbed. Figure 6-126 defines the logic for the stability of the waste form colloids in the water column and calculates a mass flux of waste form colloids available in the waste form cell for *reversible* transport, $M_{col_wf_both_WP_b}$, as a fraction of the maximum colloidal mass flux, $M_{col_wf_both_max}$, times the ratio of the concentration of Pu irreversibly bound to the maximum possible Pu irreversibly bound, $CPu_{col_wf_irrev_b} / CPu_{col_wf_irrev_max}$. The mass flux of waste form colloid is multiplied by the volume of water in the waste form cell to calculate the total mass of waste form colloid available for reversible transport. The mass of iron-(hydr)oxide and ground water colloids is calculated in the waste form cell by multiplying the volume of the waste form cell by the mass flux for each colloid type respectively (see sections above). The TSPA-SR model uses the defined Kd values to track the mass sorbed reversibly throughout the system. For CSNF packages only iron-(hydr)oxide and ground water colloids are present. Waste form colloids are only produced from CDSP packages.

Colloids in the UZ and SZ. Colloid facilitated transport is modeled through the UZ and SZ for both reversible and irreversible colloids. At the EBS-UZ interface, the irreversible colloidal mass, as tracked by individual irreversible species and their daughters (e.g., I-241, I-237), is passed to FEHM. The irreversible colloids are tracked through the UZ and passed back at the UZ-SZ interface. The irreversible colloids are tracked through the SZ and to the accessible environment. For reversible species the Kc model is used in both the UZ and SZ (see Sections 6.3.6 Unsaturated Zone Transport and Section 6.3.7 Saturated Zone Transport). Table 6-62 below lists parameters that affect the colloid mass calculation

Table 6-62. Other TSPA-SR Parameters with Colloid Generation Calculation Impacts

Description	TSPA Parameter	Parameter Value	Applicability
pH within a CDSP waste package	pH_CDSP	As defined for each local environment by the in package chemistry.	Localized to Environment
pH within a CSNF waste package	pH_CSNF	As defined for each local environment by the in package chemistry.	Localized to Environment
pH in the Invert cell	pH_Invert	As defined for each local environment by the in drift chemistry.	Localized to Environment
Ionic Strength within a CDSP waste package	Ionic_Str_CDSP	As defined for each local environment by the in package chemistry.	Localized to Environment
Ionic Strength within a CSNF waste package	Ionic_Str_CSNF	As defined for each local environment by the in package chemistry.	Localized to Environment
Ionic Strength in the Invert cell	Ionic_Str_Invert	As defined for each local environment by the in drift chemistry.	Localized to Environment
Mass Fraction Calculation	Cumulative_mass_to_waste_form_cell	Example: CDSP_AlwaysDrip.Cumulative_to_Waste_Form[Pu238]	Localized to Environment

Results and Verification

This section discusses the results and verification of the colloid component of the TSPA-SR model. All of the results presented below represent the median value simulation. Although the generation of irreversible and reversible colloids in CDSP waste packages and invert for the Always Drip environment in Bin 4 is discussed in this section, the model logic for every other bin environment is identical with one exception. CSNF waste packages do not form irreversible colloids so this calculation is omitted from CSNF environment calculations.

The ionic strength inside the waste package and invert is a key parameter in assessing the stability of the generated colloids. Figure 6-138 plots the waste package ionic strength in the Always Drip environment in Bin 4 along with the threshold limits for waste form colloids.

Colloid formation will commence once a waste package has failed and the waste form is exposed to percolating water. In the median value simulation the waste packages in the Always Drip environment in Bin 4 begin to fail at 44,500 years. The ionic strength in the waste package once waste package failure is initiated is below the low threshold for the first 1,000 years. According to the model logic the maximum concentration of plutonium irreversibly attached to colloids, 6×10^{-8} mol/L, should be generated. At 46,000 years the in-package chemistry changes from the early phase conditions to the late phase conditions (see Section 6.3.4.2 In-Package Chemistry) causing the ionic strength in the package to increase by about a factor of ten, from 0.00326 mol/L to 0.03376 mol/L. The change in chemical conditions causes the ionic strength in the package to exceed the low threshold yet remains below the high threshold. As the in package pH is 5.0091, the colloids are unstable (as tested by the stability test, $CPu_Col_Wf_Irrev_b$, ionic strength $< pH/200$, $0.03376 > 0.2505$) and the concentration of Pu irreversibly bound in the colloid reaches its minimum, $1e-11$ mol/L. By 47,000 years, the pH has adjusted and the ionic strength reaches the stable range for the duration of the simulation. The concentration of Pu irreversibly bound to the waste form colloids should equal $(-1.25 \times 10^{-6} (Ionic_Str_CDSP) + 7.25 \times 10^{-6})$ mol/l from 47,000 years to 1,000,000 years. Figure 6-139 tracks the concentration of irreversibly bound Pu on waste form colloids ($CPu_Col_Wf_Irrev_b$). As the figure shows, the concentration of Pu irreversibly bound to waste form colloids is equal to the maximum, 6×10^{-8} mol/L until 46,000 years. The concentration of irreversibly attached Pu drops to the minimum for one time step, $t = 46,000$, and then rises to equal the value calculated result of the equation $(-1.25 \times 10^{-6} (Ionic_Str_CDSP) + 7.25 \times 10^{-6})$ mol/l. Trends shown in the plot verifies that the implemented logic works appropriately.

In the invert, the changes in aqueous chemical conditions could cause the waste form colloids to become unstable. According to the implemented logic, if the ionic strength in the invert, $Ionic_Str_Invert$, exceeds the high threshold then the colloids become unstable and a change in colloidal mass available for reversible transport in the water column should occur (if $Ionic_Str_Invert > I_hi_Thresh_Col$, $CPu_Wf_Irrev_Min$). Figure 6-140 displays the ionic strength in the invert with the applicable conditions. The ionic strength in the invert exceeds the high threshold at early times, but there is no impact because at these times the waste packages have not failed and no colloids can be generated. After the first 32,000 years the ionic strength in the invert is between the low and high threshold and no change in colloidal mass is observed.

The behavior of Am irreversibly bound in the waste form colloids is quite different than that of Pu because of the relatively short half-life of Am (9.40498×10^{-5} years⁻¹, Section 6.3.4.1 Radionuclide Inventory). By the time the waste packages fail (approximately 44,500 years) all of the initial ²⁴¹Am inventory has naturally decayed and 98.5 percent of the initial ²⁴³Am inventory has naturally decayed. The mass fraction of Am to Pu is very low after package failure (3.06×10^{-5}), consequently the concentration of Am on irreversible colloids will be very low. Figure 6-141 shows both the Pu and Am species concentrations irreversibly bound to waste form colloids. The concentration of Am species irreversibly bound to waste form colloids in the waste package is on the order of 1.0×10^{-13} mol/L and lower.

The following paragraphs focus on the formation of iron-(hydr)oxide colloids in the waste package and in the invert. The results presented in Figure 6-142 show that the ionic strength in the waste package never exceeds the high threshold and is always greater than the value calculated by Equation 6-6. As can be seen in the graph (Figure 6-142), the ionic strength is below the low threshold until the elapsed time is equal to 46,000 years. The resulting explanation is identical to the threshold comparison presented earlier for the waste form colloids. Given the calculated results and in accordance with the implemented logic, Condition A equals 1 only after 46,000 years and Condition B always equals 1. During the time period when the ionic strength is below the low threshold, the in-package pH equals 5.0091, as a result, Condition C in the model logic will never equal 1. According to the flow chart logic the mass concentration of iron-(hydr)oxide colloids is at its maximum, 1mg/L, until the elapsed time equals 46,000 years. Starting at 46,000 years the mass concentration of iron-(hydr)oxide colloids is at its minimum, 0.001 mg/L.

The ionic strength comparison to the invert conditions is shown in Figure 6-143. At early times before the waste packages fail, the calculated ionic strength in the invert is greater than the high threshold. Because colloid formation is not an issue prior to waste package failure this has no impact on the calculated results. At all other times in the simulation the ionic strength in the invert is between the low and high thresholds and is always greater than the result of Equation 3. Therefore, Conditions A and B equal 1 during the period when colloid formation can occur and the formation is unstable so the minimum mass of iron-(hydr)oxide colloids is predicted in the invert. Figure 6-144 shows the calculated mass of iron-(hydr)oxide colloids in the waste package and in the invert. This is the mass available for reversible sorption of radionuclide species. From 44,500 years (initial waste package failure) until 46,000 years, the mass of iron-(hydr)oxide colloids is limited by aqueous chemical conditions in the invert.

For the groundwater colloid calculations the ionic strength conditional statements for calculating the mass of groundwater colloids are the same as the conditional statements used for calculating waste form colloids. The ionic strength comparisons for both the waste package and invert are shown in Figure 6-138 and Figure 6-140. Inside the waste package the ionic strength is below the low threshold and the pH-based threshold immediately after package failure, according to the model logic the maximum mass of groundwater colloids, 3.0×10^{-2} mg/L is expected. At 46,000 years the ionic strength is greater than the low threshold but higher than the pH-based threshold, the colloids are unstable and the minimum mass of groundwater colloids, 3e-06 mg/L, is expected. After 46,000 years the ionic strength is between the low and high threshold and lower than the pH-based threshold and the stable mass calculated by Equation 6-6 is expected.

Figure 6-145 shows the model results match the predicted results, verifying that the model logic works correctly.

The ionic strength in the invert is outside the low and high pH threshold for the first 32,000 years. This has no impact on the amount of colloids which can form because it is prior to waste package failure. Once the waste packages have begun failing, around 44,500 years, the ionic strength remains between the low and high thresholds and the mass of groundwater colloids formed per unit volume of water is calculated using Equation 6-7 with the value of *Ionic_Str_Invert* at each time step. The results are presented in Figure 6-146.

The following paragraphs describe the observed results for the additional irreversible species and the removal of an equivalent mass of soluble species from the waste form calculational cells. This discussion pertains to TSPA-SR model parameters shown in Figure 6-130, Figure 6-131, and Figure 6-136.

The mass of each soluble radionuclide species removed from the waste form cell due to irreversible entrainment within the waste form colloids is calculated as the total mass of each radionuclide entrained within irreversible colloids per unit volume of water (e.g., *Cpu_Col_Wf_Irrev_Pu239*) divided by the total mass of colloids produced per unit volume of water, *M_Col_Wf_Both_WP_Irrev* multiplied by the product of waste form cell to invert cell mass flux of colloids and the time differential (i.e., the time step length). The result of the first two terms $Cpu_Col_Wf_Irrev_Pu239 / M_Col_Wf_Both_WP_Irrev$ yields the mass of radionuclide which, if available, is bound per unit mass of colloid. The second term yields the mass of colloids which is produced in a time step. The product of the two terms yields the mass of the radionuclide leaving the waste form cell due to irreversible attachment in waste form colloids. The amount of each radionuclide entrained within irreversible colloids was added to a new species for each radionuclide. The masses of these species, *Ic238*, *Ic239*, *Ic240*, *Ic241*, and *Ic243* increase at the expense of ²³⁸Pu, ²³⁹Pu, ²⁴⁰Pu, ²⁴¹Am, and ²⁴³Am. This is depicted in Figure 6-147. The lesser of the available mass of soluble Pu in the waste form cell or the calculated mass of irreversible colloidal species is used to add irreversible colloidal mass to the waste form cell (see above for the description of the parameters called *Mass_Pu239_Irrev*, etc). A consequence generator adds and subtracts mass to the waste form cell each time step. Figure 6-147 displays that the appropriate mass is added to irreversible species. An equivalent mass is subtracted from the soluble species.

All of the calculations in the colloid component of the TSPA-SR model have been verified using hand calculations. The results of the hand calculations are used to plot the curves in the figures shown in this section. The model parameters track the predicted responses based on the conditional statements described in the flow charts in Figure 6-126 through Figure 6-128. The sorption of Pu and Am species onto reversible colloids is discussed in section 6.3.5.2 EBS Flow and Transport.

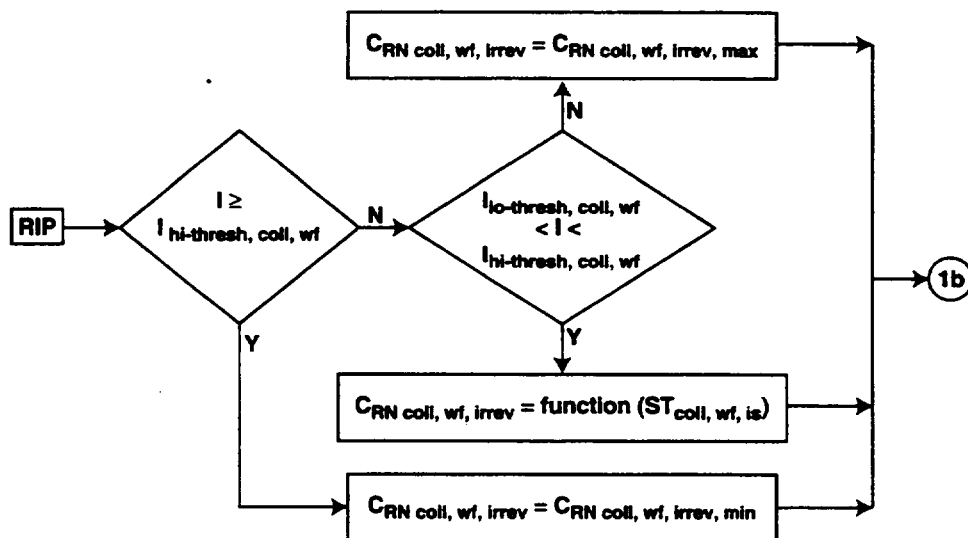


Figure 1a. Waste-form Colloids - Generation from Degradation of HLW Glass

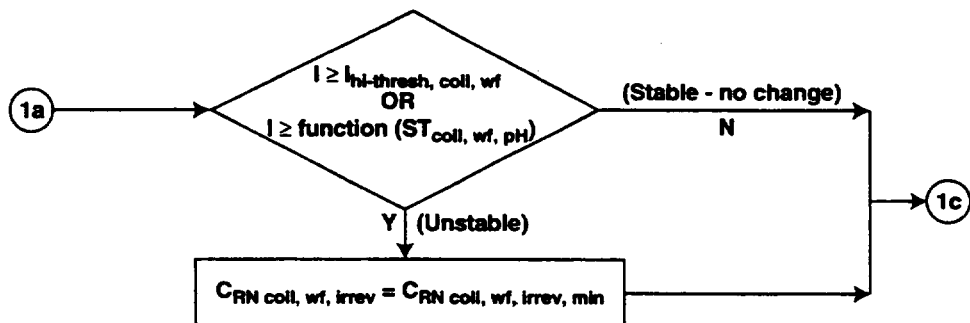


Figure 1b. Waste-form Colloids - Effect of pH and Ionic Strength on Stability

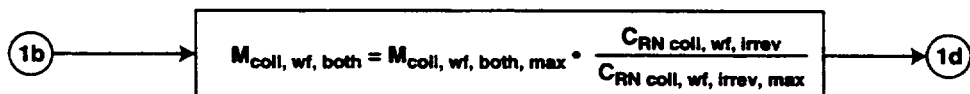


Figure 1c. Waste-form Colloids - Mobile Colloid Mass

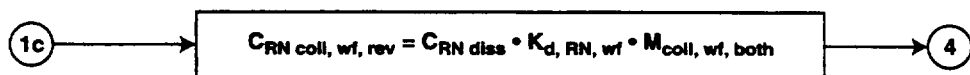


Figure 1d. Waste-form Colloids - Sorption of Radionuclides

TRI-6243-6272-0

Figure 6-126. Waste Form Colloid Formation Flow Charts of Model Logic

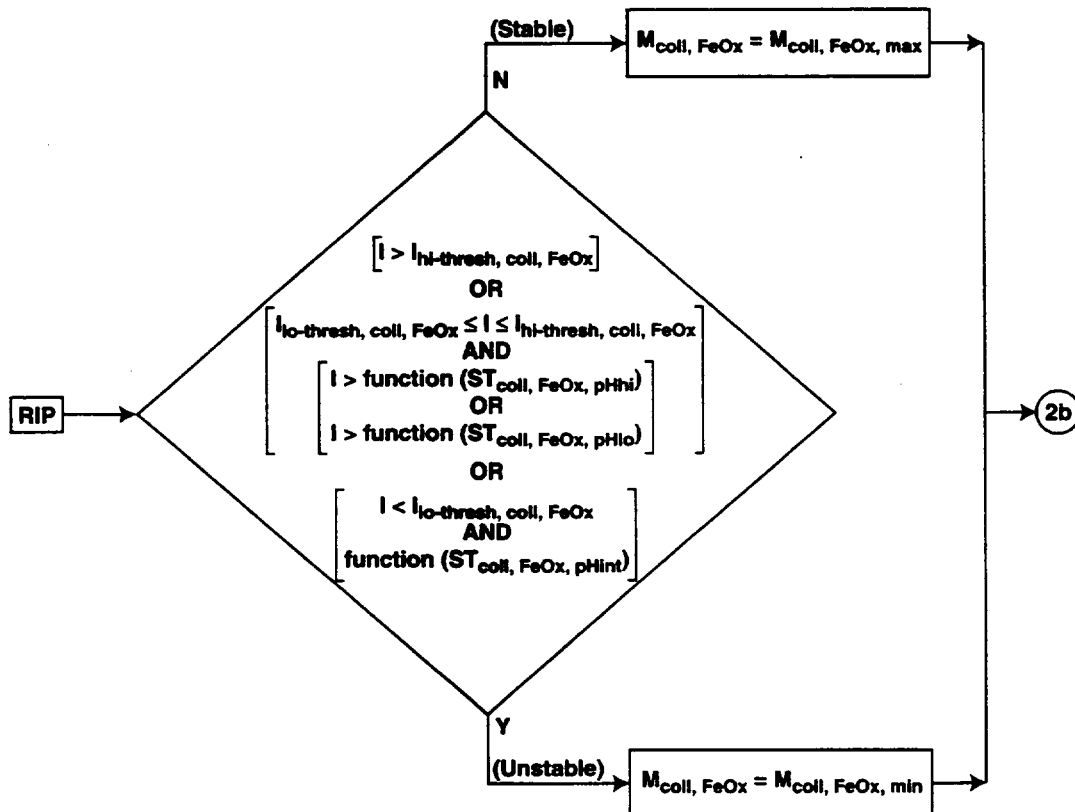


Figure 2a. Iron - (Hydr)oxide Colloids - Effect of pH and Ionic Strength on Stability



Figure 2b. Iron - (Hydr)oxide Colloids - Sorption of Radionuclides

TRI-6243-6273-0

Figure 6-127. Iron-(Hydr)oxide Colloid Formation Flow Charts of Model Logic

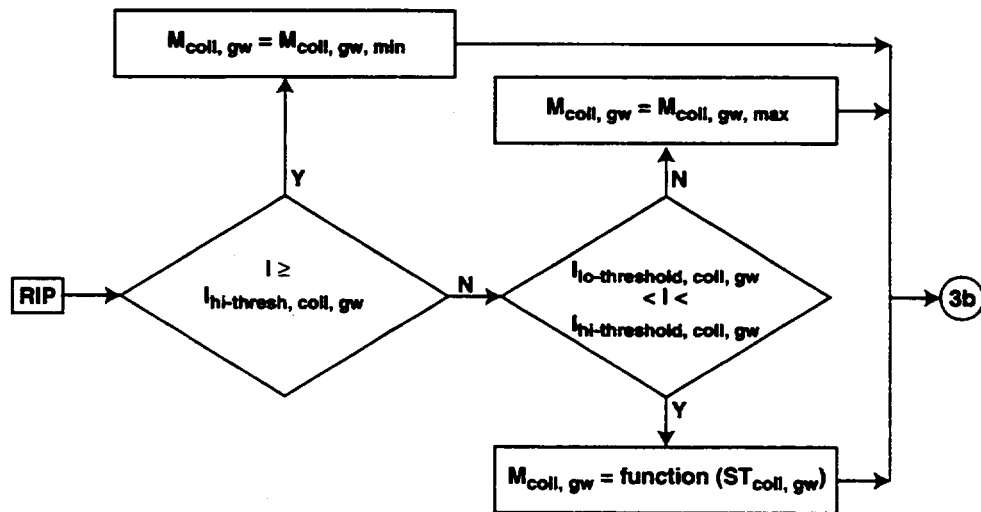


Figure 3a. Groundwater Colloids - Effect of Ionic Strength on Mobile Mass

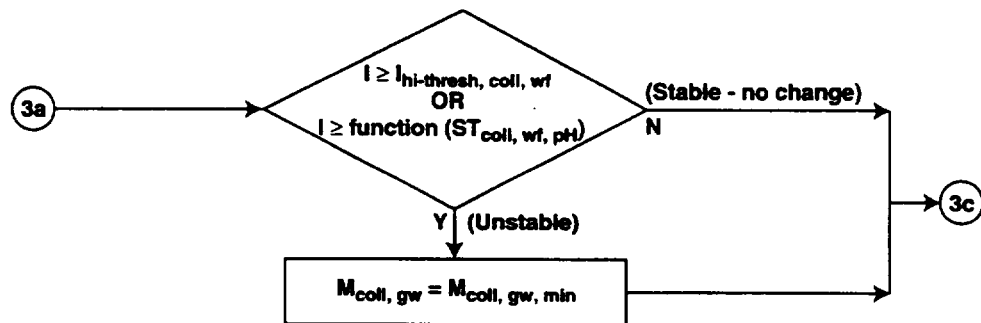


Figure 3b. Groundwater Colloids - Effect of pH on Stability

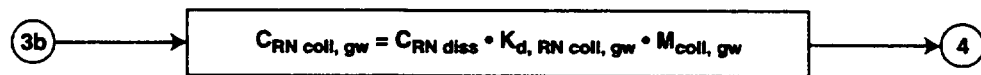


Figure 3c. Groundwater Colloids - Sorption of Radionuclides

TRI-6243-6274-0

Figure 6-128. Groundwater Colloid Formation Flow Charts of Model Logic

through water is the primary mechanism controlling the release of radionuclides from the EBS (see FEP 3.2.10.00.00 in CRWMS M&O 2000 [150806] for the screening arguments related to gaseous release). Before the radionuclide transport can occur, the waste forms must degrade, cladding must fail (for commercial spent nuclear fuel packages), and the waste packages must be breached.

In the TSPA-SR model, three primary waste package breach mechanisms are considered:

- The formation of pits (small openings formed through localized corrosion of waste packages)
- The formation of patches (large openings formed by the generalized corrosion of the waste packages)
- The formation of stress corrosion cracks (formed by the welding of the waste package lids that grow under the action of tensile stresses).

Both advection and diffusion can occur through the pits and patches while only diffusion is assumed to occur through the stress corrosion cracks (see assumption in Section 5.3.5). The stress corrosion cracks are expected to act as a barrier to the advective transport of radionuclides because of their small size and because they will fill up with corrosion products in a relatively short period of time (CRWMS M&O 2000 [129284]). The only breach mechanism considered for the drip shield is the formation of patches resulting from generalized corrosion since the formation of pits and stress corrosion cracks is ignored for the drip shield (see assumption in Section 5.3.3). Advective mass release is governed by the flux of water through the corroded drip shield and the waste package and the concentration of radionuclides in the water based on their solubilities. A flux splitting algorithm is used to determine the fluid volume that flows through the drip shield or waste package and the remainder that flows around the drip shield or waste package. The algorithm assumes that the fluid flux through a patch or pit in the drip shield or waste package is proportional to the ratio of the total length of penetration in the axial direction to the total axial length of the drip shield or waste package (see assumption in Section 5.3.5). The fractional length breached is determined by the corrosion of the drip shield and the waste package, which are presented in Section 6.3.3. It is physically unrealistic to assume that the advective flux in the waste package can occur through stress corrosion cracks, as discussed above.

For packages that do not see drips, the only pathway for release is through diffusion of radionuclides from the breached surface of waste package. Even in the absence of dripping flux, the waste form and invert material will likely have a residual saturation because of the relative humidity in the repository after closure. It is assumed that there is a continuous pathway of water for diffusive transport from the waste form, through the invert and into the surrounding rock (see assumption in Section 5.3.5). Diffusive release is a function of the diffusive mass flux area, the diffusivity of radionuclide species, and the concentration gradient. The diffusive area is proportional to the area of the waste package breached, while the concentration gradient is a function of the difference in concentration between two points.

The maximum concentration of each radionuclide in water is a function of its aqueous solubility, which is dependent on the in-package and in-drift chemistry (see Section 6.3.4.6). Both

advective and diffusive mass fluxes are affected by the aqueous solubilities. The net result is that the radionuclides with low solubility limits will have a much lower mass flux from the waste compared to the radionuclides with high solubility limits. Information about the solubilities of individual radionuclides can be found in Section 6.3.4.5 of this document.

Sorption onto colloids is also important for EBS transport. For TSPA-SR model, colloid-facilitated transport is modeled for plutonium, americium, and their daughter products. Information regarding colloidal properties is provided in Section 6.3.4.6 of this document. In general, plutonium and americium have low solubilities in water, but can readily sorb to colloids in the waste package water. Since both advective and diffusive transport of colloids can occur, the overall release of plutonium and americium is greater than the dissolved release as determined from the solubility limits. A certain portion of plutonium and americium in the waste form is assumed to be an inherent part of the colloidal structure that is formed by the breakdown of glass matrix containing the high level waste (see Section 6.3.4.6 for details). This fraction of plutonium and americium is assumed to be irreversibly sorbed to colloids (see Section 5.3.4).

Multiple pathways exist for the transport of radionuclides through the EBS and into the host rock. In the following section these pathways are described and their implementation in GoldSim code is addressed. Although several processes can affect the release of radionuclides from the EBS, only parameters that significantly affect transport through the EBS will be discussed here. The important processes, as implemented in GoldSim code, are shown graphically in Figure 6-148.

Implementation

The transport of radionuclides through the EBS is modeled within GoldSim code by defining individual mixing cells and interconnections between the cells thus representing the physical components and transport pathways respectively. A mixing cell is a well-mixed compartment represented by the volume of water (e.g., the volume of water in the invert or in a waste package) and the homogenized mass of the materials associated with the water (either dissolved or suspended via colloids) in that cell. Connections define the advective or diffusive transport properties between the cells. The following sections detail the parameters that define the cells and connections.

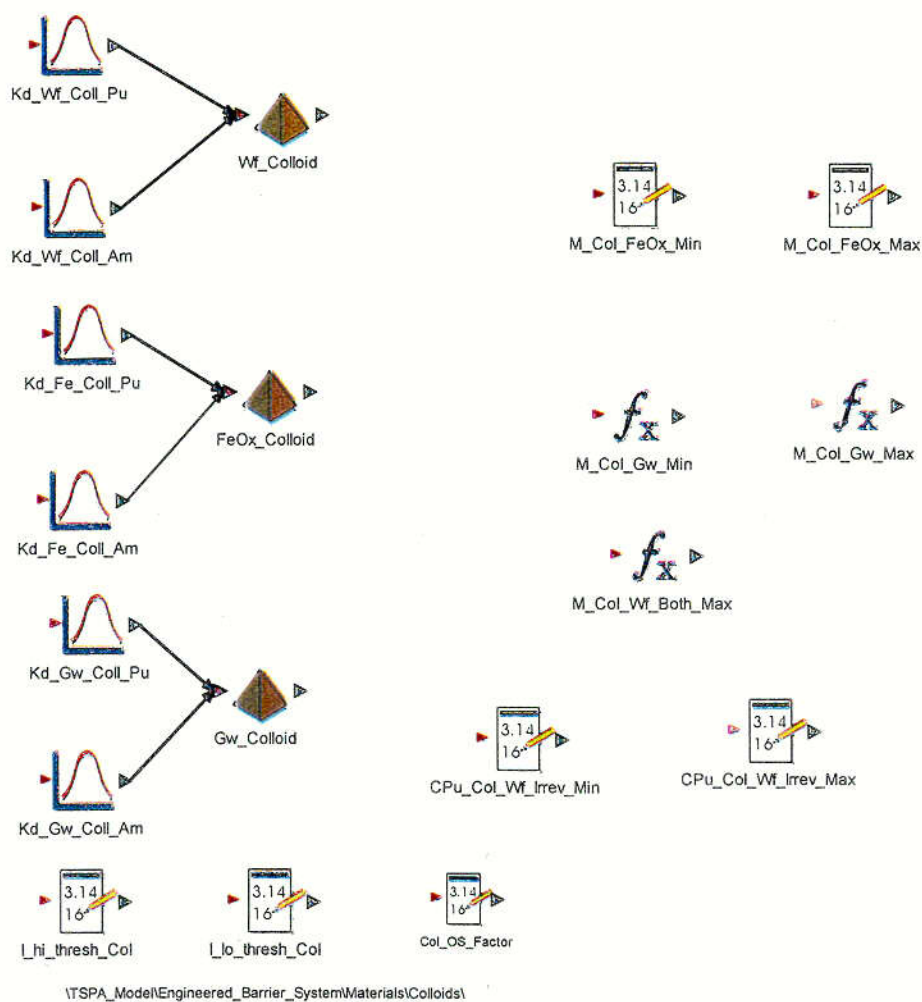
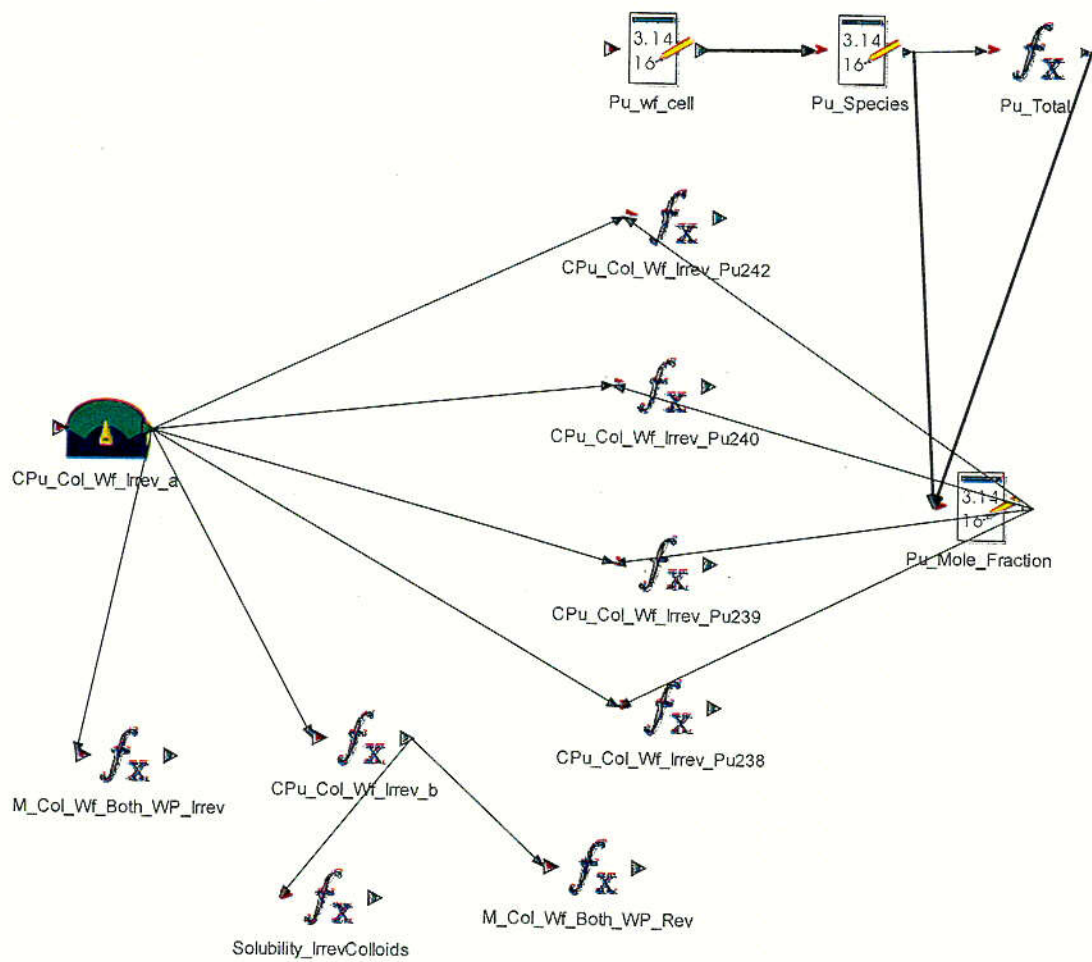


Figure 6-129. Representation of the Definition of Colloid Model Component Inputs

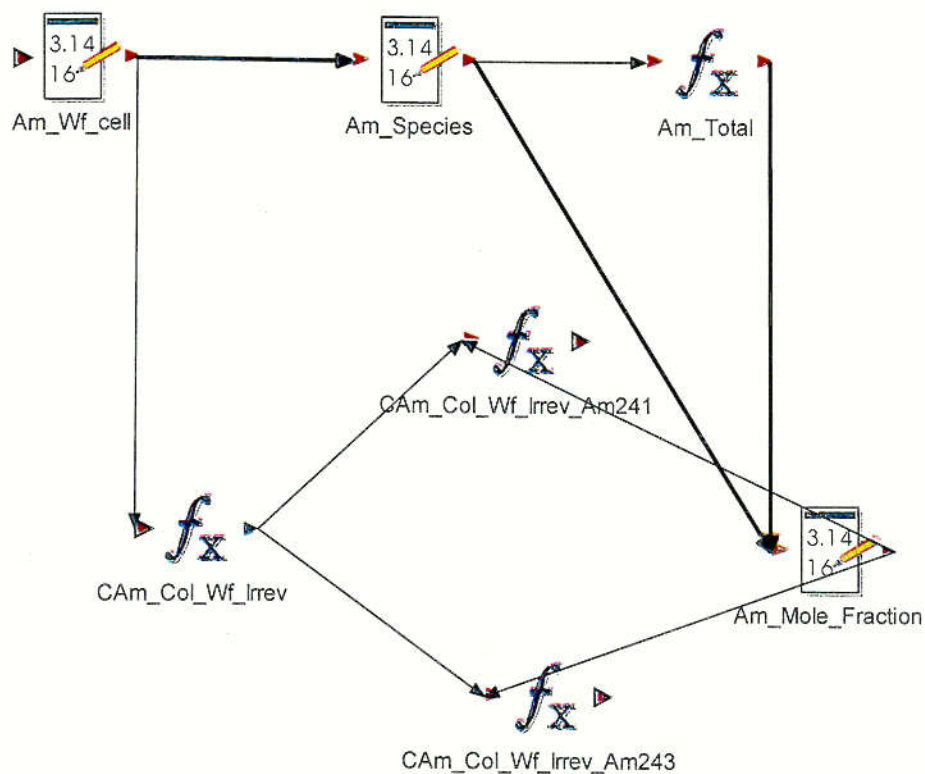
C85



\\TSPA_Model\\Disruptive_Events\\Indirect_Release_Zone1\\Intrusive_Events_CDSP_Packages\\Colloids\\WF_Colloids\\In_WP_WF_Colloids\\Pu_Colloids\\

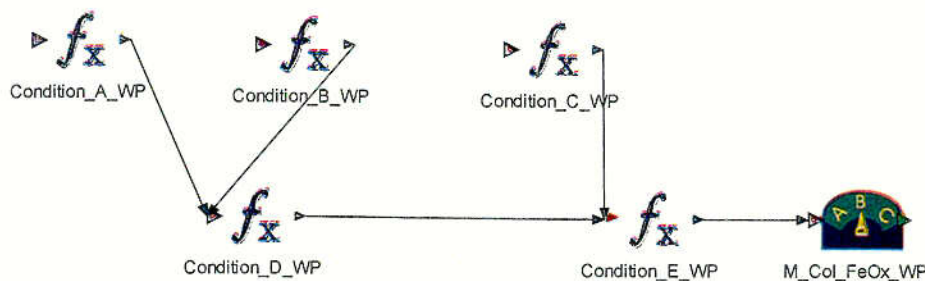
Figure 6-130. Illustration of the Waste Form Colloids Implementation

C86



\\TSPA_Model\\Disruptive_Events\\Indirect_Release_Zone1\\Intrusive_Events_CDSP_Packages\\Colloids\\WF_Colloids\\In_WP_Wf_Colloids\\Am_Colloids\\

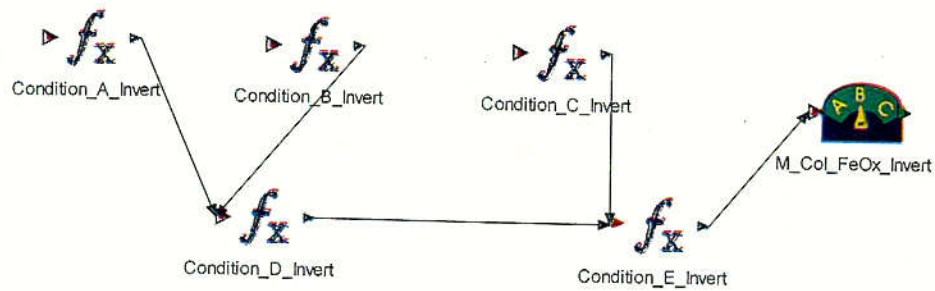
Figure 6-131. Representation of the Calculation for Irreversibly Bound Am Species



\\TSPA_Model\\Engineered_Barrier_System\\CDSP_Packages\\Infiltration_Bin_1\\Always_Drip\\Colloids\\Fe_Hydroxide_Colloids\\In_WP_FeOH_Colloids\\

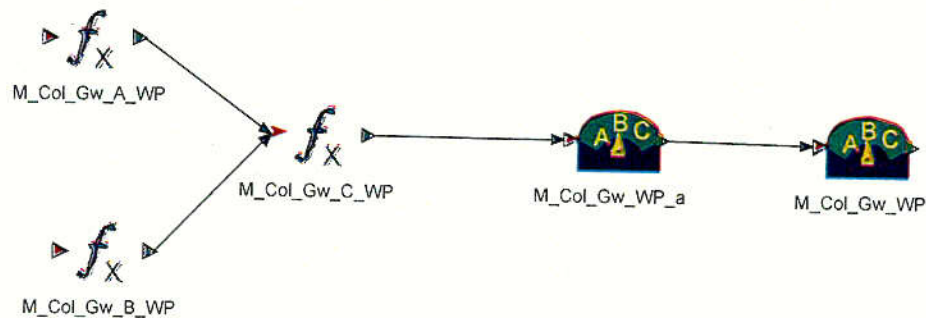
Figure 6-132. Representation of the Iron-(hydr)oxide Colloids Calculation for Waste Packages

C87



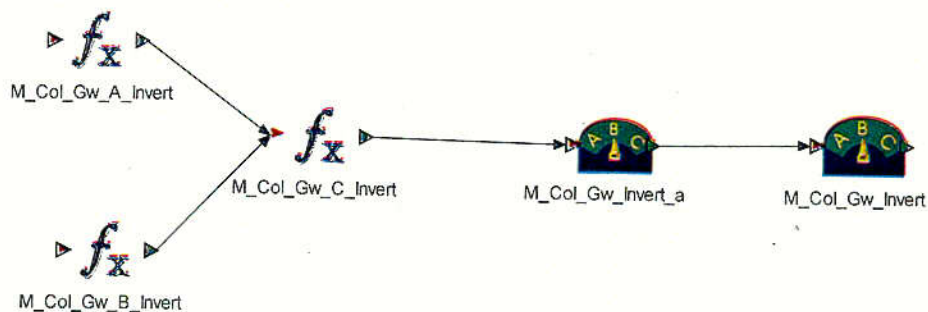
\\TSPA_Model\\Engineered_Barrier_System\\CDSP_Packages\\Infiltration_Bin_1\\Always_Drip\\Colloids\\Fe_Hydroxide_Colloids\\In_Invert_FeOH_Colloids\\

Figure 6-133. Illustration of the Iron-(hydr)oxide Colloid Formation in the Invert Cell



\\TSPA_Model\\Engineered_Barrier_System\\CDSP_Packages\\Infiltration_Bin_1\\Always_Drip\\Colloids\\Groundwater_Colloids\\In_WP_GW_Colloids\\

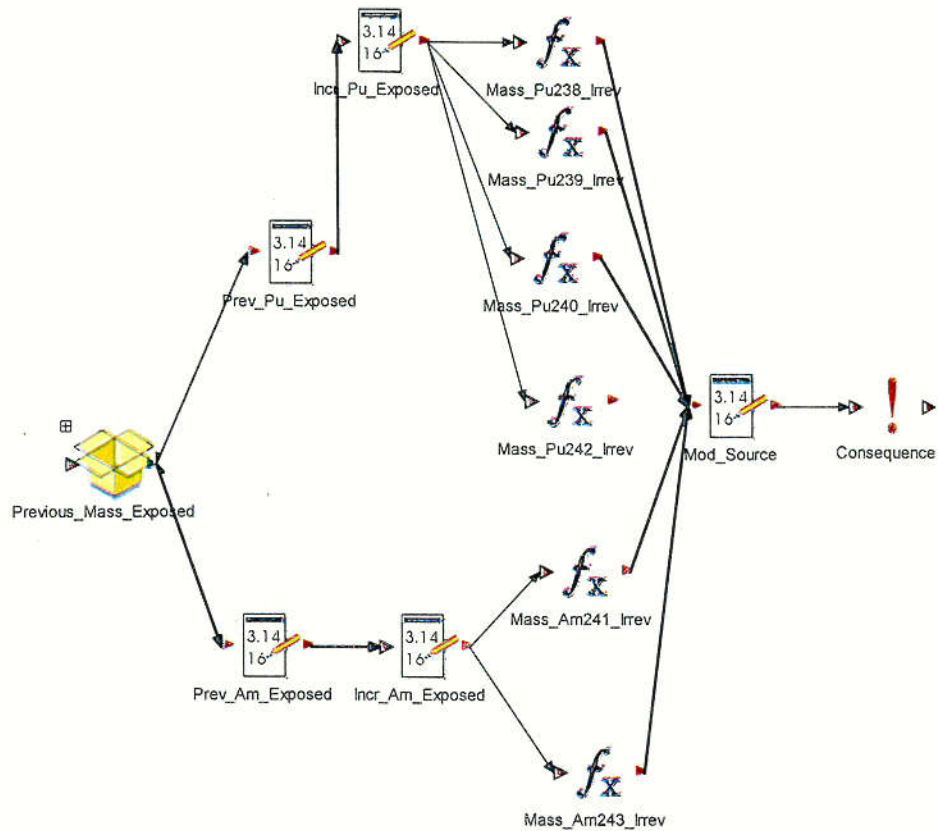
Figure 6-134. Illustration of the Groundwater Colloids Calculation for Waste Packages



\\TSPA_Model\\Engineered_Barrier_System\\CDSP_Packages\\Infiltration_Bin_1\\Always_Drip\\Colloids\\Groundwater_Colloids\\In_Invert_GW_Colloids\\

Figure 6-135. Graphical Illustration of the Groundwater Colloids Calculation for the Invert Cell

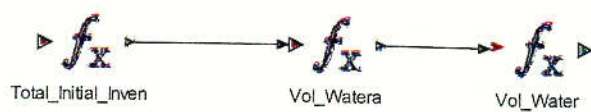
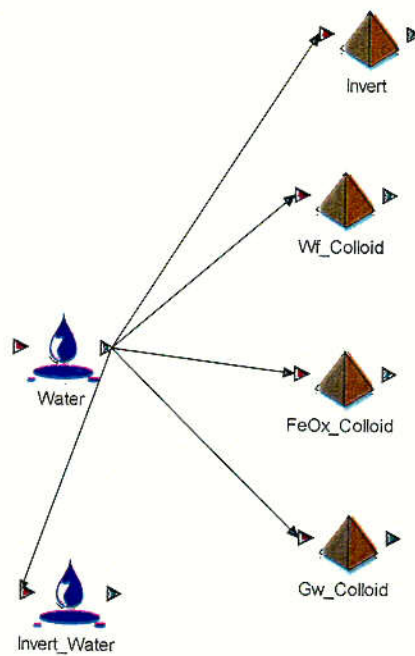
C88.



\\TSPA_Model\\Engineered_Barrier_System\\CDSP_Packages\\Infiltration_Bin_1\\Always_Drip\\GenerateColloids\\

Figure 6-136. Graphical Illustration of the Model Implementation for Removing Species Mass as Irreversible Colloids

C89



\\TSPA_Model\\Engineered_Barrier_System\\CDSP_Packages\\Infiltration_Bin_1\\Always_Drip\\Materials\\

Figure 6-137. Illustration of the Definition of Colloid Solids

c90

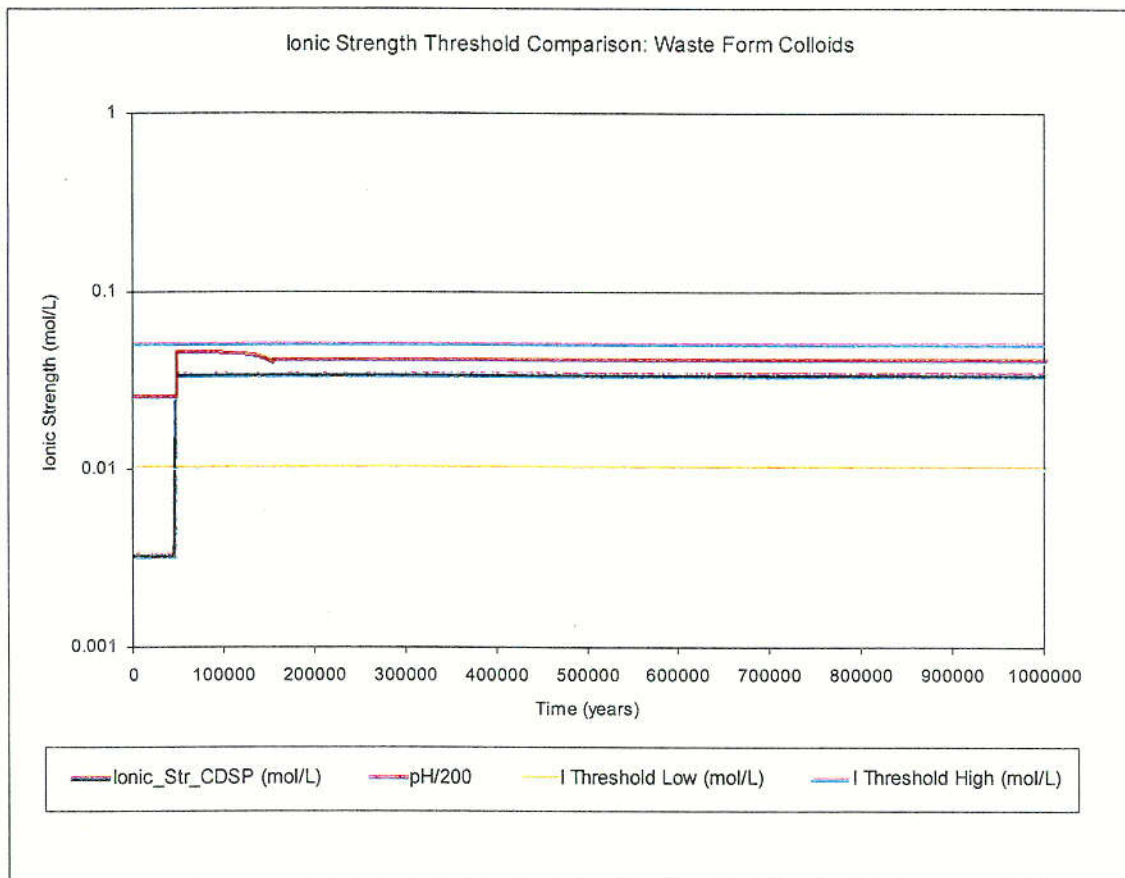


Figure 6-138. Plot of the In-Package Ionic Strength Conditional Statements for Waste Form Colloids

C91

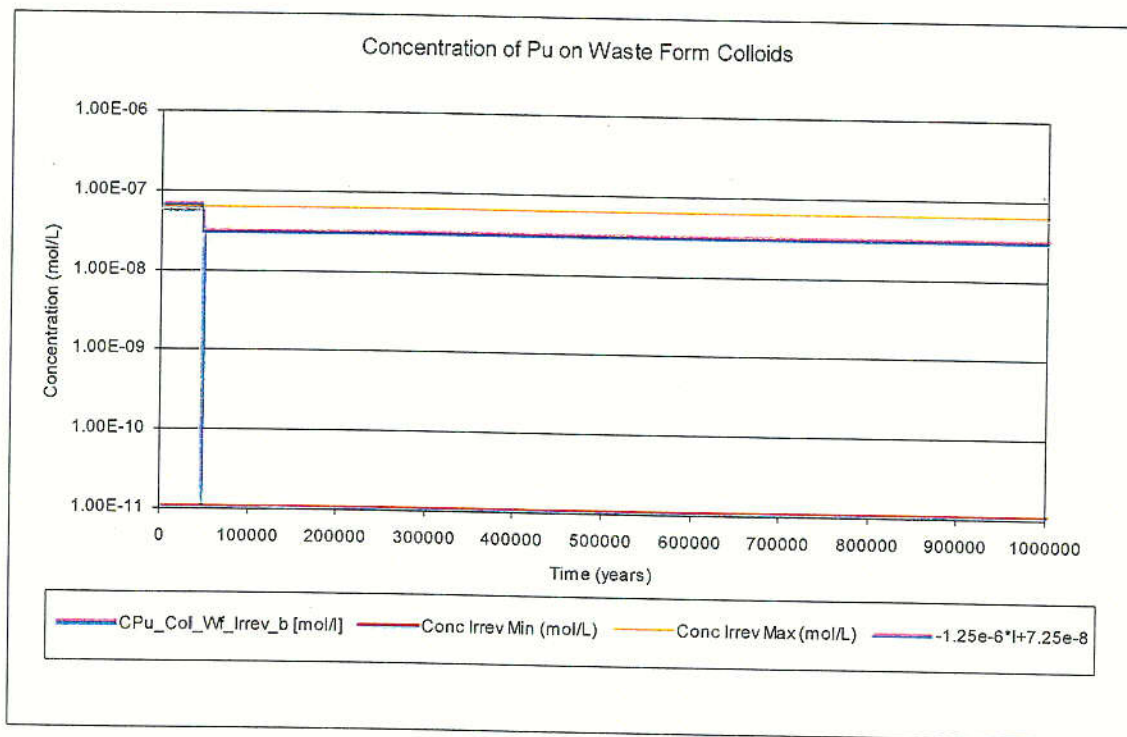


Figure 6-139. Concentration of Pu Irreversibly Bound on Waste Form Colloids in the Waste Package

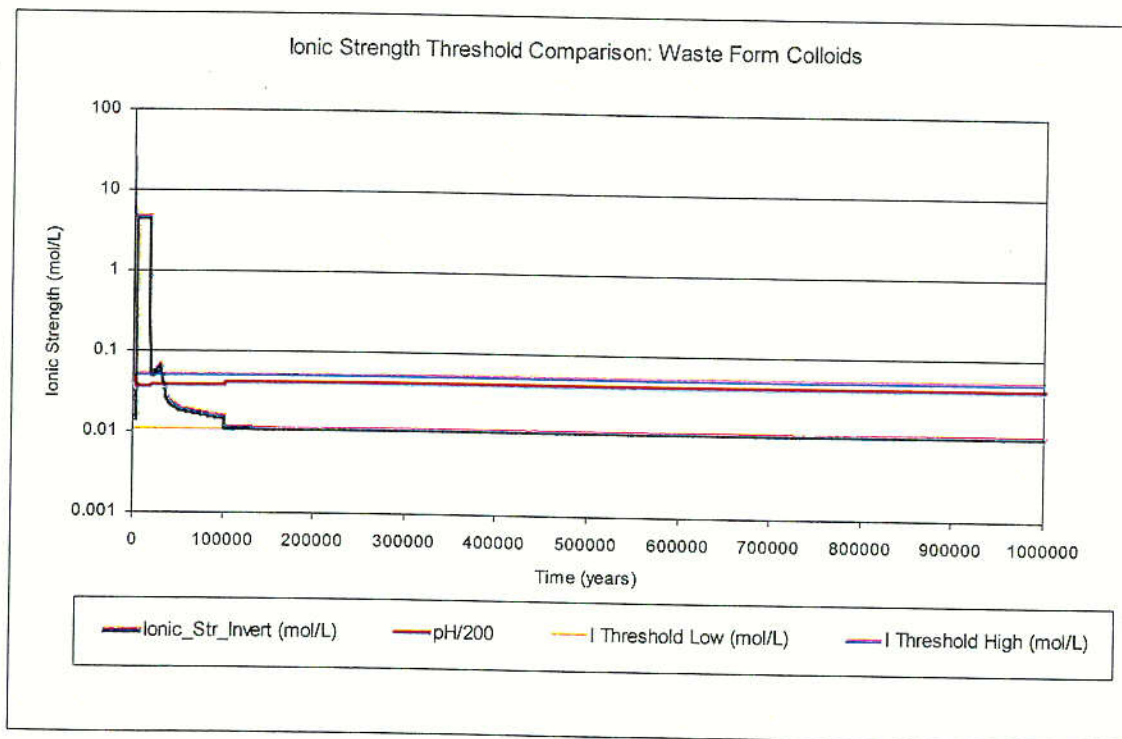


Figure 6-140. Comparison of Ionic_Str_Invert and Conditional Statements for Waste Form Colloid Formation

C92

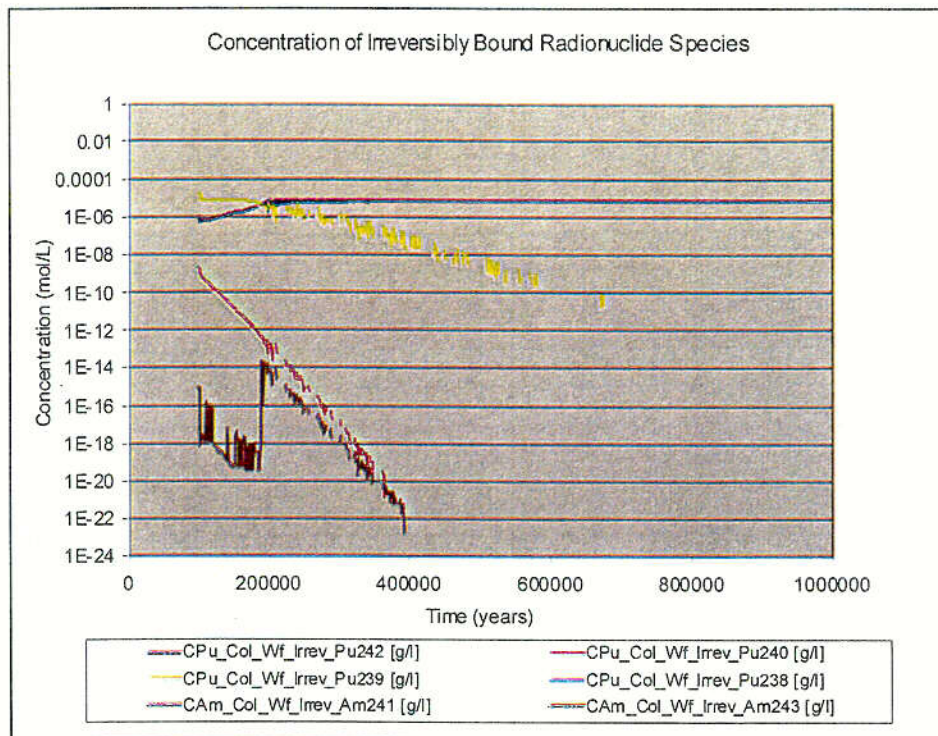


Figure 6-141. Pu and Am Species Irreversibly Bound to Waste Form Colloids in the Waste Package

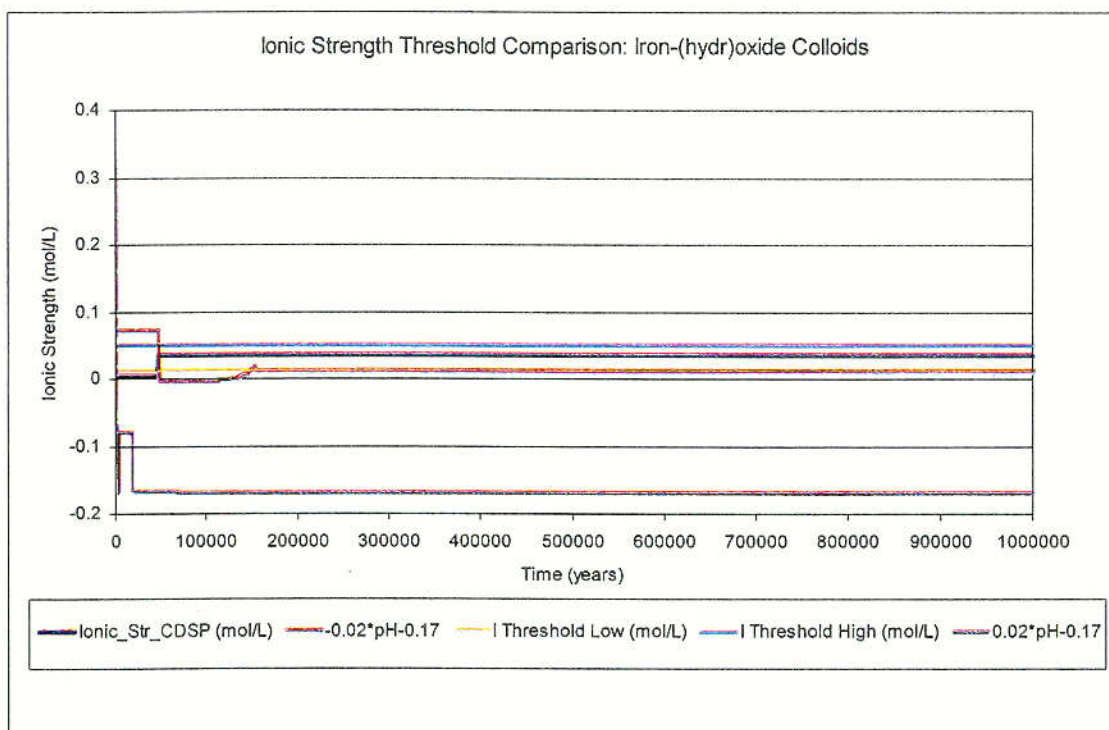


Figure 6-142. Ionic Strength Comparison to Conditional Statements for the Formation of Iron-(hydr)oxide Colloids in the Waste Package

C93

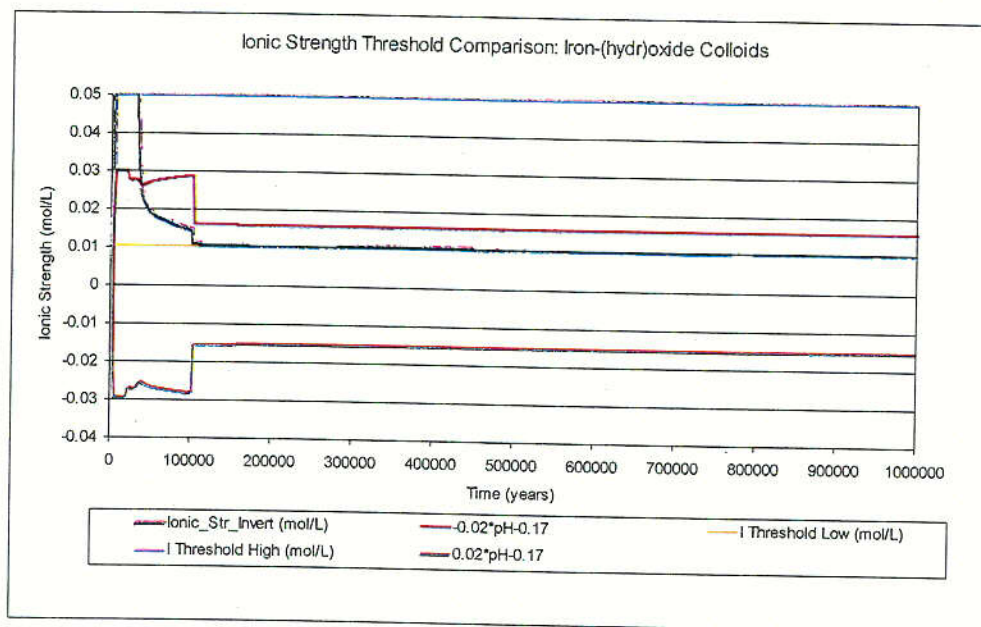
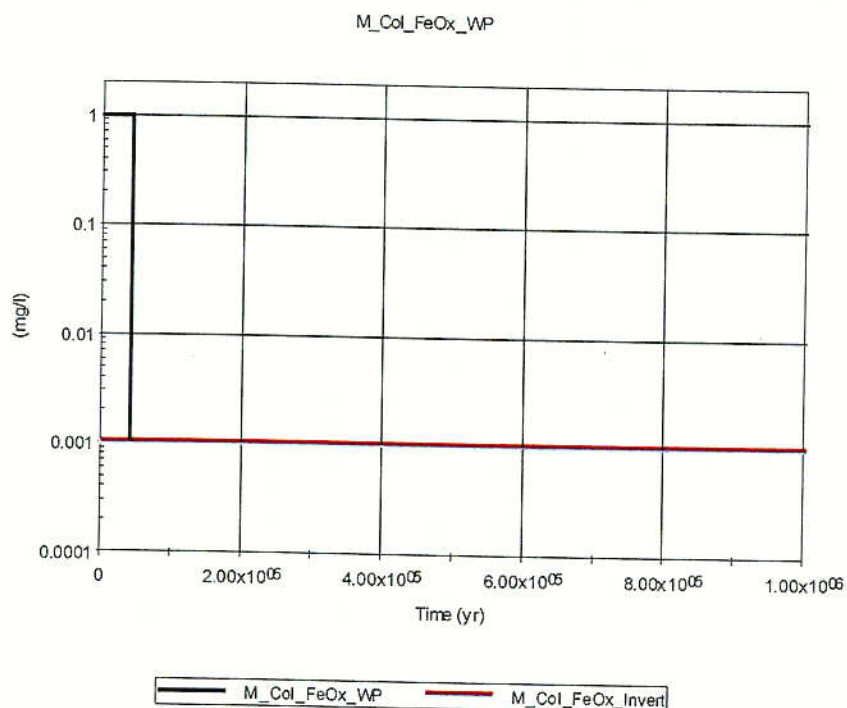


Figure 6-143. Ionic Strength Comparison to Conditional Statements for the Formation of Iron-(hydr)oxide Colloids in the Invert



\\TSPA_Model\\Engineered_Barrier_System\\CDSP_Packages\\Infiltration_Bin_4\\Always_Drip\\Colloids\\Fe_Hydroxide_Colloids\\

Figure 6-144. Mass of Stable Iron-(hydr)oxide Colloids Formed in the Waste Package and in the Invert

C94

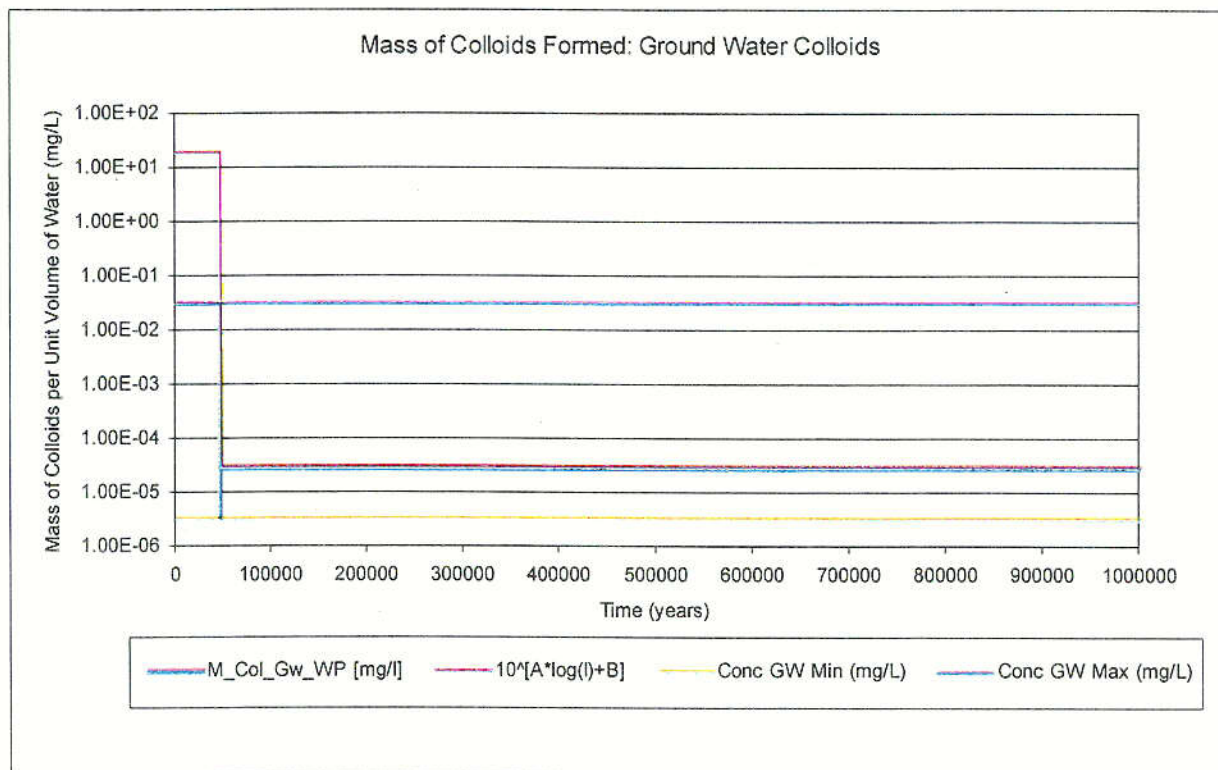


Figure 6-145. Mass of Stable Groundwater Colloids Formed in the Waste Package and in the Waste Package

C95

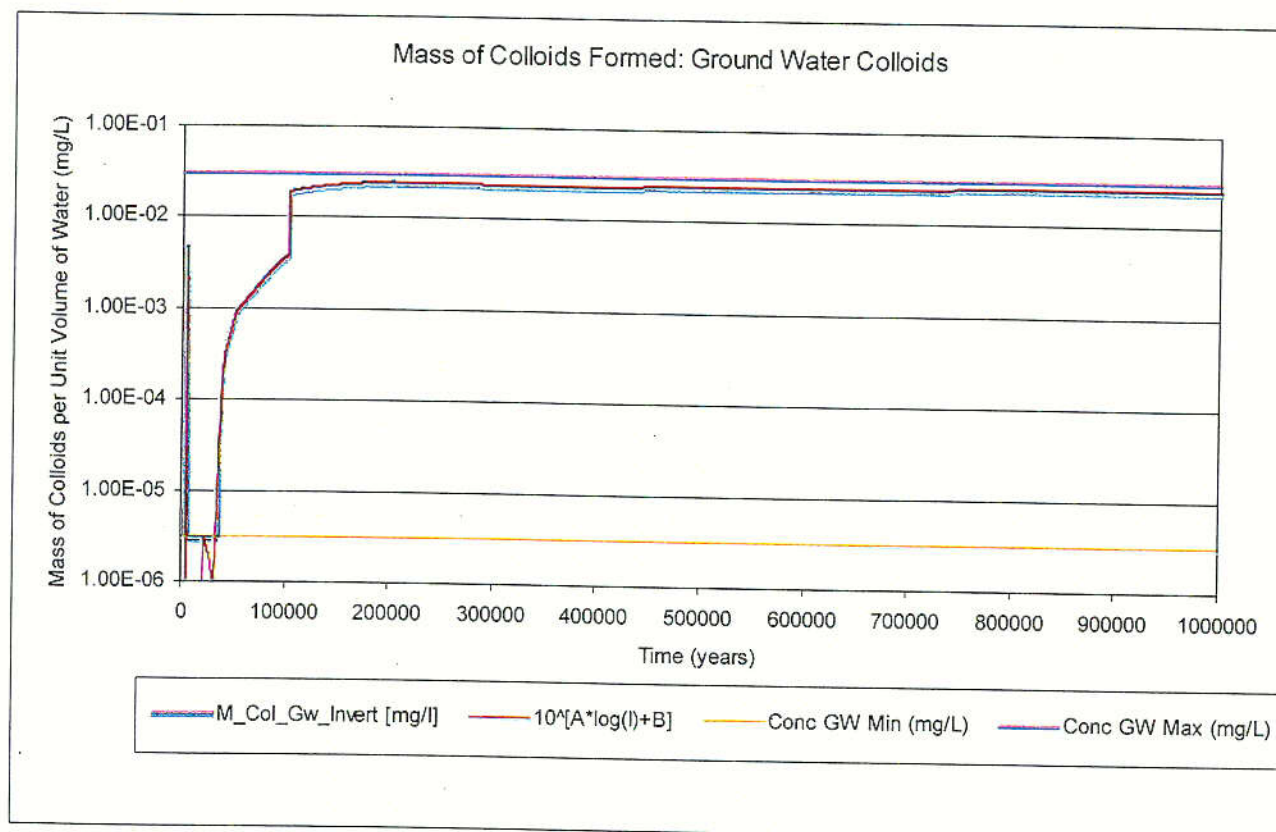


Figure 6-146. Mass of Stable Groundwater Colloids Formed in the Waste Package and in the Invert

C96

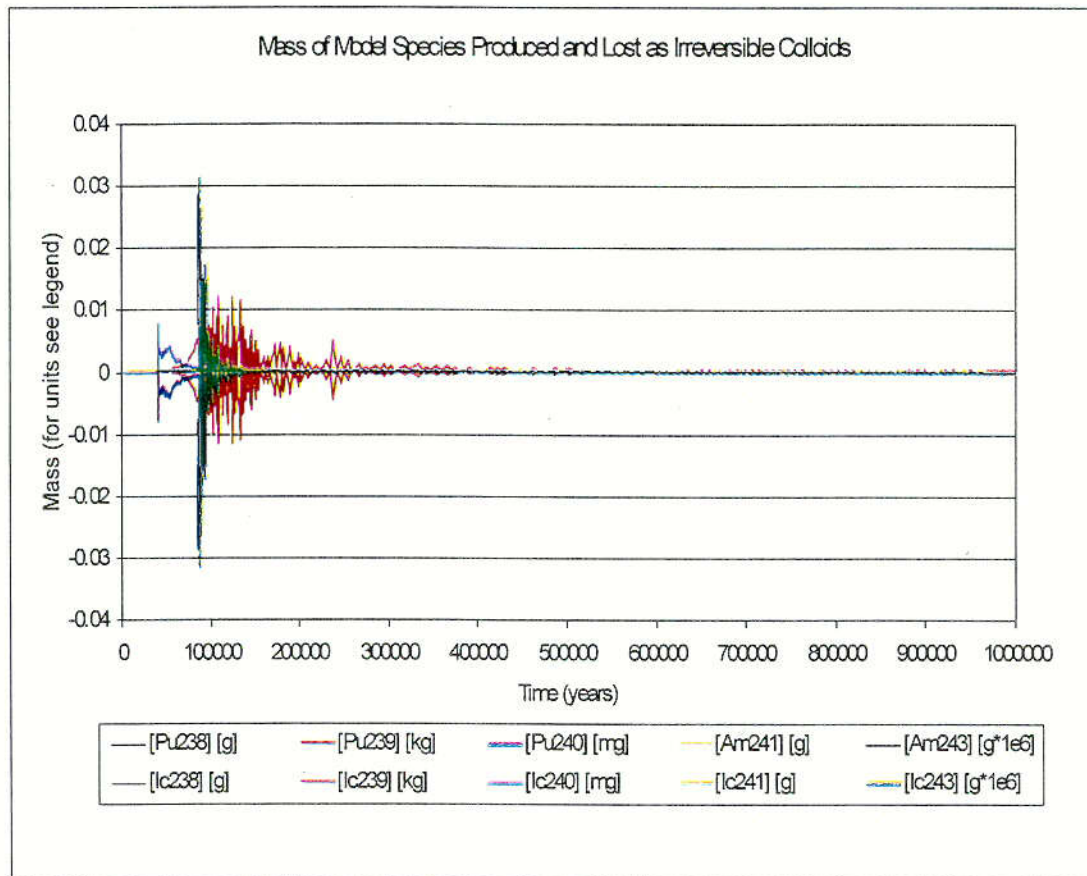


Figure 6-147. Mass of Model Species Produced and Lost Due to Irreversible Colloids

6.3.5 Engineered Barrier System Transport

The Engineered Barrier System (EBS) is the primary man-made barrier to the release of radionuclides from the proposed repository into the biosphere. The EBS comprises three major components:

- The waste packages that encase waste form
- The drip shields above the waste packages
- The crushed tuff invert below the waste packages.

The specific effects of these components on the transport of radionuclides through the EBS and a description of the transport pathways and related parameters are given in the following sections.

Overview

Once the waste form is exposed, the release of radionuclides from the EBS can occur primarily by (a) transport of radionuclides dissolved in water and (b) transport of radionuclides sorbed onto colloids. Both the dissolved and sorbed radionuclides can diffuse and advect through water within the waste packages and through the invert (crushed tuff) below the waste packages. Although other mechanisms of release can exist (e.g., gaseous carbon release), the transport

- Three dripping environments based on when a certain set of packages will experience drips (see Figure 6-150).

An additional source term (not shown in Figure 6-150) is added for all commercial spent nuclear fuel rods with stainless steel cladding. This source term is defined to be in the infiltration bin representing the largest repository area. It experiences Bin 1 seepage if the simulation infiltration scenario is set to present day infiltration (*Infiltration_Scenario* = 1) otherwise it experiences the Bin 4 seepage. A total of thirty-one source terms are modeled in TSPA-SR.

Colloids—Within each cell the colloidal mass is defined as the calculated concentration of colloids multiplied by the volume of water in the cell (see Section 6.3.4.6 for details on colloid concentration calculations). The following types of colloids are considered:

- Ground water colloids
- Iron hydroxide colloids
- Waste form colloids.

Each colloid type may have a different concentration in water. The concentration of colloids in water along with the partition coefficients of radionuclides to colloids are used to calculate the mass of radionuclides sorbed to colloids within each cell. Radionuclides sorbed to colloids are transported via advection and can diffuse between cells based on the concentration gradient between the cells. Table 6-63 through Table 6-66 provide the parameters used to define the mass of colloids within each cell in the EBS.

Table 6-63. Parameters Defining the Waste Form Cells

Waste Form Cell			
Parameter(s)	Description	Value [†]	Notes
Volumes and Masses			
Vol_waterra	Volume of water in waste form cell	If(Total_initial_inven == 0{g}, 0 {m ³ }, (Vol_Rod_CSNF or Vol_Rod_CDSP)* Porosity_Rind* Sat_Rind)*(1-#.Unexposed_Mass[U238] / Total_initial_inven)	The volume of water in the waste form cell is equal to the volume of the rind times the porosity of the rind times the saturation. U238 is used as a surrogate to determine the fraction of the waste form that has been exposed to form a rind. U238 is chosen because of its long-half life (~4.5 billion years) (see assumption in Section 5.2)
Vol_water	Volume of water in waste form cell, with error trap	If(vol_waterra <= 0, 1x10 ⁻⁶ {m ³ }, vol_waterra)	This error trap function assures that the volume is not less than 1x10 ⁻⁶ m ³ to avoid division by zero errors (see assumption in Section 5.2)
M_Col_FeOX_WP * Vol_water	Mass of iron hydroxide colloids, equal to the concentration multiplied by the volume of water	Calculated	See colloid section of this document for discussion of concentration
M_Col_GW_WP * Vol_Water	Mass of ground water colloids, equal to the concentration multiplied by the volume of water	Calculated	See colloid section of this document for discussion of concentration

Table 6-63. Parameters Defining the Waste Form Cells (Continued)

Waste Form Cell			
Parameter(s)	Description	Value [†]	Notes
Volumes and Masses			
M_Col_Wf_Both_WP_Rev*Vol_Water	Mass of waste form colloids, equal to the concentration multiplied by the volume of water (Note: only applies to CDSP packages)	Calculated	See colloid section of this document for discussion of concentration. Only applies to CDSP packages
Mass Input			
#.Cumulative_to_Waste_Form	Mass input from source term calculation	Calculated	Mass input to cell is a function of cladding degradation, waste package failure and waste form degradation.
Advective Connection (Outflows)			
QFlux_WP	Water flow to "Invert_Cell"	Calculated	See text for description and Figure 6-156 for graphical representation
Diffusive Flux (Patches)			
Thick_WP + Thick_Invert/2	Diffusive length through patches and half of invert	20 {mm} + 0.303 {m}	Diffusive length is equal to the thickness of the waste package plus half of the maximum thickness of the invert
WP_Total_Patch_Area_CSNF (or CDSP)	Diffusive area	Failure_Opening * WP_Patch_Area_CSNF (or CDSP)	Number of patches (calculated with WAPDEG) multiplied by the area of a single patch
None + Invert	Material for diffusion through patches	Diffusion Coefficient for Invert	No material specified for diffusion through the waste package as self-diffusion coefficient of water is used. Diffusion through invert based on invert diffusion coefficient
Thick_WP + Thick_Invert/2	Diffusive length through pits and half of invert	20 {mm} + 0.303 {m}	Diffusive length is equal to the thickness of the waste package plus half of the maximum thickness of the invert
WP_Total_Pit_Area	Diffusive area	Failure_Opening * WP_Pit_Area	Number of pits (calculated with WAPDEG) multiplied by the area of a single pit
None + Invert	Material for diffusion through pits	Diffusion Coefficient for Invert	No material specified for diffusion through the waste package as self-diffusion coefficient of water is used. Diffusion through invert based on invert diffusion coefficient
Diffusive Flux (Stress Corrosion Cracks)			
Thick_WP_Lid1+ Thick_WP_Lid2, Thick_Invert/2	Diffusive length	25 {mm} + 10 {mm} + 0.303 {m}	Diffusive length is equal to the combined thickness of the two waste package lids and half of the maximum thickness of the invert

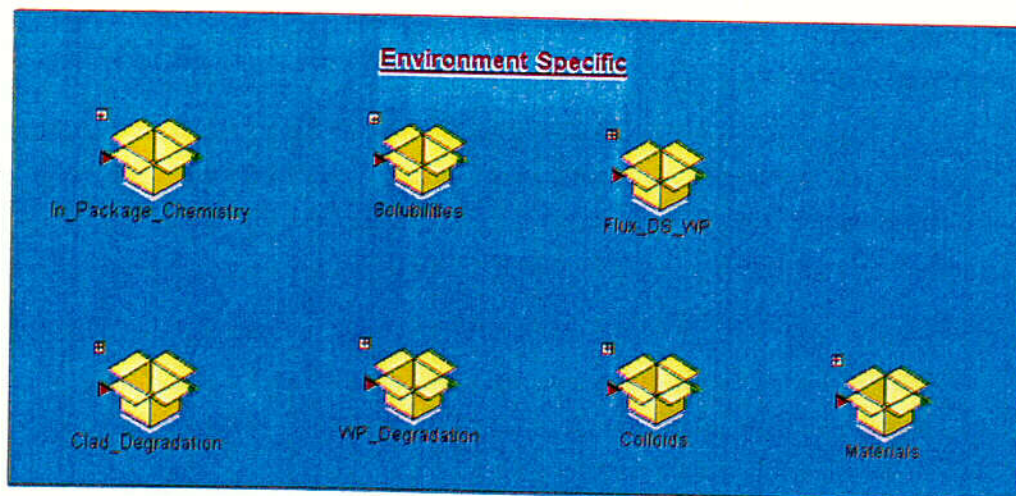


Figure 6-148. Graphical Representation of Important Processes that affect EBS Transport of Radionuclides

6.3.5.1 EBS Flow and Transport Pathways

For the TSPA-SR model, several transport pathways have been identified and modeled by mixing cells and by connections between them (Figure 6-149). A source term is defined initially (e.g., CSNF_AlwaysDrip) to characterize the inventory and to explicitly model the effects of barriers (e.g., cladding or glass matrix) on the release of radionuclides. Once the barriers bounding the waste form fail the cumulative mass released from the exposed waste form (but still held within the waste package) is modeled by using a Waste_Form cell. The Waste_Form cell is a mixing cell that represents the actual waste package in which the exposed waste form is homogeneously mixed with the volume of water available in the waste package and accessible for transport once the waste package is breached.

Advective release from the waste package (Waste_Form cell) occurs through pits and patches, while diffusive release occurs through pits, patches and stress corrosion cracks. Both advective and diffusive releases can occur through the invert. As shown in Figure 6-149, the water within the waste package is represented by a single (mixing) cell, while a second (mixing) cell represents the invert below the waste package. A third cell, referred to as the collector cell, is defined to implement a constant-flux boundary condition at the base of the invert for transport out of the EBS (see Table 6-62 through Table 6-66 for details of the parameters used to define the EBS cells). Mass releases from various collector cells representing alternate percolation flux histories are combined in a new cell called EBS Bin Out (discussed later in this section).

Each source term that can experience unique transport or environmental conditions is defined by a separate set of invert and collector cells. Thirty unique source terms are identified based on:

- Two types of waste packages (CSNF and CDSP)
- Five subdivisions of percolation fluxes into the repository

Table 6-63. Parameters Defining the Waste Form Cells (Continued)

Waste Form Cell			
Parameter(s)	Description	Value [†]	Notes
Volumes and Masses			
WP_Total_Crack_Area	Diffusive area	Failure_Opening * WP_Crack_Area	Number of cracks (calculated with WAPDEG) multiplied by the area of a single crack
None + Invert	Material for diffusion	Diffusion Coefficient for Invert	No material specified for diffusion through the waste package as self-diffusion coefficient of water is used. Diffusion through invert based on invert diffusion coefficient

NOTE: [†]For sources of values see Table 6-68.

indicates that unique parameters are used for each source term based on the differences between the infiltration bins and/or the fuel types.

Table 6-64. Parameters Defining the Invert Cells

Invert Cell			
Parameter(s)	Description	Value [†]	Notes
Volumes and Masses			
Vol_Water_Invert	Volume of water in invert cell	If(Sat_# <=0, Vol_Invert_# * Invert_Porosity * 1x10 ⁻¹² , Vol_Invert_# * Invert_Porosity * Sat_#)	Volume of invert multiplied by the porosity and saturation. Volume of the invert is based on waste package dimensions. Saturation is defined for each infiltration bin and fuel type and is provided from Thermal Hydrology. An error trap is added to assure that the saturation is greater than zero
M_col_FeOX_WP * Vol_Water_Invert	Mass of iron hydroxide colloids, equal to the concentration multiplied by the volume of water	Calculated	See colloid section of this document for discussion of concentration
M_Col_Gw_WP * Vol_Water_Invert	Mass of ground water colloids, equal to the concentration multiplied by the volume of water	Calculated	See colloid section of this document for discussion of concentration
Volumes and Masses			
M_Col_Wf_Both_WP_Rev*Vol_Water_Invert	Mass of waste form colloids, equal to the concentration multiplied by the volume of water (<i>Note: only applies to CDSP packages</i>)	Calculated	See colloid section of this document for discussion of concentration. Only applies to CDSP packages
Mass_Invert	Mass of invert	(Invert_Density * (1-Invert_Porosity)) * Vol_Invert_#	Mass of invert is a function of the density, volume and porosity. The volume is calculated based on the waste package dimensions
Mass Input			
None defined	N/a	N/a	Mass input is defined with connections from Waste Form Cell

Table 6-64. Parameters Defining the Invert Cells (Continued)

Invert Cell			
Parameter(s)	Description	Value [†]	Notes
Volumes and Masses			
Advective Connection (Outflows)			
QFlux_DS	Water flow to "Collector"	See Table 1-5	Calculated by using flux splitting algorithm: fluid flux through a patch or pit in the drip shield is proportional to the ratio of the total length of penetration in the axial direction to the total axial length of the drip shield (see Table 6-67).
Diffusive Flux (Patches/Pits/Stress Corrosion Cracks)			
See Table 6-63	See Table 6-63	See Table 6-63	Diffusive connections are bi-directional between cells. The parameters that define the connections are identical for both cells. See Table 6-63 for parameter values
Diffusive Flux (to Collector Cell)			
Thick_Invert/2	Diffusive length	0.303 {m}	Diffusive length is equal to half the thickness of the invert
DiffArea_Inv_#	Diffusive area	$\text{Pi} * (\text{Radius}_{\#} + \text{Thick_Invert}) * \text{Length}_{\#}$	Area defined as a half-cylinder with a radius of the waste package plus the invert thickness and a length equal to the length of the waste package
Invert	Material for diffusion	Diffusion Coefficient for Invert	Diffusion through invert based on invert diffusion coefficient

NOTE: '#' indicates that unique parameters are used for each source term based on the differences between the infiltration bins and/or the fuel types.

[†]For sources of values see Table 6-68.

Table 6-65. Parameters Defining the Collector Cells

Collector Cells			
Parameter(s)	Description	Value	Notes
Volumes and Masses			
Vol_Water_Collector	Volume of water in collector cells	$1 \times 10^{-6} \text{ {m}^3}$	Assumption in Section 5.2
M_col_FeOX_WP * Vol_Water_Collector	Mass of iron hydroxide colloids, equal to the concentration multiplied by the volume of water	Calculated	See colloid section of this document for discussion of concentration
M_Col_Gw_WP * Vol_Water_Collector	Mass of ground water colloids, equal to the concentration multiplied by the volume of water	Calculated	See colloid section of this document for discussion of concentration
M_Col_Wf_Both_WP_Rev*Vol_Water_Collector	Mass of waste form colloids, equal to the concentration multiplied by the volume of water (Note: only applies to CDSP packages)	Calculated	See colloid section of this document for discussion of concentration. Only applies to CDSP packages

Table 6-65. Parameters Defining the Collector Cells (Continued)

Collector Cells			
Parameter(s)	Description	Value	Notes
Volumes and Masses			
Mass Input			
None defined	n/a	n/a	Mass input is defined with connections from Invert Cell
Advective Connection (Outflows)			
Collector_Flux	Water flow to "EBS_Bin#_Out"	1×10^5 {m ³ /yr}	Assumption in Section 5.2
Diffusive Flux (Invert)			
See Table 6-64	See Table 6-64	See Table 6-64	Diffusive connections are bi-directional between cells. The parameters that define the connections are identical for both cells. See Table 6-64 for parameter values

NOTE: '#' indicates that unique parameters are used for each source term based on the differences between the infiltration bins and/or the fuel types.
For sources of values see Table 6-68.

Table 6-66. Parameters Defining the EBS Bin Out Cells

EBS_Bin_Out Cells			
Parameter(s)	Description	Value	Notes
Volumes and Masses			
Vol_Water_Collector	Volume of water in EBS_Bin#_Out cells	1×10^{-6} {m ³ }	Assumption in Section 5.2
M_Col_FeOX_WP * Vol_Water_Collector	Mass of iron hydroxide colloids, equal to the concentration multiplied by the volume of water	Calculated	See colloid section of this document for discussion of concentration
M_Col_Gw_WP * Vol_Water_Collector	Mass of ground water colloids, equal to the concentration multiplied by the volume of water	Calculated	See colloid section of this document for discussion of concentration
M_Col_Wf_Both_WP_Rev*Vol_Water_Collect or	Mass of waste form colloids, equal to the concentration multiplied by the volume of water	Calculated	See colloid section of this document for discussion of concentration.
Mass Input			
Bin#_input_indirect	Mass input from indirect volcanic releases	See Section 6.3.9.2	Mass input is defined with connections from Collector Cell and from volcanic event portion of total system model

Table 6-66. Parameters Defining the EBS Bin Out Cells (Continued)

EBS Bin Out Cells			
Parameter(s)	Description	Value	Notes
Volumes and Masses			
Volumes and Masses			
Advective Connection (Outflows)	Water flow to "FEHM_External"	$1 \times 10^5 \{m^3/yr\} *$ multiplier	Assumption in Section 5.2. Multiplier ensures a very small residence time in the Bin Out cells.
Collector_Flux* (7 for bin_1 or 6 for bin_2 or 6 for bin_3 or 7 for bin_4 or 6 for bin_5)			

NOTE: *# indicates that unique parameters are used for each source term based on the differences between the infiltration bins and/or the fuel types.
For sources of values see Table 6-68.

Waste Form Cell—The volume of water and mass of colloids within a waste package are represented by the waste form cell. The volume of water available for contact with the waste form (per waste package) is calculated to be the rind volume multiplied by the porosity of the rind and the water saturation of the rind (CRWMS M&O 2000 [144167]). The parameters *Vol_Watera* and *Vol_Water* are used to implement the abstraction (see Table 6-63 for actual values and for the list of parameters that define the waste form cells).

Invert Cell—In order to conservatively represent diffusive releases from waste packages, the entire bottom half of each waste package is defined to be in contact with the invert. The volume of the invert (*volume_invert_CSNF* and *volume_invert_CDSP*) is therefore defined as a concentric half-cylinder surrounding the waste package that has an interior radius equal to the radius of the waste package (*Radius_CSNF* and *Radius_CDSP*), a thickness equal to the maximum thickness of the invert (*thick_invert*), and a length equal to the length of the waste package (*length_CSNF* and *length_CDSP*). So

$$Vol_Invert_CSNF = (\pi / 2.0) * ((Radius_CSNF + Thick_Invert) \wedge 2 - (Radius_CSNF) \wedge 2) * Length_CSNF$$

$$Vol_Invert_CDSP = (\pi / 2.0) * ((Radius_CDSP + Thick_Invert) \wedge 2 - (Radius_CDSP) \wedge 2) * Length_CDSP$$

Collector Cells—The collector cell for each source term is used to implement a conservative near zero concentration constant-flux boundary condition at the edge of the EBS. To implement this boundary condition, the collector cells are given a small volume of water (*Vol_Water_Collector* = $1 \times 10^{-6} m^3$) and a high outgoing flux (*collector_flux* = $1 \times 10^5 m^3/yr$). This approach results in a negligible residence time for any mass transported by either advection or diffusion into the collector cell. See Table 6-65 for details of the parameters that define the collector cells.

EBS Bin Out Cells—At the edge of the EBS, five cells are defined to sum the mass flux of radionuclides out of each infiltration bin (see Figure 6-151). This step is necessary because the UZ transport model (see Section 6.3.6) requires mass flux input as a function of time from each

specified infiltration bin. Indirect release of radionuclides from volcanic events, when modeled, are added as cumulative mass input to each of the Bin_Out cells. As with the collector cells, the cells at the edge of the EBS are defined with a small volume of water ($Vol_Water_Collector = 1 \times 10^{-6} \text{ m}^3$) and a high advective outflow ($1 \times 10^5 \text{ m}^3/\text{yr}$) so that there is effectively no residence time in the cells. See Table 6-66 for details of the parameters that define the EBS bin cells.

Diffusive Transport of Radionuclides—Diffusive transport of radionuclides and colloids is controlled by the effective diffusion coefficient, the concentration gradient, and the diffusive area within the transport pathway. For diffusion out of the waste package (and into the invert), the concentration gradient is defined by the ratio of the difference in concentration between the waste form cell and the adjacent invert cell to the total diffusive length. The total diffusive area for the waste package is defined by the combination of breached areas resulting from pits, patches, and cracks ($WP_Total_Pit_Area$, $WP_Total_Patch_Area_CDSP$, $WP_Total_Patch_Area_CSNF$, and $WP_Total_Crack_Area$), respectively. In case of diffusion through pits and patches, the diffusive length is given as the thickness of the waste package outer barrier ($Thick_WP$) plus half the maximum thickness of the invert ($Thick_Invert$), while the diffusive length for diffusion through stress corrosion cracks is the combined thickness of the two waste package lids ($Thick_WP_Lid1 + Thick_WP_Lid2$) plus half the maximum thickness of the invert ($Thick_Invert$).

For diffusion through the invert, the diffusive length is equal to half the maximum thickness of the invert ($Thick_Invert$) while the diffusive area is given as the cross-sectional area of the invert ($DiffArea_Inv_CSNF$ and $DiffArea_Inv_CDSP$). Several factors can affect the effective diffusion coefficient within the invert, including porosity, liquid saturation, concentration of radionuclides in solution, and the effect of temperature on the viscosity of a fluid. For TSPA-SR, the effects of porosity, liquid saturation, and temperature are considered (CRWMS M&O 2000 [129284], Section 6.4.1). The base diffusion coefficient for all radionuclides in the TSPA-SR model is taken to be the coefficient for self-diffusion of water ($Diff_Free = 2.299 \times 10^{-5} \text{ cm}^2/\text{sec}$), which represents an upper bound for the free-water diffusivity of radionuclides considered in the TSPA-SR. The diffusion coefficient for the invert is calculated by multiplying $Diff_Free$ (Table 6-67) by the porosity to the 1.3 power and liquid saturation to the 1.849 power. This value is then modified for the effect of temperature as follows:

$$\frac{D_T}{D_{Free}} = \frac{\frac{T}{T_{Free}}}{\frac{\eta_T}{\eta_{Free}}}, \quad (\text{Eq. 6-9})$$

where T is the new temperature, T_{Free} is the temperature at which the free water diffusion coefficient is known, η_T is the viscosity of water at temperature T , and η_{Free} is the viscosity of water at temperature T_{Free} . The temperature dependence of viscosity is given by:

$$\log_{10} \left(\frac{\eta_T}{\eta_{20}} \right) = \frac{1.3272(293 - T) - 0.001053(T - 293)^2}{T - 168} \quad (\text{Eq. 6-10})$$

or

$$\eta_T = (1.002)10^{\left[\frac{1.3272(293-T) - 0.001053(T-293)^2}{T-168} \right]} \quad (\text{Eq. 6-11})$$

with $\eta_{20} = 1.002$ Centipoise.

Table 6-67. Parameters Defining Flux through Drip Shields, Waste Packages, and Invert

Parameter	Definition	Notes
DS_Frac_Patch	DS_Top_Patch_Failures/Number_DS_Patches	DS_Top_Patch_Failures is determined from WAPDEG.
DS_Frac_Pit	DS_Top_Pit_Failures/DS_Total_Length	DS_Top_Pit_Failures is determined from WAPDEG.
Qflux_DS_Patch	DS_Frac_Patch * Seepage#	Seepage is unique for each infiltration bin and each dripping environment. See Section 6.3.1.2 for details on seepage. Note: Qflux_DS_Patch also contains an error trap to assure that fractional area is not greater than 1.
Qflux_DS_Pit	DS_Frac_Pit * Seepage#	Seepage is unique for each infiltration bin and each dripping environment. See Section 6.3.1.2 for details on seepage. Note: Qflux_DS_Pit also contains an error trap to assure that fractional area is not greater than 1.
Qflux_DS	Qflux_DS_Pit + Qflux_DS_Patch	Qflux_DS also contains an error trap to assure that the total flux is not greater than seepage
WP_Frac_Patch_#	WP_Total_Patch_Length_#/Length_#	WP_Total_Patch_Length_# is determined from WAPDEG.
WP_Frac_Pit_#	WP_Total_Pit_length/Length_#	WP_Total_Pit_Length is determined from WAPDEG.
Qflux_WP_Patch	WP_Frac_Patch_# * Qflux_DS	Seepage is unique for each infiltration bin and each dripping environment. See Section 6.3.1.2 for details on seepage. Note: Qflux_WP_Patch also contains an error trap to assure that fractional area is not greater than 1.
Qflux_WP_Pit	WP_Frac_Pit_# * Qflux_DS	Seepage is unique for each infiltration bin and each dripping environment. See Section 6.3.1.2 for details on seepage. Note: Qflux_WP_Pit also contains an error trap to assure that fractional area is not greater than 1.
Qflux_WP	Qflux_WP_Pit + Qflux_WP_Patch	Qflux_WP also contains an error trap to assure that the total flux is not greater than Qflux_DS

NOTE: See Table 6-63 for parameter sources.

All temperatures are in degrees Kelvin. The above equations are broken into several parts for implementation in the GoldSim model (*Eta_A*, *Eta_B*, *Eta_C*, and *Eta* - see Parameter section for values of each parameter).

Advective Transport of Radionuclides. Advective release from the waste package to the invert is modeled to occur through pits and patches only (a significant amount of fluid does not advect through stress corrosion cracks). The flow through pits and patches are combined into a single flux (Q_{flux_WP}) that is used in mass transport calculations. This flux is primarily a function of (a) the seepage onto the waste package through the drip shield (Q_{flux_DS}) and (b) the fractional length of the waste package breached by pits and patches (WP_Frac_Patch or $WP_Frac_Patch_CSNF$ and $WP_Frac_Pit_CSNF$ or $WP_Frac_Pit_CDSP$) (see Table 6-67).

The advective flux from the invert to the collector cell is equal to the flux through the drip shield (Q_{flux_DS}), which is a function of the total seepage into the drift and the fractional area of the drip shield that is breached. This approach assumes that the seepage flux that goes around the drip shield does not travel through the invert and thus is ignored for the EBS transport calculations (see assumption in Section 5.3.5). There is no advective flux through the invert and waste package for packages that do not experience drips, discounting any condensation on the underside of the drip shield.

Advective flux out of the collector cells and EBS Bin Out cells is defined as $1 \times 10^5 \text{ m}^3/\text{yr}$ (see assumption in Section 5.2). This high flux value is used to implement the constant flux boundary condition in the collector cell and to assure that there is almost no residence time in the EBS Bin Out cells.

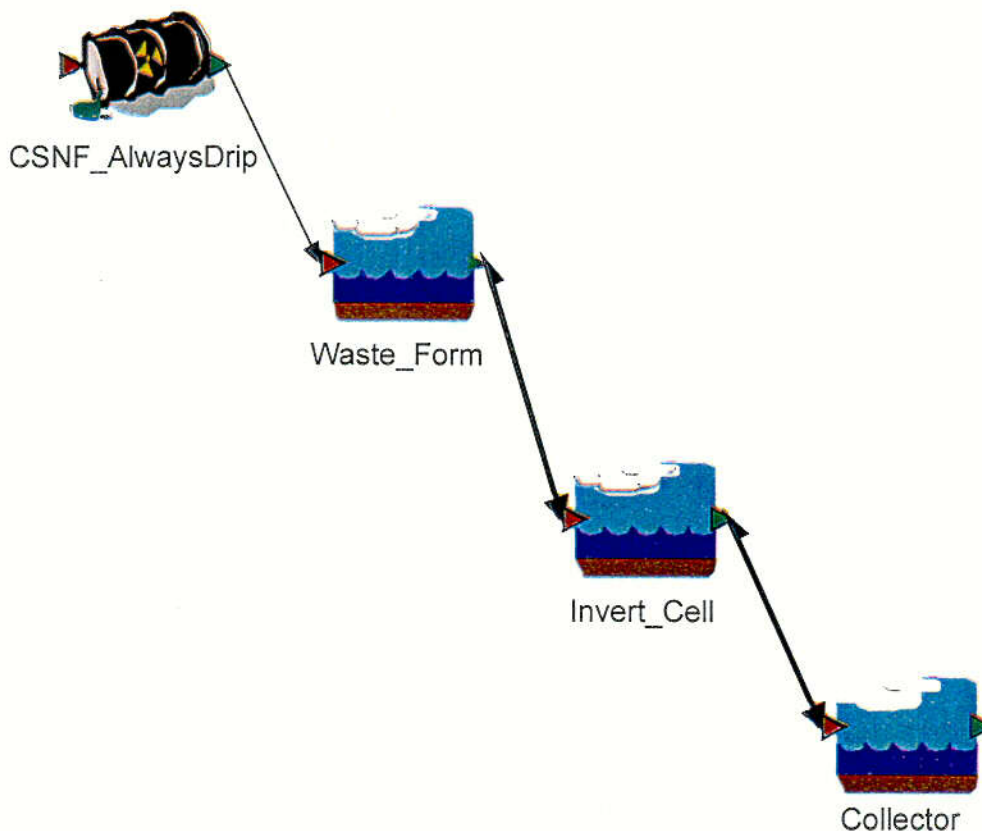


Figure 6-149. The Cells Defined for EBS Transport from Each Unique Source Term

C99

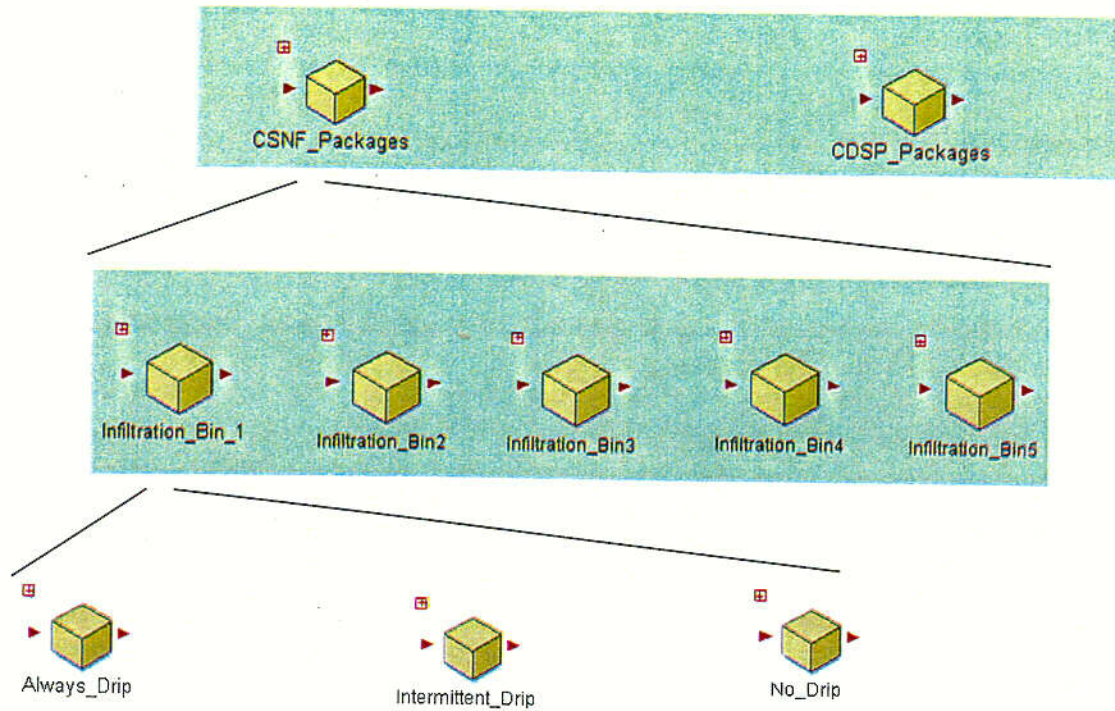


Figure 6-150. Graphical Representation of Thirty Unique Source Terms for the Total System Model in GoldSim



Figure 6-151. Cells at the Edge of the EBS that Feed The UZ Model

C100

6.3.5.2 EBS Transport Parameters

Table 6-68 summarizes the parameters that define the inputs to the EBS transport model in TSPA.

Table 6-68. Values and Sources for EBS Transport Parameters

Parameter Name	Parameter Value	Source
Eta_A	$1.3272 \cdot (293\{K\} - \text{Temp_}\#\{K\})$	CRWMS M&O 2000 [129284], Section 6.4.1.3
Eta_B	$0.001053 \cdot (\text{Temp_}\#\{K\} - 293\{K\})^2$	CRWMS M&O 2000 [129284], Section 6.4.1.3
Eta_C	$\text{Temp_}\#\{K\} - 168\{K\}$	CRWMS M&O 2000 [129284], Section 6.4.1.3
Eta	$10^{((\text{Eta_A} - \text{Eta_B}) / \text{Eta_C})}$	CRWMS M&O 2000 [129284], Section 6.4.1.3
Diff_Free	$2.299 \times 10^{-5} \text{ cm}^2/\text{sec}$	CRWMS M&O 2000 [129284], Table 1 DTN: MO0002SPASDC00.002 [148338]
Inv_Diff_Coeff	$\text{Diff_Free} \cdot (\text{Temp_}\#\{K\}) / (273 + 25\{K\}) / \text{Eta}$	CRWMS M&O 2000 [129284], Section 6.4.1.3
Invert_Porosity	0.545	CRWMS M&O 2000 [129284], Table 1 DTN: SN9908T0872799.004 [108437]
Invert_Density	2530 {kg/m ³ }	CRWMS M&O 2000 [129284], Table 1 DTN: SN9908T0872799.004 [108437]
Thick_Invert	0.606 {m}	CRWMS M&O 2000 [129284], Table 1 DTN: SN9908T0872799.004 [108437]
DiffArea_Inv_CSNF	$\pi \cdot (\text{Radius_CSNF} + \text{Thick_Invert}) \cdot \text{Length_CSNF}$	Internal GoldSim Parameter
DiffArea_Inv_CDSP	$\pi \cdot (\text{Radius_CDSP} + \text{Thick_Invert}) \cdot \text{Length_CDSP}$	Internal GoldSim Parameter
Vol_Invert_CSNF	$(\pi/2.0) \cdot ((\text{Radius_CSNF} + \text{Thick_Invert})^2 - (\text{Radius_CSNF})^2) \cdot \text{Length_CSNF}$	Internal GoldSim Parameter
Vol_Invert_CDSP	$(\pi/2.0) \cdot ((\text{Radius_CDSP} + \text{Thick_Invert})^2 - (\text{Radius_CDSP})^2) \cdot \text{Length_CDSP}$	Internal GoldSim Parameter
Vol_Water_Invert	if(Saturation <= 0, Vol_Invert * Invert_Porosity * 1×10^{-12} , Vol_Invert * Invert_Porosity * Saturation)	Internal GoldSim Parameter
Mass_Invert	$(\text{Invert_Density} \cdot (1 - \text{Invert_Porosity})) \cdot \text{Vol_Invert}$	Internal GoldSim Parameter
Length_CSNF	5.275 {m}	CRWMS M&O 2000 [129284], Table 1
Radius_CSNF	0.782 {m}	CRWMS M&O 2000 [129284], Table 1
Length_CDSP	3.73 {m}	CRWMS M&O 2000 [129284], Table 1
Radius_CDSP	1.015 {m}	CRWMS M&O 2000 [129284], Table 1
WP_SA_CSNF	$2.0 \cdot \pi \cdot \text{Radius_CSNF} \cdot \text{Length_CSNF}$	Internal GoldSim Parameter
WP_SA_CDSP	$2.0 \cdot \pi \cdot \text{Radius_CDSP} \cdot \text{Length_CDSP}$	Internal GoldSim Parameter
WP_Frac_Patch #	WP_Total_Patch_Length_#/Length_#	Internal GoldSim Parameter
WP_Frac_Pit #	WP_Total_Pit_length/Length_#	Internal GoldSim Parameter
DS_Frac_Patch	DS_Top_Patch_Failures/Number_DS_Patches	Internal GoldSim Parameter

Table 6-68. Values and Sources for EBS Transport Parameters (Continued)

Parameter Name	Parameter Value	Source
DS_Frac_Pit	DS_Top_Pit Failures/DS_Total_Length	Internal GoldSim Parameter
Qflux_WP_Patch	If(WP_Frac_Patch_# < 1, (Qflux_DS*WP_Frac_Patch_#), Qflux_DS)	Internal GoldSim Parameter
Qflux_WP_Pit	If(WP_Frac_Pit_# < 1, (Qflux_DS*WP_Frac_Pit_#), Qflux_DS)	Internal GoldSim Parameter
Qflux_DS_Patch	If(DS_Frac_Patch < 1, (SeepFlux#*DS_Frac_Patch), SeepFlux#)	Internal GoldSim Parameter
Qflux_DS_Pit	If(DS_Frac_Pit < 1, (SeepFlux#*DS_Frac_Pit), SeepFlux#)	Internal GoldSim Parameter
Qflux_WP	if((Qflux_WP_Patch + Qflux_WP_Pit) > Qflux_DS, Qflux_DS, (Qflux_WP_Patch + Qflux_WP_Pit))	Internal GoldSim Parameter
Qflux_DS	If((Qflux_DS_Patch + Qflux_DS_Pit) > SeepFlux_AI_CS NF_1, SeepFlux_AI_CS NF_1, (Qflux_DS_Patch + Qflux_DS_Pit))	Internal GoldSim Parameter
WP_Total_Pit_Area	(Failure_Opening(ETime, 23) + Failure_Opening(ETime, 26)+ Failure_Opening(ETime, 29))*WP_Pit_Area	Internal GoldSim Parameter
WP_Total_Patch_Area	(Failure_Opening(ETime, 22) + Failure_Opening(ETime, 25)+ Failure_Opening(ETime, 28))*WP_Patch_Area_#	Internal GoldSim Parameter
WP_Total_Crack_Area	(Failure_Opening(ETime, 24) + Failure_Opening(ETime, 27) + Failure_Opening(ETime, 30)) * WP_Crack_Area	Internal GoldSim Parameter
Vol_Rod_CS NF	0.94{m ³ }	CRWMS M&O 2000 [136045], calculated from parameters given in Table 2 and Attachment I-4.
Vol_Rod_CDSP	0.71{m ³ }	CRWMS M&O 2000 [143420], calculated from dimensions specified in Section 6.1.2.
Porosity_Rind	0.2	CRWMS M&O 2000 [144167], Section 6.3 suggests a value of waste form porosity of 20%, DTN: LL000207751021.119 [145940]
Sat_Rind	1.0	Assumption in Section 5.2
Vol_Watera	If(Total_initial_inven == 0{g}, 0 {m ³ }, (Vol_Rod_CS NF (or CDSP) * Porosity_Rind* Sat_Rind)*(1- #_Unexposed_Mass[U238] / Total_initial_inven) # denotes unique source term identifier	The volume of water in the waste form cell is equal to the volume of the rind times the porosity of the rind times the saturation (CRWMS M&O 2000 [144167]). U238 is used as a surrogate to determine the fraction of the waste form that has been exposed to form a rind (see assumption in Section 5.2).
Vol_Water	If(vol_watera <=0, 1x10 ⁻⁶ {m ³ }, vol_watera)	Assumption in Section 5.2
Thick_WP	20 {mm}	CRWMS M&O 2000 [129284], Table 1 (thickness of outer layer only)
Vol_Water_Collector	1x10 ⁻⁶ {m ³ }	Assumption in Section 5.2

Table 6-68. Values and Sources for EBS Transport Parameters (Continued)

Parameter Name	Parameter Value	Source
Collector_Flux	$1 \times 10^5 \{m^3/yr\}$	Assumption in Section 5.2
Number_WP_Patches	1000	Assumption in Section 5.2.
WP_Crack_Area	$4.08 \times 10^{-6} \{m^2\}$	CRWMS M&O 2000 [129284], Section 6.3.1.2.1 DTN: MO0006SPASTR01.003 [153029]
WP_Pit_area	0 $\{m^2\}$	CRWMS M&O 2000 [129284], Section 6.3.1.2. Pitting has been screened out as a plausible corrosion mechanism for Alloy C22. See assumption in Section 5.2.
Thick_WP_Lid1	25 {mm}	CRWMS M&O 2000 [144128], Attachment 1, detail A
Thick_WP_Lid2	10 {mm}	CRWMS M&O 2000 [144128], Attachment 1, detail A
DS_Total_Length	4.775 {m}	CRWMS M&O 2000 [144128], Attachment I, Inner shell length.
Number_DS_Patches	500	Assumption in Section 5.2.

NOTE: Some source parameters listed in the parameter definitions are not detailed here. Definitions for these source parameters can be found in the relevant sections of this document.

Implementation

The implementation of the parameters listed in Table 6-68 is discussed in Section 6.3.5.1, where they have been described in detail and used in calculating other parameters.

Results and Verification

The main output from the EBS transport model is the mass flux out of the engineered barrier system into the unsaturated zone. Mass releases for Np-237 and Tc-99 from each of the infiltration bins are compared in Figure 6-152 and Figure 6-153 respectively for the median value simulation. These results do not represent all of the results of the engineered barrier system, but instead are meant to be a representative sample of the EBS results for two important radionuclides.

The validation/verification for the EBS transport conceptual model can be found in the document EBS Radionuclide Transport Abstraction (CRWMS M&O 2000 [129284]). GoldSim is used as a shell program to combine all of the components and abstractions for the total system model. In order to demonstrate the validation/verification of the implementation of the components in GoldSim, it is only necessary to show that the abstractions are implemented correctly in GoldSim and that the feeds between the component models are working correctly. Table 6-69 lists the connections between the EBS transport component and some of the other total system model components.

Table 6-69. Description of the Components of the Total System Model that are Connected to EBS Transport

Component	Description of connection to EBS Transport Component
Seepage	Advective flux through waste package and drift is a function of seepage into the drift. The seepage fraction (fraction of packages experiencing drips) is also a function of the seepage rate
Climate	Seepage rates into the drift are affected by climate
Waste Package Degradation	Radionuclide transport can not occur until waste packages are breached. The advective and diffusive release out of a waste package is proportional to the fraction of the axial length failed on the waste package, among other factors. Advective fluxes through the waste package and drift are a function of the breached area of a drip shield
Concentration limit	Concentration limits affect diffusive and advective releases. The maximum advective release out of a waste package and through the engineered barrier system is the sum of the concentration limit for radionuclides dissolved in water and the concentration limit for any colloidal species that can sorb the radionuclides. The maximum gradient for diffusion is controlled by the concentration limit of a radionuclide
Colloids	Colloids can increase release of radionuclides out of a waste package. Radionuclides can reversibly and irreversibly sorb onto colloids in the engineered barrier system
Inventory	Inventory determines the total mass of radionuclides that are available for EBS transport
Waste Form Degradation and Mobilization	Cladding and waste form degradation determine the availability of radionuclides for transport through the EBS at each time step
Unsaturated Zone Transport	The mass release from the EBS is the source term for transport through the unsaturated zone

The following is a demonstration that the waste package degradation and seepage feeds to the EBS transport model are correct. For Bin 4, commercial spent nuclear fuel packages that sometimes experience drips, the advective flux through the drip shield is determined by the drip shield failure area fraction and the seepage into the drift. At 200,000 years, the number of patch failures on the top part of the drip shield is 486.92 (*DS_Top_Patch_Failures* = 486.92). Note that no pits form during the simulation. The seepage rate is equal to 0.96337 m³/yr (*SeepFlux_In_CSNF_4_median_nbf* = 0.96337 m³/yr). With the total number of the drip shield patches (*Number_DS_Patches*) equal to 500 the following is the expected flux through the drip shield:

$$\begin{aligned}\text{Flux} &= \text{seepage rate} * \text{patch failure} / \text{total patches} \\ \text{Flux} &= 0.96337 \text{ m}^3/\text{yr} * 486.92 / 500 = 0.93816 \text{ m}^3/\text{yr}\end{aligned}$$

The advective flux through the invert (*Qflux_DS*), as calculated by the model, is equal to 0.93816 m³/yr at 200,000 years, which matches with the hand calculated value.

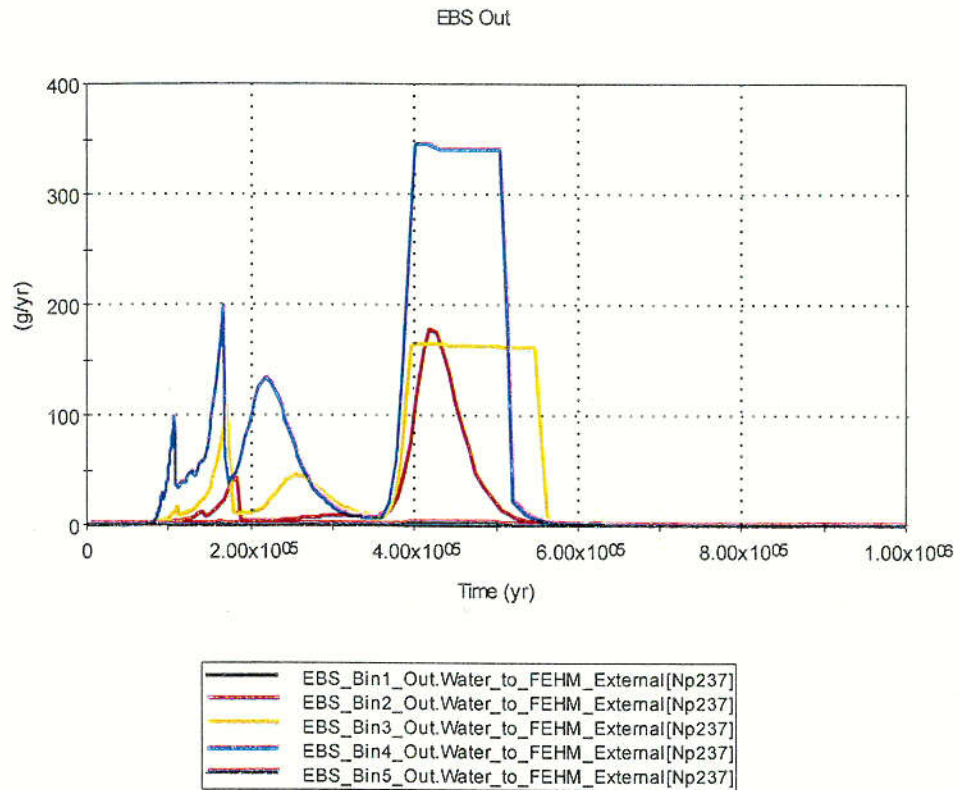


Figure 6-152. Comparison of Mass Release of Np-237 from EBS for each Infiltration Bin

C101

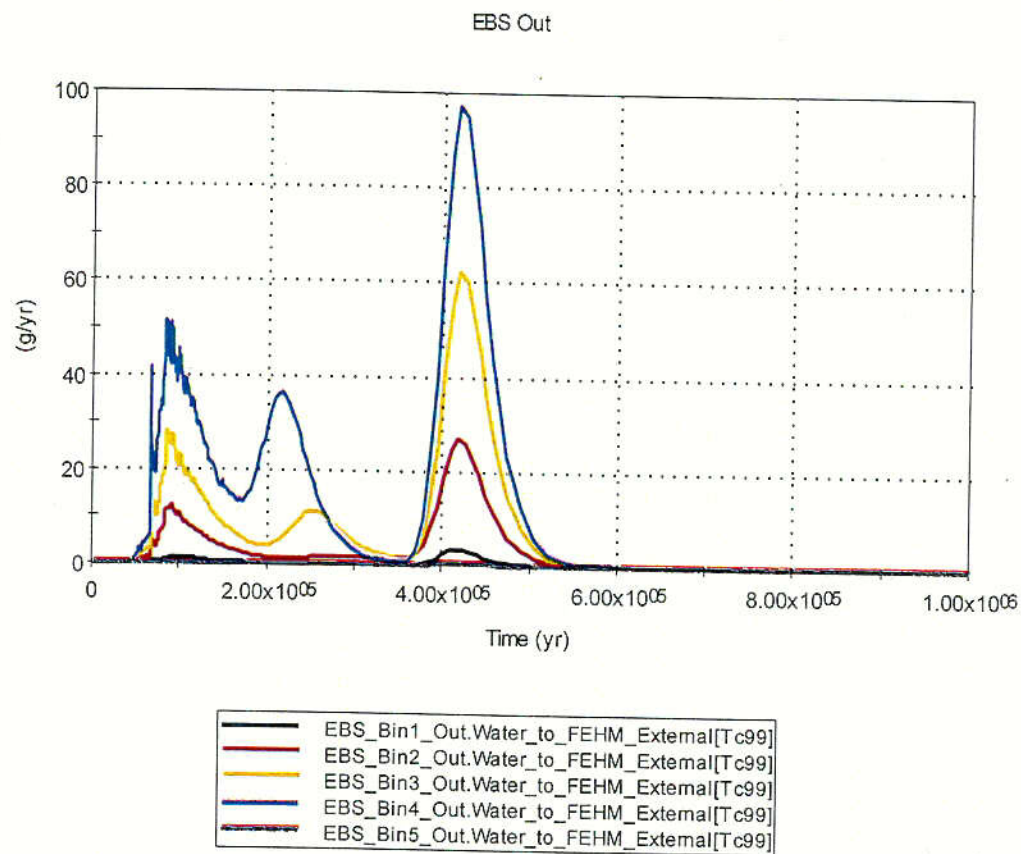


Figure 6-153. Comparison of Mass Release of Tc-99 from EBS for each Infiltration Bin